HOKKAIDO UNIVERSITY

Title	Evolution of Ecology in Crocodylians : Morphometric and Phylogenetic Approach
Author(s)	飯島, 正也
Degree Grantor	北海道大学
Degree Name	博士(理学)
Dissertation Number	甲第13134号
Issue Date	2018-03-22
DOI	https://doi.org/10.14943/doctoral.k13134
Doc URL	https://hdl.handle.net/2115/72343
Type	doctoral thesis
File Information	Masaya_Iijima.pdf

Hokkaido University Collection of Scholarly and Academic Papers : HUSCAP

博士学位論文

Evolution of Ecology in Crocodylians: Morphometric and Phylogenetic Approach

（ワニ類の生態進化史の復元：形態計測・系統学的アプローチ）

飯島 正也

北海道大学大学院理学院

自然史科学専攻

平成 30 年 3 月

Evolution of Ecology in Crocodylians: Morphometric and Phylogenetic Approach

by

Masaya Iijima

A thesis submitted in partial fulfillment of the

requirements for the degree of Doctor of Philosophy

Department of Natural History Sciences

Graduate School of Science, Hokkaido University

March 2018

Abstract

Crocodylia is a remarkably successful group of archosaurs (crocodylians, birds, and all descendants of their most recent common ancestor) which has dominated the land-water interface since the Late Cretaceous. Because extant species are available for measuring morphology, function, performance, and fitness, Crocodylia is an ideal model group for ecomorphological study. Moreover, ~80 Ma of its clade history allows us to test various evolutionary hypotheses in a geologic time scale. Meanwhile, crocodylian systematics is a classic model case in that morphological and molecular datasets provide contradictory higher-level relationships, which has not reached consensus yet. This dissertation aimed at understanding evolution of ecology in crocodylians thorough morphometrics of trophic and locomotor ecomorphology and reconsideration of the morphological phylogenetic hypothesis, using extant and fossil materials.

Comparative growth trajectories of cranial trophic ecomorphology among crocodyloid species revealed the role of postnatal development in shaping trophic diversity in crocodyloid crocodylians. Growth patterns of some traits (e.g. rostrum shape; pterygoid flange depth) are universal among all examined species, suggesting the existence of a shared size-dependent biomechanical constraint in crocodyloids. On the other hand, *Gavialis gangeticus*, a putative piscivorous taxon, shows unique ontogenies for several other traits (e.g. size of supratemporal fenestra; tooth size disparity), implying that piscivorous adaptation involves shifts in the growth trajectories of trophic ecomorphology.

Morphometrics of appendicular and axial skeletons among extant and fossil crocodylians revealed locomotor divergence between two major groups (Alligatoroidea and Crocodyloidea) and uniqueness of *G. gangeticus*. Comparative limb proportions show that crocodyloids have relatively long stylopodia (humerus and femur) than alligatoroids, indicating that two groups may differ in locomotor functions. *G. gangeticus* differs in various limb and vertebral metrics, reflecting its distinct locomotor ecology. Some of the postcranial metrics (e.g. limb proportions) are correlated with rostral shape, an indicator of trophic function, suggesting that trophic and locomotor functions might differently delimit the ecological opportunity of alligatoroids and crocodyloids in the evolution of crocodylians.

The morphological phylogeny of crocodylians was reconsidered through a new look at East Asian “tomistomines,” and a revised postcranial character sampling. Although a new analysis supported the previous morphological hypothesis of higher level relationships, the

alternative tree that was forced to fit the molecular hypothesis was only few steps longer than the unconstrained tree, and two trees were not significantly incongruent with each other. Mapped on the constrained tree that is consistent with the molecular hypothesis, cranial and postcranial characters show a gradual specialization on the lineage of *G. gangeticus*, preceding the divergence of "gavialoids" in the morphological context.

Acknowledgments

As the end of my PhD life approached, I realized that I had only achieved very small things in past five years. At the same time, I knew that none of such small progress could be made on my own.

I first express my sincere gratitude to my dissertation supervisor Yoshitsugu Kobayashi for his guidance throughout my PhD study. He opened an opportunity for studying fossil crocodylians, which was his favorite research topic. He has facilitated access to most of the important domestic crocodylian collections, allowing me to conduct a comprehensive systematic work on Japanese crocodylians. Needless to say, he is the largest contributor to this dissertation. Every piece of my work was conceptualized through our interaction, and some ideas were entirely borrowed from him. My graduate committee member Yasuhiro Iba constantly gave constructive criticisms to my research works, and a lot of valuable advice on research life. I largely owe to his encouragement over the years of hardship in my PhD. Other committee members Noriyuki Suzuki and Toru Takeshita made me realize the importance of thinking evolution in a geologic and paleoenvironmental context.

Research and technical staff in the Hokkaido University Museum provided a fun and productive working environment. I thank Masaki Eda and Junji Yamamoto for giving access to animal dissection and microscope facilities, and Hiroki Echizenya for helping with boiling and maceration of crocodylians. Current lab members of Hokkaido University Paleobiology Group (Tomonori Tanaka, Ryuji Takasaki, Tsogtobaatar Chinzorig, Junki Yoshida, Aya Kubota, Sangu An, Akira Ota, Miu Tanaka, Kota Kubo, Ryo Suzuki, and many undergraduates), as well as lab alumni (Shoji Hayashi, Yoshihiro Tanaka, Kohei Tanaka, Kentaro Chiba, Yuya Ishida, Kento Otsuka, Takumi Sakakiyama, and others) were always helpful in many ways. I hugely thank for their friendship, research advice, and technical support. Tomonori Tanaka is thanked for providing at least few hundred hours for sociality skill lessons. I can say for sure that he could publish several good papers if he spared some time for his study, but without doubt he is still a great scientist and educator. Ryuji Takasaki has been a great debater and editor as an ideal ‘desk neighbor’ in my office. Fossil prep and molding volunteers at the Hokkaido University Museum provided a relaxing atmosphere in the weekly coffee breaks, where I can get away from research. I never forget late Kei Nakano scooped me up from the bottom after I failed the PhD candidacy exam in 2015.

Tamaki Sato, my undergraduate supervisor at Tokyo Gakugei University, has been an amazing mentor since I began working on my undergraduate thesis in 2010. It was her encouragement that put me back on the right track, and saved me from quitting school. I also appreciate her willingness to write many reference letters, although I failed all the time. Takehito Ikejiri has been an excellent role model for me since I first met him in 2009. I got many tips on how to enjoy research life from him. I am also indebted to his extraordinary hospitality during my visit to Massachusetts and Connecticut in 2017.

I claim minimum level of originality in this dissertation. Most of my ideas and datasets were built through interaction with my generous collaborators. I thank Yoshikazu Hasegawa for his insightful comments on the systematics of the 'Yage' crocodylian, Tai Kubo for contributing methodology and discussion in quantifying the croc postcranial variation, Arata Momohara for leading the paleotemperature reconstruction of the croc-bearing beds, Tadahiro Ikeda, Katsunori Watanabe, and Masahiro Tanimoto for their help in compiling crocodylian fossils in Japan, Keiichi Takahashi and Shoji Hayashi for thoroughly proofreading my description manuscripts, and Riosuke Aoki, the best known crocodylian expert in Japan, for thought-provoking talks on general crocodylian biology and Asian crocodylian systematics.

Original photos, CT images, raw measurements, and geology data of some crocodylians used in this study were kindly made available by Yoshitsugu Kobayashi, Yoshikazu Hasegawa, Daisuke Suzuki, Shoji Kajima, Shogo Konishi, Keiichi Takahashi, Katsuyoshi Yamamoto, Shigeki Nanko, Toshio Isobe, Akihiro Koizumi, Ai Takekawa, Christopher Brochu, Jeremy Martin, Massimo Delfino, Stephen Jouve, Adam Yates, and Rodrigo Figueiredo. Copies of countless 'elusive' papers and dissertations were located and given by Kentaro Chiba, Seung Choi, Yan-yin Wang, Christopher Brochu, Stephen Jouve, Evan Whiting, Cholawit Thongcharoenchaikit, and Jorge Moreno-Bernal. My specimen visits were assisted by many museum curators and friends over the world. I cannot list all of them, but I would like to specifically thank David Blackburn, Coleman Sheehy, and Edward Stanley (FLMNH, Gainesville) for arranging my long-term visit and allowing me to access their micro-CT facility, Alan Resetar (FMNH, Chicago) for his exceptional generosity during my visit, Takehito Ikejiri, Juri Miyamae, Kentaro Chiba, Shinobu Kabe, and Rosemarie Tadzik for providing accommodation, and Yan-yin Wang and Mei-li Yang for their hospitality and friendship.

Finally, I thank my family and two dorm moms, Yuriko Hatsuseo and Mieko Ozaki for their understanding and support throughout seven years of my graduate study in Sapporo.

Table of contents

Abstract ii

Acknowledgment iv

Table of contents vi

General introduction 1

I. Assessment of trophic ecomorphology in non-alligatoroid crocodylians and its adaptive and taxonomic implications 5

II. Comparative limb proportions reveal differential locomotor morphofunctions of alligatoroids and crocodyloids 36

III. Comparative morphology of presacral vertebrae in extant crocodylians 56

IV. Mosaic nature in the skeleton of East Asian “tomistomines” and *Gavialis*-*Tomistoma* debate 79

V. *Toyotamaphimeia* cf. *machikanensis* (Crocodylia, Tomistominae) from the Middle Pleistocene of Osaka, Japan, and the crocodylian survivorship through the Pliocene-Pleistocene climatic oscillations 104

VI. The oldest record of *Alligator sinensis* from the Late Pliocene of Western Japan, and its biogeographic implication 132

Literature cited 148

Supplement to chapters I–VI 182

Summary (in Japanese) 256

General introduction

Why study crocodylians?

Crocodylians are large bodied predatory reptiles that dominates the land-water interface in world's tropics and subtropics. As the sole living remnants of Pseudosuchia (crocodylians and all archosaurs closer to crocodylians than to birds), which has successfully diversified during the Mesozoic (Brusatte *et al.*, 2008; Stubbs *et al.*, 2013; Toljagic & Butler, 2013), Crocodylia has survived K-Pg mass extinction and major environmental crises during the Cenozoic. Because extant species are readily available for measuring morphology, function, performance, and resource use, crocodylians have been used to estimate ecology of fossil archosaurs (Parrish, 1987; Witmer, 1997; Seebacher, Grigg, & Beard, 1999; Hutchinson & Gatesy, 2000; Farmer & Sanders, 2010; Tanaka, Zelenitsky, & Therrien, 2015). Also, observation of the ontogenetic series of extant species enables us to test adaptive, phylogenetic, and evolutionary hypotheses with developmental perspectives (Dodson, 1975; Seebacher *et al.*, 1999; Meers, 2002; Livingston *et al.*, 2009; Sadleir, 2009; Allen *et al.*, 2010; Piras *et al.*, 2010; Erickson *et al.*, 2014). Furthermore, an extensive fossil record of crocodylians, spanning 70-80 million years from the Late Cretaceous (Brochu, 2003) can be used to examine the ecological diversity pattern, history of adaptation, and interaction with environments in a geological time scale (Markwick, 1998a; Brochu, 2001; Wheatley, 2010; Mannion *et al.*, 2015; Wilberg, 2017).

Meanwhile, biological understandings such as evolutionary patterns of morphology, function, and ecology, diversity through time, and biogeography require a firmly established phylogenetic hypothesis. Recently, phylogenetic comparative methods are put force for any intra- and interspecific comparisons, and importance of reliable trees in comparative biology has been confirmed (Felsenstein, 1985; Harvey & Pagel, 1991; Pagel, 1999; Nunn, 2011). Since crocodylian systematics can benefit from both extant and fossil samples, and different data types (i.e. molecular and morphology) can be rigorously compared, Crocodylia has played a central role in providing various methodological points of view for discussing and improving vertebrate systematics (Trueman, 1998; Hillis & Wiens, 2000; Gatesy *et al.*, 2003).

Perspectives and issues in understanding crocodylian ecology and evolution

Trophic and locomotor ecomorphology: The feeding system is fundamental to individual survival and reproductive success, and under strong selection pressure (Schwenk, 2000).

Therefore, as in most of other animals, morphological variation of crocodylians is largely observed in their skulls, which have been used for taxonomic and phylogenetic purposes (Kälin, 1933; Norell, 1989; Brochu, 1997b). Generally, it has been considered that feeding habits of crocodylians are reflected to their rostrum shape, and most of its variation is explained on slender vs. broad snout shape axis (Brochu, 2001; Pierce, Angielczyk, & Rayfield, 2008; Okamoto *et al.*, 2015). This assumption of morphology-ecology correlation was supported by observation of feeding performance (Thorbjarnarson, 1990), and examination of mechanical properties of skulls (Busbey, 1995; McHenry *et al.*, 2006; Pierce *et al.*, 2008). However, except for rostrum shape, only few skull characters were proposed and assessed as the correlates of feeding function and performance (Walmsley *et al.*, 2013; Gignac & Erickson, 2015), hence impeding accurate estimation of trophic ecology in extinct crocodylomorphs. In recent years, macroevolutionary patterns of skulls were investigated for a variety of crocodylomorph taxa by using advanced analytical tools of morphometrics (Young *et al.*, 2010; Hastings, 2012; Wilberg, 2017). However, the skull geometries captured by those studies were mostly associated with rostrum shapes, and other potentially functionally relevant characters (e.g. tooth shape, morphological correlates of jaw adductor muscle mass) were not fully appreciated.

The locomotor system also directly or indirectly influences on fitness consequences, and constitutes a major component of ecomorphological studies. Nonetheless, locomotor ecomorphology of crocodylians has received little attention, due to the perceived morphological conservativeness of crocodylian postcrania. Even the interspecific osteological variation of locomotor apparatus (limbs and vertebrae) is not satisfactory known to date. Among the few quantitative comparisons attempted include Chamero et al.'s (2013, 2014) works on forelimbs and cervico-thoracic vertebrae, where they noted some morphological differences between major groups of crocodylians. Meers (2002) compared biomechanical properties of the forelimb among a wide range of species but found little, if any, variation. Even so, limb muscle properties between alligatoroids and crocodyloids were shown to be different (Allen *et al.*, 2015), thus a close look at limbs and vertebrae may reveal additional osteological differences. If the functionally and ecologically relevant morphology is established, macroevolutionary patterns of locomotor ecology can be reconstructed through morphometrics of fossils.

Phylogeny of crocodylians: Crocodylian systematics is a classic model case in that different

(molecular and morphology) datasets present conflicting higher-level phylogenetic relationships. Since the introduction of quantitative phylogenetics in 1980s, molecular analyses consistently posited that the Malayan gharial *Tomistoma schlegelii* is the living sister taxon to the Indian gharial, *Gavialis gangeticus* (e.g., Densmore, 1983; Gatesy *et al.*, 2003; McAliley *et al.*, 2006; Oaks, 2011), but morphological analyses kept suggesting that *G. gangeticus* is a sister taxon to all other living crocodylians (e.g., Norell, 1989; Brochu, 1997a, 1999a; Salisbury *et al.*, 2006). The problem is not only about the placements of these two living species, but also involves dozens of longirostris fossils considered as members of "Tomistominae" or "Gavialoidea," and confounded evolutionary and biogeographic interpretations of crocodylians.

Various potential causes of the topological mismatch between molecular and morphological hypotheses have been proposed from the standpoints of both datasets, such as rooting and long branch attraction problem, homoplastic nature in the skull morphology, heterochrony and secondary signal, character non-independence, and subjectivity involved when choosing character and assigning character state (Densmore, 1983; Norell, 1989; Hass *et al.*, 1992; Brochu, 1997a, 1999b; Trueman, 1998; Gatesy *et al.*, 2003; Harshman *et al.*, 2003). However, in recent years it is becoming increasingly difficult to ignore the strong evidence of molecular analyses, given that a large number of independent molecular datasets provided a consistent tree topology (Willis *et al.*, 2007; Brochu personal communication). Therefore, it would be prudent for morphological workers to find how morphological character evolution can be interpreted on the molecular tree.

If the molecular tree is the best estimate of crocodylian phylogenetic relationships, the largest issue in interpreting the morphological character evolution on the molecular tree is the extensive character reversal seen in "gavialoid" (Gatesy *et al.*, 2003). Although the mechanisms underlying such peculiar taxic atavism is unknown, refined taxon sampling of longirostris lineages ("tomistomines" and "gavialoids") and finding of taxonomically informative characters would be a key to resolve this issue. Meanwhile, other important technical problems of morphological phylogenetics (e.g. choice of outgroups and character non-independence: Sadleir & Makovicky, 2008; Wilberg, 2015) should also be fully taken into account.

Dissertation objectives and organization

This study attempts to reveal the evolution of ecology in crocodylians by means of

morphometric and phylogenetic approaches using extant and fossil materials. This dissertation is composed of 6 independent manuscripts (chapters 1–6). Chapters 1–3 provide morphometric comparisons of trophic and locomotor ecomorphology (skull, limbs and vertebrae). Through intra- and interspecific comparisons of ecology relevant morphology in extant and fossil species, trophic and locomotor adaptation and evolution throughout ontogeny and phylogeny are discussed. In chapter 4, a new tomistomine crocodylian is described from the Pleistocene of Japan, and its East Asian relatives are reviewed. A new look at these East Asian forms, combined with the quantitative comparisons between molecular and morphological hypotheses provides a renewed understanding of the crocodylian phylogeny. Chapters 5–6 present a thorough compilation of the late Cenozoic Japanese crocodylians. These crocodylians were living near their thermal limits during the Plio-Pleistocene, and give an insight into how ectothermic animals responded to severe orbital scale climate fluctuations in the late Cenozoic icehouse world. The following is a list of chapters that have been published or in press. The remaining chapters (chapters 3–4) will be submitted to peer-reviewed journals in the future.

Chapter 1	*Journal of Anatomy*	231:192-211 (2017)
Chapter 2	*Royal Society Open Science*	in press (2018)
Chapter 5	*Palaeogeography, Palaeoclimatology, Palaeoecology*	in press (2018)
Chapter 6	*Journal of Asian Earth Sciences*	124:94-101 (2016)

I. Assessment of trophic ecomorphology in non-alligatoroid crocodylians and its adaptive and taxonomic implications

Introduction

Ecomorphology, in its broad sense, is the study of the interaction between the organismal design and environment (Bock, 1990; Wainwright & Reilly, 1994; Motta *et al.* 1995), and the correspondence between the two is made by linking the morphology with function and performance, and by measuring the effects of the latter on fitness (Arnold, 1983; Garland, Jr. & Losos, 1994; Ricklefs & Miles, 1994; Wainwright, 1994). Since morphology can be rigorously measured based on the homologous structures and has a high repeatability of measurement, it has been used to derive ecological inferences including resource partitioning and niche relationships among taxa, community structure, and diversity within taxa (Ricklefs & Miles, 1994). Probably, the utility of ecomorphological analysis is most appreciated in paleontological researches, because direct measurements of performance and fitness are not possible in extinct animals, but the morphology of hard tissues is often available in fossils. By using morphology, we can estimate important biological aspects of extinct organisms such as feeding and locomotor habits and body size (e.g. Kubo & Benton, 2009; Zanno & Makovicky, 2011; Campione & Evans, 2012), and can get insights into the ecological diversity pattern, species or higher level interactions, and history of adaptation in an evolutionary time scale (e.g. Brusatte *et al.* 2008; Sookias *et al.* 2012; Larson *et al.* 2016).

Crocodylians are opportunistic ambush predators, feeding on a wide range of invertebrates and vertebrates, depending on the availability of their habitat (Pooley, 1989; Webb & Manolis, 1989). Generally, their feeding habits are thought to reflect the skull shapes, and most of its variation is explained by broad to slender-snouted shape axis in extant as well as extinct forms (Brochu, 2001; Pierce *et al.* 2008; Okamoto *et al.* 2015). The extreme end-member in the slender-snouted taxa is Indian gharial (*Gavialis gangeticus*), which is considered as the most predominant fish-eater in extant crocodylians (Whitaker & Basu, 1982; Trutnau & Sommerlad, 2006). Its long and narrow snout accounts for the high angular velocity of the jaw tip while lateral head sweeping (Thorbjarnarson, 1990) and jaw closure, thus favorable for catching small agile prey. However, this type of snout is mechanically

weak for stress during biting (Busbey, 1995; McHenry *et al.* 2006; Pierce *et al.* 2008; Walmsley *et al.* 2013), and hydrodynamically costly as compared to the cranial morphology of generalist-type taxa (e.g. *C. porosus* and *C. niloticus*) (McHenry *et al.*, 2006). On the other hand, experimental studies revealed that interspecific variation in crocodylian bite force is primarily explained by body mass if *G. gangeticus* is excluded, and slender-snouted forms can generate equivalent bite forces with broader-snouted forms, suggesting that slender-snouted species may reduce jaw stresses by targeting on smaller prey such as fish and crustaceans (Erickson *et al.*, 2012).

Although the snout shape has been particularly focused in the previous ecomorphological analyses of crocodylians, there are a number of other characters that have also been proposed as ecomorphological characters (Iordansky, 1973; Langston, 1973; Brochu, 2001). However, quantitative assessments of such potential ecomorphological traits have rarely been conducted (but see Walmsley *et al.* 2013; Gignac & Erickson, 2015). Crocodylians are known as the sole remnants of Pseudosuchia (the most inclusive clade containing *Crocodylus niloticus* but not *Passer domesticus*: Nesbitt, 2011), a diverse and successful group of reptilians that rivaled dinosaurs in the early Mesozoic (Brusatte *et al.*, 2008), and are often regarded as modern analogs of extinct large-bodied aquatic predators. Hence, establishment of trophic ecomorphology in living crocodylians can contribute to estimating feeding habits in extinct pseudosuchians and non-pseudosuchian reptiles such as marine crocodyliforms, dinosaurs, phytosaurs, and choristoderans (e.g. Erickson, 1972b; Hunt, 1989; Sereno *et al.* 1998; Sereno *et al.* 2001; Massare, 1987), and helps answer various ecological questions by integrating space, time, and phylogenetic perspectives. Moreover, the finding of the ecological characters and their correlation (Sadleir & Makovicky, 2008) may help better understand the crocodylian phylogeny. It should be noted that a suite of potential feeding ecomorphological traits in rostrum is indeed consistent with molecular tree rather than supporting the morphological tree (Gatesy *et al.* 2003). However, removal or proper weighting of such non-independent characters are necessary for rigorously comparing the fit of morphological data on morphological and molecular trees, and thus resolving the long-standing discussion on the placement of *G. gangeticus* in the crocodylian phylogeny (e.g. Densmore, 1983; Norell, 1989; Poe, 1996; Brochu, 1997a; Gatesy *et al.* 2003).

Meanwhile, as most of the animals do, crocodylian skulls change remarkably during the postnatal development (Mook, 1921d; Müller, 1927; Kälin, 1933; Dodson, 1975; Monteiro & Soares, 1997; Monteiro *et al.* 1997; Sadleir, 2009; Piras *et al.* 2010; Bona & Desojo, 2011;

Foth *et al.* 2015; Watanabe & Slice, 2014; Fernandez-Blanco *et al.* 2015). Previous studies demonstrated that growth trajectories of *Crocodylus* skulls can fall into some stages, and hypothesized that the breakpoints between the stages correspond to changes in diets (Hall & Portier, 1994; Radloff *et al.* 2012). Whereas an experimental study suggested that positive allometry of bite force is conserved among crocodylians regardless of snout shape variation (Erickson *et al.*, 2014). Comparisons of the developmental pathways of trophic ecomorphology among crocodylians would tell us whether dietary adaptation during growth occurs through certain morphological changes, and the role of developmental process in shaping the morphological and ecological diversity of crocodylians.

Here, using the postnatal growth series of extant crocodylians, I first assess the validity of proposed trophic ecomorphology of non-alligatoroid crocodylians, with the special focus on piscivorous ecomorphology. I then compare the growth patterns of trophic ecomorphology among non-alligatoroid crocodylians for finding differential and shared scaling patterns and discuss their adaptive and taxonomic significance. Although the current study restricts the sample to non-alligatoroid crocodylians, additional sampling of alligatoroid species may permit the generalization about the observed trends and patterns among crocodylians.

Materials and methods

Specimen sampling

For conducting species comparisons of snout shape and the associated skull characters among Crocodylia, multiple taxa with a wide range of snout shape are required. I sampled the postnatal growth series of skulls from 10 crocodylians (n = 236; 7 species of *Crocodylus*, *Mecistops cataphractus*, *Tomistoma schlegelii*, and *Gavialis gangeticus*: Fig. 1). Alligatoroid species were not included in the sample because the current study specifically focuses on piscivorous specialization. *Crocodylus* is the most diverse and species-rich genus in extant crocodylians, including 12 known species (Grigg & Kirshner, 2015) from blunt-snouted type to slender-snouted type. A recent molecular study by Oaks (2011) revealed the late Miocene divergence of this group, suggesting that *Crocodylus* snout shape is ecologically plastic and is not strongly constrained by the phylogenetic relationships. Three remaining non-*Crocodylus* species are all slender-snouted, yet they differ in the degree. In crocodylian systematics, the relationships among *Crocodylus*, and placement of *T. schlegelii* and *G. gangeticus* are still not fully settled (e.g. Densmore, 1983; Densmore & White, 1991; Brochu, 1997a, 1999a; Gatesy *et al.* 2003; McAliley *et al.* 2006; Roos et al. 2007; Oaks, 2011). However, in the current

study, I chose to use the most recent and comprehensive time-calibrated molecular tree by Oaks (2011) as a phylogenetic framework for statistical analyses because contrary to the molecular analyses, previous morphological analyses (Brochu, 2000; Brochu *et al.* 2010; Brochu & Storrs, 2012) has not resolved the phylogenetic relationships among *Crocodylus*. Nearly all (232/236) samples used in this study are wild-caught with locality information (Supporting Information Table S1). In 10 crocodylians used in this study, some species are known to have morphologically distinct cryptic populations (*C. niloticus* [Hekkala *et al.* 2011; Nestler, 2012]; *C. novaeguineae* [Hall, 1989]; *C. palustris* [Trutnau & Sommerlad, 2006], and *M. cataphractus* [Shirley *et al.* 2014]). With this in mind, I sampled individuals from a limited geographical area for *C. niloticus* (Congo basin: Hekkala *et al.* 2011; Nestler, 2012) and for *M. cataphractus* (Congolian zone: Shirley *et al.* 2014), but other species are from all available localities to increase the sample size.

Data acquisition

A list of previously proposed trophic ecomorphology in crocodylians that are functionally explained in relation with feeding behavior is shown in Table 1. Among the variables, I did not consider the tooth shape because teeth are often shed and their original positions are not available in the specimens. To assess validity of the proposed ecomorphological characters in crocodylians, I conducted regression analyses of the proposed ecomorphological characters against the established ecomorphological character (snout shape) to examine their correlations. In crocodylians, snout shape is considered as being correlated with their diet (Brochu, 2001), and is known to reflect the feeding function and performance (Taylor, 1987; Thorbjarnarson, 1990; McHenry *et al.* 2006). Therefore, if a character correlates with snout shape, then it can also be regarded as a trophic ecomorphological character.

For the quantification of the snout shape, I performed two-dimensional geometric morphometrics with 7 landmarks (type 1 and 2 of Bookstein, 1991) and 38 sliding semi-landmarks which were digitized from palates (Fig. 2A), using tpsDig v. 2.17 (Rohlf, 2013a). The current method is probably better in capturing snout shapes than previous studies that used the ratio of linear measurements from dorsal snouts (e.g. Hall & Portier, 1994; Erickson *et al.* 2012), which did not take into account subtle differences in snout outlines. Landmark and semi-landmark coordinates of the pooled samples (n = 236) were superimposed by a generalized Procrustes analysis (Gower, 1975; Rohlf & Slice, 1990), and subjected to relative warp analysis using tpsRelw v. 1.53 (Rohlf, 2013b). Since much of the snout shape variation

would be accounted for by the first axis of relative warps (RWs), RW1 scores were extracted as the snout shape proxy.

The degree of heterodonty (tooth size disparity) was calculated as the coefficient of variation (ratio of standard deviation to mean) of mesiodistal diameters of all right/left maxillary alveoli (Supporting Information Table S2). The spacing of teeth was represented as the ratio of the sum of mesiodistal diameters of all right/left maxillary alveoli to the maxillary tooth row length (Fig. 2A), which was measured in juvenile–adult specimens showing interalveolar bones. The tooth count was taken from left and right maxillae, because tooth counts in maxillae are more variable than those of premaxillae among crocodylians (Iordansky, 1973). These tooth size, tooth spacing, and tooth count patterns in upper jaw can almost certainly be generalized for lower jaw (Brown *et al.* 2015). The size of supratemporal fenestra (STF) was measured as an area enclosed by landmarks and semi-landmarks (Fig. 2D) using tpsUtil v. 1.58 (Rohlf, 2013c), based on the photos of posterior skulls taken from dorsal view, with the scale on the flat part of skull table. The measurements of other metrics are shown in Fig. 2B & E. As the body size proxy, I used the centroid size (CS) of superimposed dorsal postrostrum landmarks (Fig. 2C) of each species obtained from tpsRelw, because the postrostrum shape is more conservative compared with the rostrum (Piras *et al.*, 2014). To obtain the size information for the digitized landmark data, samples were scaled with reference to maximum skull width at jaw joint in tpsDig. Linear measurements were taken by Tresna point digital caliper (Series SC02, ID 111-203, resolution = 0.01 mm). Photos of palatal and dorsal aspects of the skulls for geometric morphometrics were taken by positioning Nikon D3100 camera (AF-S DX NIKKOR 18-55mm f/3.5-5.6G VR, 14.2 Mp resolution) perpendicular to the palatal and skull table surface respectively, consistently centering specimens in the field of view, and keeping enough distance between the lens and specimens.

Assessment of the proposed trophic ecomorphology in non-alligatoroid crocodylians

To size-normalize the dimensioned variables, linear measurements were divided by centroid size (CS), and area measurements were square rooted and then divided by CS. However even after the size-removal, various allometric trends in ecomorphological variables need to be controlled. A common approach for correcting allometry is to regress variables on size metrics using least squares regression and then to take the residuals (e.g. Foth *et al.* 2015; Piras *et al.* 2014; Watanabe & Slice, 2014), but crocodylian snout shapes are known to show

non-linear growth trajectories (Hall & Portier, 1994; Radloff *et al.* 2012; this study), thus use of such approach would be inappropriate. Therefore, I selected individuals within the arbitrarily set thresholds of log10 transformed CS (log[CS]), which correspond to subadult–adult stages for all species. For examining the correlations between proposed ecomorphological variables and snout shape (RW1 score) within the set size range, I first conducted ordinary least squares (OLS) regression with whole samples. Maxillary tooth count was not analyzed in the whole sample OLS. Secondly, species comparison was performed by phylogenetic generalized least squares (PGLS) regression, in which average species ecomorphological variable values were regressed on average species snout shape (RW1 score) within the set size range, on an assumption of Brownian motion model of trait evolution. For maxillary tooth count, mode instead of mean was used for the regression. Since PGLS regression requires a time-calibrated tree, a phylogenetic tree of 10 sampled crocodylian species (Fig. 1) was constructed with reference to a molecular study by Oaks (2011), and divergence time estimates was adopted from the species tree of the original study with a 90 myr upper limit on the root age. Additionally, a morphological tree (Supporting Information Fig. S1) was used for testing the sensitivity of the PGLS results to tree shape. PGLS regression was conducted using software R with caper package (Orme *et al.*, 2013), and a phylogenetic signal parameter (Pagel's λ) was optimized and took into account in the analysis.

Comparative growth trajectories of trophic ecomorphology in non-alligatoroid crocodylians

Prior to analyses, linear and area measurements were log10 transformed, yet dimensionless variables (snout shape, degree of heterodonty, and spacing of teeth) were left untransformed. The growth trajectories of ecomorphological variables were visualized using a bivariate plot of log(CS) of the postrostrum and each variable. Because the trajectories of snout shape were nonlinear with breakpoint(s), piecewise linear models, where two straight lines are joined at an unknown knot (breakpoint), were fit to find the breakpoint. The analysis was conducted using R with the SiZer package (Sonderegger, 2012), and the breakpoint estimate was reported with 95% confidence intervals. In the model fitting, very small individuals were excluded by setting an arbitrary size threshold for all species so as not to include individuals from relative skull growth phase I (Hall & Portier, 1994). Therefore, the first and second segments in the model correspond to the skull growth phases II and III (Hall & Portier, 1994).

Because some species do not grow larger than the assumed breakpoint or have small sample size beyond the breakpoint, the analysis was performed only in large-bodied well-sampled taxa (6 species: *C. acutus*, *C. niloticus*, *C. palustris*, *C. porosus*, *G. gangeticus*, and *T. schlegelii*). After the mean snout shape breakpoint of 6 species was obtained, I additionally tested if snout shapes differ between growth phase II (smaller than mean breakpoint) and phase III (larger than mean breakpoint) in the 6 species using Welch's t-test.

For the remaining variables, I performed reduced major axis (RMA) regression of ecomorphological variables against log(CS) with whole samples using R with smatr package (Warton *et al.*, 2012). Dimensionless variables were examined if there are significant relationships between the variables and size (log[CS]), and dimensioned variables were examined if RMA slopes for the relationships of variables (log10 transformed) and size (log[CS]) are different from the expected isometric slopes (1.0 and 2.0 for linear and area measurement variables, respectively). The growth of the variables was considered either positively or negatively allometric if 95% confidence intervals of the slopes do not overlap the expected isometric slopes. Since maxillary tooth count is different in its data type, it was separately subjected to Spearman rank correlation to test the correlation between tooth count and size. All statistical tests were carried out with R language and environment (R Core Team, 2014).

Results

Assessment of the proposed trophic ecomorphology

Because body size (log[CS]) of sampled crocodylians (10 species, $n = 236$) ranges from ~1.6–2.6, and snout shape (RW1 score) largely changes beyond log(CS) of ~2.4 for all taxa (Fig. 4), I selected individuals from the arbitrary set size range ($2.1 \leq \log[CS] \leq 2.4$), which covers a relatively stable size range of the snout shape, and secures 110–123 individuals for each variable. A summary of the whole sample OLS regression and species PGLS regression between proposed trophic ecomorphological variables and snout shape (RW1 score) are found in Fig. 3 and Table 2. Among the proposed ecomorphological variables, CV of maxillary alveolus diameter, maxillary tooth spacing, relative supratemporal fenestra (STF) area, relative pterygoid flange depth, and relative lower jaw symphysis length are significantly correlated with snout shape in both whole sample OLS and species PGLS regressions, thus verified as trophic ecomorphology. The use of an alternative tree (morphological tree) for PGLS did not significantly change the results (Supporting

Information Table S3). These indicate that generally, tooth size variability becomes smaller, maxillary teeth are more spaciously positioned, STF size increases, pterygoid flange depth increases, and lower jaw symphysis length extends in accord with the snout narrowing in the sampled crocodylians. On the contrary, relative basioccipital tubera width and mode species maxillary tooth count were not significantly correlated with snout shape in either whole sample OLS or species PGLS regression.

Growth trajectories of trophic ecomorphology

An observation of the bivariate plot of snout shape (RW1 score) and log(CS) (Fig. 4) revealed a universal trend of snout widening through growth. In most of the species, the snout shape is isometric or somewhat positively allometric in its width until reaching log(CS) of ~ 2.4, but beyond this size the snout grows increasingly wider. Although a rigorous comparison of species trajectories was not attempted because of the difficulty in comparing non-linear trajectories, this pattern seems global and unrelated with interspecific snout shape differences. The result of the snout shape breakpoint estimation by piecewise linear model fitting is shown in Fig. 5 (Supporting Information Table S4). In this analysis, individuals with log(CS) ≥ 2.0 were used for excluding very small forms that might belong to relative skull growth phase I (Hall & Portier, 1994). The estimated log(CS) breakpoints of snout shape growth trajectories are 2.31–2.46 in 6 species (*C. acutus*, *C. niloticus*, *C. palustris*, *C. porosus*, *G. gangeticus*, and *T. schlegelii*), and their mean is 2.40. Individuals with log(CS) smaller and larger than the mean snout shape breakpoint were considered as members of growth phase II and III (Hall & Portier, 1994), respectively, and Welch's t-test confirmed that snout shapes are significantly different between two phases (Table 3).

Bivariate plots of log(CS) and trophic ecomorphological variables are provided in Fig. 6, and a summary of the RMA regression between ecomorphological variables and log(CS) for whole samples is found in Table 4. Maxillary tooth size variability is significantly ($P < 0.05$) and near significantly ($P < 0.1$) correlated with size in 7 species excluding *G. gangeticus*, *C. johnsoni*, and *M. cataphractus*, all showing a positive trend through growth. Maxillary tooth spacing is significantly and near significantly correlated with size in 6 species, and all of which show a positive trend. A strong positive correlation ($R^2 > 0.6$) is found in two most longirostral taxa (*G. gangeticus* and *T. schlegelii*), indicating a significant decrease in the relative spacing of maxillary teeth through growth. The relationship of relative STF area is negatively allometric (95% CI less than 2) in 4 species, isometric (95% CI includes 2) in 5

species, and positively allometric (95% CI greater than 2) in *G. gangeticus*. The slopes for relative pterygoid flange depth are positively allometric for all taxa, and those for relative basioccipital tubera widths vary among 10 species. The relationship of relative symphysis length is positively allometric and isometric in 9 species, but negatively allometric in *G. gangeticus*.

The maxillary tooth count is stable through growth in all sampled taxa (Fig. 6). In 9 out of 10 species, maxillary tooth count varies within each species, but it is not significantly correlated with size, as confirmed by Spearman rank correlation (Table 5).

Discussion

Non-alligatoroid crocodylian trophic ecomorphology and the uniqueness of G. gangeticus

The crocodylian skulls are featured by the high level of character convergence that is thought to reflect trophic convergence (Brochu, 2001; Sadleir & Makovicky, 2008). The non-phylogenetic and phylogenetic methods in testing the correlations between the proposed trophic ecomorphology and snout shape indicated that with narrowing of the snout, maxillary tooth size disparity increases (lateral maxillary margin more festooned), maxillary teeth less packed, supratemporal fenestra (STF) enlarged, pterygoid flange deepened, and lower jaw symphysis extended. These characters are intercorrelated with each other, and supposedly transformed concurrently in the trophic specialization of non-alligatoroid crocodylians. Other variables (tooth count and relative basioccipital tubera width) yielded non-significant correlation with snout shape. However, it is possible that the character transformation of those two variables is stepwise, and increase in tooth count and enlargement of basioccipital tubera occur once snout is narrowed to a certain degree, perhaps as much as *G. gangeticus*, the most predominant fish-eater in extant crocodylians. Previous studies demonstrated that skull of *G. gangeticus* is known to occupy unique morphospace among extant adult crocodylians (Pierce *et al.* 2008; Sadleir, 2009), and its developmental pathway begins and ends in a distinct region of the morphospace (Piras *et al.*, 2010). Its bite force performance is also different from other species, because *G. gangeticus* falls outside the 95% confidence interval of the OLS regression of bite force and size (Erickson *et al.*, 2012). The current result is consistent with the previous notion that *G. gangeticus* is morphologically and functionally atypical. In the whole sample OLS regressions of ecomorphological variables against snout shape (RW1 score), *G. gangeticus* is placed outside of the 95% PI for relative STF area, relative symphysis length, and relative pterygoid flange depth among the verified trophic

ecomorphology (Fig. 3). These suggest that specialization for true piscivory involves the deviation from the conserved transformation axis of crocodylian skull characters. However, the results of the current analyses should be interpreted carefully. Inclusion of extant alligatoroids and some fossil forms, especially with relatively narrow snouts such as *C. crocodilus apaporiensis*, *Orthogenysuchus* (Mook, 1924), and *Procaimanoidea* (Gilmore, 1946) in the analyses may have significant impact on the results.

Until now, adaptation for feeding on small aquatic prey has been suggested for many taxa of large aquatic reptiles, including thalattosuchian (Langston, 1973; Massare, 1987; Hua, 1994; Young *et al.* 2010) and tethysuchian (Denton *et al.* 1997; Sereno et al. 2001; Hastings *et al.* 2011; Schwarz-Wings, 2014) crocodyliforms, phytosaurs (Hunt, 1989; Renesto & Paganoni, 1998), and choristoderans (Erickson, 1972b; Evans & Hecht, 1993), mostly on the grounds of long and narrow snouts as well as slender and pointed teeth. Establishment of trophic ecomorphology in crocodylians, and a close comparison of above-listed forms with crocodylians will reveal a degree to which the adaptation to similar ecology is driven by convergence among large aquatic reptiles.

Comparative snout shape ontogeny

Using 2D geometric morphometrics of palate shapes, I demonstrated that the snout widening is a universal trend in non-alligatoroid crocodylians, regardless of the interspecific snout shape differences. Moreover, growth trajectories of sampled crocodylians are non-linear, and beyond some size, the snout grows increasingly wider. This is evident when the trajectories of extremely slender-snouted taxa (*G. gangeticus* and *T. schlegelii*), moderately slender-snouted taxa (e.g. *C. intermedius*), and generalist-type taxa (e.g. *C. porosus* and *C. niloticus*) are compared (Fig. 4). Statistical tests supported that the mean snout shape threshold in 6 species is log(CS) of 2.40, and snout shape is significantly wider beyond the threshold in all 6 species (Fig. 7). The log(CS) of postrostrum landmarks is strongly correlated with log(skull width) for all taxa (n = 236, log[skull width] = 1.185log[CS] − 0.459, R^2 = 0.993), and the skull width predicted from the mean snout shape threshold (2.40 log[CS]) is 242 mm, with the lowest and highest estimate values of 6 species range 191–287 mm. In other words, extant non-alligatoroid crocodylians begin significant snout shape changes when their skull widths are about 242 mm during growth. Meanwhile, larger variance in the snout shape of *C. acutus* might be derived from greater geographical variation, because *C. acutus* samples were collected from Florida (United States), Mexico, and Caribbean, Central American, and

Northern South American countries.

The results are partly congruent with previous studies on comparative skull shape allometry (Piras *et al.* 2010; Watanabe & Slice, 2014), yet differ in showing a universal trend of snout widening in non-alligatoroid crocodylians. A non-linearity of the snout growth in some species of crocodylians was mentioned by Hall & Portier (1994) and Watanabe & Slice (2014). Both studies described U-shaped trajectories, in which snout narrowing occurs in early stages, followed by snout widening in late stages. Hall & Portier (1994) defined three general growth phases of skulls in *C. novaeguineae*, each characterized by snout narrowing (phase I: ≤ 60–70 mm skull length), stationary snout shape (phase II: 60–70 mm ≤ skull length ≤ 350 mm), and snout widening (phase III: ≥ 350 mm skull length), respectively. Although the boundary of the three growth phases are ambiguous, they hypothesized that the phase transitions are concomitant with dietary shifts during ontogeny. This idea was examined in *C. niloticus* using stable carbon and nitrogen isotope analyses of scute keratin, finding some support for the correlated changes of skull morphometrics and the isotopic ratios (Radloff *et al.*, 2012). The estimated snout shape breakpoint in the current samples (191 mm ≤ skull width ≤ 287 mm) is close to Hall & Portier's (1994) phase II–III boundary (estimated skull width of 188 mm), which corresponds 350 mm skull length in the current *C. novaeguineae* samples. However, since the pattern of snout shape change seems homogeneous among sampled taxa that display various dietary patterns, distinct growth phases of the skull imply the existence of a shared size-dependent biomechanical constraint, rather than the morphological response to the dietary shift in non-alligatoroid crocodylians.

The significant skull shape change in very large size classes of crocodylians has been known (Mook, 1921d; Müller, 1927; Kälin, 1933), and previous studies on extant crocodylians have concerned with the effect of ontogenetic allometry in species or larger group comparisons of skull shapes (Pierce *et al.* 2008; Sadleir & Makovicky, 2008; Piras *et al.* 2009; Piras *et al.* 2014). However, perhaps more susceptible to allometry are analyses of fossil forms, because most of the species are represented by single individuals, and their growth patterns and maximum sizes are not known. If the size-related shape change is large and samples from different size classes are used simultaneously without size correction, ecological diversity inferences such as morphological disparity metrics are spuriously calculated, and higher level analyses of disparity integrating time, phylogeny, and geography are confounded with various allometric effects. Fig. 8 illustrates the effect of size range on the rostrum shape disparity of crocodylians using the empirical dataset, by randomly

sampling 10 individuals of 10 each species from a series of size ranges. While the mean variance seems unrelated with size range, 95% CI of variance is more than doubled with the increase in the size range. A significant widening of the 95% CI of snout shape variance occurs where log(CS) > 2.4, which corresponds the skull growth phase III. Given that most of the skull shape variation is related with rostrum shape in extant crocodylians (Pierce *et al.*, 2008), analysis of skull shape disparity of fossil taxa (e.g. Young *et al.* 2010; Wilberg, 2012; Hastings & Hellmund, 2016) may need to limit the size range of samples.

Allometry of trophic ecomorphology in non-alligatoroid crocodylians

As indicated by regression slopes of ecomorphological variables against log(CS), the allometric patterns of the variables differ among species, possibly related to trophic specialization during growth. The relative maxillary tooth size variation increases with size in 7 species, yet the variation remains smaller throughout life in *G. gangeticus* and possibly in *C. johnsoni* and *M. cataphractus* (Fig. 6, Table 4). Accordingly, the lateral maxillary margin is more 'festooned' in adults of non-*Gavialis* taxa, including *T. schlegelii* (Fig. 9). The increased degree of tooth size disparity in large adults of non-*Gavialis* taxa is most likely advantageous for holding larger prey firmly (Iordansky, 1973). On the other hand, *G. gangeticus* is arguably a predominant fish-eater, although they occasionally feed on prey other than fish (Whitaker & Basu, 1982; Trutnau & Sommerlad, 2006). Thus, it is intuitive that they maintain near-homodont dentition through growth. While most of the sampled taxa acquire more heterodont dentition toward adults, interalveolar space of maxillary dentition decreases during growth in 6 species, in which two longirostrine taxa (*G. gangeticus* and *T. schlegelii*) exhibit the most significant trends (Fig. 6, Table 4). These, combined with constant tooth counts through growth, imply that at least some of the maxillary teeth exhibit positive allometric growth relative to the maxillary tooth row length in non-alligatoroid crocodylians. As expected, a qualitative observation revealed that teeth positioned near the top of the convexities of the maxillary margin grow with positive allometry (Fig. 9). A previous study agrees with this observation by showing positive allometry in the diameter of 'caniniform' tooth relative to tooth row length (maxillary tooth #5 in *C. porosus*, and #4 in *A. mississippiensis*) which is positioned at the apex of the 'first wave' of maxillary tooth row (Brown *et al.*, 2015).

Relative supratemporal fenestra (STF) area and pterygoid flange depth (PFD) are associated with the relative mass of jaw adductor muscles. Growth trends for relative STF

area are isometric or negatively allometric in most of the sampled taxa, which agree with the STF scaling in *A. mississippiensis* (Dodson, 1975), but only *G. gangeticus* exhibits a positive trend (Fig. 6, Table 4). Because enlarged STF area is correlated with the hypertrophied *Musculus pseudotemporalis*, which helps weak but rapid jaw closure (Iordansky, 1964; Endo *et al.* 2002) and hence advantageous for catching agile prey, *G. gangeticus* might be specialized for fish eating through growth. By contrast, all taxa show a positive allometric trend for relative PFD (Fig. 6, 10, Table 4) as suggested in *A. mississippiensis* (Dodson, 1975), which indicates that relative mass of *Mm. pterygoidei dorsalis* et *ventralis*, strong jaw adductor muscles (Iordansky, 1964), increases through growth in all sampled species. This is consistent with the study of adductor muscle mass and physiological cross-sectional areas (PCSA) scaling in *A. mississippiensis* (Gignac & Erickson, 2016). This study demonstrated that the mass and PCSA of both dorsal and ventral pterygoid muscles are positively allometric, in which the ventral one shows greatest relative growth of all adductor muscles. Moreover, experimental studies of bite force scaling among Crocodylia showed that a positive allometry of bite force is conserved among extant crocodylians regardless of phylogenetic relatedness and snout shape (Erickson, Lappin, & Vliet, 2003; Erickson *et al.*, 2014). The other aspect of relative ventral extension of pterygoid flange is its correlation with maximal mouth opening (Piras *et al.*, 2014). It could be possible that crocodylians, regardless of their snout shapes, achieve greater maximal mouth opening during growth.

Growth patterns of relative lower jaw symphysis length show ontogenetic convergence through growth (Fig. 6, Table 4), where patterns of *G. gangeticus* and *T. schlegelii* are negatively allometric (95% CI lower than 1) or almost negatively allometric (upper 95% CI slightly exceeds 1), respectively, whereas that of other species are isometric or positively allometric. Because shorter symphysis incurs lower strain under equivalent loads (Walmsley *et al.*, 2013), slender-snouted taxa such as *G. gangeticus* and *T. schlegelii* might be able to tolerate higher relative loads through growth. Overall, it is conceivable that non-alligatoroid crocodylian skull characters react differently towards the trophic specialization: some of the characters respond to the change in prey preference during growth, yet other characters are in keep with the conserved relationship of maximum bite force and body size among crocodylians (Erickson *et al.*, 2012, 2014).

Taxonomic implication

The occlusal pattern has been traditionally used for the classification of two large groups of

crocodylians, Alligatoroidea and Crocodyloidea: maxillary teeth of living alligatoroids occlude buccal to dentary teeth, but maxillary and dentary teeth of living crocodyloids interfinger. While fossils suggested the presence of the intermediate character state, and the character transformation history has been understood (Brochu, 1999a; Brochu, 2003), the occlusal pattern is still recognized as a popular identification key for crocodylians in academic and public scenes. The observation of the ontogenetic series of non-alligatoroid crocodylians revealed that the occlusal pattern is continuous in nature rather than discrete, and is strongly associated with growth stages and snout shape.

As the consequence of increased tooth size disparity and positive allometry of teeth at maxillary margin convexity through ontogeny, first 5 maxillary teeth and last 5–6 teeth are densely packed in large adults of generalist-type taxa (e.g. *C. acutus*; *C. niloticus*; *C. palustris*). This is also a characteristic of large adults of slender-snouted taxa, such as *C. intermedius* and *T. schlegelii* (Fig. 9). By contrast, in all taxa maxillary teeth #6–8 are widely spaced even in large adults, to occlude with large dentary teeth that are positioned at a convex margin of the dentary. The 'packed' anterior and posterior maxillary teeth lead to an unavoidable result: overbite occlusion at anterior and posterior maxilla. This is clear from the observation of live individuals (M. I. personal observation), and occlusal pits occasionally left on palates, that are placed lingual to maxillary alveoli, even in slender-snouted taxa like *T. schegelii* (Fig. 11A). Yet still, in-line occlusion is maintained at the concavity of maxillary margin (maxillary tooth # 6–8). The current study also suggested that degree of heterodonty and spacing of maxillary teeth are strongly correlated with snout shape: in taxa with wider snout, maxillary teeth are more heterodont and more packed. Considering these, it can be supposed that short-snouted taxa like *C. palustris* are prone to exhibit 'semi-overbite' (overbite at anterior and posterior maxilla) occlusion, and achieve it in younger age (with smaller size) compared to slender-snouted taxa. It might also be worthwhile to mention that a few specimens of *P. palustris* (e.g. BMNH 1848.2.5.9; BMNH 1852.5.9.45; ZSM 565/1911) examined here bear a pit between premaxilla and maxilla for reception of the fourth dentary tooth (Fig. 12), although its lateral wall is not fully formed. Formation of such pit is often associated with overbite occlusion in crocodylians (Brochu, 2003). When fossils are taken into account, the acquisition of 'semi' and 'full' overbite occlusion of maxillary and dentary teeth are common in stem Crocodylidae (Brochu, 1997b; Brochu, 1999a), also occurred repeatedly among Crocodylidae, mainly in large specimens. In subfossil remains of osteolaemine *Voay robustus* from Madagascar (Mook, 1921c; Brochu, 2007a), and the

Pleistocene remain of *Crocodylus rhombifer* from Cuba (Varona, 1984), the interalveolar space of maxillary teeth # 6–8 is much narrower than that in *C. palustris*. As a result, occlusal pits are placed lingually to maxillary teeth # 6–8, achieving a near full overbite occlusion (Fig. 11B, C), while in smaller individuals of *V. robustus*, more in-line occlusion is recognized (Mook, 1921c; Brochu, 2007a). Likewise, a various degree of overbite occlusion is observed in mekosuchine crocodiles (Willis *et al.* 1990; Megirian *et al.* 1991; Willis, 1993), probably caused by densely packed teeth. Although further studies are necessary to understand the interaction of the occlusal pattern with snout shape, tooth spacing, and tooth count, there seem to be a few barriers in the transition of 'interfingering' and 'overbite' patterns in crocodyloids, mostly in short-snouted forms.

Taxonomic characters that are related with trophic ecomorphology can be found in other parts of the skull. Associated with the ventral extension of the pterygoid flange is the extent to which basisphenoid exposes below median Eustachian opening (MEO). In the sampled taxa, it is longest in *C. palustris* (Fig. 13), the most wide-snouted taxon in genus *Crocodylus*, and shortest in slender-snouted *G. gangeticus* and *T. schlegelii*. Consequently, the posterior pterygoid process is also tallest in *C. palustris* (Fig. 13), as opposed to the shortest condition in *G. gangeticus* and *T. schlegelii*. These characters (chars. #98 and #119 in Brochu, 1999a) are highly variable even within the identical character states, and rather correlated with the pterygoid flange depth, and hence with the snout shape. The problem of ecomorphological character correlation has been debated in morphological phylogenetic analyses of crocodylians (Gatesy *et al.* 2003; Sadleir & Makovicky, 2008). Although improved taxon and character sampling is key for the better phylogenetic reconstruction, and rooting and the choice of outgroups have a great impact on the placement of ingroup taxa (Wilberg, 2015), recognition of ecomorphological characters and their inter-correlations, and evaluation of such characters in datasets will be of further help in accurately reconstructing the phylogenetic relationships of crocodylians.

This chapter was published as:

Iijima M. 2017. Assessment of trophic ecomorphology in non-alligatoroid crocodylians and its adaptive and taxonomic implications. *Journal of Anatomy* 231: 192-211.

Fig. 1. A time-calibrated molecular phylogeny of 10 sampled crocodylian species (modified from Oaks, 2011).

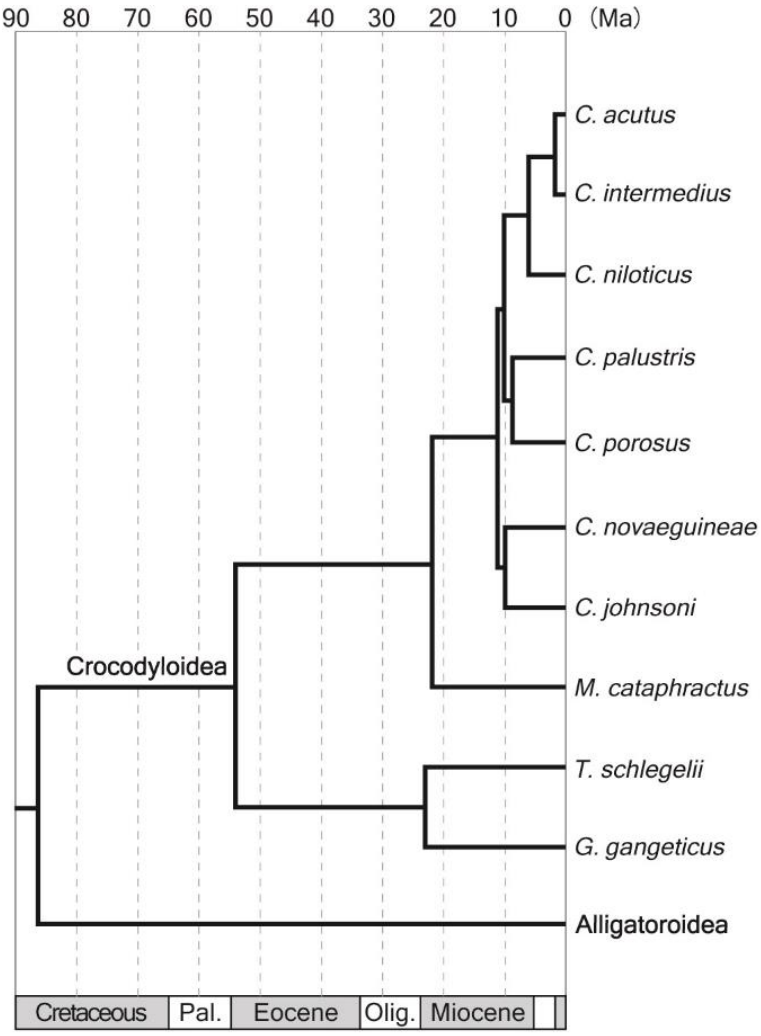


Fig. 2. (A) Rostral landmarks and semi-landmarks used in this analysis. 7 landmarks (white markers) are taken at: 1: anterior end of rostrum; 2, 3: both lateral edges of premaxillary-maxillary contact; 4, 5: both lateral edges of maxillary alveolus #5; 6, 7: both lateral edges of rostrum at the level of posterior end of last maxillary alveolus. A total of 38 semi-landmarks (gray markers) is taken on the outline of 6 palatal outline segments. (B) Measurement of lower jaw symphysis length. (C) 19 post-rostral landmarks taken at: 1: orbit-prefrontal-lacrimal contact; 2: orbit-lacrimal-jugal contact; 3: orbit-prefrontal-frontal contact; 4: orbit-frontal-postorbital contact; 5: anteroventral end of postorbital bar; 6: posteroventral end of postorbital bar; 7: anterodorsal end of postorbital bar; 8: posterodorsal end of postorbital bar; 9: infratemporal fenestra-jugal-quadratojugal contact; 10: lateral edge of skull table at postorbital-squamosal contact; 11: supratemporal fenestra-postorbital-squamosal contact; 12: triple junction of frontal-parietal-postorbital; 13: supratemporal fenestra-parietal-postorbital contact; 14: supratemporal fenestra-parietal-squamosal contact; 15: frontal-parietal contact on midline; 16: supraoccipital-parietal contact on midline; 17: posterior edge of skull table at parietal-squamosal contact; 18: posteromedial corner of quadrate jaw joint; 19; posterior end of quadrate-quadratojugal contact. (D) Landmarks and semi-landmarks for calculating area of supratemporal fenestra (STF). 4 landmarks (white markers) are taken at: 1: anterior edge of STF at postorbital-parietal contact; 2: lateral edge of STF at postorbital-squamosal contact; 3: medial-most point of STF along parietal; 4: posterior edge of STF at parietal-squamosal contact. A total of 12 semi-landmarks (gray markers) is taken on the outline of STF to calculate the STF area including its smooth floor. (E) Measurements of pterygoid flange depth and basioccipital tubera width.

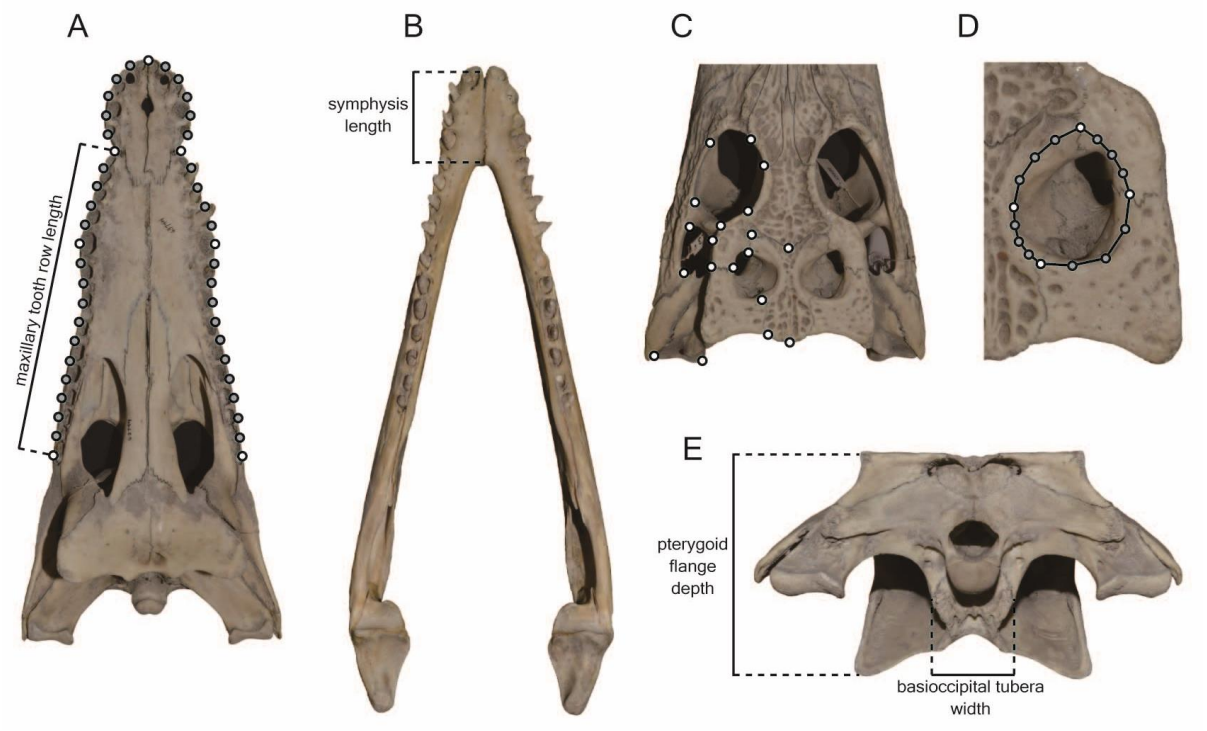


Fig. 3. (A–B, D–G) Bivariate plots of snout shape (RW1 score) and proposed ecomorphological variables for individuals within 2.1 ≤ log(CS) ≤ 2.4. Ordinary least squares (OLS) regression lines are fit on the plots. (C) Bivariate plot of mean species RW1 score and mode species maxillary tooth count for individuals within 2.1 ≤ log(CS) ≤ 2.4. CV, coefficient of variation. Dashed lines are 95% prediction intervals (PIs).

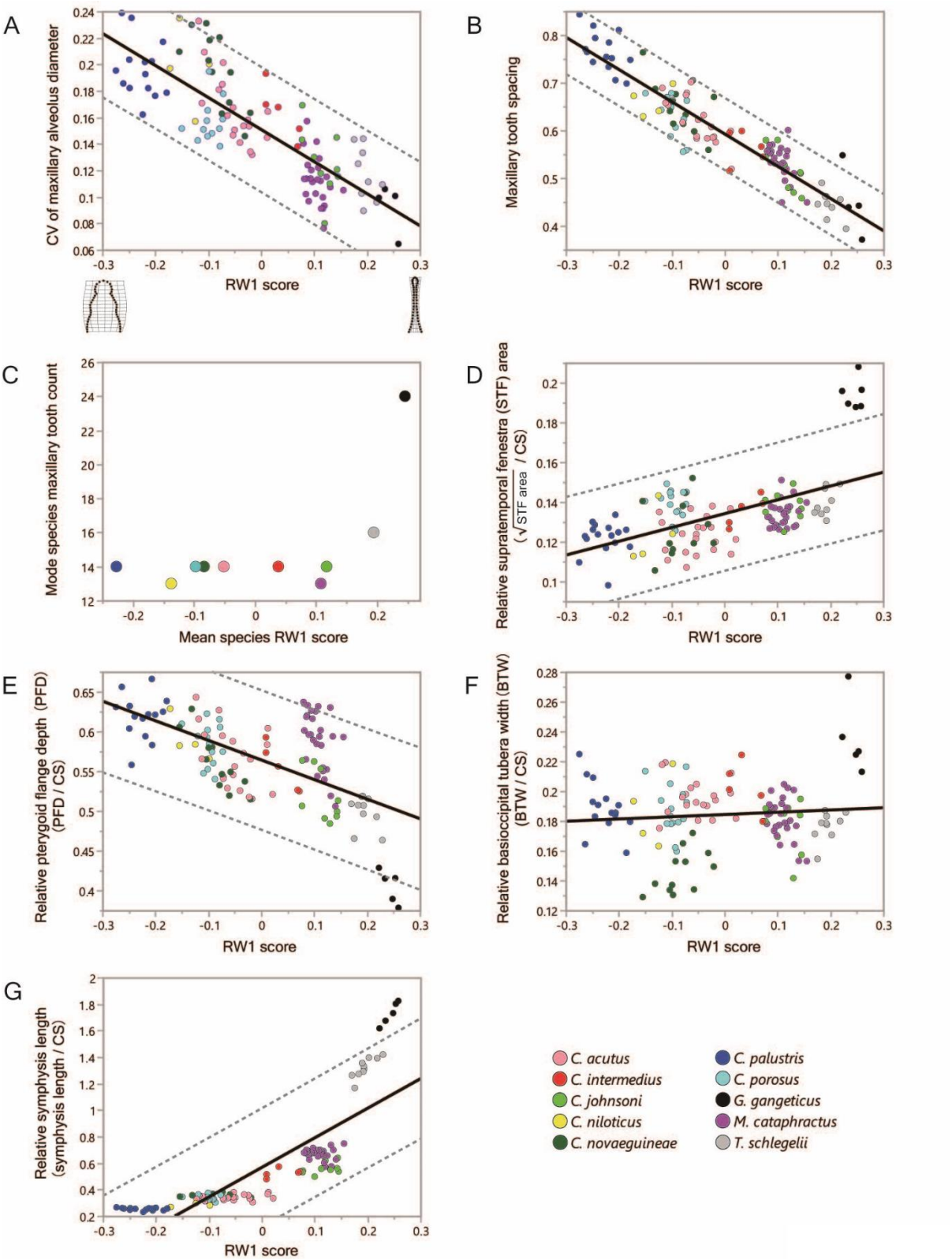


Fig. 4. Bivariate plot of log(CS) and snout shape (RW1 scores). Area with gray gradient represents the estimated range of log(CS) breakpoints of snout shape for 6 species (*C. acutus*, *C. niloticus*, *C. palustris*, *C. porosus*, *G. gangeticus*, and *T. schlegelii*), and the dashed line is their mean.

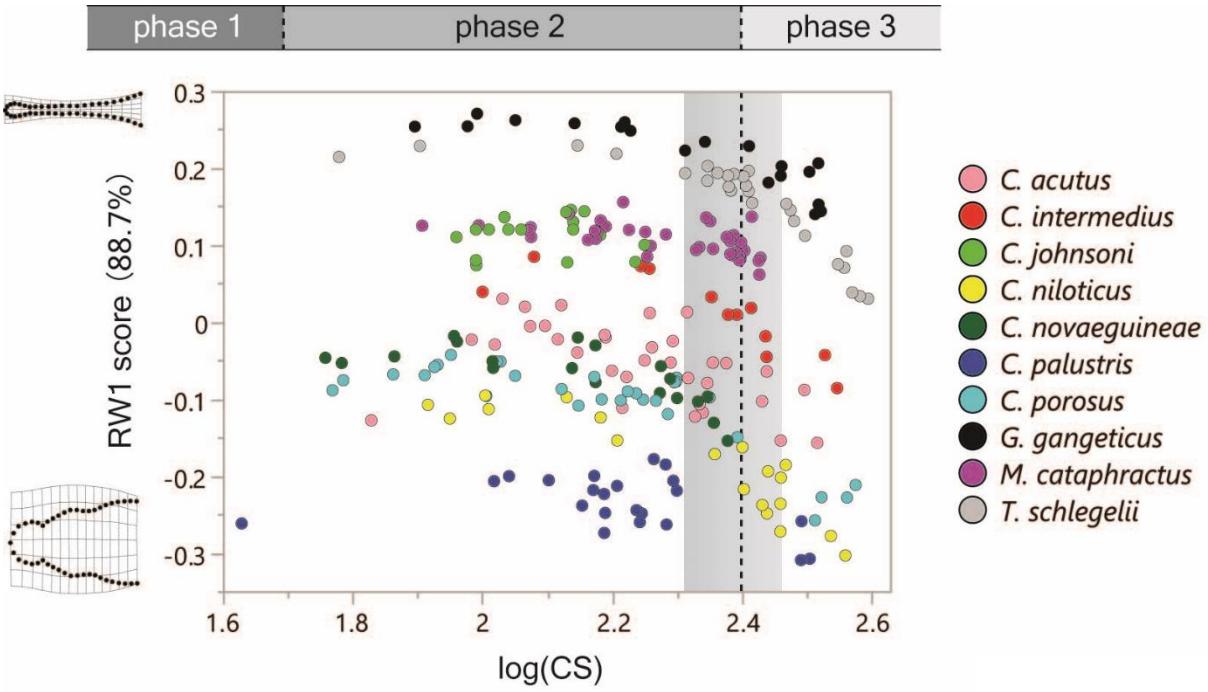


Fig. 5. Log(CS) breakpoints of snout shape growth trajectories in 6 species estimated by piecewise linear model fitting. Individuals with log(CS) ≥ 2.0 were used for this analysis. Dots are the estimated values, and bars represent their 95% confidence intervals.

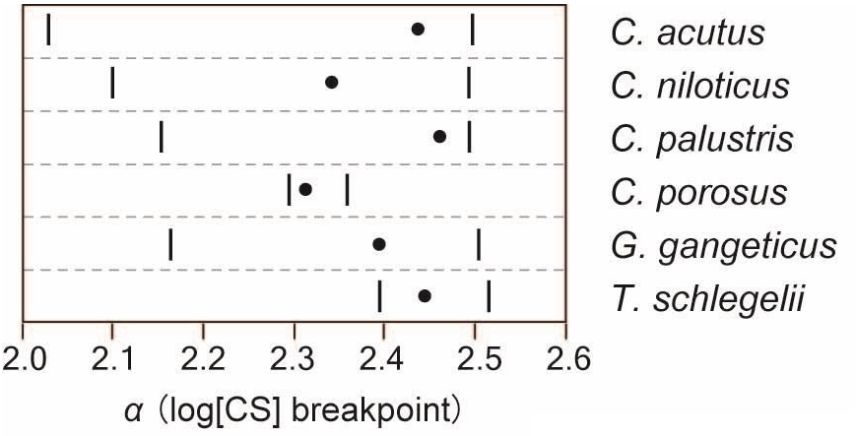


Fig. 6. (A–G) Bivariate plots of log(CS) and ecomorphological variables. Reduced major axis (RMA) regression lines are fit on the plots (A–B, D–G).

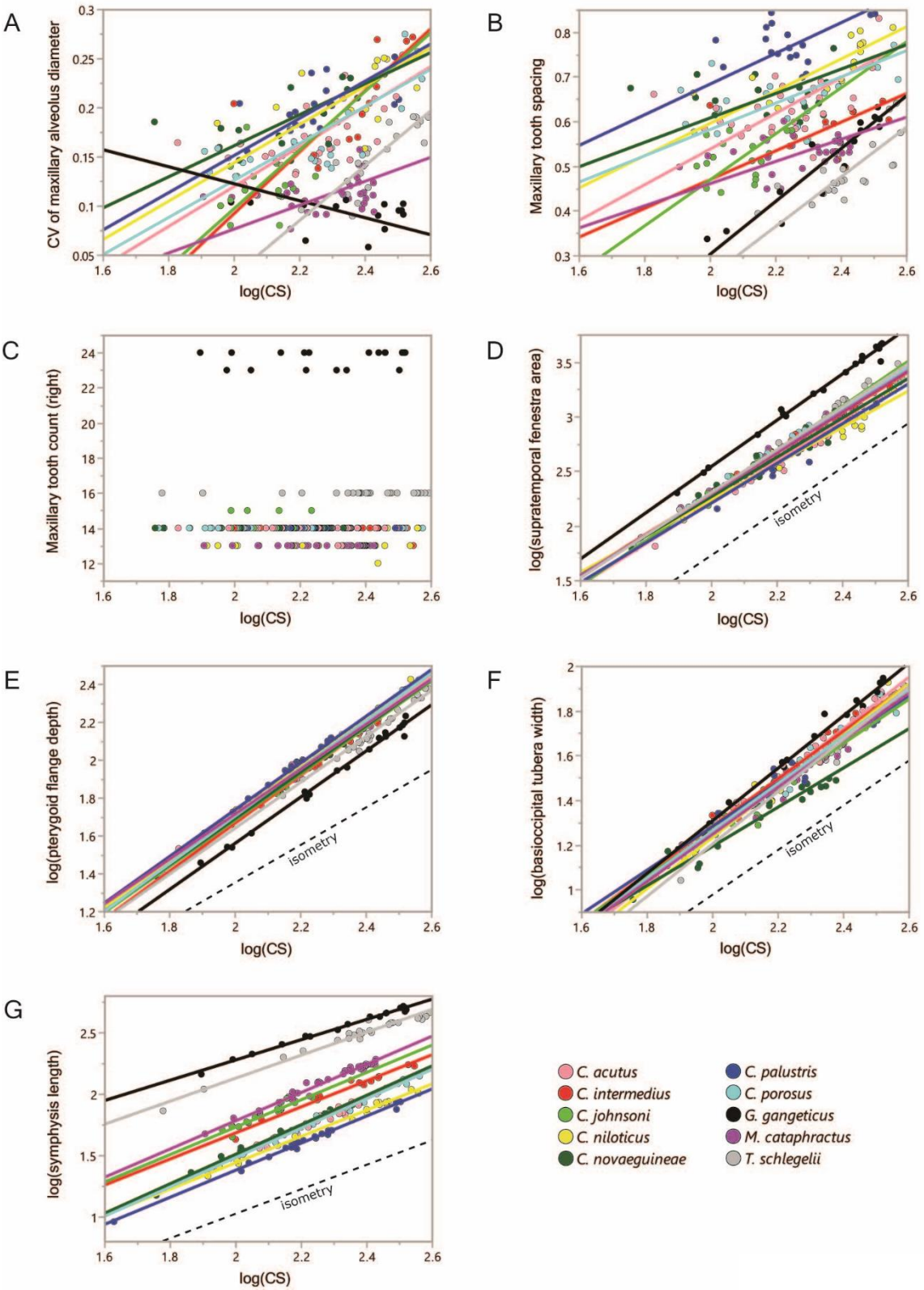


Fig. 7. Significant snout shape changes across the skull growth phases II and III. (A) *C. acutus* (from top: FMNH 20159; FMNH 59070). (B) *C. intermedius* (from top: FMNH 75659; SMF 28139). (C) *C. niloticus* (from top: IRSNB 5007; IRSNB 5012). (D) *C. palustris* (from top: BMNH 1848.2.5.9; BMNH 1868.4.9.11). (E) *C. porosus* (from top: FMNH 63744; FMNH 14071). (F) *G. gangeticus* (from top: YPM R10514; ZSM 28.1912). (G) *T. schlegelii* (from top: BMNH 1899.1.31.1; ZSM 395.1907). Ca, *C. acutus*; Ci, *C. intermedius*; Cni, *C. niloticus*; Cpa, *C. palustris*; Cpo, *C. porosus*; Gg, *G. gangeticus*; Ts, *T. schlegelii*. All scale bars are 10 cm.

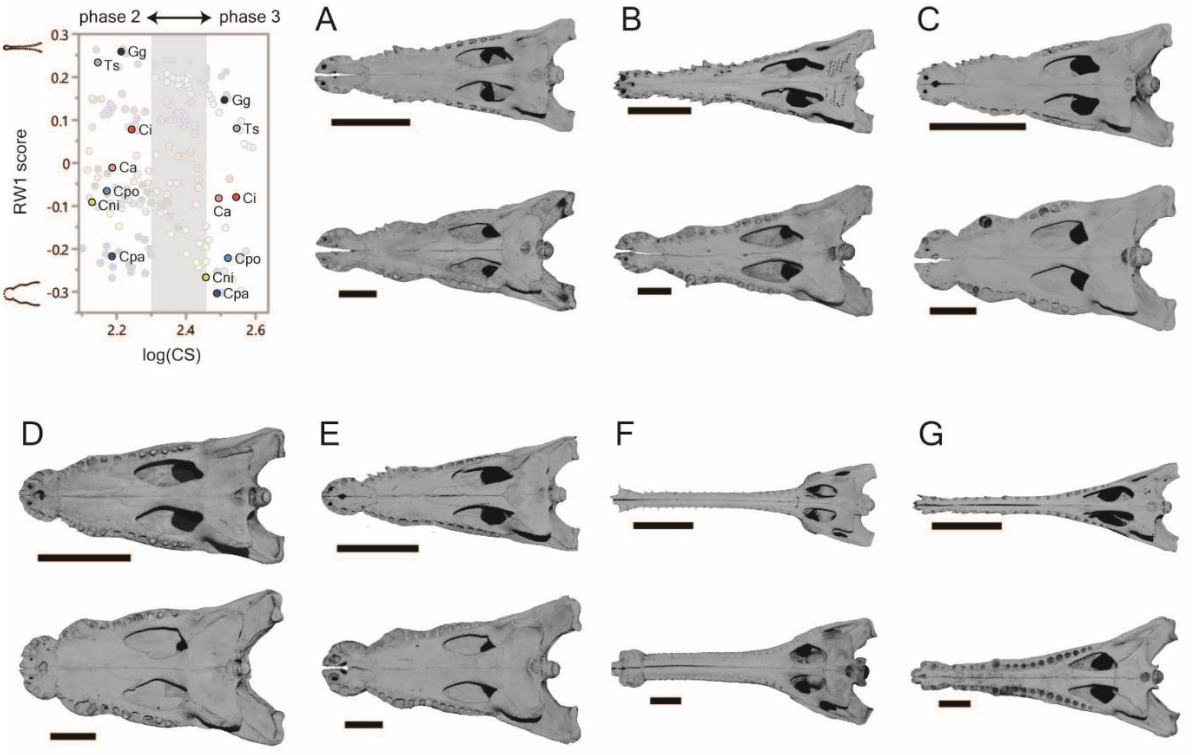


Fig. 8. Effect of size ranges on snout shape disparity tested by the empirical dataset. 10 individuals from 10 each species were randomly subsampled (10,000 replicates) without replacement, and the snout shape (RW1 scores) variance of 10 species was calculated for series of size ranges ($2.0 \leq \log(CS) \leq x$, $2.30 \leq x \leq 2.60$), with x sequentially changes by 0.01. The means and 95% confidence intervals of the variance for the series of size ranges were shown by a line chart. The subsampling and variance calculation were carried out in the software R.

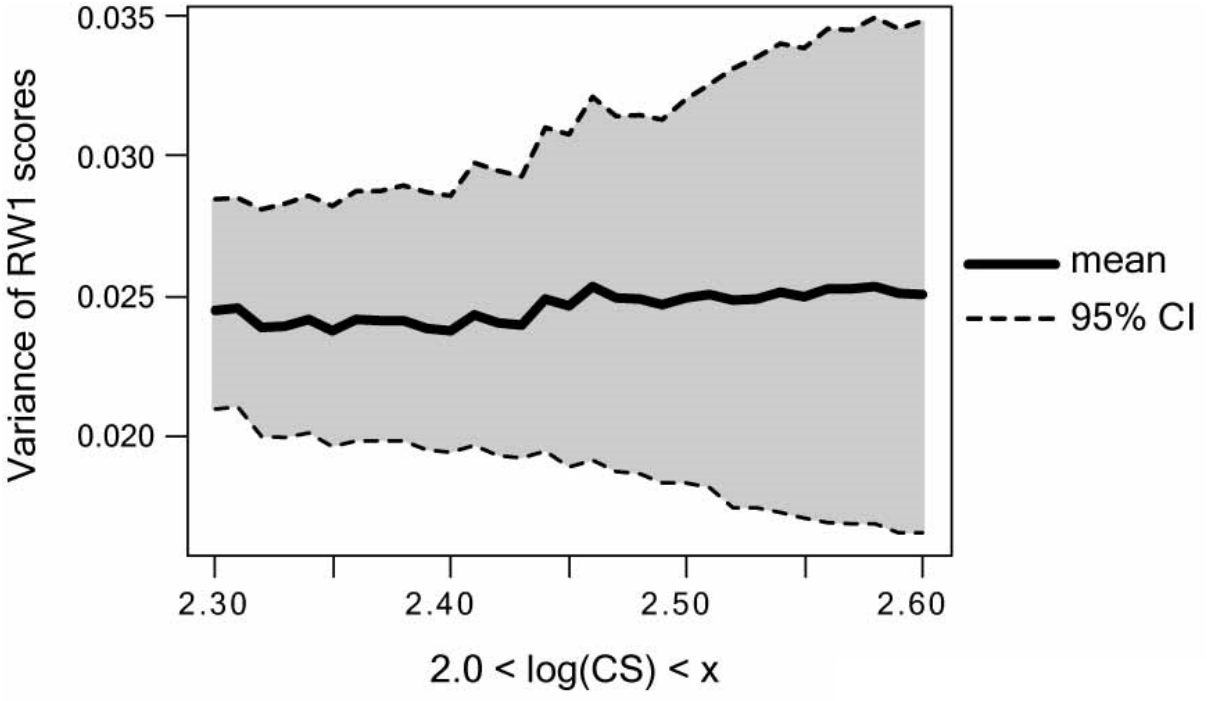


Fig. 9. Comparative growth of snout shape (right palate) in sampled crocodylians. (A) *C. palustris* (from top: ZSM 523.1911; ZSM 542.1911; BMNH 1897.12.31.1). (B) *C. acutus* (from top: USNM 52336; FMNH 11038; USNM 268760). (C) *T. schlegelii* (from top: ZSM 202.1907; SMF 28135; ZSM 375.1907). (D) *G. gangeticus* (from top: BMNH 46.1.7.3; ZSM 29.1912; BMNH 1974.3009). All scale bars are 5 cm.

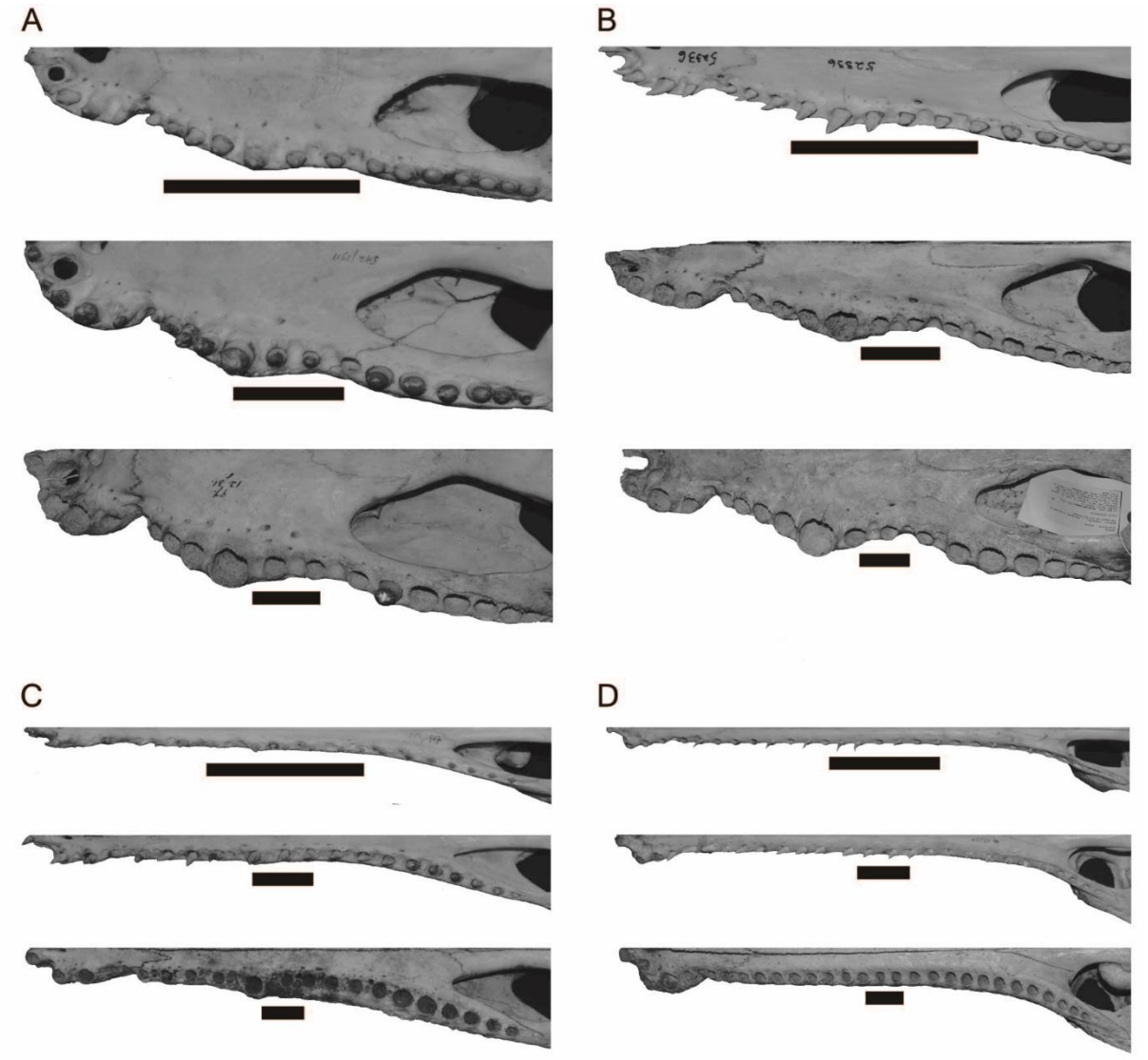


Fig. 10. Comparison of occipital part of skulls in sampled crocodylians. (A) *C. palustris* (from left: ZSM 523.1911; ZSM 517.1911; BMNH 1897.12.31.1). (B) *C. acutus* (from left: AMNH 15182; AMNH 43299; USNM 268760). (C) *T. schlegelii* (from left: ZSM 202.1907; SMF 28135; ZSM 375.1907). (D) *G. gangeticus* (from left: BMNH 1896.7.7.4; ZSM 29.1912; AMNH 7138). All scale bars are 5 cm.

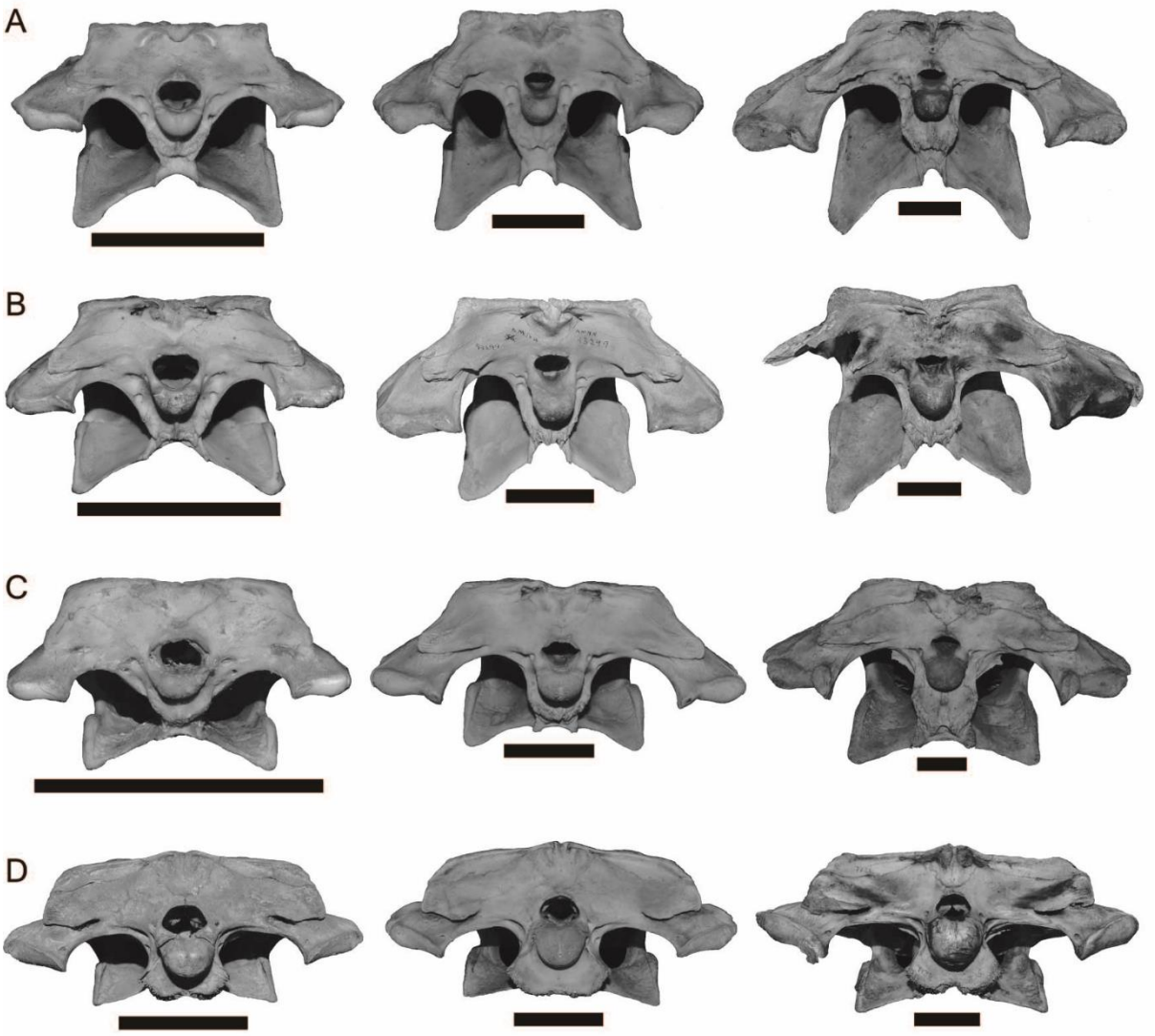


Fig. 11. Occlusal pits left on palates. (A) *T. schlegelii* (BMNH 94.2.21.1). (B) *Voay robustus* (AMNH 3101). (C) *Crocodylus rhombifer* (AMNH 6181). Arrows indicate occlusal pits placed medial to maxillary tooth row. M5, maxillary alveolus #5; SOF, suborbital fenestra. All scale bars are 10 cm.

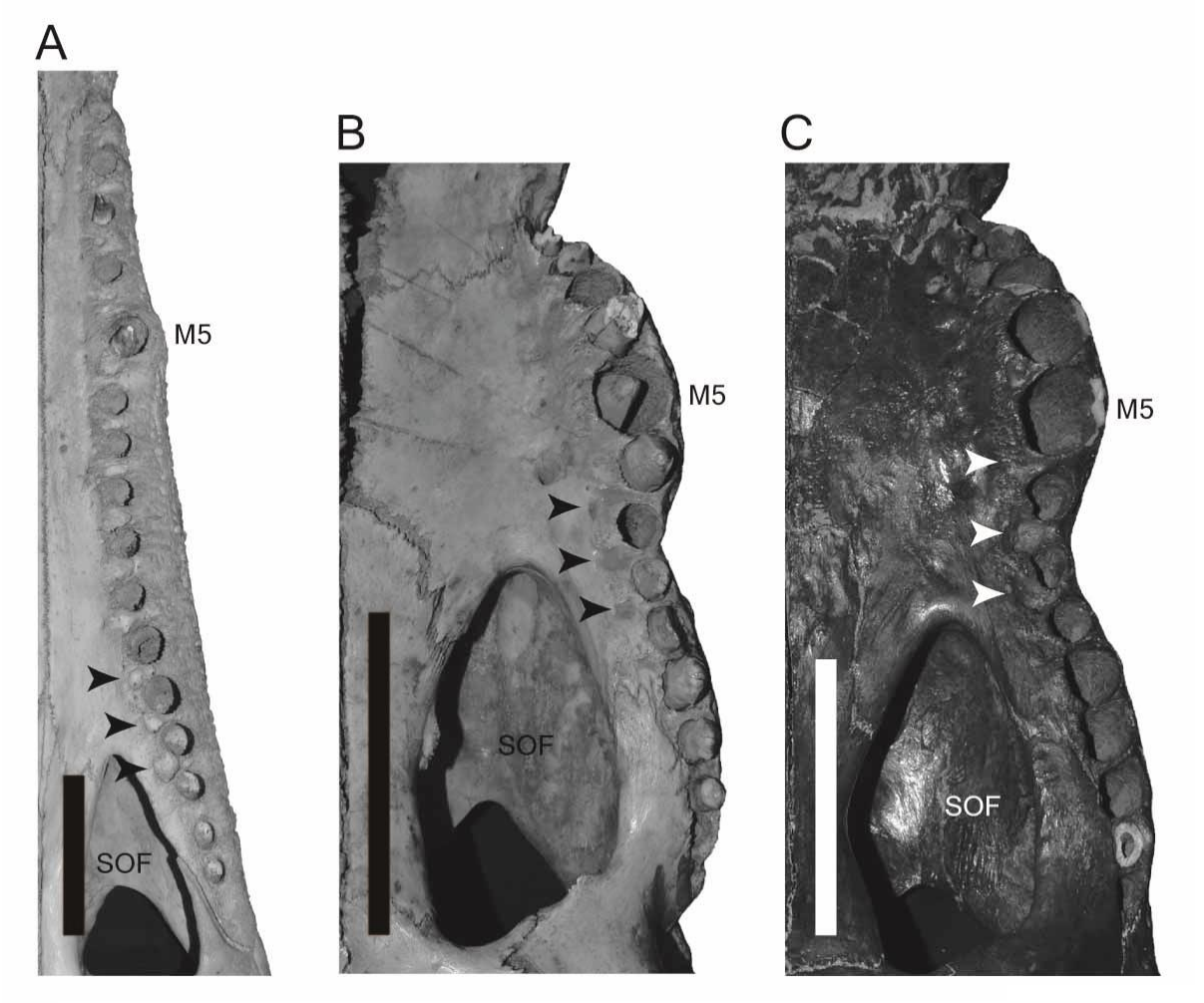


Fig. 12. A pit between premaxilla and maxilla for reception of the fourth dentary tooth (*C. palustris*: BMNH 1852.5.9.45). Arrow indicates the pit. Scale bar is 5 cm.

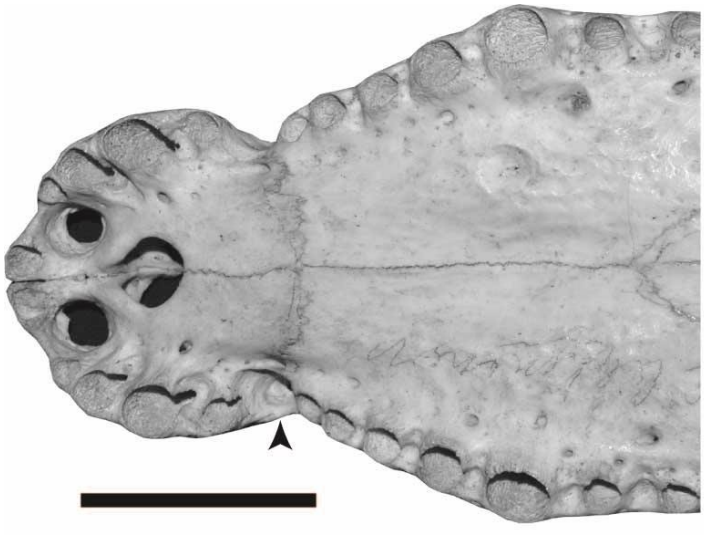


Fig. 13. Basioccipital region of the skull in *C. palustris* (BMNH 1897.12.31.1). Scale bar is 3 cm.

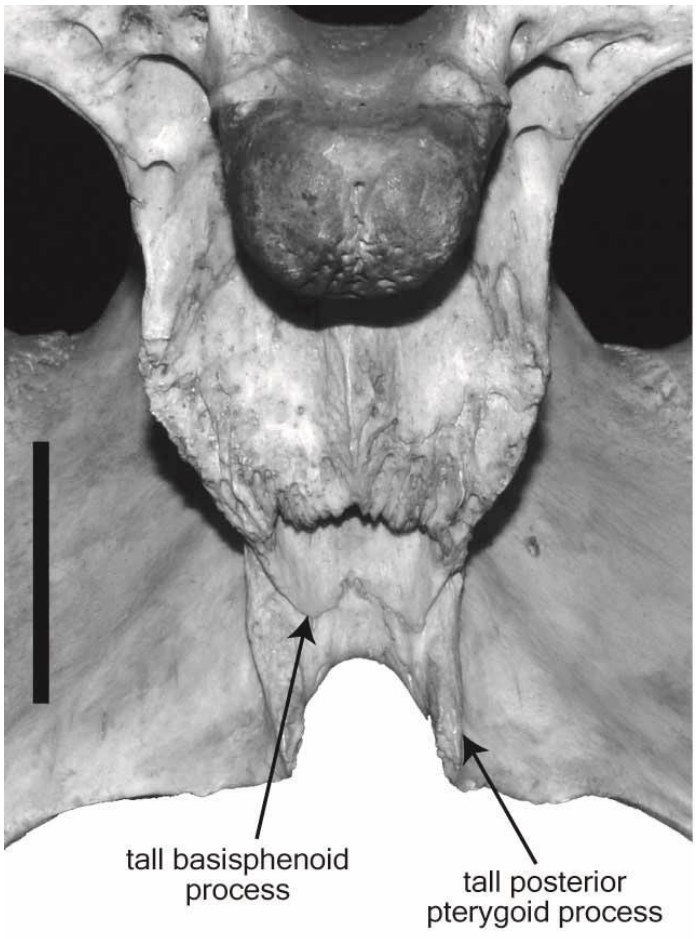


Table 1. Proposed trophic ecomorphological variables and their piscivorous states in crocodylians.

Variable	Piscivorous state	Function and performance	Reference
Snout shape	long and slender	higher angular velocity of jaw tip during lateral head sweeping and jaw closing, thus favorable for catching small agile prey	Taylor, 1987; Thorbjarnarson, 1990; McHenry et al. 2006
Degree of heterodonty (tooth size disparity)	less degree of heterodonty (coupled with less undulated jaw margin)	efficient for detaining relatively docile prey, but inefficient for holding larger prey firmly	Iordansky, 1973; Busbey, 1995
Spacing of teeth	widely spaced	striking and impaling prey	Langston, 1973
Tooth count	increased in number	increase the chance of catching prey and facilitates transport of the food items towards the pharynx (while inertial feeding)	Busbey, 1995
Tooth shape	long, slender, and recurved	striking and impaling prey, and maneuvering fish back toward gullet	Langston, 1973; Massare, 1987; Busbey, 1995
Size of supratemporal fenestra	increased	increased mass of *M. pseudotemporalis*, which is asscіated with rapid but weak jaw adduction	Iordansky, 1964; Endo et al. 2002
Ventral extension of pterygoid flange	reduced	reduced mass and moment arm of *Mm. pterygoidei dorsalis* et *ventralis* (strong jaw adductors), and reduction in maximal mouth opening	Iordansky, 1964; Endo et al. 2002; Piras et al. 2014
Development of basioccipital tubera	highly developed and pendulous	modified neck musculature (*M. longissimus capitis profundus* and *M. rectus capitis anticus major*; Tsuihiji 2007) advantageous for head motions during fish eating (e.g., lateral head sweeping)	Langston, 1973
Length of lower jaw symphysis	elongated	incur higher strain under loads used for feeding upon large prey	Walmsley et al. 2013

Table 2. Whole sample and species regressions of proposed ecomorphological variables against snout shape (RW1 score). Individuals with 2.1 ≤ log(CS) ≤ 2.4 were used for the analyses.

Variable by snout shape (RW1 score)	*n*	R^2	*P*	Slope	Intercept	Pagel's λ
Whole sample analysis with ordinary least squares (OLS) regression						
CV of maxillary alveolus diameter	111	0.668	< 0.001	-0.242	0.151	NA
Maxillary tooth spacing	111	0.860	< 0.001	-0.676	0.593	NA
Relative supratemporal fenestra (STF) area ([STF area]$^{1/2}$/CS)	123	0.315	< 0.001	0.069	0.134	NA
Relative pterygoid flange depth (PFD/CS)	120	0.376	< 0.001	-0.247	0.564	NA
Relative basioccipital tubera witdth (BTW/CS)	122	0.009	0.311	0.015	0.184	NA
Relative symphysis length (SL/CS)	110	0.667	< 0.001	2.233	0.567	NA
Species analysis with phylogenetic generalized least squares (PGLS) regression						
CV of maxillary alveolus diameter	10	0.863	< 0.001	-0.232	0.155	0.000
Maxillary tooth spacing	10	0.972	< 0.001	-0.646	0.591	0.000
Mode Maxillary tooth count	10	0.054	0.519	3.154	16.352	1.000
Relative supratemporal fenestra (STF) area ([STF area]$^{1/2}$/CS)	10	0.509	0.021	0.098	0.137	0.000
Relative pterygoid flange depth (PFD/CS)	10	0.634	0.006	-0.237	0.541	1.000
Relative basioccipital tubera witdth (BTW/CS)	10	0.130	0.306	0.053	0.187	0.000
Relative symphysis length (SL/CS)	10	0.676	0.004	1.476	0.835	1.000

CV, coefficient of variation. Mean species RW1 scores and mean variable values were used for species analysis (PGLS regression). Oaks (2011)'s molecular tree was used for PGLS regression.

Table 3. Welch's t-test of snout shape (RW1 score) between skull growth phases II and III. Individuals with log(CS) ≥ 2.0 were used for the analysis.

Taxon	*n*	*t*	df	*P*
C. acutus	31	-3.591	5.958	0.012
C. niloticus	17	-5.777	13.607	< 0.001
C. palustris	21	-3.819	2.665	0.039
C. porosus	23	-12.821	5.068	< 0.001
G. gangeticus	16	-5.696	12.045	< 0.001
T. schlegelii	25	-4.821	17.774	< 0.001

Table 4. RMA regressions of ecomorphological variables against size (log[CS]).

Taxon	*n*	R^2	*P*	Slope	Lower 95% CI	Upper 95% CI	Allometric trend
CV of maxillary alveolous diameter							
C. acutus	29	0.401	< 0.001	0.203	NA	NA	NA
C. intermedius	11	0.329	0.065	0.313	NA	NA	NA
C. johnsoni	17	0.082	0.264	0.296	NA	NA	NA
C. niloticus	15	0.221	0.077	0.195	NA	NA	NA
C. novaeguineae	17	0.303	0.022	0.158	NA	NA	NA
C. palustris	19	0.296	0.016	0.189	NA	NA	NA
C. porosus	23	0.503	< 0.001	0.188	NA	NA	NA
G. gangeticus	14	0.030	0.554	-0.086	NA	NA	NA
M. cataphractus	31	0.079	0.127	0.122	NA	NA	NA
T. schlegelii	22	0.690	< 0.001	0.279	NA	NA	NA
Maxillary tooth spacing							
C. acutus	29	0.198	0.015	0.399	NA	NA	NA
C. intermedius	11	0.000	0.982	0.322	NA	NA	NA
C. johnsoni	17	0.078	0.279	0.524	NA	NA	NA
C. niloticus	15	0.551	0.002	0.361	NA	NA	NA
C. novaeguineae	17	0.000	0.993	0.273	NA	NA	NA
C. palustris	19	0.018	0.584	0.343	NA	NA	NA
C. porosus	23	0.211	0.027	0.294	NA	NA	NA
G. gangeticus	14	0.875	< 0.001	0.592	NA	NA	NA
M. cataphractus	31	0.103	0.079	0.248	NA	NA	NA
T. schlegelii	22	0.606	< 0.001	0.557	NA	NA	NA
log(supratemporal fenestra area)							
C. acutus	33	0.958	< 0.001	1.895	1.758	2.043	=
C. intermedius	12	0.981	< 0.001	1.852	1.682	2.039	=
C. johnsoni	16	0.947	< 0.001	2.044	1.792	2.332	=
C. niloticus	19	0.964	< 0.001	1.659	1.506	1.828	−
C. novaeguineae	19	0.954	< 0.001	1.799	1.613	2.007	=
C. palustris	22	0.969	< 0.001	1.816	1.673	1.971	−
C. porosus	30	0.992	< 0.001	1.916	1.850	1.984	−
G. gangeticus	18	0.991	< 0.001	2.118	2.015	2.225	+
M. cataphractus	34	0.978	< 0.001	1.877	1.779	1.981	−
T. schlegelii	24	0.977	< 0.001	1.955	1.828	2.090	=
log(pterygoid flange depth)							
C. acutus	31	0.993	< 0.001	1.231	1.193	1.270	+
C. intermedius	12	0.996	< 0.001	1.267	1.209	1.328	+
C. johnsoni	17	0.977	< 0.001	1.222	1.125	1.327	+
C. niloticus	18	0.994	< 0.001	1.241	1.193	1.292	+
C. novaeguineae	18	0.998	< 0.001	1.225	1.193	1.258	+
C. palustris	20	0.994	< 0.001	1.236	1.190	1.283	+
C. porosus	30	0.997	< 0.001	1.261	1.236	1.286	+
G. gangeticus	18	0.992	< 0.001	1.221	1.164	1.281	+
M. cataphractus	38	0.989	< 0.001	1.191	1.149	1.234	+
T. schlegelii	27	0.994	< 0.001	1.215	1.175	1.255	+
log(basioccipital tubera width)							
C. acutus	31	0.980	< 0.001	1.151	1.091	1.215	+
C. intermedius	12	0.962	< 0.001	1.063	0.927	1.220	=
C. johnsoni	17	0.840	< 0.001	0.990	0.796	1.231	=
C. niloticus	18	0.973	< 0.001	1.147	1.052	1.251	+
C. novaeguineae	19	0.950	< 0.001	0.878	0.783	0.985	−
C. palustris	20	0.920	< 0.001	0.977	0.850	1.123	=
C. porosus	30	0.978	< 0.001	1.060	1.001	1.122	+
G. gangeticus	17	0.986	< 0.001	1.176	1.102	1.256	+
M. cataphractus	38	0.954	< 0.001	1.055	0.981	1.134	=
T. schlegelii	27	0.982	< 0.001	1.173	1.111	1.239	+
log(symphysis length)							
C. acutus	30	0.985	< 0.001	1.186	1.130	1.244	+
C. intermedius	12	0.970	< 0.001	1.061	0.939	1.198	=
C. johnsoni	17	0.897	< 0.001	1.112	0.933	1.325	=
C. niloticus	18	0.992	< 0.001	1.070	1.022	1.121	+
C. novaeguineae	13	0.989	< 0.001	1.200	1.118	1.287	+
C. palustris	20	0.992	< 0.001	1.102	1.053	1.153	+
C. porosus	24	0.995	< 0.001	1.195	1.157	1.234	+
G. gangeticus	17	0.991	< 0.001	0.825	0.784	0.868	−
M. cataphractus	37	0.976	< 0.001	1.149	1.089	1.212	+
T. schlegelii	24	0.968	< 0.001	0.936	0.864	1.013	=

CV, coefficient of variation. +, positive allometry; −, negative allometry; =, isometry.

Table 5. Spearman rank correlation of maxillary tooth count and size (log[CS]).

Taxon	*n* (right)	*n* (left)	Mode	Mean	Deviation from mode (total)	Mode tooth count frequency (%) (total)	Spearman ρ (right)	*P* (right)	Spearman ρ (left)	*P* (left)
C. acutus	33	33	14	13.94	4	93.9	-0.147	0.415	-0.187	0.298
C. intermedius	12	12	14	13.92	2	91.7	-0.194	0.545	NA	NA
C. johnsoni	17	17	14	14.18	6	82.4	0.085	0.746	0.112	0.669
C. niloticus	19	19	13	13.21	10	73.7	0.358	0.133	0.589	0.008
C. novaeguineae	19	19	14	14.00	0	100.0	NA	NA	NA	NA
C. palustris	20	20	14	13.98	1	97.5	NA	NA	-0.099	0.677
C. porosus	30	30	14	13.98	1	98.3	-0.225	0.231	NA	NA
G. gangeticus	19	19	24	23.74	10	73.7	0.269	0.266	0.165	0.500
M. cataphractus	38	38	13	13.01	1	98.7	-0.037	0.823	NA	NA
T. schlegelii	27	27	16	15.98	1	98.1	NA	NA	-0.302	0.126

II. Comparative limb proportions reveal differential locomotor morphofunctions of alligatoroids and crocodyloids

Introduction

Crocodylia is a remarkably successful group of large semi-aquatic predators, now thriving in the world's tropics and subtropics. The fossil record shows that the two living major groups, Alligatoroidea and Crocodyloidea (including *Gavialis* based on the molecular phylogeny: e.g. Gatesy *et al.*, 2003; McAliley *et al.*, 2006; Oaks, 2011) were split during the Late Cretaceous, and both have survived through several environmental crises afterwards, including the devastating K-Pg mass extinction event and the Plio-Pleistocene climatic deterioration (Brochu, 1997a, 2003).

These two crocodylian lineages are readily distinguished by the osmoregulatory organs found in the mouth. While all crocodyloids show keratinized buccal cavity and all crocodyloids except for *Gavialis gangeticus* possess lingual salt glands, alligatoroids' buccal cavity is non-keratinized, and their tongues lack lingual salt glands (Taplin *et al.*, 1982; Taplin, Grigg, & Beard, 1985; Taplin & Grigg, 1989; Leslie & Taplin, 2001). This led Taplin et al. (1985) to suggest the marine ancestry in crocodyloids, which enabled them to expand their distribution through transoceanic dispersals. Another well-known difference between the two groups is found in the sensory organs on the postcranial skin. The integumentary sense organs (Brazaitis, 1987), referring to minute dark spots on scales, detect the water vibration, low-frequency bellowing sounds, water quality (pH), and possibly change in temperatures (e.g. Soares, 2002; Brazaitis & Watanabe, 2011; Leitch & Catania, 2012; Di-Poï & Milinkovitch, 2013). These structures are present on the head as well as every postcranial scale of crocodyloids, but only on the head of alligatoroids.

Other distinctions of two major groups of crocodylians include their general differences in cranial features and minor differences in postcranial skeletons. Previous quantitative studies on cranial shape disparity of extant crocodylians demonstrated that crocodyloids occupy much larger skull morphospace than alligatoroids due to their long and narrow snouts, while the range of alligatoroids is extensively overlapped by generalized and blunt-snouted crocodyloids (Pierce, Angielczyk, & Rayfield, 2008; Sadleir, 2009). Furthermore, fossil

evidence indicated that similar slender snout shapes were acquired multiple times in distantly related lineages of crocodylians, but the slender-snouted morphotype has never evolved within alligatoroids (Brochu, 2001). Meanwhile, recent studies on postcranial skeletons revealed that forelimb and cervico-thoracic vertebrae are significantly different between alligatoroids and crocodyloids, where alligatoroids exhibit broader and shorter cervico-thoracic neural spines and stouter coracoid and humerus than crocodyloids (Chamero, Buscalioni, & Marugán-Lobón, 2013; Chamero *et al.*, 2014). Additionally, an examination of limb muscle properties in extant crocodylians found that relative muscle fascicle lengths and muscle physiological cross-sectional areas are different between the two groups, possibly reflecting the difference in their terrestrial locomotor capabilities (Allen *et al.*, 2015). Consistent with the large genetic divergence between alligatoroids and crocodyloids (Gatesy *et al.*, 2003; Oaks, 2011), the above evidence related with anatomical and physiological differences between them suggested that two groups are ecologically different (Leslie & Taplin, 2001). However, anatomical differences that indicate functional differences between two groups are still limited, and additional findings of such differences would be appreciated to further understand their ecological divergence. Moreover, an evolutionary correlation among the multiple morphofunctional systems that differentiated two groups, such as feeding and locomotor systems, have yet to be evaluated.

In the present study, appendicular morphology of extant and fossil crocodylians, exemplified by length proportion of fore- and hind limb elements, was examined. We first test if the locomotor morphology of alligatoroids and crocodyloids are different from each other, and reconstruct its evolutionary history on phylogeny. We then investigate the correlation of locomotor and feeding morphologies to see if they evolved in association, and discuss an evolutionary connection of locomotor and feeding functions, which might jointly dictate the fate of the two superfamilies.

Material and methods

Specimens and measurements

The extant crocodylian sample includes 110 individuals from 20 species (Table 1, and supplementary material, Table S1), among which three individuals were adopted from Mook (1921e). The sample represents all six known subfamilies (Alligatorinae, Caimaninae, Crocodylinae, Osteolaeminae, Gavialinae, and Tomistominae) of the living crocodylians in the context of molecular tree (Brochu, 2003) (Table 1). Sexes were not recorded for most of

the specimens and thus sexually dependent differences were not considered here, because sexes account for only limited portions of appendicular shape variation (Bonnan, Farlow, & Masters, 2008). We included individuals from juveniles to large adults with various size classes (femur length ≥ 50 mm) for each species to maximize the sample size. Unavoidably, some species are represented by relatively large individuals (e.g. *Crocodylus porosus* and *Tomistoma schlegelii*) or small individuals (e.g. two species of *Paleosuchus*) compared to others (supplementary material, Fig. S1). The fossil crocodylian sample includes taxa that are outgroup of Alligatoroidea + Crocodyloidea (*Anteophthalmosuchus hooleyi*, *Susisuchus anatoceps*, *Borealosuchus wilsoni*, *Boverisuchus vorax*, and *Boverisuchus bolcensis*), basal alligatorines (*Allognathosuchus gracilis*, *Navajosuchus mooki*, and *Wannaganosuchus brachymanus*), a derived alligatorine (*Alligator prenasalis*), caimanines (*Stangerochampsa mccabei*, *Necrosuchus ionensis*, and *Tsoabichi greenriverensis*), a basal crocodyloid (*Asiatosuchus*), and a tomistomine (*Toyotamaphimeia machikanensis*) (supplementary material, Table S3).

In this study, maximum lengths of three main forelimb segments (humerus, ulna, and metacarpal III: HL, UL, and MC3L), and three main hind limb segments (femur, tibia, and metatarsal III: FL, TL, and MT3L) were measured (Fig. 1). Measured bones were selected based on previous works on crocodylian limb proportions (Dodson, 1975; Livingston *et al.*, 2009). For forelimb, ulna instead of radius was used because ulna is much stouter than radius and is assumed to be the major weight-bearing element among forelimb zeugopodium. The olecranon process of crocodylian ulna is minute and degree of its development may have negligible effects on the total length. Measurements of fossil crocodyliforms were obtained by direct observation, through personal communications, and from literatures (supplementary material, Table S3). Only either fore- or hind limb was available for some individuals. When metacarpal III or metatarsal III length was not available, it was estimated from the average ratio of metacarpal II to III, or that of metatarsal II or IV to III of three extant taxa (*Melanosuchus niger*, *Caiman crocodilus*, and *Crocodylus acutus*: Mook, 1921e). Lengths of left and right elements were averaged when possible.

We used the trunk length (sum of 3rd cervical to 15th dorsal centrum lengths) as a body length proxy, which was measured for 55 individuals of 17 species (Table 1 and supplementary material, Table S1) among the 20 extant species for which limb bones were measured. Trunk lengths of fossil taxa were unmeasurable, and they were not included in the dataset.

Crocodylian rostral shape is known to be associated with their diets (Brochu, 2001; Erickson *et al.*, 2012), feeding function, and performance (Taylor, 1987; Thorbjarnarson, 1990; McHenry *et al.*, 2006). Here, rostral proportion, which is defined as the ratio of the palate width at the last maxillary alveoli to the length from there to the tip of the snout, was measured as a correlate of trophic function. The average rostral proportions were obtained for 20 species (Table 1 and supplementary material, Table S2). Small individuals with skull width < 100 mm were excluded from the dataset. Fossil taxa were not included in the dataset because they are represented by a single or few individuals with various size classes, and their rostral shapes would be largely dependent on size.

Data analyses

Since crocodylian limbs show ontogenetic allometry (Dodson, 1975; Livingston *et al.*, 2009), size normalization with allometric correction of the measurements is required prior to the species comparison. We used geometric mean (GM) of six limb segments ($GM = [HL \times UL \times MC3L \times FL \times TL \times MT3L]^{1/6}$) as the size index for each individual, because GM would more accurately reflect the overall body size than the length of single bone (e.g. humerus or femur). All the measurements were normalized using the equation of Elliott et al. (1995), which was adopted by recent vertebrate workers (e.g. Pierce, Clack, & Hutchinson, 2011; Molnar *et al.*, 2015; Cuff *et al.*, 2016): $M_s = M_o (L_s/L_o)^b$, where M_s is the standardized measurement, M_o is the original measurement, L_s is the overall mean GM of all individuals, L_o is the GM of each individual, and b is the regression slope of $\log_{10}M_o$ (response variable) on $\log_{10}L_o$ (predictor variable) for all individuals. If fossil taxa preserved either only fore- or hind limb, the normalization was separately done for fore- and hind limbs, using geometric means of segment lengths of forelimb (HL, UL, and MC3L) or hind limb (FL, TL, and MT3L) as size indexes.

All normalized measurements (cHL, cUL, cMC3L, cFL, cTL, and cMT3L) were log10-transformed to remedy the right-skewed distribution (Sokal & Rohlf, 1995). Principal component analysis (PCA) was used to reduce the dimensionality of the dataset, and the limb morphospace was visualized by a PC score plot. Correlations between size and the normalized measurements were tested by ordinary least squares (OLS) regressions of $\log_{10}$GM vs. first three PC axes. To examine the difference in the multivariate means between the two superfamilies (Alligatoroidea and Crocodyloidea), non-parametric multivariate analysis of variance (npMANOVA: Bray-Curtis distance, 9,999 permutations) was conducted

for the log10-transformed normalized measurements using the R package 'vegan' (Oksanen *et al.*, 2016). The analysis was run separately for smaller (GM < median GM) and larger (GM ≥ median GM) subsamples to examine the size effect on limb measurements. Because the phylogenetic placement of Gavialinae (*Gavialis gangeticus*) differs between molecular (e.g. Densmore, 1983; Densmore & White, 1991; Gatesy *et al.*, 2003; McAliley *et al.*, 2006; Oaks, 2011) and morphological (e.g. Norell, 1989; Brochu, 1997a, 1999a; Salisbury *et al.*, 2006) trees, we performed the alternative analysis excluding *Gavialis gangeticus* from the dataset. The npMANOVA was also conducted for the whole sample using the subfamily as a factor, followed by pairwise comparisons for all pairs of subfamilies (*p*-values adjusted by the Holm method).

For the species comparisons, the normalized measurements were averaged within each species. To help understand the difference in the limb proportion among 20 extant and 14 fossil species, ternary diagrams of within-forelimb and within-hind limb segment proportions, and a univariate plot of forelimb / (fore + hind limbs) were provided. Evolutionary history of fore- and hind limb proportions were reconstructed on a recent comprehensive molecular tree of Oaks (2011) using the contMap() function of the R package 'phytools' (Revell, 2012). Phylogenetic relationships of fossil taxa are based on literatures (Salisbury *et al.*, 2006; Brochu, 2013; Jouve *et al.*, 2015; Salas-Gismondi *et al.*, 2015), disregarding the inconsistent placement of *Gavialis gangeticus* between the molecular and morphological trees. Ages of fossil taxa were assumed to be the mid points of their stage ranges, and root age was set at 129.4 mya (beginning of Barremian: Cohen *et al.*, 2013), which is the first appearance datum for the basalmost taxon, *Anteophthalmosuchus hooleyi* (Martin, Delfino, & Smith, 2016). Divergence times of extant taxa were adopted from Oaks' (2011) species tree (90 mya upper limit on the root age), and that of fossil taxa were estimated by dividing the 'shared' branch lengths equally (Brusatte *et al.*, 2008). Here, *Allognathosuchus gracilis* was regarded as a close relative of *A. haupti*, and *Toyotamaphimeia machikanensis* was regarded as a sister taxon to *Tomistoma schlegelii*.

Relative lengths of total fore- and hind limbs against body length were obtained from extant crocodylians for further analyses. Allometry in trunk length (sum of 3rd cervical to 15th dorsal centrum lengths), total forelimb length (HL + UL + MC3L), and total hind limb length (FL + TL + MT3L) were corrected by the above described normalization equation, using the geometric mean (GM) of the three measurements (GM = [trunk length × total forelimb length × total hind limb length]$^{1/3}$) as a size index. Subsequently, species average

relative forelimb length (total forelimb / trunk length) and hind limb length (total hind limb / trunk length) were compared among 17 species (Table 1 and supplementary material, Table S1). We then tested if relative proximal segment lengths within fore- and hind limbs (cHL / total forelimb; cFL / total hind limb) are associated with relative fore- and hind limb lengths (total forelimb / trunk length; total hind limb / trunk length), by phylogenetically generalized least squares (PGLS) regressions for 17 species.

In order to explore the locomotor and trophic correlation in crocodylians, we performed PGLS regressions of rostral proportions (Table 1 and supplementary material, Table S2) vs. relative proximal segment lengths (cHL / total forelimb; cFL / total hind limb) using the average values of 20 extant species. Additionally, PGLS regressions of rostral proportions vs. relative overall limb length ([fore + hind limbs] / trunk length) for 17 extant species are performed. Because rostrum shape is size dependent (but not growth stage dependent) in extant crocodylians, and large forms attain increasingly wider rostrum beyond a certain size (skull width ~240 mm for crocodyloids: Iijima, 2017), we have conducted PGLS regressions twice; either using all individuals with skull width ≥ 100 mm (n = 256), or using individuals within a set size range (100 mm ≤ skull width ≤ 200 mm; n = 151), to test the effect of size range on the results. In PGLS regressions, the scaling parameter lambda was estimated by maximum likelihood method and incorporated into the regression, using the R package 'caper' (Orme *et al.*, 2013). The time-calibrated trees required for the PGLS regression were reconstructed in reference to a comprehensive molecular tree (Fig. 2*a*: Oaks, 2011), with divergence times adopted from Oaks' (Oaks, 2011) species tree (90 mya upper limit on the root age). The alternative morphological tree (Fig. 2*b*) is based on Brochu (1997a, 1999a, 2000), with divergence times estimated from first appearance data of fossils (Brochu, 1997a, 2004c). The root age (87.14 myr) is adopted from Oaks (2011). In the morphological tree, relationships within Indo-Pacific *Crocodylus* are left unresolved, and *Mecistops* is regarded as a sister taxon to *Osteolaemus* based on the recent molecular and morphological evidence (McAliley *et al.*, 2006; Oaks, 2011; Shirley *et al.*, 2014). All statistical analyses were carried out with R language and environment (R Core Team, 2016). Drawings of limbs and trunk (Figs. 1,4–7) are based on Mook (1921e) and Richardson et al. (2002).

Results

PCA of log10-transformed normalized limb measurements revealed that about 90% of the variance is explained by first three PC axes (Table 2). OLS regressions of $\log_{10}$GM against

the first three PC axes indicated non-significant relationships between size and limb measurements (p = 0.66, 0.31, 0.80 for first, second, and third axis respectively). The first PC axis accounts for relative fore- vs. hind limb length. Individuals with high PC1 scores have longer humerus, ulna and metacarpal III and shorter femur, tibia, and metatarsal III. The second PC axis describes relative contribution of stylopodium, zeugopodium, and metapodium within fore- and hind limbs. Individuals placed high on this axis have longer stylopodia (humerus and femur) and shorter metapodia (metacarpal III and metatarsal III). A three-dimentional PC score plot (Fig. 3) shows that alligatoroids (Alligatorinae and Caimaninae) and crocodyloids (Crocodylinae, Osteolaeminae, Gavialinae, and Tomistominae) are moderately separated on the first and second axes. npMANOVA of the log10-transformed normalized limb measurements with smaller (GM < median GM) and larger (GM ≥ median GM) subsamples found significant differences between Alligatoroidea and Crocodyloidea (F = 13.643, $p < 0.001$ for smaller subsample; F = 8.399, $p < 0.001$ for larger subsample). The alternative test excluding *Gavialis gangeticus* from subsamples also indicated significant differences (F = 13.833, $p < 0.001$ for smaller subsample; F = 7.342, $p < 0.001$ for larger subsample). Subfamily npMANOVA yielded the significant result (F = 13.697, $p < 0.001$). Pairwise comparisons among the subfamilies show significant differences ($p < 0.05$) for all subfamily pairs, highlighting the separation of limb morphospace among six subfamilies (supplementary material, Table S5).

Ternary diagrams of fore- and hind limbs in extant crocodylians demonstrate species' differences in within-forelimb and within-hind limb proportions (Fig. 4). As shown in the PCA for the whole sample, extant alligatoroids (Alligatorinae and Caimaninae) have relatively short humerus within the forelimb elements (50.1–51.5% in Alligatorinae and 50.0–51.3% in Caimaninae) whereas extant crocodyloids without *Gavialis* (Crocodylinae, Osteolaeminae, and Tomistominae) have relatively long humerus (50.7–52.8% in Crocodylinae, 50.7–51.8% in Osteolaeminae, and 53.6% in Tomistominae) (Fig. 4*a*). It is noteworthy that a gavialine *Gavialis gangeticus* exhibits by far the longest relative humerus within the forelimb elements (56.1%). The similar trend is observed in the hind limb, where relatively short femur within the hind limb elements characterizes extant alligatoroids (43.6–44.0% in Alligatorinae and 43.2–45.2% in Caimaninae), while relatively long femur is found in extant crocodyloids (44.5–46.8% in Crocodylinae, 44.7–45.6% in Osteolaeminae, 45.1% in Gavialinae and 45.3% in Tomistominae) (Fig. 4*b*).

Extinct species have explored much larger limb morphospace than the extant species. The

ternary diagrams of limb segment proportions for fossils (Fig. 4*c*, *d*) reveal that most of the fossil alligatoroids (basal alligatorines *Wannaganosuchus brachymanus* from the Paleocene and *Allognathosuchus gracilis* from the Eocene, and a derived alligatorine *Alligator prenasalis* from the Eocene), and three caimanines (*Stangerochampsa mccabei* from the Late Cretaceous, *Necrosuchus ionensis* from the Paleocene, and *Tsoabichi greenriverensis* from the Eocene) were plotted nearby extant alligatoroids in having relatively shorter stylopodia (cHL / total forelimb ≤ 50.8%; cFL / total hind limb ≤ 44.9%), suggesting that the modern alligatoroid limb morphology was acquired in early times of their evolution (Figs. 4*c*, *d* and 6). An exception is a basal alligatorine *Navajosuchus mooki*, which has relatively long humerus (52.1%) and femur (47.4%) similar to crocodyloids. The basal crocodyloid *Asiatosuchus* is plotted outside of the extant species range with a relatively long tibia. The tomistomine *T. machikanensis* is placed beyond the range of extant crocodyloids, in having extremely long humerus within forelimb elements (cHL / total forelimb = 58.8%). Outgroup taxa of Alligatoroidea + Crocodyloidea have diverse forelimb proportions (*Boverisuchus vorax* with relatively short humerus and long ulna) and hind limb proportions (*Susisuchus* sp. with short femur and long tibia, and *Borealosuchus wilsoni* with short tibia and long metatarsal III).

The fore- vs. hind limb proportion varies among and within subfamilies, where forelimb / (fore + hind limbs) is relatively small in Caimaninae (35.6–42.7%) and Gavialinae (41.1%), relatively large in Crocodylinae (42.2–44.5%), Osteolaeminae (43.0–43.4%), and Tomistominae (42.3%), and largely varies around the average in Alligatorinae (40.3–44.0%) (Fig. 5*a*). The outgroup taxa are diverse in forelimb / (fore + hind limbs), where *Anteophthalmosuchus hooleyi* has an extremely long forelimb (48.3%). The comparison of relative fore- and hind limb lengths to body length shows that *Gavialis gangeticus* has the shortest fore- and hind limbs relative to body length among all (Fig. 5*b*, *c*). Alligatoroids and crocodyloids occupy overlapping limb ratio ranges, but particularly in crocodyloids, it seems as though wider-snouted species (*Osteolaemus tetraspis*, *Crocodylus palustris*, *C. moreletii*, and *C. rhombifer*) have longer limbs than the slender-snouted species (*Tomistoma schlegelii*, *Crocodylus johnsoni*, *C. acutus*, and *C. porosus*: see Fig. 7*e*).

PGLS regressions of relative forelimb length (total forelimb / trunk length) on relative humerus length within forelimb (cHL / total forelimb) indicate that relative forelimb length to trunk length is significantly decreased in taxa with long humerus (adjusted $R^2 = 0.498$, $F = 16.89$, $p = 0.001$, $\lambda = 0.520$ for molecular tree; adjusted $R^2 = 0.451$, $F = 14.13$, $p = 0.002$, $\lambda =$

0.5 for morphological tree) (Fig. 7*a*). The relationship between relative hind limb length (total hind limb / trunk length) and relative femur length within hind limb (cFL / total hind limb) is non-significant (adjusted R^2 = -0.045, F = 0.316, p = 0.583, λ = 0 for molecular tree; adjusted R^2 = -0.058, F = 0.13, p = 0.724, λ = 0.541 for morphological tree) (Fig. 7*b*). Regressions of rostral proportions (individuals with skull width ≥ 100 mm) on limb ratio variables reveal significant negative correlations between rostral proportions and cHL / total forelimb (adjusted R^2 = 0.472, F = 17.95, p < 0.001, λ = 0 for both trees: Fig. 7*c*) and a weak correlation between rostral proportions and cFL / total hind limb (adjusted R^2 = 0.151, F = 4.37, p = 0.051, λ = 0.449 for molecular tree; adjusted R^2 = 0.336, F = 10.63, p = 0.004, λ = 0 for morphological tree: Fig. 7*d*). Rostral proportions show significant positive correlation with (fore + hind limbs) / trunk length (adjusted R^2 = 0.416, F = 12.4, p = 0.003, λ = 0.646 for molecular tree; adjusted R^2 = 0.471, F = 15.25, p = 0.001, λ = 0.681 for morphological tree) (Fig. 7*e*). Alternative PGLS regressions using average rostral proportion of each species with the upper size limit (100 ≤ skull width ≤ 200 mm) also show significant relationships between rostral proportions and limb ratio variables in the same manner (supplementary material, Table S6). These results indicate that slender-snouted taxa have relatively long stylopodia and short overall limbs (or long trunk).

Discussion

Difference of locomotor morphofunction between alligatoroids and crocodyloids

This study is the first to describe the interspecific variation in the limb proportion of crocodylians. Although the current sample shows a broad overall size range, the standardization procedure effectively removed size and ontogenetic allometry from the measurements, and major multivariate dimensions of limbs (PC1–3) did not show any correlation with size ($\log_{10}$GM). Therefore, if other sources of intraspecific variation, including sexual dimorphism (Prieto-Marquez, Gignac, & Joshi, 2007; Bonnan *et al.*, 2008) and phenotypic plasticity (Meers, 2002; Erickson *et al.*, 2004; Sadleir, 2009; Drumheller, Wilberg, & Sadleir, 2016; Pollard *et al.*, 2017) are set aside, observed differences in the limb proportion would be largely attributed to their locomotor ecology and phylogenetic background.

Analyses of six fore- and hind limb measurements demonstrated that crocodylian limbs are diverse, reflecting the phylogenetic history of each group. Two superfamilies as well as six subfamilies are separated in the multidimensional morphospace (Fig. 3 and supplementary

material, Table S5), contrary to the common wisdom that crocodylian postcranium is remarkably conservative (Parrish, 1987; Meers, 2003). Among the 20 species, *Gavialis gangeticus*, a crocodyloid based on the molecular phylogenetic hypothesis, is placed close to *Tomistoma schlegelii* (Tomistominae) in the limb morphospace (Fig. 3), suggesting their similarity in locomotor ecology.

With regard to locomotor function, differences in the limb proportion between the two superfamilies (Alligatoroidea and Crocodyloidea) have an important implication. The segregation of the two superfamilies is seen in PC2 scores (Fig. 3) that reflects relative contribution of stylopodia (humerus and femur) within fore- and hind limbs: alligatoroids have relatively short stylopodia, whereas crocodyloids have relatively long stylopodia within each limb (Fig. 4). In addition, the relative lengthening of humerus within forelimb is correlated with the overall forelimb length reduction (Fig. 7*a*).

The variation in the relative length of stylopodia and overall limb length observed in extant crocodylians is also seen through ontogeny of the American alligator, *Alligator mississippiensis*. Through growth, *A. mississippiensis* attains increasingly longer proximal limb segments relative to distal limb segments, with the decrease in relative overall limb lengths (Dodson, 1975; Livingston *et al.*, 2009). These ontogenetic changes are most likely associated with the reduced terrestrial locomotor capability in larger individuals of crocodylians (Zug, 1974; Singh & Bustard, 1976; Whitaker & Andrews, 1988). Generally, lengthened proximal limb segments and shortened distal limb segments move muscle mass more distally along the limb. This would increase the moment of inertia of limb about the shoulder- and hip-joint and reduce the velocity of limb protraction and retraction (Dodson, 1975; Hildebrand & Goslow, 2001), although longer proximal limb segments may also indicate longer upper arm and thigh muscle fibers that would help quick limb motion (Allen *et al.*, 2015). Moreover, shortening of overall limb length compared to trunk length leads to a reduction of stride length (Hildebrand & Goslow, 2001). Although limbs are used during slow paraxial swimming and bottom walking to some degree (Manter, 1940; Fish, 1984; Davenport & Sayer, 1989; Frey & Salisbury, 2001; Seebacher, Elsworth, & Franklin, 2003; Grigg & Kirshner, 2015), they produce negligible propulsive force in the fast axial swimming in crocodylians. Hence, short proximal limb segments and short overall limb length might be indicative of a reduced capability of terrestrial locomotion. In fact, *Gavialis gangeticus*, arguably the most aquatic of living crocodylians (Bustard & Singh, 1977; Whitaker & Basu, 1982; Stevenson & Whitaker, 2010) exhibits the longest humerus within forelimb and the

shortest fore- and hind limbs (Fig. 4). The difference in the limb proportion of alligatoroids and crocodyloids, specifically the relative contribution of stylopodia within fore- and hind limbs, indicates that alligatoroids and crocodyloids may be different in their locomotor functions and habits. In accord with our findings, the morphology of humerus-coracoid pair is clearly separated between the two living superfamilies: stouter humerus and coracoid and more abruptly emerging deltopectoral crest of alligatoroids are contrasted with the opposed character states in crocodyloids (Chamero *et al.*, 2013). Fore- and hind limb muscle properties are also different between the two groups, where extant crocodyloids generally have longer muscle fascicles especially in the pectoral limb and smaller muscle physiological cross-sectional areas than alligatoroids (Allen *et al.*, 2015). Because longer muscle fascicles can help achieve larger arcs of limb motion, this would be related to the use of asymmetrical gaits in crocodyloids (Allen *et al.*, 2015). However, smaller cross-sectional areas of crocodyloids' limb muscles may produce smaller forces, which would have an adverse effect on the terrestrial locomotion.

The divergent locomotor morphofunctions seen in alligatoroids and crocodyloids might be deeply rooted in the crocodylian phylogeny (Fig. 6). Locomotor functions of the outgroup taxa of Alligatoroidea + Crocodyloidea, reflected in proportions of their limb bones, were diverse, and some species exhibit unique limb proportions that were not taken by extant crocodylians. Remarkably, *Susisuchus* and *Boverisuchus vorax* show decoupled trends of fore- and hind limb proportions, where extremely elongated zeugopodia (ulna or tibia) is observed for only either fore- or hind limb. For the ziphodont crocodylian *B. vorax*, elongate ulna combined with other postcranial peculiarity (e.g. hoof-like ungual phalanges) (Rossmann, 2000) would suggest a terrestrial lifestyle of this taxon. After the split of Alligatoroidea and Crocodyloidea in the Late Cretaceous, most of the early alligatoroids from the Paleocene and Eocene, such as *Stangerochampsa mccabei*, *Allognathosuchus gracilis*, *Wannaganosuchus brachymanus*, *Necrosuchus ionensis*, and *Tsoabichi greenriverensis* already acquired the limb proportions that are close to extant alligatoroids (relatively short humerus and femur). Only *Navajosuchus mooki* from the Paleocene is a notable exception to this trend in having a long humerus and femur similar to crocodyloids. Therefore, it is inferred that locomotor ecology of most of the early alligatoroids were similar to their living relatives. Crocodyloids, on the other hand, might explore the limb proportions towards longer stylopodia within fore- and hind limbs, although their early evolution could not be confirmed with fossil taxa by the current sampling.

Locomotor and trophic integration

The other ecological aspect worthwhile to discuss is the significant association of limb morphology and cranial shape. With larger proportions of stylopodia within fore- and hind limbs (cHL / total forelimb; cFL / total hindlimb), and with shorter overall limbs relative to body length ([fore + hind limbs] / trunk length), rostral shapes become narrower (Fig. 7*c–e*). Relatively long stylopodia and short overall limbs may indicate reduced terrestrial locomotor capability (Dodson, 1975). Because limbs do not play major roles in fast axial swimming, changes in limb proportions may negligibly affect aquatic locomotor capability in crocodylians (Manter, 1940; Fish, 1984; Davenport & Sayer, 1989; Frey & Salisbury, 2001; Seebacher *et al.*, 2003; Grigg & Kirshner, 2015). On the other hand, the long and narrow rostrum enables higher angular velocity of jaw tip during lateral head sweeping, thus is favorable for catching small agile prey (i.e. fish) in water (Taylor, 1987; Thorbjarnarson, 1990). The correlation of appendicular and rostral proportions, which could be indicative of an association of locomotor and trophic functions, may have constrained morphofunctional diversification in crocodylians. To see if rostral shapes of crocodylians have diverged between alligatoroids and crocodyloids in similar fashion to that of the limb proportion, we here compiled the rostral proportions of 90 crocodylian species encompassing all the major clades of Alligatoroidea and Crocodyloidea (supplementary material, Table S4). Gavialoidea was not included in the dataset due to its contentious phylogenetic position (e.g. Brochu, 1997a; Gatesy *et al.*, 2003). Because most fossil species are represented by few individuals, the size related variation for each species was not accounted for here. The compilation shows that Tomistominae, Mekosuchinae, and derived crocodyloids (i.e. the least inclusive clade containing *Crocodylus*, *Mecistops*, and *Osteolaemus* in the morphological phylogenetic context) (Brochu & Storrs, 2012) have evolved slender-snouted forms beyond the range of alligatoroids (Fig. 8). On the contrary, basal alligatoroids, Alligatorinae, and Caimaninae have taken the extreme broad rostral shapes that were never explored by crocodyloids. Of course, one should be cautious in interpreting the simple rostral proportion metric used here: aside from the slender-blunt evolutionary axis, crocodylians have other ways in transforming their skull shapes (ziphodont and duck-faced morphotypes: Brochu, 2001). Even so, the morphology of extant and fossil skulls implies that trophic evolution of alligatoroids and crocodyloids are differently constrained in some way since their split in the Cretaceous, which is in accordance with the pattern of locomotor evolution illuminated by limb

morphology (Fig. 6).

Conclusion

This study examined the morphofunctional difference in the fore- and hind limbs of alligatoroids and crocodyloids. The difference in relative lengths of stylopodia indicated that alligatoroids and crocodyloids may be different in their locomotor functions, which is potentially related with terrestrial locomotor capability. Moreover, appendicular and rostral proportions are significantly correlated, where longer forelimb stylopodium and short total limb lengths evolved in association with slender snout, implying a possible connection between locomotor and trophic functions. This potential morphofunctional correlation might differently delimit the ecological opportunity of alligatoroids and crocodyloids, which seemingly have similar lifestyles in the present day water-land interface.

This chapter was accepted as:

Iijima M, Kubo T, Kobayashi Y. In press. Comparative limb proportions reveal differential locomotor morphofunctions of alligatoroids and crocodyloids. *Royal Society Open Science*.

Fig. 1. Measurements of forelimb **(*a*)** and hind limb **(*b*)** long bones. FL, femur length; MC3L, metacarpal III length; MT3L, metatarsal III length; HL, humerus length; TL, tibia length; UL, ulna length.

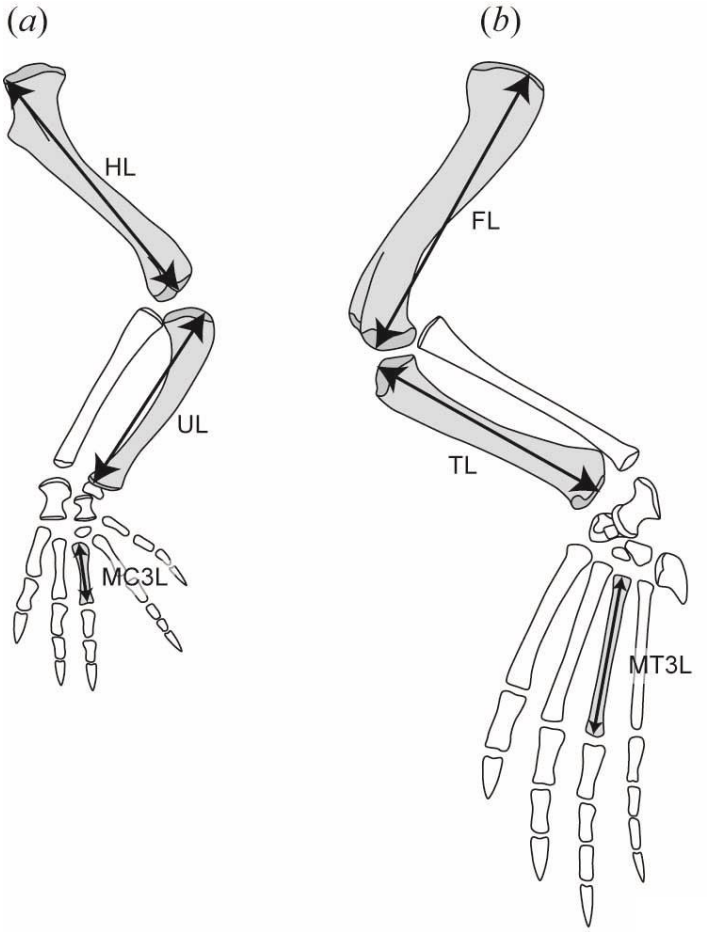


Fig. 2. Time-calibrated molecular **(*a*)** and morphological **(*b*)** trees of Crocodylia used in this study. Subfamily abbreviations: A, Alligatorinae; Ca, Caimaninae; Cr, Crocodylinae; G, Gavialinae; O, Osteolaeminae; T, Tomistominae.

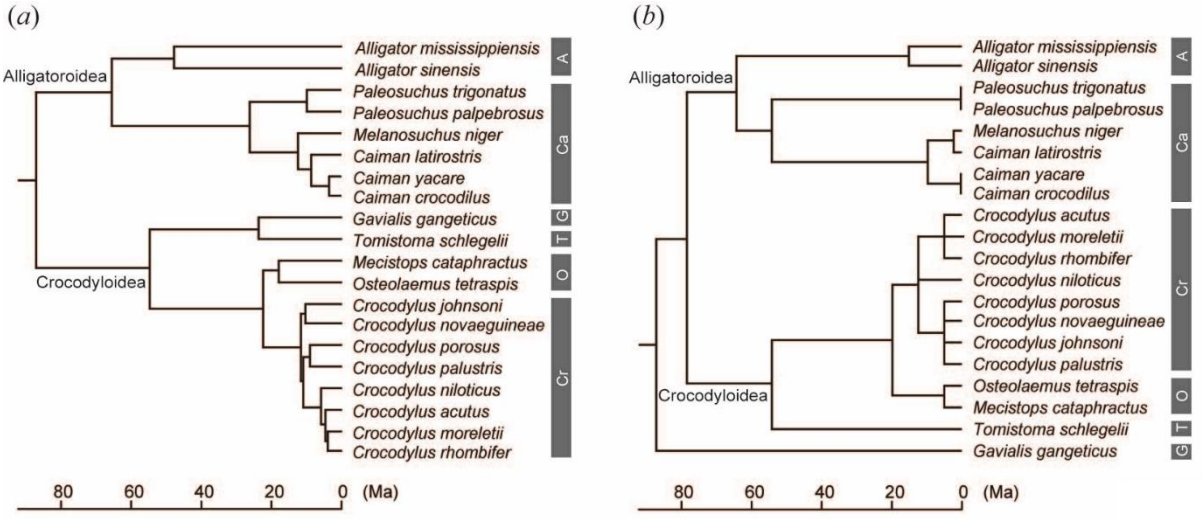


Fig. 3. Three-dimensional component score plots generated from the PCA of log10-transformed normalized limb measurements. Alli., Alligatoroidea; Croc., Crocodyloidea.

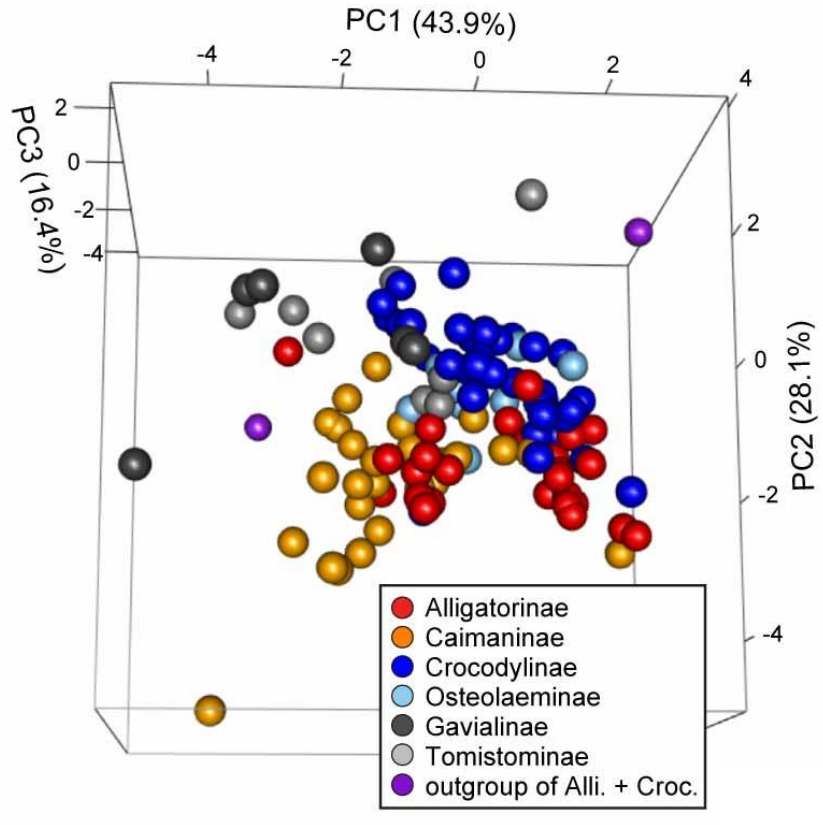


Fig. 4. Comparisons of limb proportions among crocodylian species. Ternary diagrams of within-forelimb **(*a*, *c*)** and within-hind limb **(*b*, *d*)** segment proportions for extant **(*a*, *b*)** and fossil **(*c*, *d*)** crocodylians. Alli., Alligatoroidea; Croc., Crocodyloidea. FL, femur length; MC3L, metacarpal III length; MT3L, metatarsal III length; HL, humerus length; TL, tibia length; UL, ulna length. Prefix 'c' (e.g. 'cFL') indicates normalized value. Species abbreviations: Ag, *Allognathosuchus gracilis*; Ah, *Anteophthalmosuchus hooleyi*; Am, *Alligator mississippiensis*; Ap, *Alligator prenasalis*; As, *Alligator sinensis*; Asiato, *Asiatosuchus*; Bb, *Boverisuchus bolcensis*; Bv, *Boverisuchus vorax*; Bw, *Borealosuchus wilsoni*; Ca, *Crocodylus acutus*; Cc, *Caiman crocodilus*; Cj, *Crocodylus johnsoni*; Cl, *Caiman latirostris*; Cm, *Crocodylus moreletii*; Cni, *Crocodylus niloticus*; Cno, *Crocodylus novaeguineae*; Cpa, *Crocodylus palustris*; Cpo, *Crocodylus porosus*; Cr, *Crocodylus rhombifer*; Cy, *Caiman yacare*; Gg, *Gavialis gangeticus*; Mc, *Mecistops cataphractus*; Mn, *Melanosuchus niger*; Ni, *Necrosuchus ionensis*; Nm, *Navajosuchus mooki*; Ot, *Osteolaemus tetraspis*; Pp, *Paleosuchus palpebrosus*; Pt, *Paleosuchus trigonatus*; Sa, *Susisuchus anatoceps*; Susi, *Susisuchus*; Sm, *Stangerochampsa mccabei*; Tm, *Toyotamaphimeia machikanensis*; Tg, *Tsoabichi greenriverensis*; Ts, *Tomistoma schlegelii*; Wb, *Wannaganosuchus brachymanus*.

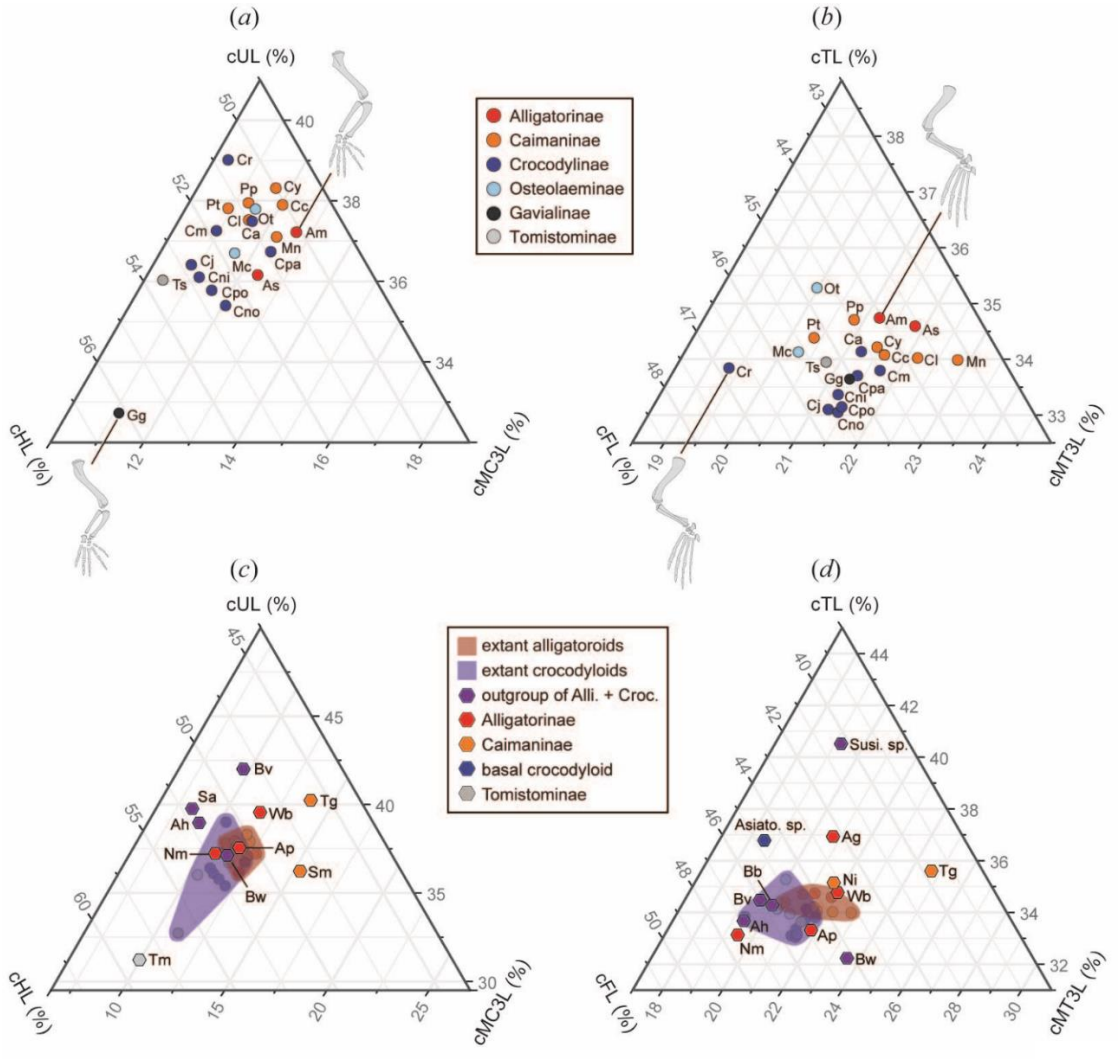


Fig. 5. Univariate plots of forelimb / (fore + hind limbs) **(*a*)**, forelimb / trunk length **(*b*)**, and hind limb / trunk length **(*c*)**. Alli., Alligatoroidea; Croc., Crocodyloidea. For species abbreviation, see legend of Fig. 4.

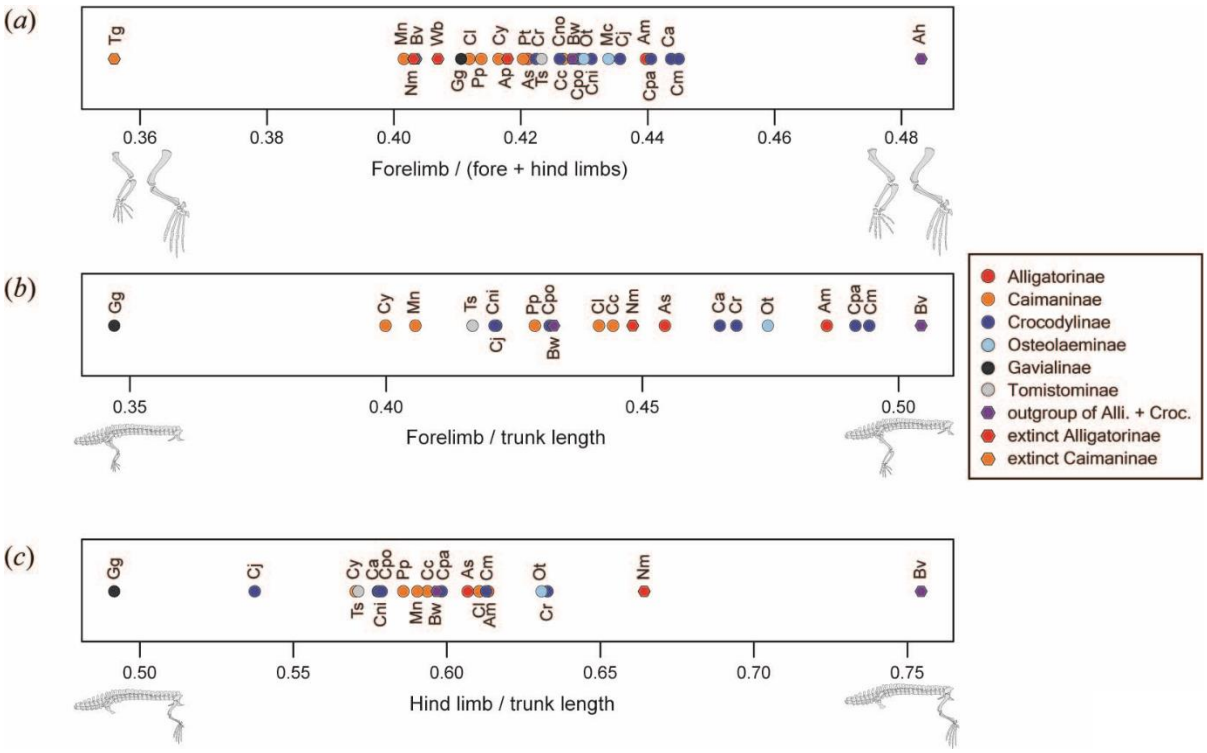


Fig. 6. Evolution of limb proportions in crocodylians mapped on the phylogenetic tree. **(*a*)** cHL / total forelimb. **(*b*)** cFL / total hind limb. FL, femur length; HL, humerus length. Prefix 'c' (e.g. 'cFL') indicates normalized value.

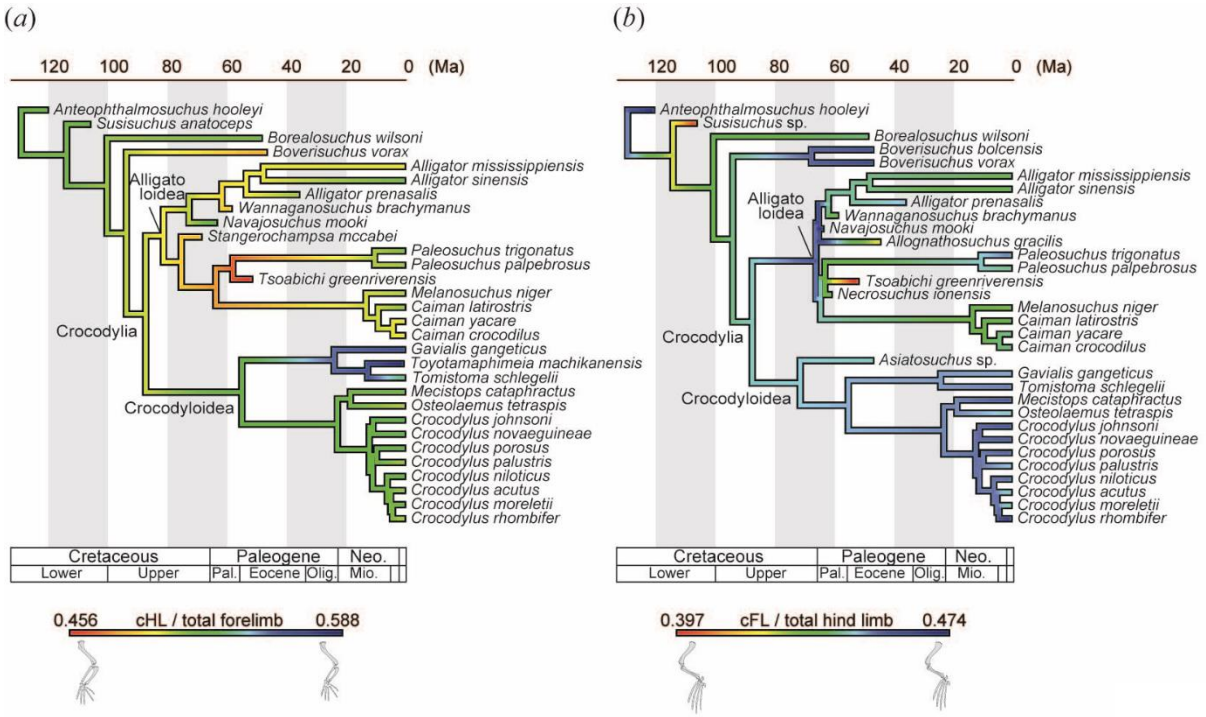


Fig. 7. Results of PGLS regressions. **(*a*)** forelimb / trunk length against cHL / total forelimb. **(*b*)** hind limb / trunk length against cFL / total hind limb. **(*c*–*e*)** rostral proportion against cHL / total forelimb **(*c*)**, cFL / total hind limb **(*d*)**, and (fore + hind limbs) / trunk length **(*e*)**. All PGLS regressions shown here used the molecular phylogeny (Fig. 2*a*: Oaks, 2011). For species abbreviations, see legend of Fig. 4. FL, femur length; HL, humerus length. Prefix 'c' (e.g. 'cFL') indicates normalized value.

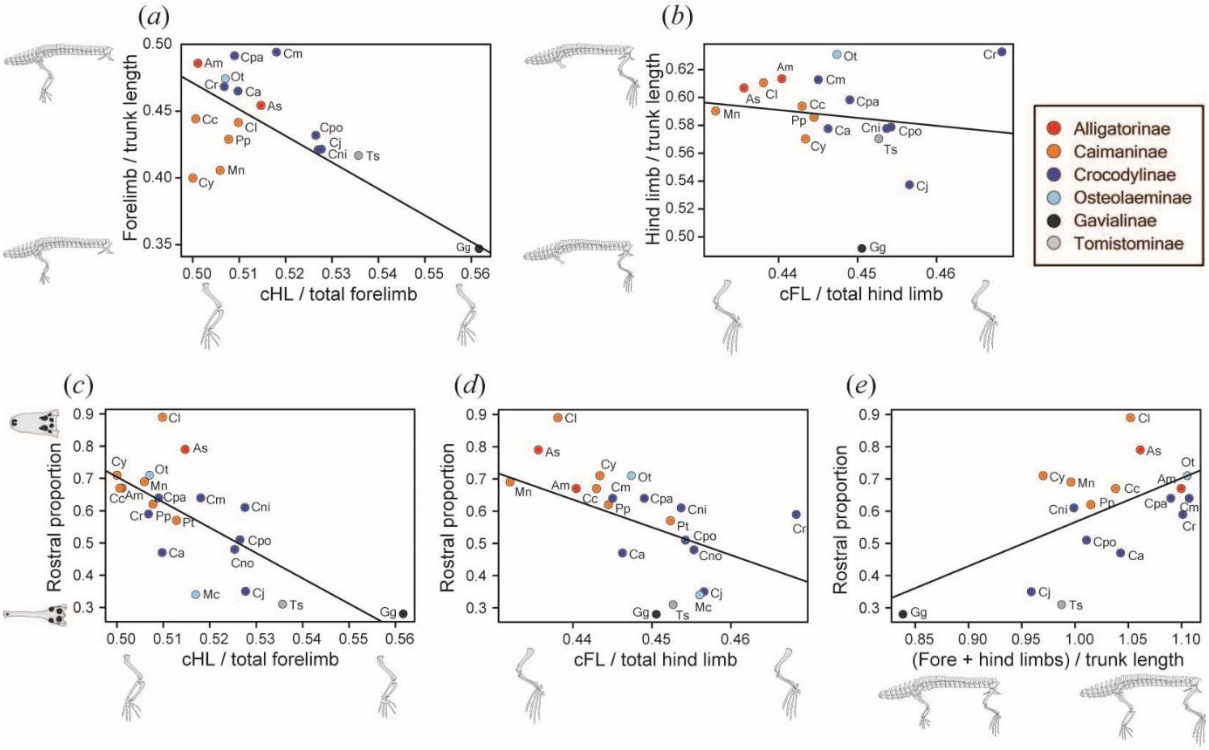


Fig. 8. Distribution of rostral proportions among crocodylian subgroups on the phylogenetic tree (e.g. Brochu & Storrs, 2012; Salas-Gismondi *et al.*, 2015). Enclosed A and C symbols refer to Alligatoroidea and Crocodyloidea respectively.

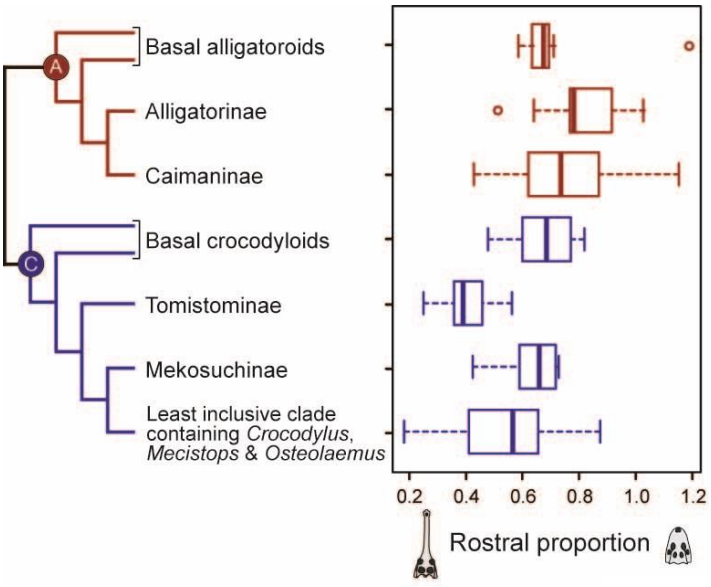


Table 1. Number of extant samples examined for each skeletal element, and average rostral proportion for each species (skull width ≥ 100 mm). **Caiman crocodilus crocodilus* + *C. c. fuscus* ; **central African species [Shirley et al. 2014]).

Subfamily	Species	*n* (fore- and hind limbs)	*n* (trunk)	*n* (rostrum)	Rostral proportion
Alligatorinae	*Alligator mississippiensis*	15	10	18	0.67
	Alligator sinensis	8	4	3	0.79
Caimaninae	*Caiman crocodilus*	9	3	10	*0.67
	Caiman yacare	5	1	9	0.71
	Caiman latirostris	2	1	5	0.89
	Melanosuchus niger	5	3	21	0.69
	Paleosuchus palpebrosus	5	3	5	0.62
	Paleosuchus trigonatus	2	NA	2	0.57
Crocodylinae	*Crocodylus acutus*	7	4	25	0.47
	Crocodylus johnsoni	7	3	6	0.35
	Crocodylus niloticus	6	1	12	0.61
	Crocodylus novaeguineae	1	NA	12	0.48
	Crocodylus palustris	3	1	17	0.64
	Crocodylus porosus	6	4	20	0.51
	Crocodylus rhombifer	4	4	2	0.59
	Crocodylus moreletii	2	1	4	0.64
Osteolaeminae	*Mecistops cataphractus*	3	NA	36	**0.34
	Osteolaemus tetraspis	6	1	5	0.71
Gavialinae	*Gavialis gangeticus*	6	5	19	0.28
Tomistominae	*Tomistoma schlegelii*	8	6	25	0.31
	Total	110	55	256	

Table 2. Factor loadings of log10-transformed normalized fore- and hind limb measurements acquired from PCA for all available individuals (*n* = 117).

log(variable)	PC1 (43.9%)	PC2 (28.1%)	PC3 (16.4%)
log(cHL)	0.250	0.800	0.492
log(cUL)	0.621	0.261	-0.692
log(cMC3L)	0.708	-0.613	0.190
log(cFL)	-0.747	0.543	-0.027
log(cTL)	-0.810	-0.135	-0.403
log(cMT3L)	-0.687	-0.535	0.254

III. Comparative morphology of presacral vertebrae in extant crocodylians

Introduction

Crocodylians are largest known living reptiles, and at least 27 species are distributed in world's tropics and subtropics (Grigg & Kirshner, 2015). As derived members of Pseudosuchia, a once diverse and successful group of reptiles that rivaled early dinosaurs in the Triassic (Brusatte *et al.*, 2008), crocodylians have survived several large environmental crises since the Cretaceous (Brochu, 2003). Because living species are readily available for measuring function and performance and for evaluating resource use, crocodylians have been widely used to infer ecology of extinct pseudosuchians and non-pseudosuchian archosaurs (e.g. Parrish, 1987; Witmer, 1997; Seebacher, Grigg, & Beard, 1999; Hutchinson & Gatesy, 2000; Farmer & Sanders, 2010; Tanaka, Zelenitsky, & Therrien, 2015).

Recent decades have seen a rise in the number of studies targeted on postcrania of extant crocodylians. Such studies often focused on girdle and limb elements, revealing their systematic importance (Chamero, Buscalioni, & Marugán-Lobón, 2013), biomechanical properties (Gatesy, 1997; Blob & Biewener, 1999, 2001; Blob, 2000; Meers, 2002; Allen *et al.*, 2015), ontogeny (Dodson, 1975; Rieppel, 1993; Brochu, 1995; Livingston *et al.*, 2009; Allen *et al.*, 2010), and sexually dimorphic patterns (Prieto-Marquez, Gignac, & Joshi, 2007; Bonnan, Farlow, & Masters, 2008). However, axial skeleton of extant crocodylians have received considerably less attention, despite its inherent taxonomic and ecological significance. This is partly because vertebral osteology and myology of extant crocodylian families are remarkably conservative (Hoffstetter & Gasc, 1969), although they have been divided for more than 70 million years (Brochu, 2003). Consequently, most previous authors have not gone beyond anatomical descriptions of few available species (Mook, 1921e; Hoffstetter & Gasc, 1969; Seidel, 1978; Frey, 1988; Cong *et al.*, 1998; Cleuren & de Vree, 2000; Tsuihiji, 2005, 2007; Böhmer, Rauhut, & Wörheide, 2015). Similarly, growth patterns (Dodson, 1975; Rieppel, 1993; Brochu, 1996; Ikejiri, 2012, 2015) and morphology-function relationship (Molnar, Pierce, & Hutchinson, 2014) of vertebrae are examined only in certain model species (e.g. *Alligator mississippiensis* and *Crocodylus niloticus*).

Insufficient interspecific comparisons to date would hinder realizing the taxonomic utility of crocodylians vertebrae (Chamero *et al.*, 2014). It would also deter establishing the linkage

between vertebral morphology and ecology in extant crocodylians, which is a basis for gaining insight into ecology of their extinct relatives (Salisbury & Frey, 2001; Hua, 2003; Molnar *et al.*, 2015). To our knowledge, Chamero et al. (2014) is the only work that provided a quantitative comparison of vertebrae among a broad range of extant species. They measured the cervical to anterior thoracic spine morphology of 15 species using 3D geometric morphometrics, indicating significant shape differences between alligatorids and crocodylids.

In this study, we provide the most comprehensive interspecific comparison of presacral (cervical, thoracic, and lumber) vertebrae among extant crocodylians thus far. By using function relevant measurements for 14 living species, we demonstrate size-dependent trends and potential taxonomic signals in the presacral vertebral morphology. We also interpret the shape variation in terms of feeding and locomotor functions, and examine the coordination between cranial and vertebral geometry, to evaluate functional coordination among multiple modules in a crocodylian skeleton.

Materials and methods

Specimen sampling and measurements

We sampled 42 individuals from 14 species (Fig. 1), which covers all six subfamilies of extant crocodylians (Alligatorinae, Caimaninae, Crocodylinae, Osteolaeminae, Tomistominae, and Gavialinae) (Brochu, 2003). Disarticulated vertebrae were primarily chosen, but articulated ones are also included to get available measurements and maximize the sample size. Here, third cervical to the last dorsal vertebrae, which show a gradual morphological change across the vertebral series, were sampled. The atlas and axis (first and second cervical vertebrae) are morphologically distinct from other cervical vertebrae and therefore were excluded (Chamero *et al.*, 2014). In the present study, first nine vertebrae are termed cervical, which have no connection with the sternum (Hoffstetter & Gasc, 1969). Following 15 vertebrae anterior to the sacrum are termed dorsal, because the number of vertebrae in thoracic and lumbar regions differ among extant species (Hoffstetter & Gasc, 1969; this study).

Seven linear measurements were taken to capture major morphofunctional differences in the presacral vertebrae: centrum length (CL); centrum height (CH); centrum width (CW); pre-zygapophyseal width (PZW); inter-zygapophyseal length (IZL); neural spine height (NSH); transverse process width (TPW), following the previous studies (e.g. Long *et al.*, 1997; Pierce, Clack, & Hutchinson, 2011; Molnar, Pierce, & Hutchinson, 2014) (Fig. 2). We

did not use 2D or 3D geometric morphometrics that are recently put force for vertebral shape quantification (Chamero *et al.*, 2014; Böhmer *et al.*, 2015; Jones, 2015; Werneburg *et al.*, 2015; Jones & Pierce, 2016; Randau *et al.*, 2017), because linear measurements have advantages in directly comparing functionally informative regions, and in readily incorporating incomplete fossil materials in the dataset. Missing measurements in the middle of the vertebral series are estimated as an average value for preceding and following vertebral positions, while that in the terminal positions are deemed to have a same value with the next position. All measurements were taken by the Tresna point digital caliper (0.01 mm resolution).

Presacral vertebrae 'Profiles'

For minimizing size effects on shape, all raw measurements were normalized using the equation of Elliott, Haskard, & Koslow (1995): $M_s = M_o (L_s/L_o)^b$, where M_s is the standardized measurement, M_o is the original measurement, L_s is the overall mean of size proxy (sum of third cervical to the last dorsal centrum lengths) for all individuals, L_o is the size proxy of each individual, and b is the regression slope of $\log_{10}M_o$ on $\log_{10}L_o$ for all individuals. The normalized measurements were averaged for each species, and the species averages were further averaged for six subfamilies. Subfamily averages of normalized measurements were 'profiled' as line charts, to visually compare serial morphological changes over entire presacral vertebrae among extant crocodylian subfamilies.

Scaling relationships and taxonomic signals in vertebral dimensions

First, four regions of presacral vertebrae are selected, namely mid cervical (cervical 5 & 6), posterior cervical (cervical 8 & 9), anterior dorsal (dorsal 5 & 6), and posterior dorsal (dorsal 10 & 11), and measurements were averaged for each region. We then obtained four size-dependent and two size-independent vertebral metrics that were made of single or composite measurement(s), from four selected regions (Table 1). These metrics are relevant to intervertebral stiffness for dorsoventral and lateral bending, and muscular leverage. Relationships between the size-dependent metrics [CL, π(CH×CW)/4, NSH, and TPW] and the body size proxy (sum of third cervical to the last dorsal centrum lengths) were analyzed by ordinary least squares (OLS) regressions. Both metrics and the size proxy were log10-transformed prior to the analyses. Two other metrics (CH/CW and IZL/PZW) are the ratio of two measurements and thus are size-independent. For these metrics, relationships between

numerator and denominator were analyzed for four presacral regions by log-log reduced major axis (RMA) regressions, which assume error in both *x* and *y* axes (Sokal & Rohlf, 1995). Relationships of *x* and *y* variables are considered either negatively or positively allometric when the 95% confidence intervals of OLS and RMA slopes do not overlap the expected isometric slopes.

To find out taxonomic signals in the presacral vertebrae, we conducted analysis of covariance (ANCOVA) with size-dependent metrics [CL, π(CH×CW)/4, NSH, and TPW] as dependent variables, two superfamilies (Alligatoroidea and Crocodyloidea) as independent variables, and the size proxy as covariate, using log-log OLS regressions. ANCOVA was also conducted for two size-independent metrics (CH/CW and IZL/PZW), with numerators as dependent variables, two superfamilies as independent variables, and denominators as covariates, using log-log RMA regressions. RMA regressions and RMA-based ANCOVA were performed with R package smatr (Warton *et al.*, 2012).

Morphofunctional integrations between presacral vertebrae and skull

We examined the relationships of presacral vertebrae and skull morphometrics to search for correlation(s) among different skeletal modules. Prior to analyses, OLS residuals (on *y* axis) for log-log regressions of CL, π(CH×CW)/4, NSH, and TPW against the size proxy were taken to control for the body size. Likewise, RMA residuals (*y* residual minus *x* residual) for log-log regressions of CH on CW, and IZL on PZW were taken to assess the direction and degree of plot deviation from the regression lines. These OLS and RMA residuals were then averaged for each species. We used rostral proportion (the ratio of the palate width at the last maxillary alveoli to the length from there to the tip of the snout) as an indicator of trophic function in crocodylians. Rostral proportions of 14 crocodylian species were adopted from Iijima et al. (2018). The correlations between OLS and RMA residuals of six vertebral metrics and rostral proportion were tested by phylogenetically generalized least squares (PGLS) regressions for 14 species. The analyses were run for four selected regions (mid cervical, posterior cervical, anterior dorsal, and posterior dorsal regions) using R package caper (Orme *et al.*, 2013). PGLS regressions were performed with a time-calibrated molecular tree, which was based on Oaks (2011). All statistical analyses were carried out with R language and environment (R Core Team, 2016).

Results

Presacral vertebrae 'profiles'

Centrum length (Figs 3 and 5A) shows a S-shape pattern along the presacral region, where the shortest and longest centra are found in posterior cervical and posterior dorsal regions. The difference in cervical and dorsal centrum lengths is most pronounced in alligatorines (*Alligator mississippiensis* and *A. sinensis*). In contrast, cervical and dorsal regions are less regionalized in *Gavialis gangeticus* and *Tomistoma schlegelii* than other subfamilies. *T. schlegelii* and a crocodyline (*Crocodylus johnsoni*) have relatively shorter anterior dorsal centra (fourth to eighth dorsal vertebra) than others.

Centrum height pattern (Fig. 5B) resembles an inverted U-shape. The highest centrum is located at fourth dorsal vertebra, which is few positions posterior to the shortest centrum (eighth or ninth cervical vertebra). Abrupt increase and decrease in the heights are found in second to fifth dorsal centra. These vertebral positions correspond to the loss of the hypapophysis. *Osteolaemus tetraspis* has higher, and *G. gangeticus* and caimanines (specifically genus *Caiman*) have lower centra. Alligatorines (*A. mississippiensis* and *A. sinensis*) are distinct in having well regionalized centrum heights with low cervical and high dorsal centra.

The serial pattern of centrum width (Fig. 5C) is S-shaped, and generally mirrors that of the centrum length. However, the widest centrum is found in second dorsal vertebra, which is two or three positions posterior to the shortest centrum position, coinciding the most elevated parapophysis on the centrum before it shifts onto the transverse process. Alligatorines (*A. mississippiensis* and *A. sinensis*), *O. tetraspis*, and two crocodylines (*Crocodylus palustris* and *C. rhombifer*) have wider centra, whereas *G. gangeticus* and two *Caiman* species have narrower centra over presacral vertebrae.

Pre-zygapophyseal width (Figs 4 and 5D) gradually increases towards sacrum in all taxa excluding *G. gangeticus*. The change rates are higher in taxa with wide centrum: alligatorines (*A. mississippiensis* and *A. sinensis*), *O. tetraspis*, and two crocodylines (*Crocodylus palustris* and *C. rhombifer*). Pre-zygapophyseal width of *G. gangeticus* is stable throughout the entire presacral vertebrae. Contrary to other taxa, the width gets slightly narrower posteriorly in the dorsal region.

Inter-zygapophyseal length (Figs 4 and 5E) exhibits a S-shaped pattern similar to the centrum length in most of the taxa except for *G. gangeticus* and *T. schlegelii*. The regionalization of cervical and dorsal vertebrae is most prominent in alligatorines (*A. mississippiensis* and *A. sinensis*) and *O. tetraspis*. Patterns in *G. gangeticus* and *T. schlegelii*

are rather linear with slight increasing trends towards sacrum.

The neural spine height profile (Figs 3 and 5F) shows an inverted V-shape in all taxa excluding *G. gangeticus*, with its peak at ninth cervical or first dorsal vertebrae. Cervical neural spines of *O. tetraspis* is remarkably longer than other non-*Gavialis* taxa. Neural spines of *G. gangeticus* remain low along cervical to dorsal regions, and its difference from other taxa is most evident in cervical to anterior dorsal regions.

The profile of transverse process width (Figs 4 and 5G) is an inverted S-shape with its plateau in the mid dorsal region. The pattern in the cervical region is uniform except for *G. gangeticus*, which has shorter cervical transverse processes compared to other taxa, matching its narrow cervical centra. In the dorsal region, all crocodylines and *O. tetraspis* show weaker increasing trends, whereas others (alligatorines, caimanines, *G. gangeticus* and *T. schlegelii*) demonstrate stronger increasing trends.

Scaling of morphofunctional dimensions

Log-log OLS regressions of size-dependent vertebral metrics [CL, π(CH×CW)/4, NSH, and TPW] on size proxy for four presacral regions (mid and posterior cervical regions, and anterior and posterior dorsal regions) revealed evolutionary (and/or ontogenetic) allometry of the metrics (Table 2 and Fig. 6). All metrics are strongly and significantly correlated with size ($r^2 > 0.89$, $p < 0.001$). CL of all regions, NSH and TPW of mid and posterior cervical vertebrae showed isometric scaling. On the contrary, π(CH×CW)/4 for all regions, and NSH and TPW for anterior and posterior dorsal vertebrae scale with positive allometry, indicating that inter-central joints of all presacral centra become relatively larger, and neural spines and transverse processes of dorsal vertebrae get relatively longer with increasing size.

Log-log RMA regressions of CH on CW, and IZL on PZW for four presacral regions revealed that CH scales positively with CW in anterior and posterior dorsal vertebrae (Table 2 and Fig. 7A-D), suggesting that dorsal centra become relatively taller with increasing size. The scaling relationship of IZL against PZW (Table 2 & Fig. 7E-H) is not significantly different from isometric pattern.

Taxonomic signals in presacral vertebrae dimensions

ANCOVA was designed to test differences in the slope and elevation of OLS and RMA regressions between two superfamilies (Alligatoroidea and Crocodyloidea) (Table 3). The results indicate that slope differences between two groups are insignificant for all cases.

Significant superfamily-level elevation differences in vertebral metrics against size are found for CL in mid cervical and anterior and posterior dorsal regions, π(CH×CW)/4 in mid cervical region, NSH in posterior cervical region, and TPW in anterior dorsal region. Additionally, elevation differences of IZL against PZW in mid and posterior cervical and posterior dorsal regions are significant. These suggest that alligatoroids have shorter mid cervical and dorsal centra, smaller mid cervical inter-central joint area, longer posterior cervical neural spines, longer anterior dorsal transverse processes, and more widely placed cervical and posterior dorsal zygapophyses than crocodyloids.

Morphofunctional integrations between vertebrae and skull

PGLS regressions of rostral proportions on the OLS and RMA residuals using a widely agreed molecular phylogeny suggested that several vertebral metrics are potentially correlated with rostral proportion, a trophic indicator (Table 4 and Fig. 8). Significant correlations with rostral proportions (Holm adjusted $p < 0.05$) were found for OLS residuals of π(CH×CW)/4 in anterior and posterior dorsal regions, NSH in posterior cervical and anterior and posterior dorsal regions, TPW in posterior cervical region, and RMA residuals of CH on CW in anterior and posterior dorsal regions, and IZL on PZW in mid and posterior cervical regions. These imply that in cervical region, inter-zygapophyseal length is shortened compared to pre-zygapophyseal width, neural spine becomes longer, and transverse processes are lengthened with broader rostrum. In dorsal region, inter-central joints are enlarged, centrum width is increased compared to height, and neural spine becomes longer with broader rostrum.

Discussion

Allometry in vertebral dimensions

Previous studies have revealed the ontogenetic allometric trends of presacral vertebral dimensions in American alligators, *A. mississippiensis*. (Dodson, 1975) examined the relative growth of four linear measurements to an overall size proxy (axis-sacrum length) of a mid thoracic and an anterior lumber vertebrae. He found that vertebral height (from the bottom of centrum to the top of neural arch) and transverse process width scale with strong positive allometry to the size proxy, and allometric coefficients of centrum length is much smaller than that of centrum width. (Ikejiri, 2015) selected seven presacral vertebral positions and observed the allometric trends of 12 linear measurements, demonstrating that all dimensions

except for diameters of neural canal scale with positive allometry to a size proxy (femur length). Among the dimensions, neural arch height (from the ceiling of neural canal to the top of the neural arch) and transverse process width scale with the strongest positive allometry (allometric coefficient ~1.38). However, overall positive allometry of vertebral dimensions proposed by Ikejiri (2015) should be interpreted carefully, because femur length, against which vertebral dimensions were scaled, is known to show negative allometry relative to axis-sacrum length (Dodson, 1975). On the other hand, Chamero *et al.* (2014) compared 3D geometry of cervico-thracic vertebrae in extant crocodylians and exemplified that the intra- and inter-specific allometry is shared for extant species, where large individuals (of any species) tend to exhibit shorter centrum length to the height and width, and longer neural spine (Chamero *et al.*, 2014: Fig. 7C).

Although we did not isolate ontogenetic and interspecific allometry in this study, we showed size-related vertebral shape changes in crocodylians that are largely congruous with these previous works. Essentially, crocodylian dorsal vertebrae attain increasingly larger inter-central joint area relative to centrum length, and higher ratio of centrum height/width with larger size. When the dorsal vertebrae are assumed to be a beam supported by two pillars (fore- and hind limbs), the trunk vertebrae incur dorsiflexion bending moment which maximally acts at the midst of the trunk, and this load is mostly countered by axial compression (Macpherson & Ye, 1998; Smit, 2002). The larger and deeper cross-sectional shape of dorsal centra in large individuals of crocodylians would resist the increased dorsiflexion bending and axial compression loads of the trunk (Jones, 2015; Jones & Pierce, 2016). Moreover, longer vertebral processes (i.e. neural spines and transverse processes) in large crocodylians would accommodate greater epaxial and hypaxial muscle masses. This increases the muscular leverages for dorsoventral and mediolateral flexions (Shapiro, 2007), but also enhances intervertebral stiffness due to larger cross-sectional area of trunk (Long *et al.*, 1997). The allometric trend of vertebrae, specifically centrum dimensions in crocodylians, is similar to terrestrial mammals such as felids and bovids, but unlike aquatic pinnipeds, in the latter of which body support role of the trunk is diminished (Jones, 2015; Jones & Pierce, 2016). Aside from vertebrae, width and cross-sectional area of humeral and femoral mid-shafts in *A. mississippiensis* scale with positive allometry to the shaft lengths and trunk length, which is most likely to resist increased bending and torsional moments of limbs during the terrestrial locomotion (Dodson, 1975; Meers, 2002). The allometry of the vertebral and limb mechanical properties in crocodylians may reflect the sustained necessity

of terrestrial locomotion throughout life, although all crocodylians spend most of the time in or near water (Grigg & Kirshner, 2015).

Taxonomic signals and functional and ecological implications

Chamero et al. (2014) suggested superfamily level differences in cervico-thoracic vertebrae of extant crocodylians. Compared to alligatoroids, crocodyloid necks are characterized by anteroposteriorly broader and dorsoventrally longer neural spines that are oriented more orthogonal to the coronal plane, and shorter hypapophyses that are oriented more ventrally (Chamero *et al.*, 2014). By examining entire presacral vertebrae, our quantitative analyses demonstrated additional morphological differences between two superfamilies. One notable difference is the transverse process width of anterior dorsal vertebrae, where alligatoroids have longer processes than crocodyloids. This difference arises by the rapid increase in the transverse process widths at anterior dorsal vertebrae from the preceding cervical vertebrae in alligatoroids, which increases mediolateral flexion leverages but also increases the trunk stiffness due to the large cross-sectional area (Long *et al.*, 1997; Shapiro, 2007). For other vertebral metrics that show significant superfamily differences, alligatoroids and crocodyloids are often largely overlapped, and their clear separations are hardly seen. For instance, alligatoroids have generally shorter mid cervical centra and more widely placed cervical zygapophyses than crocodyloids, although for both dimensions a crocodyloid *Osteolaemus tetraspis* exhibits a similarity with alligatoroids.

Species level differences of presacral vertebrae have been proposed qualitatively as characters for phylogenetic analyses, which are mostly about shape, size, position, and orientation differences in neural spines, hypapophyses and diapophyses in anterior cervical vertebrae (e.g. Norell & Clark, 1990; Clark, 1994; Brochu, 1997b). Our interspecific comparisons found that *G. gangeticus* is unique and different from other extant crocodylians in many respects. In particular, differences of centrum lengths, pre-zygapophyseal widths, inter-zygapophyseal lengths, and neural spine heights between cervical and dorsal regions are less pronounced in *G. gangeticus* than other species, indicating the reduced degree of regionalization in presacral vertebrae. Interestingly, *Tomistoma schlegelii* shares a similar serial pattern of inter-zygapophyseal length with *G. gangeticus* by its relative stableness over presacral vertebrae. *G. gangeticus* is considered as the most aquatic species (Bustard & Singh, 1977; Whitaker & Basu, 1982; Stevenson & Whitaker, 2010) with the short overall limb and long stylopodia (humerus and femur) within fore- and hind limbs (Iijima *et al.*,

2018). More uniform presacral vertebrae of *G. gangeticus* might increase the efficiency of aquatic locomotion by generating constant undulatory waves, although tail is the main propulsive organ in crocodylians (Manter, 1940; Fish, 1984; Davenport & Sayer, 1989; Frey & Salisbury, 2001). One exceptional dimension which does show a marked regionalization between cervical and dorsal regions in *G. gangeticus* is the transverse process width: it is elongated in dorsal regions similar to or even greater than other crocodylians.

The neck of *G. gangeticus* is distinct among extant crocodylians with short vertebral processes (neural spines and transverse processes) and larger ratios of inter-zygapophyseal length to width. The former decreases the cross-sectional area of neck (Long *et al.*, 1997) and the latter allows greater displacement of the column during flexion, same as the longer and more spool-shaped centrum can achieve a larger column displacement (Buchholtz, 1998, 2001b). These altogether increase the neck intervertebral mobility. The more flexible neck of *G. gangeticus* would be favorable to catch small agile preys by lateral head sweeping in water (Thorbjarnarson, 1990). Nonetheless, relatively long cervical vertebrae of *G. gangeticus* does not fit the typical trend of neck reduction seen in the secondary aquatic adaptation of mammals (Buchholtz, 1998, 2001b). As opposed to *G. gangeticus*, a few species such as *O. tetraspis* and two *Alligator* have relatively short cervical vertebrae, long vertebral processes, and smaller ratios of zygapophyseal length to width, which are indicative of reduced neck flexibility. Moreover, longer cervical neural spines that are oriented dorsally or even anterodorsally in these species suggest the larger extensor leverage for the epaxial musculature to support a head. These cervical features might be beneficial when animals are out of water and under terrestrial gravity.

For dorsal vertebrae, *G. gangeticus* stands out among extant species by its narrowly placed zygapophyses, which would increase the intervertebral mobility. Additionally, as mentioned by Hoffstetter & Gasc (1969), the count of ribless dorsal vertebrae (lumber vertebrae) in *G. gangeticus* is three, which is fewer as compared to other extant species (four or five).

Integration of skull and axial modules

Our recent study revealed locomotor and trophic integration in extant crocodylians, by examining correlation between appendicular and skull morphometrics on phylogeny (Iijima *et al.*, 2018). We demonstrated that overall fore- and hind limb lengths become shorter and relative stylopodial (humerus and femur) lengths get longer with narrower rostrum shape, indicating the reduced terrestrial locomotor capability in long-snouted species, such as *G.*

gangeticus. The current study provides potential integration between snout shape (a trophic indicator) and vertebral dimensions.

In cervical vertebrae, particularly at posterior positions, slender-snouted species tend to exhibit shorter neural spines and shorter transverse processes, which decrease the cross-sectional area of neck and reduce passive intervertebral stiffness (Long *et al.*, 1997). In addition, more narrowly placed pre- and post- zygapophyses in slender-snouted taxa increase the intervertebral mobility. These suggest that slender snouts might evolve with more flexible neck in crocodylians, together enhancing the food capturing efficiency while laterally sweeping the head in water (Thorbjarnarson, 1990).

In dorsal vertebrae, slender-snouted taxa show smaller and taller inter-central joints and shorter neural spines. It is conceivable that smaller inter-central joints of slender-snouted taxa are less favorable to resist compression force and dorsiflexion bending moment that act on mid trunk under terrestrial circumstances (Macpherson & Ye, 1998; Smit, 2002; Jones, 2015; Jones & Pierce, 2016). On the other hand, tall centrum would better counter the mid-trunk dorsiflexion moment on land, while in turn assist axial swimming using laterally undulating trunk in water (Davenport & Sayer, 1989), and increase the underwater foraging efficiency.

Conclusion

Despite its systematic and functional importance, axial skeleton of crocodylians has gained considerably less attention than cranial and appendicular skeleton, probably owing to its evolutionary conservativeness. The current study provides comprehensive quantitative comparisons of presacral vertebrae in extant crocodylians to understand size-dependent shape changes, and to obtain taxonomic and ecological inferences. The scaling relationships of vertebral dimensions show that dorsal vertebrae become stiffer with increasing body size by larger and taller inter-central joints and longer vertebral processes (neural spines and transverse processes). These structural changes are to resist increasing compression loads and dorsiflexion bending moment in the trunk of larger individuals on land, reflecting the sustained necessity of terrestrial locomotion throughout life. Species level comparisons highlighted the uniqueness of the Indian gharial, *G. gangeticus*. The presacral vertebrae of *G. gangeticus* are characterized by reduced level of regionalization and increased inter-vertebral mobility in the neck (more narrowly placed zygapophyses and short vertebral processes), which would help lateral head sweeping under water for foraging. Conversely, *O. tetraspis* and two species of *Alligator* exhibit stiffer neck (more widely placed zygapophyses and long

vertebral processes), which might be favorable to support the head on land. The analyses of correlation between vertebral dimensions and snout shape indicate that slender-snouted species tend to have more mobile neck, implying the potential integration of cranial and neck modules to optimize the foraging strategy.

Fig. 1. A time-calibrated molecular tree used in this study [adopted from Oaks (2011)]. Subfamily abbreviations: A, Alligatorinae; Ca, Caimaninae; Cr, Crocodylinae; G, Gavialinae; O, Osteolaeminae; T, Tomistominae.

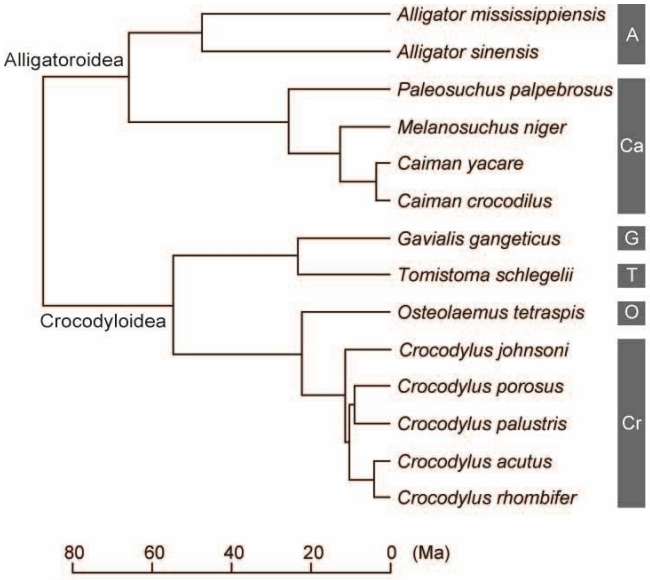


Fig. 2. Measurements of vertebral dimensions. CH, centrum height; CL, centrum length; CW, centrum width; IZL, inter-zygapophyseal length; NSH, neural spine height; PZW, pre-zygapophyseal width; TPW, transverse process width.

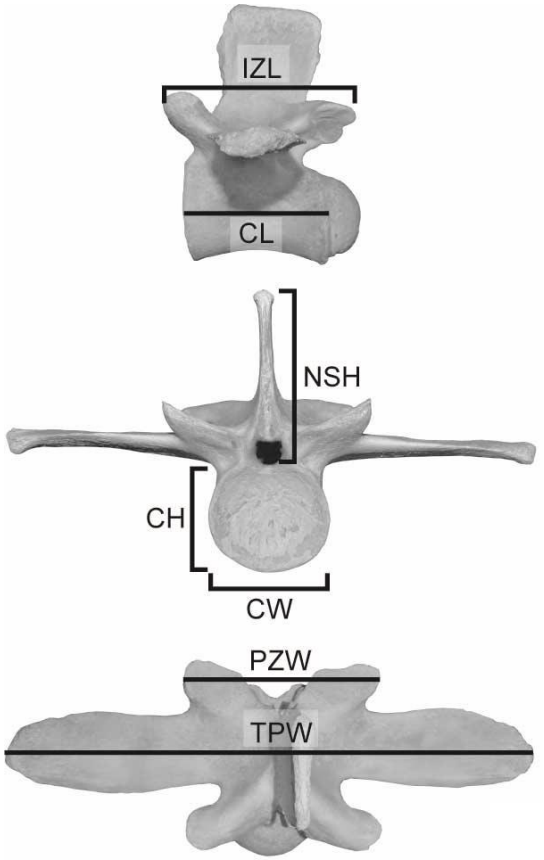


Fig. 3. Comparative presacral vertebrae (left lateral view). A, *Alligator mississippiensis* (AMNH 43315); B, *Caiman crocodilus* (USNM 102874); C, *Paleosuchus palpebrosus* (AMNH 78976); D, *Crocodylus acutus* (USNM 247943); E, *Crocodylus johnsoni* (QM J58446); F, *Osteolaemus tetraspis* (AMNH 69057); G, *Tomistoma schlegelii* (USNM 52972); H, *Gavialis gangeticus* (USNM 576261). Scale bars equal 5 cm.

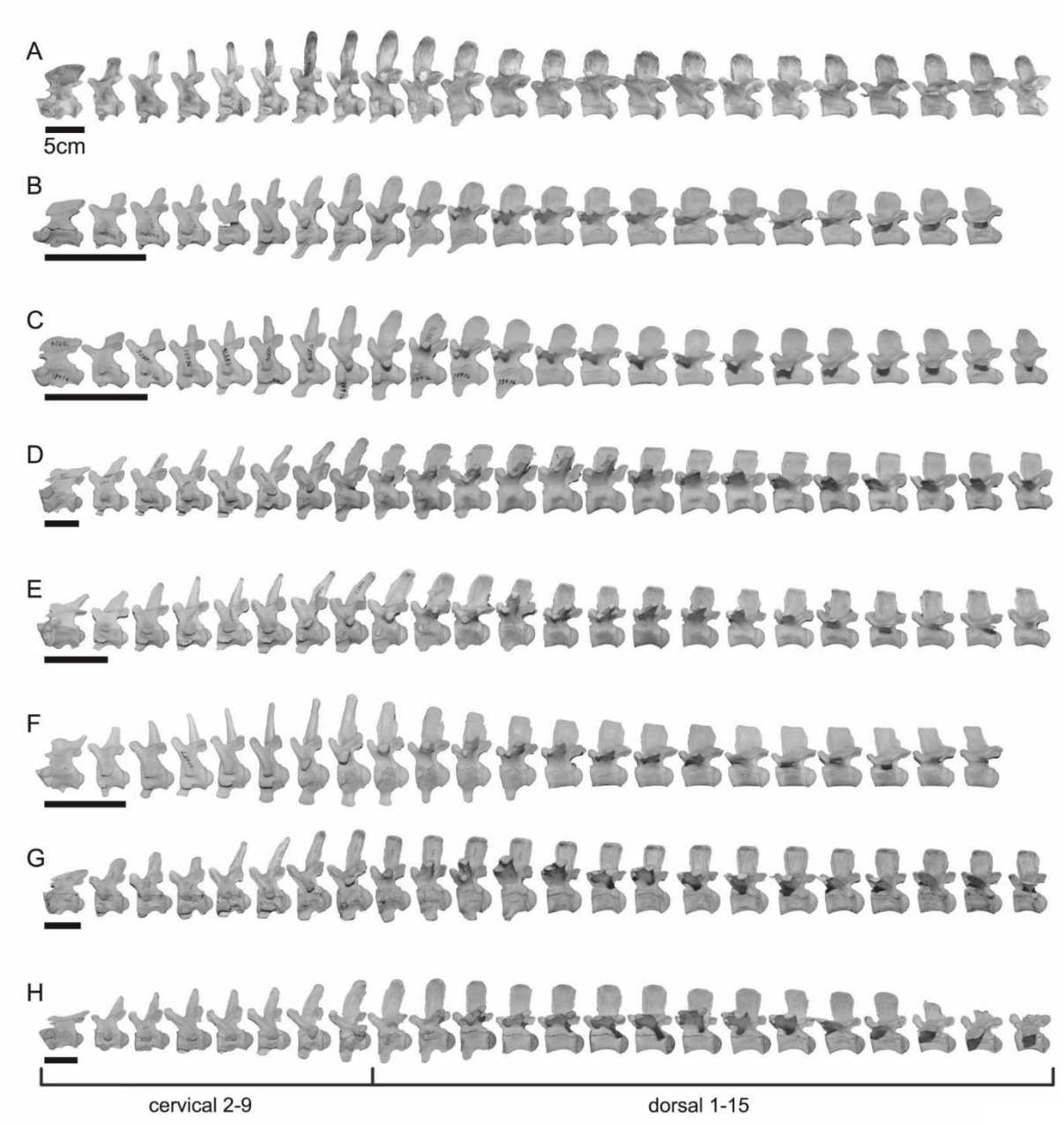


Fig. 4. Comparative presacral vertebrae (dorsal view). A, *Alligator mississippiensis* (AMNH 43315); B, *Caiman crocodilus* (USNM 102874); C, *Paleosuchus palpebrosus* (AMNH 78976); D, *Crocodylus acutus* (USNM 247943); E, *Crocodylus johnsoni* (QM J58446); F, *Osteolaemus tetraspis* (AMNH 69057); G, *Tomistoma schlegelii* (USNM 52972); H, *Gavialis gangeticus* (USNM 576261). Scale bars equal 5 cm.

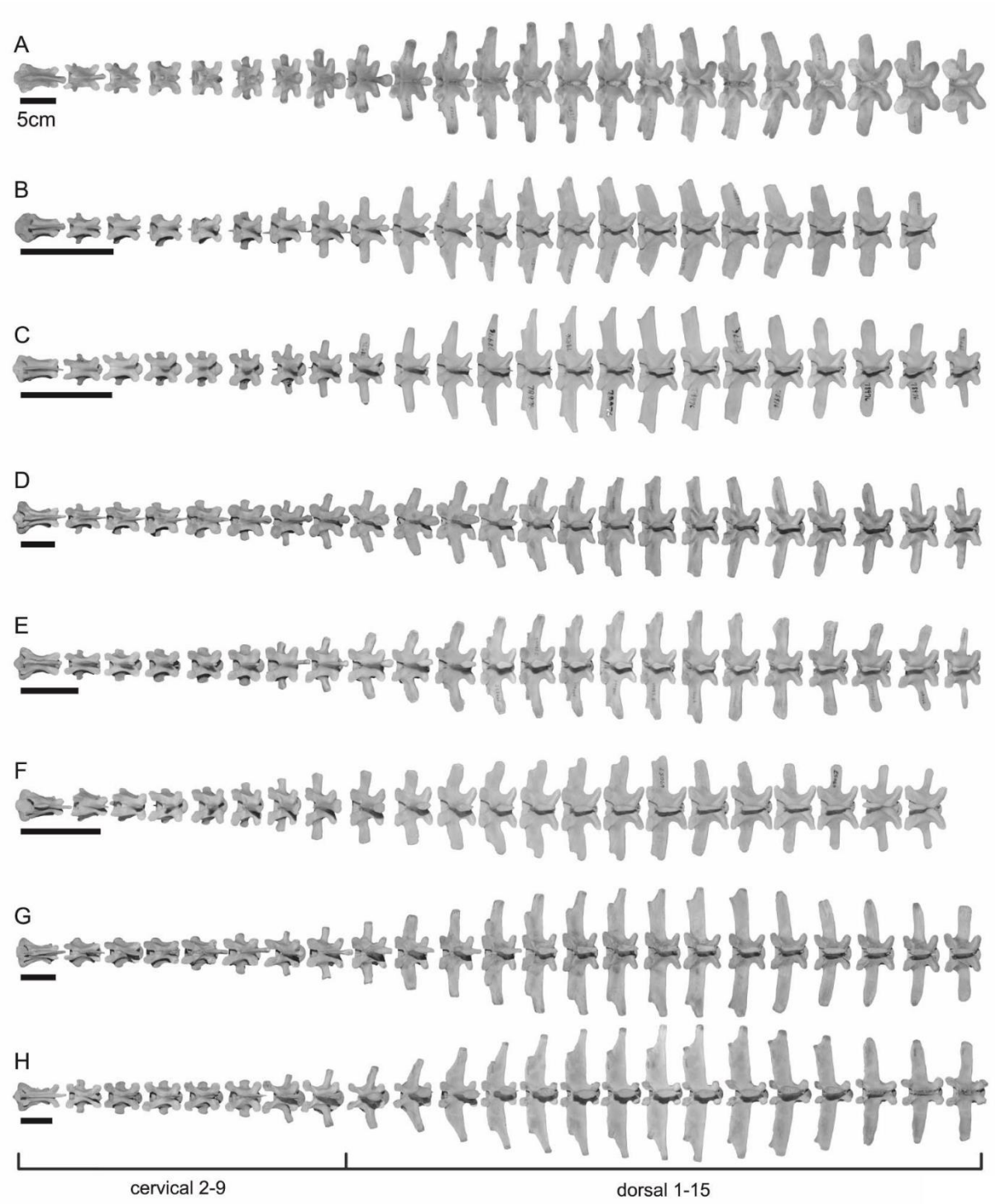


Fig. 5. Presacral vertebrae 'profiles' for A, centrum length; B, centrum height; C, centrum width; D, pre-zygapophyseal width; E, inter-zygapophyseal length; F, neural spine height; G, transverse process width.

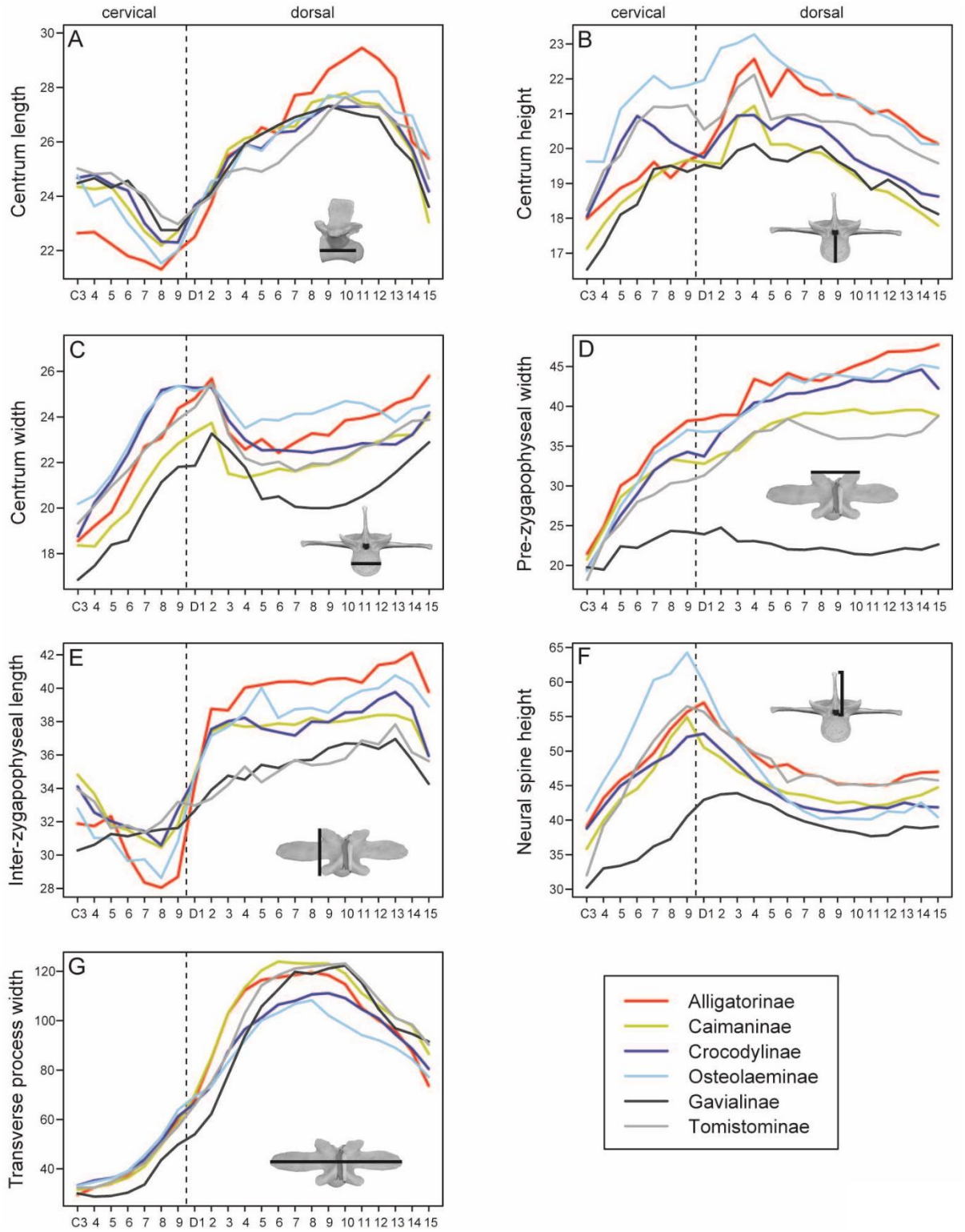


Fig. 6. Ordinary least squares (OLS) regressions of vertebral metrics against size for four vertebral regions (mid and posterior cervical, and anterior and posterior dorsal regions). A-D, log(CL); E-H, log[π(CH×CW)/4]; I-L, log(NSH); M-P, log(TPW) on log(size).

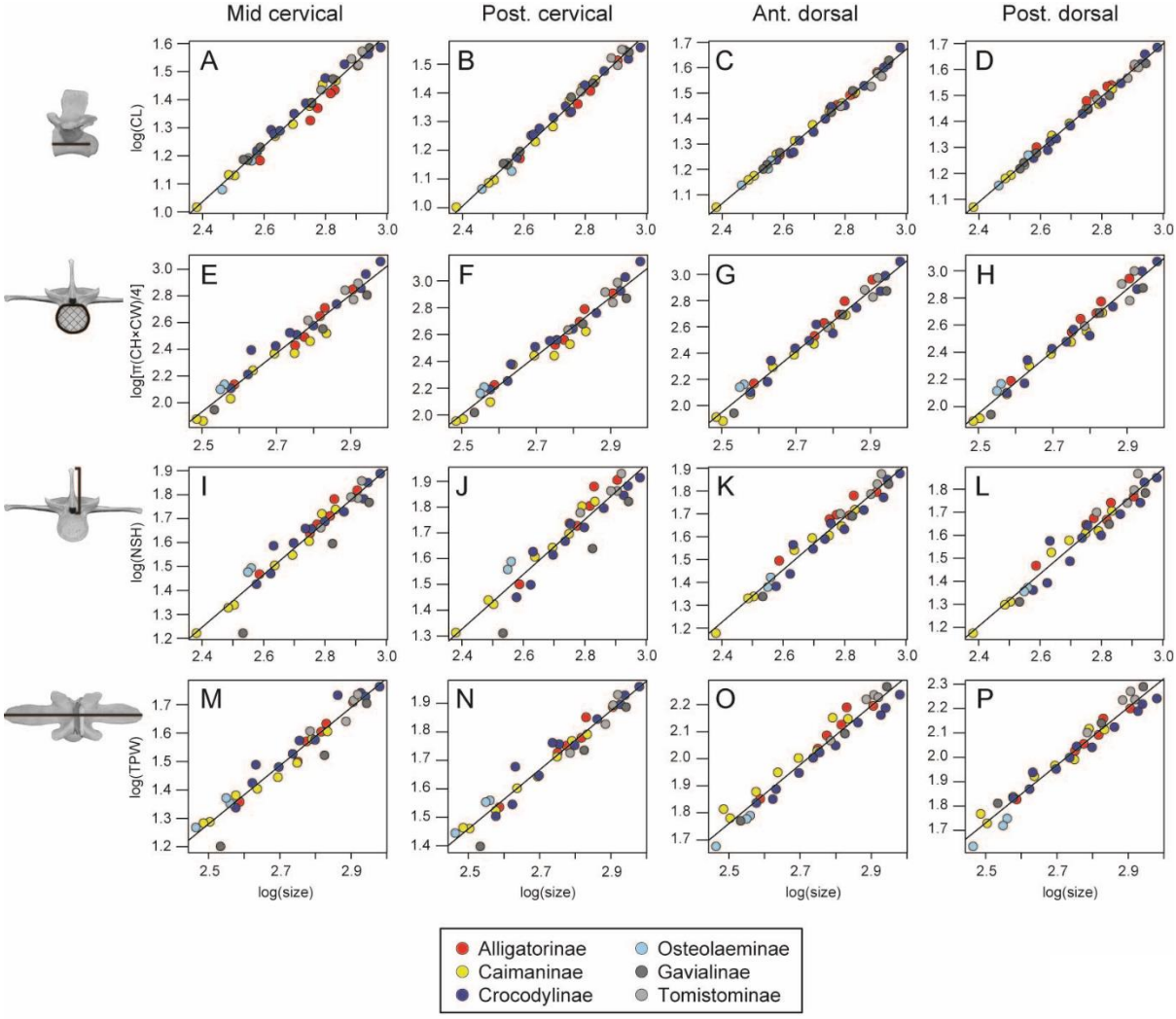


Fig. 7. Reduced major axis (RMA) regressions between vertebral dimensions for four vertebral regions (mid and posterior cervical, and anterior and posterior dorsal regions). A-D, log(CH) on log(CW); E-H, log(IZL) on log(PZW).

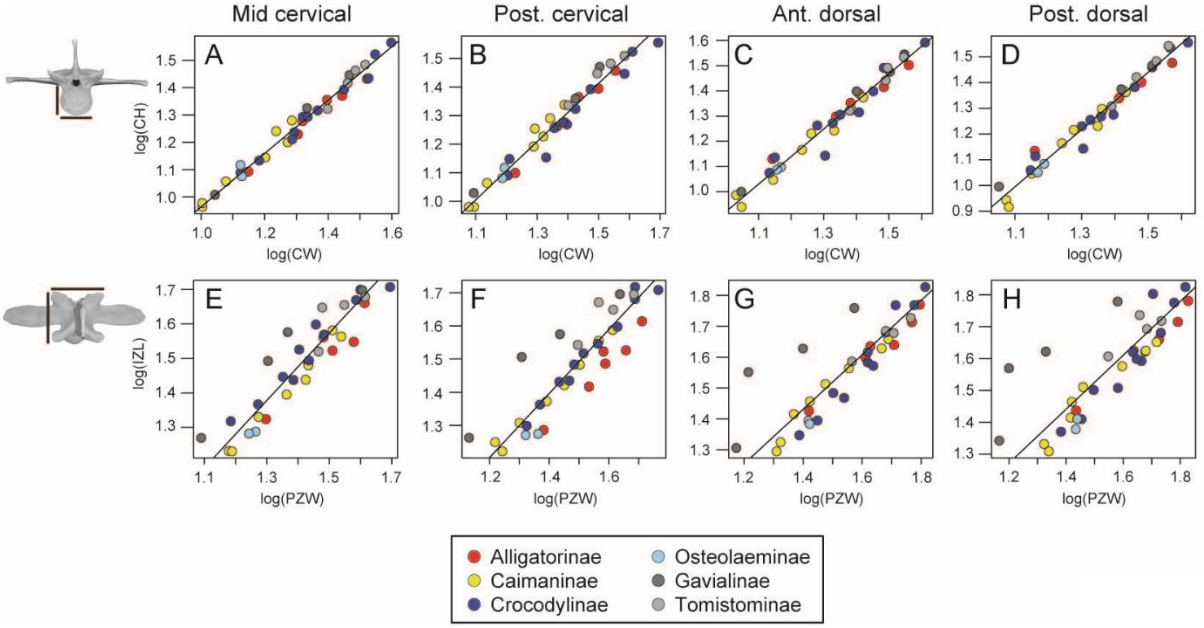


Fig. 8. Phylogenetically generalized least squares (PGLS) regressions of rostral proportion against OLS and RMA residuals of vertebral metrics. ant. dor., anterior dorsal; post. cer., posterior cervical; post. dor., posterior dorsal.

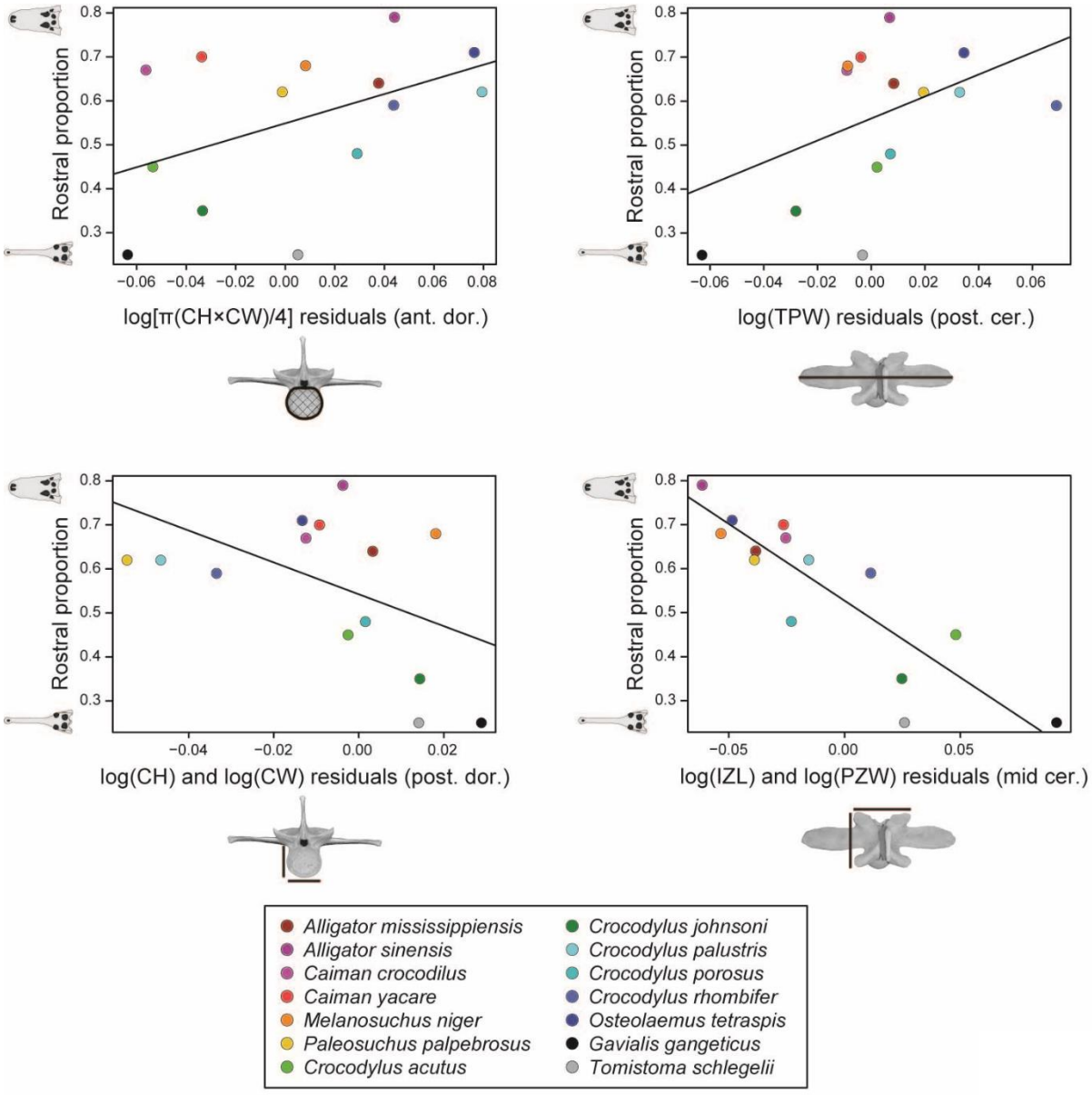


Table 1. Vertebral metrics and their functional relevance.

Vertebral metric	Functional relevance	Previous study
centrum length (CL)	longer: decreased stiffness for dorsoventral and lateral flexion	Shapiro 1995, 2007; Buchholtz 1998, 2001a, b; Boszczyk et al. 2001; Buchholtz and Schur 2004; Shapiro et al. 2005; Lindgren et al. 2007; Pierce et al. 2011; Molnar et al. 2014, 2015; Jones 2015
inter-central joint area (π(CH×CW)/4)	larger: increased stiffness for dorsoventral and lateral flexion	Shapiro 2007; Jones and Pierce 2016
neural spine height (NSH)	longer: increased muscular leverage for dorsal flexion, but increased stiffness due to larger cross-sectional area of body	Shapiro 1995, 2007; Long et al. 1997; Shapiro et al. 2005; Pierce et al. 2011; Molnar et al. 2014, 2015
transverse process width (TPW)	wider: increased muscular leverage for lateral flexion, but increased stiffness due to larger cross-sectional area of body	Long et al. 1997; Shapiro 2007; Pierce et al. 2011; Molnar et al. 2014, 2015
relative centrum height/width (CH/CW)	relative stiffness for dorsoventral vs. lateral flexion	Buchholtz 1998, 2001a, b; Lindgren et al. 2007; Jones and Pierce 2016
relative inter-zygapophyseal length/width (IZL/PZW)	larger: decreased stiffness for lateral flexion	proposed in this study

Table 2. OLS regressions of vertebral metrics [CL, π(CH×CW)/4, NSH and TPW] on size (sum of third cervical to the last dorsal centrum lengths), and RMA regressions of CH on CW and IZL on PZW.

y on *x*	*n*	r^2	*p*	Slope	Lower 95% CI	Upper 95% CI	Allometric trend
log(CL) on log(size)							
cervical 5&6	40	0.981	< 0.001	0.993	0.947	1.039	=
cervical 8&9	40	0.987	< 0.001	1.004	0.966	1.042	=
dorsal 5&6	40	0.992	< 0.001	1.013	0.983	1.042	=
dorsal 10&11	40	0.992	< 0.001	1.015	0.985	1.046	=
log[π(CH×CW)/4] on log(size)							
cervical 5&6	34	0.955	< 0.001	2.193	2.021	2.365	+
cervical 8&9	34	0.964	< 0.001	2.183	2.032	2.334	+
dorsal 5&6	34	0.974	< 0.001	2.318	2.181	2.454	+
dorsal 10&11	34	0.971	< 0.001	2.292	2.148	2.436	+
log(NSH) on log(size)							
cervical 5&6	34	0.920	< 0.001	1.098	0.981	1.214	=
cervical 8&9	34	0.892	< 0.001	1.063	0.929	1.196	=
dorsal 5&6	34	0.961	< 0.001	1.151	1.068	1.234	+
dorsal 10&11	34	0.945	< 0.001	1.138	1.039	1.237	+
log(TPW) on log(size)							
cervical 5&6	35	0.942	< 0.001	1.025	0.936	1.115	=
cervical 8&9	35	0.953	< 0.001	1.036	0.955	1.117	=
dorsal 5&6	35	0.954	< 0.001	1.089	1.004	1.174	+
dorsal 10&11	35	0.962	< 0.001	1.185	1.101	1.269	+
log(CH) on log(CW)							
cervical 5&6	34	0.978	< 0.001	0.976	0.925	1.029	=
cervical 8&9	34	0.962	< 0.001	1.020	0.950	1.094	=
dorsal 5&6	34	0.964	< 0.001	1.095	1.023	1.172	+
dorsal 10&11	34	0.969	< 0.001	1.112	1.043	1.185	+
log(IZL) on log(PZW)							
cervical 5&6	35	0.866	< 0.001	0.978	0.859	1.113	=
cervical 8&9	35	0.792	< 0.001	0.965	0.822	1.134	=
dorsal 5&6	35	0.743	< 0.001	0.882	0.738	1.055	=
dorsal 10&11	35	0.661	< 0.001	0.846	0.689	1.038	=

Table 3. ANCOVA testing the between-superfamily (Alligatoroidea and Crocodyloidea) differences in vertebral metrics. Analyses using log(size) as covariate are OLS-based, and others are RMA-based.

Dependent variable	Covariate	Covariate x superfamily *p*-value	Superfamily *p*-value
log(CL)	log(size)		
cervical 5&6		0.351	0.002
cervical 8&9		0.874	0.200
dorsal 5&6		0.582	0.028
dorsal 10&11		0.649	0.003
log[π(CH×CW)/4]	log(size)		
cervical 5&6		0.502	0.011
cervical 8&9		0.955	0.059
dorsal 5&6		0.089	0.832
dorsal 10&11		0.226	0.580
log(NSH)	log(size)		
cervical 5&6		0.298	0.462
cervical 8&9		0.295	0.039
dorsal 5&6		0.948	0.083
dorsal 10&11		0.872	0.075
log(TPW)	log(size)		
cervical 5&6		0.812	0.502
cervical 8&9		0.690	0.837
dorsal 5&6		0.289	< 0.001
dorsal 10&11		0.313	0.342
log(CH)	log(CW)		
cervical 5&6		0.260	0.551
cervical 8&9		0.732	0.680
dorsal 5&6		0.421	0.513
dorsal 10&11		0.920	0.508
log(IZL)	log(PZW)		
cervical 5&6		0.780	< 0.001
cervical 8&9		0.229	< 0.001
dorsal 5&6		0.953	0.140
dorsal 10&11		0.987	0.015

Table 4. PGLS regressions of rostral proportion against OLS and RMA residuals of six vertebral metrics. Rostral proportions of 14 species are adopted from Iijima and Kubo (in review). A time-calibrated molecular tree of Oaks (2011) is used for the analyses.

y-residual for OLS regression of	*n*	r^2	Holm-corrected *p*	Slope	Intercept	Pagel's λ
log(CL) on log(size)						
cervical 5&6	14	0.282	0.248	-4.370	0.533	0.742
cervical 8&9	14	0.147	0.578	-2.858	0.552	0.753
dorsal 5&6	14	0.101	0.384	3.020	0.554	0.802
dorsal 10&11	14	0.182	0.293	5.240	0.535	0.733
log[π(CH×CW)/4] on log(size)						
cervical 5&6	14	0.081	0.694	0.604	0.571	0.927
cervical 8&9	14	0.020	0.645	0.377	0.567	0.866
dorsal 5&6	14	0.637	0.006	1.664	0.549	1.000
dorsal 10&11	14	0.575	0.016	1.809	0.545	1.000
log(NSH) on log(size)						
cervical 5&6	14	0.453	0.059	1.515	0.564	1.000
cervical 8&9	14	0.505	0.026	1.661	0.558	0.998
dorsal 5&6	14	0.469	0.039	2.141	0.551	1.000
dorsal 10&11	14	0.487	0.032	1.602	0.556	1.000
log(TPW) on log(size)						
cervical 5&6	14	0.131	0.671	1.564	0.560	0.759
cervical 8&9	14	0.603	0.011	2.501	0.560	1.000
dorsal 5&6	14	0.150	0.384	2.349	0.535	1.000
dorsal 10&11	14	0.088	0.324	1.027	0.556	1.000
y-residual minus *x*-residual for RMA regression of						
log(CH) on log(CW)						
cervical 5&6	14	0.061	0.694	1.685	0.556	0.912
cervical 8&9	14	0.149	0.578	-2.149	0.562	0.833
dorsal 5&6	14	0.514	0.029	-2.221	0.572	1.000
dorsal 10&11	14	0.542	0.021	-3.622	0.542	1.000
log(IZL) on log(PZW)						
cervical 5&6	14	0.745	0.001	-3.491	0.527	0.000
cervical 8&9	14	0.533	0.023	-2.051	0.539	0.142
dorsal 5&6	14	0.221	0.314	-0.868	0.561	1.000
dorsal 10&11	14	0.359	0.091	-1.119	0.546	0.398

IV. Mosaic nature in the skeleton of East Asian "tomistomines" and *Gavialis-Tomistoma* debate

Introduction

Since modern quantitative techniques were applied to crocodylian systematics, the phylogenetic placement of *Gavialis* within Crocodylia has been a long-standing subject of discussion. The morphological analyses consistently suggested that the lineage of *Gavialis* is outgroup to all other Crocodylia, which has withstood the increased taxon and character sampling in recent decades (e.g. Norell, 1989; Brochu, 1997a,b, 1999a, 2004b; Hua & Jouve, 2004; Salisbury *et al.*, 2006; Jouve *et al.*, 2008, 2015; Brochu *et al.*, 2012). On the contrary, molecular analyses robustly indicated that *Gavialis* is sister taxon to *Tomistoma*, and this clade is closer to Crocodylinae than to Alligatoroidea, by using antigenic distance matrices, nuclear and mitochondrial DNA sequences, and restriction fragment length polymorphism matrices independently and compositely (Densmore, 1983; Densmore & Dessauer, 1984; Densmore & White, 1991; Gatesy & Amato, 1992; Hass *et al.*, 1992; Gatesy *et al.*, 2003; Gatesy, Baker, & Hayashi, 2004; Harshman *et al.*, 2003; Janke *et al.*, 2005; McAliley *et al.*, 2006; Roos, Aggarwal, & Janke, 2007; Willis *et al.*, 2007; Oaks, 2011).

The inconsistent placement of *Gavialis* between the two datasets is often highlighted in the study of crocodylian systematics, because except for this conflict, morphology and molecular hypotheses are remarkably congruent (Brochu, 1997a; Gatesy *et al.*, 2003). Various potential causes of the topological mismatch between two hypotheses, such as rooting and long branch attraction problem, homoplastic nature in the skull morphology, heterochrony and secondary signal, character non-independence, taxon and character sampling, subjectivity involved when choosing character and assigning character state, and analytical methods (Densmore, 1983; Norell, 1989; Hass *et al.*, 1992; Brochu, 1997a, 1999b; Trueman, 1998; Gatesy *et al.*, 2003; Harshman *et al.*, 2003) have been proposed. However, both datasets have advantage and disadvantage, and both hypotheses have defied explanation, thus this conflict represents one of a few examples that one hypothesis cannot eliminate the other (Hillis & Wiens, 2000).

One intriguing pattern recognized in the morphological dataset is the existence of competing hierarchical signals, of which the hidden secondary signal supports the molecular tree. Trueman (1998) first exemplified this by using reverse successive weighting of morphological characters, in which non-homoplastic characters found in the unweighted

parsimony analysis were excluded, and analysis was rerun with the remaining characters. Brochu (1999b) counterargued that the secondary signal did not appear when the fossil forms, especially from the most basal positions were included in the analysis. Later analysis by Gatesy et al. (2003) used different metric for hidden character support which does not need the character weighting and removal. They detected a massive hidden character support for the molecular tree in both morphology and molecular datasets, when the combined dataset, with or without fossils, was analyzed.

Willis et al. (2007:793) made a closing remark in their molecular study "…it is becoming increasingly difficult to ignore the consistent results of the molecular data sets…" by taking into account the congruent tree topology drawn from a large number of independent molecular datasets. As suggested by Oaks (2011), recent morphological studies used the molecular tree as a framework on which morphological and functional evolution was analyzed (Erickson *et al.*, 2012; Tanaka, Zelenitsky, & Therrien, 2015). Otherwise, both morphological and molecular trees were used for the comparison, or a combined tree that is congruent with molecular tree was chosen (Sadleir & Makovicky, 2008; Sadleir, 2009; Gold, Brochu, & Norell, 2014; Piras *et al.*, 2014; Watanabe & Slice, 2014).

If molecular tree is assumed as the best estimate of crocodylian phylogeny, a few issues remain and need to be addressed. The most peculiar among those is the extensive character reversal occurring in Gavialinae. More than a dozen of characters are reverted in Gavialinae to the primitive states that are otherwise only found in the outgroup of Crocodylia (Gatesy *et al.*, 2003). The mechanism of this extreme case of taxic atavism is currently unexplained, but it is suggested that developmental changes experienced in Gavialinae might be the cause, and the inclusion of fossils from basal Gavialinae and Tomistominae will help clarify the true character transformation history in these groups (Gatesy *et al.*, 2003).

Here, we report a solid evidence of the gavialine-specific atavistic characters from "Tomistominae," by describing a new species from the Pleistocene of Japan and by reexamining the skeletal characters of the previously described taxa from East Asia. A morphological tree that was forced to fit the molecular hypothesis, as well as a total evidence tree incorporating the molecular data recovered these East Asian "tomistomines" as basal Gavialinae, and "Tomistominae" of the morphological tree context was collapsed as successive sister groups of Gavialinae.

Methods

Taxonomy

We used Brochu's (2003) definition of crocodylian taxa based on the phylogenetic context. Longirostres, which is the last common ancestor of *C. niloticus* and *G. gangeticus* and all of its descendants is adopted from Harshman et al. (2003), and used in the molecular tree context. For some taxa (Crocodylidae, Crocodylinae, Gavialidae, and Tomistominae), definitions are different between morphological and molecular tree contexts. In this study, taxa and taxonomic constituents defined by the morphological tree context are represented with “ ”.

Phylogenetic analysis

The parsimony analysis of the morphology dataset was performed in PAUP 4.0a147 (Swofford, 2002). The current morphology matrix (66 taxa and 241 characters) is based on Jouve et al.'s (2015) matrix with revision of one character (chr. 22), addition of three new characters (chr. 239-241), modification of the character coding in *T. machikanensis* and *P. pani*, and inclusion of a new taxon. *Bernissartia fagesii* was designated to the outgroup, and a heuristic search was run with 100 random addition sequence replicates and tree bisection reconnection branch swapping. 10 trees per replication were saved. All characters were unordered and equally weighted. Nodal support was evaluated by a bootstrap resampling analysis, which conducted a separate heuristic analysis with 100 random addition sequence replicates, but without utilizing branch swapping algorism to save computation time. 10 trees per replication were saved. Bootstrap percentages larger than 50% were shown on the nodes.

In the second parsimony analysis, a “backbone constraint,” which defines the relationship among 9 extant taxa plus the ourgroup (*B. fagesii*), but allows remaining extinct taxa to float among the tree, was imposed. The topology of the extant taxa is based on the recent molecular analysis (Oaks, 2011), while the relationship of 5 crocodylid species was left unresolved. The same matrix and analytical options with the first analysis were used for this analysis. To assess the significant difference in the character state distribution between the two sets of most parsimonious trees (MPTs) that were generated by first and second analyses, non-parametric Templeton test and Kishino-Hasegawa (KH) test were performed in PAUP 4.0a147, using ten bootstrap sampled pairs of MPTs. *P* values less than 0.05 indicate significant conflict between the two trees.

Cranial shape correlates and weighted analysis

Character non-independence is known to violate the basic assumption of phylogenetic analysis, spuriously overweight the correlated characters, and give misleading phylogenetic estimate (Kluge & Farris, 1969; Felsenstein, 1973; Kluge & Wolf, 1993; Chippindale & Wiens, 1994). In the crocodylian systematics, similar snout shapes were repeatedly acquired in distantly related lineages, probably reflecting trophic convergence (Clark, 1994; Brochu, 2001; Wilberg, 2012). Because many of the cranial characters are thought to be correlated with the snout shape, phylogenetic analysis without downweighting the correlated characters would effectively overweight on snout shape, thus may produce a wrong tree. One of the few attempts made so far to alleviate this problem is by Clark (1994), who conducted the parsimony analysis eliminating all but one of the shared characters of *Gavialis*, thalattosuchians, dyrosaurs, and pholidosaurs. Meanwhile, Sadleir and Makovicky (2008) detected several snout shape correlates by testing the association of two discrete variables (snout shape and cranial characters), but later phylogenetic works did not utilize their methods as the basis for *a priori* or *a posteriori* weighting. Gatesy et al. (2003) argued that since large snout shape variation is observed even within the long-snouted groups, and potential snout shape correlates show widely different phylogenetic distribution, the use of such methods for finding character correlation may not be valid. To address this difficulty, we took the rostrum shape as continuous variable and cranial characters as discrete variable, and tested if the two are significantly correlated on phylogeny, using a phylogenetic logistic regression.

The rostrum shape of 59 out of 66 species used in the current phylogenetic analysis was quantified, by measuring the ratio of palate width at the last maxillary alveoli and the midline palate length between the tip of the skull to the line connected by the last maxillary alveoli. The ratio data were collected both by direct observation of specimens and the literature survey. For cranial discrete character matrix (66 taxa × 183 characters), characters with over 50% missing state were excluded, and the multistate characters were re-coded as binary characters to keep the requirement of the analysis. The remaining characters with the fewer observed state counts less than 10% of the total available state counts were removed, because such characters may not be informative as the snout shape correlates: as the result of this procedure, 101 cranial characters were left for the analysis. The missing terminal node states were estimated using the parsimony state reconstruction in Mesquite (Maddison & Maddison, 2011), on the strict consensus tree acquired in the unconstrained morphological and constrained morphological analysis (first and second parsimony analysis), respectively.

Equivocal terminal node states were further estimated by using ACCTRAN and DELTRAN optimization manually, applying the internal node state optimization procedure. The ambiguous root node states were treated as having state 0. Because a phylogenetic logistic regression requires a tree with internal branch length, both unconstrained morphological tree (UMT) and constrained morphological tree (CMT) with 59 taxa were time-calibrated by using R version 3.1.2 (R Development Core Team 2014) with strap package v. 1.4 (Bell & Lloyd, 2014, 2015), choosing "equal" option (Brusatte *et al.*, 2008) and setting root length as 5 million years. The first and last appearance data of each taxon is collected from the original literatures and the Paleobiology database (https://paleobiodb.org/). Finally, with the time-calibrated trees (UMT and CMT), quantified rostrum shape (continuous variable), and cranial characters (discrete variable) for 59 taxa, phylogenetic logistic regression was conducted using R with phylolm package v. 2.4 (Ho & Ané, 2014), choosing "logistic_MPLE" method, and setting btol and boot of 100 respectively. The significant correlation of two variables was evaluated by *p* values of less than 0.05. The detected shared snout shape correlates for both UMT and CMT were then downweighted such that each character was weighted to 1 / number of shared snout shape correlates, and the phylogenetic analysis was rerun.

Simultaneous analysis with morphology and molecular data

Lastly, a simultaneous parsimony analysis of the supermatrix constructed by the morphology dataset (66 taxa, 241 characters; mentioned above) and the molecular dataset (9 extant taxa, 7282 characters: Oaks 2011) was performed without imposing weight. All characters were unordered and equally weighted, and indels in the sequence alignments were treated as a fifth character state. Since Oaks (2011) sampled multiple individuals for each extant species, we selected one individual for each species for the current analysis (see Supplementary data). A heuristic analysis with 1000 Wagner tree replicates and tree bisection reconnection branch swapping, which holds 10 trees per replicates was executed in TNT 1.1 (Goloboff, Farris, & Nixon, 2003), assigning *B. fagesii* as an outgroup.

Test for stratigraphic congruence

Stratigraphic congruence metrics have been used for the purpose of comparing conflicting or alternative hypotheses of phylogenetic relationships (e.g. Brochu, 1997a; Brochu & Norell, 2000; Pol & Norell, 2006; Brusatte & Sereno, 2008; Boyd *et al.*, 2011), taking advantage of several metrics which have been developed and modified since early 1990s (Norell &

Novacek, 1992; Benton & Storrs, 1994; Huelsenbeck, 1994; Siddall, 1998; Wills, 1999; Pol & Norell, 2001, 2006; Wills, Barrett, & Heathcote, 2008; Boyd *et al.*, 2011). We here used the modified Manhattan stratigraphic measure (MSM*: Pol & Norell, 2001) and the Gap excess ratio (GER: Wills 1999) which need the exact first appearance datum (FAD), as well as the range measures (MSMp* range and GERp range: Pol & Norell, 2006; Boyd *et al.*, 2011) which take into account the age uncertainty of FAD and the alternative methods of resolving polytomies in phylogeny by a randomization procedure. These metrics are relatively less sensitive to tree balance, thus suited for comparing competing trees (Pol, Norell, & Siddall, 2004).

To calculate the metrics, both UMT and CMT were time-calibrated, incorporating FAD and LAD of 66 taxa (see above section). The analysis was executed with the StratPhyloCongruence function in R with strap package (Bell & Lloyd, 2014, 2015), by choosing the following options (hard=F, randomly.sample.ages=T, samp.perm=100, rand.perm=100, fix.topology=T, fix.outgroup=T). *P* values of MSM* and GER less than 0.05 indicate that trees show better fit to stratigraphy than random. Significant difference of stratigraphic fit between the alternative hypotheses (UMT and CMT) was judged by overlap or non-overlap of the MSMp* range and GERp range.

Results

Systematic Paleontology

Crocodylia Gmelin, 1789 (*sensu* Clark in Benton and Clark, 1988)

Gavialidae Adams, 1854

Gavialinae Nopcsa, 1923 (*sensu* Brochu, 2003)

Toyotamaphimeia Aoki, 1983

Toyotamaphimeia enshuensis, sp. nov.

Holotype

[GMNH XX-XXX], including at least 15 individuals, because 15 left femora had been found (Nakajima, 1983).

Locality and horizon

F3 Bed of the lower Yage Formation (Middle Pleistocene, Marine isotope stage 11-8.2), Yage, Inasa-cho, Hamamatsu City, Shizuoka, Japan (Tomida, 1978; Nojima, 2002; Nojima *et al.*,

2014).

Diagnosis

Posterior and lateral bar of the supratemporal fenestra near equal in thickness, absence of deep excavation on the ventral jugal near the jugal-ectopterygoid suture (differs from *Toyotamaphimeia machikanensis*); axial hypapophysis widely forked; third cervical centrum lacks prominent hypapophysis; iliac anterior process prominent; dorsal or pelvic midline osteoderm flat, rectangular in shape, and without an anterior process, and convex posterior articular facet of the second sacral centrum (potentially due to abnormality).

General description

The partial rostrum, near complete preorbital elements, complete skull table, partial infratemporal and suspensorium elements, partial occipital elements are preserved (Fig. 1). The palatal side of right posterior maxilla has six alveoli. The occlusal pits are placed in line with the alveoli as in non-alligatoroid crocodylians, yet differing from the overbite occlusal pattern of the posterior maxillary and dentary dentition in *T. machikanensis* (Aoki, 1983; Kobayashi *et al.*, 2006). The lacrimal extends far anteriorly than the prefrontal, and the lacrimal is wider than the prefrontal. The anterior extension of the frontal process is shorter than prefrontals. The frontal-nasal contact has a complex zig-zag sutural pattern, similar to *P. pani* (Shan *et al.*, 2009). The skull table broadened posteriorly, and the anterolateral edge is rounded. The shape of supratemporal fenestra is sub-circular to anteroposteriorly long oval, and the lateral and posterior bars of supratemporal fenestra are equally thick, unlike of *T. machikanensis* and derived gavialines in which the posterior bar is extremely narrow. The sutural contact of the parietal and frontal is concave anteriorly. On the lateral surface of the skull table, the shallow squamosal groove flares anteriorly. The descending process of postorbital, the dorsal half of the postorbital bar, is laterally compressed and missing the ventral extension. On the ventral surface of left jugal, near the jugal-ectopterygoid suture, a shallow concavity is present, which is much less prominent than that in *T. machikanensis*.

Large portion of the mandible except for the coronoid is preserved (Fig. 1). The right posterior dentary preserves the widely and evenly spaced seven alveoli. The occlusal pits are placed in line with the alveoli. The left splenial shows that the symphysis extends the length of at least three adjacent alveoli, but the shape of the symphysis is uncertain. The right splenial exhibits the small foramen intermandibularis oralis near the caudal end of the

symphysis, as in *T. machikanensis* and *G. gangeticus*. The surangular is medially perforated by the lingual foramen for the articular artery and alveolar nerve. The descending process of the articular contacts with surangular by simple linear suture, and there is no prominent sulcus between them. The retroarticular process is slender, which is roughly three times longer than the glenoid in dorsal view.

The axial skeleton of *T. enshuensis* includes cervical, dorsal, sacral, and caudal vertebrae, cervical, dorsal, and sacral ribs, and chevrons. All the presacral centra except for the atlas and axis are procoelous. On the ventral surface of axial centrum, forked hypapophyses are more widely bifurcated than in gavialoids, which are placed in the anteroventral surface of the centrum (Fig. 2A-C). The third or fourth cervical centrum also has forked hypapophyses (Fig. 2D-F), which converges anteriorly with the ventral median keel, as in *P. pani* and *T. machikanensis*. The keel is widened and rugose anterior to the convex intervertebral joint surface of the centrum. The second sacral centrum has platy anterior and convex posterior intervertebral joint surfaces unlike in typical crocodylians. The dorsal margin of the iliac blade is broadly convex (Fig. 2G, H), and there is a prominent anterior process as in gavialoids, *P. pani* and *T. machikanensis* (Kobayashi *et al.*, 2006; Shan *et al.*, 2009). The flat, rectangular and mediolaterally wide osteoderms (Fig. 2I-L) are of midline dorsal or pelvic osteoderms, usually with serrate joints on both sides. Those osteoderms are without keel on the dorsal surface.

Reexamination of other East Asian "tomistomines"

A small number of gavialine-specific atavistic characters were previously described in Asian "tomistomines:" *Penghusuchus pani* from the Miocene of Taiwan, and *Toyotamaphimeia machikanensis* from the Pleistocene of Japan (Kobayashi *et al.*, 2006; Shan *et al.*, 2009). Our reassessment revealed much increased assembly of such characters in those "tomistomine" species.

A small lump, which would be an axial diapophysis, is present on either side of the axial neural arch in *T. machikanensis* (Fig. 3D: Kobayashi et al. 2006), and a similar lump is also found in the axial neural arch of *P. pani* (Fig. 3A). Except for these species, the "axial diapophysis" is found exclusively in gavialines within the crown Crocodylia (e.g., *E. minor*; *T. neocesariensis*; *A. krebsi*; *G. gangeticus*: Brochu, 1997b, 2006; Jouve *et al.*, 2006; USNM 576261). Kobayashi et al. (2006) and Shan et al. (2009) noted there is a pair of ridges on the anterior portion of the ventral surface of the axial centrum in *P. pani* and *T. machikanensis*

(Fig. 3B, D), but supposed that the keeled posterior portion of the ventral surface might represent the hypapophysis, if any. We interpret the anterior paired ridges to be the true hypapophyses. Although those are much more widely bifurcated than gavialine species (e.g., *E. minor*; *T. macrorhynchus*; *G. bengawanicus*: Troedsson, 1924; Brochu, 2006; Delfino & de Vos, 2010), such ridges other than hypapophyses are not known. The weak posterior ventral keel might represent the common origin of hypaxial muscles with the hypapophysis of the successive vertebrae. Similarly, a flattened and knob-like prominence in the anterior portion of the ventral surface of third cervical centrum in *T. machikanensis* (Fig. 3F) is here interpreted as a hypapophysis, instead of a posterior ventral keel that was originally regarded as such. The absence of keel-like hypapophysis in third cervical centrum is characteristic in gavialines, *Borealosuchus*, and Planocraniidae within Crocodylia. The fourth cervical centrum is also missing the prominent keel-like hypapophysis in *T. machikanensis*. In *P. pani*, third through fifth cervical centra have widely forked ridges, but they converge with the prominent anterior boss, together forming a hypapophysis.

The iliac blade of *P. pani* and *T. machikanensis* is known to possess a prominent anterior process (Fig. 3G, H) as in gavialines, *Borealosuchus* and Planocraniidae (Kobayashi *et al.*, 2006; Shan *et al.*, 2009). Additionally, the dorsal margin of the iliac blade is smooth and nearly straight in *P. pani* as in gavialines, *Borealosuchus*, and some species of Alligatoroidea. *T. machikanensis* shows slightly more rounded and indented dorsal margin of ilium. The humerus of *P. pani* possesses a less developed deltopectoral crest (Fig. 3I), which is less pointed than most of the non-gavialine crocodylians including *T. machikanensis*, and its proximal edge is smooth without a concavity.

The wider than long, rectangular shaped midline dorsal or pelvic osteoderms of *P. pani* and *T. machikanensis* (Fig. 3K-P) actually possess an anterior process as in gavialines (*E. minor*, *E. mississippiensis*, *T. macrorhynchus*, *E. africanum*, *G. bengawanicus*: Troedsson 1924; Brochu 2004a, 2006; Delfino and de Vos 2010; BMNH R3335), *Borealosuchus*, and some species of *Diplocynodon* within Crocodylia (Brochu, 1997b). The lateral dorsal or pelvic osteoderms, which are without serrate joints on either side, are also considerably wider than long in *P. pani* and *T. machikanensis*, similar to *G. gangeticus* than to *T. schlegelii* (FMNH 98864; FMNH 206755).

The basioccipital tubera of *T. machikanensis* is massive (Fig. 4A: Kobayashi et al. 2006). It is thrusted posterodorsally, thus the posterior surface of basioccipital below the occipital condyle is significantly concave. The exoccipital sends a robust and anteroposteriorly wide

descending process to the basioccipital as in most species of Gavialinae. Although the sutural relationship of exoccipital and basioccipital is hard to trace, this seems also true in *P. pani*. On the occipital surface of skull, there is a prominent convex process of the exoccipital hanging over the cranio-quadrate passage in *P. pani*, as in some gavialine crocodylians (*E. mississippiensis*; *G. gangeticus*: Brochu 2004a; ZSM 29.1912). The splenial symphysis shape of *P. pani* (Fig. 4B) is similar to that of basal gavialine species, in extending the length of 5 to 7 dentary teeth, and forming wide "V" without a constriction. The splenial symphysis of *T. machikanensis* is slightly constricted but still forms a wide "V" as in the gavialine *S. venezuelensis* (Brochu & Rincón, 2004).

Unweighted phylogenetic analysis of morphology data

The first parsimony analysis of the morphology dataset without imposing topological constraint recovered 96 most parsimonious trees (MPTs), with the tree length of 867, consistency index (CI) excluding uninformative characters of 0.359, and retention index (RI) of 0.709. The strict consensus tree (Fig. 5) shows that *T. enshuensis* is deeply nested in "Tomistominae," and forms an unresolved polytomy with *P. pani* and *T. machikanensis*. This clade is supported by 14 unambiguous synapomorphies: (Chr. 4, 19, 34, 43, 45, 60, 89, 128, 147, 151, 162, 223, 227, 235): axial neural arch possesses diapophysis; axial hypapophysis with deep fork; iliac anterior process prominent; splenial symphysis extends over the length of five to seven teeth and forms wide "V"; lingual foramen for articular artery and alveolar nerve perforates surangular entirely; articular flush against surangular; largest maxillary alveolus in the "first wave" is No. 7; lateral carotid foramen opens lateral to basisphenoid lateral exposure at maturity; lateral Eustachian canals open lateral to medial Eustachian canal; occipitals send robust process ventrally and participate in basioccipital tubera; surangular-articular suture oriented anteroposteriorly within glenoid fossa; anterior tip of frontal forms broad complex sutural contact with the nasals; large maxillary tooth in the "second wave" 12th or posterior; maxillary teeth not widely spaced, and 7th and 8th teeth not more spaced than other teeth. Except for the addition of the new taxon, the rest of the tree topology is wholly consistent with the previous analysis (Jouve *et al.*, 2015), in which Gavialoidea is the outgroup of all other Crocodylia, and Tomistominae is the sister taxon to Crocodylinae. The close relationship between this East Asian clade and North American *Thecachampsa* is retained.

The second parsimony analysis of the morphology dataset with the backbone constraint on

modern taxa recovered 96 MPTs, with the tree length of 873, CI of 0.356, and RI of 0.706. The strict consensus tree (Fig. 6) shows that *Borealosuchus*, Planocraniidae, *A. germanicus*, *P. langi*, *C. depressifrons*, *C. affinis*, *C. acer*, and *B. eversolei* are posited as the successive outgroups to Longirostres. Within Gavialoidea, *M. zennaroi*, *K. spenceri*, *M. arduini*, and *D. densmorei* are successive sister taxa to Gavialidae, and Tomistominae (*T. schlegelii* and all crocodylians closer to it than to *G. gangeticus*) are small clade including only four species (*T. coppensi*, *T. schlegelii*, *T. lusitanica*, *G. eggenburgensis*). *T. cairense*, *Penghusuchus* + *Toyotamaphimeia*, and *P. courti* are basal members of Gavialinae, which are more closely related to *G. gangeticus* than to *T. schlegelii*. The tree lengths of UMT and CMT are different by only 6 steps (0.69 %). The tests of tree incongruence indicated that the difference is not significant enough (p = 0.497-0.521 for Templeton test; p= 0.498-0.524 for KH test).

Weighted analysis of morphology data

The phylogenetic logistic regression of cranial binary characters and the rostrum shape detected a large number of cranial shape correlates in our dataset. The regression analysis was run four times with the combination of two alternative trees (UMT and CMT) and two optimization criterions (ACCTRAN and DELTRAN). The analysis yielded 19-25 potential correlates, and 16 of which are shared by all analyses (Table 1). Most of the characters within the list are related with the degree of symphysis extension, relative cranial bone extension in sagittal direction, and the tooth size variation. When weight of the 16 characters was reduced to 1/16, weighted unconstrained morphological analysis recovered 12 MPTs, with the tree length of 730.125, CI of 0.38, and RI of 0.718. The strict consensus tree (Supplementary Fig. 9) is mostly congruent with the unweighted UMT, just differs in the resolution of basal "Gavialoidea" and Planocraniidae. Weighted constrained morphological analysis recovered 24 MPTs, with the tree length of 744.625, CI of 0.372, and RI of 0.709. In the strict consensus tree (Supplementary Fig. 10), *P. courti* and the clade of *P. pani*, *T. machikanensis*, and *T. enshuensis* were still posited within Gavialinae, but *T. cairense* moved to a more basal position out of Gavialinae. The tree length of weighted unconstrained morphological tree (WUMT) differs from weighted constrained morphological tree (WCMT) by 14.5 steps (1.947 %), although this difference is insignificant in both of the tree incongruence tests (p = 0.087-0.107 for Templeton test; p= 0.081-0.094 for KH test).

Simultaneous analysis

The parsimony analysis of combined morphology and molecular datasets without imposing weight produced 48 most parsimonious trees, with the tree length of 4427, CI of 0.703, and RI of 0.679. The strict consensus tree (Supplementary Fig. 11) is largely congruent with CMT, which only differed in the resolution of genus *Crocodylus* and the placement of *M. cataphractus*.

Stratigraphic congruence

Both UMT and CMT show significant fit to stratigraphy (Table 2). Although MSM* measure values were relatively low (0.168 for UMT and 0.131 for CMT), this can be attributed to large number of taxa in the current dataset (Pol *et al.*, 2004). When fit of the conflicting trees were compared, UMT exhibits better fit to stratigraphy than CMT overall, and MSMp* range and GERp range measures have no overlap between two trees, suggesting that the difference of stratigraphic fit between two trees is significant.

Discussion

Bridging the morphological gap between "Tomistominae" and "Gavialoidea"

The assessment of the skeletal characters in East Asian "tomistomines" *Penghusuchus pani* and two species of *Toyotamaphimeia* revealed the previously unknown distribution of gavialine characters in "tomistomines" (Fig. 6). Postcranial characters such as the presence of axial diapophysis [char. 4(1)], third cervical centrum without prominent hypapophysis [char. 8(1)], axial hypapophysis with deep fork [char. 19(1)], proximal edge of deltopectoral crest emerges smoothly from proximal end of humerus [char. 26(0)], dorsal margin of iliac blade rounded with smooth border [char. 28(0)], iliac anterior process prominent [char. 34(0)], and midline osteoderms with anterior process[char. 40(0)] have been widely recognized in Gavialinae, otherwise only known in Planocraniidae and *Borealosuchus* that are the members of stem Longirostres, some of the alligatoroids, and the outgroup of Crocodylia in the CMT and the combined tree. The pronounced character reversal recognized in Gavialinae is noted by Gatesy et al. (2003) as "most troubling." That the atavistic characters are not found in "Tomistominae," a sister group of Gavialinae in the molecular tree, and that the outgroup of Crocodylia shows primitive states of those characters may support the morphological hypothesis of crocodylian phylogeny. In the morphological tree, "Gavialoidea" is placed as a sister taxon of all other Crocodylia, thus it is simply regarded that "gavialoids" retained the primitive character states from the ancestors. Our UMT posited *P. pani* plus

Toyotamaphimeia, which possesses a set of Gavialine-specific atavistic characters, deeply within “Tomistominae,” a sister group to Crocodylinae. However, the CMT, and the combined tree recovered *P. pani* plus *Toyotamaphimeia* as well as African “tomistomines” *T. cairense* and *P. courti* as basal gavialines, which are more closely related to *G. gangeticus* than to *T. schlegelii*. These imply that some of the “tomistomines” including the East Asian taxa are intermediate between “Tomistominae” and “Gavialoidea,” characterized by the mosaic of “tomistomine” and “gavialoid” features.

Other postcranial features that are not incorporated in the phylogenetic analysis support this view. Limb and vertebral measurements in *T. machikanensis*, a basal member of Gavialine in molecular tree suggest that traits potentially related with the increased aquatic adaptation of gavialine crocodylians are evident in this taxon. Comparison of allometry corrected ulna length / humerus length (UL_c / HL_c) and zygapophyseal length / width (ZL / PZW) of dorsal vertebrae (Fig. 7) revealed that *G. gangeticus* is different from other groups of extant crocodylians (Alligatoridae, Crocodylidae, and Tomistominae) in those metrics. *G. gangeticus* possesses shorter epipodial (ulna) relative to propodial (humerus), and more narrowly placed zygapophyses of dorsal vertebrae among other extant crocodylians. *T. machikanensis* shows similarity with *G. gangeticus* in both limb and vertebral metrics, suggested by a discriminant analysis (see Supplementary information). The forelimb reduction associated with the marine adaptation is known in thalattosuchians, where reduction in the relative epipodial (ulna and radius) length leads to plate-like epipodials and flipper like manus in derived metriorhynchoids, whereas relative epipodial length varies among teleosauroids (Fraas, 1902; Andrews, 1915; Wilberg, 2015). Meanwhile, allometric scaling of limb elements in the extant crocodylian *A. mississippiensis* indicates that distal elements (epipodials and metapodials) grow increasingly shorter through growth (Dodson, 1975; Livingston *et al.*, 2009), which suggests decreased terrestrial locomotor capability in large forms. The narrowly placed zygapophyses of dorsal vertebrae increase the mediolateral intervertebral flexibility, and are characteristic of semi-fully aquatic thalattosuchians, but also of other terrestrial crocodylomorphs (Molnar *et al.*, 2015).

Our CMT and combined tree show the gradual specialization of cranial characters on the lineage of *G. gangeticus* (Fig. 8). In the morphological tree context, the potential slender snout correlates such as extended mandibular symphysis, reduced anterior extension of nasals, and homodont dentition are considered as independently derived in “gavialoids” and “tomistomines.” On the contrary, in the molecular tree context, those characters are regarded

to be derived by a single event within Gavialoidea and shared by the descendants (Gatesy *et al.*, 2003). The character states of the slender snout correlates (e.g., Chr. 43, 95) derives stepwise within Gavialoidea, and some character state changes are located at basal and stem Gavialinae, preceding the divergence of "gavialoids" of the morphological tree context. The cranial, as well as postcranial evidence discussed above altogether implies that the unique skeletal features of *G. gangeticus* among the extant crocodylians (Tarsitano, Frey, & Riess, 1989; Pierce, Angielczyk, & Rayfield, 2008; Piras *et al.*, 2010) were gradually assembled on the lineage leading to *G. gangeticus*, making it "the most thoroughly aquatic of the extant crocodylians" (Stevenson & Whitaker, 2010).

Congruence vs. incongruence between morphological and molecular trees

Although the unconstrained morphological tree (UMT) obtained from the current morphological dataset (241 characters × 66 taxa) was consistent with previously presented morphological trees in the placement of *Gavialis* (e.g. Norell, 1989; Brochu, 1997a, 1999a; Hua & Jouve, 2004; Salisbury *et al.*, 2006; Jouve *et al.*, 2015), the constrained morphological tree (CMT) that is congruent with the molecular hypothesis did not disagree with the UMT, which was supported by both Templeton test and KH sites test. The previous study that used the matrix of 164 characters × 15 extant plus 46 extinct taxa indicated the significant difference in the character state distribution between the unconstrained tree and constrained tree which was forced to match the molecular hypothesis, and the same result was obtained when only extant taxa were used (Brochu, 1997a). The current dataset is pruned with many of the alligatoroid species, but this group is relatively stable (Brochu, 1997a,b, 1999a, 2004b, 2011) and could minimally affect the result. It is conceivable that the increased character sampling and the addition of several fossil "gavialoids" and "tomistomines" might help more parsimoniously explain the character distribution within the CMT. On the contrary, fit of the molecular characters on the morphological tree was proven to be significantly worse than on the molecular tree, when examined with independent nuclear and mitochondrial DNA dataset (Gatesy *et al.*, 2003). Because morphological data can fit the molecular tree but reverse does not work, it would be more prudent to use the molecular tree as the phylogenetic framework of crocodylians (Oaks, 2011), and discuss the cause of any inconsistency between the datasets.

However, as pointed out by Trueman (1998) and later corroborated by Gatesy et al. (2003), characters supporting the close relationship of *G. gangeticus and T. schlegelii* are mostly

related with rostrum, which are hidden behind the primary phylogenetic signal in the morphology-only tree. If these characters are correlates of snout shape, trees produced by phylogenetic analysis may be unwarrantedly heavily weighted on snout shape, and thus are misleading. The use of phylogenetic logistic regression detected over a dozen of potential snout shape correlates on phylogeny. Slender snout states of these characters: tooth size homodonty [chr. 89(5), 227(2)]; extended lower jaw symphysis [chr. 43(4-6), 176(1, 2), 195(2)] are suggested to be functionally advantageous in catching docile preys instead of larger preys (Iordansky, 1973; Busbey, 1995; Walmsley *et al.*, 2013). Since slender snout is favorable in achieving higher angular velocity of jaw tip during lateral head sweeping and jaw closing to strike on small agile preys (Taylor, 1987; Thorbjarnarson, 1990; McHenry *et al.*, 2006), such adaptive characters are likely considered as being correlatedly acquired during the trophic specialization. Functional significance of other potential snout shape correlates that are associated with the relative shortening-lengthening of cranial bones in sagittal direction is currently unknown, but such change in the sutural relationships would also be a biomechanical response to the trophic adaptation.

When potential snout shape correlates (16 characters) were downweighted *a posteriori*, resulted WUMT and UMT, and WCMT and CMT are largely congruent. Tree length difference between WUMT and WCMT (1.95 %) is larger than that between UMT and CMT (0.69 %), but both tree incongruence tests (Templeton test and KH test) yielded insignificant difference between WUMT and WCMT ($p > 0.05$). Our result would partly support the claim that snout shape correlates helped to place *G. gangeticus* and *T. schlegelii* close to each other, yet such secondary phylogenetic signal cannot overwhelm the primary signal in the morphological tree (Brochu, 1999b). However, the result of weighted analysis should be carefully discussed. More than a half of the downweighted characters originally consisted of multiple states that were forced to re-code binary in the phylogenetic logistic regression. Consequently, some taxonomical signal might be lost in the weighted analysis. For example, degree of splenial symphysis extension is over the length of 5 to 7 dentary teeth in both state 4 and 5 of character 43 (combined and re-coded to state 1 in binary coding), although they differ in the symphysis shape: the former and latter states describe wide “V” and narrow “V” shape respectively. Both states are observed within “Tomistominae,” yet the former state is only found within “Gavialoidea.”

When fossils were fitted to the molecular hypothesis of crocodylian phylogeny, one remaining inconsistency is a large stratigraphic gap recognized in “Tomistominae” (Fig. 9).

Although the CMT shows significant fit to stratigraphy, the fit is significantly worse than that of UMT. In both CMT and the combined tree, “Tomistominae” was collapsed as successive sister groups of Gavialinae, and the appearance of the first “tomistomine” postdated the first “gavialoids” by about 15 Ma. In the Maastrictian to Eocene of Africa, both “tomistomine” and “gavialoid” fossils have been recovered from the Oulad Abdoun Basin, Morocco (Jonet & Wouters, 1977; Hua & Jouve, 2004; Jouve *et al.*, 2008, 2015) and Fayum Province of Egypt (Andrews, 1901; Müller, 1927; Brochu & Gingerich, 2000). Intriguingly, CMT and the combined tree recovered two of the Eocene Egyptian “tomistomines” (*T. cairense* and *P. courti*) within Gavialinae, reflecting the gavialine characters possessed by these species (char. 89, 123, 128, 165: maxillary teeth homodont, sloped skull table surface; lateral carotid foramen opens lateral to basisphenoid lateral exposure at maturity; edge of maxillary tooth higher than the space between the tooth rows). A careful reexamination of “tomistomines” and “gavialoids” from both regions and the improved taxon sampling from the Maastrichtian through Eocene deposits of North Africa might help further filling the morphological and time gap between “tomistomines” and “gavialoids.”

Fig. 1. Composite skull and mandible reconstructions of *Toyotamaphimeia enshuensis* in A, dorsal, B, left lateral views. an, angular; art, articular; d, dentary; f, frontal; j, jugal; l, lacrimal; m, maxilla; n, nasal; p, parietal; pm, premaxilla; po, postorbital; q, quadrate; qj, quadratojugal; sa, surangular; soc, supraoccipital; sq, squamosal. Scale bar is 10 cm.

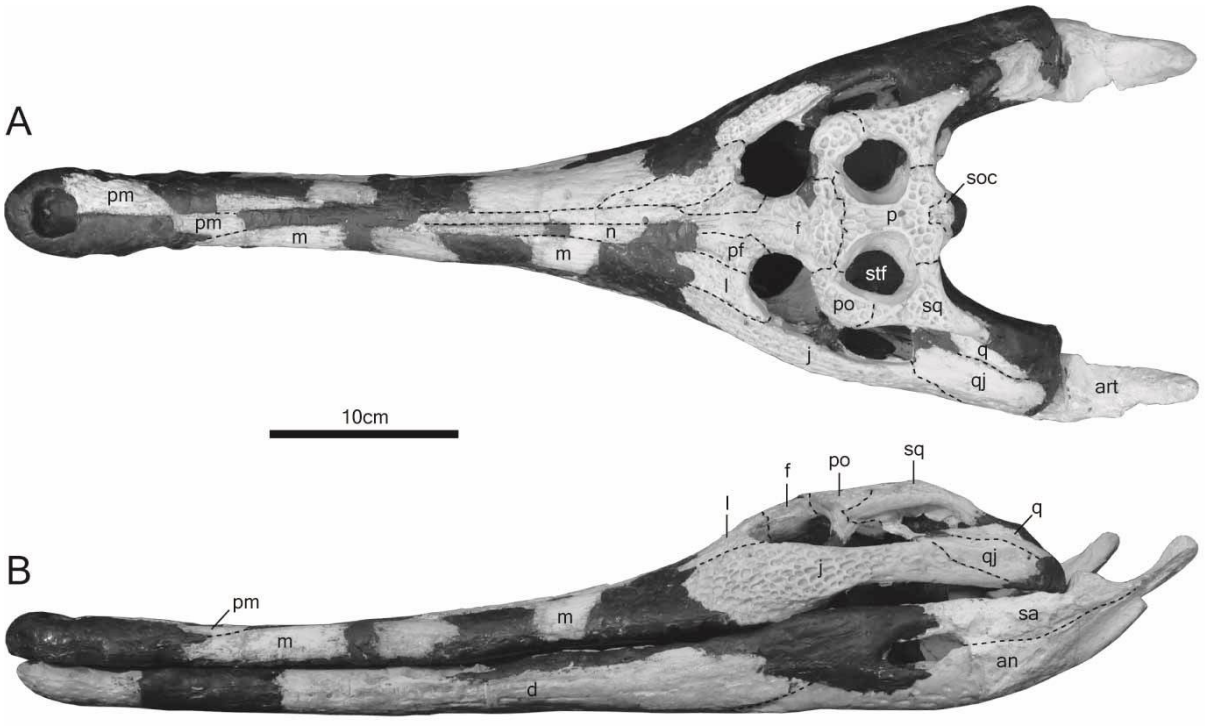


Fig. 2. Selected postcrania of *Toyotamaphimeia enshuensis*. A-C, axial centrum (T114) in A, left lateral, and B, C, ventral views. D-F, third or fourth cervical centrum (HH376) in D, left lateral and E, F, ventral views. G, H, right ilia (G: HH713; H: HH560) in lateral view. I-L, osteoderms (I: SH1; J: HH327; K: HH531; L: HH496) in external view. hp, hypapophysis; iac, iliac anterior process; pp, parapophysis; vmk, ventral median keel. Scale bars are 2 cm.

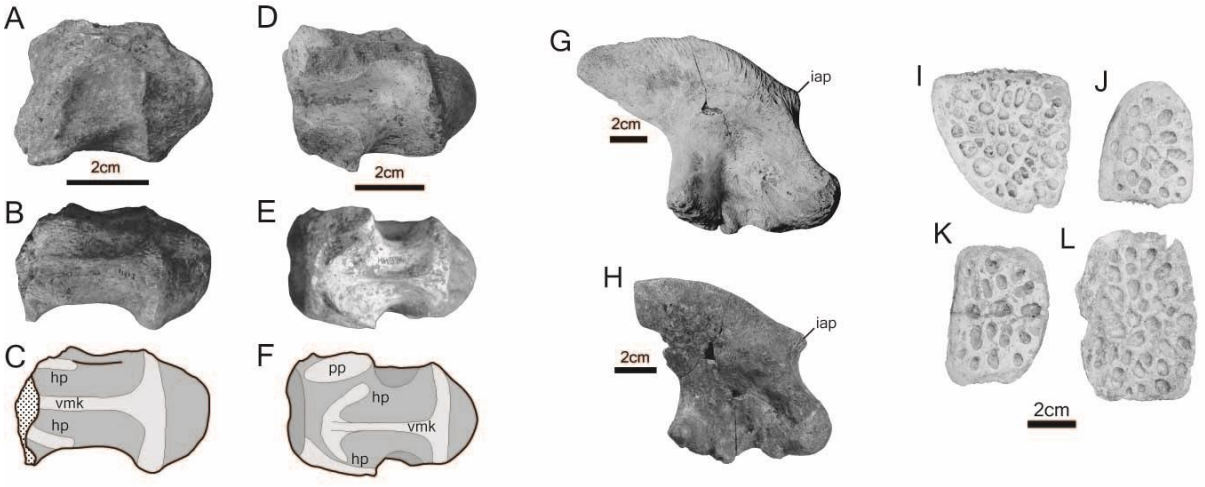


Fig. 3. Selected postcrania of *Penghusuchus pani* (NMNS-005645) and *Toyotamaphimeia machikanensis* (MOUF 00001). A-D, axial centrum (A, B: *P. pani*; C, D: *T. machikanensis*) in A, C, right lateral, and B, D, ventral views. E, F, third cervical centrum (E: *P. pani*; F: *T. machikanensis*) in ventral view. G, H, left ilium (G: *P. pani*; H: *T. machikanensis*) in lateral view. I, J, left humerus (I: *P. pani*; J: *T. machikanensis*) in lateral view. K-P, dorsal or pelvic midline osteoderms (K-M: *P. pani*; N-P: *T. machikanensis*) in external view. dp, diapophysis; dpc, deltopectoral crest; hp, hypapophysis; iac, iliac anterior process; pp, parapophysis. Arrow indicates anterior process of osteoderm. Scale bars are 5 cm.

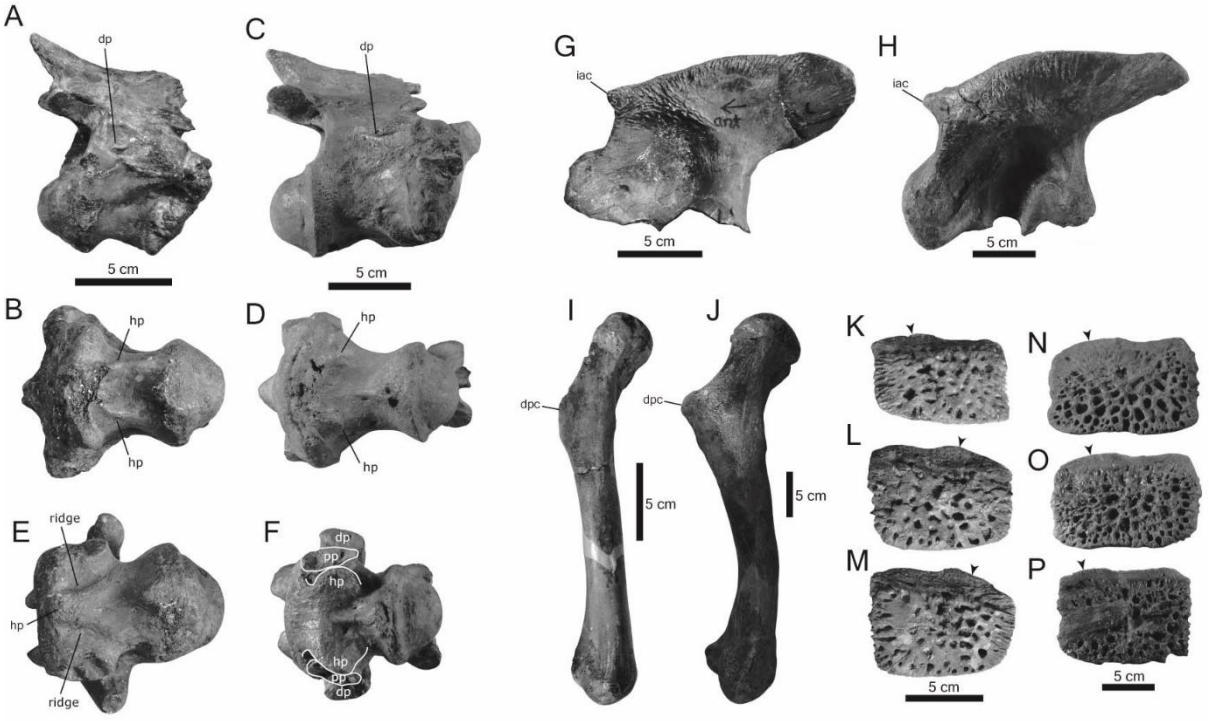


Fig. 4. A, occipital region of *Toyotamaphimeia machikanensis* (MOUF 00001). B, splenial symphysis of *Penghusuchus pani* (NMNS-005645) in dorsal view. bo, basioccipital; cn X, exit of cranial nerve X; cn XII, exit of cranial nerve XII; eo, exoccipital; leu, lateral Eustachian opening; meu, medial Eustachian opening. Scale bar for B is 5 cm.

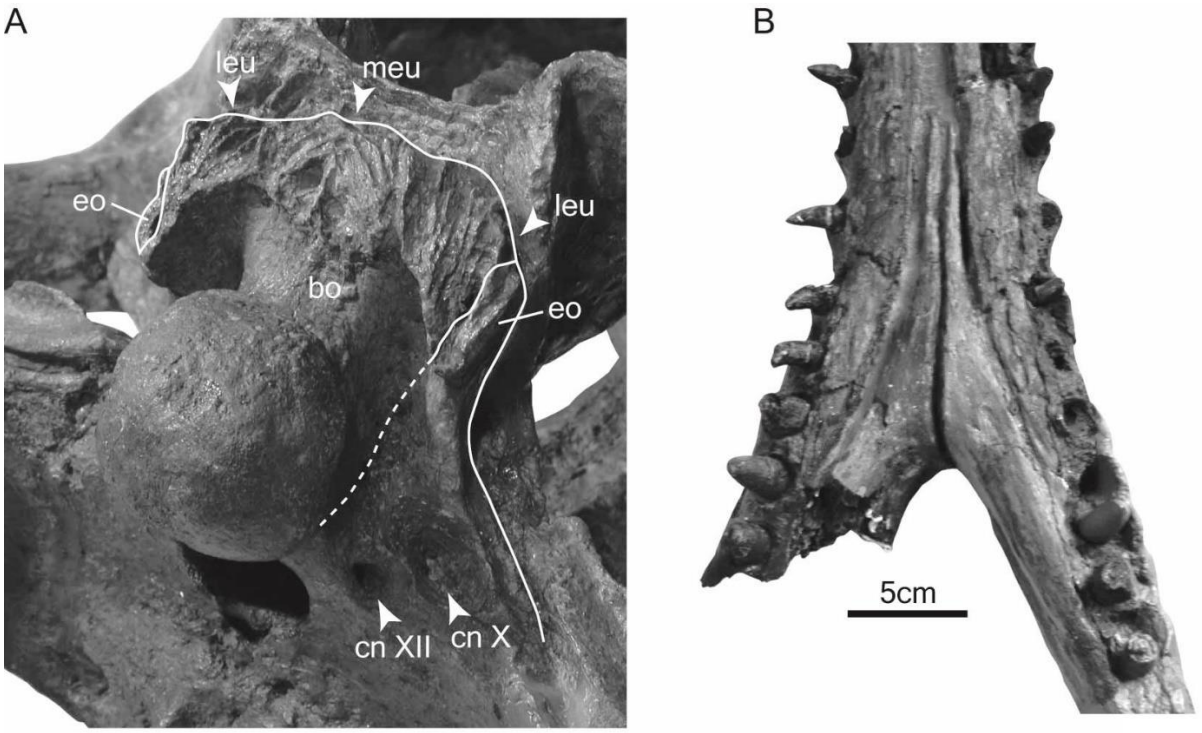


Fig. 5. A strict consensus tree obtained from the parsimony analysis of the morphology dataset without imposing topological constraint. Numbers at nodes are bootstrap percentages.

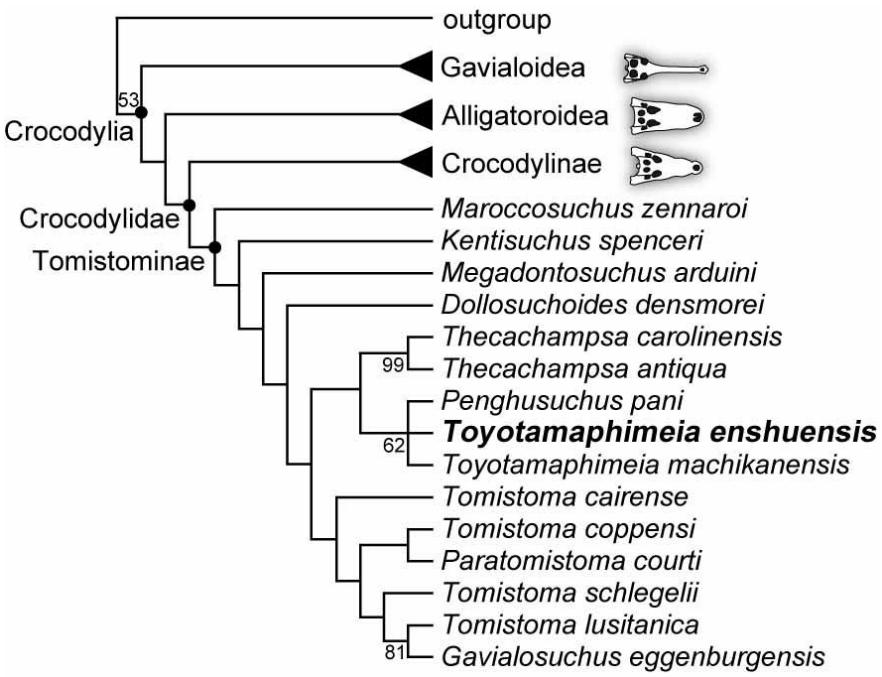


Fig. 6. A strict consensus tree obtained from the parsimony analysis with the backbone constraint on modern taxa. Numbers at nodes are bootstrap percentages. Character state distribution of Gavialine-specific atavistic characters is shown.

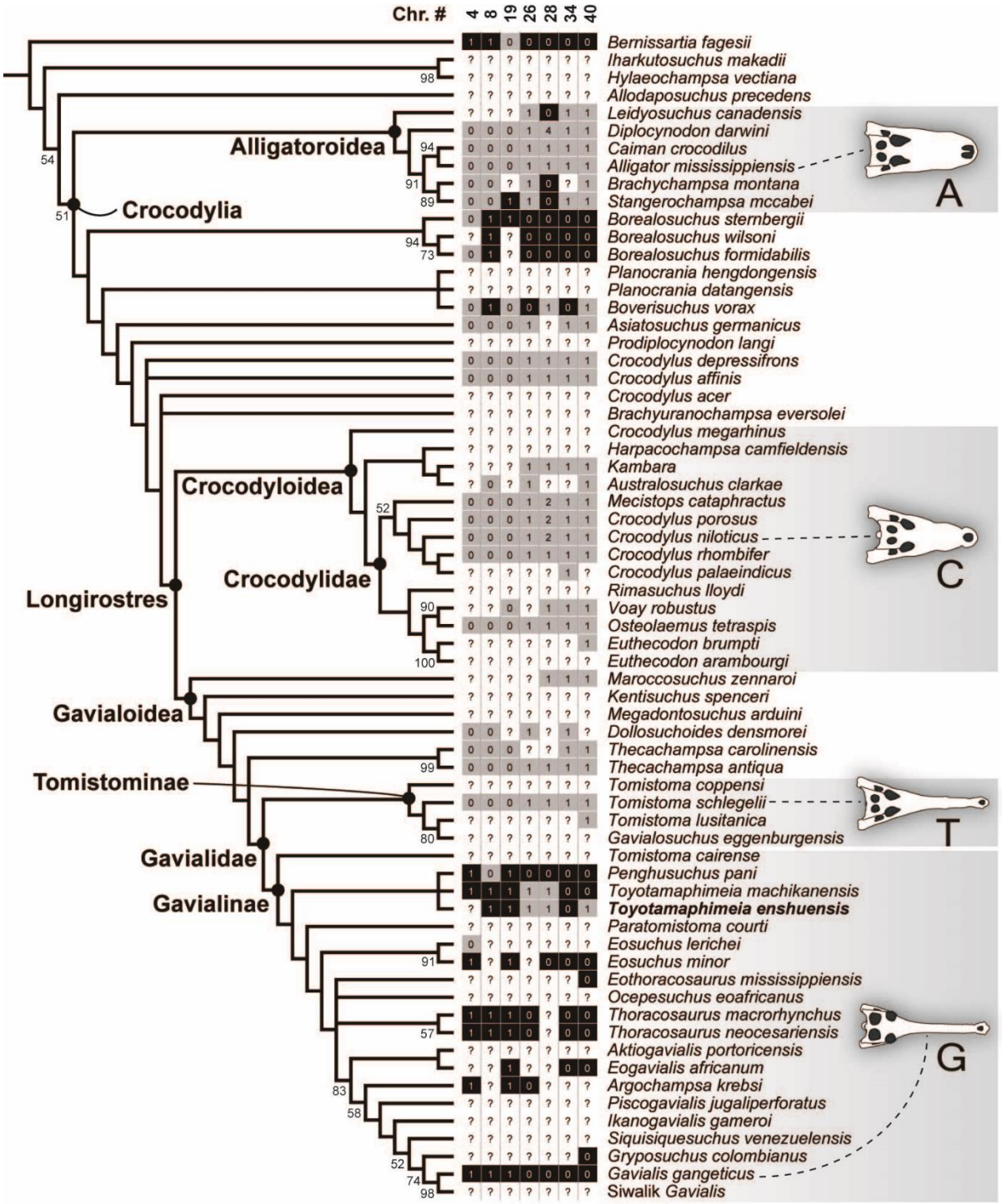


Fig. 7. Comparison of limb metric (UL_c/HL_c: allometry corrected ulna length / humerus length) and vertebral metric [posterior dorsal vertebrae (D6-D15) average zygapophyseal length (ZL) / pre-zygapophyseal width (PZW) ratio] among four groups of extant crocodylians plus *Toyotamaphimeia machikanensis* (MOUF 00001). Asterisks indicate significant difference in the mean. Single asterisk indicates $p < 0.05$, and double asterisks indicate $p < 0.001$.

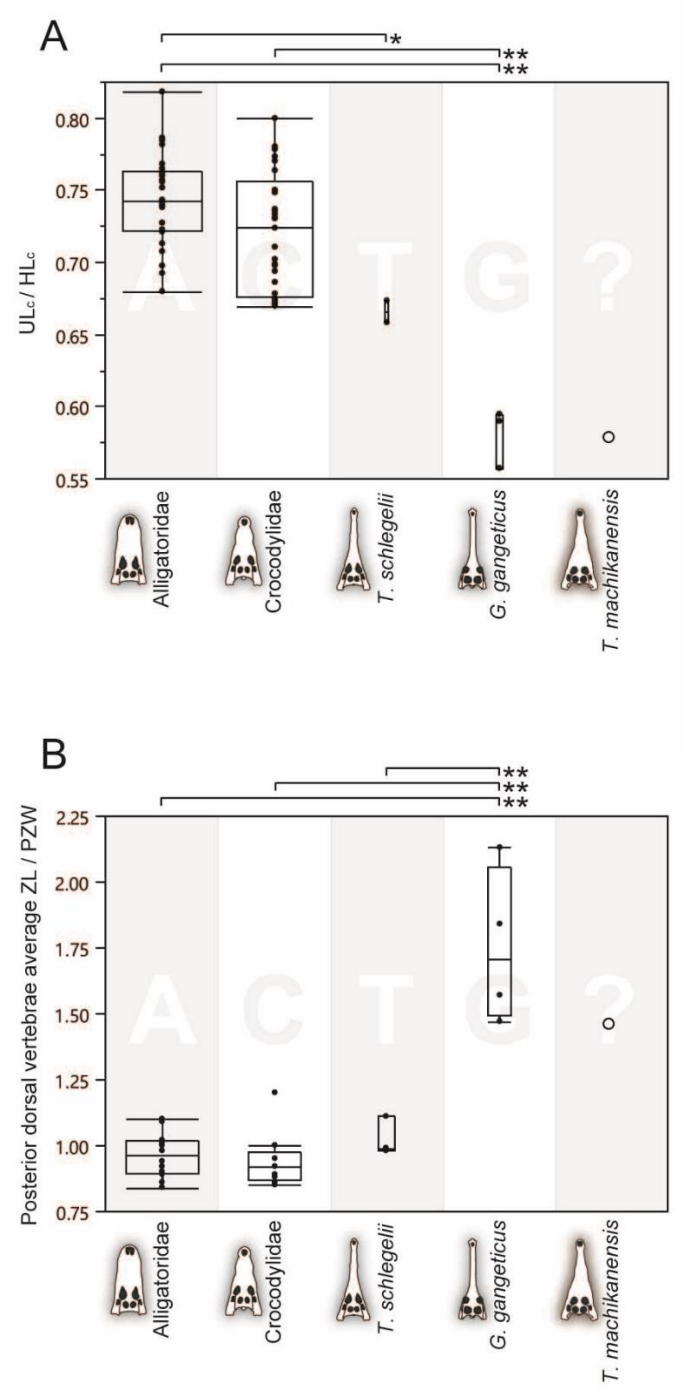


Fig. 8. Gradual specialization of cranial characters on the lineage of *Gavialis gangeticus* mapped on the constrained morphological tree (CMT) that is consistent with the molecular hypothesis.

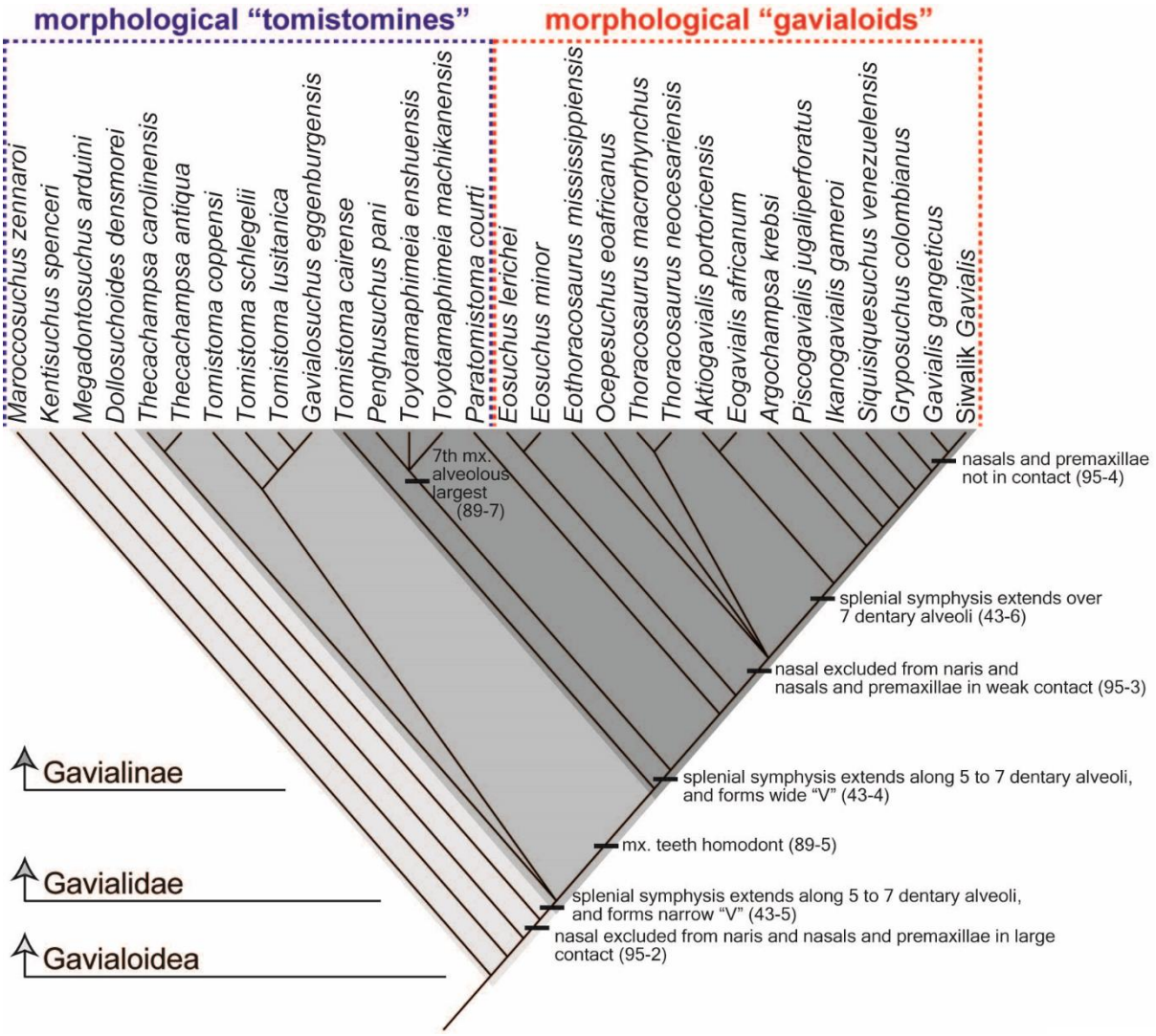


Fig. 9. A time calibrated tree of Gavialoidea, based on the constrained morphological tree (CMT) that is consistent with the molecular hypothesis.

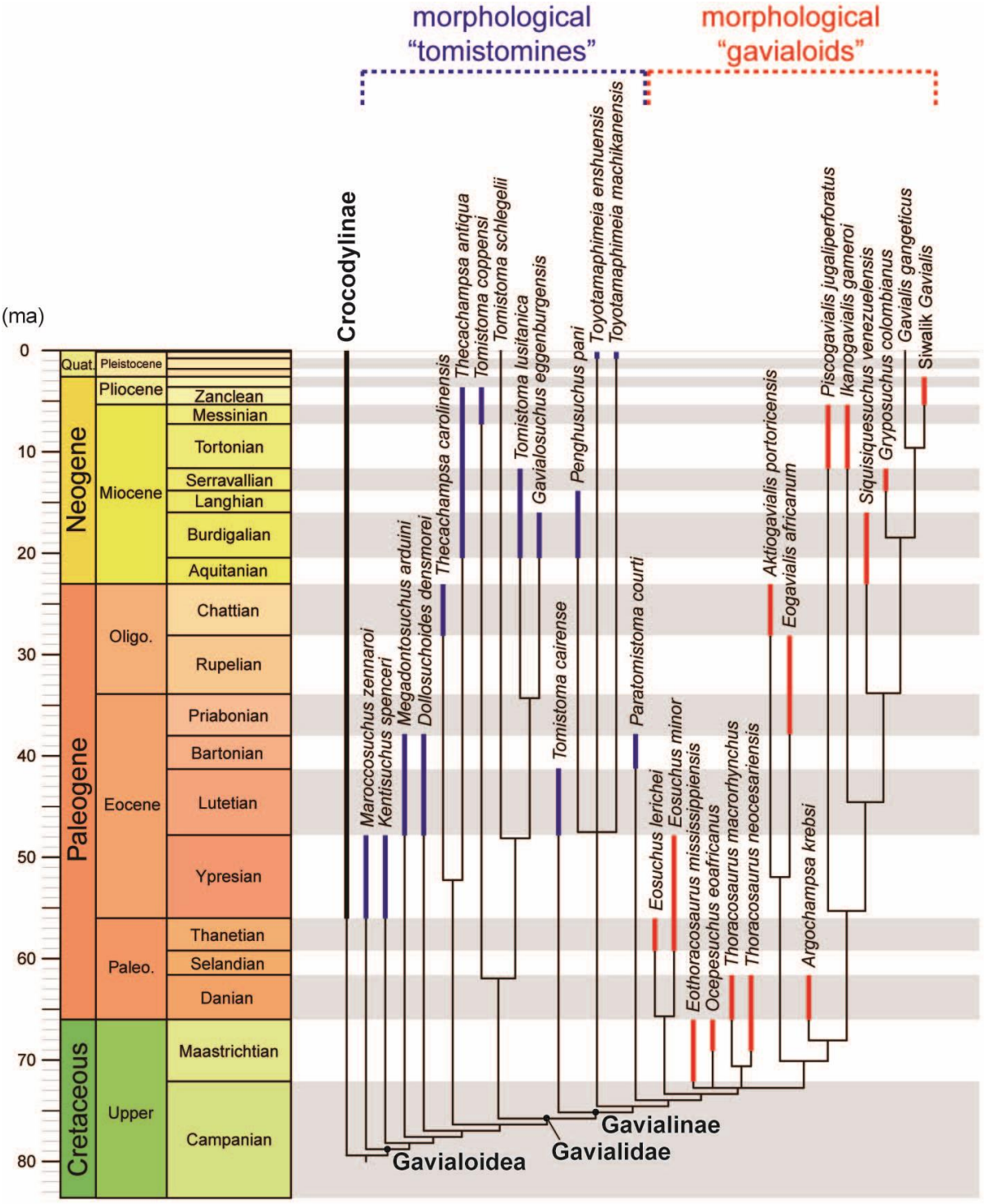


Table 1. Potential rostrum shape correlates detected by phylogenetic logistic regression.

Chracter No. and longirostrine states	Description of longirostrine states
43 (3,4,5)	splenial symphysis participates in the mandibular symphysis over the length of 5 tooth positions
77 (0)	dentary tooth 4 occludes in notch between premaxilla and maxilla early in ontogeny
89 (5)	maxillary alveoli in the "first wave" equal in size
95 (3,4)	nasals excluded from naris and nasals and premaxillae in weak or no contact
153 (2,3)	caudal margin of the foramen incisivum anterior to the caudal margin of penultimate premaxillary tooth
171 (1,2)	frontal ends at the same level or extends well anterior to the anterior extension of the prefrontal
176 (1,2)	mandibular symphysis extends posterior to the level of 14th dentary tooth
184 (1)	postorbital bar vertical and not visible in dorsal view
192 (1)	length between the posterior margin of external nares and to the posterodorsal extremity of premaxilla at least twice longer than the length between tip of snout to the posterior margin of external nare
195 (2)	dentary symphysis extends behind 8th dentary tooth
204 (2)	last premaxillary tooth placed posteromedial to the penultimate premaxillary tooth
205 (1)	premaxillae contact largely each other posterior to the external nare
208 (0)	parasagittal line extending from the lateral margin of orbit passes lateral to the maxillary teeth 3-6
223 (0)	anterior tip of frontal forms simple acute point
225 (2)	penultimate and antepenultimate premaxillary teeth nearly equal in size
227 (2)	maxillary alveoli in the "second wave" equal in size

Table 2. Result of the stratigraphic congruence tests.

	GER	MSM*	GERp range	MSMp* range
Unconstrained morphological tree	0.894 ($p < 0.001$)	0.168 ($p < 0.001$)	0.888 - 0.909	0.162 - 0.192
Constrained morphological tree	0.858 ($p < 0.001$)	0.131 ($p < 0.001$)	0.854 - 0.880	0.127 - 0.160

V. *Toyotamaphimeia* cf. *machikanensis* (Crocodylia, Tomistominae) from the Middle Pleistocene of Osaka, Japan, and crocodylian survivorship through the Pliocene-Pleistocene climatic oscillations

Introduction

Crocodylians rely on an external source of heat, and metabolic heat production minimally contributes to their thermal budget (Seebacher, Grigg, & Beard, 1999). Although extant crocodylian species can tolerate a wide range of temperatures, they may not survive with the body temperatures below 4–5°C, which is the critical minimum temperature measured for American alligators (Brisbin, Standora, & Vargo, 1982). Under freezing air temperatures with ice covering the water surface, large American alligators make small breathing holes around their noses and stay underwater until the air gets warm enough (Brisbin *et al.*, 1982; Hagan, Smithson, & Doerr, 1983; Brandt & Mazzotti, 1990; Grigg & Kirshner, 2015). Meanwhile, the minimum ambient environmental (water) temperature for American alligators is reported as 2–4°C (Brisbin *et al.*, 1982; Hagan *et al.*, 1983), which is close to the critical minimum body temperature for the same species, suggesting that extremely low environmental temperature limits individual survival. In the long run, prolonged cold temperatures delay and shorten the breeding seasons (Joanen & McNease, 1989), hence hindering reproductive success. Growth rates are also decreased in colder areas due to the longer periods of suppressed appetite, thus northern populations of the American alligator take longer time to reach maturity (Lance, 2003).

As consistent with these observations, temperature as well as the presence of standing water are principal factors determining the distribution of crocodylians (Markwick, 1998a). Modern crocodylians, including 27+ species in nine genera (Grigg & Kirshner, 2015) are mostly restricted to the tropics and subtropics. Their northern and southern distribution limits are ~36°N for *Alligator mississippiensis* in northeastern North Carolina (Elsey & Woodward, 2010) and ~33–34°S for *Caiman latirostris* in central Argentina and Uruguay (Verdade, Larriera, & Piña, 2010), while several other species polewardly extend their ranges to 30°N or 30°S (*Alligator sinensis*, *Caiman yacare*, *Crocodylus palustris*, *Crocodylus niloticus*, and

Gavialis gangeticus: Campos *et al.*, 2010; da Silva & Lenin, 2010; Jiang, 2010; Stevenson & Whitaker, 2010). As expected from extant species, the fossil record suggests that climate, and in particular temperature, contributed to biodiversity and evolution of crocodylomorphs (Markwick, 1998b; Carvalho *et al.*, 2010; Martin *et al.*, 2014; Mannion *et al.*, 2015). For the crown-group crocodylians, it has been known that their latitudinal ranges have been greatly changed since the Cretaceous Period, being much wider in warmer times and narrower in colder times (Berg, 1964). Using a large dataset of fossil crocodylians, Markwick (1998a, b, 2007) showed that during the Cretaceous–Middle Eocene, their distribution was extended to 60°N and higher paleolatitudes, with the most poleward record found in the Early Eocene of Ellesmere Island, Canadian Arctic Archipelago (Estes & Hutchison, 1980). After the appearance of the major ice sheets in the Late Eocene, their latitudinal range has gradually contracted. Through the rapid climatic deterioration over the late Pliocene–Pleistocene, they had been constrained to low latitudes and coastal regions of mid latitudes (Markwick, 1994, 1998a, b, 2007), similar to the Present. Because the late Pliocene–Pleistocene is characterized by the large orbital-scale climate oscillations, a number of studies has examined the effect of such large climate fluctuations on animal and plant biogeography and evolution, using both fossils and DNA (e.g., Hewitt, 2000; Davis & Shaw, 2001; Sommer & Zachos, 2009). However, for Pliocene-Pleistocene crocodylians, a chronologically continuous fossil record of geographically marginal populations in the mid-latitudes is yet to be provided, and the interplay of their distribution and climate patterns is rarely discussed.

The Japanese archipelago is rich in Pliocene-Pleistocene deposits, which are mainly distributed in the coastal areas of the Pacific Ocean and the Japan Sea (Itihara, 1993; Satoguchi & Nagahashi, 2012). Pliocene-Pleistocene crocodylians were abundantly found on the Pacific side of the Honshu Island, as best represented by a nearly complete skeleton of a tomistomine, *Toyotamaphimeia machikanensis* from the Middle Pleistocene Osaka Group (Kobatake *et al.*, 1965; Aoki, 1983; Kobayashi *et al.*, 2006). The Osaka Group, as well as other crocodylian bearing units (Kobiwako, Tokai, and Kazusa Groups) are located at 34–36°N that roughly equals the northern distribution limit of extant crocodylians. These deposits are intercalated by numerous tephra beds, and the local tephras are correlated with each other (Satoguchi & Nagahashi, 2012), thus crocodylian occurrences can be sequentially ordered. Moreover, for many rock units, local climates are reconstructed by using pollen and plant fossil records (e.g., Iwauchi, 1994; Momohara, 1994; Nakagawa *et al.*, 2002), therefore the crocodylian record can be discussed with the regional climate patterns.

In this paper, we describe a well preserved crocodylian from the Middle Pleistocene of Kishiwada City, Osaka Prefecture, which was preliminarily examined and briefly discussed in Taruno (1999) and Kobayashi et al. (2006). We also compile a well-dated fossil record of Japanese Pliocene-Pleistocene crocodylians. In reference to global and local climate data, crocodylian response and survival potential during the Pliocene-Pleistocene climate deterioration are discussed.

Materials and methods

Description and phylogenetic analysis

We describe the osteology of a new crocodylian material from the Middle Pleistocene of Osaka, Japan (KSNHM-F7-6) accessioned in the Natural History Museum, Kishiwada City, Osaka, Japan. A phylogenetic analysis was performed by adding KSNHM-F7-6 into Shan et al.'s (2017) taxon-character matrix that is largely based on Jouve et al. (2015), using TNT 1.5-beta (Goloboff, Farris, & Nixon, 2003). 67 ingroup taxa and 238 characters were employed in the analysis. *Bernissartia fagesii* was used as an outgroup, and a heuristic search was run with 1000 random addition sequence replicates of Wagner trees, and tree bisection reconnection branch swapping. 10 trees per replication were saved. All characters were unordered and equally weighted. Character scorings of the holotype of *Toyotamaphimeia machikanensis* (MOU F00001) and *Penghusuchus pani* (NMNS-005645) were modified based on the direct observation (see supplementary data).

Paleotemperature reconstruction

We reconstructed the coldest-month mean temperature (CMMT), warmest-month mean temperature (WMMT), and mean annual temperature (MAT) of the crocodylian-bearing interglacial stages (MIS 35, 31, 17 and 13) in the Kinki district of Japan, based on the climatic requirements of the nearest living relatives of the plant macrofossil (mainly fruit and seed fossils) assemblage components (Mosbrugger & Utescher, 1997; Yamakawa *et al.*, 2017). To reconstruct paleotemperatures at the site of fossil deposition, we selected the most thermophilous and the most cold-loving plants. These plants provide the warmest temperature values among the coldest limit temperatures and the coldest temperature values among the warmest limit temperatures respectively, of the macrofossil assemblage components. Paleotemperatures at the site of fossil deposition are warmer than the coldest temperature limit of the most thermophilous plants, while the warmest limit temperatures of the most

cold-loving plants constrains the warmest limit of estimated paleotemperature (Mosbrugger & Utescher, 1997). However, temperature estimates using the cold-loving plants should be interpreted carefully because such taxa could be transported from higher altitudes (Yamakawa *et al.*, 2017). Using the climate databases (IDBMC, 1984; JMA, 2002), we obtained the temperature variables at the selected plant's current northern/southern distribution limit in reference to local floras in which the distribution of taxa is described and/or mapped on an altitudinal scale of at least 100 m based on herbarium specimens and/or field observations.

Systematic paleontology

Crocodylia Gmelin, 1789 (*sensu* Benton & Clark, 1988)

Tomistominae Kälin, 1955 (*sensu* Brochu, 2003)

Toyotamaphimeia Aoki, 1983

Toyotamaphimeia cf. *machikanensis* Kamei *et* Matsumoto in Kobatake *et al.*, 1965

Material

KSNHM-F7-6, incomplete skull, mandible, tooth, hyoid, humerus, pubis, femur, vertebrae, rib and dorsal osteoderms.

Institutional abbreviations used in text

GMNH, Gunma Museum of Natural History, Gunma, Japan; IRSNB, Royal Belgian Institute of Natural Sciences, Brussels, Belgium; KSNHM, Natural History Museum, Kishiwada City, Osaka, Japan; LBM, Lake Biwa Museum, Shiga, Japan; MOU, Museum of Osaka University, Osaka, Japan; NMNS, National Museum of Natural Science, Taichung, Taiwan; OMNH, Osaka Museum of Natural History, Osaka, Japan.

Locality and horizon

A tomistomine fossil was discovered 7.5 m below the pavement at an intersection (N34.440119, E135.389582) in Nagareki-cho, Kishiwada City, Osaka prefecture in 1994, during a sewerage construction. The stratigraphic section of the locality (Fig. 1) shows that the specimen is derived from the sandy silt layer near the bottom of the marine bed 5 (Ma 5) of the Senpoku Formation of the upper part of the Osaka Group (Taruno, 1999). The Osaka Group is the Pliocene and the Pleistocene unit, which is exposed on the hills and terraces in the Osaka Basin. The lower to upper parts of the unit are characterized by cycles of fluvio-

lacustrine beds and 12 marine beds intercalated by a number of volcanic ash layers, in which the marine and volcanic ash layers serve as key beds (Itihara, 1993). As to the age of the fossil bearing horizon (Ma 5), Azuki tephra, the volcanic ash layer in the lower part of Ma 3 that is 20 m below Ma 5 was dated at 0.87±0.07 Ma by fission track dating (Nishimura & Sasajima, 1970). Recent correlation of the Osaka Group with the oxygen isotope record showed that Ma 5 was assignable to the marine isotope stage 17 (Masuda & Ito, 1999; Yoshikawa & Mitamura, 1999), which started at 712 ka (Lisiecki & Raymo, 2005).

Integrity of specimen

Remains can be attributed to a single individual (Taruno, 1999) because (1) most of the post-rostral skull elements were sutured when discovered, (2) all the skeletal elements were found in the small area (vertical shaft of 2.4 m diameter), and (3) all elements are compatible in size without element duplication. Here, cranial elements are described only. Description of hyoid and postcranial elements can be found in the supplementary information.

Skull description

In the skull, middle to posterior portion of the rostrum, skull table, infratemporal region, upper portion of the occipital are preserved (Fig. 2).

The maxillae preserve their middle to posterior portion, while the dorsal and palatal parts are separated. The dorsal surface of the maxillae is relatively smooth and is not ornamented with pits or grooves. In the dorsal part of maxillae, several alveoli are recognized. For the left maxilla, the fourth alveolus from the front is the largest. The palatal part of maxillae shows the anterolateral boarder of the suborbital fenestrae (SOF). In the left maxilla, the seventh alveolus anterior to the SOF is surrounded by the slightly elevated ridge, representing the largest maxillary tooth position. Except for this alveolus, the palatal surface of the maxillae is flat and at the same level with alveolar margins. Anterior to the left SOF, the suture for the palatine extends anteromedially. Medial to the third alveolus anterior to the SOF, a large oval shape foramen (11.2 mm long) for the exit of the cranial nerve V is present.

The nasals are rod-like anteriorly. Posteriorly near the level of the maxilla-lacrimal suture, the nasals widen and become sheet-like, and pinch the anterior frontal process.

The lacrimals form the anterior margin of the orbits, and extend far more anterior than the prefrontals and frontal, although their anterior extremities are broken.

Each prefrontal forms the anteromedial corner of the orbit. It is widest at the orbital

margin, and tapers anteriorly, with its anterior extremity projecting further forward than the frontal. On the dorsal surface, a small perforation is seen in the middle of this element.

The frontal forms the posteromedial corners of the orbits. It is narrow at the contact with the prefrontals, and sends a slender process anteriorly. Although its sutural contact with the nasals are damaged, its anterior tip seems to form a simple acute point. The shallowly pitted interorbital space is slightly concave, and its width is about twice wider than the space between supratemporal fenestrae (STF). The frontal-parietal suture is concave anteriorly, and the suture does not enter the STF. The frontal-postorbital suture is zigzag shaped.

The skull table is much shorter than that of *Toyotamaphimeia machikanensis* (MOU F00001), but this is most likely due to the reconstruction error in MOU F00001 (discussed later). The anterolateral corners of the table at the level of the postorbitals are rounded, and the lateral sides are nearly straight and are widened posteriorly. Each supratemporal fenestra is wider than long, and its size is about the same as the orbit. In dorsal view, the posterior border of the STF is straight, and its anterior border is angled near the parietal-postorbital suture. The posterior bar of the STF is thinner than the lateral bar in dorsal view, as in derived gavialoids and in some tomistomines including *T. machikanensis* (MOU F00001). On the posterior wall of the fenestra, the upper half of the temporal canal is preserved.

Each postorbital forms the anterolateral region of the skull table. It is wider than long, and the outer margin above the descending process is rounded. The anterolaterally oriented descending process of the postorbital is inset from the skull table, and bears a prominent projection dorsally (Fig. 3). The postorbital bar is generally massive, anteroposteriorly thick, and oriented nearly horizontally. The upper half or the bar is triangular in section, whereas the bottom half is more dorsoventrally compressed.

In lateral view, each squamosal sends a wedged anterior process into the postorbital bar (Fig. 3). The groove for the external ear valve musculature is shallow and is flared anteriorly. Posteriorly, a significant squamosal prong extends posterolaterally.

The parietal merges with the squamosal and both contribute to a thin posterior margin of the STF, and the constricted medial border of STF (Fig. 2C and E). Its dorsal surface near the posterior margin is slightly concave and ornamented with large pits.

Each jugal sends a dorsoventrally thin ascending process, which borders the posterolateral corner of the orbit. The ascending process is inset from the main body of the jugal, separated by a deep gutter (Fig. 2C and E). Medially, the suture for the ectopterygoid extends up to the middle of the postorbital bar. The dorsal margin of the jugal lateral to the postorbital bar is

straight, while the ventral margin is concave (Fig. 3). Ventrally, just posterior to the suture of the ectopterygoid, a large depression (about 15.0 mm long axis: Fig. 4A) is present, and the bottom of the fossa is perforated as in *T. machikanensis* (MOU F00001). This perforation is interconnected with a large foramen on the dorsal surface of the jugal at the base of the postorbital bar. On the medial surface, a medial jugal foramen cannot be observed because this part is crushed.

The quadratojugals are incomplete and do not preserve the spina quadratojugalis, or the ascending process which would dorsally border the infratemporal fenestra. The posterolateral angle of the infratemporal fenestra is bordered by the quadratojugal-jugal suture, or quadratojugal alone. Ventrally, each quadratojugal bears a large foramen (about 5 mm diameter) near its posterior end (Fig. 4A).

The dorsal surface of the quadrates is damaged, whereas their ventral surfaces preserve muscle scars (crest B and B' in Iordansky, 1973: Fig. 4A). Posteriorly, the quadrate shows the lateral half of the cranio-quadrate opening (Fig. 2A and B). The quadrate foramen aëreum seems large, and opens at the dorsomedial corner of the medial hemicondyle.

In posterior view, the supraoccipital is triangular in shape, and much wider than deep (Fig. 2A and B). It is exposed on the posterior border of the skull table. The lateral posterior tuberosity is not prominent, and is not largely visible from a dorsal view. Lateral to the tuberosity, the postemporal fenestrae are damaged, but they appear to be tear drop shaped and widened laterally. The ventral portion of the right exoccipital shows the vagus foramen, which would be positioned lateral to the foramen magnum.

The only preserved tooth (Fig. 2F) is sharp and recurved. Its crown height and mesiodistal width at the base are 25.5 mm and 10.3 mm, respectively, and the sectional shape is conical. There are two carinae on the opposed sides of the crown, and numerous striations run between them.

Mandible description

Fragments of the anterior portion of the mandible, and most of the posterior mandibular elements (dentary, surangular, angular, articular) are preserved (Fig. 5).

The anterior and middle portions of the left dentary preserve fourteen alveoli in total. Each alveolus projects anterodorsally, but the anterior alveoli are nearly horizontally oriented. In medial view, the level of alveoli ascends posteriorly, and the groove below the alveoli widens and deepens accordingly. Laterally, there are a series of foramina below the tooth row, and

the foramina are larger posteriorly. In the posterior most part of the dentary, shallow grooves extend to the posterior dentary process between the bifurcated anterior processes of the surangular, and to the anterior corner of the external mandibular fenestra (Fig. 5A and B).

The symphyseal part of the left splenial is adjacent to at least four dentary alveoli (Fig. 5C and D). When its broken anterior and posterior extents are taken into account, it is most likely adjacent to five alveoli. In dorsal view, the splenial forms a slightly constricted V-shape as in *T. machikanensis* and *P. pani* (Kobayashi *et al.*, 2006; Shan *et al.*, 2009). Posterior to the symphysis, four alveoli are present, as inferred from a series of concavity on the lateral surface of the splenial.

The anterior processes of the surangular are unequal in length, and the dorsal one extends far anteriorly than the ventral one. The lateral surface of the surangular is flat posterior to the external mandibular fenestra. Posterior to it, the surangular forms a lateral wall of the glenoid fossa, which continues to its dorsal tip. Immediately lateral to the glenoid fossa is a series of vertically placed depressions. Medially, the surangular-articular suture is simple (articular does not have an anterior process) and the lingual foramen is entirely on the surangular (Fig. 5E and F).

The angular borders the external mandibular fenestra ventrally, and sutures with the ventral process of the dentary near the anterior end of the fenestra. The anterior process of the angular wedges between the dentary and splenial at the level of the last dentary alveolus.

The articular preserves a glenoid fossa with two depressions, in which the lateral one is larger than the medial one. The surangular-articular suture within the glenoid fossa is anteroposteriorly straight (Fig. 5C–D). The anterior surface of the articular is flat without the sulcus between the surangular-articular suture (Fig. 5E and F).

The external mandibular fenestra is long and narrow (Fig. 5A and B). The posterior process of the dentary intersects with the surangular anterior to the dorsal apex of the fenestra. The ventral margin of the fenestra is straight anteriorly and rounded posteriorly. The posterior corner of the fenestra is bordered by the surangular, and slightly ventral to it the surangular-angular suture intersects with the fenestra.

Taxonomic identification

The crocodylian from Kishiwada City, Osaka prefecture, Japan (hereafter the Kishiwada specimen) exhibits tooth size heterodonty, and 7th maxillary tooth anterior to the suborbital fenestra is largest, as in slender-snouted taxa including tomistomines (e.g., *Kentisuchus*

spenceri, *Thecachampsa antiqua*, *Maomingosuchus petrolica*, *Penghusuchus pani*, and *Toyotamaphimeia machikanensis*: Owen, 1850; Kobayashi *et al.*, 2006; Shan *et al.*, 2009, 2017). The splenial symphysis of the Kishiwada specimen forms slightly constricted but relatively broad V-shape, which extends about 4–5 dentary tooth positions as in moderately longirostorine gavialoids and tomistomines, including Taiwanese *P. pani* and Japanese *T. machikanensis* (Kobayashi *et al.*, 2006; Shan *et al.*, 2009). In an extant tomistomine *Tomistoma schlegelii*, the symphysis is more narrowly constricted. On the skull table, the posterior supratemporal bar of the Kishiwada specimen is thinner than the lateral bar, but is not extremely thin as in gavialoids, similar to some tomistomines (e.g., *Thecachampsa antiqua*, *Gavialosuchus eggenburgensis*, *Tomistoma lusitanica*, and *T. machikanensis*: Toula & Kail, 1885; Antunes, 1961; Myrick, 2001; Kobayashi *et al.*, 2006). Posterior part of the skull table is damaged in *P. pani* (Shan *et al.*, 2009). Along with the above characters, the Kishiwada specimen shares a unique character with the holotype of *T. machikanensis* (MOU F00001): deep and large depression with bottom perforations on the ventral part of the jugal at the base of postorbital bar (Fig. 4A). Our observation revealed that a similar character is also present in the extant crocodylian *Mecistops cataphractus* (both in West and Central African lineages proposed by Shirley *et al.*, 2014: Fig. 4B) and *Crocodylus intermedius*. In these species, the ventral jugal depression is shallower than that in the holotype of *T. machikanensis* and the Kishiwada specimen, while the bottom perforation leads to a large internal room at the base of the postorbital bar, and this room is interconnected with the medial and dorsal jugal foramina. This character is unobservable in *P. pani* (Shan *et al.*, 2009). In other crocodylians including *T. schlegelii*, a ventral jugal depression is not seen, yet there is a series of small perforations on the ventral jugal at the base of the postorbital bar, which may be interconnected with the dorsal and medial jugal foramina.

Among Asian tomistomines, Japanese materials (the Kishiwada specimen and the holotype of *T. machikanensis*) and Chinese and Taiwanese materials (*Maomingosuchus petrolica* and *Penghusuchus pani*) differ in the sutural pattern of the antorbital part. The degree of anterior extension of antorbital elements are frontal < prefrontal < jugal < lacrimal in Japanese materials (anterior tip of jugal missing in the Kishiwada specimen), consistent with an extant tomistomine *T. schlegelii*. On the other hand, the relationship is frontal < prefrontal = jugal = lacrimal in *P. pani* (Shan *et al.*, 2009) and frontal = prefrontal = jugal < lacrimal in *M. petrolica* (Shan *et al.*, 2017).

Since the original report by Taruno (1999), the taxonomic status of the Kishiwada

specimen remained obscure until now. Taruno (1999) tentatively concluded that the Kishiwada specimen could be referred to as *T. machikanensis* based on the following similarities: narrow snout; orbit sub-circular in shape; orbit and supratemporal fenestra is subequal in size; short interorbital width; large supratemporal fenestrae. He also stated that both forms may also be similar in: nasals excluded from external naris; mandibular symphysis long, extending to the level of ?13th and ?14th tooth (alveolus); large 7th maxillary tooth. However, most of the characters he mentioned were symplesiomorphic and not diagnostic at lower taxonomic levels (Kobayashi *et al.*, 2006). Only the large 7th maxillary tooth (alveolus) is diagnostic of the clade of *Penghusuchus pani* from the Miocene of Taiwan plus *T. machikanensis* (Jouve *et al.*, 2015), although the character state in the Kishiwada specimen is not confirmed from the preserved parts. Taruno (1999) also pointed out some differences between the two forms, which were additionally discussed in Kobayashi et al. (2006). They argued that the Kishiwada specimen has a slenderer snout and wider skull table compared to the holotype of *T. machikanensis*. Furthermore, the Kishiwada specimen's supratemporal fenestrae are wider than long, and frontal-parietal suture is concavo-convex, different from the holotype of *T. machikanensis* (Kobayashi *et al.*, 2006) (Fig. 6).

Among these differences, slenderness of snout is not taxonomically informative because living tomistomine *Tomistoma schlegelii* develops more robust snout in the later growth stages (Müller, 1927; Iijima, 2017; Fig. 7 and supplementary data). The large adults [BMNH 94.2.21.1 (skull length 839 mm, width 409 mm); USNM 211322 (skull length 783 mm, width 354 mm)] have wide and nearly triangular skulls as in the holotype of *T. machikanensis*. Since the skull of Kishiwada specimen is smaller than the holotype (skull width of the Kishiwada specimen is about 83% of that in the holotype of *T. machikanensis*), the difference in the snout slenderness is likely attributed to the different ontogenetic stages.

The remaining incongruence between the two specimens was probably brought when reconstructing the skull table of the holotype of *T. machikanensis*. The region in between the possible frontal-parietal suture and the interfenestral bar is filled with plaster in the holotype (Kobayashi *et al.*, 2006; Fig. 6). Our observation of the holotype shows that the medial edge of the supratemporal fenestra (STF) is unnaturally angled, suggesting that the STF shape as well as the skull table would be much shorter. Accordingly, the frontal-parietal suture cannot be observed, and the state of this character is questionable.

An additional feature pointed by Furui et al. (2012) is a foramen on the ventral surface of the quadratojugal in the Kishiwada specimen (Fig. 4A). Observation on recent crocodylian

species reveals that this character is widely present in Crocodylia including *Tomistoma*, and large adults have reasonably large foramina (BMNH 94.2.21.1; USNM 211322). Although the absence of such foramina in the holotype of *T. machikanensis* cannot be explained, this character is probably not diagnostically important.

To confirm the phylogenetic position of the Kishiwada specimen (KSNHM-F7-6), a phylogenetic analysis was performed by adding the Kishiwada specimen into Jouve et al.'s (2015) taxon-character matrix. Although many skeletal elements are missing in the Kishiwada specimen, all codable characters are consistent with the holotype of *T. machikanensis.* The analysis recovered 232 equally parsimonious trees (tree length, 893; CI, 0.346; RI, 0.7). The Kishiwada specimen is deeply nested in the subfamily Tomistominae, and forms a sister-taxon relationship with the holotype of *T. machikanensis* (Fig. 8), supported by one unambiguous synapomorphy [character 47 (1): Angular-surangular suture passes broadly along ventral margin of external mandibular fenestra in the late ontogeny].

In sum, (1) character comparison combined with a phylogenetic analysis, (2) assessment of ontogenetic change in the skull shape using the modern relative *Tomistoma*, and (3) taking into account the reconstruction error in the holotype of *T. machikanensis* (MOU F00001) together warrant the taxonomic status of the Kishiwada specimen (KSNHM-F7-6) as *Toyotamaphimeia* cf. *machikanensis*.

Discussion: Pliocene-Pleistocene crocodylian record in Japan

Pliocene

Four localities in Honshu Island, and one locality in Kyushu island are known for Pliocene crocodylians (Fig. 9 and Table 1). Hattorigawa River floor in Iga City, Mie Prefecture yields numerous fragmentary elements including a right premaxilla, teeth, postcranial fragments, and trace fossils. The right premaxilla (Tanimoto and Okuyama, 1998; Fig. 10) is mediolaterally narrow, and its lateral margin is subparallel to the midline. The premaxillary tooth count is five as in *Toyotamaphimeia machikanensis* (Kobatake *et al.*, 1965; Aoki, 1983; Kobayashi *et al.*, 2006), in which 2nd to 5th alveoli are preserved. This narrow premaxilla, with several slender and recurved teeth from ~3.5 Ma of Iga (below Hattorigawa II tephra: Satoguchi & Nagahashi, 2012) suggest that a slender-snouted crocodylian, possibly a relative of *T. machikanensis*, was present in the Late Pliocene of Japan. Crocodylian materials from the similar age include the posterior portion of a skull, axial and limb fragments, and footprints from ~3.5 Ma of Suzukagawa River floor in Kameyama City, Mie Prefecture

(Kobayashi, 2009; Okamura, 2009; Tanaka & Mikami, 2009; Tsumura, 2009; Nakagawa, 2014), teeth and osteoderms from 3.6–3.1 Ma of Isshinden-Kozubeta, Tsu City, Mie Prefecture (Mie Prefectural Museum, 2011; Hoshi, 2016), isolated teeth from ~2.7 Ma of Koka City, Shiga Prefecture (Matsuoka, Okamura, & Tamura, 1991; Satoguchi & Nagahashi, 2012), and multitaxic bonebeds from ~3.0 Ma of Fukami River bank and floor, Ajimu, Usa City, Oita Prefecture (Aoki, 1983; Hoshizumi & Morishita, 1993; Hase *et al.*, 2001; Satoguchi, 2001, 2008; Iijima, Tahakashi, & Kobayashi, 2016). The last locality produced a number of sharp pointed teeth as well as *Alligator sinensis* materials, demonstrating the existence of a slender- and broad snouted crocodylians in the Late Pliocene of Kyushu.

Pleistocene

The Pleistocene crocodylian record is divided into early–mid Early Pleistocene (2.4–1.4 Ma) and late Early and Middle Pleistocene (1.2–0.3 Ma) (Figs. 8 and Table 1). The former includes teeth from 2.5–2.3 Ma of Goshiki Town, Hyogo Prefecture (above Kenjyogaoka II tephra: Nanko, 1996; Katoh et al., 2004) and isolated teeth from 2.1–1.9 Ma of four localities in Shiga Prefecture (below Narutani tephra, below Hara tephra, and around Kiryu I tephra: Isobe, 1990; Matsuoka *et al.*, 1991; Takahashi, 1998; Yamamoto, 1998; Watanabe & Tanimoto, 2005; Abe, 2011). All of these teeth are slender and recurved. The other material is postcrania from ~1.4 Ma of Tama River floor, Kawasaki City, Kanagawa Prefecture (around Nishikubo tephra: Koizumi, 1995; Suzuki & Murata, 2011). This material is represented by a midline dorsal or pelvic osteoderm that is significantly wider than long without keel on its dorsal surface, being consistent with *T. machikanensis*.

The late Early and Middle Pleistocene crocodylians include several well dated materials from the Osaka Group of Osaka and Hyogo Prefectures, the oldest of which is an isolated vertebra from ~1.2 Ma of Yagi, Akashi City, Hyogo Prefecture (Byobugaura clay bed of the Osaka Group: Taruno, 1979). A bonebed material from ~1.1 Ma of Kaminokuchi, Takatsuki City, Osaka Prefecture (above Ma 1 bed of the Osaka Group: Kobayashi, 1977; Taruno, 1979) consists of a tooth, cervical to caudal vertebrae, ribs, and pelvic girdle elements (Fig. 11). The left iliac blade has a rounded dorsal margin without strong indentation, and there is a prominent anterior process, which is characteristic of *Bernissartia*, gavialoids, *Borealosuchus*, basal alligatoroids, and some “tomistomines,” such as *Penghusuchus* and *Toyotamaphimeia* (Brochu, 1997b; Kobayashi *et al.*, 2006; Shan *et al.*, 2009). Hence, this specimen might be a close relative of *T. machikanensis*. Two *Toyotamaphimeia* specimens

from ~0.7 Ma of Nagareki-cho, Kishiwada City and ~0.5 Ma of Machikaneyama-cho, Toyonaka City, Osaka Prefecture (Bottom of Ma 5 and below Ma 8 beds of the Osaka Group: Kobatake *et al.*, 1965; Aoki, 1983; Taruno, 1999; Kobayashi *et al.*, 2006; this study) are among the best preserved specimens of Japanese Plio-Pleistocene crocodylians. The youngest crocodylian record from Japan consists of more than a thousand skeletal fragments from ~0.4–0.3 Ma of the limestone fissure deposit in Inasa-cho, Hamamatsu City, Shizuoka Prefecture (below Yage tephra of the lower "Yage" Formation: Nojima, 2002; Lisiecki & Raymo, 2005; Nojima *et al.*, 2014). Nojima (2002) suggested a close affinity of this specimen with extant *Tomistoma* based on the cranial and tooth morphology.

Japanese crocodylian survivorship in the Plio-Pleistocene climatic oscillations

Our review of Pliocene-Pleistocene records of Japanese crocodylians (Figs. 9 and 12, Table 1) reveals the continuous occurrence of crocodylians in the Kinki, Tokai, and Kanto districts since the Pliocene until the late Middle Pleistocene. Those occurrences are chronologically well constrained by use of tephro- and magnetostratigraphy (Satoguchi & Nagahashi, 2012). Furthermore, the upper part of the Osaka Group was correlated with oxygen isotope stages (e.g., Masuda & Ito, 1999; Yoshikawa & Mitamura, 1999), by assigning marine clay beds into interglacial stages of the oxygen isotope curve (Lisiecki & Raymo, 2005). Ma0 and Ma1 marine clay beds, which yield the late Early Pleistocene crocodylians, are correlated with MIS 35 and MIS 31, respectively (Yoshikawa & Mitamura, 1999). Ma5 marine clay bed, from which the *Toyotamaphimeia* from Kishiwada was obtained, is correlated with MIS 17 (Yoshikawa & Mitamura, 1999; Masuda & Ito, 1999). A sandy clay bed including the Kasuri tephra, from which another *Toyotamaphimeia* crocodylian occurred, is one meter below Ma8 marine clay bed that is assigned to MIS 13 (Yoshikawa & Mitamura, 1999). A potential *Toyotamaphimeia* record from the Shizuoka Prefecture (F3 bed of the lower "Yage" Formation) is correlated with MIS 9 (Nojima *et al.*, 2014).

These crocodylian bearing horizons are situated in and/or near the marine clay beds in the Osaka Group, suggesting interglacial sea-level highstands. Even sediments associated with the Kasuri tephra below Ma8 marine clay bed were deposited under an interglacial condition because many thermophilous trees were found below the tephra bed (Ito, Momohara, & Zhou, 2017). Thus, paleotemperature reconstruction of the corresponding interglacial stages is important for discussing the crocodylian survivorship during the Early to Middle Pleistocene of Japan. The temperature estimates (see 2.2. for methodology) of the crocodylian

bearing beds in the lower and upper parts of the Osaka Group based on the thermophilous taxa are CMMT of 0.7–3.0°C, MAT of 13.4–13.6°C, and WMMT of 24.2–25.0°C (Table 2). The alternative temperature estimates using the cold-loving taxa (CMMT: -1.5–1.8°C; MAT: 9.8–12.2°C; WMMT: 21.9–23.1°C) should be interpreted carefully because such taxa could be transported from higher altitudes.

The previous analysis of recent crocodylian distribution indicated that temperature is the principal component limiting their distribution, although the presence of standing water is also important for their survival (Markwick, 1998a). According to his study, three temperature indices, 1) CMMT of at least 5.5°C, 2) MAT of at least 14.2°C, and 3) relatively lower mean annual range of temperature (Markwick, 1998a) together influence crocodylian distribution, thereby fossil crocodylians have been used as an climate proxy in the past (Markwick, 1994, 1998a, b, 2007). However, living species' current distribution, which is the basis for the thermal limit estimation of crocodylians, differ slightly from the historical distribution during the last few centuries (Markwick, 1998a). For instance, the Chinese alligator *Alligator sinensis* showed much wider distribution before mid 19th through early 20th centuries along the lower reach of the Yangtze River (Wen *et al.*, 1981). Recent climate data of China (IDBMC, 1984) suggests that the historical population of *A. sinensis* might tolerate increased seasonality and severe winter at some localities including Nanjing, Jiangsu (CMMT: 2.1°C; MAT: 15.3°C; WMMT: 27.9°C), Hefei, Anhui (CMMT: 2.1°C; MAT: 15.7°C; WMMT: 28.3°C), and Wuhu, Anhui (CMMT: 2.9°C; MAT: 16.0°C; WMMT: 28.7°C). Thus, it is conceivable that crocodylians could cope with slightly more severe climate than previously perceived. Nonetheless, Japanese Pleistocene crocodylians in the Kinki district were supposed to be living near the lower thermal limit of crocodylians during the interglacial stages.

Climate deterioration during glacial stages, which became severer in the late Quaternary, would have impacted the crocodylian population in Japan. Paleotemperatures during a glacial stage in 1.9–1.8 Ma reconstructed from plant macrofossil assemblages in the Kobiwako Group in the central Kinki district were estimated as CMMT of -9–-1.6°C, MAT of 5.1–10.2°C, and WMMT of 17.3–23.4°C (Yamakawa *et al.*, 2017). The subfreezing winter and low mean annual temperature prevented crocodylian survival in the central Kinki district during the glacial stages. They had most likely moved to the refugia along the Pacific coast and the exposed shelf along the Ryukyu islands, extending southwest from Kyushu.

The potential glacial refugia of crocodylians can be inferred based on the refugia position

of plants whose thermal requirements are similar to crocodylians. *Elaeocarpus sylvestris* var. *ellipticus* (Elaeocarpaceae) and *Prunus zippeliana* (Rosaceae) are evergreen broadleaved trees with their northern distribution limits in the southern Boso Peninsula (Fig. 9), where the temperature condition is close to the crocodylian thermal limit (e.g., CMMT: 5.7°C; MAT: 15.7°C; WMMT: 26.7°C in Chiba City, Chiba Prefecture) (JMA, 2002). Their refugia during the last glacial maximum was distributed along the Pacific coast between the Muroto Peninsula and south Kyushu (Fig. 9), where rare haplotypes are found from the current local populations (Aoki *et al.*, 2004). This molecular evidence demonstrates the crocodylian survival in lowlands along the Pacific coast south of the Muroto Peninsula during the glacial stages.

After the end of each glacial period, crocodylians had perhaps re-expanded the distribution to the north, because their record in the central Honshu extends over multiple prominent isotopic glacial peaks (MIS 12 and 16) in the Middle Pleistocene (Fig. 12). Long term monitoring surveys on once depleted populations of the saltwater crocodiles demonstrated that there was a rapid increase in the population density after the hunting stopped (Webb *et al.*, 2000; Fukuda *et al.*, 2011). This strong recovery, with the ability of long distance travel in both freshwater and estuarine habitats (Campos *et al.*, 2006; Read *et al.*, 2007; Lance *et al.*, 2011) could help the multiple range re-expansion over the Plio-Pleistocene.

It is also possible that crocodylians had died out from Japan during glacial periods, but they had migrated from the Asian continent through a land bridge or by coasting when the climate was moderate. Stratigraphic distribution of warm-water diatoms, foraminifers, and mollusks in the Plio-Pleistocene deposits along the coast of the Japan Sea suggests that the southern channel of the Japan Sea was periodically opened for few interglacial intervals during 3.5–1.7 Ma, but for almost all interglacial intervals after 1.7 Ma (Kitamura *et al.*, 2001; Kitamura & Kimoto, 2006). Hence, crocodylians might have been able to disperse from the mainland Asia into Japan across the land bridge until 1.7 Ma. Even without the formation of a land bridge, they would migrate across ocean via fluvial capture on the shallow shelf, as proposed for the *Gavialis* dispersal from the mainland Asia into Java in the Pleistocene (Martin *et al.*, 2012). In support of this view, relative abundance data of a warm-water planktonic foraminifera through time suggested that the Tsushima Current, which passes the southern channel of Japan through the Japan Sea, was much lower in salinity during interglacial periods until 1.7 Ma (Kitamura & Kimoto, 2006), probably due to the freshwater delivered from the eastwardly extended Chinese mainland (Nakamura *et al.*,

1999).

Because of the constantly opened southern channel of the Japan Sea, and increased volume and higher salinity of the Tsushima Current during interglacial highstands after 1.7 Ma (Kitamura & Kimoto, 2006), crocodylian migrations between the Asian continent and Japan became restricted by means of transoceanic travels in saline water. Among Japanese crocodylians, a tomistomine *Toyotamaphimeia* might have salt tolerance because many of the fossil tomistomines have been recovered from estuarine and coastal settings (e.g., Brochu, 2003; Piras *et al.*, 2007; Jouve *et al.*, 2015), although the living relative *Tomistoma* is restricted to freshwater. On the other hand, the Pliocene *Alligator sinensis* from Japan (Iijima *et al.*, 2016) most likely lacked lingual salt gland as in extant *Alligator* (Taplin & Grigg, 1989). This prevented Japanese *A. sinensis* from migrating across ocean after severe glacial periods, although short offshore travels could be possible, as rarely reported in extant alligatorids (Elsey, 2005; Grigg & Kirshner, 2015). In the future, stable isotope analyses on fossil teeth, as implemented in previous works (Wheatley, 2010; Martin *et al.*, 2015; Whiting, Steadman, & Krigbaum, 2016) will be helpful to discuss the physiology and dispersal potential of Japanese crocodylians.

During the Plio-Pleistocene, both of two Japanese crocodylian lineages (*Toyotamaphimeia* and *Alligator*) had wider distributions in the East Asia across the East China Sea. Fossil crocodylians showing affinity with East Asian tomistomines (large 7th maxillary tooth: synapomorphy of *Toyotamaphimeia* + *Penghusuchus*) were found in the Plio-Pleistocene of Taiwan (Takekawa *et al.*, 2017) and the Holocene of Guangdong Province in China (Zhao, Zong, & Ma, 1986). Similarly, definite and potential *A. sinensis* fossils were recovered from the Pleistocene of Taiwan (Shan, Cheng, & Wu, 2013), Guangdong Province in China (Huang *et al.*, 1988), and ?Late Miocene-Pleistocene of Thailand (Claude *et al.*, 2011). Geographical ranges of these two East Asian crocodylian lineages were largely contracted by the climate deterioration during the Plio-Pleistocene and anthropogenic effects after the rise of humans, leaving only *A. sinensis* in Anhui Province, China at present (Zhao *et al.*, 1986; Thorbjarnarson & Wang, 2010). Comparable range contraction of crocodylians occurred globally in the Plio-Pleistocene, and crocodylians were progressively restricted to major river systems and coastal plains in lower latitudes towards the Recent (Markwick, 1994, 1998a, 1998b, 2007).

Conclusions

A description of a crocodylian material from the Middle Pleistocene of Japan, and compilation of the fossil record of Japanese Pliocene-Pleistocene crocodylians shows that crocodylians including a tomistomine *Toyotamaphimeia* had continuously existed from ~3.5 Ma in the Pliocene through ~0.3 Ma in the Pleistocene in Japan. Paleotemperature estimates of the crocodylian-bearing interglacial beds suggest that Japanese Pleistocene crocodylians were living near their perceived lower thermal limit. During glacial periods, they might have survived in the southern refugia, or became locally extinct from Japan. The strong population recovery, combined with potential dispersals from the mainland Asia across land bridges and through oceans could explain the continuity of the Japanese crocodylian record during the Pliocene-Pleistocene. However, repeated range contractions in the glacial periods might have reduced the genetic diversity of crocodylians, leading to their final demise in Japan.

This chapter was accepted as:

Iijima M, Momohara A, Kobayashi Y, Hayashi S, Ikeda T, Taruno H, Watanabe K, Tanimoto M, Furui S. In press. *Toyotamaphimeia* cf. *machikanensis* (Crocodylia, Tomistominae) from the Middle Pleistocene of Osaka, Japan, and crocodylian survivorship through the Pliocene-Pleistocene climatic oscillation. *Palaeogeography, Palaeoclimatology, Palaeoecology*.

Fig. 1. A, localities of two Japanese tomistomine specimens (MOU F00001 and KSNHM-F7-6). B, stratigraphic column of the locality of the Kishiwada specimen (based on Yoshikawa, 1993; Taruno, 1999). Ma, marine bed in the Osaka Group. A crocodylian silhouette modified from Kobayashi et al. (2006).

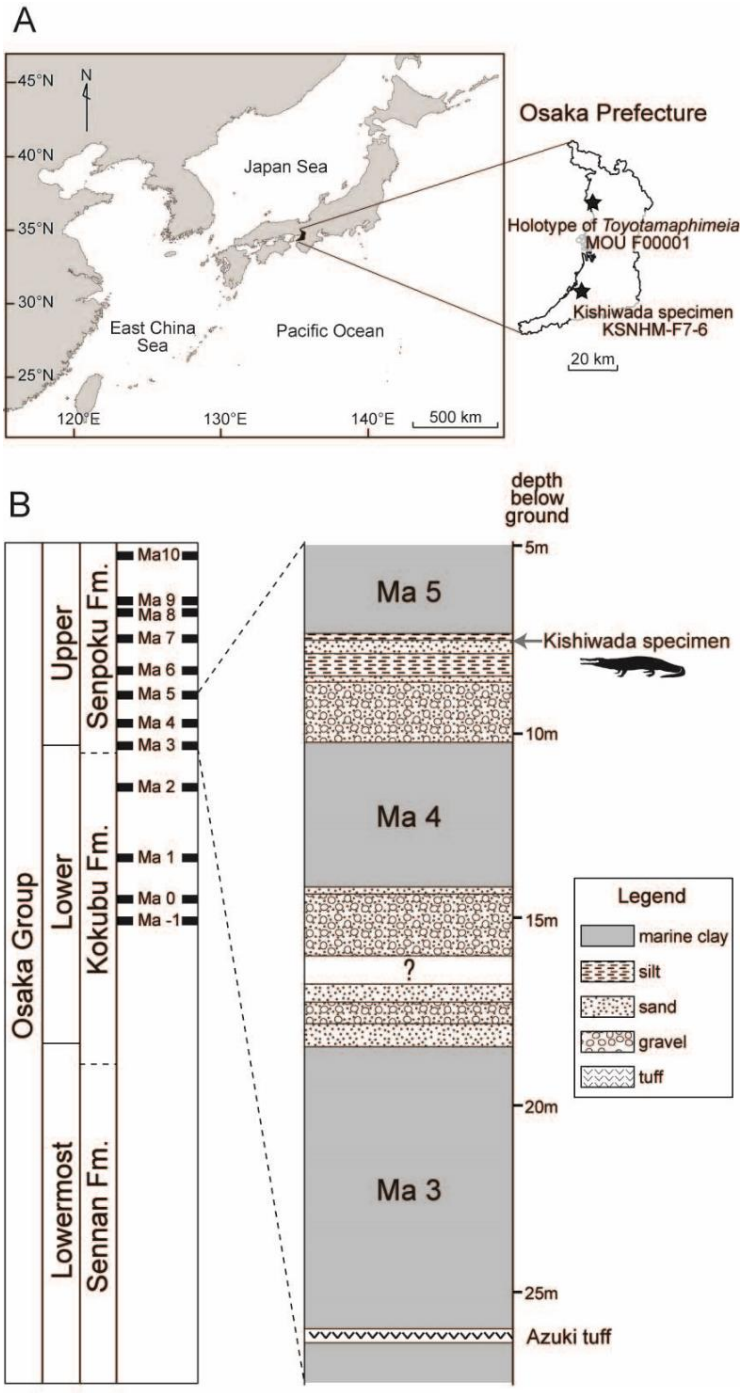


Fig. 2. KSNHM-F7-6 (Kishiwada specimen), A and B, skull in posterior view; C and E, skull in dorsal view; D, palatal maxillae in ventral view; F, tooth in mesial (distal) view. Stippled area indicates damaged bone. cnV, exit for cranial nerve V; cqo, cranio-quadrate opening; eoc, exoccipital; f, frontal; fae.q, quadrate foramen aëreum; j, jugal; lac, lacrimal; mx, maxilla; n, nasal; p, parietal; po, postorbital; perf, perforation; prf, prefrontal; ptf, postemporal fenestra; q, quadrate; qj, quadratojugal; soc, supraoccipital; sof, suborbital fenestra; sq, squamosal; vf, vagus foramen. Scale bars are 10 cm (A–E) and 2 cm (F).

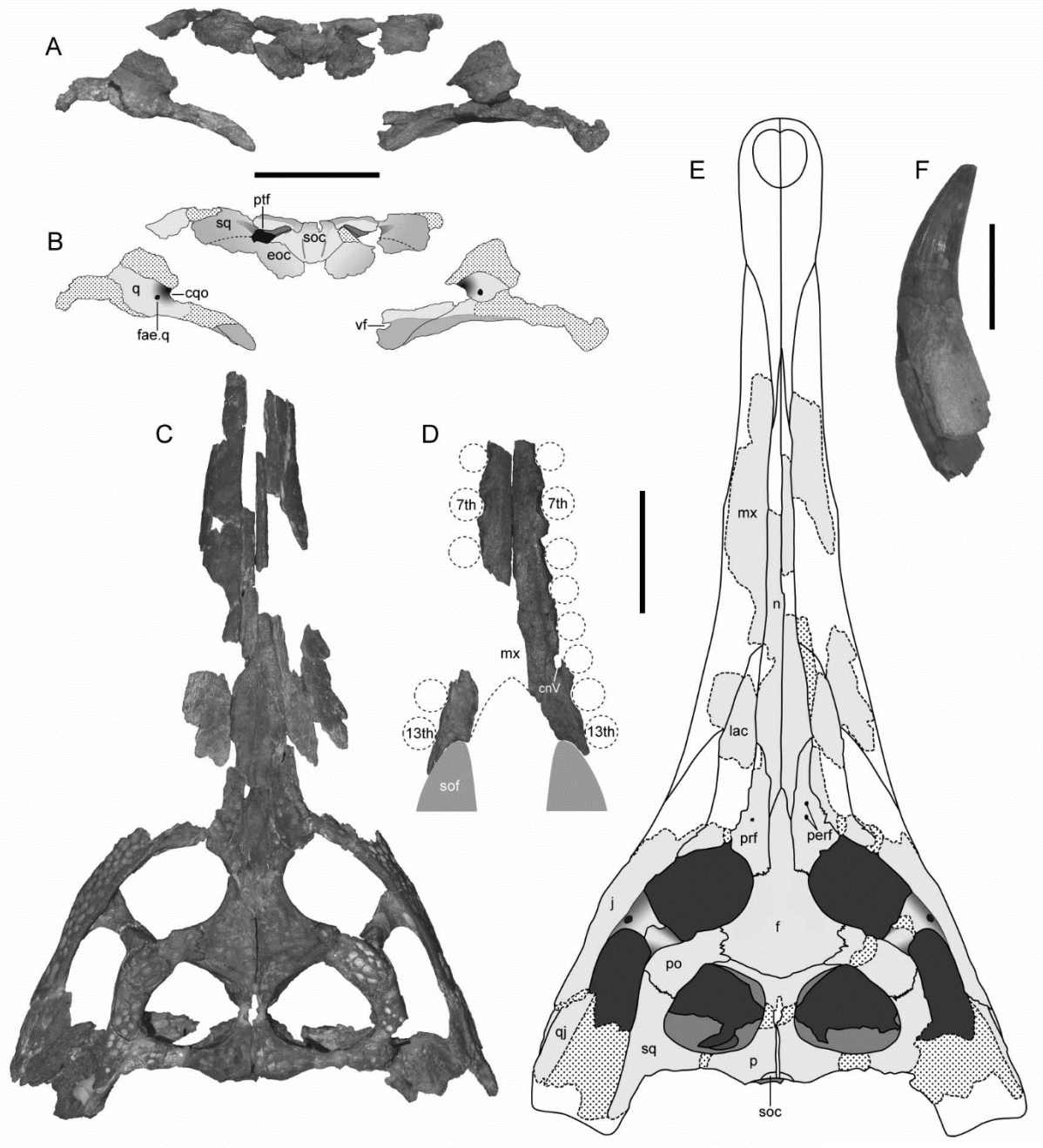


Fig. 3. KSNHM-F7-6 (Kishiwada specimen), posterior part of skull in left lateral view. j, jugal; po, postorbital; proj, projection; sq, squamosal. Scale bar is 5 cm.

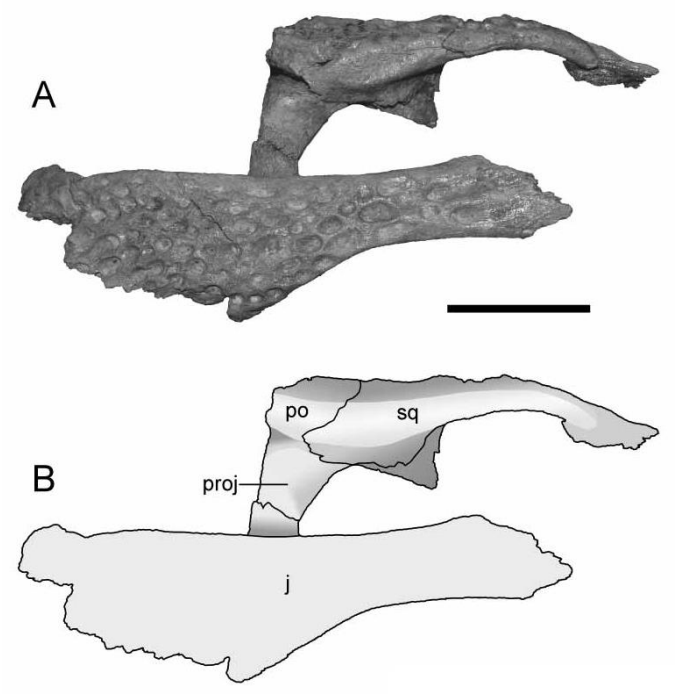


Fig. 4. Comparison of left jugal, quadratojugal, and quadrate in ventral view. A, KSNHM-F7-6 (Kishiwada specimen) and B, *Mecistops* cf. *cataphractus* (IRSNB 17962). dep, depression; fo, foramen; j, jugal; q, quadrate; qj, quadratojugal. Scale bars are 5 cm.

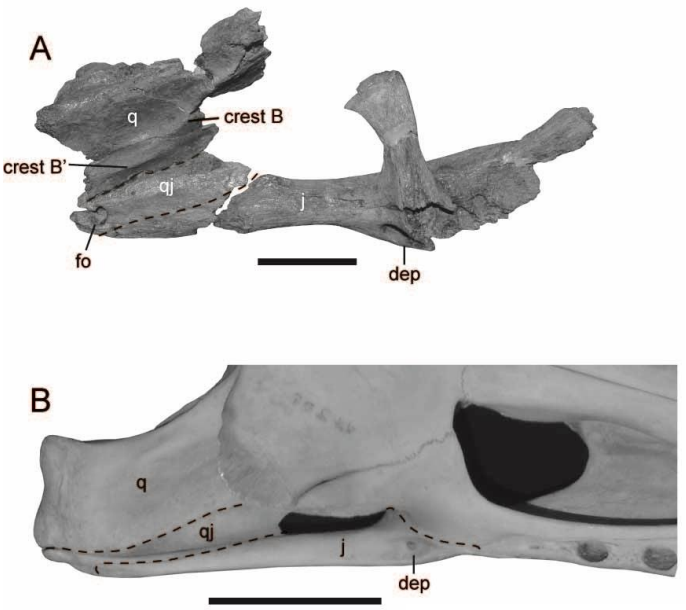


Fig. 5. KSNHM-F7-6 (Kishiwada specimen), left mandible in A and B, lateral views; C and D, dorsal views; E and F, posterior part in dorsomedial view. Alveolar positions are marked with filled circles. Stippled area indicates damaged bone. an, angular; art, articular; emf, external mandibular fenestra; d, dentary; lf, lingual foramen for articular artery and alveolar nerve; sa, surangular; sp, splenial. Scale bars are 10 cm (A–D) and 5 cm (E–F).

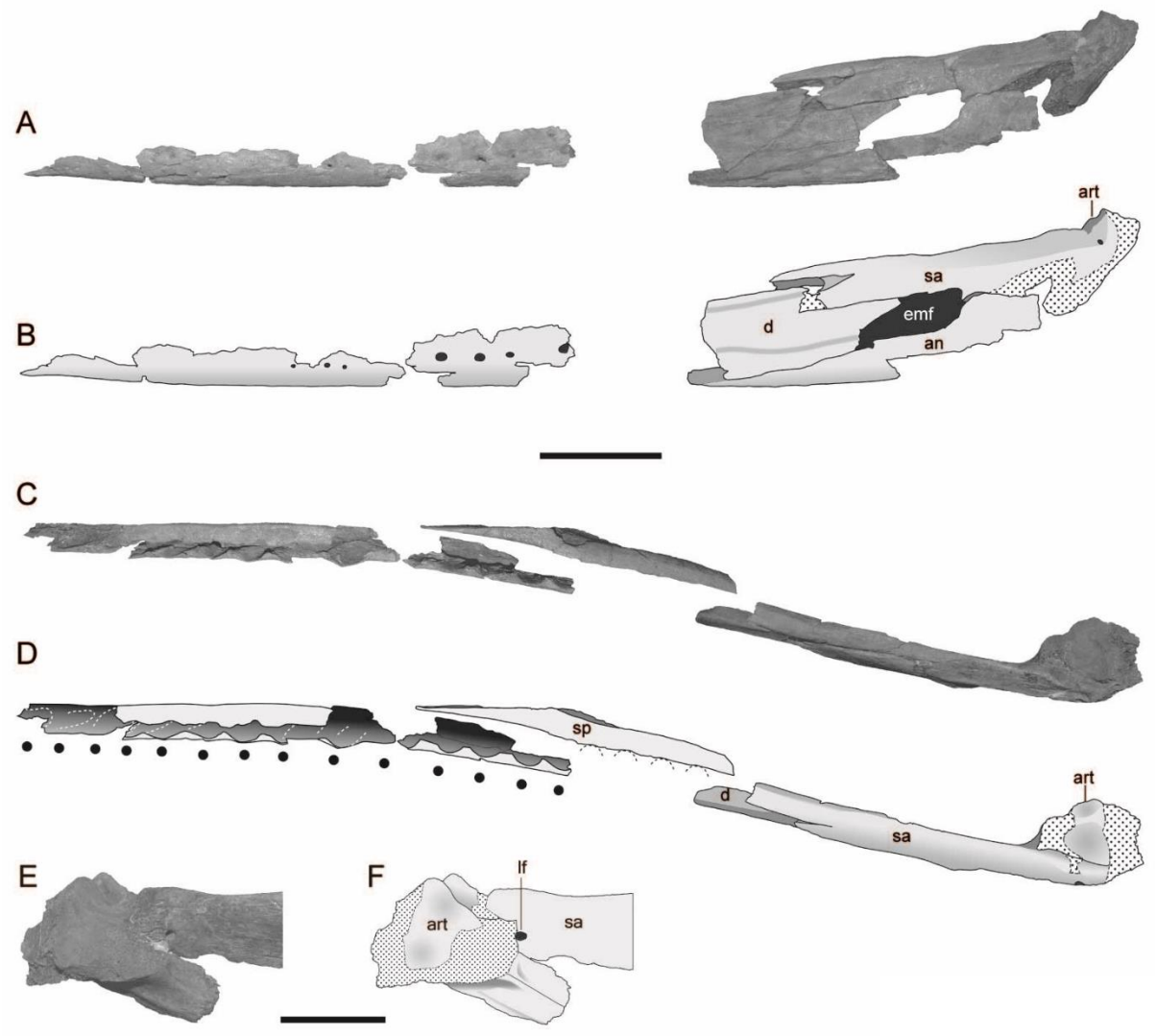


Fig. 6. Comparison of the skulls of A, MOU F00001 (holotype of *Toyotamaphimeia machikanensis*) (modified from Kobayashi et al., 2006) and B, KSNHM-F7-6 (Kishiwada specimen). Stippled area indicates damaged bone. Scale bar is 10 cm.

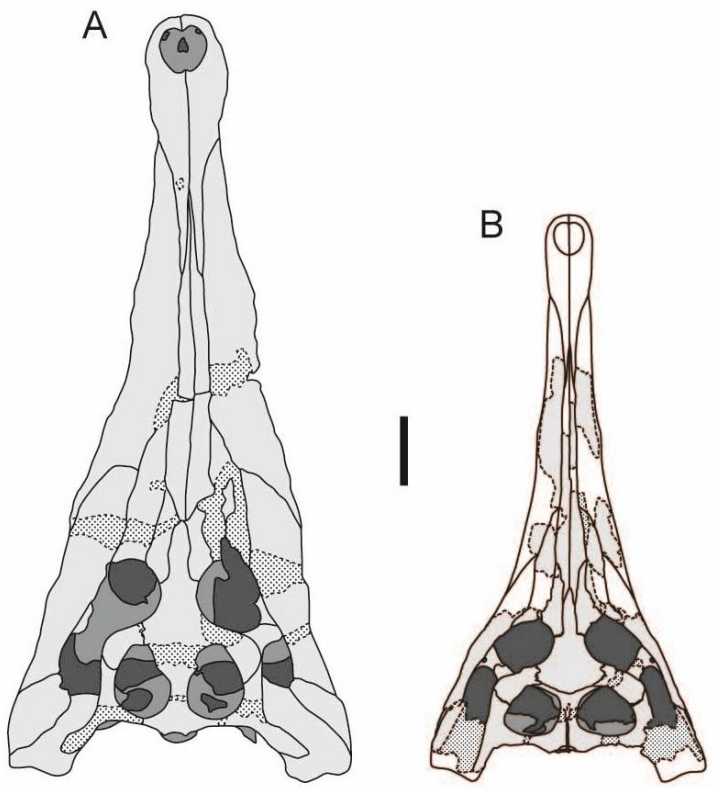


Fig. 7. Relationship of skull width and rostral proportion in Tomistoma schlegelii. AOW, width at anterior end of orbit; M5W, width at 5th maxillary alveolus; RL, rostral length (snout tip to anterior end of orbit). Star symbols are of the holotype of *Toyotamaphimeia machikanensis* (MOU F00001).

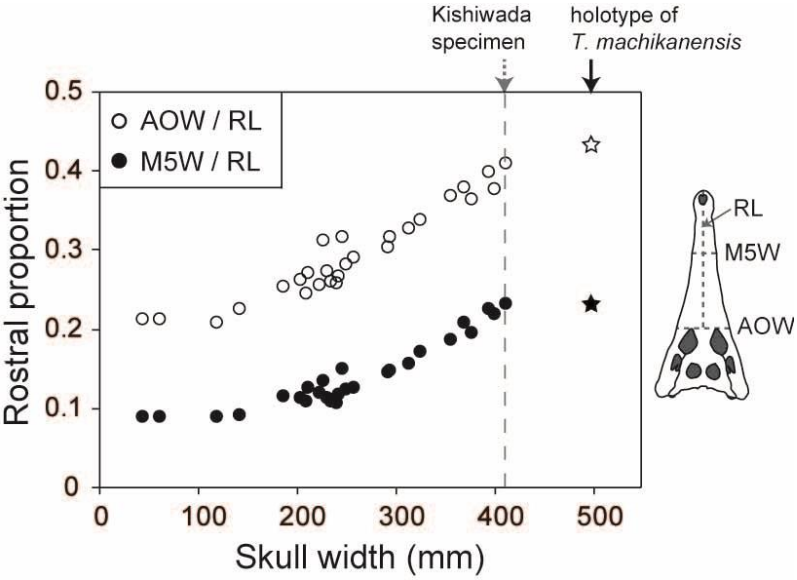


Fig. 8. Strict consensus of 232 equally parsimonious trees (tree length, 893; CI, 0.346; RI, 0.7). AF, Africa; AS, Asia; EU, Europe, NA, North America.

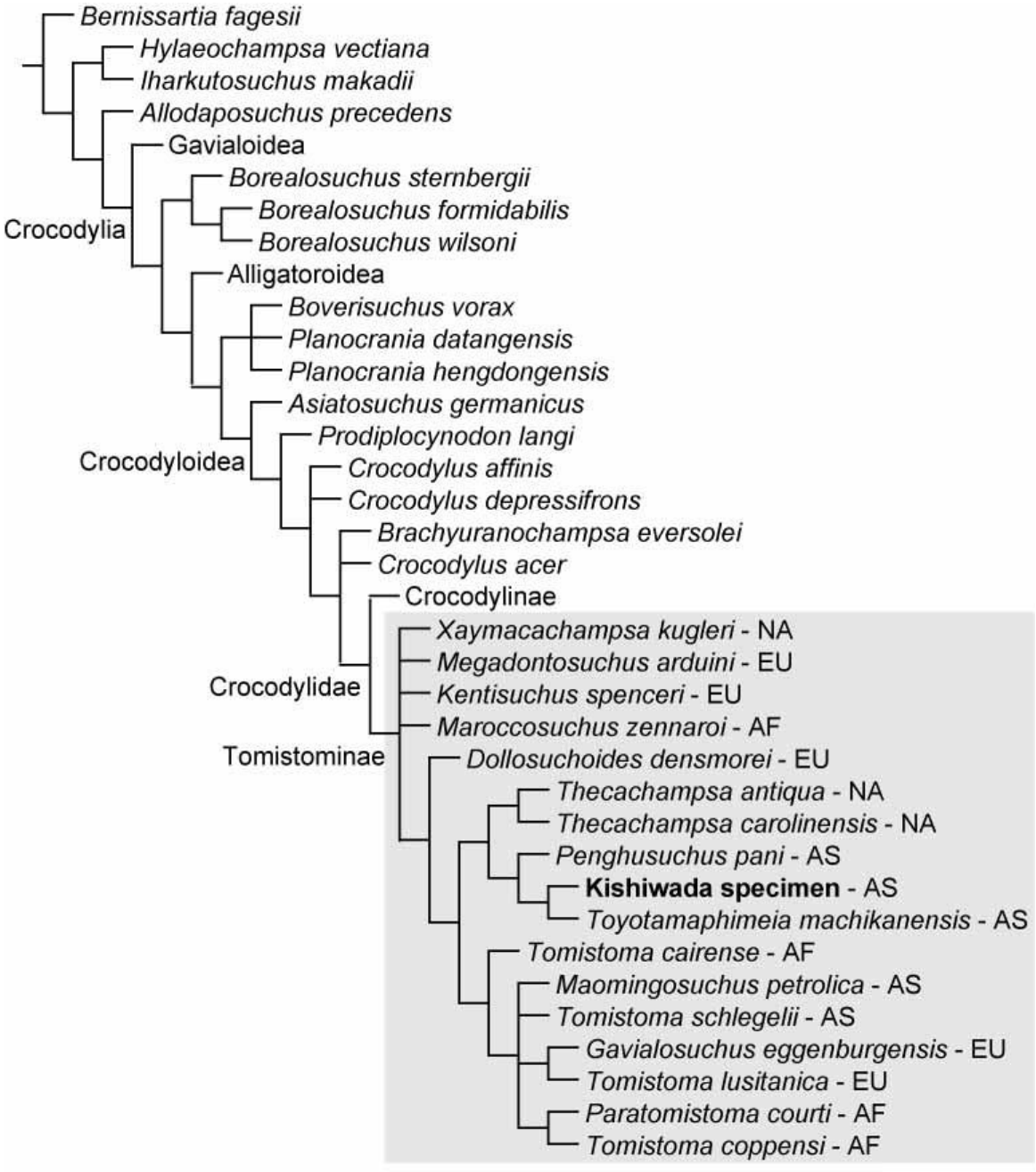


Fig. 9. Locality map of Japanese Pliocene-Pleistocene crocodylians. Number corresponds to Fig. 12 and Table 1. pen, peninsula.

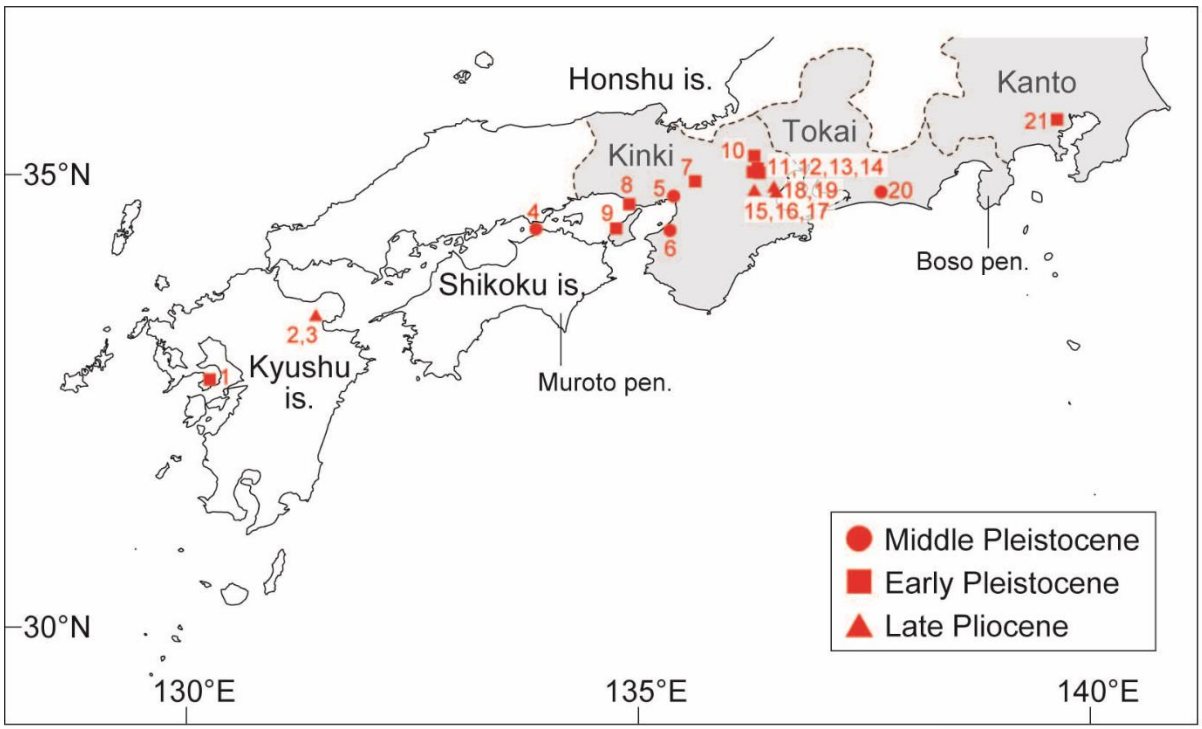


Fig. 10. A crocodylian right premaxilla (LBM 0142001118) from the mid Pliocene of Iga City, Mie Prefecture. A and B, dorsal views; C and D, ventral views. Scale bar is 2 cm.

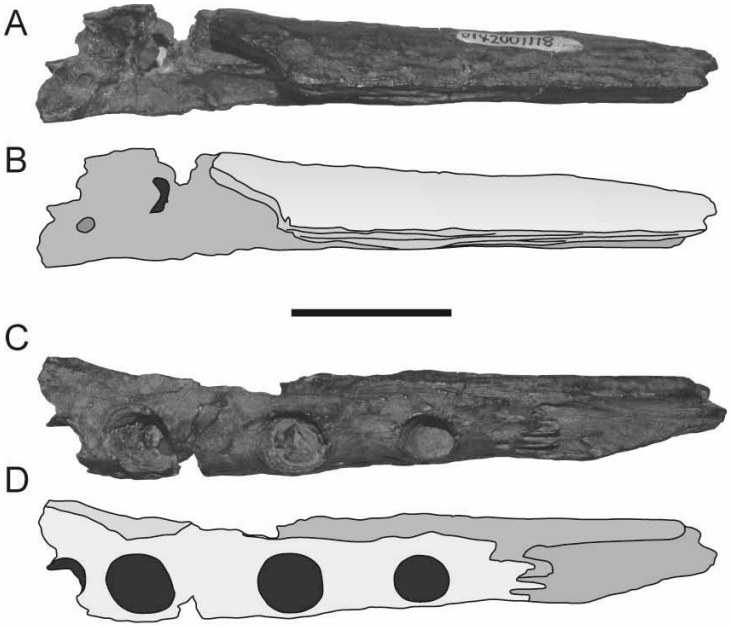


Fig. 11. Partial crocodylian skeleton from the Early Pleistocene of Takatsuki City, Osaka Prefecture. A and B, tooth crown (OMNH-QV 0278) in lingual (A) and apical (B) views; C, left ilium (OMNH-QV 0279) in lateral view; D, dorsal vertebra (OMNH-QV 0280) in dorsal view; E, second sacral vertebra (OMNH-QV 0281) in dorsal view. ap, anterior process of ilium. Scale bars are 1 cm (A and B) and 5 cm (C–E).

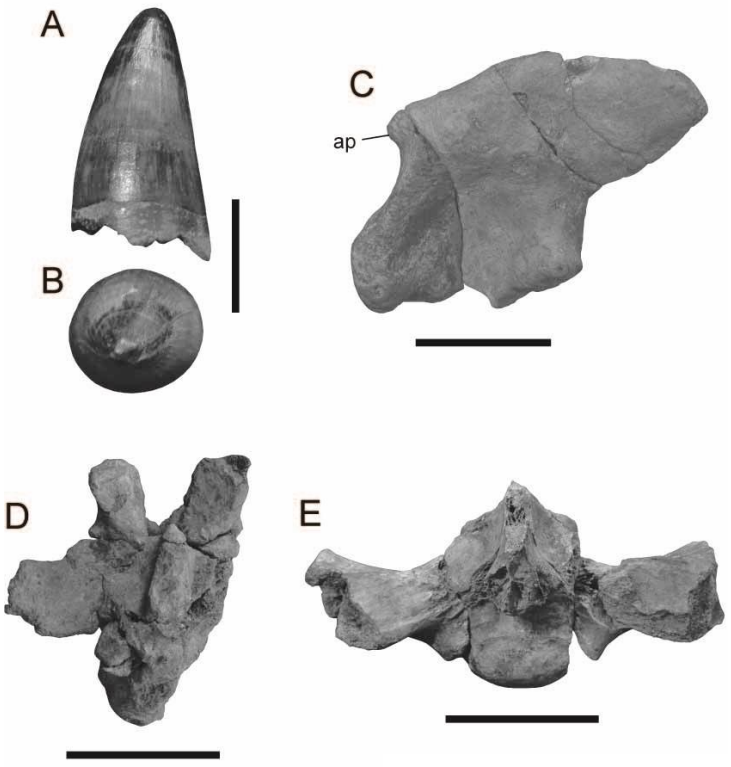


Fig. 12. Stratigraphic distribution of Plio-Pleistocene crocodylians from the Kinki, Tokai, and Kanto districts in Japan. Number corresponds to Fig. 9 and Table 1. The Plio-Pleistocene Series of these districts are time calibrated by tephro- and magnetostratigraphy (Satoguchi & Nagahashi, 2012) and oxygen isotope stratigraphy (Yoshikawa & Mitamura, 1999). The oxygen isotope record is adopted from Lisiecki and Raymo (2005). Im, Iimuro Formation; Kk, Kakio Formation; Oz, Ozenji Formation; Tk, Takatsu Formation; Tr, Tsurukawa Formation; Kz. Gp., Kazusa Group.

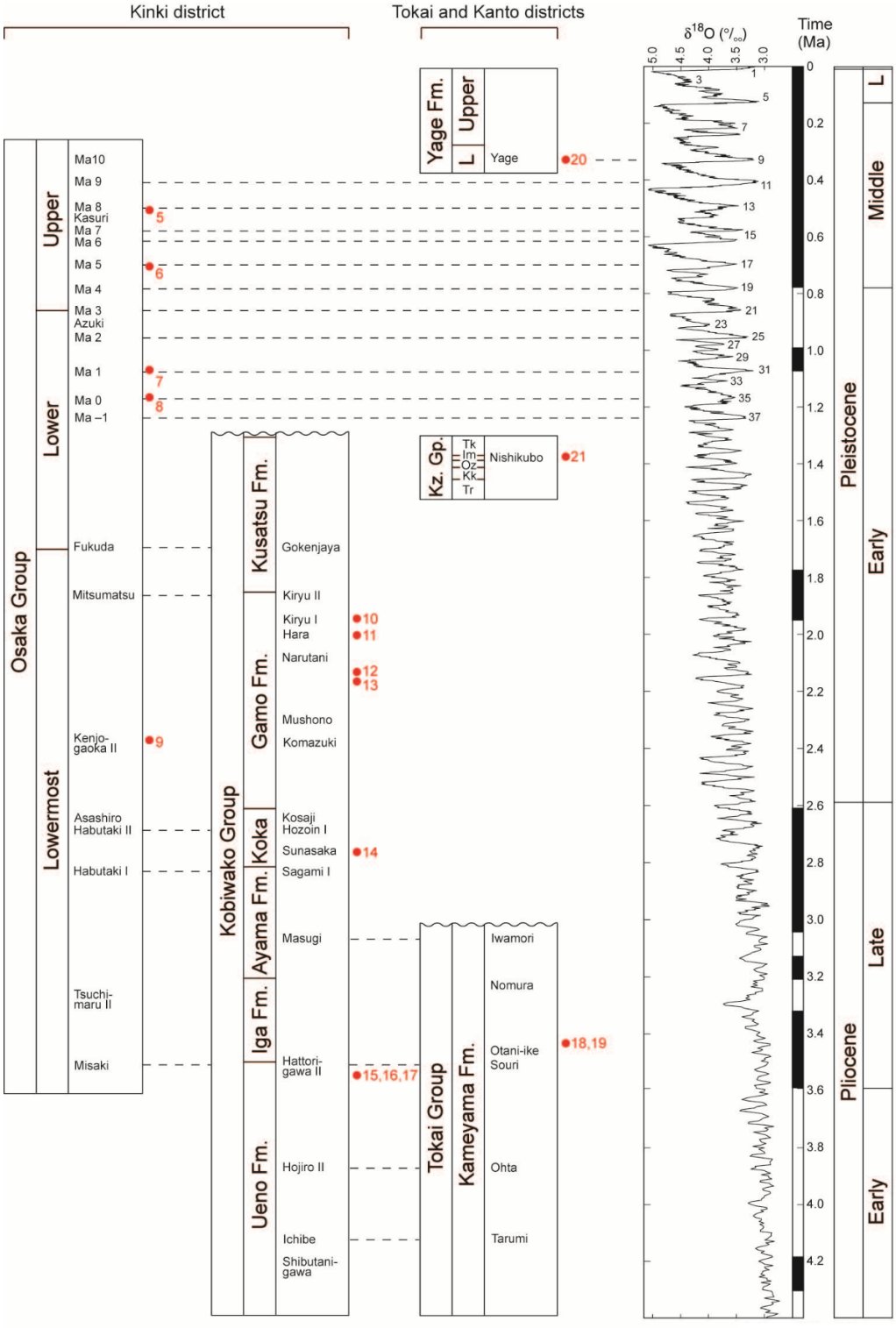


Table 1. The Plio-Pleistocene crocodylians from Japan.

No.	Taxon	Age	Locality	Horizon	Element	Reference
1	Crocodylia indet.	Early Pleistocene	Kazusa-cho, Minamishimabara City, Nagasaki Prefecture	upper Kazusa Formation of Kuchinotsu Group	teeth and vertebrae	Otsuka 1969
2	*Alligator sinensis*	Late Pliocene	Fukami River bank and floor in Ajimu-machi, Usa City, Oita Prefecture	middle Tsubusagawa Formation	partial skull, lower jaw, limbs, vertebrae, osteoderms, and teeth	Aoki 2001; Iijima et al. 2016
3	Crocodylidae cf. *Toyotamaphimeia*	Late Pliocene	Ajimu-machi and Innai-machi, Usa City, Oita Prefecture	middle Tsubusagawa Formation	teeth	Aoki 2001
4	Crocodylia indet.	?Middle to Late Pleistocene	Bisan-Seto Sea, in Seto Inland Sea	Bisan-Seto Group	femur	Taruno 1988
5	*Toyotamaphimeia machikanensis*	Middle Pleistocene	Machikaneyama-cho, Toyonaka City, Osaka Prefecture	below Ma8 Bed (Kasuri tephra), Ibaraki Formation of Osaka Group	a nearly complete skeleton	Kobatake et al. 1965; Kobatake and Kamei 1966; Aoki 1983; Kobayashi et al. 2006
6	*Toyotamaphimeia* cf. *machikanensis*	Middle Pleistocene	Nagareki-cho, Kishiwada City, Osaka Prefecture	near bottom of Ma5, Senpoku Formation of Osaka Group	partial skull, lower jaw, limbs, vertebrae, osteoderms, and tooth	Taruno 1999; This study
7	Crocodylia indet.	Early Pleistocene	Kaminokuchi, Takatsuki City, Osaka Prefecture	above Ma1 Bed, lower Osaka Group	tooth, vertebrae, ribs, and pelvis	Kobayashi 1977; Taruno 1979
8	Crocodylia indet.	Early Pleistocene	Yagi, Akashi City, Hyogo Prefecture	Byobugaura Clay Bed (Ma0), lower Osaka Group	vertebra	Taruno 1979
9	Crocodylia indet.	Early Pleistocene	Tsushi-saisaki, Goshiki Town, Hyogo Prefecture	above Kenjyogaoka II tephra, Atago Formation of Osaka Group	teeth	Nanko 1996
10	Crocodylia indet.	Early Pleistocene	Taga Town, Inukami-gun, Shiga Prefecture	Shide tephra (correlated with Kiryu tephra I), Gamo Formation of Kobiwako Group	teeth	Tamura et al. 1993; Abe 2011; Tanimoto and Iijima 2017
11	Crocodylia indet.	Early Pleistocene	Shinden, Toriidaira, Hino Town, Gamo-gun, Shiga Prefecture	above Hara tephra, Gamo Formation of Kobiwako Group	teeth	Isobe 1990; Takahashi 1998
12	Crocodylia indet.	Early Pleistocene	Mikumo, Kosei-cho, Konan City, Shiga Prefecture	clay bed 80m below Narutani tephra, Gamo Formation of Kobiwako Group	teeth	Watanabe and Tanimoto 2005; Yamamoto 1998
13	Crocodylia indet.	Early Pleistocene	Utta, Minakuchi-cho, Koka City, Shiga Prefecture	clay bed 150m above Mushono tephra, Gamo Formation of Kobiwako Group	tooth	Watanabe and Tanimoto 2005; Konishi 2015 personal communication
14	Crocodylia indet.	Late Pliocene	Kibogaoka, Terasho, and Oki, Koka City, Shiga Prefecture	clay bed containing Sunasaka tephra, Koka Formation of Kobiwako Group	teeth	Matsuoka et al. 1991
15	Crocodylia indet.	mid Pliocene	Hattorigawa River floor in Hirata, Iga City, Mie Prefecture	below Hattorigawa II tephra, Ueno Formation of Kobiwako Group	footprint	Okuyama and Ochiai 1993; Okuyama 1994
16	Crocodylia indet.	mid Pliocene	Hattorigawa River floor in Hatamura and Kawara, Iga City, Mie Prefecture	between Hattorigawa I and II tephra, Ueno Formation of Kobiwako Group	teeth, ?pes, vertebrae, osteoderms, and coprolites	Okuyama 1981, 1983, 1984, 1985, 1988; Kawaguchi and Kitada 1982; Matsuoka et al. 1990; Matsuoka et al. 1991; Tanimoto and Kaede 2000; Yamamoto 1997
17	Crocodylidae indet.	mid Pliocene	Hattorigawa River floor in Hatamura, Iga City, Mie Prefecture	between Hattorigawa I and II tephra, Ueno Formation of Kobiwako Group	premaxilla	Tanimoto and Okuyama 1998
18	Crocodylia indet.	mid Pliocene	Suzukagawa River floor in Nomura-cho, Kameyama City, Mie Prefecture	clay bed 150m below Nomura tephra, Kameyama Formation, Tokai Group	posterior skull, vertebra, footprints	Kobayashi 2009; Okamura 2009; Nakagawa 2014
19	Crocodylia indet.	mid Pliocene	Isshinden-kozubeta, Tsu City, Mie Prefecture	above Otani-ike tephra, Kameyama Formation, Tokai Group	teeth, osteoderms	Mie Prefectural Museum. 2011
20	Crocodylidae indet.	Middle Pleistocene	Yage, Inasa-cho, Hamamatsu City, Shizuoka Prefecture	lower 'Yage' Formation	skull, lower jaw, teeth, limbs, vertebrae, and osteoderms	Nojima 2002; Nojima and Itoigawa 2017; Nojima et al. 2007; Nojima et al. 2014
21	Crocodylia indet.	Early Pleistocene	Near Nikaryo Syukugawara, Tama Ward, Kawasaki City, Kanagawa Prefecture	above Nishikubo tephra, Iimuro Formation of Kazusa Group	vertebrae, libs, limbs, pelvis, and osteoderms	GMNH Koizumi collection; Koizumi 1995

Table 2. Paleotemperature estimates using the thermophilous and cold-loving taxa in the plant macrofossil assemblages from Ma0, Ma1, Ma5, and Ma8 marine clay beds in the Osaka Group. Abbreviations: J, Japan; Ch, China; CMMT, coldest-month mean temperature; MAT, mean annual temperature; WMMT, warmest-month mean temperature. Temperature values in bold letters were accepted and those in italics were rejected.

Taxon	Locality of distribution limit				Temperature (°C)			Reference	Occurrence in the Osaka Group
	Locality	Altitude (m)	Latitude N	Longitude E	CMMT	MAT	WMMT		
Thermophilous taxon									
Ficus pumila	Tsukushino, S. Fukuoka, J.	350	33°31'	130°34'	**3.0**	**13.4**	**24.2**	Tsutsui, 1992	Ma0, Ma8
Syzygium buxifolium	Mt. Huang, S. Anhui, Ch.	750	30°05'	118°10'	**1.5**	**13.4**	**24.3**	Hu and Liang, 1996	Ma8
Paliurus hemsleyanus	Sennojia, W. Hubei, Ch.	950	31°45'	110°45'	**0.7**	*14.5*	**25.0**	Zhu and Song, 1999	Ma0, Ma1, Ma5, Ma8
	Mt.Tianmu, Zhejiang, Ch.	550	30°20'	129°26'	*1.6*	**13.6**	*25.5*	Ding et al., 2009	
Cold-loving taxon									
Thuja standishii	Sasazu, Toyama, J.	550	36°29'	137°17'	**-1.5**	**9.8**	**22.8**	Takahashi, 1962	Ma0
Picea polita	Igawa, C. Shizuoka, J.	750	35°11'	138°12'	**0.6**	**11.1**	**21.9**	Hayashi, 1952	Ma1, Ma5
Fagus japonica	Igawa, C. Shizuoka, J.	550	35°10'	138°11'	**1.8**	**12.2**	**23.1**	Takahashi, 1962	Ma8

VI. The oldest record of *Alligator sinensis* from the Late Pliocene of Western Japan, and its paleobiogeographic implication

Introduction

Alligator sinensis is the only extant alligatorid species found outside the Americas, which is one of the critically endangered species among the world's crocodylians and now restricted to a small area in Anhui Province, China (Thorbjarnarson & Wang, 1999; Jiang, 2010). Fossil and archaeological evidences (Fig. 1; Table 1) indicate that its past distribution was extended to the north at Wangyin, Shandong Province of China (Fig. 1: marker #10), and to the south at Penghu Channel, west of Taiwan (Fig. 1: marker #4). If the potential *A. sinensis* materials are included, the distribution is extended to further south at Ban Si Liam, Nakhon Ratchasima Province of Thailand (Fig. 1: marker #1). *Alligator* bones and skins were also collected in other Neolithic and Bronze Age sites of China (Dawenkou cultural site in Tai'an, Shandong Province; Longshan cultural sites in Linqu and Sishui, Shandong Province, and Linfen, Shanxi Province; Shang Dynasty royal tombs in Anyang, Henan Province), while those remains were related with burials of high-ranked people and could be brought from other regions (Liu, 1994; Thorbjarnarson & Wang, 2010). However, compared with the solid archaeological evidence, fossil records of *A. sinensis* hinting the origin and past distribution of the species are still limited; the sole definitive *A. sinensis* is the skull from the Late Pleistocene of Taiwan (Shan, Cheng, & Wu, 2013).

In late 1990s, a series of excavations of the Pliocene Tsubusagawa Formation at Ajimu-machi, Usa City, Oita Prefecture, Japan had yielded numerous vertebrate fossils including fishes (Cyprinidae and Bagridae), a salamander (Cryptobranchidae), crocodylians (Alligatoridae and Crocodylidae), turtles (Platysternidae, Trionychoidae, and Bataguridae), birds (Pelecaniformes, Falconiformes, Anseriformes, and Gruiformes), and mammals (Stegodontidae, Cervidae, Ursidae, and Rhinocerotidae) (Aoki, 2001; Hirayama, 2001; Kato, 2001; Matsui *et al.*, 2001; Matsuoka, 2001; Nakajima & Kitabayashi, 2001; Takahashi & Kitabayashi, 2001; Watanabe & Kitabayashi, 2001), and this fossil assemblage was named "Ajimu fauna" (Takahashi, 2001). Aoki (2001) suggested the presence of *Alligator sinensis* among the Ajimu fauna based on the fragmentary skull and postcranial elements, but it lacks

thorough description and taxonomic assessment. Because any fossil *A. sinensis* or its potential kin from the Cenozoic of East Asia is crucial in the study of *Alligator* biogeography, we here provide a detailed description and a firm basis for the taxonomic identification of the Ajimu *Alligator*, and discuss its paleobiogeographic significance.

Geologic setting

The Tsubusagawa Formation distributes over Ajimu-machi and Innai-machi, Usa City, Oita Prefecture in Kyushu Region, which consists of lacustrine (Matsumoto, Murata, & Imanaka, 1984; Iwauchi & Hase, 1986) and fluvial and marsh deposits (Satoguchi, 2001), intercalated by numerous volcanic ash beds. Iwauchi and Hase (1986) divided the formation into three parts: the lower part characterized by peaty mudstone with lignite beds and tuffaceous sand-silitstone; the middle part characterized by massive mudstone and tuff; the upper part characterized by coarse sandstone and conglomerate. The total thickness of the Tsubusagawa Formation is roughly 150 m, and is uncorformably overlaid and underlay by the igneous Higashishiiya Formation and Usa Formation, respectively (Matsumoto *et al.*, 1984).

All the crocodylian materials described here were recovered from very fine sandstone (Matsuoka, 2001) of the lowermost part of the middle Tsubusagawa Formation, which crops out at river-bank and -floor of the Fukami River, upstream of Shiromaru-bashi Bridge, Ajimu-machi, Usa City, Oita Prefecture (Fig. 2).

Matsuoka and Kitabayashi (2001) described six freshwater molluscs (*Margarya*, *Anodonta*, *Lanceolaria*, *Pronodularia*, *Semisulcospira*, and *Inversiunio*) from the lowermost part of the middle Tsubusagawa Formation, and suggested that the molluscan assemblage of the Tsubusagawa Formation is comparable with that of the Plio-Pleistocene Gamo Formation of the Kobiwako Group, which distributes in the Kinki Region of Japan. Multiple tuff beds intercalated in the lower Tsubusagawa Formation was dated at 4.9-3.1 Ma by fission track method (Hase *et al.*, 2001; Satoguchi, 2001), while the tuff bed in the upper Tsubusagawa Formation is dated at 3.2 Ma (Hoshizumi & Morishita, 1993). A recent correlation of those beds with regional tephras in the other part of Kyushu region indicates that the lower boundary of Tsubusagawa Formation is at ~3.5 Ma (Satoguchi, 2008). Additionally, the andesite lava in the overlying Higashishiiya Formation is dated at 2.4 Ma (Kamata & Muraoka, 1984) by K-Ar dating. Although some age estimates and their stratigraphic levels are inconsistent, the age of the alligator fossil bearing horizon is most likely at ~3.0 Ma in the Late Pliocene.

Systematic paleontology

Crocodylia Gmelin, 1789 (*sensu* Clark in Benton & Clark, 1988)

Alligatoridae Cuvier, 1807 (*sensu* Brochu, 2003)

Alligatorinae Gray, 1844 (*sensu* Brochu, 2003)

Alligator sinensis Fauvel, 1879

Material: left quadrate (LBM 0142000027), left dentary (LBM 0142000753), left angular (LBM 0142000754), left articular (LBM 0142000756). The left mandible elements belong to a single individual.

Crocodylia indet. Gmelin, 1789 (sensu Clark in Benton & Clark, 1988)

cf. *Alligator sinensis* Fauvel, 1879

Material: left jugal (LBM 0142000054), isolated teeth (LBM 0142000020; LBM 0142000023; LBM 0142000036; LBM 0142000039; LBM 0142000042; LBM 0142000044; LBM 0142000047; LBM 0142000049; LBM 0142000050), right ilium (LBM 0142000025), osteoderms (LBM 0142000030; LBM 0142000032; LBM 0142000035; LBM 0142000043; LBM 0142000046; LBM 0142000051). See Aoki (2001) for other materials from the same and other localities, which are potentially assigned to *Alligator sinensis*.

Description

Alligator sinensis Fauvel, 1879

The left quadrate (Fig. 3A-E) is nearly complete. Dorsally near the quadrate condyles, scarf-joint suture for the quadratojugal is transversely broad, which tapers anteriorly and becomes butt-joint suture. In lateral view, a ventral half of the otic aperture and lateral wall of the cranio-quadrate passage are preserved. Anterior to the otic aperture, a large preotic foramen is present within a shallow depression. Near the caudal end of the cranio-quadrate passage, quadrate foramen aëreum is set in from the mediodorsal angle of quadrate condyles and placed on the dorsal surface. Of the two quadrate hemicondyles, the medial one is less deep than the lateral one, and the dorsal surface of the element is smooth without notch between the condyles. On the ventral surface, a keel for the attachment of jaw adductor muscles (crest A – A') extends along the quadrate-quadratojugal suture, and medial to the crest A, a weak rugosity represents the crest B (Iordansky, 1973).

In the left mandible (Fig. 3F, G), the external mandibular fenestra is large such that the

foramen intermandibularis caudalis is largely visible laterally as in derived members of the genus *Alligator*. Among the extant members of Alligatoroidea, *M. niger* (e.g., ZSM 3.1911; ZSM 19.1911) and some individuals of the genus *Caiman* (*C. crocodilus crocodilus*; *C. crocodilus fuscus*; *C. latirostris*; *C. yacare*) (e.g., ZSM 104.1911; ZSM 81.1937; ZSM 73.1926; ZSM 168.1929) also have relatively large EMF, through which FIC is partially visible in side view. The dorsal posterior process of the dentary extends near the dorsal apex of the external mandibular fenestra. The ventral posterior process of the dentary is broken, but the dentary-angular sutural facet on the angular suggests that it extends to the posterior half of the external mandibular fenestra. The angular-surangular suture terminates horizontally at the posterior corner of the external mandibular fenestra.

The left dentary (Fig. 3J, K) is missing the anterior portion and preserves posterior 13 alveoli, corresponding to the seventh to nineteenth alveoli. The seventh to eleventh alveoli are small in size and labio-lingually compressed oval in shape, whereas alveoli posterior to the twelfth are abruptly enlarged and sub-circular in shape (Table 2). In lateral view, the dorsal rim of the dentary is gently downturned at the level of the thirteenth alveolous, and the dentary shallows anteriorly. On the dorsal surface, sutural facets for the anterior processes of the surangular are preserved, showing these processes are nearly same in length.

The left angular (Fig. 3F-I) is almost complete, missing its anterior tip. The lateral surface is densely sculptured by large pits, and caudal part posterior to the glenoid fossa is smoothed for the insertion of M. pterygoideus ventralis (Holliday & Witmer, 2007). The sutural surface for the surangular is pinched off and does not reach to the posterior tip of the retroarticular process. The medial wall of the mandibular adductor fossa at the level of the posterior end of the external mandibular fenestra is swollen for the tendinous insertion of M. pterigoideus dorsalis (Holliday & Witmer, 2007). Anterior to this muscle insertion, the angular forms the posterior half of the foramen intermandibularis caudalis, of which the dorsal and ventral rims are nearly parallel.

The left articular is preserved, but missing the descending process (Fig. 3H, I, L, M). The retroarticular process is projected posterodorsally and its dorsal surface is divided into two concavities by a low longitudinal ridge. In dorsal view, the process is triangular shape with a medially flared margin. The flared margin ends posterior to the articular foramen aëreum and is separated from the posterior wall of the glenoid fossa. The articular foramen aëreum is fully set in from the medial margin of articular. The articular-surangular suture within the glenoid fossa is bowed laterally in dorsal view. In lateral view, the suture for the surangular

extends to near the dorsal tip of the glenoid posterior wall.

cf. Alligator sinensis Fauvel, 1879

The main body of the left jugal (Fig. 4A, B) is preserved, missing the ascending process of postorbital bar and the lateral bar of infratemporal fenestra. The body is broad dorsoventrally, and widened anteriorly, as generally in blunt-snouted crocodylians. Its dorsal edge, the lateral border of the orbit, is straight and gently downturns posteriorly at the place of postorbital bar. The lateral surface of the body is ornamented by longitudinally oriented pits, and the margin of each pit is obscured, as Aoki (2001) mentioned. However, the ornamentation pattern of jugal is individually variable in extant *A. sinensis* (e.g., FMNH 31303; USNM 52557; USNM 292078). On the lateral surface immediately above the jugal-ectopterygoid suture, a ridge extends longitudinally, which is placed more dorsally in generalized and more slender snouted crocodylians. On the medial surface, two small foramina (medial jugal foramina) are present near the base of postorbital bar.

Several isolated teeth, often without root, are categorized into two morphotypes. One is conical with a blunt tip and has a ratio of crown height to width greater than 1 (Fig. 5A-D). This type generally has low mesial and distal carinae and faint linear striations from the base of the crowns to near the apex on the labial and lingual surfaces. The other type is globular with low crown (height/width less than 1) (Fig. 5E-H). These teeth lack mesial or distal carina, and enamel ridges on the labial and lingual surfaces are short and anastomosing.

The right ilium (LBM 0142000025: Fig. 6) is missing the pubic and ischiac peduncles. The iliac blade lacks the anterior process. The posterior portion of the iliac blade is broken, but remaining part indicates that its dorsal margin has a modest indentation. The posterior portion of the blade is shallow. Dorsal to the shallow and large acetabulum, supraacetabular crest is weakly developed to the level of mid-acetabulum.

All of preserved osteoderms are flat with a single keel (Fig. 7). Its external surface is sculptured by dense large pits, and the ventral surface is smooth with small nutrient foramina. Large rectangular-shaped osteoderms are probably dorsal or pelvic osteoderms, with complex serrate-joint on either or both sides. In those osteoderms, a facet along its anterior margin is smooth for a contact with a successive osteoderm. Small and more rounded osteoderms lacks this anterior facet and probably represent lateral or caudal osteoderms (Cong *et al.*, 1998: Fig. 4).

Discussion

Taxonomic status of the Ajimu specimen

Aoki's (2001) identification of *A. sinensis* from Ajimu is based on the following characters in the fragmentary skull and postcranial elements: non-significant "twist" of medial and lateral quadrate hemicondyles, referring to the relatively shallower medial hemicondyle; laterally displaced quadrate foramen aëreum; jugal width widest at the level of the anterior end of orbit; absence of longitudinal ridge on the lateral surface of jugal; dorsal margin of jugal downturned like "cutting edge" at the level of anteroventral corner of lower temporal fenestra; distinct ornamentation pattern on the lateral surface of jugal; non-significant orbital rim elevation of jugal; presence of globular teeth. He also discussed the patterns of the development of crests for the attachments of jaw adductor muscles on the ventral surface of quadrate and the iliac blade shape, finding an overall morphological congruence between the Ajimu specimen and *A. sinensis*.

Among these, first two characters are a synapomophy or a widely observed trait in more inclusive groups of Alligatoroidea (Brochu, 1997b, 1999a). The last character, low-crowned globular teeth, is present in *A. sinensis* (described as "mushroom-shaped" in Cong *et al.*, 1998) as well as the Paleogene blunt-snouted alligatorids (e.g., *Allognathosuchus polyodon*: Mook, 1921a; *Navajosuchus mooki*: AMNH 6780). Similarly, "massive crushing teeth" are also prevalent in the genus *Alligator* (Wu, Brinkman, & Russell, 1996). Other characters of the jugal are considered by Aoki (2001) as diagnostic for alligatorids or alligatorines, or at least consistent with *A. sinensis* while species comparison is not conducted. Provided these, a solid basis for the identification of Ajimu specimen at lower taxonomic levels has to be shown. Moreover, there is an inherent problem in using the bone bed materials that include isolated skeletal elements from multiple taxa. We here assess the taxonomic status of the Ajimu specimen based on the lower jaw elements (left dentary, angular, and articular) from a single individual.

The dentary and articular of the Ajimu specimen show two unambiguous synapomorphies of Alligatoroidea, suggested by a phylogenetic analysis by (Brochu, 1999a): subequal anterior processes of the surangular; articular foramen aëreum set in from medial margin of the articular. Additionally, posterior extension of the surangular is pinched off before the caudal tip of retroarticular process, which is present in non-caiman alligatoroids (Brochu, 1999a). The large external mandibular fenestra such that the foramen intermandibularis caudalis is visible in lateral view, is an unambiguous synapomorphy of the derived *Alligator* clade: *A.*

olseni + *A. sinensis* + *A. mefferdi* + *A. mississippiensis* + *A. thompsoni* (Brochu, 1999a) which is otherwise only known in Caimaninae *Prussaurus nievensis* (Brochu, 1997b).

Among the derived *Alligator* clade, pattern of dentary alveolar size in the Ajimu specimen is consistent with *A. sinensis*, while different from the rest of the clade members (*A. olseni*, *A. mefferdi*, *A. mississippiensis,* and *A. thompsoni*). In all species of the clade and the Ajimu specimen, twelfth alveolous is abruptly enlarged in its diameter from the preceding alveoli, and posterior to the twelfth, there are 8, 7, 9, 7-8, and 6-7 tooth positions for *A. olseni*, *A. sinensis*, *A. mefferdi*, *A. mississippiensis*, *A. thompsoni* respectively (Iordansky, 1973; Mook, 1923, 1946; White, 1942). The Ajimu specimen has 7 tooth positions posterior to the twelfth, which is congruent with *A. sinensis*, *A. mississippiensis*, and *A. thompsoni*. Additionally, the large posterior alveoli from twelfth to nineteenth are similar in size except for the last alveoli as in *A. sinensis* (USNM 52577: Cong *et al.*, 1998) as well as Paleogene alligatorids with blunt snout (e.g., *Allognathosuchus polyodon*: Mook, 1921a; *Navajosuchus mooki*: AMNH 6780) (Brochu, 2004b). In other species of the derived *Alligator* clade, posterior dentary alveoli progressively become smaller posteriorly (AMNH 7016; YPM R10503; Mook, 1923; White, 1942).

Furthermore, angular bar ventral to the external mandibular fenestra is much shallower than the surangular bar dorsal to the fenestra such that the ventral border of the fenestra is near the level of the adductor fossa floor in *A. mississippiensis*, contrasting the similar depth of both bars in *A. sinensis* (Shan *et al.*, 2013). The Ajimu specimen resembles *A. sinensis* in this regard. These lines of evidence indicate that the Ajimu specimen is referable to *A. sinensis*.

Body size of the Ajimu Alligator

Aoki (2001) preliminary estimated the total length of the Ajimu *Alligator* based on two cranial fragments by scaling those elements with drawings of *A. sinensis* (IVPP 1335: Cong *et al.*, 1998) and his personal collections of this species: 180 cm based on the left quadrate (LBM 0142000027) and 240 cm based on the left dentary (LBM 0142000753). He also suggested that the latter estimate was indicative of the largest *A. sinensis* ever known.

Here we re-estimated the total length of the Ajimu *Alligator* from the left mandible of a single individual (LBM 0142000753; LBM 0142000754; LBM 0142000756: Fig. 3F-I) instead of one element, with a consideration of an allometry of the dorsal cranial length (DCL) and the total length (TL). First, the mandibular length of the Ajimu *Alligator* is

estimated as 337.9 mm based on the proportion of the length between the posterior tip of mandible to the apex of jaw margin convexity at the thirteenth alveolous and the mandibular length of *A. sinensis* (FMNH 31303; USNM 52577). Second, the estimated mandibular length is scaled to DCL, using the average proportion of the two measurements in *A. sinensis* provided in Cong et al. (1984), resulted in 276.2 mm as the predicted DCL. We then modeled the relationship of DCL and TL in *A. sinensis* using the literature data (Wermuth, 1964; Cong *et al.*, 1998) of seven adult individuals > 150 cm TL (Table A.1). Both variables (DCL and TL) are log-transformed, and ordinary least square regression is fitted. The regression equation ($\log TL = 0.787 \log DCL + 1.38$, $r^2 = 0.950$) indicates strong negative allometry of TL against DCL in adult *A. sinensis*, and yields the TL estimate for the Ajimu *Alligator* of 201.0 cm (Fig. 8).

Our estimate TL of the Ajimu *Alligator* is smaller by roughly 15% than Aoki's (2001). Thorbjarnarson and Wang (2010) reported that the maximum TL of wild *A. sinensis* is about 200 cm for adult males, which nearly equal the Ajimu *Alligator*. Although our estimate is smaller than Aoki's (2001), it is still in the degree of the largest size for *Alligator sinensis*.

Asian Alligator biogeography

The origin of *Alligator sinensis* has been a subject of discussion in the study of vertebrate biogeography. Molecular analyses estimated the divergence time of the two extant alligators (*A. mississippiensis*; *A. sinensis*) during the Paleogene: 50.9 Ma (Wu *et al.*, 2003); 53-47 Ma (Roos, Aggarwal, & Janke, 2007); 58-31 Ma (Oaks, 2011), and the Late Cretaceous: 89-64 Ma (Janke *et al.*, 2005). On the other hand, fossil evidence indicates that the two extant taxa splitted by the mid-Miocene because *A. thompsoni*, a probable sister taxon of *A. mississippiensis* first appeared at around 14 Ma (Brochu, 1999a). Considering the lack of salt tolerance in living alligatorids (Taplin & Grigg, 1989), *Alligator* might disperse from North America to Asia across the Bering land bridge prior to 14 Ma (Brochu, 1999a, 2003; Snyder, 2007), concordant with the oldest occurrence of a definitive *Alligator* in Asia, *Alligator luicus*, from the mid Miocene of Linqu, Shandong Province, China (Li & Wang, 1987). Claude et al. (2011) preliminarily reported an occurrence of *Alligator* cf. *sinensis* from ?Late Miocene- Pleistocene in Thailand, which is potentially the oldest record of *A. sinensis,* but this specimen needs detailed description and better resolution of the age of its rock unit. Therefore, the Ajimu *Alligator* described herein is the oldest record of definitive *A. sinensis*, suggesting that the origin of this species in Asia was 3.0 Ma in the Pliocene or prior. *A.*

sinensis is probably derived from the Asian *Alligator* stock including *A. luicus*, and might get to Japan before back-arc opening of the Japan Sea and isolation from the Asian continent during 25-15 Ma (Maruyama *et al.*, 1997), or after the reconnection with the Asian continent at around 10 Ma (Tada, 1994).

Iwauchi (1994) and Yamakawa (2001) reconstructed the paleoclimate of Ajimu, Oita Prefecture, Kyushu Region during the Late Pliocene. The mean annual temperature (MAT) estimates of the lower and middle Tsubusagwa Formation, which includes the horizon of the Ajimu *Alligator*, are at 11.0~12.5 °C for the lower part and 14.5 °C for the middle part, respectively. These temperatures are near or even lower than the minimum MAT limit (14.2 °C) for the survival of crocodylians (Markwick, 1998a, 2007). During the Late Pliocene through the Pleistocene, the MAT of Kyushu, the southernmost main island of Japan, had often shifted to below 10 °C (Iwauchi, 1994), with which crocodylians might not have survived. This Plio-Pleistocene climatic deterioration, combined with the repeated opening of the southern channel of the Japan Sea after 3.5 Ma (Tada, 1994; Kitamura & Kimoto, 2006) might isolate the Japanese *A. sinensis* population, which was finally wiped out from Japan. On the contrary, the Chinese mainland population of *A. sinensis* assumedly responded the Plio-Pleistocene climatic oscillation by repeated north-south range expansion and retraction (Thorbjarnarson & Wang, 2010) and has survived till the present.

This chapter was published as:

Iijima M, Takahashi K, Kobayashi Y. 2016. The oldest record of *Alligator sinensis* from the Late Pliocene of Western Japan, and its biogeographic implication. *Journal of Asian Earth Sciences* 124: 94-101.

Fig. 1. Distribution of *A. sinensis* over time. Historical time and current distributions are modified from Thorbjarnarson and Wang (1999). See Table 1 for the locality information of paleontological and archaeological sites that produced *A. sinensis* (marker 1-10).

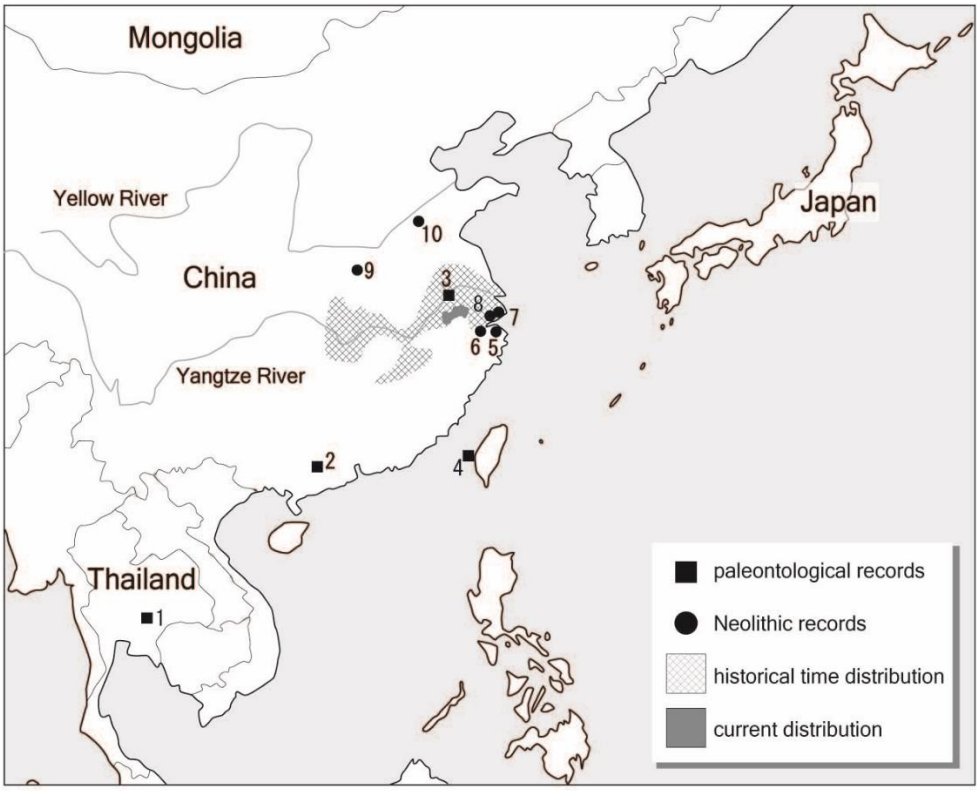


Fig. 2. (A) locality map of Ajimu Alligator (modified from Iwauchi and Hase, 1986), (B) stratigraphic column of the locality (modified from Matsuoka and Kitabayashi 2001). Star indicates the *A. sinensis* fossil locality. Sr bridge is Shiromaru-bashi bridge.

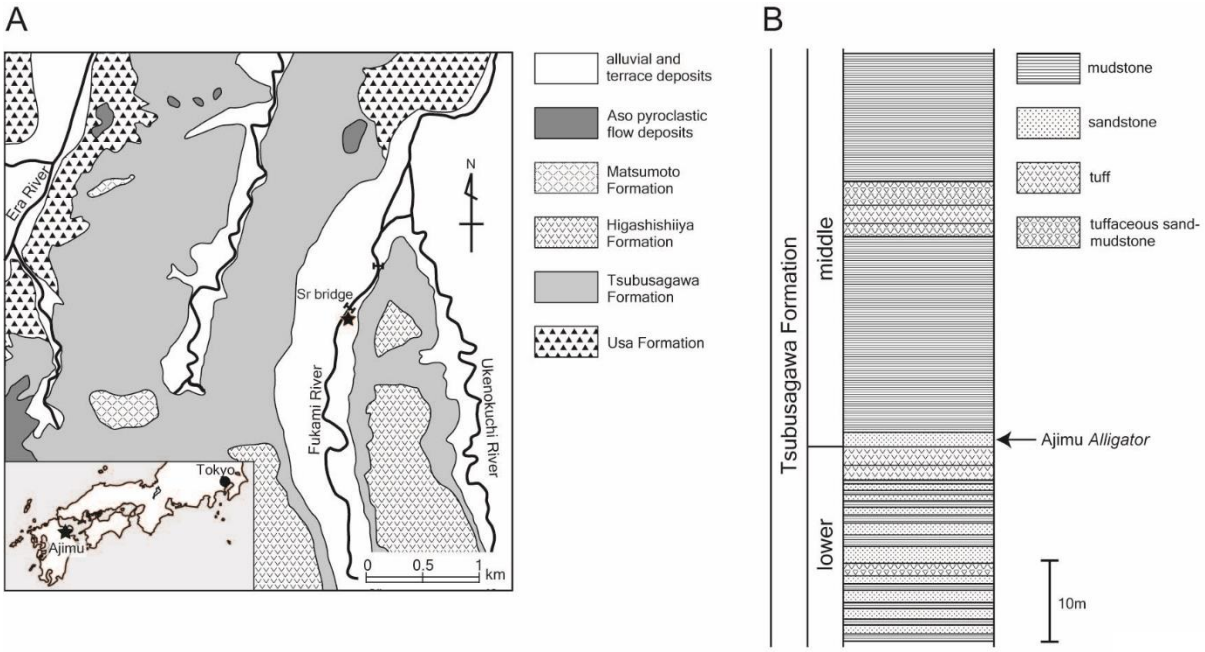


Fig. 3. Skull and mandible elements of Ajimu Alligator (*A. sinensis*). A-E, left quadrate (LBM 0142000027) in (A) lateral, (B, C) dorsal, (D) ventral, and (E) quadrate condyles in posterodorsal views. F-I, left mandible (LBM 0142000753, LBM 0142000754, LBM 0142000756) in (F, G) lateral, and (H, I) medial views. (J, K) left dentary (LBM 0142000753) in dorsal view. (L, M) left articular (LBM 0142000756) in dorsal view. Meshed area indicates sutural surface and dotted area indicates damaged surface. an, angular; ar, articular, d, dentary; EMF, external mandibular fenestra; FIC, foramen intermandibularis caudalis. Scale bars for A-E equal 2 cm, and F-M equal 5 cm.

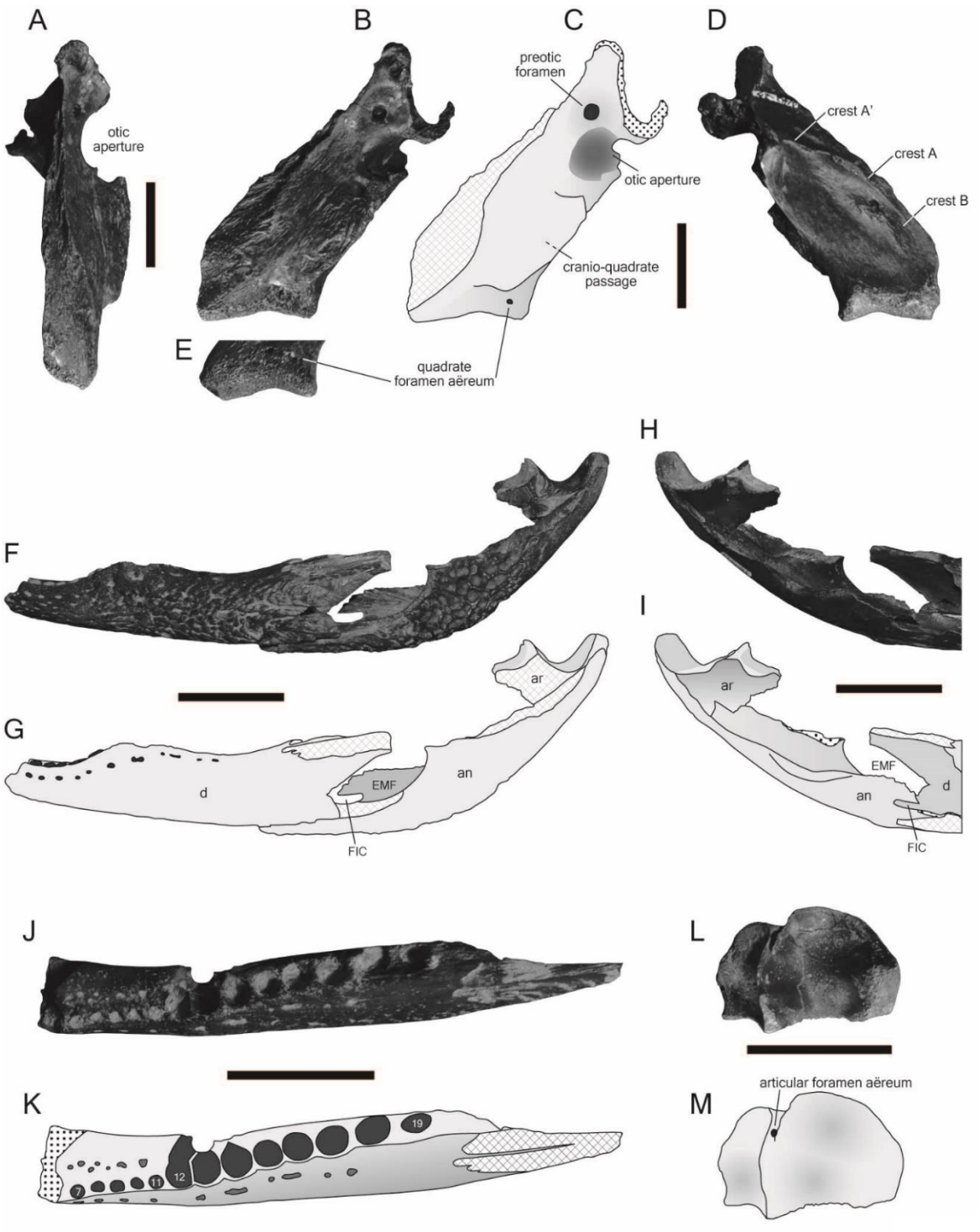


Fig. 4. Left jugal (LBM 0142000054) of Ajimu Alligator (cf. *A. sinensis*) in (A) lateral, and (B) medial views. Scale bar equals 2 cm.

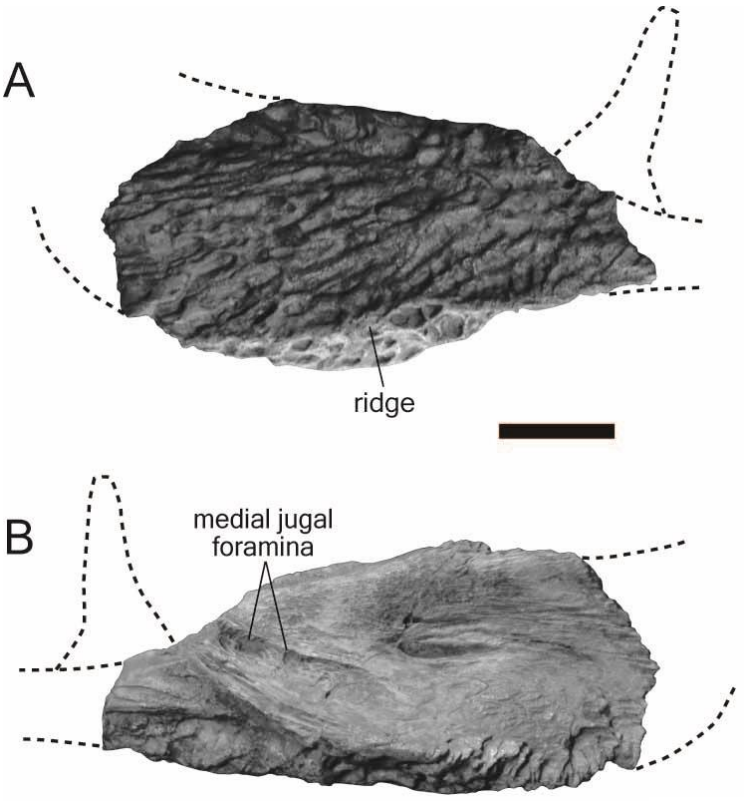


Fig. 5. Teeth of Ajimu Alligator (cf. *A. sinensis*). (A, B) LBM 0142000042, (C, D) LBM 0142000050), (E, F) LBM 0142000020, (G, H) LBM 0142000044 in (A, C, E, G) labial (lingual) and (B, D, F, H) apical views. All scale bars equal 5 mm.

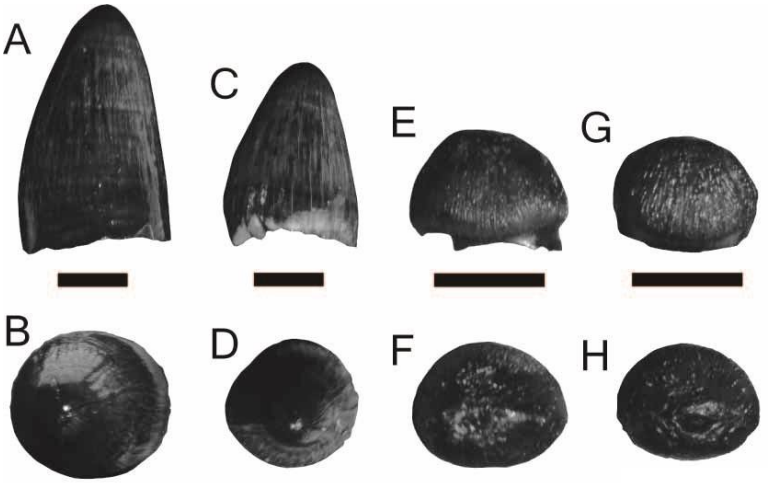


Fig. 6. Right ilium (LBM 0142000025) of Ajimu Alligator (cf. *A. sinensis*) in lateral view. Scale bar equals 2 cm.

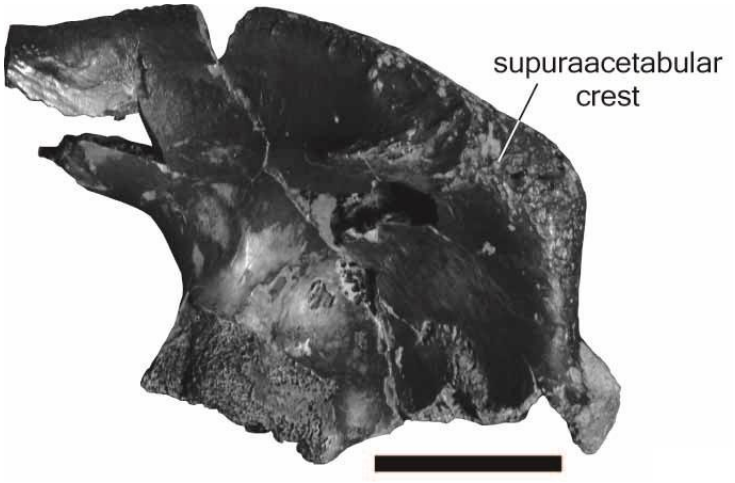


Fig. 7. Osteoderms of Ajimu Alligator (cf. *A. sinensis*) in external view. (A) LBM 0142000030, (B) LBM 0142000043, (C) LBM 0142000035, (D, F) LBM 0142000032, (E) LBM 0142000051, (G) LBM 0142000046. All scale bars equal 2 cm.

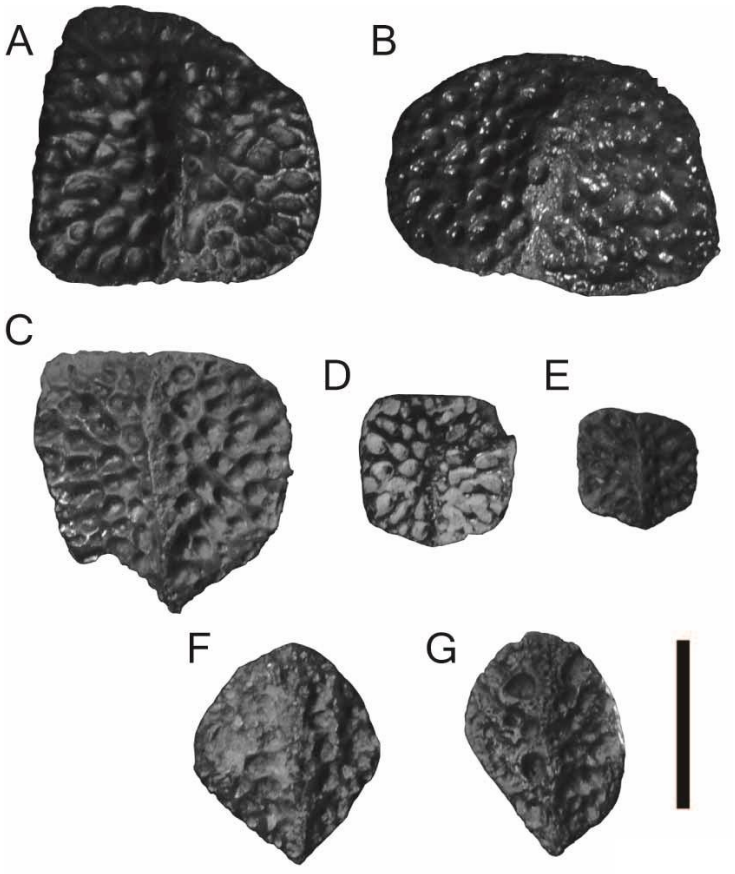


Fig. 8. Relationship of dorsal cranial length and total length in *A. sinensis*. Solid markers are extant *A. sinensis*.

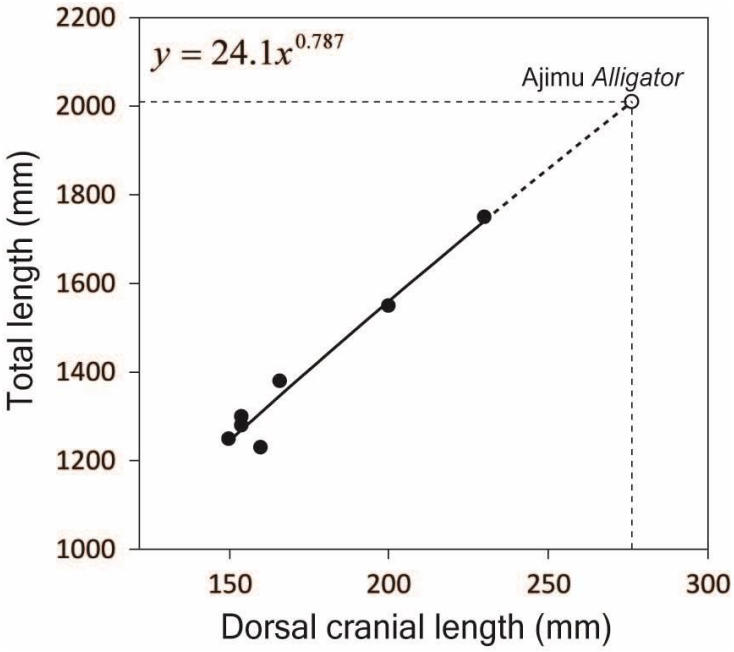


Table 1. Paleontological and Archaeological records of *A. sinensis* (*A*. cf. *sinensis* and cf. *A. sinensis* are also included).

	Locality	Geological time/ Archaeological period	Reference
1	Ban Si Liam, Mai Subdistrict, Non Sung District, Nakhon Ratchasima Province, Thailand	?Late Miocene-Pleistocene	Claude et al. 2011
2	Xiashan Cave, Pingtang, Luoding City, Guangdong Province, China	Middle Pleistocene	Huang et al. 1988
3	Longtandong Cave, northern slope of Wangjia Mountain, Hexian County, Anhui Province, China	Middle Pleistocene	Huang et al. 1982; Liu and Chen 1993
4	Penghu Channel, west of Taiwan	Late Pleistocene	Shan et al. 2013
5	Hemudu site, along the southern shore of Hangzhou Bay, Yuyao County, Zhejiang Province, China	Neolithic	NHSCPM 1978; Wei and Xu 1981; ZPICRA 2003
6	Kuahuqiao site, Xianghucun in Xiaoshan District, Hangzhou City, Zhejiang Province, China	Neolithic	Jiang and Liu 2005
7	Maqiao site, Maqiao, Minhang District, Shanghai City, China	Neolithic	Cao 1984
8	Majiabang site, Nanhu District, Jiaxing City, Zhejiang Province, China	Neolithic	Chang 1986
9	Jiahu site, Jiahu Village, Wuyang County, Henan Province, China	Neolithic	HPICRA 1999
10	Wangyin site, Yanzhou District, Jining City, Shandong Province, China	Neolithic	Zhou 1982; IACASS 2000

Table 2. Measurements of mandibular alveoli in the left dentary of Ajimu specimen (LBM 0142000753).

Mandibular alveolous #	7	8	9	10	11	12	13	14	15	16	17	18	19
Mesiodistal diameter (mm)	5.5	5.3	4.6	4.8	5.6	—	9.7	9.2	8.5	9.4	10.2	—	—
Labiolingual diameter (mm)	4.5	3.9	3.6	3.7	4.8	—	—	—	9.2	9.3	8.8	—	—

Literature cited

Abe Y. 2011. A crocodylian tooth from the Kobiwako Group, Taga Town. In: Taga Town Museum, ed. Abstracts of the Taga Town Museum Research Meeting 2010–2011., 9.

Aguilera OA, Riff D & Bocquentin-Villanueva J. 2006. A new giant *Purussaurus* (Crocodyliformes, Alligatoridae) from the Upper Miocene Urumaco Formation, Venezuela. Journal of Systematic Palaeontology 4: 221–232.

Allen V, Elsey RM, Jones N, et al. 2010. Functional specialization and ontogenetic scaling of limb anatomy in *Alligator mississippiensis*. Journal of Anatomy 216: 423–445.

Allen V, Molnar J, Parker W, et al. 2015. Comparative architectural properties of limb muscles in Crocodylidae and Alligatoridae and their relevance to divergent use of asymmetrical gaits in extant Crocodylia. Journal of Anatomy 225: 569–582.

Andrews CW. 1901. II.—Preliminary note on some recently discovered extinct vertebrates from Egypt. (Part II). Geological Magazine 8: 436–444.

Andrews CW. 1915. Note on a fore-paddle of *Metriorhynchus* from the Oxford Clay of Peterborough. Geological Magazine 2: 444–447.

Antunes MT. 1961. *Tomistoma lusitanica*, crocodilien du Miocène du Portugal. Revista da Faculdade de Ciências Universidad de Lisboa, Serie II 9: 5–88.

Aoki K, Suzuki T, Hsu TW, et al. 2004. Phylogeography of the component species of broad-leaved evergreen forests in Japan, based on chloroplast DNA variation. Journal of Plant Research 117: 77–94.

Aoki R. 1983. A new generic allocation of *Tomistoma machikanense*, a fossil crocodilian from the Pleistocene of Japan. Copeia 1: 89–95.

Aoki R. 2001. The crocodilian fossils from the Tsubusagawa Formation (Pliocene) of Japan. Research Report of the Lake Biwa Museum 18: 97–109.

Arnold SJ. 1983. Morphology, performance and fitness. American Zoologist 23: 347–361.

Bartels WS. 1984. Osteology and systematic affinities of the horned alligator *Ceratosuchus* (Reptilia, Crocodilia). Journal of Paleontology 58: 1347–1353.

Bell MA & Lloyd GT. 2014. strap: Stratigraphic Tree Analysis for Palaeontology. Available at: https://CRAN.R-project.org/package=strap.

Bell MA & Lloyd GT. 2015. strap: an R package for plotting phylogenies against stratigraphy and assessing their stratigraphic congruence. Palaeontology 58: 379–389.

Benton MJ & Clark JM. 1988. Archosaur phylogeny and the relationships of the Crocodylia. In: Benton MJ, ed. The Phylogeny and classification of the tetrapods, vol. 1., 295–338.

Benton MJ & Storrs GW. 1994. Testing the quality of the fossil record: paleontological knowledge is improving. Geology 22: 111–114.

Berg DE. 1964. Krokodile als Klimazeugen. Geologische Rundschau 54: 328–333.

Berg DE. 1966. Die Krokodile, insbesondere *Asiatosuchus* und aff. Sebecus?, aus dem Eozän von Messel bei Darmstadt/Hessen. Abhandlungen des Hessischen Landesamtes für Bodenforschung 52: 1–105.

Blob RW. 2000. Interspecific scaling of the hindlimb skeleton in lizards, crocodilians, felids and canids: does limb bone shape correlate with limb posture? Journal of Zoology 250: 507–531.

Blob RW & Biewener AA. 1999. In vivo locomotor strain in the hindlimb bones of *Alligator mississippiensis* and *Iguana iguana*: implications for the evolution of limb bone safety factor and non-sprawling limb posture. Journal of Experimental Biology 202: 1023‑1046.

Blob RW & Biewener AA. 2001. Mechanics of limb bone loading during terrestrial locomotion in the green iguana (*Iguana iguana*) and American alligator (*Alligator mississippiensis*). Journal of Experimental Biology 204: 1099–1122.

Bock WJ. 1990. From biologische anatomie to ecomorphology. Netherland Journal of Zoology 40: 254–277.

Bocquentin-Villanueva J, de Souza Filho JP, Buffetaut E, et al. 1991. Nova interpretacao do genero *Purussaurus* (Crocodylia, Alligatoridae). Anais do XI Congresso Brasiliero de Paleontologia: 427–438.

Bona P & Desojo JB. 2011. Osteology and cranial musculature of *Caiman latirostris* (Crocodylia: Alligatoridae). Journal of Morphology 272: 780–795.

Bonnan MF, Farlow JO & Masters SL. 2008. Using linear and geometric morphometrics to detect intraspecific variability and sexual dimorphism in femoral shape in *Alligator mississippiensis* and its implications for sexing fossil archosaurs. Journal of Vertebrate Paleontology 28: 422–431.

Bookstein FL. 1991. Morphometric tools for landmark data. Cambridge: Cambridge University Press.

Boszczyk BM, Boszczyk AA & Putz R. 2001. Comparative and functional anatomy of the mammalian lumbar spine. Anatomical Record 264: 157–168.

Boyd CA, Cleland TP, Marrero NL, et al. 2011. Exploring the effects of phylogenetic uncertainty and consensus trees on stratigraphic consistency scores: A new program and a standardized method. Cladistics 27: 52–60.

Brandt LA & Mazzotti FJ. 1990. The behavior of juvenile *Alligator mississippiensis* and *Caiman crocodilus* exposed to low temperature. Copeia 3: 867–871.

Brazaitis P. 1987. Identification of crocodilian skins and products. In: Webb GJW, Manolis CS, Whitehead PJ, eds. Wildlife management: crocodiles and alligators. Sydney: Surrey Beatty & Sons, 373–386.

Brazaitis P & Watanabe ME. 2011. Crocodilian behaviour: a window to dinosaur behaviour? Historical Biology 23: 73–90.

Brisbin IL, Standora EA & Vargo MJ. 1982. Body temperatures and behavior of American alligators during cold winter weather. The American Midland Naturalist 107: 209–218.

Brochu CA. 1995. Heterochrony in the crocodylian scapulocoracoid. Journal of Herpetology 29: 464–468.

Brochu CA. 1996. Closure of neurocentral sutures during crocodilian ontogeny: Implications for maturity assessment in fossil archosaurs. Journal of Vertebrate Paleontology 16: 49–62.

Brochu CA. 1997a. Morphology, fossils, divergence timing, and the phylogenetic relationships of *Gavialis*. Systematic Biology 46: 479–522.

Brochu CA. 1997b. Phylogenetic systematics and taxonomy of Crocodylia. Ph.D. dissertation, University of Texas, Austin. 540 pp.

Brochu CA. 1999a. Phylogenetics, taxonomy, and historical biogeography of Alligatoroidea. Journal of Vertebrate Paleontology 19: 9–100.

Brochu CA. 1999b. Taxon sampling and reverse successive weighting. Systematic Biology 48: 808–813.

Brochu CA. 2000. Phylogenetic relationships and divergence timing of *Crocodylus* based on morphology and the fossil record. Copeia 3: 657–673.

Brochu CA. 2001. Crocodylian snouts in space and time: phylogenetic approaches toward adaptive radiation. American Zoologist 41: 564–585.

Brochu CA. 2003. Phylogenetic approaches toward crocodylian history. Annual Review of Earth and Planetary Sciences 31: 357–397.

Brochu CA. 2004a. A new Late Cretaceous gavialoid crocodylian from Eastern North America and the phylogenetic relationships of thoracosaurs. Journal of Vertebrate Paleontology 24: 610–633.

Brochu CA. 2004b. Alligatorine phylogeny and the status of *Allognathosuchus Mook*, 1921. Journal of Vertebrate Paleontology 24: 857–873.

Brochu CA. 2004c. Patterns of calibration age sensitivity with quartet dating methods. Journal of Paleontology 78: 7–30.

Brochu CA. 2006. Osteology and phylogenetic significance of *Eosuchus minor* (Marsh, 1870) New combination, a longirostrine crocodylian from the Late Paleocene of North America. Journal of Paleontology 80: 162–186.

Brochu CA. 2007a. Morphology, relationships, and biogeographical significance of an extinct horned crocodile (Crocodylia, Crocodylidae) from the Quaternary of Madagascar. Zoological Journal of the Linnean Society 150: 835–863.

Brochu CA. 2007b. Systematics and taxonomy of Eocene tomistomine crocodylians from Britain and northern Europe. Palaeontology 50: 917–928.

Brochu CA. 2010. A new alligatorid from the Lower Eocene Green River Formation of Wyoming and the origin of caimans. Journal of Vertebrate Paleontology 30: 1109–1126.

Brochu CA. 2011. Phylogenetic relationships of *Necrosuchus ionensis* Simpson, 1937 and the early history of caimanines. Zoological Journal of the Linnean Society 163: S228–S256.

Brochu CA. 2013. Phylogenetic relationships of Palaeogene ziphodont eusuchians and the status of *Pristichampsus* Gervais, 1853. Earth and Environmental Science Transactions of the Royal Society of Edinburgh 103: 521–550.

Brochu CA & Gingerich PD. 2000. New tomistomine crocodylian from the Middle Eocene (Bartonian) of Wadi Hitan, Fayum Province, Egypt. Contributions from the Museum of Paleontology, the University of Michigan 30: 251–268.

Brochu CA & Norell MA. 2000. Temporal congruence and the origin of birds. Journal of Vertebrate Paleontology 20: 197–200.

Brochu CA & Rincón AD. 2004. A gavialoid crocodylian from the Lower Miocene of Venezuela. Special Papers in Palaeontology, Fossils of the Miocene Castillo Formation, Venezuela: Contributions in Neotropical Palaeontology 71: 61–79.

Brochu CA & Storrs GW. 2012. A giant crocodile from the Plio-Pleistocene of Kenya, the phylogenetic relationships of Neogene African crocodylines, and the antiquity of *Crocodylus* in Africa. Journal of Vertebrate Paleontology 32: 587–602.

Brochu CA, Njau J, Blumenschine RJ, et al. 2010. A new horned crocodile from the Plio-Pleistocene hominid sites at Olduvai Gorge, Tanzania. PLoS ONE 5: e9333.

Brochu CA, Parris DC, Grandstaff BS, et al. 2012. A new species of *Borealosuchus* (Crocodyliformes, Eusuchia) from the Late Cretaceous-Early Paleogene of New Jersey. Journal of Vertebrate Paleontology 32: 105–116.

Brown CM, VanBuren CS, Larson DW, et al. 2015. Tooth counts through growth in diapsid reptiles: implications for interpreting individual and size-related variation in the fossil record. Journal of Anatomy 226: 322–333.

Brusatte SL & Sereno PC. 2008. Phylogeny of Allosauroidea (Dinosauria: Theropoda): comparative analysis and resolution. Journal of Systematic Palaeontology 6: 155–182.

Brusatte SL, Benton MJ, Ruta M, et al. 2008. Superiority, competition, and opportunism in the evolutionary radiation of dinosaurs. Science 321: 1485–1488.

Buchholtz EA. 1998. Implications of vertebral morphology for locomotor evolution in early Cetacea. In: Thewissen JGM, ed. The Emergence of Whales: Evolutionary Patterns in the Origin of Cetacea. New York and London: Plenum Press, 325–351.

Buchholtz EA. 2001a. Swimming styles in Jurassic ichthyosaurs. Journal of Vertebrate Paleontology 21: 61–73.

Buchholtz EA. 2001b. Vertebral osteology and swimming style in living and fossil whales (Order: Cetacea). Journal of Zoology, London 253: 175–190.

Buchholtz EA & Schur SA. 2004. Vertebral osteology in Delphinidae (Cetacea). Zoological Journal of the Linnean Society 140: 383–401.

Busbey AB. 1995. The structural consequences of skull flattening in crocodilians. In: Thomason JJ, ed. Functional morphology in vertebrate paleontology. Cambridge: Cambridge University Press, 173–192.

Buscalioni ÁD & Sanz JL. 1990. The small crocodile *Bernissartia fagesii* from the Lower Cretaceous of Galve (Teruel, Spain). Bulletin de l'Institut royal des sciences naturelles de Belgique. Sciences de la Terre 60: 129–150.

Buscalioni ÁD, Ortega F, Weishampel DB, et al. 2001. A revision of the crocodyliform *Allodaposuchus precedens* from the Upper Cretaceous of the Hateg basin, Romania. Its relevance in the phylogeny of Eusuchia. Journal of Vertebrate Paleontology 21: 74–86.

Buscalioni ÁD, Piras P, Vullo R, et al. 2011. Buscalioni et al. 2011. Early eusuchia crocodylomorpha from the vertebrate-rich Plattenkalk of Pietraroia (Lower Albian, southern Appennines, Italy). Zoological Journal of the Linnean Society 163: S199–S227.

Buscalioni ÁD, Sanz JL & Casanovas ML. 1992. A new species of the eusuchian crocodile *Diplocynodon* from the Eocene of Spain. Neues Jahrbuch für Geologie und Paläontologie Abhandlungen 187: 1–29.

Bustard HR & Singh LAK. 1977. Studies on the Indian gharial *Gavialis gangeticus* (Gmelin) (Reptilia, Crocodilia) change in terrestrial locomotory pattern with age. Journal of Bombay Natural History Society 74: 534–537.

Böhmer C, Rauhut OWM & Wörheide G. 2015. Correlation between Hox code and vertebral morphology in archosaurs. Proceedings of the Royal Society B 282: 20150077.

Campione NE & Evans DC. 2012. A universal scaling relationship between body mass and proximal limb bone dimensions in quadrupedal terrestrial tetrapods. BMC Biology 10: doi:10.1186/1741-7007-10-60.

Campos Z, Coutinho M, Mourão G, et al. 2006. Long distance movement by *Caiman crocodilus* yacare: implications for management of the species in the Brazilian pantanal. Herpetological Journal 16: 123–132.

Campos Z, Llobet A, Piña CI, et al. 2010. Yacare caiman *Caiman yacare*. In: Manolis CS, Stevenson C, eds. Crocodiles. Status Survey and Conservation Action Plan, 3rd Edition. Darwin: Crocodile Specialist Group, 23–28.

Cao K. 1984. On the geographical and historical origins and the reasons for the decline of *Alligator sinensis* in China. Acta Herpetologica Sinica 3: 73–76.

Carvalho I de S, de Gasparini ZB, Salgado L, et al. 2010. Climate's role in the distribution of the Cretaceous terrestrial Crocodyliformes throughout Gondwana. Palaeogeography, Palaeoclimatology, Palaeoecology 297: 252–262.

Chamero B, Buscalioni ÁD & Marugán-Lobón J. 2013. Pectoral girdle and forelimb variation in extant Crocodylia: the coracoid-humerus pair as an evolutionary module. Biological Journal of the Linnean Society 108: 600–618.

Chamero B, Buscalioni ÁD, Marugán-Lobón J, et al. 2014. 3D geometry and quantitative variation of the cervico-thoracic region in Crocodylia. Anatomical Record 297: 1278–1291.

Chang K-C. 1986. The archaeology of ancient China. New Haven: Yale University Press.

Chippindale PT & Wiens JJ. 1994. Weighting, partitioning, and combining characters in phylogenetic analysis. Systematic Biology 43: 278–287.

Clark JM. 1994. Patterns of evolution in Mesozoic Crocodyliformes. In: Fraser NC, Sues HD, eds. In the shadow of the dinosaurs: early Mesozoic tetrapods. New York: Cambridge University Press, 84–97.

Claude J, Naksri W, Boonchai N, et al. 2011. Neogene reptiles of northeastern Thailand and their paleogeographical significance. Annales de Paléontologie 97: 113–131.

Cleuren J & de Vree F. 2000. Feeding in crocodilians. In: Schwent K, ed. Feeding: Form, Function, and Evolution in Tetrapod Vertebrates. San Diego, California: Academic Press, 337–358.

Cohen K, Finney S, Gibbard P, et al. 2013. The ICS International Chronostratigraphic Chart. Episodes 36: 199–204.

Cong L, Hou L & Wu X-chun. 1984. Age variation in the skull of *Alligator sinensis* Fauvel in topographic anatomy. Acta Herpetologica Sinica 3: 1–13.

Cong L, Hou L, Wu X-chun, et al. 1998. The gross anatomy of *Alligator sinensis* Fauvel. Beijing: Science Press.

Conrad JL, Jenkins K, Lehmann T, et al. 2013. New specimens of '*Crocodylus*' *pigotti* (Crocodylidae) from Rusinga Island, Kenya, and generic reallocation of the species. Journal of Vertebrate Paleontology 33: 629–646.

Cuff AR, Sparkes EL, Randau M, et al. 2016. The scaling of postcranial muscles in cats (Felidae) II: hindlimb and lumbosacral muscles. Journal of Anatomy 229: 128–141.

Davenport J & Sayer MDJ. 1989. Observations on the aquatic locomotion of young salt-water crocodiles (*Crocodylus porosus* Schneider). Herpetological Journal 1: 356–361.

Davis MB & Shaw RG. 2001. Range shifts and adaptive responses to Quaternary climate change. Science 292: 673–679.

Delfino M & de Vos J. 2010. A revision of the Dubois crocodylians, *Gavialis bengawanicus* and *Crocodylus ossifragus*, from the Pleistocene Homo erectus beds of Java. Journal of Vertebrate Paleontology 30: 427–441.

Delfino M, Codrea V, Folie A, et al. 2008. A complete skull of *Allodaposuchus precedens* Nopcsa, 1928 (Eusuchia) and a reassessment of the morphology of the taxon based on the Romanian remains. Journal of Vertebrate Paleontology 28: 111–122.

Delfino M, Piras P & Smith T. 2005. Anatomy and phylogeny of the gavialoid crocodylian *Eosuchus lerichei* from the Paleocene of Europe. Acta Palaeontologica Polonica 50: 565–580.

Delfino M & Smith T. 2009. A reassessment of the morphology and taxonomic status of '*Crocodylus' depressifrons* Blainville, 1855 (Crocodylia, Crocodyloidea) based on the Early Eocene remains from Belgium. Zoological Journal of the Linnean Society 156: 140–167.

Densmore LD. 1983. Biochemical and immunological systematics of the order Crocodilia. In: Hechet MK, Wallace B, Prance GH, eds. Evolutionary Biology. New York: Plenum, 397–465.

Densmore LD & Dessauer HC. 1984. Low levels of protein divergence detected between *Gavialis* and *Tomistoma*: Evidence for crocodilian monophyly? Comparative Biochemistry and Physiology Part B 77: 715–720.

Densmore LD & White PS. 1991. The systematics and evolution of the Crocodilia as suggested by restriction endonuclease analysis of mitochondrial and nuclear ribosomal DNA. Copeia: 602–615.

Denton Jr. RK, Dobie JL & Parris DC. 1997. The marine croocdilian *Hyposaurus* in North America. In: Callaway JM, Nicholls EL, eds. Ancient Marine Reptiles. London: Academic Press, 375–397.

Di-Poï N & Milinkovitch MC. 2013. Crocodylians evolved scattered multi-sensory micro-organs. EvoDevo 4: 1–15.

Ding BY, Li GY, Fu CX, et al. 2009. Flora of Tianmu Mountain, 1. Zhejiang University Press.

Dodson P. 1975. Functional and ecological significance of relative growth in *Alligator*. Journal of Zoology, London 175: 315–355.

Drumheller SK, Wilberg EW & Sadleir RW. 2016. The utility of captive animals in actualistic research: A geometric morphometric exploration of the tooth row of *Alligator mississippiensis* suggesting ecophenotypic influences and functional constraints. Journal of Morphology 277: 866–878.

Elliott NG, Haskard K & Koslow JA. 1995. Morphometric analysis of orange roughy (*Hoplostethus atalanticus*) off the continental slope of southern Australia. Journal of Fish Biology 46: 202–220.

Elsey RM. 2005. Unusual offshore occurrence of an American *Alligator*. Southeastern Naturalist 4: 533–536.

Elsey RM & Woodward AR. 2010. American alligator *Alligator mississippiensis*. In: Manolis CS, Stevenson C, eds. Crocodiles. Status Survey and Conservation Action Plan, 3rd Edition. Darwin: Crocodile Specialist Group, 1–4.

Endo H, Aoki R, Taru H, et al. 2002. Comparative functional morphology of the masticatory apparatus in the long-snouted crocodiles. Anatomia, Histologia, Embryologia 31: 206–213.

Erickson BR. 1972a. *Albertochampsa langstoni*, gen. et sp. nov., a new alligator from the Cretaceous of Alberta. The Scientific Publications of the Science Museum of Minnesota, New Series 2: 1–13.

Erickson BR. 1972b. The lepidosaurian reptile *Champsosaurus* in North America. The Science Museum of Minnesota, Monograph (Paleontology) 1: 1–91.

Erickson BR. 1982. *Wannaganosuchus*, a new alligator from the Paleocene of North America. Journal of Paleontology 56: 492–506.

Erickson BR, Sawyer GT. 1996. The estuarine crocodile *Gavialosuchus carolinensis* n. sp. (Crocodylia: Eusuchia) from the late Oligocene of South Carolina, North America. The Science Museum of Minnesota, Monograph (Paleontology) 3: 1–47.

Erickson GM, Gignac PM, Lappin AK, et al. 2014. A comparative analysis of ontogenetic bite-force scaling among Crocodylia. Journal of Zoology 292: 48–55.

Erickson GM, Gignac PM, Steppan SJ, et al. 2012. Insights into the ecology and evolutionary success of crocodilians revealed through bite-force and tooth-pressure experimentation. PLoS ONE 7: e31781.

Erickson GM, Lappin AK & Vliet KA. 2003. The ontogeny of bite-force performance in American alligator (*Alligator mississippiensis*). Journal of Zoology 260: 317–327.

Erickson GM, Lappin AK, Parker T, et al. 2004. Comparison of bite-force performance between long-term captive and wild American alligators (*Alligator mississippiensis*). Journal of Zoology 262: 21–28.

Estes R & Hutchison JH. 1980. Eocene lower vertebrates from Ellesmere Island, Canadian Arctic Archipelago. Palaeogeography, Palaeoclimatology, Palaeoecology 30: 325–347.

Evans SE & Hecht MK. 1993. A history of an extinct reptilian clade, the Choristodera: longevity, Lazarus-taxa, and the fossil record. Evolutionary Biology 27: 323–338.

Fabiani R. 1912. Contributi alla conoscenza dei vertebrati terziari e quaternari del Veneto: I. Il tipo del *Crocodilus vicetinus* Lioy. Memorie dell'Istituto geologico della R. Università di Padova 1.

Farmer CG & Sanders K. 2010. Unidirectional airflow in the lungs of alligators. Science 327: 338–340.

Fauvel AA. 1879. Alligators in China. Journal of the North-China Branch of the Royal Asiatic Society 13: 1–36.

Felsenstein J. 1973. Maximum likelihood and minimum-steps methods for estimating evolutionary trees from data on discrete characters. Systematic Biology 22: 240–249.

Felsenstein J. 1985. Phylogenies and the comparative methods. American Naturalist 125: 1–15.

Harvey PH & Pagel M. 1991. The Comparative Method in Evolutionary Biology. Oxford: Oxford University Press.

Fernandez-Blanco M V, Bona P, Olivares AI, et al. 2015. Ontogenetic variation in the skulls of Caiman: the case of *Caiman latirostris* and *Caiman yacare* (Alligatoridae, Caimaninae). Herpetological Journal 25: 65–73.

Figueiredo RG, Kellner AWA. 2009. A new crocodylomorph specimen from the Araripe Basin (Crato Member, Santana Formation), northeastern Brazil. Palaontologische Zeitschrift 83: 323–331.

Figueiredo RG, Moreira JKR, Saraiva AÁF, Kellner AWA. 2011. Description of a new specimen of *Susisuchus anatoceps* (Crocodylomorpha: Mesoeucrocodylia) from the Crato Formation (Santana Group) with comments on Neosuchia. Zoological Journal of the Linnean Society 163: S273-288.

Fish FE. 1984. Kinematics of undulatory swimming in the American alligator. Copeia: 839–843.

Foth C, Bona P & Desojo JB. 2015. Intraspecific variation in the skull morphology of the black caiman *Melanosuchus niger* (Alligatoridae, Caimaninae). Acta Zoologica 96: 1–13.

Fourtau R. 1920. Un nouveau genre de gavialidés. In: Department ES, ed. Contribution à l'étude des vertébrés Miocènes de l'Égypte. Cairo: Government Press, 116–121.

Fraas E. 1902. Die Meer-Crocodilier (Thalattosuchia) des oberen Jura unter specieller Berücksichtigung von Dacosaurus und Geosaurus. Palaeontographica 49: 1–72.

Frey E & Salisbury SW. 2001. The kinematics of aquatic locomotion in *Osteolaemus tetraspis* Cope. In: Grigg GC, Seebacher F, Franklin CE, eds. Crocodilian Biology and Evolution. Chipping Norton: Surrey Beatty & Sons, 165–179.

Frey E. 1988. Anatomie des Körperstammes von *Alligator mississippiensis* Daudin. Stuttgarter Beiträge zur Naturkunde A (Biologie) 424: 1–106.

Fukuda Y, Webb GJW, Manolis CS, et al. 2011. Recovery of saltwater crocodiles following unregulated hunting in tidal rivers of the Northern Territory, Australia. Journal of Wildlife Management 75: 1253–1266.

Furui S, Kobayashi Y & Chiba K. 2012. A new tomistomine from the Osaka Group in Kishiwada City, Osaka Prefecture, Japan. Journal of Vertebrate Paleontology 32 (supple: 98.

Garland, Jr. T & Losos JB. 1994. Ecological morphology of locomotor performance in squamate reptiles. In: Wainwright PC, Reilly SM, eds. Ecological Morphology. Chicago: The University of Chicago Press, 240–302.

Gatesy J & Amato GD. 1992. Sequence similarity of 12s ribosomal segment of mitochondrial DNAs of gharial and false gharial. Copeia: 241–243.

Gatesy J, Amato GD, Norell MA, et al. 2003. Combined support for wholesale taxic atavism in gavialine crocodylians. Systematic Biology 52: 403–422.

Gatesy J, Baker RH & Hayashi C. 2004. Inconsistencies in arguments for the supertree approach: supermatrices versus supertrees of Crocodylia. Systematic Biology 53: 342–355.

Gatesy SM. 1997. An electromyographic analysis of hindlimb function in *Alligator* during terrestrial locomotion. Journal of Morphology 234: 197–212.

Gignac PM & Erickson GM. 2015. Ontogenetic changes in dental form and tooth pressures facilitate developmental niche shifts in American alligators. Journal of Zoology 295: 132–142.

Gignac PM & Erickson GM. 2016. Ontogenetic bite-force modeling of *Alligator mississippiensis*: implications for dietary transitions in a large-bodied vertebrate and the evolution of crocodylian feeding. Journal of Zoology 299: 229–238.

Gilmore CW. 1946. A new crocodilian from the Eocene of Utah. Journal of Paleontology 20: 62–67.

Gmelin JF. 1789. Regnum animal. In: Bear GE, ed. Caroli a Linne. Systema naturae per regna tria naturae, secundum classes, ordines, genera, species, cum characteribus, differentiis, synonymis, locis., 1033–1516.

Gold MEL, Brochu CA & Norell MA. 2014. An expanded combined evidence approach to the *Gavialis* problem using geometric morphometric data from crocodylian braincases and Eustachian systems. PLoS ONE 9: e105793.

Goloboff PA, Farris JS & Nixon KC. 2003. T.N.T.: Tree analysis using new technology. Available at: http://www.lillo.org.ar/phylogeny/tnt/.

Gower JC. 1975. Generalized Procrustes analysis. Psychometrika 40: 33–51.

Grigg GC & Kirshner D. 2015. Biology and Evolution of Crocodylians. Clayton South, VIC, Australia: CSIRO Publishing.

Hagan JM, Smithson P & Doerr PD. 1983. Behavioral response of the American alligator to freezing weather. Journal of Herpetology 17: 402–404.

Hall PM. 1989. Variation in geographic isolates of the New Guinea crocodile (*Crocodylus novaeguineae* Schmidt) compared with the similar, allopatric, Philippine crocodile (*C. mindorensis* Schmidt). Copeia 1: 71–80.

Hall PM & Portier KM. 1994. Cranial morphometry of New Guinea crocodiles (*Crocodylus*

novaeguineae): ontogenetic variation in relative growth of the skull and an assessment of its utility as a predictor of the sex and size of individuals. Herpetological Monographs 8: 203–225.

Handa N. 2015. A Pleistocene rhinocerotid (Mammalia, Perissodactyla) from Yage, Shizuoka Prefecture, central Japan. Paleontological Research 19: 139–142.

Harshman J, Huddleston CJ, Bollback JP, et al. 2003. True and false gharials: a nuclear gene phylogeny of crocodylia. Systematic Biology 52: 386–402.

Hase Y, Danhara T, Shiihara M, et al. 2001. Stratigraphy and fission-track ages of the Tsubusagawa Formation in the Ajimu area of Northern Kyushu, Japan. Research Report of the Lake Biwa Museum 18: 5–15.

Hass CA, Hoffman, MA, Densmore III LD, et al. 1992. Crocodilian evolution: insights from immunological data. Molecular Phylogenetics and Evolution 1: 193–201.

Hastings AK. 2012. Early Paleogene crocodyliform evolution in the Neotropics: evidence from northeastern Colombia. Ph.D. dissertation, University of Florida, Gainesville. 250 pp.

Hastings AK & Hellmund M. 2017. Evidence for prey preference partitioning in the middle Eocene high-diversity crocodylian assemblage of the Geiseltal-Fossillagerstätte, Germany utilizing skull shape analysis. Geological Magazine 154: 119–146.

Hastings AK, Bloch JI & Jaramillo CA. 2011. A new longirostrine dyrosaurid (Crocodylomorpha, Mesoeucrocodylia) from the Paleocene of north-eastern Colombia: Biogeographic and behavioural implications for New-World Dyrosauridae. Palaeontology 54: 1095–1116.

Hayashi Y. 1952. The natural distribution of important trees, indigenous to Japan. Bulletin of the Government Forest Experiment Station 55: 1–251.

Hekkala ER, Shirley MH, Amato GD, et al. 2011. An ancient icon reveals new mysteries: Mummy DNA resurrects a cryptic species within the Nile crocodile. Molecular Ecology 20: 4199–4215.

Henan Provincial Institute of Cultural Relics and Archaeology. 1999. Wuyang Jiahu, Volume I & II. Beijing: Science Press.

Hewitt G. 2000. The genetic legacy of the Quaternary ice ages. Nature 405: 907–913.

Hildebrand M & Goslow G. 2001. Analysis of Vertebrate Structure. 5th edition. New York: John Wiley & Sons, Inc.

Hillis DM & Wiens JJ. 2000. Molecules versus morphology in systematics–Conflicts, artifacts, and misconceptions. In: Wiens JJ, ed. Phylogenetic analysis of morphological data. Washington D. C.: Smithsonian Institution Press, 1–19.

Hirayama R. 2001. Fossil turtles from the Tsubusagawa Formation (Pliocene) of Ajimu-cho, Oita Prefecture, Northern Kyushu, Japan. Research Report of the Lake Biwa Museum 18: 79–96.

Ho L si T & Ané C. 2014. A linear-time algorithm for Gaussian and non-Gaussian trait evolution

models. Systematic Biology 63: 397–408.

Hoffstetter R & Gasc JP. 1969. Vertebrae and ribs of modern reptiles. In: Gans C, Parson TS, eds. Biology of the Reptilia, Vol. 1. New York: Academic Press, 201–310.

Holliday CM & Witmer LM. 2007. Archosaur adductor chamber evolution: Integration of musculoskeletal and topological criteria in jaw muscle homology. Journal of Morphology 268: 457–484.

Hoshi H. 2016. Paleomagnetic dating of a fossiliferous bed of the Tokai Group at the construction site of the new Mie Prefectural Museum, Tsu City. Mie Prefectural Museum Research Bulletin 2: 1–6.

Hoshizumi H & Morishita Y. 1993. Geology of the Toyooka district with geological sheet map at 1:50,000. Fukuoka: Geological Survey of Japan.

Hu C & Liang S. 1996. Plants of Huang Shan Mountain. Fudan University Press.

Hua S. 1994. Hydrodynamique et modalitée d'allègement chez *Metrorhynchus supercilosus* (Crocodylia, Thalattosuchia): implications paléologique. Neues Jahrbuch für Geologie und Palaontologie Abhandlungen 193: 1–19.

Hua S. 2003. Locomotion in marine mesosuchians (Crocodylia): the contribution of the 'locomotion profiles'. Neues Jahrbuch für Geologie und Palaontologie Abhandlungen 227: 139–152.

Hua S & Jouve S. 2004. A primitive marine gavialoid from the Paleocene of Morocco. Journal of Vertebrate Paleontology 24: 341–350.

Huang W. 1982. Preliminary study on the fossil hominid skull and fauna of Hexian, Anhui. Vertebrata PalAsiatica 20: 248–256.

Huang W, Song F, Guo X, et al. 1988. First discovery of *Megalovis guangxiensis* and *Alligator* cf. *sinensis* in Guangdong. Vertebrata PalAsiatica 26: 227–231.

Huelsenbeck JP. 1994. Comparing the stratigraphic record to estimates of phylogeny. Paleobiology 20: 470–483.

Hunt AP. 1989. Cranial morphology and ecology among phytosaurs. In: Lucas SG, Hunt AP, eds. Dawn of the age of dinosaurs in the American Southwest. New Mexico Museum of Natural History, Albuquerque, 349–354.

Hutchinson JR & Gatesy SM. 2000. Adductors, abductors, and the evolution of archosaur locomotion. Paleobiology 26: 734–751.

Iijima M. 2017. Assessment of trophic ecomorphology in non-alligatoroid crocodylians and its adaptive and taxonomic implications. Journal of Anatomy 231: 192–211.

Iijima M, Kubo T & Kobayashi Y. 2018. Comparative limb proportions reveal differential locomotor morphofunctions of alligatoroids and crocodyloids. Royal Society Open Science.

Iijima M, Momohara A, Kobayashi Y, et al. 2018. *Toyotamaphimeia* cf. *machikanensis* (Crocodylia,

Tomistominae) from the Middle Pleistocene of Osaka, Japan, and crocodylian survivorship through the Pliocene-Pleistocene climatic oscillations. Palaeogeography, Palaeoclimatology, Palaeoecology.

Iijima M, Takahashi K & Kobayashi Y. 2016. The oldest record of *Alligator sinensis* from the Late Pliocene of Western Japan, and its biogeographic implication. Journal of Asian Earth Sciences 124: 94–101.

Ikejiri T. 2012. Histology-based morphology of the neurocentral synchondrosis in *Alligator mississippiensis* (Archosauria, Crocodylia). Anatomical Record 295: 18–31.

Ikejiri T. 2015. Modes of ontogenetic allometric shifts in crocodylian vertebrae. Biological Journal of the Linnean Society 116: 649–670.

Information Department of Beijing Meteorological Center. 1984. Land climate data of China (1951–1980). Beijing: China Meteorological Press.

Institute of Archaeology in Chinese Academy of Social Sciences. 2000. Excavations of the Wangyin site in Shandong. Beijing: Science Press.

International Commission on Zoological Nomenclature. 1999. International code of zoological nomenclature. The International Trust for Zoological Nomenclature 1999.

Iordansky NN. 1964. The jaw muscles of the crocodiles and some relating structures of the crocodilian skull. Anatomischer Anzeiger 115: 256–280.

Iordansky NN. 1973. The skull of the Crocodilia. In: Gans C, Parson TS, eds. Biology of the Reptilia, Vol. 4; Morphology D. New York: Academic Press, 201–262.

Isobe T. 1990. Shigaken sanchi annai sono 2. Kyoto Chigaku-kai Kaishi 44: 18–26.

Itihara M. 1993. Introduction–Geology and geomorphology, and a historical review of researches–. In: Itihara M, ed. The Osaka Group. Osaka: Sogen-sha, 3–10.

Ito A, Momohara A & Zhou Z. 2017. Pleistocene fossil leaflets of *Albizia kalkora* (Roxb.) Prain (Leguminosae subfamily Mimosoideae) from central Honshu, Japan, and its implication for historical biogeography. Japanese Journal of Historical Botany 26: 3–13.

Iwauchi A. 1994. Late Cenozoic vegetational and climatic changes in Kyushu, Japan. Palaeogeography, Palaeoclimatology, Palaeoecology 108: 229–280.

Iwauchi A & Hase Y. 1986. Late Cenozoic vegetation and paleoenvironment of northern and central Kyushu, Japan—Part 2 Ajimu-Innai area (Upper Pliocene)—. Journal of the Geological Society of Japan 92: 591–598.

Janke A, Gullberg A, Hughes S, et al. 2005. Mitogenomic analyses place the gharial (*Gavialis gangeticus*) on the crocodile tree and provide pre-K/T divergence times for most crocodilians. Journal of Molecular Evolution 61: 620–626.

Japan Meteorological Agency. 2002. Mesh Meteorological Values 2000.

Jiang HX. 2010. Chinese alligator *Alligator sinensis*. In: Manolis CS, Stevenson C, eds. Crocodiles. Status Survey and Conservation Action Plan, 3rd Edition. Darwin: Crocodile Specialist Group, 5–9.

Jiang L & Liu L. 2005. The discovery of an 8000-year-old dugout canoe at Kuahuqiao in the Lower Yangzi River, China. Antiquity 79.

Joanen T & McNease LL. 1989. Ecology and physiology of nesting and early development of the American alligator. American Zoologist 29: 987–998.

Jones KE. 2015. Evolutionary allometry of the thoracolumbar centra in felids and bovids. Journal of Morphology 276: 818–831.

Jones KE & Pierce SE. 2016. Axial allometry in a neutrally buoyant environment: effects of the terrestrial-aquatic transition on vertebral scaling. Journal of Evolutionary Biology 29: 594–601.

Jonet S & Wouters G. 1977. *Maroccosuchus zennaroi*, crocodilien eusuchien nouveau des phosphates du Maroc. Notes et Mémoires du Service géologique du Maroc 38: 177–202.

Jouve S. 2004. Study of the Crocodyliformes from the latest Cretaceous-Paleogene of the Oulad Abdoun Basin (Morocco) and comparison with contemporaneous African faunas: systematic, phylogeny and paleobiogeography. Ph.D. dissertation, Muséum National d'Histoire Naturelle, Paris. 651 pp.

Jouve S, Bardet N, Jalil NE, et al. 2008. The oldest African crocodylian: phylogeny, paleobiogeography, and differential survivorship of marine reptiles through the Cretaceous-Tertiary boundary. Journal of Vertebrate Paleontology 28: 409–421.

Jouve S, Bouya B, Amaghzaz M, et al. 2015. *Maroccosuchus zennaroi* (Crocodylia: Tomistominae) from the Eocene of Morocco: phylogenetic and palaeobiogeographical implications of the basalmost tomistomine. Journal of Systematic Palaeontology 13: 421–445.

Jouve S, Iarochene M, Bouya B, et al. 2006. New material of *Argochampsa krebsi* (Crocodylia: Gavialoidea) from the Lower Paleocene of the Oulad Abdoun Basin (Morocco): phylogenetic implications. Geobios 39: 817–832.

Kamata H & Muraoka H. 1984. K-Ar ages of the andesite lava from Ajimu district in Oita Prefecture, southwestern Japan. Journal of the Geological Society of Japan 90: 125–128.

Kato T. 2001. Discovery of the Pliocene Rhinocerotidae (Perissodactyla) from the Tsubusagawa Formation, Oita Prefecture. Research Report of the Lake Biwa Museum 18: 164–168.

Katoh S, Danhara T & Hyodo M. 2004. Re-examination of the Plio-Pleistocene boundary in the Osaka Group in Central Awaji Island, Western Japan. The Quaternary Research 43: 213–224.

Kawaguchi M & Kitada M. 1982. Crocodylian and cyprinid fish fossils from the Iga Formation.

Kansai Shizen-Kagaku 33: 16–18.

Kitamura A & Kimoto K. 2006. History of the inflow of the warm Tsushima Current into the Sea of Japan between 3.5 and 0.8 Ma. Palaeogeography, Palaeoclimatology, Palaeoecology 236: 355–366.

Kitamura A, Takano O, Takata H, et al. 2001. Late Pliocene-early Pleistocene paleoceanographic evolution of the Sea of Japan. Palaeogeography, Palaeoclimatology, Palaeoecology 172: 81–98.

Kluge AG & Farris JS. 1969. Quantitative phyletics and the evolution of anurans. Systematic Biology 18: 1–32.

Kluge AG & Wolf AJ. 1993. Cladistics: What's in a word? Cladistics 9: 183–199.

Kobatake N & Kamei T. 1966. The first discovery of fossil crocodile from central Honshu, Japan. Proceedings of the Japan Academy 42: 264–269.

Kobatake N, Chiji M, Ikebe N, et al. 1965. Discovery of crocodile fossil from the Osaka Group. The Quaternary Research 4: 49–58.

Kobayashi K. 1977. Geological and geographical history of Takatsuki City. In: Editorial Committee of 'History of Takatsuki City, ed. History of Takatsuki City. Kyoto: Nissha Printing, 47–90.

Kobayashi Y. 2009. A crocodylian fossil from the Pliocene Tokai Group distributed in the riverbed of the Suzuka-gawa, Kameyama City, Central Japan. In: Geology Group of the Editorial Committee of 'History of Kameyama City', ed. Excavation report on fossils from the Pliocene Tokai Group distributed in the riverbed of the Suzuka-gawa, Kameyama City, Central Japan. Mie: Kameyama City Historical Museum, 53–54.

Kobayashi Y, Tomida Y, Kamei T, et al. 2006. Anatomy of a Japanese tomistomine crocodylian, *Toyotamaphimeia machikanensis* (Kamei et Matsumoto, 1965), from the Middle Pleistocene of Osaka Prefecture: The reassessment of its phylogenetic status within Crocodylia. National Science Museum Monographs 35: 1–121.

Koizumi A. 1995. Lower Pleistocene tephrostratigraphy of the Iimuro Formation, Kazusa Group, in the eastern part of the Tama Hills, central Japan. Bulletin of the Kawasaki Municipal Science Museum for Youth 6: 41–47.

Kraus R. 1998. The cranium of *Piscogavialis jugaliperforatus* n.gen., n.sp. (Gavialidae, Crocodylia) from the Miocene of Peru. Paläontologische Zeitschrift 72: 389–406.

Kubo T & Benton MJ. 2009. Tetrapod postural shift estimated from Permian and Triassic trackways. Palaeontology 52: 1029–1037.

Kälin JA. 1933. Beiträge zur vergleichenden Osteologie des Crocodiliden-schädels. Zoologische Jahrbücher, Abteilung für Anatomie und Ontogenie der Tiere 57: 535–714.

Lance VA. 2003. *Alligator* physiology and life history: The importance of temperature. Experimental

Gerontology 38: 801–805.

Lance VA, Elsey RM, Trosclair III PL, et al. 2011. Long-distance movement by American alligators in southwest Louisiana. Southeastern Naturalist 10: 389–398.

Langston WJ. 1965. Fossil crocodilians from Colombia and the Cenozoic history of the Crocodylia in South America. University of California Publications in Geological Sciences 52: 1–152.

Langston WJ. 1973. The crocodilian skull in historical perspective. In: Gans C, Parson TS, eds. Biology of the Reptilia, Vol. 4. New York: Academic Press, 263–289.

Langston WJ & Gasparini Z. 1997. Crocodilians, *Gryposuchus*, and the South American gavials. In: Kay RF, Madden RH, Cifelli RL, Flynn JJ, eds. Vertebrate Paleontology in the Neotropics: The Miocene Fauna of La Venta, Colombia. Washington D. C.: Smithsonian Institution, 113–154.

Larson DW, Brown CM & Evans DC. 2016. Dental disparity and ecological stability in bird-like dinosaurs prior to the end-Cretaceous mass extinction. Current Biology 26: 1325–1333.

Leitch DB & Catania KC. 2012. Structure, innervation and response properties of integumentary sensory organs in crocodilians. Journal of Experimental Biology 215: 4217–4230.

Leslie AJ & Taplin LE. 2001. Recent development in osmoregulation of crocodiles. In: Grigg GC, Seebacher F, Franklin CE, eds. Crocodilian Biology and Evolution. Chipping Norton: Surrey Beatty & Sons, 265–279.

Li J & Wang B. 1987. A new species of *Alligator* from Shanwang, Shandong. Vertebrata PalAsiatica 25: 199–207.

Lindgren J, Jagt JWM & Caldwell MW. 2007. A fishy mosasaur: The axial skeleton of *Plotosaurus* (Reptilia, Squamata) reassessed. Lethaia 40: 153–160.

Lisiecki LE & Raymo ME. 2005. A Pliocene-Pleistocene stack of 57 globally distributed benthic $\delta^{18}O$ records. Paleoceanography 20: PA1003.

Liu G & Chen G. 1993. Late Cenozoic Crocodilia fossils from Jiangsu. Vertebrata PalAsiatica 31: 61–64.

Liu L. 1994. Development of chiefdom societies in the middle and lower Yellow River valley in Neolithic China—A study of the Longshan culture from the perspective of settlement patterns. Ph.D. dissertation, Harvard University, Cambridge, Massachusetts. 539 pp.

Livingston VJ, Bonnan MF, Elsey RM, et al. 2009. Differential limb scaling in the American alligator (*Alligator mississippiensis*) and its implications for archosaur locomotor evolution. Anatomical Record 292: 787–797.

Long JH, Pabst DA, Shepherd WR, et al. 1997. Locomotor design of dolphin vertebral columns: Bending mechanics and morphology of *Delphinus delphis*. Journal of Experimental Biology 200: 65–81.

Lucas SG & Estep JW. 2000. Osteology of *Allognathosuchus mooki* Simpson, a Paleocene crocodilian from the San Juan Basin, New Mexico, and the monophyly of *Allognathosuchus*. New Mexico Museum of Natural History and Science Bulletin 16: 155–168.

Maccagno AM. 1948. Descrizione di una nuova specie di '*Crocodilus*' del giacimiento di Sahabi (Sirtica). Atti della Reale Accademia Nazionale dei Lincei: Memorie della Classe di Scienze Fisiche, Serie 8 1: 61–96.

Macpherson JM & Ye Y. 1998. The cat vertebral column: Stance configuration and range of motion. Experimental Brain Research 119: 324–332.

Maddison WP & Maddison DR. 2011. Mesquite: modular system for evolutionary analysis, Version 2.75. Available at: http://mesquiteproject.wikispaces.com/.

Man Z, Yishu W, Peng Y, et al. 2011. Crocodilian phylogeny inferred from twelve mitochondrial protein-coding genes, with new complete mitochondrial genomic sequences for *Crocodylus acutus* and *Crocodylus novaeguineae*. Molecular Phylogenetics and Evolution 60: 62–67.

Mannion PD, Benson RBJ, Carrano MT, et al. 2015. Climate constrains the evolutionary history and biodiversity of crocodylians. Nature Communications 6: 8438: doi:10.1038/ncomms9438.

Manter JT. 1940. The mechanics of swimming in the alligator. Journal of Experimental Zoology 83: 345–358.

Markwick PJ. 1994. 'Equability,' continentality, and Tertiary 'climate': The crocodilian perspective. Geology 22: 613–616.

Markwick PJ. 1998a. Fossil crocodilians as indicators of Late Cretaceous and Cenozoic climates: implications for using palaeontological data in reconstructing palaeoclimate. Palaeogeography, Palaeoclimatology, Palaeoecology 137: 205–271.

Markwick PJ. 1998b. Crocodilian diversity in space and time: the role of climate in paleoecology and its implication for understanding K/T extinctions. Paleobiology 24: 470–497.

Markwick PJ. 2007. The palaeogeographic and palaeoclimatic significance of climate proxies for data-model comparisons. In: Williams M, Haywood AM, Gregory FJ, et al., eds. Deep-Time Perspectives on Climate Change: Marrying the Signal from Computer Models and Biological Proxies. The Micropalaeontological Society Special Publications. The Geological Society, London, 251–312.

Martin JE. 2007. New material of the Late Cretaceous globidontan *Acynodon iberoccitanus* (Crocodylia) from southern France. Journal of Vertebrate Paleontology 27: 362–372.

Martin JE, Amiot R, Lécuyer C, et al. 2014. Sea surface temperature contributes to marine crocodylomorph evolution. Nature Communications 5: 4658: doi:10.1038/ncomms5658.

Martin JE, Buffetaut E, Naksri W, et al. 2012. *Gavialis* from the Pleistocene of Thailand and its relevance for drainage connections from India to Java. PLoS ONE 7: e44541.

Martin JE, Deesri U, Liard R, et al. 2015. Strontium isotopes and the long-term residency of thalattosuchians in the freshwater environment. Paleobiology 42: 143–156.

Martin JE, Delfino M & Smith T. 2016. Osteology and affinities of Dollo's goniopholidid (Mesoeucrocodylia) from the Early Cretaceous of Bernissart, Belgium. Journal of Vertebrate Paleontology 1222534: e1222534.

Maruyama S, Isozaki Y, Kimura G, et al. 1997. Paleogeographic maps of the Japanese Islands: Plate tectonic synthesis from 750 Ma to the present. Island Arc 6: 121–142.

Massare JA. 1987. Tooth morphology and prey preference of Mesozoic marine reptiles. Journal of Vertebrate Paleontology 7: 121–137.

Masuda F & Ito M. 1999. Contribution to sequence stratigraphy from the Quaternary studies in Japan. The Quaternary Research 38: 184–193.

Matsui M, Kitabayashi E, Takahashi K, et al. 2001. A fossil giant salamander of the genus *Andrias* from Kyushu, Southern Japan. Research Report of the Lake Biwa Museum 18: 72–78.

Matsumoto H, Murata M & Imanaka H. 1984. Late Cenozoic volcano-stratigraphy in the northern part of Oita Prefecture, Japan I. Usa-Ajimu and Yabakei areas. Kumamoto Journal of Science (Geology) 13: 1–24.

Matsuoka C, Okamura Y & Tamura M. 1991. Vertebrate fossils found in Shiga Prefecture. In: Foundation of the Nature Conservation in Shiga Prefecture, ed. Landscape and environment of Shiga: Scientific studies of Shiga Prefecture, Japan., 543–625.

Matsuoka H. 2001. The Pliocene paleoavifauna of Ajimu, Oita, Japan, reconstructed from the fossils of the lacustrine deposit Tsubusagawa Formation. Research Report of the Lake Biwa Museum 18: 110–125.

Matsuoka K & Kitabayashi E. 2001. Fossil freshwater molluscs from the Tsubusagawa Formation in Ajimu Basin, Oita Prefecture, Japan. Research Report of the Lake Biwa Museum 18: 42–50.

Matsuoka K, Yoshida T & Okuyama S. 1990. Coprolites from the Iga Formation. In: Abstracts of the 139th Regular Meeting of the Palaeontological Society of Japan., 34.

McAliley LR, Willis RE, Ray DA, et al. 2006. Are crocodiles really monophyletic? –Evidence for subdivisions from sequence and morphological data. Molecular Phylogenetics and Evolution 39: 16–32.

McHenry CR, Clausen PD, Daniel WJT, et al. 2006. Biomechanics of the rostrum in crocodilians: a comparative analysis using finite-element modeling. The Anatomical Record Part A 288: 827–849.

Medina CJ. 1976. Crocodilians from the late Tertiary of northwestern Venezuela: *Melanosuchus fisheri* sp. nov. Breviora 438: 1–14.

Meers MB. 2002. Cross-sectional geometric properties of the crocodylian humerus: an exception to Wolff's Law? Journal of Zoology, London 258: 405–418.

Meers MB. 2003. Crocodylian forelimb musculature and its relevance to Archosauria. The Anatomical Record Part A 274A: 891–916.

Meganathan PR, Dubey B, Batzer MA, et al. 2010. Molecular phylogenetic analyses of genus *Crocodylus* (Eusuchia, Crocodylia, Crocodylidae) and the taxonomic position of *Crocodylus porosus*. Molecular Phylogenetics and Evolution 57: 393–402.

Megirian D, Murray PF & Willis PMA. 1991. A new crocodile of the gavial ecomorph morphology from the Miocene of Northern Australia. The Beagle: Records of The Northern Territory Museum of Arts and Sciences 8: 135–158.

Meredith RW, Hekkala ER, Amato GD, et al. 2011. A phylogenetic hypothesis for *Crocodylus* (Crocodylia) based on mitochondrial DNA: Evidence for a trans-Atlantic voyage from Africa to the New World. Molecular Phylogenetics and Evolution 60: 183–191.

Mie Prefectural Museum. 2011. Kaseki ga detazo!: Minna de shirabeta Shinkenritsuhakubutsukan kensetsuchi. Tsu: Mie Prefectural Museum.

Molnar JL, Pierce SE & Hutchinson JR. 2014. An experimental and morphometric test of the relationship between vertebral morphology and joint stiffness in Nile crocodiles (*Crocodylus niloticus*). Journal of Experimental Biology 217: 758–768.

Molnar JL, Pierce SE, Bhullar BAS, et al. 2015. Morphological and functional changes in the vertebral column with increasing aquatic adaptation in crocodylomorphs. Royal Society Open Science 2: 150439: doi:10.1098/rsos.150439.

Momohara A. 1994. Floral and paleoenvironmental history from the late Pliocene to middle Pleistocene in and around central Japan. Palaeogeography, Palaeoclimatology, Palaeoecology 108: 281–293.

Monteiro LR & Soares M. 1997. Allometric analysis of the ontogenetic variation and evolution of the skull in *Caiman* Spix, 1825 (Crocodylia: Alligatoridae). Herpetologica 53: 62–69.

Monteiro LR, Cavalcanti MJ & Sommer HJS. 1997. Comparative ontogenetic shape changes in the skull of *Caiman* species (Crocodylia, Alligatoridae). Journal of Morphology 231: 53–62.

Mook CC. 1921a. *Allognathosuchus*, a new genus of Eocene crocodilians. Bulletin of the American Museum of Natural History 44: 105–110.

Mook CC. 1921b. Description of a skull of a Bridger crocodilian. Bulletin American Museum of Natural History 8: 111–116.

Mook CC. 1921c. Description of a skull of the extinct Madagascar crocodile, *Crocodilus robustus* Vaillant and Grandidier. Bulletin of the American Museum of Natural History 44: 25–33.

Mook CC. 1921d. Individual and age variations in the skulls of Recent Crocodilia. Bulletin of the American Museum of Natural History 44: 51–66.

Mook CC. 1921e. Notes on the postcranial skeleton in the Crocodilia. Bulletin of the American Museum of Natural History 44: 67–100.

Mook CC. 1921f. The skull of *Crocodilus acer* Cope. Bulletin American Museum of Natural History 9: 117–121.

Mook CC. 1923. A new species of *Alligator* from the Snake Creek Beds. American Museum Novitates 73: 1–13.

Mook CC. 1924. A new crocodilian from the Wasatch beds. American Museum Novitates 137: 1–4.

Mook CC. 1932. A study of the osteology of A study of the osteology of *Alligator prenasalis* (Loomis). Bulletin of the Museum of Comparative Zoology 74: 19–41.

Mook CC. 1946. A new Pliocene alligator from Nebraska. American Museum Novitates 1311: 1–12.

Mosbrugger V & Utescher T. 1997. The coexistence approach–a method for quantitative reconstructions of Tertiary terrestrial palaeoclimate data using plant fossils. Palaeogeography, Palaeoclimatology, Palaeoecology 134: 61–86.

Motta PJ, Norton SF & Luczkovich JJ. 1995. Perspectives on the ecomorphology of bony fishes. Environmental Biology of Fishes 44: 11–20.

Myrick AC. 2001. *Thecachampsa antiqua* (Leidy, 1852) (Crocodylidae: Thoracosaurinae) from fossil marine deposits at Lee Creek Mine, Aurora, North Carolina, USA. Smithsonian Contributions to Paleontology 90: 219–225.

Müller L. 1927. Ergebnisse der Forschungsreisen Prof. E. Stromers in den Wüsten Ägyptens. V. Tertiäre Wirbeltiere: 1. Beiträge zur Kenntnis der Krokodilier des ägyptischen Tertiärs. Abhandlungen der Bayerischen Akademie der Wissenschaften 31: 1–97.

Nakagawa T, Tarasov PE, Nishida K, et al. 2002. Quantitative pollen-based climate reconstruction in central Japan: Application to surface and Late Quaternary spectra. Quaternary Science Reviews 21: 2099–2113.

Nakagawa Y. 2014. Dekaizo Miezou!: Kaseki ga Kataru Kyodaizou no sekai. Tsu: Mie Prefectural Museum.

Nakajima S. 1983. A study on a crocodylian fossil from Yage, Inasa-cho, Shizuoka Prefecture. M.Sc. thesis, Yokohama National University, Yokohama City. 150 pp.

Nakajima T & Kitabayashi E. 2001. Fossil pharyngeal teeth of cyprinids from the Pliocene Tsubusagawa Formation in the Ajimu, Oita Prefecture, Kyushu Island, Japan. Research Report of the Lake Biwa Museum 18: 57–65.

Nakamura Y, Kameo K, Asahara Y, et al. 1999. Stratigraphy and geologic age of the Neogene

Shimajiri Group in Kumejima Island, Ryukyu Islands, southwestern Japan. Journal of the Geological Society of Japan 105: 757–770.

Nanko S. 1996. Fossils of Awaji Island. Kyoto: Nissha Printing.

Natural History Section in Chekiang Provincial Museum. 1978. A study of the animal and plant remains unearthed at Ho-mu-tu. Acta Archaeologica Sinica 1: 95–107.

Nestler JH. 2012. A geometric morphometric analysis of *Crocodylus niloticus*: evidence for a cryptic species complex. M.Sc. thesis, University of Iowa, Iowa City. 70 pp.

Nishimura S & Sasajima S. 1970. Fission-track age of volcanic ash-layers of the Plio-Pleistocene Series in Kinki District, Japan. Chikyukagaku 24: 222–224.

Nojima K. 2002. The Pleistocene vertebrate faunas from the 'Yage' Limestone Fissure Deposits in Shizuoka Prefecture. Geoscience Reports of Shizuoka University 29: 1–11.

Nojima K & Itoigawa J. 2017. Tomistominae gen. et sp. indet. (Crocodylia: Crocodylidae) from the Lower Yage Formation (Middle Pleistocene) in Hamamatsu City, Shizuoka Prefecture, Japan. Bulletin of the Mizunami Fossil Museum 43: 35–46.

Nojima K, Aoshima A, Masuda K, et al. 2007. A new crocodylian with cyprinid fish fossils from the Middle Pleistocene of Yage, Inasa-cho, Hamamatsu City. Bulletin of the Hamamatsu City Museum 20: 1–16.

Nojima K, Aoshima A, Masuda K, et al. 2014. Geological age and paleovegetation of the Middle Pleistocene Lower Yage Formation, Shizuoka, Central Japan. Memoir of the Fukui Prefectural Dinosaur Museum 13: 37–45.

Norell MA. 1989. The higher level relationships of the extant Crocodylia. Journal of Herpetology 23: 325–335.

Norell MA & Clark JM. 1990. A reanalysis of *Bernissartia fagesii*, with comments on its phylogenetic position and its bearing on the origin and diagnosis of the Eusuchia. Bulletin de l'Institut royal des sciences naturelles de Belgique. Sciences de la Terre 60: 115–128.

Norell MA & Novacek MJ. 1992. The fossil record and evolution: comparing cladistic and paleontologic evidence for vertebrate history. Science 255: 1690–3.

Nunn CL. 2011. The Comparative Approach in Evolutionary Anthropology and Biology. Chicago: University of Chicago Press.

Oaks JR. 2011. A time-calibrated species tree of Crocodylia reveals a recent radiation of the true crocodiles. Evolution 65: 1–13.

Okamoto KW, Langerhans RB, Rashid R, et al. 2015. Microevolutionary patterns in the common caiman predict macroevolutionary trends across extant crocodilians. Biological Journal of the Linnean Society 116: 834–846.

Okamura Y. 2009. Pliocene fossil footprints from the riverbed of the Suzuka river, Kameyama City, Mie Prefecture, Central Japan. In: Geology Group of the Editorial Committee of 'History of Kameyama City', ed. Excavation report on fossils from the Pliocene Tokai Group distributed in the riverbed of the Suzuka-gawa, Kameyama City, Central Japan. Mie: Kameyama City Historical Museum, 63–76.

Oksanen J, Blanchet FG, Friendly M, et al. 2016. vegan: Community Ecology Package. Available at: https://CRAN.R-project.org/package=vegan.

Okuyama S. 1981. Atlas of fossils from Iga Basin, Mie Prefecture, Japan, No. 2. Self publishing.

Okuyama S. 1983. Atlas of fossils from Iga Basin, Mie Prefecture, Japan, No. 3. Self publishing.

Okuyama S. 1984. Atlas of fossils from Iga Basin, Mie Prefecture, Japan, No. 4. Self publishing.

Okuyama S. 1985. Atlas of fossils from Iga Basin, Mie Prefecture, Japan, No. 5. Self publishing.

Okuyama S. 1988. Atlas of fossils from Iga Basin, Mie Prefecture, Japan, No. 8. Self publishing.

Okuyama S. 1994. Concave epirelief fossils of crocodilian found from the Iga-Aburahi Formation in palaeo lake Biwa Group. Journal of the Society of EarthScientists and Amateurs of Japan 43: 83–90.

Okuyama S & Ochiai H. 1993. Fossils concave epirelief of crocodilian found from the Iga/Aburahi Formation in palaeo lake Biwa Group. Oyamada Village Board of Education.

Orme D, Freckleton R, Thomas G, et al. 2013. caper: Comparative Analyses of Phylogenetics and Evolution in R. Available at https://CRAN.R-project.org/package=caper.

Ortega F, Gasparini Z, Buscalioni ÁD, et al. 2000. A new species of *Araripesuchus* (Crocodylomorpha, mesoeucrocodylia) from the Lower Cretaceous of Patagonia (Argentina). Journal of Vertebrate Paleontology 20: 57–76.

Ősi A, Clark JM & Weishampel DB. 2007. First report on a new basal eusuchian crocodyliform with multicusped teeth from the Upper Cretaceous (Santonian) of Hungary. Neues Jahrbuch für Geologie und Paläontologie - Abhandlungen 243: 169–177.

Otsuka H. 1969. Pleistocene vertebrate fauna from the Kuchinotsu Group of West Kyushu. Reports of the Faculty of Science, Kagoshima University 2: 53–84.

Owen R. 1850. Monograph on the fossil Reptilia of the London Clay, and of the Bracklesham and other Tertiary beds, part II: Crocodilia (*Crocodilus*, etc.). In: Monograph of the Palaeontographical Society, London., 50.

Pagel M. 1999. Inferring the historical patterns of biological evolution. Nature 401: 877–884.

Parrish JM. 1987. The origin of crocodilian locomotion. Paleobiology 13: 396–414.

Pickford M. 1994. Late Cenozoic crocodiles (Reptilia: Crocodylidae) from the Western Rift, Uganda. Geology and Palaeobiology of the Albertine Rift Valley, Uganda-Zaire, Vol. II–Palaeobiology.

Orleans: CIFEG Occas Publication, 137–155.

Pickford M. 2003. A new species of crocodile from Early and Middle Miocene deposits of the lower Orange River Valley, Namibia, and the origins of the Nile crocodile (*Crocodylus niloticus*). Memoir of the Geological Survey of Namibia 19: 51–65.

Pierce SE, Angielczyk KD & Rayfield EJ. 2008. Patterns of morphospace occupation and mechanical performance in extant crocodilian skulls: A combined geometric morphometric and finite element modeling approach. Journal of Morphology 269: 840–864.

Pierce SE, Clack JA & Hutchinson JR. 2011. Comparative axial morphology in pinnipeds and its correlation with aquatic locomotory behaviour. Journal of Anatomy 219: 502–14.

Piras P & Buscalioni AD. 2006. *Diplocynodon muelleri* comb. nov., an Oligocene diplocynodontine alligatoroid from Catalonia (Ebro Basin, Lleida Province, Spain). Journal of Vertebrate Paleontology 26: 608–620.

Piras P, Buscalioni ÁD, Teresi L, et al. 2014. Morphological integration and functional modularity in the crocodilian skull. Integrative Zoology 9: 498–516.

Piras P, Colangelo P, Adams DC, et al. 2010. The *Gavialis-Tomistoma* debate: The contribution of skull ontogenetic allometry and growth trajectories to the study of crocodylian relationships. Evolution and Development 12: 568–579.

Piras P, Delfino M, Favero, Letizia D, et al. 2007. Phylogenetic position of the crocodylian *Megadontosuchus arduini* and tomistomine palaeobiogeography. Acta Palaeontologica Polonica 52: 315–328.

Piras P, Teresi L, Buscalioni ÁD, et al. 2009. The shadow of forgotten ancestors differently constrains the fate of Alligatoroidea and Crocodyloidea. Global Ecology and Biogeography 18: 30–40.

Pol D & Norell MA. 2001. Comments on the Manhattan Stratigraphic Measure. Cladistics 17: 285–289.

Pol D & Norell MA. 2006. Uncertainty in the age of fossils and the stratigraphic fit to phylogenies. Systematic Biology 55: 512–521.

Pol D, Norell MA & Siddall ME. 2004. Measures of stratigraphic fit to phylogeny and their sensitivity to tree size, tree shape, and scale. Cladistics 20: 64–75.

Pol D, Turner AH & Norell MA. 2009. Morphology of the Late Cretaceous crocodylomorph *Shamosuchus djadochtaensis* and a discussion of neosuchian phylogeny as related to the origin of Eusuchia. Bulletin of the American Museum of Natural History 324: 1–103.

Pollard AS, Charlton BG, Hutchinson JR, et al. 2017. Limb proportions show developmental plasticity in response to embryo movement. Scientific Reports 7: 41926: doi:10.1038/srep41926.

Price LI. 1964. Sóbre o crânio de um grande crocodilideo extinto do alto rio Juruá, Estado do Acre.

Anais da Academia Brasiliera de Ciencias 36: 59–66.

Prieto-Marquez A, Gignac PM & Joshi S. 2007. Neontological evaluation of pelvic skeletal attributes purported to reflect sex in extinct non-avian archosaurs. Journal of Vertebrate Paleontology 27: 603–609.

R Core Team. 2016. R: A Language and Environment for Statistical Computing. Vienna, Austria: R Foundation of Statistical Computing. Available at https://www.R-project.org/.

Radloff FGT, Hobson KA & Leslie AJ. 2012. Characterizing ontogenetic niche shifts in Nile crocodile using stable isotope ($\delta^{13}C$, $\delta^{15}N$) analyses of scute keratin. Isotopes in Environmental and Health Studies 48: 439–456.

Randau M, Cuff AR, Hutchinson JR, et al. 2017. Regional differentiation of felid vertebral column evolution: a study of 3D shape trajectories. Organisms Diversity and Evolution 17: 305–319.

Rauhe M, Rossmann T. 1995. News about fossil crocodiles from the Middle Eocene of Messel and Geiseltal, Germany. Hallesches Jahrbuch für Geowissenschaften 17: 81–92.

Read MA, Grigg GC, Irwin SR, et al. 2007. Satellite tracking reveals long distance coastal travel and homing by translocated estuarine crocodiles, *Crocodylus porosus*. PLoS ONE 2: e949.

Renesto S & Paganoni A. 1998. A phytosaur skull from the Norian (Late Triassic) of Lombardy (northern Italy). Rivista Italiana di Paleontologia e Stratigrafia 104: 115–122.

Revell LJ. 2012. phytools: An R package for phylogenetic comparative biology (and other things). Methods in Ecology and Evolution 3: 217–223.

Richardson KC, Webb GJW & Manolis CS. 2002. Crocodiles: Inside out. Chipping Norton: Surrey Beatty & Sons.

Ricklefs RE & Miles DB. 1994. Ecological and evolutionary inferences from morphology: An ecological perspective. In: Wainwright PC, Reilly SM, eds. Ecological Morphology. Chicago: The University of Chicago Press, 13–41.

Rieppel O. 1993. Studies on skeleton formation in reptiles. v. Patterns of ossification in the skeleton of *Alligator mississippiensis* Daudin (Reptilia, Crocodylia). Zoological Journal of the Linnean Society 109: 301–325.

Riff D, Aguilera OA. 2008. The world's largest gharials *Gryposuchus*: description of *G. croizati* n. sp (Crocodylia, Gavialidae) from the Upper Miocene Urumaco Formation, Venezuela. Paläontologische Zeitschrift 82: 178–195.

Rohlf FJ & Slice D. 1990. Extensions of the Procrustes method for the optimal superimposition of landmarks. Systematic Zoology 39: 40–59.

Rohlf FJ. 2013a. tpsDig version 2.17. Department of Ecology and Evolution, State University of New York, Stony Brook, NY.

Rohlf FJ. 2013b. tpsRelw version 1.53. Department of Ecology and Evolution, State University of New York, Stony Brook, NY.

Rohlf FJ. 2013c. tpsUtil version 1.58. Department of Ecology and Evolution, State University of New York, Stony Brook, NY.

Roos J, Aggarwal RK & Janke A. 2007. Extended mitogenomic phylogenetic analyses yield new insight into crocodylian evolution and their survival of the Cretaceous–Tertiary boundary. Molecular Phylogenetics and Evolution 45: 663–673.

Rossmann T. 1998. Studien an känozoischen Krokodilen: 2. Taxonomische Revision der Familie Pristichampsidae Efimov (Crocodilia: Eusuchia). Neues Jahrbuch für Geologie und Palaontologie Abhandlungen 210: 85-128.

Rossmann T. 2000. Studien an känozoischen Krokodilen: 5. Biomechanische Untersuchung am postkranialen Skelett des paläogenen Krokodils *Pristichampsus rollintii* (Eusuchia: Pristichampsidae). Neues Jahrbuch für Geologie und Paläontologie Abhandlungen 217: 289–330.

Sacco F. 1896. I coccodrilli del Monte Bolca. Memorie della Reale Accademia delle Scienze de Torino, Ser. 2 45: 75–88.

Sadleir RW & Makovicky PJ. 2008. Cranial shape and correlated characters in crocodilian evolution. Journal of Evolutionary Biology 21: 1578–1596.

Sadleir RW. 2009. A morphometric study of crocodylian ecomorphology through ontogeny and phylogeny. Ph.D. dissertation, the University of Chicago, Chicago. 229 pp.

Salas-Gismondi R, Flynn JJ, Baby P, et al. 2015. A Miocene hyperdiverse crocodylian community reveals peculiar trophic dynamics in proto-Amazonian mega-wetlands. Proceedings of the Royal Society B 282: 20142490.

Salas-Gismondi R, Flynn JJ, Baby P, et al. 2016. A new 13 million year old gavialoid crocodylian from proto-amazonian mega-wetlands reveals parallel evolutionary trends in skull shape linked to longirostry. PLoS ONE 11: e0152453.

Salisbury SW & Frey E. 2001. Biomechanical transformation model for the evolution of semi-spheroidal articulations between adjoining vertebral bodies in crocodilians. In: Grigg GC, Seebacher F, Franklin CE, eds. Crocodilian Biology and Evolution. Chipping Norton: Surrey Beatty & Sons, 85–134.

Salisbury SW, Molnar RE, Frey E, et al. 2006. The origin of modern crocodyliforms: new evidence from the Cretaceous of Australia. Proceedings of the Royal Society B 273: 2439–2448.

Salisbury SW, Willis PMA. 1996. A new crocodylian from the Early Eocene of southeastern Queensland and a preliminary investigation of the phylogenetic relationships of crocodyloids. Alcheringa 20: 179–226.

Satoguchi Y. 2001. Geological stratigraphy and volcanic ash beds in the Mori district, Ajimu-cho,

Japan. Research Report of the Lake Biwa Museum 18: 16–24.

Satoguchi Y. 2008. Depositional age of the Tsubusagawa Formation based on correlations of tephras between in the Miyazaki Group, Kyushu Island, Japan. In: Abstracts of 115st Annual Meeting of the Geological Society of Japan., 81.

Satoguchi Y & Nagahashi Y. 2012. Tephrostratigraphy of the Pliocene to Middle Pleistocene Series in Honshu and Kyushu Islands, Japan. Island Arc 21: 149–169.

Scheyer TM, Delfino M. 2016. The late Miocene caimanine fauna (Crocodylia: Alligatoroidea) of the Urumaco Formation, Venezuela. Palaeontologia Electronica 19.3.48A: 1–57.

Schwarz-Wings D. 2014. The feeding apparatus of dyrosaurids (Crocodyliformes). Geological Magazine 151: 144–166.

Schwenk K. 2000. Tetrapod feeding in the context of vertebrate morphology. In: Schwenk K, ed. Feeding: Form, Function, and Evolution in Tetrapod Vertebrates. San Diego, California: Academic Press, 3–20.

Seebacher F, Elsworth PG & Franklin CE. 2003. Ontogenetic changes of swimming kinematics in a semi-aquatic reptile (*Crocodylus porosus*). Australian Journal of Zoology 51: 15–24.

Seebacher F, Grigg GC & Beard LA. 1999. Crocodiles as dinosaurs: behavioural thermoregulation in very large ectotherms leads to high and stable body temperatures. The Journal of Experimental Biology 202: 77–86.

Seidel MR. 1978. The somatic musculature of the cervical and occipital regions of Alligator mississippiensis. Ph.D. dissertation, The City University of New York, New York. 327 pp.

Sereno PC, Beck AL, Dutheil DB, et al. 1998. A long-snouted predatory dinosaur from Africa and the evolution of spinosaurids. Science 282: 1298–1302.

Sereno PC, Larsson HCE, Sidor CA, et al. 2001. The giant crocodyliform *Sarcosuchus* from the Cretaceous of Africa. Science 294: 1516–1519.

Shan H-yin, Cheng Y-nien & Wu X-chun. 2013. The first fossil skull of *Alligator sinensis* from the Pleistocene, Taiwan, with a paleogeographic implication of the species. Journal of Asian Earth Sciences 69: 17–25.

Shan H-yin, Wu X-chun, Cheng Y-nien, et al. 2009. A new tomistomine (Crocodylia) from the Miocene of Taiwan. Canadian Journal of Earth Sciences 46: 529–555.

Shan H-yin, Wu X-chun, Cheng Y-nien, et al. 2017. *Maomingosuchus petrolica*, a restudy of '*Tomistoma*' *petrolica* Yeh, 1958. Palaeoworld 26: 672–690.

Shapiro LJ. 1995. Functional morphology of lndrid lumbar vertebrae. American Journal of Physical Anthropology 98: 323–342.

Shapiro LJ. 2007. Morphological and functional differentiation in the lumber spine of lorisids and

galagids. American Journal of Primatology 69: 86–102.

Shapiro LJ, Seiffert CVM, Godfrey LR, et al. 2005. Morphometric analysis of lumbar vertebrae in extinct Malagasy strepsirrhines. American Journal of Physical Anthropology 128: 823–839.

Shikama T & Shimaoka Y. 1955. Shizuoka-ken Mikatahara-Chihou no rekkataisekibutsu to sono kasekisou. Journal of the Geological Society of Japan 61: 325.

Shirley MH, Vliet KA, Carr AN, et al. 2014. Rigorous approaches to species delimitation have significant implications for African crocodilian systematics and conservation. Proceedings of the Royal Society B 281: 20132483.

Siddall ME. 1998. Forum. Stratigraphic fit to phylogenies: A proposed solution. Cladistics 14: 201–208.

Sill WD. 1970. Nota preliminar sobre un nuevo gavial del Plioceno de Venezuela y una discusion de los gaviales sudamericanos. Ameghiniana 7: 151–159.

da Silva A & Lenin J. 2010. Mugger crocodile *Crocodylus palustris*. In: Manolis CS, Stevenson C, eds. Crocodiles. Status Survey and Conservation Action Plan, 3rd Edition. Darwin: Crocodile Specialist Group, 94–98.

Singh LAK & Bustard HR. 1976. Locomotory behaviour during basking and spoor formation in the gharial (*Gavialis gangeticus*). British Journal of Herpetology 5: 673–676.

Smit TH. 2002. The use of a quadruped as an in vivo model for the study of the spine–Biomechanical considerations. European Spine Journal 11: 137–144.

Snyder D. 2007. Morphology and systematics of two Miocene alligators from Florida, with a discussion of *Alligator* biogeography. Journal of Paleontology 81: 917–928.

Soares D. 2002. Neurology: an ancient sensory organ in crocodilians. Nature 417: 241–242.

Sokal RR & Rohlf FJ. 1995. Biometry. New York: Freeman and Company.

Sommer RS & Zachos FE. 2009. Fossil evidence and phylogeography of temperate species: ‘glacial refugia’ and post-glacial recolonization. Journal of Biogeography 36: 2013–2020.

Sonderegger DL. 2012. SiZer: Significant Zero Crossings. Available at https://CRAN.R-project.org/package=SiZer.

Sookias RB, Butler RJ & Benson RBJ. 2012. Rise of dinosaurs reveals major body-size transitions are driven by passive processes of trait evolution. Proceedings of the Royal Society B 279: doi:10.1098/rspb.2011.2441.

Sternberg CM. 1932. The skull of *Leidyosuchus canadensis*. The American Midland Naturalist 13: 157–169.

Stevenson C & Whitaker R. 2010. Indian gharial *Gavialis gangeticus*. In: Manolis CS, Stevenson C, eds. Crocodiles. Status Survey and Conservation Action Plan, 3rd Edition. Darwin: Crocodile

Specialist Group, 139–143.

Storrs GW. 2003. Late Miocene–Early Pliocene crocodilian fauna of Lothagam, southwest Turkana Basin, Kenya. In: Leakey MG, Harris JM, eds. Lothagam: the dawn of humanity in Eastern Africa. New York: Columbia University Press, 137–159.

Stubbs TL, Pierce, Stephanie E, Rayfield EJ, et al. 2013. Morphological and biomechanical disparity of crocodile-line archosaurs following the end-Triassic extinction. Proceedings of the Royal Society B: Biological Sciences 280: 20131940.

Suzuki T & Murata M. 2011. Stratigraphy and correlation of tephras in the Lower Pleistocene Kiwada Formation and its correlative beds, Kanto, Central Japan. Journal of the Geological Society of Japan 117: 379–397.

Swofford DL. 2002. PAUP*. Phylogenetic analysis using parsimony (*and other methods). Version 4.

Tada R. 1994. Paleoceanographic evolution of the Japan Sea. Palaeogeography, Palaeoclimatology, Palaeoecology 108: 487–508.

Takahashi K. 1962. Studies on vertical distribution of the forest in middle Honshu. Bulletin of the Government Forest Experiment Station 142: 1–171.

Takahashi K. 1998. Vertebrate fossils and their origins. Urban Kubota 37: 46–57.

Takahashi K. 2001. The environment of the Tsubusagawa Formation and the significance of the Ajimu fauna. Research Report of the Lake Biwa Museum 18: 188–193.

Takahashi K & Kitabayashi E. 2001. Elephant fossils and other mammalian fossils from Mori, Ajimu-cho, Oita Prefecture, Japan. Research Report of the Lake Biwa Museum 18: 126–163.

Takai F, Shikama T, Inoue M, et al. 1958. On fossil milk teeth of elephant from Iinoya-mura, Inasa-gun, Shizuoka. The Quaternary Research 1: 58–61.

Takekawa A, Aoki R, Hirayama R, et al. 2017. Taxonomical reexamination of a large crocodylian from Tsochin, Taiwan. In: Abstracts with programs, the 166th Regular Meeting, the Palaeontological Society of Japan., 48.

Tamura M, Amemori K, Kohayakawa T, et al. 1993. On the Kobiwako Group at the Lake Biwa Eastern Industrial Park. In: Taga Town B of E, ed. Research report on the cultural and natural heritage of Taga Town No. 3 (Taga Town, Inukami-gun, Shiga Prefecture): Report on the geological survey associated with the construction of the Lake Biwa Eastern Industrial Park (Part I)., 26–82.

Tanaka K, Zelenitsky DK & Therrien F. 2015. Eggshell porosity provides insight on evolution of nesting in dinosaurs. PLoS ONE 10: e0142829.

Tanaka S & Mikami T. 2009. Geology and sedimentary environments of the Pliocene Kameyama Formation, Tokai Group distributed in the Suzuka-gawa riverbed, Kameyama City, Central Japan.

In: Geology Group of the Editorial Committee of 'History of Kameyama City', ed. Excavation report on fossils from the Pliocene Tokai Group distributed in the riverbed of the Suzuka-gawa, Kameyama City, Central Japan. Mie: Kameyama City Historical Museum, 17–26.

Tanimoto M & Iijima M. 2017. A fossil crocodylian tooth discovered during the 4th excavation of Taga Ancient Elephant Excavation Project. In: Office of Taga Ancient Elephant Excavation Project, Takahashi K, eds. Reports on the Taga Ancient Elephant Excavation Project: Exploring the Paleoenvironment 1.8–1.9 Million Years Ago. Taga, Shiga: Taga Town Board of Education, 77–82.

Tanimoto M & Kaede T. 2000. A Pliocene crocodilian vertebra from Iga Basin, Mie Prefecture, southwest Japan. Journal of the Society of EarthScientists and Amateurs of Japan 49: 97–100.

Tanimoto M & Okuyama S. 1998. A premaxillary fossil of a longirostral crocodile (Crocodylidae gen, sp. indet.) from the Lower Pliocene Ueno Formation of the Kobiwako Group at Ohyamada-mura, Ayama-gun, Mie Prefecture, Southwest Japan. Journal of the Society of EarthScientists and Amateurs of Japan 47: 83–90.

Taplin LE & Grigg GC. 1989. Historical zoogeography of the eusuchian crocodilians: A physiological perspective. American Zoologist 29: 885–901.

Taplin LE, Grigg GC & Beard LA. 1985. Salt gland function in fresh water crocodiles: evidence for a marine phase in eusuchian evolution? In: Grigg GC, Shine R, Ehmann H, eds. Biology of Australasian Frogs and Reptiles. Chipping Norton: Surrey Beatty & Sons, 403–410.

Taplin LE, Grigg GC, Harlow P, et al. 1982. Lingual salt glands in *Crocodylus acutus* and *C. johnstoni* and their absence from *Alligator mississippiensis* and *Caiman crocodilus*. Journal of Comparative Physiology B 149: 43–47.

Tarsitano SF, Frey E & Riess J. 1989. The evolution of the Crocodilia: A conflict between morphological and biochemical data. American Zoologist 29: 843–856.

Taruno H. 1979. Vertebrate fossils from the Osaka Group. In: Osaka M of NH, ed. Fossils of Osaka. Osaka: Osaka Museum of Natural History, 29–33.

Taruno H. 1988. Vertebrate fossils from Bisan-Seto Sea. In: Kurashiki M of NH, ed. Vertebrate fossils from the Kurashiki Museum of Natural History: Research report of Yamamoto collection (Part I)., 11–61.

Taruno H. 1999. A fossil crocodile from Nagareki-cho, Kishiwada City. In: Excavation report on a fossil crocodile from Nagareki-cho, Kishiwada City. Osaka: Kishiwad City Board of Education and Natural History Museum of Kishiwada City, 36.

Taylor MA. 1987. How tetrapods feed in water: a functional analysis by paradigm. Zoological Journal of the Linnean Society 91: 171–195.

Tchernov E. 1986. Evolution of the crocodiles in East and North Africa. Paris: Editions du CNRS.

Thorbjarnarson JB. 1990. Notes on the feeding behavior of the gharial (*Gavialis gangeticus*) under semi-natural conditions. Journal of Herpetology 24: 99–100.

Thorbjarnarson JB & Wang X. 1999. The conservation status of the Chinese alligator. Oryx 33: 152–159.

Thorbjarnarson JB & Wang X. 2010. The Chinese Alligator: Ecology, Behavior, Conservation, and Culture. Baltimore: The Johns Hopkins University Press.

Toljagic O & Butler RJ. 2013. Triassic–Jurassic mass extinction as trigger for the Mesozoic radiation of crocodylomorphs. Biology Letters 9: 20130095.

Tomida S. 1978. On the Quaternary cave and fissure deposits and vertebrate fossils from Yage Quarry, near Lake Hamana, Central Japan. Bulletin of the Mizunami Fossil Museum 5: 113–141.

Toula F & Kail JA. 1885. Über einen Krokodil-Schädel aus den Tertiärablagerungen von Eggenburg in Niederösterreich: eine paläontologische studie. Denkschriften der Kaiserlichen Akademie der Wissenschaften von Wien, Mathematisch-naturwissenschaftliche Klasse 50: 299–355.

Troedsson GT. 1924. On crocodilian remains from the Danian of Sweden. Lunds Universitet Årsskrift. N. F. 20: 1–75.

Trueman JWH. 1998. Reverse successive weighting. Systematic Biology 47: 733–737.

Trutnau L & Sommerlad R. 2006. Crocodilians: their natural history & captive husbandry. Frankfurt: Edition Chimaira.

Tsuihiji T. 2005. Homologies of the transversospinalis muscles in the anterior presacral region of Sauria (Crown Diapsida). Journal of Morphology 263: 151–178.

Tsuihiji T. 2007. Homologies of the longissimus, iliocostalis, and hypaxial muscles in the anterior presacral region of extant Diapsida. Journal of Morphology 268: 986–1020.

Tsumura Y. 2009. Shell fossils from the Tokai Group distributed in the Suzuka-gawa riverbed, Kameyama City, Central Japan. In: Geology Group of the Editorial Committee of 'History of Kameyama City', ed. Excavation report on fossils from the Pliocene Tokai Group distributed in the riverbed of the Suzuka-gawa, Kameyama City, Central Japan. Mie: Kameyama City Historical Museum, 35–39.

Tsutsui S. 1992. Enumeration of vascular plants in Fukuoka Prefecture Japan, vol. 2, Spermatophyta. Fukuoka: Botanical Society of Fukuoka.

Uyeno T. 1965. On a cyprinid fish from a Pleistocene bed in Shizuoka Prefecture, Japan, and ‘fossil species’ problem. Report of the Japanese Society of Systematic Zoology 1: 27–29.

Vaillant L. 1872. Étude zoologique sur les crocodiliens fossiles tertiaires de Saint-Gérand-le-Puy. Annales de la Société Géologique de France 3: 1–58.

Varona LS. 1984. Los cocodrilos fosiles de Cuba (Reptilia: Crocodylidae). Caribbean Journal of

Science 20: 13–18.

Verdade LM, Larriera A & Piña CI. 2010. Broad-snouted caiman *Caiman latirostris*. In: Manolis CS, Stevenson C, eds. Crocodiles. Status Survey and Conservation Action Plan, 3rd Edition. Darwin: Crocodile Specialist Group, 18–22.

Wainwright PC. 1994. Functional morphology as a tool in ecological research. In: Wainwright PC, Reilly SM, eds. Ecological Morphology. Chicago: The University of Chicago Press, 42–59.

Wainwright PC & Reilly SM. 1994. Introduction. In: Wainwright PC, Reilly SM, eds. Ecological Morphology. Chicago: The University of Chicago Press, 1–9.

Walmsley CW, Smits PD, Quayle MR, et al. 2013. Why the long face? The mechanics of mandibular symphysis proportions in crocodiles. PLoS ONE 8: e53873.

Warton DI, Duursma RA, Falster DS, et al. 2012. SMATR 3 – an R package for estimation and inference about allometric lines. Methods in Ecology and Evolution 3: 257–259.

Watanabe A & Slice DE. 2014. The utility of cranial ontogeny for phylogenetic inference: A case study in crocodylians using geometric morphometrics. Journal of Evolutionary Biology 27: 1078–1092.

Watanabe K & Kitabayashi E. 2001. A fossil bagrid from the Pliocene Tsubusagawa Formation in Ajimu Basin, Oita Prefecture. Research Report of the Lake Biwa Museum 18: 66–71.

Watanabe K & Tanimoto M. 2005. Kishiwada wani to sono nakamatachi (M Kazama, S Hirata, K Murakami, et al., Eds.). Kishiwada: Kishiwada City Board of Education and Natural History Museum of Kishiwada City.

Webb GJW, Britton ARC, Manolis CS, et al. 2000. The recovery of *Crocodylus porosus* in the Northern Territory of Australia: 1971-1998. In: IUCN, ed. Crocodiles. Proceedings of the 15th working meeting of the IUCN-SSC Crocodile Specialist Group. Gland, Switzerland, 195–234.

Wei F & Xu Y. 1981. On the occurrence of *Alligator* from Homutu Yu-yao. Vertebrata PalAsiatica 19: 375–377.

Wen H ran, Huang C chien, He Y heng, et al. 1981. On the changes of geographic distribution of the Chinese alligator. Natural Science Journal of Xiangtan University: 112–122.

Wermuth H. 1964. Das Verhältnis zwischen Kopf-, Rumpf- und Schwanzlänge bei den rezenten Krokodilen. Senckenbergiana biologica 45: 369–385.

Werneburg I, Wilson LAB, Parr WCH, et al. 2015. Evolution of neck vertebral shape and neck retraction at the transition to modern turtles: An integrated geometric morphometric approach. Systematic Biology 64: 187–204.

Wheatley P V. 2010. Understanding saltwater tolerance and marine resource use in the Crocodylia: A stable isotope approach. Ph.D. dissertation, University of California Santa Cruz. 167 pp.

Whitaker R & Andrews H. 1988. Notes on crocodilian locomotion. Journal of Bombay Natural History Society 85: 621–622.

Whitaker R & Basu D. 1982. The gharial (*Gavialis gangeticus*): a review. Journal of Bombay Natural History Society 79: 531–548.

White TE. 1942. A new *Alligator* from the Miocene of Florida. Copeia: 3–7.

Whiting ET, Steadman DW & Krigbaum J. 2016. Paleoecology of Miocene crocodylians in Florida: Insights from stable isotope analysis. Palaeogeography, Palaeoclimatology, Palaeoecology 451: 23–34.

Wilberg EW. 2012. Phylogenetic and morphometric assessment of the evolution of the longirostrine crocodylomorphs. Ph.D. dissertation, University of Iowa, Iowa City. 250 pp.

Wilberg EW. 2015. What's in an outgroup? The impact of outgroup choice on the phylogenetic position of Thalattosuchia (Crocodylomorpha) and the origin of Crocodyliformes. Systematic Biology 64: 621–637.

Wilberg EW. 2017. Investigating patterns of crocodyliform cranial disparity through the Mesozoic and Cenozoic. Zoological Journal of the Linnean Society 181: 189–208.

Willis PMA. 1993. *Trilophosuchus rackhami* gen. et sp. nov., a new crocodilian from the early Miocene limestones of Riversleigh, northwestern Queensland. Journal of Vertebrate Paleontology 13: 90–98.

Willis PMA. 1997. New crocodilians from the Late Oligocene White Hunter Site, Riversleigh, northwestern Queensland. Memoirs of the Queensland Museum 41: 423–438.

Willis PMA, Molnar RE, Scanlon JD. 1993. An Early Eocene crocodilian from Murgon, southeastern Queensland. Kaupia 3: 27–33.

Willis PMA, Molnar RE. 1991. A new Middle Tertiary crocodile from Lake Palankarinna, south Australia. Records of the South Australian Museum 25: 39–55.

Willis PMA, Molnar RE. 1997. A review of the Plio-Pleistocene crocodilian genus *Pallimnarchus*. Proceedings of the Linnean Society of New South Wales 117: 224–242.

Willis PMA, Murray PF & Megirian D. 1990. *Baru darrowi* gen. et sp. nov., a large broad-snouted crocodyline (Eusuchia: Crocodylidae) from mid-Tertiary freshwater limestones in northern Australia. Memoirs of the Queensland Museum 29: 521–540.

Willis RE, McAliley LR, Neeley ED, et al. 2007. Evidence for placing the false gharial (*Tomistoma schlegelii*) into the family Gavialidae: Inferences from nuclear gene sequences. Molecular Phylogenetics and Evolution 43: 787–794.

Wills MA. 1999. Congruence between phylogeny and stratigraphy: randomization tests and the gap excess ratio. Systematic Biology 48: 559–580.

Wills MA, Barrett PM & Heathcote JF. 2008. The modified gap excess ratio (GER*) and the stratigraphic congruence of dinosaur phylogenies. Systematic Biology 57: 891–904.

Witmer LM. 1997. The evolution of the antorbital cavity of archosaurs: A study in soft-tissue reconstruction in the fossil record with an analysis of the function of pneumaticity. Journal of Vertebrate Paleontology 17: 1–73.

Wu X-chun, Brinkman DB & Russell AP. 1996. A new alligator from the Upper Cretaceous of Canada and the relationships of early eusuchians. Palaeontology 39: 351–375.

Wu X-chun, Russell AP & Brinkman DB. 2001. A review of *Leidyosuchus canadensis* Lambe, 1907 (Archosauria: Crocodylia) and an assessment of cranial variation upon new material. Canadian Journal of Earth Sciences 38: 1665–1687.

Wu X, Wang Y, Zhou K, et al. 2003. Complete mitochondrial DNA sequence of Chinese alligator, *Alligator sinensis*, and phylogeny of crocodiles. Chinese Science Bulletin 48: 2050–2054.

Yamakawa C. 2001. Plant macrofossils obtained with animal fossils from the Tsubusagawa Formation in Ajimu, northern Kyushu, Japan. Research Report of the Lake Biwa Museum 18: 25–35.

Yamakawa C, Momohara A, Saito T, et al. 2017. Composition and paleoenvironment of wetland forests dominated by *Glyptostrobus* and *Metasequoia* in the latest Pliocene (2.6 Ma) in central Japan. Palaeogeography, Palaeoclimatology, Palaeoecology 467: 191–210.

Yamamoto K. 1997. Vertebrate fossils from Oyamada clay beds, Kobiwako Group. Konseki 20: 67–75.

Yamamoto K. 1998. On the first occurrence of *Mesocyprinus* from the Gamo Formation of the Kobiwako Group. Konseki 21: 2–5.

Yoshikawa S. 1993. The southern part of Osaka basin. In: Itihara M, ed. The Osaka Group. Osaka: Sogen-sha, 49–67.

Yoshikawa S & Mitamura M. 1999. Quaternary stratigraphy of the Osaka Plain, central Japan and its correlation with oxygen isotope record from deep sea cores. Journal of the Geological Society of Japan 105: 332–340.

Young MT, Brusatte SL, Ruta M, et al. 2010. The evolution of Metriorhynchoidea (Mesoeucrocodylia, Thalattosuchia): An integrated approach using geometric morphometrics, analysis of disparity, and biomechanics. Zoological Journal of the Linnean Society 158: 801–859.

Zangerl R. 1944. *Brachyuranochampsa eversolei*, gen. et sp. nov., a new crocodilian from the Washakie Eocene of Wyoming. Annals of the Carnegie Museum 30: 77–84.

Zanno LE & Makovicky PJ. 2011. Herbivorous ecomorphology and specialization patterns in theropod dinosaur evolution. Proceedings of the National Academy of Sciences of the United States of America 108: 232–237.

Zhao K, Zong Y & Ma J. 1986. On the ancient crocodiles of Guangdong Province. Acta Herpetologica Sinica 5: 161–165.

Zhejiang Provincial Institute of Cultural Relics and Archaeology. 2003. Hemudu: A Neolithic site and its archaeological excavations, Volume I & II. Beijing: Cultural Relics Publishing House.

Zhou B. 1982. Skeletal remains of the Yangtze alligator discovered at the Wangyin Neolithic site, Yanzhou, Shandong. Acta Archaeologica Sinica 2: 251–260.

Zhu ZQ & Song ZS. 1999. Scientific Survey of Shennongjia Nature Reserve. Beijing: China Forestry Press.

Zug GR. 1974. Crocodilian Galloping: An unique gait for reptiles. Copeia 2: 550–552.

Supplement to chapter I

Fig. S1. A time-calibrated morphological phylogeny of 10 sampled crocodylian species. The phylogenetic relationships are based on published trees (Brochu, 2000; Brochu & Storrs, 2012), while the relationships within Indo-pacific Crocodylus are unresolved. Node ages are constrained with reference to Brochu (1997, 2004), and the root age (87.14 myr) is adopted from Oaks (2011).

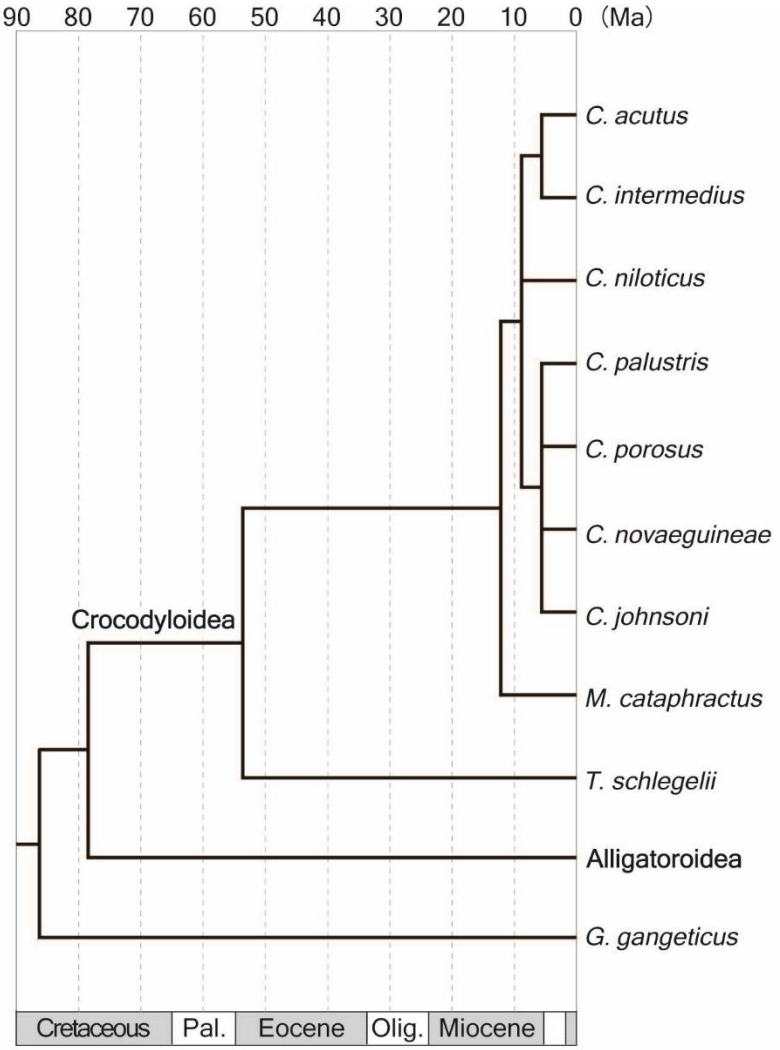


Table S1. Specimens, locality information, and raw data used in the current study. BTW; basiooccipital tubera width; CS, centroid size; CV, coefficient of variation; PFD; pterygoid flange depth; SL; symphysis length; STF, supratemporal fenestra.

Taxon	Specimen #	Locality	skull length (mm)	skull width (mm)	centroid size	log(CS)	RW1 score	Maxillary tooth row length (mm)	Coefficient of variation (CV) of maxillary alveolus diameters	Sum of maxillary alveolus diameters/maxillary tooth row length	STF area (mm2)	log(STF area)	STF^0.5/CS	Symphysis length (mm)	log(SL)	SL/CS	Pterygoid flange depth (mm)	log(PFD)	PFD/CS	Basioccipital tubera width (mm)	log(BTW)	BTW/CS	Maxillary tooth count (right)	Maxillary tooth count (left)
C. acutus	AMNH R 114503	Belize	113.1	54.3	67.4	1.829	-0.128	61.7	0.164	0.661	64.9	1.812	0.119	19.3	1.285	0.286	34.0	1.532	0.504	11.3	1.053	0.167	14	14
C. acutus	AMNH R 15182	Nicaragua	190.4	83.8	104.5	2.019	-0.030	114.3	0.163	0.630	216.5	2.336	0.141	33.9	1.530	0.324	52.2	1.718	0.500	18.3	1.263	0.175	14	14
C. acutus	AMNH R 43299	Florida, Miami-Dade	396.0	199.2	212.8	2.328	-0.123	210.7	NA	NA	825.0	2.916	0.135	70.0	1.845	0.329	136.8	2.136	0.643	37.3	1.571	0.175	13	13
C. acutus	AMNH R 9659	Florida	400.0	212.0	218.6	2.340	-0.118	220.5	0.233	0.689	803.2	2.905	0.130	77.7	1.890	0.355	134.6	2.129	0.616	47.6	1.678	0.218	14	13
C. acutus	FMNH 11038	Honduras, Lake Ticamaya	404.0	212.8	216.1	2.335	-0.107	238.5	0.209	0.653	571.8	2.757	0.111	67.6	1.830	0.313	128.8	2.110	0.596	40.2	1.604	0.186	14	14
C. acutus	FMNH 11041	Belize, Belize	341.0	159.7	177.8	2.250	-0.050	202.6	0.151	0.623	513.4	2.710	0.127	60.3	1.781	0.339	98.9	1.995	0.556	32.1	1.506	0.180	14	14
C. acutus	FMNH 13220	Honduras, Lake Ticamaya	370.0	184.5	195.1	2.290	-0.053	223.4	0.167	0.583	582.9	2.766	0.124	62.3	1.794	0.319	106.5	2.027	0.546	39.9	1.601	0.205	14	14
C. acutus	FMNH 20159	Guatemala, Escuintla, Tiquisate, Conception del Mar	294.0	135.7	154.4	2.189	-0.017	179.8	0.132	0.576	342.7	2.535	0.120	47.0	1.672	0.305	79.5	1.901	0.515	30.0	1.476	0.194	14	14
C. acutus	FMNH 5775	Honduras, Lake Ticamaya	235.2	108.7	124.9	2.096	-0.005	140.7	0.150	0.568	240.5	2.381	0.124	36.5	1.563	0.293	65.8	1.818	0.527	24.8	1.394	0.198	14	14
C. acutus	FMNH 5776	Honduras, Lake Ticamaya	244.0	113.1	130.7	2.116	-0.023	150.0	0.153	0.585	325.3	2.512	0.138	43.6	1.639	0.333	67.6	1.830	0.517	23.6	1.373	0.180	14	14
C. acutus	FMNH 59070	Panama, Canal Zone	591.0	301.0	313.6	2.496	-0.089	342.4	0.211	0.720	1651.6	3.218	0.130	121.2	2.084	0.387	207.9	2.318	0.663	71.5	1.854	0.228	14	14
C. acutus	FMNH 59071	Panama, Canal Zone, Chagres River, near Juan Mina	600.0	323.0	328.2	2.516	-0.157	334.9	0.253	0.831	1443.7	3.159	0.116	NA	NA	NA	216.3	2.335	0.659	76.5	1.884	0.233	14	14
C. acutus	FMNH 69886	Colombia, Magdalena, Cienaga Grande, Cano de Las	486.0	267.7	269.9	2.431	-0.103	290.8	0.209	0.630	960.4	2.982	0.115	99.9	2.000	0.370	177.3	2.249	0.657	57.6	1.761	0.214	14	14
C. acutus	FMNH 73755	Colombia, Magdalena	526.0	289.0	288.4	2.460	-0.154	297.3	0.199	0.767	1242.3	3.094	0.122	111.1	2.046	0.385	185.3	2.268	0.643	63.2	1.801	0.219	14	14
C. acutus	FMNH 74923	Colombia, Bolivar, Isla Fuerte	357.0	161.0	182.6	2.261	-0.033	218.0	0.154	0.583	587.9	2.769	0.133	66.1	1.820	0.362	104.5	2.019	0.573	34.7	1.541	0.190	14	14
C. acutus	FMNH 74924	Colombia, Bolivar, Isla Fuerte	259.5	107.1	132.3	2.122	0.022	157.8	NA	NA	257.2	2.410	0.121	44.3	1.646	0.334	68.9	1.838	0.521	24.0	1.381	0.182	14	14
C. acutus	FMNH 74925	Colombia, Bolivar, Isla Fuerte	210.7	86.0	107.4	2.031	0.030	125.4	0.121	0.600	222.3	2.347	0.139	34.2	1.535	0.319	56.2	1.750	0.523	20.7	1.316	0.193	14	14
C. acutus	SMF 28142	Ecuador, Bodegas	416.0	199.1	206.8	2.316	0.013	251.1	0.164	0.519	553.1	2.743	0.114	78.5	1.895	0.380	124.9	2.097	0.604	43.9	1.642	0.212	14	14
C. acutus	SMF 28143	Ecuador, Rio Daule	224.9	99.8	116.3	2.066	0.020	136.4	0.111	0.593	274.8	2.439	0.143	38.5	1.585	0.331	58.9	1.770	0.506	23.1	1.363	0.198	14	14
C. acutus	SMF 30007	Cuba	316.3	149.1	166.8	2.222	-0.072	184.3	0.201	0.679	319.2	2.504	0.107	53.6	1.729	0.321	90.2	1.955	0.541	31.8	1.502	0.191	14	14
C. acutus	SMF 42808	El Salvador	230.6	103.6	118.5	2.074	-0.006	138.0	NA	NA	204.7	2.311	0.121	36.2	1.558	0.305	64.0	1.806	0.540	24.5	1.389	0.207	14	14
C. acutus	SMF 42956	El Salvador	299.0	142.3	154.8	2.190	-0.020	181.4	0.134	0.587	322.9	2.509	0.116	52.4	1.719	0.338	87.5	1.942	0.565	30.5	1.484	0.197	14	14
C. acutus	USNM 115353	Mexico, Guerrero, Acapulco, Laguna Coyuca	420.0	215.0	222.1	2.347	-0.080	246.9	0.181	0.617	759.1	2.880	0.124	NA	NA	NA	139.3	2.144	0.627	43.5	1.639	0.196	14	14
C. acutus	USNM 247943	Panama, Colon, Barro Colorado Island, Barbour Point	443.0	216.6	237.6	2.376	-0.054	253.6	NA	NA	834.7	2.922	0.122	81.2	1.910	0.342	139.7	2.145	0.588	45.7	1.660	0.192	14	14
C. acutus	USNM 258735	Belize, Stann Creek	309.8	151.9	164.3	2.216	-0.112	181.8	0.171	0.658	362.3	2.559	0.116	57.3	1.758	0.349	92.9	1.968	0.566	36.0	1.557	0.219	14	14
C. acutus	USNM 52336	Mexico, Colima, Manzanillo	178.2	76.5	96.3	1.983	-0.023	104.9	0.149	0.584	156.1	2.194	0.130	29.7	1.473	0.309	47.7	1.678	0.495	17.2	1.235	0.178	14	14
C. acutus	YPM R 10726	Florida, Dade County, Miami	400.0	188.8	207.4	2.317	-0.073	223.0	0.185	0.675	566.1	2.753	0.115	69.0	1.839	0.333	123.4	2.091	0.595	41.1	1.613	0.198	13	14
C. acutus	YPM R 15100	Mexico, Jalisco State, Chamela Bay West	288.9	124.9	140.1	2.146	-0.040	158.4	0.141	0.632	316.6	2.501	0.127	NA	NA	NA	73.6	1.867	0.526	26.7	1.427	0.191	14	14
C. acutus	ZSM 122/1908	Jamaica	297.1	138.9	158.4	2.200	-0.064	172.3	0.161	0.702	468.4	2.671	0.137	53.4	1.728	0.337	83.8	1.923	0.529	32.0	1.505	0.202	14	14
C. acutus	ZSM 137/1926	Columbia, Rio Lebrija	434.0	216.1	226.6	2.355	-0.053	259.8	0.147	0.588	654.3	2.816	0.113	86.0	1.935	0.380	NA	NA	NA	NA	NA	NA	14	14
C. acutus	ZSM 72/1929	Nicaragua, Lake Managua	540.0	271.5	274.3	2.438	-0.065	316.5	0.165	0.652	1019.7	3.008	0.116	103.7	2.016	0.378	175.9	2.245	0.641	54.2	1.734	0.198	14	14
C. acutus	ZSM 73/1937	Colombia, Jesus del Rio, Dep. Bolivar	366.0	178.3	196.6	2.294	-0.025	225.9	0.158	0.607	626.5	2.797	0.127	70.2	1.846	0.357	NA	NA	NA	NA	NA	NA	14	14
C. acutus	ZSM 74/1937	Colombia, Jesus del Rio, Dep. Bolivar	347.0	167.2	181.1	2.258	0.011	202.0	0.145	0.599	612.8	2.787	0.137	66.2	1.821	0.366	105.7	2.024	0.584	36.0	1.556	0.199	14	14
C. intermedius	BMNH 1.85.1.8.25.29	Orinoco	516.0	242.5	259.5	2.414	0.018	288.7	0.204	0.498	983.7	2.993	0.121	127.1	2.104	0.490	160.4	2.205	0.618	51.8	1.714	0.200	14	14
C. intermedius	BMNH 62.10.19.1	Orinoco	670.0	335.0	337.2	2.528	-0.043	365.9	0.267	0.645	2034.8	3.309	0.134	172.8	2.237	0.512	221.5	2.345	0.657	64.1	1.807	0.190	14	14
C. intermedius	FMNH 75658	Colombia, Meta Intendencia, Rio Ariari	243.4	102.7	120.1	2.080	0.084	137.6	NA	NA	296.9	2.473	0.143	61.5	1.789	0.512	57.8	1.762	0.481	20.8	1.317	0.173	14	14
C. intermedius	FMNH 75659	Colombia, Meta Intendencia, Rio Ariari	357.0	156.2	175.6	2.245	0.072	206.6	0.151	0.545	597.9	2.777	0.139	94.1	1.974	0.536	92.2	1.965	0.525	31.6	1.499	0.180	14	14
C. intermedius	FMNH 75660	Colombia, Meta Intendencia, Rio Ariari	473.0	219.4	225.5	2.353	0.032	270.3	0.168	0.599	965.9	2.985	0.138	129.2	2.111	0.573	125.4	2.098	0.556	50.6	1.704	0.224	14	14
C. intermedius	FMNH 75661	Colombia, Meta Intendencia, Rio Ariari, ca 250m	367.0	164.8	181.0	2.258	0.069	207.0	0.138	0.566	688.0	2.838	0.145	95.8	1.981	0.529	95.3	1.979	0.526	35.7	1.552	0.197	13	14
C. intermedius	FMNH 75662	Colombia, Meta Intendencia, Rio Guejar	530.0	282.3	274.2	2.438	-0.046	297.1	0.269	0.622	1245.4	3.095	0.129	138.1	2.140	0.504	164.6	2.216	0.600	61.5	1.789	0.224	14	14
C. intermedius	FMNH 75663	Colombia	478.0	233.2	239.3	2.379	0.009	266.9	0.170	0.595	962.9	2.984	0.130	123.1	2.090	0.515	137.2	2.137	0.574	50.7	1.705	0.212	14	14
C. intermedius	SMF 28139	Orinoco	649.0	361.0	352.2	2.547	-0.086	361.3	0.272	0.603	1861.0	3.270	0.122	168.5	2.227	0.478	236.1	2.373	0.671	68.5	1.836	0.194	13	14
C. intermedius	SMF 55155	Colombia	526.0	263.2	273.2	2.437	-0.019	296.9	0.221	0.622	1252.4	3.098	0.130	135.4	2.132	0.496	156.8	2.195	0.574	57.4	1.759	0.210	14	14
C. intermedius	USNM 211281	Venezuela, Orinoco River	490.0	226.3	246.8	2.392	0.009	271.9	0.193	0.515	973.7	2.988	0.126	118.3	2.073	0.479	146.3	2.165	0.593	49.7	1.696	0.201	14	14
C. intermedius	ZSM 80/1935	Venezuela, San Fernando de Apure	193.1	81.6	100.1	2.000	0.039	110.8	0.204	0.636	171.6	2.235	0.131	42.6	1.630	0.426	48.7	1.688	0.487	21.5	1.332	0.215	14	14
C. johnsoni	AMNH R 86540	Australia, Queensland	393.0	165.7	172.1	2.236	0.078	236.5	0.169	0.580	539.7	2.732	0.135	93.2	1.970	0.542	97.0	1.987	0.564	32.4	1.511	0.188	15	14
C. johnsoni	NTM R12626	Australia, Northern Territory: Finniss River	210.9	80.0	97.3	1.988	0.123	124.7	0.076	0.447	170.1	2.231	0.134	54.8	1.739	0.563	45.7	1.660	0.469	18.4	1.264	0.189	14	14
C. johnsoni	NTM R12627	Australia, Northern Territory: Finniss River	304.0	124.6	138.5	2.141	0.125	189.3	0.084	0.477	353.4	2.548	0.136	85.6	1.933	0.618	68.0	1.832	0.491	26.1	1.417	0.189	14	14
C. johnsoni	NTM R12630	Australia, Northern Territory: Daly River	200.3	77.1	90.9	1.958	0.106	122.3	0.099	0.501	166.8	2.222	0.142	50.9	1.707	0.560	46.3	1.665	0.509	16.4	1.215	0.181	14	14
C. johnsoni	NTM R12631	Australia, Northern Territory: Daly River	209.8	84.0	98.4	1.993	0.080	129.8	0.142	0.574	197.8	2.296	0.143	54.3	1.734	0.552	47.6	1.678	0.484	18.3	1.262	0.186	15	14
C. johnsoni	QM J39230	Australia, northern Queensland	384.0	174.8	178.9	2.253	0.102	234.0	0.131	0.579	655.5	2.817	0.143	89.0	1.950	0.498	100.6	2.003	0.562	30.3	1.481	0.169	14	14
C. johnsoni	QM J47916	Australia, Queensland: Elizabeth Gorge, Bowthorn Station	297.8	119.8	136.8	2.136	0.132	182.4	0.111	0.466	417.2	2.620	0.149	75.2	1.876	0.549	66.2	1.821	0.484	19.4	1.287	0.142	14	15
C. johnsoni	QM J60590	Australia, Queensland: Amber Station, pool 1	241.8	96.6	110.7	2.044	0.124	153.4	0.178	0.547	NA	NA	NA	58.2	1.765	0.526	53.4	1.728	0.482	21.3	1.328	0.192	15	14
C. johnsoni	QM J60591	Australia, Queensland: Springfield Station, pool 5	253.6	98.4	114.8	2.060	0.116	154.6	0.131	0.582	282.6	2.451	0.146	64.5	1.809	0.562	57.4	1.759	0.500	19.7	1.294	0.172	14	14
C. johnsoni	QM J84415	Australia, Queensland: Donkey Springs, Bulleringa NP	225.4	85.3	102.1	2.009	0.121	139.1	0.127	0.519	209.6	2.321	0.142	54.1	1.733	0.530	48.8	1.689	0.478	17.6	1.245	0.172	14	14
C. johnsoni	SMF 25484	Australia, Western Australia: Drysdale River	230.7	91.0	108.2	2.034	0.136	141.0	0.116	0.441	202.1	2.306	0.131	59.1	1.771	0.546	54.8	1.739	0.506	20.6	1.313	0.190	14	14
C. johnsoni	SMF 54424	Australia, Queensland	304.0	122.1	134.7	2.129	0.143	191.4	0.145	0.512	358.8	2.555	0.141	75.4	1.878	0.560	66.4	1.822	0.493	24.8	1.394	0.184	14	14
C. johnsoni	SMF 54425	Australia, Queensland	304.0	123.6	137.0	2.137	0.145	193.3	0.115	0.458	350.2	2.544	0.137	73.6	1.867	0.537	70.3	1.847	0.513	21.6	1.333	0.157	15	14
C. johnsoni	SMF 54426	Australia, Queensland	342.0	141.4	151.9	2.182	0.113	215.9	0.118	0.528	360.7	2.557	0.125	84.6	1.927	0.557	84.0	1.924	0.553	28.1	1.449	0.185	14	14
C. johnsoni	SMF 54427	Australia, Queensland	341.0	129.7	143.6	2.157	0.144	217.1	0.121	0.510	364.5	2.562	0.133	91.8	1.963	0.640	71.7	1.855	0.499	28.0	1.447	0.195	14	14
C. johnsoni	USNM 299810	Australia, Western Territory: Mckinlay River	281.2	123.3	135.2	2.131	0.077	169.7	0.143	0.544	363.2	2.560	0.141	71.8	1.856	0.531	68.5	1.835	0.506	24.3	1.386	0.180	14	15
C. johnsoni	USNM 64091	Australia, Western Australia: Derby, 32 miles SE of Fitzroy River	201.7	79.0	97.9	1.991	0.073	117.3	0.106	0.506	153.0	2.185	0.126	44.5	1.648	0.454	45.8	1.661	0.468	19.3	1.285	0.197	14	14
C. niloticus	IRSNB 17961	Democratic Republic of Congo, Delta Semliki, Kivu, Albert National Park	474.0	294.0	293.5	2.468	-0.186	266.9	0.249	0.776	986.1	2.994	0.107	86.8	1.939	0.296	185.0	2.267	0.630	52.9	1.724	0.180	14	14
C. niloticus	IRSNB 3307	Democratic Republic of Congo, Pweto, Haut-Katanga	134.5	61.7	82.4	1.916	-0.108	71.7	NA	NA	112.7	2.052	0.129	21.4	1.331	0.260	39.2	1.593	0.475	13.7	1.137	0.166	13	13
C. niloticus	IRSNB 3308	Democratic Republic of Congo, Asa	176.7	84.2	101.1	2.005	-0.096	101.2	NA	NA	184.8	2.267	0.135	28.5	1.455	0.282	54.7	1.738	0.542	NA	NA	NA	13	13
C. niloticus	IRSNB 3310	Democratic Republic of Congo, Pweto, Haut-Katanga	409.0	239.1	251.6	2.401	-0.163	215.9	0.158	0.696	732.7	2.865	0.108	74.6	1.873	0.296	156.3	2.194	0.621	46.1	1.664	0.183	13	13
C. niloticus	IRSNB 3313	Democratic Republic of Congo, Pweto, Haut-Katanga	590.0	387.0	362.6	2.559	-0.304	314.4	0.220	0.810	1728.3	3.238	0.115	100.9	2.004	0.278	261.6	2.418	0.721	75.7	1.879	0.209	14	14
C. niloticus	IRSNB 3633	Tanzania, Rukwa Lake	591.0	393.0	344.5	2.537	-0.278	310.3	NA	NA	1618.3	3.209	0.117	108.8	2.037	0.316	267.4	2.427	0.776	84.5	1.927	0.245	13	13
C. niloticus	IRSNB 5002	Tanzania, Luapula	475.0	280.0	288.2	2.460	-0.237	256.2	0.234	0.773	771.9	2.888	0.096	85.5	1.932	0.297	191.0	2.281	0.663	57.0	1.756	0.198	13	13
C. niloticus	IRSNB 5003	Tanzania, Luapula	424.0	262.3	270.0	2.431	-0.238	233.3	0.242	0.793	906.3	2.957	0.111	84.8	1.928	0.314	166.4	2.221	0.616	55.7	1.746	0.206	13	13
C. niloticus	IRSNB 5005	Tanzania, Luapula	147.5	68.2	89.1	1.950	-0.126	82.1	0.184	0.664	145.8	2.164	0.136	25.4	1.405	0.285	45.1	1.654	0.506	14.3	1.156	0.161	13	13
C. niloticus	IRSNB 5006	Tanzania, Luapula	279.0	146.9	161.4	2.208	-0.154	164.5	0.235	0.629	338.0	2.529	0.114	NA	NA	NA	94.0	1.973	0.582	27.7	1.443	0.172	13	13
C. niloticus	IRSNB 5007	Tanzania, Luapula	239.1	118.6	134.9	2.130	-0.098	141.3	0.200	0.698	279.6	2.447	0.124	38.0	1.579	0.282	76.3	1.883	0.566	29.5	1.469	0.218	14	13
C. niloticus	IRSNB 5008	Tanzania, Luapula	433.0	266.3	274.5	2.439	-0.249	235.3	0.248	0.721	824.3	2.916	0.105	85.5	1.932	0.311	188.6	2.275	0.687	50.1	1.700	0.183	12	13
C. niloticus	IRSNB 5009	Tanzania, Luapula	457.0	280.3	288.5	2.460	-0.202	258.4	0.234	0.756	1045.6	3.019	0.112	83.2	1.920	0.288	185.9	2.269	0.644	56.9	1.755	0.197	14	14
C. niloticus	IRSNB 5010	Tanzania, Luapula	411.0	237.6	253.0	2.403	-0.218	227.4	0.198	0.691	650.9	2.813	0.101	69.1	1.839	0.273	157.9	2.198	0.624	45.5	1.658	0.180	13	13
C. niloticus	IRSNB 5011	Tanzania, Luapula	374.0	214.1	228.1	2.358	-0.172	206.3	0.197	0.673	661.8	2.821	0.113	61.1	1.786	0.268	143.4	2.157	0.629	44.1	1.644	0.193	13	13
C. niloticus	IRSNB 5012	Democratic Republic of Congo, Luapula	461.0	294.8	288.0	2.459	-0.273	258.2	0.250	0.803	812.5	2.910	0.099	85.1	1.930	0.295	195.5	2.291	0.679	56.8	1.755	0.197	13	13
C. niloticus	IRSNB 5859	Democratic Republic of Congo, Semliki, Kivu, Albert National Park, sect. Liboma	429.0	266.0	275.6	2.440	-0.194	245.5	0.188	0.733	1112.9	3.046	0.121	81.9	1.913	0.297	173.4	2.239	0.629	55.0	1.740	0.199	14	14
C. niloticus	IRSNB 6036	Democratic Republic of Congo, Senze	261.2	137.7	152.1	2.182	-0.124	145.3	0.157	0.641	474.8	2.677	0.143	45.1	1.655	0.297	88.8	1.949	0.584	24.8	1.395	0.163	13	13
C. niloticus	IRSNB 6037	Democratic Republic of Congo, Senze	171.7	83.2	102.3	2.010	-0.113	99.2	NA	NA	206.3	2.315	0.140	27.0	1.431	0.264	NA	NA	NA	19.3	1.285	0.188	13	13
C. novaeguineae	BMNH 1886.5.20.1	New Guinea, Fly River	250.1	130.3	149.4	2.174	-0.079	148.8	0.220	0.614	425.2	2.629	0.138	NA	NA	NA	79.6	1.901	0.532	24.7	1.392	0.165	14	14
C. novaeguineae	BMNH 1886.5.20.2	New Guinea	177.2	84.7	103.9	2.017	-0.060	102.1	0.146	0.646	235.7	2.372	0.148	36.5	1.562	0.351	51.0	1.708	0.491	15.6	1.193	0.150	14	14
C. novaeguineae	FMNH 13966	New Guinea, Sepik River	186.4	88.0	103.7	2.016	-0.051	109.9	0.177	0.614	215.7	2.334	0.142	34.2	1.534	0.330	49.6	1.695	0.478	16.3	1.211	0.157	14	14
C. novaeguineae	FMNH 14039	Papua New Guinea, Nyourangai, Lagoon village, middle Sepik	391.0	206.7	222.4	2.347	-0.097	232.1	0.218	0.614	667.3	2.824	0.116	NA	NA	NA	NA	NA	NA	29.0	1.462	0.130	14	14
C. novaeguineae	FMNH 14040	New Guinea	329.0	169.6	188.4	2.275	-0.058	195.7	0.194	0.598	504.9	2.703	0.119	NA	NA	NA	103.5	2.015	0.549	25.3	1.402	0.134	14	14
C. novaeguineae	FMNH 14043	Papua New Guinea, Nyourangai, Lagoon village, middle Sepik	349.0	195.4	215.0	2.332	-0.104	209.6	0.231	0.641	656.1	2.817	0.119	NA	NA	NA	121.4	2.084	0.565	28.7	1.458	0.134	14	14
C. novaeguineae	FMNH 14044	New Guinea, Koraqu, middle Sepik River	374.0	217.8	227.3	2.357	-0.131	217.7	0.230	0.687	575.7	2.760	0.106	81.3	1.910	0.358	142.9	2.155	0.628	31.4	1.496	0.138	14	14
C. novaeguineae	FMNH 14047	New Guinea, Koraqu, middle Sepik River	276.6	131.8	149.4	2.174	-0.031	164.2	0.146	0.559	370.6	2.569	0.129	NA	NA	NA	80.3	1.904	0.537	23.7	1.374	0.159	14	14
C. novaeguineae	FMNH 14048	New Guinea, Koraqu, middle Sepik River	351.0	185.8	199.6	2.300	-0.099	206.7	0.203	0.661	519.8	2.716	0.114	NA	NA	NA	115.7	2.063	0.579	27.4	1.437	0.137	14	14
C. novaeguineae	FMNH 14053	New Guinea, Koraqu, middle Sepik River	92.7	40.9	57.3	1.758	-0.047	54.0	0.185	0.675	61.1	1.786	0.136	14.9	1.173	0.260	24.4	1.387	0.426	9.0	0.954	0.157	14	14

C. novaeguineae	FMNH 34491	New Guinea	132.8	54.8	73.2	1.864	-0.045	76.8	NA	NA	100.6	2.003	0.137	22.9	1.360	0.313	34.5	1.538	0.471	14.8	1.171	0.202	14	14
C. novaeguineae	SMF 53300	New Guinea, Sepik	258.1	123.8	140.3	2.147	-0.020	153.2	0.163	0.670	280.6	2.448	0.119	47.5	1.677	0.338	72.2	1.859	0.515	21.0	1.321	0.149	14	14
C. novaeguineae	SMF 56415	New Guinea, Ramu River near Atemble	100.7	44.9	60.7	1.783	-0.054	57.8	NA	NA	67.1	1.827	0.135	16.7	1.222	0.275	27.5	1.439	0.453	9.9	0.997	0.163	14	14
C. novaeguineae	SMF 60031	New Guinea, middle Sepik, between Angoram and Ambunti	338.0	177.4	187.7	2.274	-0.093	200.6	0.194	0.676	555.9	2.745	0.126	69.1	1.839	0.368	109.0	2.037	0.580	28.7	1.458	0.153	14	14
C. novaeguineae	USNM 211290	Papua New Guinea, Western Prov., Balimo Subprov., Aramia River lagoon	372.0	223.2	238.8	2.378	-0.155	212.2	0.210	0.764	1124.9	3.051	0.140	82.9	1.919	0.347	144.6	2.160	0.606	30.8	1.488	0.129	14	14
C. novaeguineae	USNM 211293	Papua New Guinea, Western Prov., Balimo Subprov., Soari River, Aramia River Drainage	161.1	71.6	90.5	1.956	-0.018	91.2	0.159	0.654	160.1	2.204	0.140	31.0	1.491	0.342	43.1	1.635	0.477	12.5	1.097	0.138	14	14
C. novaeguineae	USNM 211295	Papua New Guinea, Western Prov., Balimo Subprov., Makapa Village and Soari River, between, Aramia River	154.0	71.6	91.4	1.961	-0.026	88.5	0.179	0.705	189.8	2.278	0.151	28.8	1.460	0.315	43.8	1.641	0.479	13.0	1.115	0.142	14	14
C. novaeguineae	USNM 211298	Papua New Guinea, Western Prov., Balimo Subprob., Makapa Village Lagoon, Aramia River	238.0	119.7	137.5	2.138	-0.060	135.3	0.171	0.705	437.0	2.640	0.152	49.8	1.697	0.362	71.4	1.854	0.519	23.6	1.374	0.172	14	14
C. novaeguineae	USNM 211301	Papua New Guinea, Western Prov., Balimo Subprov., Samacki River, mouth of Aramia River drainage	335.9	166.8	194.8	2.290	-0.074	191.9	0.163	0.633	792.8	2.899	0.145	74.3	1.871	0.382	106.4	2.027	0.546	29.7	1.473	0.153	14	14
C. palustris	BMNH 1848.2.5.9	India, River Raptee	250.2	138.3	154.1	2.188	-0.224	138.2	0.162	0.754	324.3	2.511	0.117	35.6	1.551	0.231	95.0	1.978	0.616	30.0	1.478	0.195	14	14
C. palustris	BMNH 1852.5.9.46	Sri Lanka, Ceylon	274.9	156.3	172.9	2.238	-0.245	154.3	0.235	0.794	493.2	2.693	0.128	NA	NA	NA	96.5	1.984	0.558	31.6	1.500	0.183	14	14
C. palustris	BMNH 1868.4.9.11	India	497.0	311.0	309.8	2.491	-0.310	268.7	0.203	0.839	1180.3	3.072	0.111	85.1	1.930	0.275	215.1	2.333	0.694	63.8	1.805	0.206	14	14
C. palustris	BMNH 1897.12.31.1	Sri Lanka, Ceylon	505.0	319.0	310.4	2.492	-0.259	285.1	0.251	0.728	1183.9	3.073	0.111	74.8	1.874	0.241	210.7	2.324	0.679	54.7	1.738	0.176	14	14
C. palustris	BMNH 1929.8.6.2	India, Kamara, Mysore, South India	325.0	187.3	199.4	2.300	-0.220	183.0	0.202	0.733	382.4	2.582	0.098	NA	NA	NA	NA	NA	NA	NA	NA	NA	NA	NA
C. palustris	FMNH 31537	Pakistan, Sindh	500.0	308.0	319.5	2.504	-0.308	262.5	0.208	0.841	1311.5	3.118	0.113	86.2	1.935	0.270	220.6	2.344	0.690	57.2	1.757	0.179	14	14
C. palustris	SMF 36999	Ceylon	58.8	30.5	42.6	1.629	-0.262	31.8	NA	NA	32.9	1.517	0.135	9.1	0.959	0.214	18.1	1.257	0.425	NA	NA	NA	NA	NA
C. palustris	SMF 28168	India	285.6	170.2	174.8	2.243	-0.260	157.4	0.186	0.765	451.4	2.655	0.122	44.9	1.652	0.257	NA	NA	NA	36.9	1.568	0.211	14	14
C. palustris	SMF 49663	NA	244.0	156.2	154.1	2.188	-0.274	134.1	0.195	0.843	285.6	2.456	0.110	41.0	1.613	0.266	97.2	1.988	0.631	34.7	1.540	0.225	14	14
C. palustris	ZSM 231/0	India	249.0	152.8	154.7	2.189	-0.248	140.3	0.182	0.820	380.4	2.580	0.126	40.2	1.604	0.260	97.8	1.990	0.632	32.3	1.510	0.209	14	14
C. palustris	ZSM 2534/0	India (from a forestman)	248.3	143.9	148.8	2.172	-0.200	134.8	0.176	0.811	344.5	2.537	0.125	39.1	1.592	0.263	92.4	1.966	0.621	28.4	1.453	0.191	14	14
C. palustris	ZSM 274/1912	Sri Lanka, Hambantota	281.7	150.8	161.3	2.208	-0.213	157.3	0.182	0.751	394.6	2.596	0.123	41.7	1.621	0.259	100.3	2.001	0.622	29.9	1.476	0.185	14	14
C. palustris	ZSM 30/1912	India, Ganoesmünduna bei Calcutta	227.2	129.1	142.5	2.154	-0.239	121.4	NA	NA	310.5	2.492	0.124	36.3	1.559	0.254	88.2	1.945	0.619	27.2	1.434	0.191	14	14
C. palustris	ZSM 34/1912	Pakistan, Purali-Fluss, Südost-Baluchistan	157.4	88.8	104.2	2.018	-0.207	87.6	0.204	0.782	142.9	2.155	0.115	23.5	1.372	0.226	55.1	1.741	0.529	21.9	1.341	0.210	14	14
C. palustris	ZSM 380/1907	East India	310.8	164.0	183.8	2.264	-0.178	170.7	0.179	0.748	466.1	2.668	0.117	47.3	1.674	0.257	117.3	2.069	0.638	33.0	1.518	0.179	14	13
C. palustris	ZSM 389/1907	Sri Lanka, Ceylon	318.0	170.2	191.6	2.282	-0.185	185.5	0.217	0.699	583.2	2.766	0.126	46.5	1.668	0.243	119.7	2.078	0.625	30.4	1.483	0.159	14	14
C. palustris	ZSM 517/1911	Sri Lanka, Kahatagasdigiliya	339.0	181.4	197.0	2.294	-0.207	183.5	0.202	0.706	554.2	2.744	0.120	50.5	1.703	0.256	131.2	2.118	0.666	36.3	1.559	0.184	14	14
C. palustris	ZSM 523/1911	Sri Lanka, Hambantota	181.1	97.0	109.9	2.041	-0.201	101.7	0.155	0.722	233.7	2.369	0.139	27.5	1.439	0.250	62.5	1.796	0.569	19.6	1.292	0.178	14	14
C. palustris	ZSM 542/1911	Sri Lanka, Hambantota	317.0	184.7	192.2	2.284	-0.263	172.6	0.239	0.771	557.0	2.746	0.123	50.1	1.700	0.261	126.1	2.101	0.656	31.6	1.500	0.164	14	14
C. palustris	ZSM 559/1911	Sri Lanka, Hambantota	296.0	162.6	176.1	2.246	-0.249	165.4	0.204	0.744	524.3	2.720	0.130	43.6	1.639	0.247	106.3	2.027	0.604	34.0	1.531	0.193	14	14
C. palustris	ZSM 565/1911	Sri Lanka, Hambantota	213.0	114.1	126.6	2.102	-0.206	115.1	NA	NA	285.9	2.456	0.134	30.7	1.487	0.242	73.8	1.868	0.583	23.5	1.371	0.186	NA	NA
C. palustris	ZSM 612/1911	Sri Lanka, Hambantota	251.1	139.0	148.2	2.171	-0.219	138.7	0.193	0.784	354.3	2.549	0.127	36.7	1.565	0.248	88.0	1.945	0.594	26.5	1.423	0.179	14	14
C. porosus	FMNH 14031	Papua New Guinea, edge of river above Kubka	349.0	168.4	185.2	2.268	-0.103	201.0	0.158	0.588	719.1	2.857	0.145	NA	NA	NA	115.3	2.062	0.622	38.0	1.579	0.205	14	14
C. porosus	FMNH 14034	Papua New Guinea, Nyourangai, Lagoon village, middle Sepik	366.0	172.6	199.2	2.299	-0.073	211.7	0.159	0.559	765.8	2.884	0.139	NA	NA	NA	114.5	2.059	0.575	43.1	1.635	0.216	14	14
C. porosus	FMNH 14035	Papua New Guinea, Nyourangai, Lagoon village, middle Sepik	200.0	86.6	112.4	2.051	-0.070	113.6	0.147	0.646	283.0	2.452	0.150	NA	NA	NA	56.6	1.753	0.504	20.8	1.318	0.185	14	14
C. porosus	FMNH 14036	New Guinea, middle Sepic	191.9	79.4	105.3	2.022	-0.052	110.0	0.164	0.572	212.4	2.327	0.138	32.1	1.506	0.304	51.4	1.711	0.488	21.9	1.340	0.208	14	14
C. porosus	FMNH 14037	New Guinea, Sepic River	148.5	60.5	84.4	1.926	-0.059	81.2	0.134	0.594	137.9	2.139	0.139	23.9	1.379	0.284	40.2	1.605	0.477	15.2	1.182	0.180	14	14
C. porosus	FMNH 14038	New Guinea, Sepic River, Terr	159.9	65.0	89.4	1.951	-0.043	90.3	0.158	0.577	160.6	2.206	0.142	25.3	1.403	0.283	42.4	1.627	0.474	15.1	1.179	0.169	14	14
C. porosus	FMNH 14052	Papua New Guinea, Koraqu, middle Sepick Sepick River	365.0	176.7	197.7	2.296	-0.079	207.2	0.151	0.555	696.4	2.843	0.133	NA	NA	NA	121.7	2.085	0.615	39.1	1.592	0.198	14	14
C. porosus	FMNH 14071	Papua New Guinea, Gologapa, Keram River, south of Sepik River	564.0	357.0	333.3	2.523	-0.228	299.3	0.275	0.744	1914.2	3.282	0.131	120.3	2.080	0.361	237.1	2.375	0.711	67.6	1.830	0.203	14	14
C. porosus	FMNH 15222	North Borneo, Sandakan	99.8	40.7	58.8	1.769	-0.089	57.3	NA	NA	61.8	1.791	0.134	NA	NA	NA	25.8	1.411	0.439	10.6	1.023	0.180	14	14
C. porosus	FMNH 15223	North Borneo, Sandakan	105.8	42.9	61.0	1.786	-0.076	58.6	NA	NA	77.9	1.892	0.145	17.1	1.234	0.280	28.5	1.455	0.467	10.8	1.035	0.177	14	14
C. porosus	FMNH 15224	North Borneo, Sandakan	131.0	52.6	72.9	1.863	-0.068	74.3	NA	NA	103.6	2.015	0.140	20.4	1.310	0.280	35.5	1.550	0.487	12.7	1.105	0.175	14	14
C. porosus	FMNH 15225	North Borneo, Sandakan	145.2	59.2	81.5	1.911	-0.069	81.6	0.155	0.670	129.5	2.112	0.140	23.8	1.377	0.293	38.8	1.589	0.477	14.6	1.164	0.179	14	14
C. porosus	FMNH 15226	North Borneo, Sandakan	156.4	64.4	85.3	1.931	-0.056	87.5	NA	NA	148.5	2.172	0.143	25.6	1.408	0.300	41.2	1.615	0.483	15.9	1.201	0.186	14	14
C. porosus	FMNH 15228	North Borneo, Sandakan	202.9	86.5	106.7	2.028	-0.052	117.7	0.144	0.628	213.8	2.330	0.137	33.4	1.524	0.313	53.9	1.732	0.505	20.0	1.302	0.188	14	14
C. porosus	FMNH 15229	North Borneo, Sandakan	254.8	124.3	140.7	2.148	-0.109	144.3	0.151	0.670	440.3	2.644	0.149	46.3	1.666	0.329	77.0	1.887	0.547	25.1	1.399	0.178	14	14
C. porosus	FMNH 15230	North Borneo, Sandakan	287.0	132.6	152.7	2.184	-0.101	163.7	0.165	0.678	476.9	2.678	0.143	49.3	1.692	0.323	84.4	1.926	0.553	28.7	1.458	0.188	14	14
C. porosus	FMNH 15231	North Borneo, Sandakan	338.0	157.7	176.9	2.248	-0.101	191.3	0.146	0.649	664.0	2.822	0.146	66.4	1.822	0.375	106.5	2.027	0.602	31.5	1.498	0.178	14	14
C. porosus	FMNH 15232	North Borneo, Sandakan	378.0	181.4	198.9	2.299	-0.078	222.9	0.138	0.624	830.8	2.919	0.145	71.5	1.854	0.360	120.4	2.081	0.605	36.1	1.557	0.181	14	14
C. porosus	FMNH 21905	Philippines, Mindoro	177.3	81.1	101.4	2.006	-0.096	99.7	0.130	0.730	196.9	2.294	0.138	30.2	1.479	0.297	53.9	1.731	0.531	20.5	1.311	0.202	14	14
C. porosus	FMNH 21907	Philippines, Mindoro, Lake Naujan	235.6	112.7	132.5	2.122	-0.087	136.3	NA	NA	322.2	2.508	0.135	40.2	1.604	0.303	71.6	1.855	0.540	23.8	1.376	0.179	14	14
C. porosus	FMNH 28465	Philippines	307.6	148.2	172.6	2.237	-0.093	174.8	0.148	0.607	469.8	2.672	0.126	56.4	1.751	0.326	99.1	1.996	0.574	28.0	1.447	0.162	14	14
C. porosus	FMNH 28466	Philippines	311.0	148.0	163.5	2.213	-0.102	176.6	NA	NA	513.8	2.711	0.139	56.2	1.750	0.344	96.9	1.986	0.593	30.0	1.477	0.183	14	14
C. porosus	FMNH 28467	Philippines	302.0	143.8	167.5	2.224	-0.090	175.2	NA	NA	511.9	2.709	0.135	55.0	1.741	0.329	93.8	1.972	0.560	26.8	1.427	0.160	14	14
C. porosus	FMNH 28469	Philippines	394.0	197.1	223.9	2.350	-0.098	220.3	0.195	0.663	815.1	2.911	0.127	72.8	1.862	0.325	130.9	2.117	0.585	40.0	1.602	0.179	14	14
C. porosus	FMNH 63744	North Borneo, Labuk Bay, Tikus Island	281.3	129.0	148.8	2.173	-0.072	160.7	0.178	0.663	465.5	2.668	0.145	50.5	1.703	0.340	80.8	1.907	0.543	28.6	1.457	0.192	14	14
C. porosus	USNM 228412	Philippines, Mindanao Island	604.0	365.0	376.0	2.575	-0.212	350.0	0.229	0.694	2065.1	3.315	0.121	NA	NA	NA	262.6	2.419	0.698	68.7	1.837	0.183	14	14
C. porosus	USNM 228416	Philippines, Mindanao Island	544.0	351.0	325.6	2.513	-0.258	295.2	0.199	0.721	1863.1	3.270	0.133	131.1	2.117	0.403	235.1	2.371	0.722	74.8	1.874	0.230	14	14
C. porosus	USNM 38081	Philippines	360.0	178.0	193.2	2.286	-0.120	198.6	0.143	0.643	751.6	2.876	0.142	69.9	1.845	0.362	114.8	2.060	0.594	37.4	1.573	0.194	14	14
C. porosus	USNM 509454	Papua New Guinea, East Sepic Prov.	612.0	357.0	364.8	2.562	-0.228	320.7	0.257	0.771	2218.1	3.346	0.129	139.3	2.144	0.382	265.6	2.424	0.728	61.6	1.790	0.169	14	14
C. porosus	USNM 61206	Indonesia, Celebes	430.0	237.5	247.2	2.393	-0.150	241.3	0.152	0.678	1204.9	3.081	0.140	85.2	1.930	0.345	150.7	2.178	0.610	52.8	1.722	0.213	13	14
G. gangeticus	AMNH R 7138	India	690.0	292.8	329.4	2.518	0.206	433.6	0.102	0.588	3193.1	3.504	0.172	468.0	2.670	1.421	133.6	2.126	0.406	74.5	1.872	0.226	24	24
G. gangeticus	BMNH 1847.12.20.4	India	734.0	307.5	332.6	2.522	0.144	441.5	NA	NA	4675.4	3.670	0.206	484.0	2.685	1.455	171.1	2.233	0.515	88.3	1.946	0.266	24	24
G. gangeticus	BMNH 1935.6.4.1	India, Ramganga River, Bareilly, U.P.	605.0	229.0	257.7	2.411	0.228	390.8	0.058	0.500	2542.0	3.405	0.196	425.0	2.628	1.650	114.1	2.057	0.443	60.5	1.782	0.235	24	24
G. gangeticus	BMNH 1974.3009	India, Ganges	738.0	314.0	329.7	2.518	0.153	455.1	0.091	0.605	4552.0	3.658	0.205	504.0	2.702	1.529	157.5	2.197	0.478	73.5	1.866	0.223	24	24
G. gangeticus	BMNH 2005.1601	India	722.0	289.6	319.1	2.504	0.195	451.9	0.095	0.610	4348.6	3.638	0.207	502.0	2.701	1.573	148.7	2.172	0.466	76.4	1.883	0.239	23	23
G. gangeticus	BMNH 46.1.7.3 (specimen t in Gray 1873)	India	275.3	69.8	98.1	1.992	0.270	191.8	0.104	0.337	340.0	2.531	0.188	190.8	2.281	1.944	34.5	1.538	0.351	19.7	1.295	0.201	24	24
G. gangeticus	BMNH 96.7.7.4	India, Jumna River, 30 miles below Delhi	424.0	139.7	169.2	2.228	0.248	286.5	NA	NA	1009.5	3.004	0.188	293.0	2.467	1.732	65.9	1.819	0.389	38.0	1.580	0.225	24	24
G. gangeticus	BMNH specimen S in Gray 1873	India	427.0	134.1	165.7	2.219	0.259	295.5	0.065	0.371	1060.3	3.025	0.196	NA	NA	NA	62.7	1.797	0.378	35.3	1.548	0.213	23	24
G. gangeticus	found with BMNH 96.7.7.4	NA	247.4	71.2	94.9	1.977	0.254	178.6	NA	NA	305.5	2.485	0.184	NA	NA	NA	34.7	1.540	0.366	17.7	1.247	0.186	23	23
G. gangeticus	SMF 28132	NA	298.8	83.2	112.4	2.051	0.262	212.7	0.103	0.354	NA	NA	NA	211.1	2.324	1.877	41.0	1.613	0.365	24.5	1.389	0.218	23	23
G. gangeticus	SMF 37951	India, Jumna River	673.0	273.8	289.2	2.461	0.202	424.6	0.076	0.580	3578.4	3.554	0.207	456.0	2.659	1.577	133.2	2.124	0.461	NA	NA	NA	24	24
G. gangeticus	SMF 40144	NA	214.0	58.5	78.7	1.896	0.254	148.1	NA	NA	199.6	2.300	0.180	144.4	2.160	1.835	28.6	1.457	0.364	15.1	1.180	0.192	24	24
G. gangeticus	SMF 49529	Pakistan, Indus, bei dem Dorfe Buaqsar, Baharvalpur State	674.0	263.6	288.4	2.460	0.190	428.7	0.101	0.597	3247.3	3.512	0.198	454.0	2.657	1.574	139.9	2.146	0.485	66.2	1.821	0.230	24	24
G. gangeticus	USNM 72562	India, Uttar Pradesh Allahabad, near River Tons, Ganges River tributary	371.0	111.3	138.7	2.142	0.258	257.5	NA	NA	681.8	2.834	0.188	253.0	2.403	1.824	NA	NA	NA	NA	NA	NA	24	24
G. gangeticus	YPM R 10514	India	418.0	139.6	163.6	2.214	0.253	272.5	0.101	0.442	1159.2	3.064	0.208	295.0	2.470	1.803	68.0	1.832	0.415	37.1	1.569	0.227	24	24
G. gangeticus	ZSM 28/1912	India, Ganges	744.0	320.0	325.6	2.513	0.140	459.4	0.095	0.632	4197.3	3.623	0.199	517.0	2.713	1.588	153.1	2.185	0.470	84.2	1.925	0.259	24	24
G. gangeticus	ZSM 29/1912	India, Ganges	540.0	197.6	220.3	2.343	0.234	363.7	0.106	0.439	1742.7	3.241	0.189	369.0	2.567	1.675	91.4	1.961	0.415	61.0	1.785	0.277	23	24
G. gangeticus	ZSM 29/1938	India, Indus, Vorder Indien (West India)	483.0	174.6	205.3	2.312	0.223	314.7	0.099	0.548	1616.7	3.209	0.196	332.0	2.521	1.617	88.0	1.944	0.429	48.5	1.686	0.236	23	24
G. gangeticus	ZSM 621/1959	Nepal, Girwa River, near Bardia (West-Nepal)	634.0	262.4	276.0	2.441	0.181	427.9	0.090	0.556	3038.3	3.483	0.200	425.0	2.628	1.540	130.8	2.117	0.474	70.2	1.846	0.254	24	23
M. cataphractus	AMNH R 10074	Democratic Republic of Congo, Haut-Uele	175.0	65.5	80.8	1.907	0.125	104.8	0.109	0.498	146.5	2.166	0.150	47.2	1.674	0.585	41.2	1.615	0.510	15.8	1.199	0.196	13	13
M. cataphractus	AMNH R 10075	Democratic Republic of Congo	396.0	155.4	164.8	2.217	0.155	234.2	0.105	0.449	530.3	2.725	0.140	123.1	2.090	0.747	97.7	1.990	0.593	25.2	1.402	0.153	13	13
M. cataphractus	AMNH R 160902	Democratic Republic of Congo	349.0	139.2	149.5	2.175	0.108	204.6	0.122	0.449	509.5	2.707	0.151	103.7	2.016	0.694	94.4	1.975	0.632	28.6	1.457	0.192	13	13
M. cataphractus	AMNH R 75424	Cameroon	225.0	81.3	98.7	1.994	0.125	128.9	0.109	0.523	207.7	2.317	0.146	63.6	1.804	0.645	53.1	1.725	0.538	17.2	1.237	0.175	13	13
M. cataphractus	BMNH 1900.2.27.1	Gabon, Ogowe	488.0	215.1	221.2	2.345	0.135	283.6	NA	NA	804.1	2.905	0.128	154.7	2.189	0.699	131.4	2.119	0.594	39.1	1.592	0.177	13	13
M. cataphractus	BMNH 1924.5.10.1	Tanzania, Kigoma, Tanganyika	581.0	236.5	260.1	2.415	0.137	NA	NA	NA	1346.2	3.129	0.141	174.0	2.240	0.669	151.0	2.179	0.580	42.4	1.627	0.163	13	13
M. cataphractus	IRSNB 17962	Democratic Republic of Congo, Semliki Delta, Kivu	423.0	180.8	191.8	2.283	0.114	246.1	0.091	0.495	621.8	2.794	0.130	131.0	2.117	0.683	111.7	2.048	0.583	34.3	1.535	0.179	13	13
M. cataphractus	IRSNB 17963	Democratic Republic of Congo, Semliki Delta, Kivu	548.0	253.0	249.0	2.396	0.080	324.1	0.140	0.557	NA	NA	NA	169.2	2.228	0.679	158.6	2.200	0.637	44.4	1.647	0.178	13	13
M. cataphractus	IRSNB 17964	Democratic Republic of Congo, Semliki Delta, Kivu	576.0	270.5	266.6	2.426	0.079	340.7	0.111	0.531	1204.5	3.081	0.130	183.2	2.263	0.687	167.1	2.223	0.627	53.8	1.731	0.202	13	13
M. cataphractus	IRSNB 17967	Democratic Republic of Congo, Semliki Delta, Kivu	550.0	246.3	249.4	2.397	0.086	313.8	0.114	0.552	998.4	2.999	0.127	170.8	2.232	0.685	154.3	2.188	0.619	46.2	1.664	0.185	13	13
M. cataphractus	IRSNB 3302	Democratic Republic of Congo, Moero	544.0	247.0	250.5	2.399	0.103	301.9	0.102	0.553	1000.4	3.000	0.126	174.8	2.243	0.698	156.7	2.195	0.625	44.4	1.647	0.177	13	13

M. cataphractus	IRSNB 4976	Democratic Republic of Congo, Kasenga, Haut-Katanga	295.8	116.4	136.0	2.133	0.140	174.7	NA	NA	338.9	2.530	0.135	85.4	1.931	0.628	68.8	1.838	0.506	20.8	1.319	0.153	13	13
M. cataphractus	IRSNB 4977	Democratic Republic of Congo, Kasenga, Haut-Katanga	343.0	136.8	154.9	2.190	0.124	200.1	0.115	0.481	455.4	2.658	0.138	101.7	2.007	0.656	85.6	1.932	0.552	27.9	1.446	0.180	13	13
M. cataphractus	IRSNB 4979	Tanzania, Luapula	364.0	153.0	168.3	2.226	0.119	203.2	0.093	0.601	534.0	2.728	0.137	96.0	1.982	0.570	90.8	1.958	0.540	34.0	1.532	0.202	13	13
M. cataphractus	IRSNB 4980	Tanzania, Luapula	325.0	137.1	150.4	2.177	0.117	192.6	0.100	0.519	414.5	2.618	0.135	98.5	1.994	0.655	82.8	1.918	0.550	26.8	1.428	0.178	13	13
M. cataphractus	IRSNB 4981	Tanzania, Luapula	386.0	165.3	178.3	2.251	0.117	224.9	0.091	0.546	556.0	2.745	0.132	123.0	2.090	0.690	98.8	1.995	0.554	33.7	1.527	0.189	13	13
M. cataphractus	IRSNB 4982	Tanzania, Luapula	330.0	133.7	149.1	2.174	0.118	185.1	0.076	0.558	356.2	2.552	0.127	89.9	1.954	0.603	82.4	1.916	0.553	26.1	1.417	0.175	13	13
M. cataphractus	IRSNB 4983	Tanzania, Luapula	316.4	134.4	145.5	2.163	0.106	182.7	0.113	0.563	429.0	2.632	0.142	94.7	1.976	0.651	79.1	1.898	0.544	26.9	1.430	0.185	13	13
M. cataphractus	IRSNB 4984	Tanzania, Luapula	256.7	102.0	118.7	2.074	0.123	147.5	NA	NA	249.2	2.397	0.133	70.4	1.848	0.593	61.0	1.785	0.514	22.5	1.351	0.189	13	13
M. cataphractus	IRSNB 4985	Tanzania, Luapula	256.8	103.0	118.1	2.072	0.119	148.7	0.110	0.532	NA	NA	NA	72.9	1.863	0.617	62.7	1.797	0.531	21.6	1.334	0.183	13	13
M. cataphractus	IRSNB 4986	Tanzania, Luapula	594.0	268.9	268.3	2.429	0.083	349.6	0.094	0.544	NA	NA	NA	191.4	2.282	0.713	165.0	2.218	0.615	50.5	1.703	0.188	13	13
M. cataphractus	IRSNB 4987	Tanzania, Luapula	528.0	239.2	246.4	2.392	0.090	288.8	0.097	0.570	1035.6	3.015	0.131	154.6	2.189	0.627	146.9	2.167	0.596	46.3	1.666	0.188	13	13
M. cataphractus	IRSNB 4988	Tanzania, Luapula	537.0	246.7	249.8	2.398	0.082	296.9	0.114	0.558	1097.0	3.040	0.133	168.9	2.228	0.676	150.2	2.177	0.601	46.0	1.663	0.184	13	13
M. cataphractus	IRSNB 4989	Tanzania, Luapula	454.0	199.8	213.5	2.329	0.093	252.6	0.114	0.543	737.7	2.868	0.127	145.2	2.162	0.680	127.3	2.105	0.596	37.0	1.569	0.174	13	13
M. cataphractus	IRSNB 4990	Tanzania, Luapula	518.0	238.3	241.1	2.382	0.088	283.4	0.124	0.556	1101.6	3.042	0.138	160.1	2.204	0.664	152.6	2.184	0.633	48.3	1.684	0.200	13	13
M. cataphractus	IRSNB 4991	Tanzania, Luapula	388.0	171.2	179.5	2.254	0.085	212.0	0.102	0.569	564.6	2.752	0.132	125.6	2.099	0.700	101.4	2.006	0.565	34.3	1.535	0.191	13	13
M. cataphractus	IRSNB 4993	Tanzania, Luapula	537.0	239.9	238.0	2.377	0.110	295.2	0.129	0.532	950.9	2.978	0.130	166.5	2.221	0.700	141.3	2.150	0.594	46.6	1.668	0.196	13	13
M. cataphractus	IRSNB 4994	Tanzania, Luapula	540.0	243.8	242.6	2.385	0.087	320.6	0.157	0.533	NA	NA	NA	168.1	2.226	0.693	150.4	2.177	0.620	45.9	1.662	0.189	13	13
M. cataphractus	IRSNB 4996	Tanzania, Luapula	502.0	230.5	226.8	2.356	0.095	281.5	0.120	0.531	965.0	2.985	0.137	152.7	2.184	0.673	142.1	2.152	0.626	42.9	1.632	0.189	13	13
M. cataphractus	IRSNB 4997	Tanzania, Luapula	571.0	268.7	267.3	2.427	0.061	328.3	0.123	0.561	1312.0	3.118	0.136	171.7	2.235	0.642	171.7	2.235	0.642	49.8	1.697	0.186	13	13
M. cataphractus	IRSNB 4998	Tanzania, Luapula	481.0	209.2	215.9	2.334	0.097	275.5	0.111	0.530	770.2	2.887	0.129	154.2	2.188	0.714	133.0	2.124	0.616	38.1	1.580	0.176	13	13
M. cataphractus	IRSNB 4999	Tanzania, Luapula	516.0	224.1	224.5	2.351	0.131	291.4	0.107	0.510	1060.7	3.026	0.145	165.3	2.218	0.736	141.4	2.151	0.630	45.1	1.654	0.201	13	13
M. cataphractus	IRSNB 5000	Tanzania, Luapula	562.0	250.4	253.4	2.404	0.092	334.6	0.107	0.529	1081.1	3.034	0.130	173.1	2.238	0.683	153.4	2.186	0.605	46.5	1.667	0.184	13	13
M. cataphractus	IRSNB 5001	Tanzania, Luapula	552.0	244.4	243.9	2.387	0.112	320.8	0.112	0.513	1068.7	3.029	0.134	163.6	2.214	0.671	146.7	2.166	0.602	49.9	1.698	0.205	13	13
M. cataphractus	IRSNB 5225	Democratic Republic of Congo, Toa	514.0	226.7	241.1	2.382	0.105	281.6	0.142	0.528	1081.3	3.034	0.136	NA	NA	NA	140.9	2.149	0.584	39.5	1.597	0.164	13	13
M. cataphractus	IRSNB 5233	Democratic Republic of Congo, Alvertville	378.0	178.5	181.8	2.260	0.099	217.3	NA	NA	542.9	2.735	0.128	123.2	2.091	0.678	107.1	2.030	0.589	31.0	1.491	0.170	14	13
M. cataphractus	IRSNB 6031	Democratic Republic of Congo, Malbwe, Katanga, Upemba National Park	245.4	106.7	118.9	2.075	0.110	136.6	NA	NA	258.1	2.412	0.135	67.1	1.827	0.564	65.4	1.816	0.550	22.2	1.346	0.186	13	13
M. cataphractus	SMF 43977	Cameroon, Bonambassi	327.0	132.4	152.1	2.182	0.132	186.7	NA	NA	376.3	2.576	0.128	87.5	1.942	0.575	79.0	1.897	0.519	25.0	1.398	0.164	13	13
T. schlegelii	BMNH 1860.11.6.8	Borneo	574.0	244.6	260.4	2.416	0.154	330.3	NA	NA	983.8	2.993	0.120	315.0	2.498	1.210	134.5	2.129	0.516	49.7	1.697	0.191	16	16
T. schlegelii	BMNH 1899.1.31.1	Borneo, Sadong River	344.6	117.2	140.2	2.147	0.229	227.7	0.109	0.394	NA	NA	NA	198.9	2.299	1.419	65.0	1.813	0.463	26.0	1.416	0.186	16	16
T. schlegelii	BMNH 48.10.31.19	Borneo	542.0	224.9	241.6	2.383	0.170	313.9	NA	NA	1059.0	3.025	0.135	305.0	2.484	1.263	123.0	2.090	0.509	41.4	1.617	0.171	16	16
T. schlegelii	BMNH 94.2.21.1	Borneo	839.0	409.0	393.1	2.594	0.030	460.6	0.190	0.580	2732.2	3.437	0.133	459.0	2.662	1.168	238.0	2.377	0.606	81.0	1.908	0.206	16	16
T. schlegelii	FMNH 11084	Sumatra, upper Ogan River	135.3	42.5	60.1	1.779	0.214	80.0	NA	NA	68.4	1.835	0.138	72.8	1.862	1.211	25.0	1.398	0.416	10.0	1.000	0.166	16	16
T. schlegelii	IRSNB 154C	Borneo	753.0	398.0	371.6	2.570	0.038	419.1	0.186	0.641	3044.6	3.484	0.148	404.0	2.606	1.087	213.1	2.329	0.573	73.8	1.868	0.199	16	16
T. schlegelii	SMF 28134	Borneo, Baram-fluss	530.0	201.2	230.5	2.363	0.193	296.2	0.089	0.446	984.5	2.993	0.136	302.0	2.480	1.310	116.8	2.068	0.507	40.9	1.612	0.178	16	16
T. schlegelii	SMF 28135	Sumatra, Perbaungan	499.0	209.9	222.3	2.347	0.183	300.8	0.125	0.490	886.8	2.948	0.134	283.0	2.452	1.273	112.8	2.052	0.507	39.7	1.599	0.179	16	16
T. schlegelii	SMF unknown	Sumatra, Sinallino-fluss	382.0	141.3	160.9	2.207	0.218	231.1	0.096	0.455	575.8	2.760	0.149	224.0	2.350	1.392	79.3	1.899	0.493	29.0	1.462	0.180	16	16
T. schlegelii	USNM 211322	Borneo, Sarawak River	783.0	354.0	364.1	2.561	0.092	436.3	0.182	0.503	2109.4	3.324	0.126	426.0	2.629	1.170	212.4	2.327	0.583	66.4	1.822	0.182	16	16
T. schlegelii	USNM 211323	Indonesia, Kalimantan Sanggau, Kapuas River	665.0	289.4	294.2	2.469	0.153	385.9	0.158	0.467	1913.7	3.282	0.149	367.0	2.565	1.247	158.4	2.200	0.538	57.4	1.759	0.195	16	16
T. schlegelii	USNM 52972	Borneo, Samarinda	510.0	220.1	240.0	2.380	0.176	306.1	0.143	0.445	1080.6	3.034	0.137	280.0	2.447	1.167	111.6	2.048	0.465	37.1	1.569	0.155	16	16
T. schlegelii	ZSM 1/0	Borneo	674.0	311.4	302.3	2.480	0.131	393.2	NA	NA	2118.9	3.326	0.152	380.0	2.580	1.257	166.0	2.220	0.549	63.7	1.804	0.211	16	16
T. schlegelii	ZSM 200/1907	Central Borneo, Poetos Libau	557.0	232.4	244.1	2.388	0.192	329.9	0.133	0.462	1320.4	3.121	0.149	315.0	2.498	1.290	126.6	2.103	0.519	43.5	1.639	0.178	16	16
T. schlegelii	ZSM 201/1907	Central Borneo, Sungai Mendalam	562.0	228.8	239.2	2.379	0.190	332.2	0.103	0.462	1233.7	3.091	0.147	324.0	2.511	1.355	123.9	2.093	0.518	44.8	1.651	0.187	16	16
T. schlegelii	ZSM 202/1907	Sumatra, Sultanat Deli, Batang Koewis	196.7	59.6	80.1	1.904	0.229	124.8	NA	NA	140.6	2.148	0.148	109.4	2.039	1.365	34.2	1.534	0.427	11.0	1.041	0.137	16	16
T. schlegelii	ZSM 203/1907	Central Borneo, Sungai Mendalam	584.0	254.9	257.2	2.410	0.170	347.5	0.158	0.424	1419.4	3.152	0.146	327.0	2.515	1.271	138.9	2.143	0.540	51.3	1.710	0.199	16	16
T. schlegelii	ZSM 232/1909	Sumatra, Sultanat Deli, Sungai Rampah	483.0	184.5	205.2	2.312	0.193	284.6	0.144	0.413	718.7	2.857	0.131	273.2	2.437	1.331	101.9	2.008	0.496	37.6	1.575	0.183	16	16
T. schlegelii	ZSM 252/1907	Central Borneo, Bika	686.0	323.0	314.3	2.497	0.112	390.0	0.171	0.548	1903.3	3.280	0.139	380.0	2.580	1.209	184.8	2.267	0.588	61.3	1.788	0.195	16	16
T. schlegelii	ZSM 370/1907	Central Borneo	812.0	392.0	382.0	2.582	0.033	453.8	0.164	0.575	2247.4	3.352	0.124	428.0	2.631	1.120	239.2	2.379	0.626	82.7	1.917	0.216	16	15
T. schlegelii	ZSM 371/1907	Central Borneo, Kapoeas Gebeit	602.0	237.3	257.3	2.410	0.196	359.2	0.119	0.469	1196.9	3.078	0.134	NA	NA	NA	127.9	2.107	0.497	49.0	1.690	0.190	16	16
T. schlegelii	ZSM 372/1907	Central Borneo, Batang Loepar-seen	767.0	367.0	361.1	2.558	0.070	458.0	0.190	0.501	NA	NA	NA	411.0	2.614	1.138	221.9	2.346	0.615	74.5	1.872	0.206	16	16
T. schlegelii	ZSM 374/1907	Central Borneo, Kapoeas Gebeit	594.0	247.5	255.1	2.407	0.177	352.0	0.153	0.494	1442.3	3.159	0.149	400.5	2.603	1.570	132.9	2.124	0.521	47.5	1.677	0.186	16	16
T. schlegelii	ZSM 376/1907	Central Borneo, Kapoeas Gebeit	681.0	291.0	298.5	2.475	0.145	424.9	0.185	0.464	NA	NA	NA	379.0	2.579	1.270	165.3	2.218	0.554	59.7	1.776	0.200	16	16
T. schlegelii	ZSM 385/1907	Central Borneo, Kapoeas Gebeit	590.0	240.1	252.7	2.403	0.189	357.3	0.143	0.466	1424.4	3.154	0.149	NA	NA	NA	129.9	2.114	0.514	45.2	1.655	0.179	16	16
T. schlegelii	ZSM 395/1907	Central Borneo, Kapoeas Gebeit	748.0	375.0	353.4	2.548	0.075	426.8	0.190	0.628	2105.0	3.323	0.130	NA	NA	NA	207.1	2.316	0.586	72.9	1.863	0.206	16	16
T. schlegelii	ZSM 523/1909	Borneo	527.0	207.7	222.4	2.347	0.202	317.9	0.111	0.439	980.2	2.991	0.141	310.5	2.492	1.396	114.6	2.059	0.515	38.0	1.579	0.171	16	16

Table S2. Measurements of mesiodistal diameters of all right/left maxillary alveoli. All measurements are in mm.

Taxon	Specimen #	R/L	M1	M2	M3	M4	M5	M6	M7	M8	M9	M10	M11	M12	M13	M14	M15	M16	M17	M18	M19	M20	M21	M22	M23	M24
C. acutus	AMNH R 114503	R	2.11	2.71	2.76	2.76	3.80	2.57	2.90	2.69	3.24	3.61	3.34	3.24	2.75	2.30										
C. acutus	AMNH R 15182	R	3.62	4.36	4.84	5.35	6.53	4.85	5.25	4.68	5.64	6.00	5.81	5.63	5.65	3.77										
C. acutus	AMNH R 9659	R	7.31	8.58	9.62	11.72	17.01	10.78	9.67	10.91	12.05	13.92	12.23	10.94	9.22	7.99										
C. acutus	FMNH 11038	R	9.57	10.96	11.30	12.43	17.87	9.96	9.63	9.99	10.57	12.56	12.29	10.99	9.44	8.09										
C. acutus	FMNH 11041	R	6.77	8.23	8.29	9.37	11.75	8.04	7.95	8.21	9.75	10.42	10.69	10.03	8.14	8.49										
C. acutus	FMNH 13220	R	7.74	8.51	9.34	10.14	13.20	8.99	8.35	8.01	8.96	11.19	10.42	9.47	8.91	7.11										
C. acutus	FMNH 20159	R	6.97	7.21	7.28	7.77	9.85	7.63	6.43	6.57	7.69	8.27	7.94	7.33	6.82	5.72										
C. acutus	FMNH 5775	R	4.77	4.99	4.93	6.12	7.32	5.81	5.30	5.86	6.32	6.78	6.29	6.07	5.08	4.23										
C. acutus	FMNH 5776	R	4.93	5.59	5.49	6.60	7.61	6.13	5.89	5.90	6.98	7.78	7.21	6.93	6.14	4.59										
C. acutus	FMNH 59070	R	13.29	15.45	16.34	19.52	25.84	17.40	14.79	15.29	19.06	21.88	21.31	18.66	15.69	12.04										
C. acutus	FMNH 59071	R	14.52	16.24	18.20	22.98	31.69	19.45	16.13	18.45	21.05	26.75	23.34	19.89	16.41	13.04										
C. acutus	FMNH 69886	R	11.39	11.61	11.87	13.81	20.20	13.80	11.47	11.28	13.87	15.92	15.29	12.56	10.72	9.40										
C. acutus	FMNH 73755	R	12.64	14.32	14.74	16.53	23.64	15.44	14.11	14.24	20.03	20.65	18.70	15.24	14.90	12.96										
C. acutus	FMNH 74923	L	6.75	7.84	8.61	9.64	12.12	9.55	8.42	7.90	9.45	10.50	10.08	9.81	9.13	7.40										
C. acutus	FMNH 74925	R	4.60	4.53	5.02	5.11	6.22	5.63	5.23	5.24	6.06	6.20	6.30	5.73	4.85	4.49										
C. acutus	SMF 28142	R	8.15	9.52	9.63	10.14	13.20	9.17	7.56	8.09	9.28	10.77	10.13	8.93	8.83	6.98										
C. acutus	SMF 28143	R	5.24	5.34	5.54	5.59	6.96	5.36	5.69	6.03	5.62	6.79	6.49	6.19	5.48	4.62										
C. acutus	SMF 30007	R	6.00	6.91	7.88	9.62	12.32	8.65	8.36	9.00	10.09	11.41	10.55	9.22	8.50	6.58										
C. acutus	SMF 42956	R	6.27	7.17	7.50	8.24	9.87	7.08	6.86	6.80	7.68	9.04	8.45	7.93	7.12	6.43										
C. acutus	USNM 115353	R	8.11	9.73	10.50	12.28	15.59	11.03	9.86	9.67	11.05	12.28	12.71	11.45	10.09	8.00										
C. acutus	USNM 258735	R	6.45	6.89	7.37	8.04	10.91	7.61	7.40	8.09	9.49	10.27	10.67	10.04	8.26	8.09										
C. acutus	USNM 52336	R	2.98	3.88	4.05	4.36	5.66	4.79	4.16	4.13	4.54	5.06	5.03	4.63	4.13	3.89										
C. acutus	YPM R 10726	R	8.70	10.13	10.19	11.55	16.80	10.41	10.05	10.95	12.71	14.31	12.67	11.56	10.40											
C. acutus	YPM R 15100	R	5.61	6.07	6.43	7.09	9.00	6.97	6.61	6.61	7.30	8.21	8.37	8.32	7.43	6.13										
C. acutus	ZSM 122/1908	R	6.53	7.50	7.40	8.33	10.09	8.73	7.97	8.05	9.52	10.89	10.19	9.92	9.27	6.48										
C. acutus	ZSM 137/1926	R	9.09	9.84	10.11	10.75	15.73	10.65	10.96	10.09	10.52	12.09	11.91	10.54	10.63	9.75										
C. acutus	ZSM 72/1929	R	12.00	13.72	14.91	16.93	20.74	15.16	13.23	12.05	14.21	16.51	16.37	15.49	13.65	11.53										
C. acutus	ZSM 73/1937	R	8.53	8.93	9.51	10.01	13.63	9.80	8.72	9.57	10.13	11.43	11.10	10.21	8.26	7.39										
C. acutus	ZSM 74/1937	R	7.38	8.26	8.34	8.77	11.13	8.59	8.77	9.07	9.74	9.59	9.41	8.68	7.42	5.83										
C. intermedius	BMNH 1851.8.25.29	R	10.69	9.60	9.82	10.59	16.08	10.10	9.96	8.43	10.93	11.81	10.91	9.67	7.96	7.10										
C. intermedius	BMNH 62.10.19.1	R	12.98	14.35	15.02	19.32	29.26	17.80	13.95	15.62	17.13	20.99	18.74	16.35	14.05	10.52										
C. intermedius	FMNH 75659	R	6.44	7.19	7.41	8.29	10.51	8.35	7.74	7.31	8.25	10.46	8.53	8.07	7.41	6.57										
C. intermedius	FMNH 75660	R	10.54	10.99	11.51	12.06	16.23	10.39	11.09	9.41	12.61	13.10	13.50	12.03	9.82	8.60										
C. intermedius	FMNH 75661	R	8.20	8.13	8.63	8.82	12.05	8.67	8.22	8.65	9.62	11.17	8.78	7.77	8.52											
C. intermedius	FMNH 75662	R	10.86	13.12	13.78	13.50	20.83	13.99	12.23	12.11	15.90	17.30	14.77	11.59	8.39	6.50										
C. intermedius	FMNH 75663	R	10.93	11.73	10.97	12.29	16.35	11.49	9.12	10.38	11.68	12.09	12.36	11.97	8.98	8.48										
C. intermedius	SMF 28139	R	12.75	13.37	13.90	18.35	29.34	16.27	13.36	13.63	18.21	19.93	18.95	16.89	13.06											
C. intermedius	SMF 55155	R	10.49	12.34	12.36	14.88	20.63	12.43	11.43	11.38	14.87	15.49	15.02	13.88	10.12	9.29										
C. intermedius	USNM 211281	R	9.05	9.60	9.73	10.85	14.20	9.57	9.01	8.20	10.72	12.52	11.11	10.46	8.95	6.10										
C. intermedius	ZSM 80/1935	R	4.60	5.13	4.77	5.05	6.24	4.93	4.74	4.61	5.91	6.31	5.97	6.00	3.10	3.10										
C. johnsoni	AMNH R 86540	R	7.19	7.82	8.45	8.57	11.36	9.10	8.68	8.18	9.37	10.04	11.34	11.63	9.88	9.27	6.21									
C. johnsoni	NTM R12626	R	3.59	3.58	3.91	3.80	4.31	3.73	3.83	3.80	4.18	4.29	4.61	4.25	4.02	3.87										
C. johnsoni	NTM R12627	R	5.58	6.16	5.85	5.95	6.93	6.25	6.62	6.29	7.16	6.96	7.18	7.03	6.46	5.83										
C. johnsoni	NTM R12630	R	3.76	3.87	4.12	4.41	4.92	4.36	3.93	4.35	4.51	4.88	5.02	4.54	4.82	3.80										
C. johnsoni	NTM R12631	R	4.04	4.03	4.59	4.71	5.71	4.89	4.76	4.70	4.82	5.50	6.19	6.05	5.77	4.37	4.35									
C. johnsoni	QM J39230	R	7.34	8.30	9.82	10.03	12.38	9.38	10.21	8.82	10.35	10.41	9.61	10.92	9.72	8.17										
C. johnsoni	QM J47916	R	4.95	5.39	5.36	5.93	7.47	6.12	6.00	5.69	6.16	6.63	6.92	6.36	6.46	5.58										
C. johnsoni	QM J60590	R	4.26	4.85	5.03	5.22	6.26	5.83	5.12	5.52	6.21	6.61	7.72	6.47	5.86	5.21	3.74									
C. johnsoni	QM J60591	R	4.82	5.66	5.37	5.88	6.85	5.93	6.07	6.27	6.97	7.29	7.62	6.88	7.51	6.89										
C. johnsoni	QM J84415	R	4.15	4.19	4.47	4.84	5.30	4.91	4.95	4.89	5.15	5.64	6.17	6.09	5.95	5.53										
C. johnsoni	SMF 25484	R	3.81	3.66	4.09	4.18	4.36	4.35	4.28	4.60	4.45	5.08	5.37	5.04	4.96	3.92										
C. johnsoni	SMF 54424	R	5.43	4.74	6.14	6.72	8.19	7.40	7.23	7.90	7.26	7.51	8.34	7.07	7.49	6.59										
C. johnsoni	SMF 54425	R	4.74	4.88	5.69	5.68	6.11	6.09	6.37	5.61	6.32	6.84	6.87	6.34	5.93	6.30	4.77									
C. johnsoni	SMF 54426	R	6.79	7.05	7.82	7.98	10.26	8.57	7.65	7.69	8.03	9.03	9.73	7.81	8.02	7.64										
C. johnsoni	SMF 54427	R	6.15	6.59	6.98	7.56	8.67	7.85	7.22	7.44	8.11	8.93	9.26	8.67	8.91	8.42										
C. johnsoni	USNM 299810	R	5.36	5.52	5.99	6.12	7.49	6.36	5.95	6.19	6.05	6.67	7.10	6.98	6.60	6.22	3.73									
C. johnsoni	USNM 64091	R	3.68	3.77	4.01	4.05	4.74	3.97	4.10	3.68	4.44	4.82	5.09	4.71	4.22	4.10										
C. niloticus	IRSNB 17961	R	10.38	11.59	12.14	14.56	23.14	14.62	12.77	14.45	16.91	20.24	17.02	16.15	13.23	10.03										
C. niloticus	IRSNB 3310	R	9.00	9.91	10.26	11.72	15.71	11.66	10.28	11.37	12.68	14.05	12.23	11.23	10.08											
C. niloticus	IRSNB 3313	R	12.62	14.06	15.90	21.37	21.07	20.88	15.75	16.57	20.09	24.24	23.23	20.16	17.82	11.03										
C. niloticus	IRSNB 5002	R	10.85	10.98	12.36	15.06	23.85	15.64	13.38	14.37	17.10	19.73	16.52	14.72	13.46											
C. niloticus	IRSNB 5003	R	9.59	11.56	12.25	15.62	22.45	12.81	10.37	12.95	14.76	17.89	16.84	14.67	13.28											
C. niloticus	IRSNB 5005	R	2.63	3.27	3.39	3.93	4.64	4.08	4.12	4.37	4.17	5.30	5.30	4.66	4.65											
C. niloticus	IRSNB 5006	R	5.09	4.85	6.34	7.06	9.49	7.41	7.49	7.25	9.43	10.36	10.18	9.95	8.65											
C. niloticus	IRSNB 5007	R	5.47	5.40	5.64	6.60	8.82	7.08	6.23	7.72	8.58	9.21	8.76	7.75	5.99	5.42										
C. niloticus	IRSNB 5008	R	10.34	10.95	12.03	13.39	22.52	—	11.83	13.50	16.23	17.78	15.56	14.39	11.02											
C. niloticus	IRSNB 5009	R	10.47	11.28	11.96	14.45	22.74	14.61	12.06	13.05	15.21	16.29	16.25	14.87	12.27	9.88										
C. niloticus	IRSNB 5010	R	8.49	9.75	10.40	11.20	17.38	11.88	10.62	11.51	13.78	15.21	13.71	12.21	11.03											
C. niloticus	IRSNB 5011	R	7.90	8.33	9.10	10.77	13.85	9.87	8.65	9.92	12.22	13.76	12.97	12.27	9.17											
C. niloticus	IRSNB 5012	R	11.07	12.05	12.81	15.60	25.23	15.43	12.76	14.17	16.16	21.32	19.23	16.83	14.60											
C. niloticus	IRSNB 5859	R	9.87	11.10	12.42	13.77	18.18	12.16	11.20	12.20	13.88	16.06	15.07	13.54	10.60	9.85										
C. niloticus	IRSNB 6036	R	5.78	6.43	6.10	6.96	9.53	6.76	6.02	7.47	8.50	8.14	8.09	7.10	6.27											
C. novaeguineae	BMNH 1886.5.20.1	R	4.47	5.30	5.71	7.14	9.45	6.91	6.00	6.97	7.99	8.07	7.44	5.56	5.86	4.48										
C. novaeguineae	BMNH 1886.5.20.2	R	3.84	4.34	4.20	4.75	6.10	4.66	4.15	4.77	5.50	5.48	5.29	4.89	4.33	3.69										
C. novaeguineae	FMNH 13966	R	3.94	4.38	4.41	5.27	6.49	4.74	4.55	4.60	5.11	6.24	5.31	5.01	4.22	3.25										
C. novaeguineae	FMNH 14039	R	8.33	9.19	9.31	10.61	14.31	10.01	8.85	9.68	12.18	13.70	11.75	9.79	9.11	5.75										
C. novaeguineae	FMNH 14040	R	7.52	7.90	8.01	8.90	11.47	8.30	7.69	8.07	10.08	10.47	8.87	7.85	7.24	4.69										
C. novaeguineae	FMNH 14043	R	8.12	8.83	8.82	10.08	13.47	9.48	8.45	8.73	11.13	12.84	12.26	9.22	7.67	5.20										
C. novaeguineae	FMNH 14044	R	8.81	9.54	9.55	11.29	15.78	10.66	9.14	9.90	12.25	15.02	12.16	10.02	8.71	6.78										
C. novaeguineae	FMNH 14047	R	6.00	6.69	6.75	6.83	8.06	6.05	5.92	6.32	7.05	8.07	7.10	6.89	5.79	4.33										
C. novaeguineae	FMNH 14048	R	8.41	8.82	9.16	10.10	13.18	9.48	8.47	9.11	11.81	12.66	11.84	9.57	7.98	6.04										

C. novaeguineae	FMNH 14053	R	2.11	2.33	2.27	2.46	2.97	2.56	2.54	2.84	3.11	3.18	3.40	2.84	2.17	1.65											
C. novaeguineae	SMF 53300	R	6.81	6.81	6.78	8.83	9.03	7.35	7.10	6.71	7.90	9.21	7.58	7.64	6.30	4.65											
C. novaeguineae	SMF 60031	R	8.79	8.97	9.33	10.51	13.82	9.57	9.33	9.03	10.94	11.77	10.84	9.34	7.47	5.94											
C. novaeguineae	USNM 211290	R	9.25	9.79	10.20	13.67	16.59	10.59	10.21	11.47	13.90	14.97	12.90	10.62	9.30	8.60											
C. novaeguineae	USNM 211293	L	3.02	3.55	3.72	4.61	5.10	4.19	3.92	4.45	5.14	5.10	4.71	4.63	4.11	3.35											
C. novaeguineae	USNM 211295	R	3.10	3.62	3.98	4.46	5.79	4.43	4.25	4.73	5.17	5.43	5.17	4.93	3.97	3.38											
C. novaeguineae	USNM 211298	L	5.38	5.85	5.88	7.48	8.88	6.98	6.45	6.84	8.02	8.69	7.46	6.46	5.87	5.21											
C. novaeguineae	USNM 211301	R	7.37	8.68	8.53	9.48	11.86	7.88	8.05	8.70	10.10	10.41	8.72	8.20	6.90	6.67											
C. palustris	BMNH 1848.2.5.9	R	5.28	6.05	6.52	7.79	9.69	7.71	7.20	7.35	8.26	8.90	8.41	8.01	7.05	6.04											
C. palustris	BMNH 1852.5.9.46	R	5.62	6.45	7.90	9.62	12.80	8.35	6.95	8.62	10.23	11.77	10.58	8.68	8.02	6.90											
C. palustris	BMNH 1868.4.9.11	R	9.93	12.42	13.18	17.84	21.94	17.11	13.98	15.43	17.90	15.90	20.54	19.12	15.86	14.23											
C. palustris	BMNH 1897.12.31.1	R	9.69	11.76	13.56	16.86	24.07	14.82	13.35	13.97	16.86	18.53	16.98	14.65	12.48	10.04											
C. palustris	BMNH 1929.8.6.2	R	6.98	7.46	9.15	10.64	14.36	9.27	8.24	9.48	11.19	11.74	9.80	9.50	8.42	7.95											
C. palustris	FMNH 31537	R	9.60	12.86	14.53	18.07	22.14	16.54	13.52	14.41	17.76	18.62	19.29	16.60	14.48	12.34											
C. palustris	SMF 28168	R	6.05	7.28	7.68	8.36	12.60	9.43	9.03	8.95	8.86	9.71	9.47	8.65	7.68	6.59											
C. palustris	SMF 49663	R	6.06	6.53	7.25	8.64	11.43	8.22	7.89	8.05	8.96	9.92	9.54	8.20	6.57	5.84											
C. palustris	ZSM 231/0	R	5.47	6.84	7.18	8.40	10.74	8.78	8.49	8.56	9.06	10.78	7.97	9.03	6.84	6.88											
C. palustris	ZSM 2534/0	R	5.34	6.31	7.00	8.25	10.32	7.56	7.13	7.92	9.30	9.42	8.93	8.12	7.37	6.32											
C. palustris	ZSM 274/1912	R	6.11	6.48	7.42	8.84	11.88	8.35	7.77	7.66	9.32	10.21	9.62	9.27	7.83	7.45											
C. palustris	ZSM 34/1912	R	3.44	4.15	4.48	4.79	6.24	5.18	5.13	5.10	6.01	6.40	6.02	4.05	3.80	3.70											
C. palustris	ZSM 380/1907	R	6.15	7.52	8.67	10.06	12.40	8.42	8.13	9.33	10.08	11.69	8.84	9.91	8.30	8.19											
C. palustris	ZSM 389/1907	L	5.75	6.68	8.31	10.27	13.80	8.67	8.16	8.43	10.03	10.40	11.09	10.35	9.79	7.85											
C. palustris	ZSM 517/1911	R	7.22	7.22	8.29	10.25	13.40	8.67	7.53	8.51	10.45	12.19	10.24	9.27	8.71	7.54											
C. palustris	ZSM 523/1911	R	3.66	3.86	4.78	5.66	6.36	5.29	5.41	5.31	6.01	6.30	5.85	5.35	4.85	4.70											
C. palustris	ZSM 542/1911	R	5.89	6.88	8.84	9.53	13.99	8.55	8.16	9.78	11.43	12.16	11.41	10.63	9.04	6.72											
C. palustris	ZSM 559/1911	R	6.83	7.01	7.46	9.95	12.71	7.95	8.10	8.89	10.13	10.81	9.97	8.70	8.44	6.05											
C. palustris	ZSM 612/1911	R	5.56	5.84	6.75	8.26	11.61	7.36	7.02	8.11	8.75	9.07	7.91	7.74	8.01	6.81											
C. porosus	FMNH 14031	R	7.36	7.84	8.32	9.80	11.74	8.98	7.85	7.88	8.88	9.58	8.55	7.85	6.89	6.58											
C. porosus	FMNH 14034	R	6.84	7.26	7.87	9.46	11.59	8.40	7.52	8.20	9.12	9.66	9.66	8.52	7.34	6.84											
C. porosus	FMNH 14035	R	3.83	4.45	4.89	5.64	7.03	5.10	4.97	4.91	5.61	6.26	5.49	5.23	5.16	4.82											
C. porosus	FMNH 14036	R	4.00	4.52	4.64	4.97	6.31	4.64	3.89	4.34	4.39	4.85	5.00	4.61	3.62	3.19											
C. porosus	FMNH 14037	R	2.87	2.78	3.20	3.82	4.40	3.54	3.27	3.56	3.67	3.99	3.70	3.33	3.24	2.84											
C. porosus	FMNH 14038	R	3.12	2.96	3.61	4.15	4.62	3.69	3.15	3.87	4.53	4.23	4.00	4.02	3.41	2.70											
C. porosus	FMNH 14052	R	6.54	7.20	7.76	9.21	11.27	8.46	7.30	7.92	8.72	9.24	9.13	8.14	7.27	6.89											
C. porosus	FMNH 14071	R	12.88	14.05	15.32	20.19	27.92	13.88	13.35	13.95	17.55	18.06	17.09	15.63	13.64	9.26											
C. porosus	FMNH 15225	R	3.26	3.57	3.47	3.81	4.81	3.84	3.80	3.68	4.40	4.76	4.55	4.23	3.88	2.61											
C. porosus	FMNH 15228	R	4.19	4.20	4.78	5.57	6.72	5.24	4.61	6.02	5.78	6.17	5.72	5.22	5.03	4.63											
C. porosus	FMNH 15229	R	5.66	6.19	6.30	8.11	9.74	6.91	6.24	6.54	6.88	7.47	7.41	6.85	6.36	6.04											
C. porosus	FMNH 15230	R	5.93	6.69	6.85	8.65	11.03	8.22	7.20	7.07	8.55	9.47	8.53	8.30	7.30	7.23											
C. porosus	FMNH 15231	R	7.27	7.39	7.92	10.45	11.77	8.43	8.15	7.86	9.77	9.56	9.84	9.36	8.28	8.09											
C. porosus	FMNH 15232	R	7.44	8.53	9.47	10.60	13.06	9.77	9.38	9.71	10.42	11.53	10.46	10.38	9.81	8.45											
C. porosus	FMNH 21905	R	4.16	4.86	4.72	5.56	6.70	5.01	4.64	5.03	5.83	5.84	5.62	5.26	5.22	4.33											
C. porosus	FMNH 28465	R	6.21	6.67	7.09	8.45	10.39	7.14	6.90	6.71	7.36	8.17	8.75	8.37	6.99	6.82											
C. porosus	FMNH 28469	R	8.90	9.46	9.69	12.37	16.55	10.47	9.72	9.24	10.64	11.21	10.27	9.73	9.74	8.17											
C. porosus	FMNH 63744	R	5.68	6.68	6.53	7.66	11.32	6.99	6.86	7.20	8.59	8.85	7.96	7.89	7.12	7.17											
C. porosus	USNM 228412	L	15.33	16.35	17.15	23.46	28.07	16.15	13.73	14.60	17.67	18.97	16.91	15.95	15.11	13.37											
C. porosus	USNM 228416	R	12.10	14.36	13.91	17.39	23.27	14.95	12.73	13.44	16.26	17.80	16.44	14.88	14.11	11.10											
C. porosus	USNM 38081	R	7.31	7.92	8.39	10.38	12.31	9.08	7.81	8.20	9.72	10.29	9.50	9.13	9.30	8.41											
C. porosus	USNM 509454	R	14.27	16.10	18.32	21.98	28.40	19.25	14.10	14.23	17.68	18.14	23.40	16.73	13.04	11.58											
C. porosus	USNM 61206	R	9.63	10.84	12.35	15.26	16.60	11.53	11.33	10.82	12.89	12.93	13.37	13.92	12.16												
G. gangeticus	AMNH R 7138	R	9.49	10.22	10.00	11.12	10.19	10.96	10.52	10.76	9.62	11.06	10.20	10.33	11.59	11.57	11.25	12.55	12.03	12.16	11.37	10.42	10.39	10.75	8.53	7.83
G. gangeticus	BMNH 1935.6.4.1	R	7.37	7.56	7.89	8.14	8.45	8.71	8.99	7.48	7.99	7.32	8.06	7.63	8.40	8.51	8.11	8.70	8.65	8.58	8.46	8.33	8.38	8.12	7.85	7.58
G. gangeticus	BMNH 1974.3009	R	10.86	11.75	11.74	10.91	11.89	12.70	11.09	11.25	11.53	11.72	10.44	11.51	11.52	12.00	12.09	12.54	12.93	12.68	12.19	12.06	12.06	10.16	9.33	8.57
G. gangeticus	BMNH 2005.1601	R	10.38	11.32	11.70	11.55	11.95	11.89	11.19	10.98	12.11	11.58	11.76	11.53	12.30	11.60	14.36	12.08	13.18	13.43	13.71	14.34	11.67	11.00	9.94	
G. gangeticus	BMNH 46.1.7.3 (specimen t in Gray 1873)	R	2.73	2.70	2.63	2.31	2.34	2.46	2.54	2.32	2.39	2.63	2.44	2.63	2.56	2.64	3.15	3.11	3.27	2.94	2.49	2.80	2.85	3.04	3.05	2.60
G. gangeticus	BMNH specimen S in Gray 1873	R	4.38	5.00	5.22	4.93	4.62	4.53	4.55	4.67	4.66	4.69	4.31	4.50	4.79	4.56	4.47	4.87	4.57	4.72	5.50	5.37	5.01	5.03	4.73	
G. gangeticus	SMF 28132	R	2.97	2.87	2.82	2.96	2.88	3.20	2.74	2.80	3.15	3.05	3.18	3.45	3.59	3.32	3.56	3.71	3.29	3.64	3.68	3.66	3.52	3.66	3.67	
G. gangeticus	SMF 37951	R	8.87	9.37	9.98	10.34	10.30	10.23	10.29	10.40	9.91	9.87	10.31	10.16	10.03	10.66	10.59	11.25	9.62	11.27	12.43	11.51	9.66	9.23	10.26	9.58
G. gangeticus	SMF 49529	R	10.41	10.39	10.30	10.87	10.59	10.07	10.78	10.96	10.62	10.57	9.75	10.13	10.65	10.30	10.25	12.32	11.78	12.22	13.16	12.12	11.21	8.59	9.15	8.90
G. gangeticus	YPM R10514	R	4.00	4.64	4.76	4.87	4.85	4.50	4.72	4.92	4.87	4.80	5.09	5.17	5.87	5.49	5.51	5.98	5.37	5.43	5.71	5.60	4.55	4.92	4.63	4.30
G. gangeticus	ZSM 28/1912	R	10.04	11.15	11.33	12.36	12.46	12.15	12.51	12.39	12.60	13.70	12.34	11.96	13.25	13.04	12.60	12.56	12.45	13.02	13.45	12.50	12.44	10.98	10.13	8.85
G. gangeticus	ZSM 29/1912	R	6.56	6.73	7.93	7.64	6.92	6.92	7.09	6.72	7.47	7.74	6.98	6.14	7.22	7.05	7.21	7.50	8.27	7.61	6.15	6.24	6.50	6.10	4.97	
G. gangeticus	ZSM 29/1938	R	7.00	6.33	7.52	7.53	7.22	6.92	6.72	6.45	6.49	6.62	7.33	7.02	8.58	7.84	8.47	8.51	8.20	8.77	7.94	7.90	8.20	7.14	7.80	
G. gangeticus	ZSM 62/1959	R	9.07	10.19	11.71	10.11	9.84	9.99	9.52	9.22	9.19	9.26	9.34	9.55	10.83	10.07	10.56	10.26	10.67	11.01	11.56	10.06	9.61	9.45	9.16	7.59
M. cataphractus	AMNH R 10074	R	3.23	3.33	3.53	4.10	4.48	3.98	3.83	4.02	4.16	4.39	4.54	4.55	4.07												
M. cataphractus	AMNH R 10075	R	7.32	6.89	7.73	8.14	10.07	7.92	7.29	7.51	8.78	8.83	8.76	8.19	7.78												
M. cataphractus	AMNH R 160902	R	5.81	6.33	6.44	6.93	8.69	6.54	6.12	6.73	7.57	8.33	7.70	7.53	7.14												
M. cataphractus	AMNH R 75424	R	4.48	4.28	4.78	4.70	5.79	4.89	5.02	4.93	5.59	5.88	5.89	5.79	5.36												
M. cataphractus	IRSNB 17962	R	8.11	9.06	9.22	9.23	11.53	8.64	8.65	8.70	9.89	9.89	9.81	9.71	9.30												
M. cataphractus	IRSNB 17963	R	12.65	12.15	13.99	14.50	19.74	14.25	12.76	12.72	14.17	14.17	13.62	13.57	12.10												
M. cataphractus	IRSNB 17964	R	12.20	12.93	13.72	15.31	17.65	13.51	12.37	12.73	15.01	14.28	15.09	13.60	12.55												
M. cataphractus	IRSNB 17967	R	11.14	12.19	13.37	13.37	17.24	12.81	12.26	13.01	14.12	14.34	13.99	13.72	11.77												
M. cataphractus	IRSNB 3302	R	11.20	12.20	13.13	14.34	15.84	12.20	12.09	11.84	13.91	13.23	13.38	12.06	11.38												
M. cataphractus	IRSNB 4977	R	5.97	7.23	7.21	7.76	9.01	6.01	6.61	7.26	8.19	7.95	7.98	7.45	7.61												
M. cataphractus	IRSNB 4979	R	7.52	8.88	8.75	9.36	11.02	9.05	9.43	9.00	9.94	10.11	10.09	10.09	8.83												
M. cataphractus	IRSNB 4980	R	6.56	6.68	6.73	7.40	8.51	7.55	7.39	7.24	8.13	8.26	8.44	8.85	8.27												
M. cataphractus	IRSNB 4981	R	8.27	8.45	8.49	9.09	10.95	9.32	9.14	8.95	9.78	10.39	10.70	9.97	9.31												
M. cataphractus	IRSNB 4982	R	7.05	7.14	7.28	7.80	8.70	7.84	8.01	8.11	8.48	8.48	8.51	8.61	7.21												
M. cataphractus	IRSNB 4983	R	6.50	6.91	7.20	7.14	8.91	7.54	7.75	7.73	8.09	8.77	9.46	8.98	7.87												
M. cataphractus	IRSNB 4985	R	4.74	5.72	5.50	5.58	7.09	6.04	5.74	5.93	6.45	6.82	6.81	6.80	5.93												
M. cataphractus	IRSNB 4986	R	13.56	13.58	14.56	16.00	18.31	13.72	13.54	13.55	14.81	15.48	15.01	14.22	13.83												
M. cataphractus	IRSNB 4987	R	10.52	11.69	12.72	13.03	15.54	12.71	12.04	11.52	13.02	13.54	13.26	13.28	11.81												

M. cataphractus	IRSNB 4988	R	11.50	11.35	11.77	13.37	16.29	12.87	11.58	11.86	13.89	13.66	13.35	13.25	11.06				
M. cataphractus	IRSNB 4989	R	9.46	10.54	10.50	11.62	13.97	9.76	9.39	10.05	10.13	10.81	10.62	10.54	9.67				
M. cataphractus	IRSNB 4990	R	10.85	11.29	11.97	13.12	16.37	12.12	10.88	11.03	12.09	13.06	12.15	11.91	10.69				
M. cataphractus	IRSNB 4991	R	7.66	8.74	8.78	9.45	11.35	8.90	8.50	8.86	9.89	9.44	10.29	10.09	8.74				
M. cataphractus	IRSNB 4993	R	10.57	11.05	11.99	12.53	16.79	11.66	11.21	11.11	12.27	12.84	12.30	11.47	11.37				
M. cataphractus	IRSNB 4994	R	11.77	11.44	12.54	14.02	18.94	12.79	12.18	12.75	14.18	14.25	13.24	12.36	10.40				
M. cataphractus	IRSNB 4996	R	8.95	10.40	10.58	12.44	14.70	11.56	10.93	10.68	12.41	11.98	12.21	11.85	10.76				
M. cataphractus	IRSNB 4997	R	12.38	13.73	13.98	15.43	19.07	14.86	13.25	12.46	13.99	15.08	13.58	13.73	12.76				
M. cataphractus	IRSNB 4998	R	9.61	10.58	10.68	12.03	14.74	11.79	10.37	10.32	10.99	11.33	11.76	11.17	10.74				
M. cataphractus	IRSNB 4999	R	10.25	10.55	11.07	11.47	15.00	10.66	10.59	10.65	11.48	12.12	11.97	11.84	11.00				
M. cataphractus	IRSNB 5000	R	12.16	14.65	13.26	14.89	16.57	12.32	12.45	11.13	14.88	14.13	14.09	13.69	12.79				
M. cataphractus	IRSNB 5001	R	12.60	12.05	12.40	13.27	16.72	12.66	11.69	10.57	13.13	13.04	12.25	12.64	11.64				
M. cataphractus	IRSNB 5225	R	10.25	10.61	10.79	11.94	15.71	10.45	9.70	9.93	11.91	12.38	12.35	12.47	10.31				
T. schlegelii	BMNH 1899.1.31.1	R	5.26	5.25	5.06	5.31	5.64	4.81	5.12	5.68	5.96	6.03	6.95	6.58	6.24	5.71	4.91	5.20	
T. schlegelii	BMNH 94.2.21.1	R	14.47	16.22	16.39	16.32	24.42	15.16	14.52	14.30	15.06	15.08	21.35	21.24	18.62	16.82	14.62	12.53	
T. schlegelii	IRSNB 154C	R	13.76	14.35	16.73	15.01	23.53	13.87	14.55	15.58	15.91	19.37	20.60	21.69	19.11	16.12	15.23	13.18	
T. schlegelii	SMF 28134	R	7.07	7.56	7.58	7.75	8.91	7.65	8.13	8.47	8.37	8.36	9.53	9.54	9.15	8.45	8.17	7.49	
T. schlegelii	SMF 28135	R	9.04	9.10	9.32	8.96	11.16	8.48	8.56	9.46	9.76	9.81	10.31	10.94	9.63	8.92	7.33	6.70	
T. schlegelii	SMF unknown	R	6.81	6.53	6.82	6.30	7.54	6.25	6.17	6.50	6.13	6.36	7.48	7.26	6.90	7.21	5.76	5.21	
T. schlegelii	USNM 211322	R	12.33	11.60	11.79	13.22	18.55	12.75	11.71	12.30	12.69	12.84	17.84	18.55	15.38	13.90	12.75	11.10	
T. schlegelii	USNM 211323	R	9.43	10.45	10.62	11.44	14.61	9.50	10.75	10.68	10.59	10.29	14.43	14.43	12.33	10.97	10.52	9.11	
T. schlegelii	USNM 52972	R	7.53	7.73	7.81	7.73	9.98	8.00	8.19	8.10	8.52	8.53	10.86	10.73	9.70	8.65	7.97	6.31	
T. schlegelii	ZSM 200/1907	R	8.97	8.65	9.18	8.93	12.10	8.66	9.30	8.58	9.14	9.25	11.42	11.92	10.42	9.32	8.70	7.74	
T. schlegelii	ZSM 201/1907	R	8.80	8.93	9.24	9.65	12.00	8.69	8.87	8.96	9.72	9.52	10.95	11.09	9.78	9.76	8.90	8.53	
T. schlegelii	ZSM 203/1907	R	8.59	9.83	9.80	9.78	12.20	8.59	8.77	9.02	8.47	9.76	11.23	10.86	8.52	8.14	7.49	6.31	
T. schlegelii	ZSM 232/1909	R	7.76	7.55	6.93	6.49	8.05	6.83	6.42	6.65	5.74	5.69	7.53	7.97	8.08	7.07	7.61	6.81	4.33
T. schlegelii	ZSM 252/1907	R	11.82	11.45	11.98	11.80	18.66	12.00	12.30	12.37	12.59	13.40	15.90	17.01	15.99	12.95	13.11	10.49	
T. schlegelii	ZSM 370/1907	R	13.35	14.79	14.82	15.59	21.56	14.02	13.48	14.50	15.31	16.09	20.61	20.79	18.30	17.55	15.64	14.40	
T. schlegelii	ZSM 371/1907	R	9.37	9.94	9.43	9.12	12.15	10.22	9.58	10.37	10.56	10.86	13.11	12.33	11.72	10.72	10.09	8.76	
T. schlegelii	ZSM 372/1907	R	12.47	14.10	14.00	13.23	20.82	11.58	12.68	13.31	12.92	13.15	19.11	17.77	16.10	14.24	12.99	11.11	
T. schlegelii	ZSM 374/1907	R	8.77	9.45	9.55	9.69	12.52	10.92	10.35	10.33	10.94	10.39	13.60	14.61	12.34	11.10	10.59	8.66	
T. schlegelii	ZSM 376/1907	R	12.46	10.61	11.01	10.38	14.62	10.42	11.19	10.48	11.23	11.25	15.13	17.38	16.03	12.69	12.64	9.83	
T. schlegelii	ZSM 385/1907	R	8.96	8.91	9.74	9.58	11.75	9.50	9.26	10.50	9.72	10.60	12.94	13.17	12.66	10.58	10.34	8.39	
T. schlegelii	ZSM 395/1907	R	12.97	13.88	14.37	15.54	20.98	13.48	14.13	14.71	15.32	17.29	22.34	22.86	19.36	18.36	17.25	15.08	
T. schlegelii	ZSM 523/1909	R	8.12	8.51	8.65	8.02	10.24	8.88	7.83	9.24	8.93	7.83	9.30	10.29	9.72	9.24	8.04	6.61	

Table S3. Phylogenetic generalized least squares (PGLS) regressions of proposed ecomorphological variables against snout shape (RW1 score), using an alternative (morphological) tree (Fig. S1).

Variable by snout shape (RW1 score)	*n*	R^2	*P*	Slope	Intercept	Pagel's λ
CV of maxillary alveolus diameter	10	0.863	< 0.001	-0.232	0.155	0.000
Maxillary tooth spacing	10	0.972	< 0.001	-0.646	0.591	0.000
Mode Maxillary tooth count	10	0.021	0.686	1.037	18.237	1.000
Relative supratemporal fenestra (STF) area ($[\text{STF area}]^{1/2}$/CS)	10	0.419	0.043	0.049	0.151	0.990
Relative pterygoid flange depth (PFD/CS)	10	0.730	0.002	-0.243	0.523	1.000
Relative basioccipital tubera witdth (BTW/CS)	10	0.130	0.306	0.053	0.187	0.000
Relative symphysis length (SL/CS)	10	0.716	0.002	1.207	1.027	1.000

CV, coefficient of variation. Mean species RW1 scores and mean variable values were used for species analysis (PGLS regression).

Table S4. Complete results of piecewise linear model fitting for the relationship of snout shape (RW1 score) and size (log[CS]). Individuals with log(CS) ≥ 2.0 were used for this analysis.

Taxon	*n*	Intercept	log(CS) breakpoint (α)	Lower CI (α)	Upper CI (α)	Initial slope (β1)	Lower CI (β 1)	Upper CI (β 1)	Slope change (β2)	Lower CI (β 2)	Upper CI (β 2)
C. acutus	31	0.513	2.438	2.028	2.499	-0.250	-0.604	5.575	-0.330	-6.399	0.503
C. niloticus	17	0.255	2.343	2.099	2.495	-0.176	-0.350	0.170	-0.444	-1.137	-0.172
C. palustris	21	-0.103	2.462	2.154	2.494	-0.055	-0.264	0.178	-1.532	-4.205	0.777
C. porosus	23	0.092	2.312	2.296	2.358	-0.082	-0.177	0.020	-0.484	-0.828	-0.293
G. gangeticus	16	0.524	2.395	2.164	2.504	-0.124	-0.233	0.062	-0.373	-2.907	-0.119
T. schlegelii	25	0.660	2.444	2.396	2.516	-0.200	-0.321	-0.124	-0.729	-1.235	-0.492

Supplement to chapter II

Fig. S1. Species comparison of log10-transformed geometric mean (GM) of humerus, ulna, metacarpal III, femur, tibia, and metatarsal III lengths. Number in parentheses is sample size for each species.

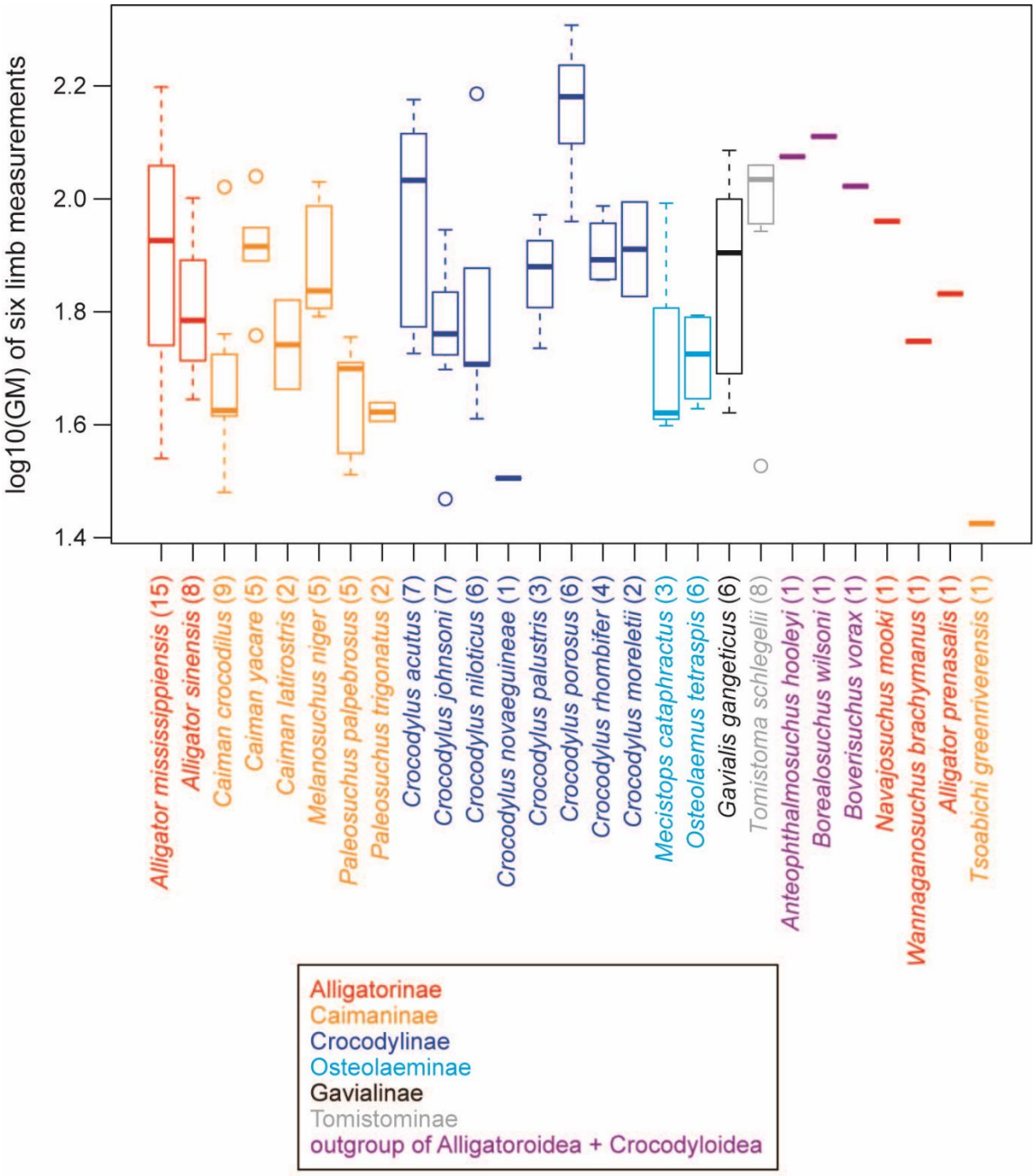


Table S1. Specimens, locality information, and raw measurements for limbs and trunk. All measurements are in mm.

Taxon	Specimen #	Locality	Humerus length	Ulna length	Metacarpal III length	Femur length	Tibia length	Metatarsal III length	Trunk length (C3-D15)
Alligator mississippiensis	AMNH 31563	NA	192.6	140.8	48.4	208.2	162.2	98.1	804.5
Alligator mississippiensis	AMNH 43315	USA, Florida	183.5	126.0	42.9	204.0	156.6	87.0	676.5
Alligator mississippiensis	AMNH 43316	NA	140.5	107.6	39.5	157.1	121.0	75.8	563.07
Alligator mississippiensis	UF 34788	USA, Florida, Alachua Co., Gainesville	125.9	93.7	30.3	137.8	110.8	65.9	NA
Alligator mississippiensis	UF 35129	USA, Florida, Alachua Co., Gainesville, Lake Alice	231.6	165.7	54.5	247.8	182.2	107.1	895.45
Alligator mississippiensis	UF 37231	USA, Florida, Palm Beach Co., Loxahatchee Refuge	92.7	71.6	24.7	105.7	85.5	53.9	388.1
Alligator mississippiensis	UF 39098	USA, Florida, Palm Beach Co., Loxahatchee Refuge	61.2	46.3	15.2	70.9	58.7	35.8	NA
Alligator mississippiensis	UF 39106	USA, South Carolina, Aiken Co., Svannah River Plant	165.7	121.4	41.2	185.2	141.0	84.9	684.4
Alligator mississippiensis	UF 39622	USA, Florida, Palm Beach Co., Loxahatchee Refuge	78.7	59.1	20.3	89.5	72.9	45.3	324.2
Alligator mississippiensis	UF 40535	USA, Florida, Palm Beach Co., Loxahatchee Refuge	58.0	45.4	15.7	66.7	57.2	35.1	NA
Alligator mississippiensis	UF 42474	USA, Florida, Palm Beach Co., Loxahatchee Refuge	48.4	36.9	12.9	55.6	46.1	29.5	NA
Alligator mississippiensis	UF 134586	NA	254.2	163.4	57.2	283.0	188.0	122.1	1166.3
Alligator mississippiensis	YPM R10503	USA, Georgia, Chatham County	162.3	117.0	37.8	172.0	135.2	79.6	655.615
Alligator mississippiensis	YPM R17123	USA, Louisiana, Cameron Parish	97.7	75.6	25.3	112.3	91.3	54.8	386.52
Alligator mississippiensis	ZSM 12/1951	NA	76.2	61.4	21.2	86.4	70.8	45.4	NA
Alligator sinensis	AMNH 23903	China, Anhwei, Wuhu	73.9	52.6	18.0	86.7	72.8	46.8	318.7
Alligator sinensis	AMNH 23904	China, Anhwei, Wuhu	83.5	58.8	19.7	97.6	80.3	50.9	371.3
Alligator sinensis	AMNH139673	NA	91.6	65.9	22.1	107.8	86.6	54.2	NA
Alligator sinensis	BMNH 1954.1.7.30	NA	148.3	110.3	37.6	164.1	128.6	78.7	595.7
Alligator sinensis	FMNH 31302	China, Anhwei	62.6	44.6	14.8	73.9	61.2	39.5	NA
Alligator sinensis	MCZ 17550	China, Anhwei, Wuhu	70.9	50.3	18.1	85.5	70.3	45.4	317.6
Alligator sinensis	UF 67829	NA	102.6	73.4	25.5	123.2	97.2	62.5	NA
Alligator sinensis	USNM 292078	NA	122.3	84.3	28.4	147.1	113.7	70.6	NA
Caiman crocodilus	AMNH 5239	Colombia	63.0	49.8	14.9	77.1	62.3	40.8	NA
Caiman crocodilus	AMNH 20584	NA	150.6	119.6	41.1	165.7	132.0	82.3	NA
Caiman crocodilus	AMNH 137179	NA	57.8	45.1	14.2	69.6	55.2	36.6	NA
Caiman crocodilus	FMNH 13062	Venezuela	79.3	61.2	19.4	98.6	78.9	50.2	NA
Caiman crocodilus	MCZ 5082 (Mook 1921)	Central America	58.8	45.9	14.0	72.5	57.0	36.0	NA
Caiman crocodilus	UF 19067	NA	55.2	44.0	14.0	70.0	58.2	35.6	259.7
Caiman crocodilus	UF 99067	South America	44.0	34.6	10.7	53.8	44.9	29.4	202.5
Caiman crocodilus	USNM 102874	Panama, Madden Lake	73.8	57.7	16.9	91.6	72.5	46.6	318.89
Caiman crocodilus	ZIT Rept. 85	Surinam	40.1	32.2	10.9	51.4	40.3	26.1	NA
Caiman yacare	AMNH 97296	Bolivia, Beni	105.8	80.8	26.0	138.7	106.1	67.1	NA
Caiman yacare	AMNH 97297	Bolivia, Beni	79.3	62.7	17.1	102.4	80.9	50.0	NA
Caiman yacare	AMNH 97300	Bolivia, Beni	122.4	94.8	29.7	153.9	120.7	77.5	617.45
Caiman yacare	AMNH 97305	Bolivia, Beni	114.0	86.4	27.5	148.1	110.8	70.1	NA
Caiman yacare	FMNH 9150	Brazil, Matto Grosso, Paraguay River	172.2	126.2	38.1	182.2	138.0	83.4	NA
Caiman latirostris	MCZ 2854a	Brazil	91.9	69.3	21.2	115.3	91.1	59.3	NA
Caiman latirostris	MCZ 4981	Brazil	63.4	48.0	14.6	79.1	63.9	42.2	283.8
Melanosuchus niger	AMNH 97325	Bolivia, Beni	85.3	62.9	21.7	110.6	86.7	61.5	NA
Melanosuchus niger	FMNH 218507	Equador, Napo Province	92.8	68.3	23.2	116.9	94.5	64.9	433.5
Melanosuchus niger	MCZ 4043 (Mook 1921)	Brazil, Amazonas/Rondonia, Madeira?	149.4	106.2	36.0	190.2	152.0	92.0	NA
Melanosuchus niger	UF 66428	NA	85.6	61.8	19.9	110.7	84.2	57.4	410.5
Melanosuchus niger	UF 72914	NA	134.2	102.1	32.1	166.5	130.1	88.1	692.8
Paleosuchus palpebrosus	FMNH 42703	Colombia, Villavicencio	48.2	38.2	11.1	61.3	49.8	31.7	240.4
Paleosuchus palpebrosus	AMNH 78976	Colombia, Amazonas, Cano Negro	70.8	53.1	15.3	89.2	72.7	42.1	305.8
Paleosuchus palpebrosus	AMNH 93812	NA	71.2	55.6	15.2	91.0	74.0	44.9	NA
Paleosuchus palpebrosus	AMNH 97326	Brazil, Rondonia	78.6	59.7	18.2	101.7	81.0	48.3	NA
Paleosuchus palpebrosus	UF 87980	NA	42.0	34.5	11.0	54.6	46.7	28.8	200.1

Paleosuchus trigonatus	AMNH 66391	NA	60.4	46.9	14.1	76.9	60.8	36.5	NA
Paleosuchus trigonatus	ZSM 149/1911	Brazil	57.3	44.1	12.0	71.4	57.8	34.6	NA
Crocodylus acutus	AMNH 7121	NA	182.4	131.4	42.0	201.4	144.4	91.6	NA
Crocodylus acutus	AMNH 7168	NA	167.8	119.4	37.5	184.5	135.2	83.8	727.7
Crocodylus acutus	AMNH 15182 (Mook 1921)	Nicaragua	80.4	59.6	18.0	90.1	69.0	42.5	NA
Crocodylus acutus	FMNH 22030	Honduras, Lake Ticamaya	228.9	166.8	49.6	238.2	180.8	111.7	NA
Crocodylus acutus	UF 54208	Haiti, Dept. du Sud	87.7	63.4	18.3	96.8	75.8	45.7	353
Crocodylus acutus	UF 56580	USA, Florida, Dade Co., Turkey Pt.	233.3	169.5	55.1	248.9	184.5	113.4	1014.7
Crocodylus acutus	UF 150402	USA, Florida, Monroe Co., Key Largo	93.2	68.6	21.4	100.8	79.6	50.7	377.7
Crocodylus johnsoni	NTM R25705	NA	135.4	97.1	29.4	152.7	110.4	72.0	629.61
Crocodylus johnsoni	NTM R26850	Australia, Northern Territory: Bullita Station, Homestead	43.9	30.7	9.1	52.3	39.7	25.6	NA
Crocodylus johnsoni	QM J47916	Australia, Queensland: Elizabeth Gorge, Bowthorn Station	103.9	72.7	21.2	116.4	86.0	55.5	NA
Crocodylus johnsoni	QM J58446	Australia, Queensland: Cooper Creek, ~6 km south of Windorah	108.2	77.4	23.1	120.7	88.3	56.8	498.35
Crocodylus johnsoni	QM J60590	Australia, Queensland: Amber Station, pool 1	86.0	59.3	17.8	99.0	73.3	47.7	377.65
Crocodylus johnsoni	QM J60591	Australia, Queensland: Springfield Station, pool 5	88.6	61.6	18.6	100.6	75.2	48.0	NA
Crocodylus johnsoni	QM J84415	Australia, Queensland: Donkey Springs, Bulleringa NP	75.2	54.8	15.4	86.1	66.0	42.5	NA
Crocodylus moreletii	UF 54813	NA	152.2	109.4	35.8	168.3	123.7	74.5	602
Crocodylus moreletii	UF 99071	NA	107.0	76.5	20.0	110.7	86.2	58.7	NA
Crocodylus niloticus	AMNH 73047	Kenya	59.9	42.4	13.1	70.3	55.0	35.8	NA
Crocodylus niloticus	AMNH 88634	Kenya, Garissa	77.2	54.2	16.4	86.7	67.5	43.6	NA
Crocodylus niloticus	BMNH 1969.1565	Ethiopia, southwestern Lake Abaya	251.5	165.9	47.0	295.3	193.0	116.8	1107.9
Crocodylus niloticus	IRSNB 6036	Democratic Republic of Congo, Senze	116.8	78.9	24.9	130.7	98.4	62.3	NA
Crocodylus niloticus	IRSNB 6037	Democratic Republic of Congo, Senze	74.3	53.7	17.7	84.4	65.2	43.2	NA
Crocodylus nilocitus	USNM 42150	Kenya	175.0	135.0	39.7	201.2	163.9	98.5	NA
Crocodylus novaeguineae	USNM 211292	Papua-New Guinea, Western Prov., Ali Village	45.0	32.4	10.9	55.2	43.1	28.4	NA
Crocodylus palustris	AMNH 77632	NA	79.4	58.0	19.3	93.2	70.5	44.3	NA
Crocodylus palustris	FMNH 51691	India	141.3	102.0	36.4	149.6	116.4	74.3	569
Crocodylus palustris	ZSM 2534/0	India	114.3	82.7	26.4	130.5	95.5	61.1	NA
Crocodylus porosus	AMNH 7115	NA	138.9	94.9	33.0	151.4	114.2	76.4	NA
Crocodylus porosus	FMNH 22026	India	222.7	146.1	39.9	249.7	173.8	108.9	954.7
Crocodylus porosus	NTM R16036	Australia, Northern Territory: Mary River, Jimmy's Creek	320.5	222.0	74.1	360.5	241.5	153.0	1335.39
Crocodylus porosus	QM J48126	Australia, Queensland: Murray River mouth, northern Tully	285.0	167.1	56.8	317.0	212.2	132.0	1266.38
Crocodylus porosus	USNM 61206	Indonesia, Celebes	201.7	130.0	43.2	221.2	155.5	99.7	871
Crocodylus porosus	ZIT Mamm. 196	Indonesia, Celebes	283.4	178.4	59.2	311.6	209.0	134.7	NA
Crocodylus rhombifer	AMNH 57773	Cuba	128.3	93.2	25.9	157.2	115.0	64.3	544.6
Crocodylus rhombifer	AMNH 77595	NA	106.0	83.1	21.5	136.1	97.9	56.1	428.9
Crocodylus rhombifer	FMNH 34677	Cuba	105.9	83.0	21.9	129.3	98.3	56.1	448.1
Crocodylus rhombifer	UF 45189	Cuba, Isle of Pines	144.3	112.2	28.9	189.6	127.8	74.2	619.9
Gavialis gangeticus	AMNH 88316	NA	112.6	67.5	24.1	127.5	95.4	59.2	568.9
Gavialis gangeticus	AMNH 110145	NA	164.0	91.7	30.0	189.9	137.6	84.3	875.3
Gavialis gangeticus	FMNH 82681	NA	75.0	46.0	16.5	86.4	65.8	42.8	386.8
Gavialis gangeticus	UF 70592	Nepal, Narayani River, Chituun National Park	66.2	39.9	12.8	75.7	56.6	36.8	339.1
Gavialis gangeticus	UF 118998	NA	188.5	110.5	35.4	217.5	176.9	115.3	966.5
Gavialis gangeticus	ZIT Rept. 53	India, Indus Bay, Dera Ismail Khan	146.2	80.8	28.2	173.9	122.9	75.7	NA
Mecistops cataphractus	AMNH 73803	NA	58.1	43.0	14.0	66.9	52.6	31.6	NA
Mecistops cataphractus	IRSNB 5233	Democratic Republic of Congo, Alvertville	146.5	105.0	32.1	176.3	130.9	78.8	NA
Mecistops cataphractus	MCZ 175004	West Africa	61.6	45.1	14.1	72.1	56.5	33.3	NA
Osteolaemus tetraspis osborni	AMNH 10083	Congo, Niapu	84.4	65.9	19.5	103.4	81.1	46.8	NA
Osteolaemus tetraspis	AMNH 69057	NA	85.8	65.6	21.5	105.4	84.3	48.9	363.2
Osteolaemus tetraspis	BMNH 1983.1130	NA	89.3	70.2	21.4	105.7	84.3	48.5	NA
Osteolaemus tetraspis	UF 34784	NA	61.7	46.6	13.6	71.3	61.0	34.6	NA
Osteolaemus tetrapsis	UF 99068	NA	108.2	81.0	24.3	122.6	97.5	56.2	NA

Osteolaemus tetraspis	USNM 194448	Ivory Coast	66.3	50.9	14.7	81.0	65.4	36.6	NA
Tomistoma schlegelii	AMNH 113078	NA	143.2	100.0	29.9	161.0	126.1	75.3	687.3
Tomistoma schlegelii	FMNH 206755	NA	183.1	119.3	38.0	200.9	150.1	91.0	806.7
Tomistoma schlegelii	HoUM unnumbered	NA	162.8	107.6	30.0	199.2	142.1	84.4	NA
Tomistoma schlegelii	MCZ 12459	Borneo, Sarawak River	181.5	117.6	31.7	221.1	157.8	97.0	801.4
Tomistoma schlegelii	UF 54210	NA	132.8	94.3	28.1	152.0	114.0	73.9	609.5
Tomistoma schlegelii	UF 72817	NA	54.6	35.9	10.3	58.5	44.1	27.9	NA
Tomistoma schlegelii	UF 107493	NA	190.5	124.6	34.0	209.4	155.1	87.0	830.8
Tomistoma schlegelii	USNM 52972	Indonesia, Borneo, Samarinda	179.6	115.0	33.4	208.3	150.1	95.1	767.6

Table S2. Measurements of rostral proportions (RPs: ratio of the palate width at the last maxillary alveoli to the length from there to the tip of the snout) in extant crocodylian individuals. Species RPs (Table 1) were obtained by averaging individual RPs for each species (skull width ≥ 100 mm).

Taxon	Specimen #	Locality	Skull length (mm)	Skull width (mm)	Rostral proportion
Alligator mississippiensis	YPM R 17123	USA, Lousiana, Cameron Parish, Rockefeller Wildlife Refuge	210.1	103.4	0.58
Alligator mississippiensis	UF 50125	USA, Florida, Wakulla Co., US 319, at Ochlocknae River	262.3	146.6	0.69
Alligator mississippiensis	UF 87885	USA, Florida, Broward County, Water Conservation Area #3	268.0	136.9	0.62
Alligator mississippiensis	UF 121384	USA, Florida, Pasco Co.	269.3	141.0	0.63
Alligator mississippiensis	UF 43151	USA, Florida, Wakulla Co., US 319, at Ochlocknae River	326.0	173.5	0.68
Alligator mississippiensis	YPM R 10503	USA, Georgia, Chatham County, Savannah River	348.0	188.0	0.66
Alligator mississippiensis	ZSM 4/1921	USA	355.0	192.3	0.71
Alligator mississippiensis	UF 67824	USA, Florida, Putnam County, 4 Km SE Melrose	358.0	200.6	0.69
Alligator mississippiensis	UF 105541	USA, Florida, Broward County, Water Conservation Area #3	367.0	192.4	0.62
Alligator mississippiensis	ZMB 36624	NA	368.0	189.3	0.62
Alligator mississippiensis	UF 98341	USA, Florida, Broward County, Water Conservation Area #3	425.0	234.0	0.62
Alligator mississippiensis	UF 42872	USA, Florida, Walulla Co., Sopchoppy River	446.0	258.3	0.67
Alligator mississippiensis	UF 33552	USA, Florida, Lake Co., Lake Griffin	465.0	288.0	0.74
Alligator mississippiensis	ZSM 2530/0	USA, Mississippi River	474.0	281.7	0.72
Alligator mississippiensis	UF 10941	USA, Florida, Evergrades	495.0	282.0	0.69
Alligator mississippiensis	UF 39618	USA, Florida, Orange Co., Lake Apopka	504.0	319.0	0.70
Alligator mississippiensis	UF 42548	USA, Florida, Clay Co., St. John River at Green Cove Springs	508.0	318.0	0.74
Alligator mississippiensis	UF 84197	USA, Florida, Polk Co.	525.0	293.0	0.69
Alligator sinensis	ZSM 178/1947	China	188.8	118.1	0.86
Alligator sinensis	IVPP 1335	China	214.3	136.2	0.78
Alligator sinensis	USNM 52557	China, Zhejiang Huchow, near Moffett, L. J.	165.1	100.9	0.72
Caiman crocodilus crocodilus	ZSM 100/1911	Brasil, Insel Marajo, Fazenda Arary am oberen Rio Arary	169.3	105.0	0.64
Caiman crocodilus crocodilus	ZSM 56/1936	Venezuela, Maracay	175.5	108.9	0.70
Caiman crocodilus crocodilus	ZSM 206/1925	Bolivia, Rio Madidi	188.7	111.1	0.62
Caiman crocodilus crocodilus	ZSM 109/1933	Venezuela, Maracay	195.7	114.2	0.65
Caiman crocodilus crocodilus	ZSM 112/1933	Venezuela, Maracay	215.0	131.7	0.63
Caiman crocodilus crocodilus	ZSM 10/1911	Brasil, Insel Marajo, Fazenda Menino Jesus am oberen Rio Arary	237.6	148.6	0.66
Caiman crocodilus crocodilus	ZSM 104/1911	Brasil, Insel Marajo, Fazenda Coniciras (2 Stunden landeinwärts vom Ararysee)	252.0	167.5	0.70
Caiman crocodilus crocodilus	ZSM 4/1911	Brasil, Insel Mexiana, Fazenda Sta. Maria	290.1	179.3	0.65
Caiman crocodilus fuscus	ZSM 70/1937	Colombia, Jesus del Rio, Dep. Bolivar	181.2	110.3	0.74
Caiman crocodilus fuscus	ZSM 69/1937	Colombia, Jesus del Rio, Dep. Bolivar	213.9	130.6	0.73
Caiman yacare	ZSM 168/1929	Argentina, Lapango, Gob. Formosa	181.3	107.8	0.70
Caiman yacare	ZSM 170/1933	Paraguay, Puerto Sastre am Rio Paraguay	227.3	142.4	0.66
Caiman yacare	USNM 281821	Bolivia, Beni, Vacadiez, Tumi Chucua, Lago Tumi Chucua	246.6	155.3	0.70
Caiman yacare	USNM 281809	Bolivia, Beni, Vacadiez, Tumi Chucua, Lago Tumi Chucua	300.6	175.1	0.66
Caiman yacare	ZSM 164/1929	Bolivia, San Pedro, Chiquitos	270.2	186.7	0.72
Caiman yacare	ZSM 163/1933	Bolivia, Trinidad, Chiquitos	288.0	189.3	0.72
Caiman yacare	ZSM 163/1929	Paraguay, Rio Paraguay bei Puerto Casado	269.0	189.9	0.78
Caiman yacare	ZSM 162/1929	Argentina, Mittellauf des Bermejo Norvanns?, Gob. Formosa	310.5	209.8	0.78
Caiman yacare	ZSM 169/1933	Paraguay, Rio Paraguay bei Puerto Casado, Estancia Sta Casilva	319.0	213.1	0.72
Caiman latirostris	ZSM 435/1911	NA	171.1	110.3	0.81
Caiman latirostris	ZMB 36629	Paraguay	177.6	118.1	0.86
Caiman latirostris	ZSM 73/1926	Argentina, La Victoria, Formosa	179.1	121.5	0.94
Caiman latirostris	ZMB 36628	Brasil, Rio Grande do Sul	209.7	144.8	0.92

Caiman latirostris	ZMB 42396	Brasil, Rio Grande do Sul	249.7	184.0	0.94
Melanosuchus niger	BMNH 1872.6.4.1	Peru, eastern Peru	212.4	110.3	0.71
Melanosuchus niger	ZSM 80/1911	Brasil, Insel Marajo, Igarapi bei der Fazenda Arary am mittleren Rio Arary	297.0	152.0	0.63
Melanosuchus niger	ZSM 87/1911	Brasil, Insel Marajo, Fazenda Menino Jesus am oberen Rio Arary	290.0	155.2	0.64
Melanosuchus niger	ZSM 79/1911	Brasil, Insel Marajo, Fazenda Menino Jesus am oberen Rio Arary	301.3	165.1	0.68
Melanosuchus niger	ZSM 76/1911	Brasil, Insel Marajo, Lago Camaleaosal bei Cachoeira am Rio Arary	296.2	166.2	0.69
Melanosuchus niger	ZSM 85/1911	Brasil, Insel Marajo, Fazenda Menino Jesus am oberen Rio Arary	307.0	169.1	0.74
Melanosuchus niger	ZSM 84/1911	Brasil, Insel Marajo, Fazenda Menino Jesus am oberen Rio Arary	310.0	172.1	0.67
Melanosuchus niger	ZSM 73/1911	Brasil, Insel Marajo, Fazenda Menino Jesus am oberen Rio Arary	340.0	177.7	0.68
Melanosuchus niger	ZSM 86/1911	Brasil, Insel Marajo, Fazenda Menino Jesus am oberen Rio Arary	328.0	179.8	0.69
Melanosuchus niger	ZSM 90/1911	Brasil, Insel Marajo, Fazenda Menino Jesus am oberen Rio Arary	331.0	183.5	0.71
Melanosuchus niger	ZSM 3/1911	Brasil, Insel Marajo, Fazenda Menino Jesus am oberen Rio Arary	364.0	198.5	0.68
Melanosuchus niger	ZSM 89/1911	Brasil, Insel Marajo, Fazenda Menino Jesus am oberen Rio Arary	351.0	200.0	0.71
Melanosuchus niger	ZSM 68/1911	Brazil, Marajo Island, Fazenda Menino Jesus on the upper Rio Arary	351.0	201.8	0.73
Melanosuchus niger	ZSM 75/1911	Brazil, Marajo Island, Fazenda Menino Jesus on the upper Rio Arary	352.0	203.9	0.71
Melanosuchus niger	ZSM 46/1911	Brazil, Marajo Island, Fazenda Menino Jesus on the upper Rio Arary	380.0	202.6	0.64
Melanosuchus niger	ZSM 64/1911	Brazil, Marajo Island, Fazenda Menino Jesus on the upper Rio Arary	394.0	228.2	0.70
Melanosuchus niger	ZSM 62/1911	Brazil, Marajo Island, Fazenda Menino Jesus on the upper Rio Arary	414.0	233.9	0.68
Melanosuchus niger	ZSM 57/1911	Brazil, Marajo Island, Fazenda Menino Jesus on the upper Rio Arary	431.0	255.4	0.70
Melanosuchus niger	ZSM 52/1911	Brazil, Marajo Island, Fazenda Menino Jesus on the upper Rio Arary	441.0	262.0	0.67
Melanosuchus niger	ZSM 63/1911	Brazil, Marajo Island, Cachoeira on the middle Rio Array	494.0	305.0	0.71
Melanosuchus niger	ZSM 223/1925	Bolivia, Cachouela Esparanga (10 h from Ribralta), Rio Beni	513.0	337.0	0.75
Paleosuchus palpebrosus	ZSM 42/1938	Brasil, Rio Ivinheima (Oberhalb Lager 4), ca. 28 km flussaufwärts von der Mündung in den Parana	180.4	104.7	0.62
Paleosuchus palpebrosus	ZSM 44/1938	Brasil, Rio Ivinheima (Oberhalb Lager 4), ca. 28 km flussaufwärts von der Mündung in den Parana	175.5	104.8	0.60
Paleosuchus palpebrosus	ZSM 43/1938	Brasil, Rio Ivinheima (Oberhalb Lager 4), ca. 28 km flussaufwärts von der Mündung in den Parana	189.2	112.8	0.63
Paleosuchus palpebrosus	ZSM 207/1925	Brasil, Manacapuru am Solimoeus, Staat Amazonas	209.1	123.1	0.58
Paleosuchus palpebrosus	ZSM 41/1938	Brasil, Rio Ivinheima (Oberhalb Lager 4), ca. 28 km flussaufwärts von der Mündung in den Parana	200.0	126.0	0.66
Paleosuchus trigonatus	FMNH 69882	Colombia, Amazonas Intendencia, Rio Apaporis	203.8	101.9	0.53
Paleosuchus trigonatus	ZSM 520/1911	Surinam	244.8	133.8	0.61
Crocodylus acutus	SMF 42808	El Salvador	230.6	103.6	0.44
Crocodylus acutus	FMNH 5775	Honduras, Lake Ticamaya	235.2	108.7	0.44
Crocodylus acutus	FMNH 5776	Honduras, Lake Ticamaya	244.0	113.1	0.44
Crocodylus acutus	FMNH 74924	Colombia, Bolívar, Isla Fuerte	259.5	107.1	0.40
Crocodylus acutus	YPM R15100	Mexico, Jalisco State, Chamela Bay West	268.9	124.9	0.47
Crocodylus acutus	FMNH 20159	Guatemala, Escuintla, Tiquisate, Conception del Mar	294.0	135.7	0.43
Crocodylus acutus	ZSM 122/1908	Jamaica	297.1	138.9	0.49
Crocodylus acutus	SMF 42956	El Salvador	299.0	142.3	0.44
Crocodylus acutus	USNM 258735	Belize, Stann Creek	309.8	151.9	0.50
Crocodylus acutus	SMF 30007	Cuba	316.3	149.1	0.48
Crocodylus acutus	FMNH 11041	Belize, Belize	341.0	159.7	0.44
Crocodylus acutus	ZSM 74/1937	Colombia, Jesus del Rio, Dep. Bolívar	347.0	167.2	0.43
Crocodylus acutus	FMNH 74923	Colombia, Bolívar, Isla Fuerte	357.0	161.0	0.45
Crocodylus acutus	ZSM 73/1937	Colombia, Jesus del Rio, Dep. Bolívar	366.0	178.3	0.46
Crocodylus acutus	FMNH 13220	Honduras, Lake Ticamaya	370.0	184.5	0.45
Crocodylus acutus	AMNH R 9659	Florida	400.0	212.0	0.53
Crocodylus acutus	FMNH 11038	Honduras, Lake Ticamaya	404.0	212.8	0.50
Crocodylus acutus	USNM 115353	Mexico, Guerrero, Acapulco, Laguna Coyuca	420.0	215.0	0.49
Crocodylus acutus	ZSM 137/1926	Columbia, Rio Lebrija	434.0	216.1	0.50

Crocodylus acutus	USNM 247943	Panama, Colon, Barro Colorado Island, Barbour Point	443.0	216.6	0.46
Crocodylus acutus	FMNH 69886	Colombia, Magdalena, Cienaga Grande, Cano de Las Mujeres	486.0	267.7	0.53
Crocodylus acutus	FMNH 73755	Colombia, Magdalena	526.0	289.0	0.56
Crocodylus acutus	ZSM 72/1929	Nicaragua, Lake Managua	540.0	271.5	0.45
Crocodylus acutus	FMNH 59070	Panama, Canal Zone	591.0	301.0	0.47
Crocodylus acutus	FMNH 59071	Panama, Canal Zone, Chagres River, near Juan Mina	600.0	323.0	0.53
Crocodylus johnsoni	USNM 299810	Australia, Western territory, Mckinlay River	281.2	123.3	0.40
Crocodylus johnsoni	SMF 54424	Australia, Queensland	304.0	122.1	0.33
Crocodylus johnsoni	SMF 54425	Australia, Queensland	304.0	123.6	0.34
Crocodylus johnsoni	SMF 54427	Australia, Queensland	341.0	129.7	0.32
Crocodylus johnsoni	SMF 54426	Australia, Queensland	342.0	141.4	0.36
Crocodylus johnsoni	AMNH R86540	Australia, Queensland	393.0	165.7	0.37
Crocodylus niloticus	IRSNB 5007	Tanzania, Luapula	239.1	118.6	0.51
Crocodylus niloticus	IRSNB 6036	Democratic Republic of Congo, Senze	261.2	137.7	0.51
Crocodylus niloticus	IRSNB 5006	Tanzania, Luapula	279.0	146.9	0.58
Crocodylus niloticus	IRSNB 5011	Tanzania, Luapula	374.0	214.1	0.59
Crocodylus niloticus	IRSNB 5010	Tanzania, Luapula	411.0	237.6	0.63
Crocodylus niloticus	IRSNB 3310	Democratic Republic of Congo, Pweto, Haut-Katanga	409.0	239.1	0.55
Crocodylus niloticus	IRSNB 5003	Tanzania, Luapula	424.0	262.3	0.63
Crocodylus niloticus	IRSNB 5008	Tanzania, Luapula	433.0	266.3	0.67
Crocodylus niloticus	IRSNB 5002	Tanzania, Luapula	475.0	280.0	0.64
Crocodylus niloticus	IRSNB 5009	Tanzania, Luapula	457.0	280.3	0.60
Crocodylus niloticus	IRSNB 5012	Democratic Republic of Congo, Luapula	461.0	294.8	0.69
Crocodylus niloticus	IRSNB 3633	Tanzania, Rukwa Lake	591.0	393.0	0.68
Crocodylus novaeguineae	USNM 211298	Papua New Guinea, Western Prov., Balimo Subprob., Makapa Village Lagoon, Aramia River	238.0	119.7	0.46
Crocodylus novaeguineae	BMNH 1886.5.20.1	New Guinea, Fly River	250.1	130.3	0.50
Crocodylus novaeguineae	SMF 53300	New Guinea, Sepik	258.1	123.8	0.43
Crocodylus novaeguineae	FMNH 14047	New Guinea, Koragu, middle Sepik River	276.6	131.8	0.44
Crocodylus novaeguineae	FMNH 14040	New Guinea	329.0	169.6	0.46
Crocodylus novaeguineae	USNM 211301	Papua New Guinea, Western Prov., Balimo Subprov., Samacki River, mouth of Aramia River drainage	335.9	166.8	0.46
Crocodylus novaeguineae	SMF 60031	New Guinea, middle Sepik, between Angoram and Ambunti	338.0	177.4	0.47
Crocodylus novaeguineae	FMNH 14048	New Guinea, Koragu, middle Sepik River	351.0	185.8	0.50
Crocodylus novaeguineae	FMNH 14043	Papua New Guinea, Nyourangai, Lagoon village, middle Sepik	349.0	195.4	0.51
Crocodylus novaeguineae	FMNH 14039	Papua New Guinea, Nyourangai, Lagoon village, middle Sepik	391.0	206.7	0.50
Crocodylus novaeguineae	FMNH 14044	New Guinea, Koragu, middle Sepik River	374.0	217.8	0.53
Crocodylus novaeguineae	USNM 211290	Papua New Guinea, Western Prov., Balimo Subprov., Aramia River lagoon	372.0	223.2	0.56
Crocodylus palustris	ZSM 565/1911	Sri Lanka, Hambantota	213.0	114.1	0.58
Crocodylus palustris	ZSM 30/1912	India, Gangesmündung bei Calcutta	227.2	129.1	0.68
Crocodylus palustris	ZSM 2534/0	India (from a forestman)	248.3	143.9	0.60
Crocodylus palustris	ZSM 231/0	India	249.0	152.8	0.68
Crocodylus palustris	BMNH 1848.2.5.9	India, River Raptee	250.2	138.3	0.62
Crocodylus palustris	ZSM 612/1911	Sri Lanka, Hambantota	251.1	139.0	0.62
Crocodylus palustris	BMNH 1852.5.9.46	Sri Lanka, Ceylon	274.9	156.3	0.62
Crocodylus palustris	ZSM 274/1912	Sri Lanka, Hambantota	281.7	150.8	0.59
Crocodylus palustris	SMF 28168	India	285.6	170.2	0.71
Crocodylus palustris	ZSM 559/1911	Sri Lanka, Hambantota	296.0	162.6	0.63
Crocodylus palustris	ZSM 542/1911	Sri Lanka, Hambantota	317.0	184.7	0.66
Crocodylus palustris	ZSM 389/1907	Sri Lanka, Ceylon	318.0	170.2	0.55

Crocodylus palustris	BMNH 1929.8.6.2	India, Kamara, Mysore, South India	325.0	187.3	0.59
Crocodylus palustris	ZSM 517/1911	Sri Lanka, Kahatagasdigiliya	339.0	181.4	0.57
Crocodylus palustris	BMNH 1868.4.9.11	India	497.0	311.0	0.73
Crocodylus palustris	FMNH 31537	Pakistan, Sindh	500.0	308.0	0.74
Crocodylus palustris	BMNH 1897.12.31.1	Sri Lanka, Ceylon	505.0	319.0	0.67
Crocodylus porosus	FMNH 21907	Philippines, Mindoro, Lake Naujan	235.6	112.7	0.49
Crocodylus porosus	FMNH 15229	North Borneo, Sandakan	254.8	124.3	0.50
Crocodylus porosus	FMNH 63744	North Borneo, Labuk Bay, Tikus Island	281.3	129.0	0.47
Crocodylus porosus	FMNH 15230	North Borneo, Sandakan	287.0	132.6	0.49
Crocodylus porosus	FMNH 28467	Philippines	302.0	143.8	0.48
Crocodylus porosus	FMNH 28465	Philippines	307.6	148.2	0.46
Crocodylus porosus	FMNH 28466	Philippines	311.0	148.0	0.49
Crocodylus porosus	ZMB 36700	Indonesia, Sumatra	319.0	151.4	0.48
Crocodylus porosus	FMNH 15231	North Borneo, Sandakan	338.0	157.7	0.48
Crocodylus porosus	FMNH 14031	Papua New Guinea, edge of river above Kubka	349.0	168.4	0.46
Crocodylus porosus	USNM 38081	Philippines	360.0	178.0	0.50
Crocodylus porosus	FMNH 14052	Papua New Guinea, Koragu, middle Sepick River	365.0	176.7	0.45
Crocodylus porosus	FMNH 14034	Papua New Guinea, Nyourangai, Lagoon village, middle Sepik	366.0	172.6	0.44
Crocodylus porosus	FMNH 15232	North Borneo, Sandakan	378.0	181.4	0.47
Crocodylus porosus	FMNH 28469	Philippines	394.0	197.1	0.47
Crocodylus porosus	USNM 61206	Indonesia, Celebes	430.0	237.5	0.51
Crocodylus porosus	USNM 228416	Philippines, Mindanao Island	544.0	351.0	0.66
Crocodylus porosus	FMNH 14071	Papua New Guinea, Gologapa, Keram River, south of Sepik River	564.0	357.0	0.58
Crocodylus porosus	USNM 228412	Philippines, Mindanao Island	604.0	365.0	0.63
Crocodylus porosus	USNM 509454	Papua New Guinea, East Sepic Prov.	612.0	357.0	0.62
Crocodylus rhombifer	AMNH 57773	Cuba	262.0	152.0	0.57
Crocodylus rhombifer	SMF 37081	Cuba, Ciénaga de Zapata	237.6	133.7	0.60
Crocodylus moreletii	SMF 28170	NA	240.5	157.5	0.68
Crocodylus moreletii	SMF 28169	NA (Acquired from Kochkunst Museum)	258.7	137.5	0.58
Crocodylus moreletii	SMF 56317	Mexico	399.0	274.4	0.69
Crocodylus moreletii	ZSM 3038/0	Mexico, La Antigua	432.0	273.1	0.62
Mecistops cataphractus	IRSNB 6031	Democratic Republic of Congo, Mabwe, Katanga, Upemba National Park	245.4	106.7	0.32
Mecistops cataphractus	IRSNB 4984	Tanzania, Luapula	256.7	102.0	0.32
Mecistops cataphractus	IRSNB 4985	Tanzania, Luapula	256.8	103.0	0.32
Mecistops cataphractus	IRSNB 4976	Democratic Republic of Congo, Kasenga, Haut-Katanga	295.8	116.4	0.30
Mecistops cataphractus	IRSNB 4983	Tanzania, Luapula	316.4	134.4	0.34
Mecistops cataphractus	IRSNB 4980	Tanzania, Luapula	325.0	137.1	0.32
Mecistops cataphractus	SMF 43977	Cameroon, Bonambassi	327.0	132.4	0.30
Mecistops cataphractus	IRSNB 4982	Tanzania, Luapula	330.0	133.7	0.32
Mecistops cataphractus	IRSNB 4977	Democratic Republic of Congo, Kasenga, Haut-Katanga	343.0	136.8	0.32
Mecistops cataphractus	AMNH R160902	Democratic Republic of Congo	349.0	139.2	0.33
Mecistops cataphractus	IRSNB 4979	Tanzania, Luapula	364.0	153.0	0.32
Mecistops cataphractus	IRSNB 5233	Democratic Republic of Congo, Alvertville	378.0	178.5	0.33
Mecistops cataphractus	IRSNB 4981	Tanzania, Luapula	386.0	165.3	0.33
Mecistops cataphractus	IRSNB 4991	Tanzania, Luapula	388.0	171.2	0.37
Mecistops cataphractus	AMNH R10075	Democratic Republic of Congo	396.0	155.4	0.30
Mecistops cataphractus	IRSNB 17962	Democratic Republic of Congo, Semliki Delta, Kivu	423.0	180.8	0.34
Mecistops cataphractus	IRSNB 4989	Tanzania, Luapula	454.0	199.8	0.36

Mecistops cataphractus	IRSNB 4998	Tanzania, Luapula	481.0	209.2	0.35
Mecistops cataphractus	BMNH 1900.2.27.1	Gabon, Ogowe	488.0	215.1	0.31
Mecistops cataphractus	IRSNB 4996	Tanzania, Luapula	502.0	230.5	0.36
Mecistops cataphractus	IRSNB 5225	Democratic Republic of Congo, Toa	514.0	226.7	0.35
Mecistops cataphractus	IRSNB 4999	Tanzania, Luapula	516.0	224.1	0.32
Mecistops cataphractus	IRSNB 4990	Tanzania, Luapula	518.0	238.3	0.37
Mecistops cataphractus	IRSNB 4987	Tanzania, Luapula	528.0	239.2	0.36
Mecistops cataphractus	IRSNB 4988	Tanzania, Luapula	537.0	246.7	0.37
Mecistops cataphractus	IRSNB 4993	Tanzania, Luapula	537.0	239.9	0.34
Mecistops cataphractus	IRSNB 4994	Tanzania, Luapula	540.0	243.8	0.36
Mecistops cataphractus	IRSNB 3302	Democratic Republic of Congo, Moero	544.0	247.0	0.36
Mecistops cataphractus	IRSNB 17963	Democratic Republic of Congo, Semliki Delta, Kivu	548.0	253.0	0.38
Mecistops cataphractus	IRSNB 17967	Democratic Republic of Congo, Semliki Delta, Kivu	550.0	246.3	0.35
Mecistops cataphractus	IRSNB 5001	Tanzania, Luapula	552.0	244.4	0.34
Mecistops cataphractus	IRSNB 5000	Tanzania, Luapula	562.0	250.4	0.37
Mecistops cataphractus	IRSNB 4997	Tanzania, Luapula	571.0	268.7	0.38
Mecistops cataphractus	IRSNB 17964	Democratic Republic of Congo, Semliki Delta, Kivu	576.0	270.5	0.37
Mecistops cataphractus	BMNH 1924.5.10.1	Tanzania, Kigoma, Tanganyika	581.0	236.5	0.32
Mecistops cataphractus	IRSNB 4986	Tanzania, Luapula	594.0	268.9	0.38
Osteolaemus osborni	AMNH 10083	Democratic Republic of Congo	177.4	106.8	0.74
Osteolaemus tetraspis	ZMB 36638	Cameroon, Osidinge	176.8	105.7	0.71
Osteolaemus tetraspis	ZMB 54447	NA	191.5	109.6	0.66
Osteolaemus tetraspis	ZMB 36639	Cameroon, Mundami	189.5	114.8	0.69
Osteolaemus tetraspis	SMF 59521	NA	196.7	117.4	0.73
Gavialis gangeticus	USNM 72562	India, Uttar Pradesh Allahabad, near River Tons, Ganges River tributary	371.0	111.3	0.23
Gavialis gangeticus	YPM R10514	India	418.0	139.6	0.22
Gavialis gangeticus	BMNH 96.7.7.4	India, Jumna River, 30 miles below Delhi	424.0	139.7	0.24
Gavialis gangeticus	BMNH specimen S of Gray 1873	India	427.0	134.1	0.23
Gavialis gangeticus	ZIT Rept. 53	Pakistan, Indus Bay (Dera Ismail Khan)	449.0	158.5	0.28
Gavialis gangeticus	ZSM 29/1938	India,Indus, Vorder Indien (West India)	483.0	174.6	0.27
Gavialis gangeticus	ZSM 29/1912	India, Ganges	540.0	197.6	0.27
Gavialis gangeticus	BMNH 61.4.1.2	India	566.0	209.4	0.27
Gavialis gangeticus	BMNH 1935.6.4.1	India, Ramganga River, Bareilly, U.P.	605.0	229.0	0.27
Gavialis gangeticus	ZSM 62/1959	Nepal, Girwa River, near Bardia (West-Nepal)	634.0	262.4	0.30
Gavialis gangeticus	ZMB 36678	India, Ganges	652.0	256.5	0.26
Gavialis gangeticus	ZIT Rept. 40	Pakistan, Indus Bay (Dera Ismail Khan)	668.0	278.1	0.32
Gavialis gangeticus	SMF 37951	India, Jumna River	673.0	273.8	0.30
Gavialis gangeticus	SMF 49529	Pakistan, Indus, bei dem Dorfe Buagsar, Baharvalpur State	674.0	263.6	0.30
Gavialis gangeticus	AMNH R 7138	India	690.0	292.8	0.29
Gavialis gangeticus	BMNH 2005.1601	India	722.0	289.6	0.28
Gavialis gangeticus	BMNH 1847.12.20.4	India	734.0	307.5	0.32
Gavialis gangeticus	BMNH 1974.3009	India, Ganges	738.0	314.0	0.32
Gavialis gangeticus	ZSM 28/1912	India, Ganges	744.0	320.0	0.33
Tomistoma schlegelii	BMNH 1899.1.31.1	Borneo, Sadong River	344.6	117.2	0.23
Tomistoma schlegelii	SMF unknown	Sumatra, Singilino-fluss	382.0	141.3	0.25
Tomistoma schlegelii	ZSM 232/1909	Sumatra, Sultanat Deli, Sungai Rampah	483.0	184.5	0.26
Tomistoma schlegelii	SMF 28135	Sumatra, Perbaungan	499.0	209.9	0.27
Tomistoma schlegelii	USNM 52972	Borneo, Samarinda	510.0	220.1	0.29

Tomistoma schlegelii	ZSM 523/1909	Borneo	527.0	207.7	0.26
Tomistoma schlegelii	SMF 28134	Borneo, Baram-fluss	530.0	201.2	0.26
Tomistoma schlegelii	BMNH 48.10.31.19	Borneo	542.0	224.9	0.32
Tomistoma schlegelii	ZSM 200/1907	Central Borneo, Poctos Libau	557.0	232.4	0.28
Tomistoma schlegelii	ZSM 201/1907	Central Borneo, Sungai Mendalam	562.0	228.8	0.28
Tomistoma schlegelii	BMNH 1860.11.6.8	Borneo	574.0	244.6	0.31
Tomistoma schlegelii	ZSM 203/1907	Central Borneo, Sungai Mendalam	584.0	254.9	0.31
Tomistoma schlegelii	ZSM 385/1907	Central Borneo, Kapoeas Gebeit	590.0	240.1	0.27
Tomistoma schlegelii	ZSM 374/1907	Central Borneo, Kapoeas Gebeit	594.0	247.5	0.29
Tomistoma schlegelii	ZSM 371/1907	Central Borneo, Kapoeas Gebeit	602.0	237.3	0.27
Tomistoma schlegelii	USNM 211323	Indonesia, Kalimantan Sanggau, Kapuas River	665.0	289.4	0.32
Tomistoma schlegelii	ZSM 1/0	Borneo	674.0	311.4	0.34
Tomistoma schlegelii	ZSM 376/1907	Central Borneo, Kapoeas Gebeit	681.0	291.0	0.32
Tomistoma schlegelii	ZSM 252/1907	Central Borneo, Bika	686.0	323.0	0.34
Tomistoma schlegelii	ZSM 395/1907	Central Borneo, Kapoeas Gebeit	748.0	375.0	0.38
Tomistoma schlegelii	IRSNB 154C	Borneo	753.0	398.0	0.40
Tomistoma schlegelii	ZSM 372/1907	Central Borneo, Batang Loepar-seen	767.0	367.0	0.38
Tomistoma schlegelii	USNM 211322	Borneo, Sarawak River	783.0	354.0	0.36
Tomistoma schlegelii	ZSM 370/1907	Central Borneo	812.0	392.0	0.40
Tomistoma schlegelii	BMNH 94.2.21.1	Borneo	839.0	409.0	0.39
Caiman crocodilus apaporiensis	ZMB 37253	Colombia, Upper Rio Apaporis	248.1	147.7	0.57
Crocodylus intermedius	FMNH 75658	Colombia, Meta Intendencia, Rio Ariari	243.4	102.7	0.36
Crocodylus intermedius	FMNH 75659	Colombia, Meta Intendencia, Rio Ariari	357.0	156.2	0.37
Crocodylus intermedius	FMNH 75661	Colombia, Meta Intendencia, Rio Ariari, ca 250m	367.0	164.8	0.38
Crocodylus intermedius	FMNH 75660	Colombia, Meta Intendencia, Rio Ariari	473.0	219.4	0.40
Crocodylus intermedius	FMNH 75663	Colombia	478.0	233.2	0.42
Crocodylus intermedius	USNM 211281	Venezuela, Orinoco River	490.0	226.3	0.44
Crocodylus intermedius	BMNH 1851.8.25.29	Orinoco	516.0	242.5	0.43
Crocodylus intermedius	SMF 55155	Colombia	526.0	263.2	0.45
Crocodylus intermedius	FMNH 75662	Colombia, Meta Intendencia, Rio Guejar	530.0	282.3	0.50
Crocodylus intermedius	SMF 28139	Orinoco	649.0	361.0	0.50
Crocodylus intermedius	BMNH 62.10.19.1	Orinoco	670.0	335.0	0.45
Crocodylus mindorensis	USNM 37435	Philippines, Mindanao Island, Zamboanga	233.5	135.1	0.57
Crocodylus mindorensis	USNM 228407	Philippines, Luzon Island, Laguna, Siniloan, near Laguna de Bay	324.0	194.2	0.58
Crocodylus siamensis	BMNH 1920.1.20.1626	Vietnam, Saigon, Cochinchina	345.9	199.6	0.57
Crocodylus siamensis	USNM 509430	NA (Hatched in captivity)	282.4	162.5	0.60
Crocodylus suchus	USNM 248848	Sierra Leone, Northern Bombali, Outamba-Kilimi National Park, Kilimi Section, southern Kilimi	260.5	129.2	0.48
Crocodylus suchus	USNM 194833	Ivory Coast, Sud Abidjan, near Mcintyre	343.0	171.7	0.51
Crocodylus suchus	USNM 194831	Ivory Coast, Sud Abidjan, near Mcintyre	373.0	186.0	0.53

Table S3. Fore- and hind limb measurements for fossil taxa. Measurements are in mm.

Taxon	Specimen #	Reference	Humerus length	Ulna length	Metacarpal III length	Femur length	Tibia length	Metatarsal III length	Trunk length (C3-D15)
Anteophthalmosuchus hooleyi	IRSNB R47	Martin et al. 2016; Martin 2017 personal communication	208.0	156.0	36.0	201.0	144.0	83.0	NA
Susisuchus anatoceps	MPSC-R1136	Figueiredo et al. 2011; Figueiredo 2017 personal communication	42.2	32.3	6.7	NA	NA	NA	NA
Susisuchus sp.	MPSC-R1137	Figueiredo and Kellner 2009	NA	NA	NA	37.6	37.8	17.9	NA
Borealosuchus wilsoni	USNM 12990	Direct observation	191.9	138.1	42.1	219.7	160.3	117.0	862
Boverisuchus vorax	USNM 12957	Direct observation (Rossmann 1998, 2000)	143.7	125.0	28.7	202.4	151.8	85.9	590
Boverisuchus bolcensis	MGP-PD 27567	Sacco 1896; Berg 1966; Rossmann 1998; Brochu 2013	NA	NA	NA	160.0	120.0	70.0	NA
Allognathosuchus gracilis	HLMD ME 8008	Rauhe and Rossmann 1995	NA	NA	NA	47.0	41.0	23.0	NA
Navajosuchus mooki	AMNH 6780	Direct observation (Lucas and Estep 2000)	133.4	95.5	27.3	179.8	125.8	73.7	572
Wannaganosuchus brachymanus	SMM P76.28.246	Erickson 1982	75.0	60.9	18.0	97.0	78.1	49.2	NA
Alligator prenasalis	YPM PU 13799	Direct observation	97.5	72.1	22.4	120.0	89.1	58.3	NA
Stangerochampsa mccabei	RTMP.86.61.0	Wu et al. 1996	107.0	80.0	33.8	NA	NA	NA	NA
Necrosuchus ionensis	AMNH 3219	Direct observation (Brochu 2011)	NA	NA	NA	153.2	124.7	76.7	NA
Tsoabichi greenriverensis	FMNH unnumbered	Direct observation	29.0	25.6	9.0	45.7	41.0	28.4	NA
Asiatosuchus sp.	MGP-PD 27568 (holotype of *Crocodylus vicetinus*)	Sacco 1896; Fabiani 1912; Berg 1966; Rauhe and Rossmann 1995	NA	NA	NA	170.0	140.0	70.4	NA
Toyotamaphimeia machikanensis	MOU F00001	Kobayashi et al. 2006	403.0	214.0	68.3	NA	NA	NA	1733

Table S4. Rostral proportions (ratio of the palate width at the last maxillary alveoli to the length from there to the tip of the snout) of fossil and extant species for the comparisons among crocodylian subgroups (figure 8).

Taxonomic group	Species	Specimen	Reference	Rostral proportion
basal alligatoroid	*Leidyosuchus canadensis*	NMC 8543	Sternberg 1932	0.68
basal alligatoroid	*Diplocynodon darwini*	reconstruction	Berg 1966	0.63
basal alligatoroid	*Diplocynodon hantoniensis*	BMNH 30392	direct observation	0.64
basal alligatoroid	*Diplocynodon ratelii*	MNHN SG12853	Vaillant 1872	0.67
basal alligatoroid	*Diplocynodon muelleri*	Spa 4 T2	Piras and Buscalioni 2006	0.71
basal alligatoroid	*Diplocynodon tormis*	IPS-9001	Buscalioni et al. 1992	0.59
basal alligatoroid	*Acynodon iberoccitanus*	ACAP-FX1	Martin 2007	1.19
Alligatorinae	*Ceratosuchus burdoshi*	FMNH P 15576	Bartels 1984	1.03
Alligatorinae	*Navajosuchus mooki*	AMNH 5186	direct observation	0.76
Alligatorinae	*Procaimanoidea utahensis*	USNM 15996	Gilmore 1946	0.51
Alligatorinae	*Wannaganosuchus brachymanus*	SMM P76.28.247	Erickson 1982	0.99
Alligatorinae	*Alligator prenasalis*	MCZ 1015	Mook 1932	0.78
Alligatorinae	*Alligator mcgrewi*	AMNH 7905	direct observation	1.02
Alligatorinae	*Alligator olseni*	MCZ 1887	White 1942	0.78
Alligatorinae	*Alligator thompsoni*	AMNH 1736	Mook 1923	0.84
Alligatorinae	*Alligator mefferdi*	AMNH 7016	direct observation	0.77
Alligatorinae	*Alligator mississippiensis*	Multiple individuals	direct observation	0.64
Alligatorinae	*Alligator sinensis*	Multiple individuals	Cong et al. 1998	0.79
Caimaninae	*Brachychampsa montana*	AMNH 5032	direct observation	0.94
Caimaninae	*Stangerochampsa mccabei*	RTMP.86.61.1	Wu et al. 1996	0.94
Caimaninae	*Albertochampsa langstoni*	SMM P67.15.3	Erickson 1972	0.73
Caimaninae	*Paleosuchus palpebrosus*	Multiple individuals	direct observation	0.62
Caimaninae	*Paleosuchus trigonatus*	Multiple individuals	direct observation	0.57
Caimaninae	*Orthogenysuchus olseni*	AMNH 5178	Mook 1924	0.43
Caimaninae	*Mourasuchus amazonensis*	DGM 526-R	Price 1964	0.58
Caimaninae	*Mourasuchus arendsi*	UNEFM-CIAAP-1297	Scheyer and Delfino 2016	0.51
Caimaninae	*Purussaurus mirandai*	UNEFM-CIAAP-1369	Aguilera et al. 2006	0.77
Caimaninae	*Purussaurus neivensis*	UCMP 39074	Langston 1965	0.78
Caimaninae	*Purussaurus brasiliensis*	UFAC 1403	Bocquentin-Villanueva et al. 1991	0.87
Caimaninae	*Gnatusuchus pebasensis*	MUSM 990	Salas-Gismondi et al. 2015	1.15
Caimaninae	*Kuttanacaiman iquitosensis*	MUSM 1490	Salas-Gismondi et al. 2015	1.09
Caimaninae	*Caiman yacare*	Multiple individuals	direct observation	0.70
Caimaninae	*Caiman crocodilus apaporiensis*	ZMB 37253	direct observation	0.57
Caimaninae	*Caiman crocodilus crocodilus*	Multiple individuals	direct observation	0.65
Caimaninae	*Caiman crocodilus fuscus*	Multiple individuals	direct observation	0.73
Caimaninae	*Caiman latirostris*	Multiple individuals	direct observation	0.89
Caimaninae	*Caiman lutescens*	UCMP 39978	Langston 1965	0.87
Caimaninae	*Melanosuchus fisheri*	MCZ 4336	Medina 1976	0.85
Caimaninae	*Melanosuchus niger*	Multiple individuals	direct observation	0.68
basal crocodyloid	*Prodiplocynodon langi*	AMNH 108	direct observation	0.82
basal crocodyloid	*Asiatosuchus germanicus*	reconstruction	Berg 1966	0.77

basal crocodyloid	*Crocodylus affinis*	AMNH 6177	Mook 1921	0.74
basal crocodyloid	*Crocodylus depressifrons*	IRSNB R251	Delfino and Smith 2009	0.63
basal crocodyloid	*Crocodylus acer*	AMNH 1240	Mook 1921	0.48
basal crocodyloid	*Brachyuranochampsa eversolei*	CM 9372	Zangerl 1944	0.60
Tomistominae	*Maroccosuchus zennaroi*	MHNT.PAL.2006.80.11	Jouve et al. 2015	0.56
Tomistominae	*Kentisuchus spenceri*	BMNH 38974	direct observation	0.37
Tomistominae	*Megadontosuchus arduini*	MGPD 1Z	Piras et al. 2007	0.44
Tomistominae	*Dollosuchoides densmorei*	IRSNB 1748	Brochu 2007	0.38
Tomistominae	*Thecachampsa carolinense*	ChM PV 4279	Erickson and Sawyer 1996	0.52
Tomistominae	*Thecachampsa antiqua*	USNM 25243	direct observation	0.35
Tomistominae	*Toyotamaphimeia machikanensis*	MOUF 00001	direct observation	0.46
Tomistominae	*Penghusuchus pani*	NMNS-005645	Shan et al. 2009	0.45
Tomistominae	*Tomistoma coppensi*	NK 527'88	Pickford 1994	0.33
Tomistominae	*Tomistoma schlegelii*	Multiple individuals	direct observation	0.25
Tomistominae	*Gavialosuchus eggenburgensis*	NHM R 767 cast of holotype	direct observation	0.40
Tomistominae	*Tomistoma lusitanica*	Lisbon specimen	Antunes 1961	0.36
Crocodylus megarhinus	*Crocodylus megarhinus*	AMNH 5061	direct observation	0.56
Mekosuchinae	*Kambara murgonensis*	QM F21115	Willis et al. 1993	0.59
Mekosuchinae	*Kambara implexidens*	QM F29662	Salisbury and Willis 1996	0.59
Mekosuchinae	*Baru darrowi*	NTM P8695-8	Willis et al. 1990	0.73
Mekosuchinae	*Baru huberi*	QM F31060	Willis 1997	0.71
Mekosuchinae	*Baru wickeni*	QM F16822	Willis 1997	0.72
Mekosuchinae	*Australosuchus clarkae*	reconstruction (mainly of UCMP 71396)	Willis and Molnar 1991	0.61
Mekosuchinae	*Pallimnarchus gracilis*	QM F1752	Willis and Molnar 1997	0.71
Mekosuchinae	*Harpacochampsa camfieldensis*	reconstruction	Megirian et al. 1991	0.42
least inclusive clade containing *Crocodylus* , *Mecistops* , & *Osteolaemus*	*Euthecodon nitriae*	Holotype	Fourtau 1920	0.18
least inclusive clade containing *Crocodylus* , *Mecistops* , & *Osteolaemus*	*Euthecodon arambourgii*	MNHN ZEL001	Tchernov 1986	0.28
least inclusive clade containing *Crocodylus* , *Mecistops* , & *Osteolaemus*	*Euthecodon brumpti*	KNM-ER1773	Tchernov 1986	0.27
least inclusive clade containing *Crocodylus* , *Mecistops* , & *Osteolaemus*	*Brochuchus pigotti*	reconstruction	Conrad et al. 2013	0.53
least inclusive clade containing *Crocodylus* , *Mecistops* , & *Osteolaemus*	*Crocodylus gariepensis*	PQ AD1856	Pickford 2003	0.61
least inclusive clade containing *Crocodylus* , *Mecistops* , & *Osteolaemus*	*Voay robustus*	AMNH 3101	direct observation	0.84
least inclusive clade containing *Crocodylus* , *Mecistops* , & *Osteolaemus*	*Osteolaemus tetraspis*	Multiple individuals	direct observation	0.70
least inclusive clade containing *Crocodylus* , *Mecistops* , & *Osteolaemus*	*Osteolaemus osborni*	AMNH 10083	direct observation	0.74
least inclusive clade containing *Crocodylus* , *Mecistops* , & *Osteolaemus*	*Rimasuchus lloydi*	KNM-ER1682	Storrs 2003	0.87
least inclusive clade containing *Crocodylus* , *Mecistops* , & *Osteolaemus*	*Mecistops cataphractus* (central African species)	Multiple individuals	direct observation	0.33
least inclusive clade containing *Crocodylus* , *Mecistops* , & *Osteolaemus*	*Crocodylus palaeindicus*	BMNH 39795	direct observation	0.68
least inclusive clade containing *Crocodylus* , *Mecistops* , & *Osteolaemus*	*Crocodylus thorbjarnarsoni*	KNM-ER1683	Brochu and Storrs 2012	0.84
least inclusive clade containing *Crocodylus* , *Mecistops* , & *Osteolaemus*	*Crocodylus checchiai*	unnumbered	Maccagno 1948	0.55
least inclusive clade containing *Crocodylus* , *Mecistops* , & *Osteolaemus*	*Crocodylus niloticus*	IRSNB 5011	direct observation	0.54
least inclusive clade containing *Crocodylus* , *Mecistops* , & *Osteolaemus*	*Crocodylus acutus*	AMNH 9569	direct observation	0.45
least inclusive clade containing *Crocodylus* , *Mecistops* , & *Osteolaemus*	*Crocodylus intermedius*	Multiple individuals	direct observation	0.37
least inclusive clade containing *Crocodylus* , *Mecistops* , & *Osteolaemus*	*Crocodylus rhombifer*	Multiple individuals	direct observation	0.59
least inclusive clade containing *Crocodylus* , *Mecistops* , & *Osteolaemus*	*Crocodylus moreletii*	Multiple individuals	direct observation	0.63

least inclusive clade containing *Crocodylus* , *Mecistops* , & *Osteolaemus*	*Crocodylus siamensis*	Multiple individuals	direct observation	0.59
least inclusive clade containing *Crocodylus* , *Mecistops* , & *Osteolaemus*	*Crocodylus porosus*	Multiple individuals	direct observation	0.48
least inclusive clade containing *Crocodylus* , *Mecistops* , & *Osteolaemus*	*Crocodylus johnsoni*	Multiple individuals	direct observation	0.35
least inclusive clade containing *Crocodylus* , *Mecistops* , & *Osteolaemus*	*Crocodylus novaeguineae*	Multiple individuals	direct observation	0.46
least inclusive clade containing *Crocodylus* , *Mecistops* , & *Osteolaemus*	*Crocodylus mindorensis*	Multiple individuals	direct observation	0.58
least inclusive clade containing *Crocodylus* , *Mecistops* , & *Osteolaemus*	*Crocodylus palustris*	Multiple individuals	direct observation	0.62

Table S5. Pairwise npMANOVAs for all pairs of crocodylian subfamilies, using log10-transformed normalized limb measurements. Holm adjusted *p*-values are in the upper right, and *F*-values are in the bottom left. Number in parentheses is sample size for each species. Italicized *p*-values indicate significant results ($p < 0.05$).

	Alligatorinae	Caimaninae	Crocodylinae	Osteolaeminae	Gavialinae	Tomistominae
Alligatorinae (26)		*0.002*	*0.002*	*0.008*	*0.002*	*0.002*
Caimaninae (29)	14.089		*0.002*	*0.002*	*0.002*	*0.002*
Crocodylinae (36)	13.117	19.474		*0.010*	*0.002*	*0.002*
Osteolaeminae (9)	5.981	8.303	3.869		*0.002*	*0.002*
Gavialinae (6)	28.344	14.850	19.555	23.439		*0.008*
Tomistominae (8)	18.735	9.617	7.595	9.874	4.789	

Table S6. Alternative PGLS regressions using individuals within a set size range (100 mm ≤ skull width ≤ 200 mm; n = 151).

Rostral proportion vs.	n	*adjusted* R^2	F	p	Slope	Intercept	Pagel's lambda
with molecular tree							
cHL/entire forelimb	20	0.507	20.520	0.000	-8.558	4.979	0.000
cFL/entire hind limb	20	0.103	3.178	0.092	-7.487	3.901	0.601
(Fore+hind limbs) / trunk length	17	0.440	13.58	0.002	1.409	-0.864	0.796
with morphological tree							
cHL/entire forelimb	20	0.507	20.520	0.000	-8.558	4.979	0.000
cFL/entire hind limb	20	0.326	10.180	0.005	-12.308	6.078	0.000
(Fore+hind limbs) / trunk length	17	0.500	16.970	0.001	1.707	-1.177	0.764

Supplement to chapter III

Table S1. Measurements of centrum length (CL) in mm. Red color indicates estimated value.

Taxon	Specimen #	Locality	C3	C4	C5	C6	C7	C8	C9	D1	D2	D3	D4	D5	D6	D7	D8	D9	D10	D11	D12	D13	D14	D15
Alligator mississippiensis	AMNH 31563		32.8	32.4	33.3	33.1	32.8	32.1	33.1	33.0	34.4	37.7	38.9	38.0	38.5	40.0	40.1	41.4	40.3	41.1	39.4	39.4	38.3	34.4
Alligator mississippiensis	AMNH 43315	USA, Florida	27.0	26.9	27.2	27.2	26.2	26.9	27.7	28.4	29.0	33.3	32.3	31.1	31.9	33.4	33.7	34.9	33.2	36.0	34.8	34.9	31.0	29.5
Alligator mississippiensis	AMNH R43316		21.6	22.1	21.3	21.1	20.5	20.8	22.2	22.8	24.8	25.5	27.0	27.6	27.4	28.7	28.7	30.2	29.8	30.3	29.2	28.7	27.6	25.1
Alligator mississippiensis	YPM R10503	USA, Georgia, Chatham County	26.8	26.3	26.5	26.5	25.6	25.7	25.3	27.3	29.2	29.5	30.5	30.7	31.5	31.7	32.4	32.9	34.5	34.0	34.8	33.7	30.9	29.5
Alligator mississippiensis	YPM R17123	USA, Louisiana, Cameron Parish	16.2	15.6	15.5	15.0	15.4	15.0	14.8	15.8	17.1	17.7	18.4	17.9	18.1	18.6	19.5	19.1	20.1	19.9	20.0	19.3	18.8	18.8
Alligator sinensis	BMNH 1954.1.7.30		24.3	24.7	23.8	23.1	23.0	22.5	23.5	23.7	24.9	27.1	27.0	28.8	28.0	30.1	29.7	30.9	31.7	32.0	31.6	30.6	27.3	27.4
Caiman crocodilus	USNM 102874	Panama, Madden Lake	13.9	13.8	13.6	13.3	12.7	12.4	12.6	13.2	13.7	14.0	14.9	15.1	14.8	15.2	18.6	16.6	15.9	15.3	16.0	15.4	13.9	13.9
Caiman crocodilus	USNM 313860	Panama, Bocas del Toro	16.4	16.6	16.7	16.0	15.7	15.2	15.0	16.1	16.5	17.6	18.1	17.9	18.4	18.0	18.3	18.9	18.8	18.5	18.1	17.9	17.5	15.3
Caiman yacare	AMNH 97300	Bolivia, Beni	28.4	28.2	29.1	27.8	26.6	26.0	26.6	26.9	28.1	29.7	29.9	29.5	28.3	27.5	28.9	28.7	29.4	29.2	29.5	28.7	27.2	23.3
Caiman yacare	UF 121268	Paraguay, Pres. Hayes Dept.	30.3	29.4	29.9	29.0	27.1	27.0	28.8	30.0	30.4	32.4	35.3	32.1	31.8	32.7	32.9	33.4	34.0	33.0	31.9	31.4	30.6	28.5
Caiman yacare	UF 120653	Paraguay, Alto Paraguay	24.6	24.4	24.6	23.1	22.3	23.7	23.6	23.9	23.5	25.5	26.3	26.1	27.5	27.4	27.5	26.8	27.9	28.1	27.9	25.6	26.8	23.5
Melanosuchus niger	FMNH 218507	Ecuador, Napo Province	19.1	18.9	18.9	18.4	17.6	16.7	17.3	18.0	19.0	19.5	20.2	20.6	20.5	20.9	21.2	22.1	22.1	22.2	21.5	20.9	19.8	18.1
Melanosuchus niger	USNM 257786	Peru, Madre De Dios, Manu National Park	21.6	21.2	20.9	20.2	19.8	18.6	19.7	21.1	22.2	22.2	22.2	23.6	23.8	23.6	23.9	25.0	24.7	24.6	25.3	24.2	24.8	22.0
Paleosuchus palpebrosus	FMNH 42703	Colombia, Villavicencio	10.8	11.0	10.6	10.2	10.7	10.1	10.0	9.6	9.9	10.7	11.0	11.2	11.3	11.3	11.5	11.5	11.8	11.7	12.0	11.5	11.2	10.8
Paleosuchus palpebrosus	AMNH 78976	Colombia, Amazonas, Cano Negro	14.1	13.5	13.8	13.3	12.8	11.8	12.6	12.9	13.2	14.0	13.8	14.2	14.6	14.5	14.5	14.9	15.3	15.0	14.9	15.2	14.0	12.9
Crocodylus acutus	AMNH 7168		31.3	32.9	33.2	34.0	31.5	30.3	29.6	31.9	32.8	34.3	33.3	33.6	34.1	34.8	35.3	34.6	34.9	35.4	35.1	32.9	31.8	30.1
Crocodylus acutus	USNM 247943	Panama, Barro Colorado Island, Barbour Point	36.1	37.0	36.8	36.3	35.1	35.2	35.6	35.5	36.3	37.1	38.9	39.7	40.2	40.9	39.7	41.2	41.3	42.2	41.1	41.0	39.4	38.4
Crocodylus johnsoni	NTM JA076		19.7	19.9	19.4	19.8	18.7	17.9	17.8	18.3	18.8	18.8	18.7	17.9	18.7	19.0	19.3	19.6	19.5	19.4	20.0	20.3	19.8	18.9
Crocodylus johnsoni	NTM R25705		31.2	30.8	29.6	30.5	28.5	26.7	26.7	27.3	28.2	27.6	27.7	28.7	28.0	29.1	29.2	29.0	29.7	29.8	29.6	28.3	27.4	26.1
Crocodylus johnsoni	QM J58446	Australia, Queensland: Cooper Creek, ~6 km south of Windorah	22.6	22.3	22.4	22.5	21.8	20.8	20.5	22.0	21.9	22.5	21.7	21.8	22.8	22.9	22.7	23.2	23.8	24.6	24.5	24.3	24.0	23.2
Crocodylus johnsoni	QM J60590	Australia, Queensland: Amber Station, pool 1	17.2	16.8	16.5	16.5	16.5	14.5	15.5	16.2	16.6	16.6	16.9	16.9	17.7	17.2	17.7	18.3	17.9	18.4	18.9	18.6	18.3	18.0
Crocodylus palustris	FMNH 51691	India (captive)	25.0	26.0	24.5	24.2	23.0	22.4	20.8	23.7	24.6	27.8	28.1	28.1	27.9	27.9	29.0	29.1	28.7	27.1	26.5	26.1	25.1	23.4
Crocodylus porosus	FMNH 22026	India	41.0	38.8	39.5	37.6	34.2	35.9	36.4	39.9	41.2	44.7	46.1	46.1	49.6	49.2	49.2	49.2	48.7	48.0	49.9	47.1	45.2	37.2
Crocodylus porosus	USNM 61206	Indonesia, Celebes	35.7	36.1	36.7	36.3	34.5	32.5	33.4	36.0	37.6	38.9	40.0	40.5	41.6	40.9	43.6	44.2	45.1	46.1	45.8	44.9	43.0	37.6
Crocodylus rhombifer	AMNH 57773	Cuba	24.1	24.4	24.8	24.0	22.7	21.9	23.2	23.4	23.5	24.0	25.0	24.3	25.8	25.2	25.4	26.5	27.1	26.7	27.4	26.5	25.4	23.3
Crocodylus rhombifer	AMNH 77595		20.4	19.3	19.1	18.8	17.6	17.5	18.5	18.6	18.4	19.7	21.4	18.7	18.3	18.9	19.1	20.0	20.7	21.4	21.0	21.2	20.3	20.0
Crocodylus rhombifer	FMNH 34677	Cuba	19.7	19.8	19.6	19.3	18.5	19.0	18.8	19.5	19.1	20.0	19.5	19.9	21.3	21.0	21.4	22.6	21.0	22.1	22.1	22.1	21.0	20.8
Osteolaemus tetraspis	AMNH 69057		16.5	15.6	15.4	15.0	14.0	13.6	13.2	15.1	15.9	15.1	16.8	16.9	17.4	17.7	18.1	19.0	18.5	18.7	18.3	18.4	17.0	17.0
Osteolaemus tetraspis	YPM R16944	Cameroon	13.3	12.0	12.4	11.6	12.0	11.5	11.7	11.8	12.8	12.8	13.2	13.6	13.9	14.0	14.1	14.3	14.1	14.3	14.7	14.5	14.5	13.8
Osteolaemus tetraspis	UF 33749?		16.1	15.9	15.9	15.2	15.1	13.7	14.9	15.2	15.5	15.9	16.9	15.8	16.1	16.4	16.7	16.7	17.1	17.1	17.4	16.3	17.4	16.8
Gavialis gangeticus	AMNH 88316		25.4	24.4	24.5	24.6	24.4	24.3	24.2	24.9	25.0	26.9	26.1	26.6	26.6	26.6	27.5	27.8	28.1	28.2	27.5	26.0	25.5	23.8
Gavialis gangeticus	FMNH 82681		17.0	17.2	17.0	17.0	16.6	15.4	16.0	16.4	16.5	17.3	18.1	18.4	18.5	18.4	19.1	19.0	19.0	19.0	18.7	18.3	17.5	16.4
Gavialis gangeticus	FMNH 98864		15.7	15.2	15.4	15.2	15.0	14.3	13.9	14.8	14.8	14.6	16.2	16.6	16.5	17.1	17.1	17.2	17.3	17.5	17.4	17.1	16.5	16.0
Gavialis gangeticus	UF 70592		14.6	15.6	14.9	15.8	15.3	14.4	14.1	14.4	14.1	14.7	16.2	15.9	15.9	16.9	16.4	16.8	16.5	16.5	16.6	15.8	15.5	14.7
Gavialis gangeticus	USNM 576261		37.7	38.7	37.8	39.1	37.3	34.3	35.3	36.9	39.2	40.4	40.7	41.8	43.4	43.2	43.2	42.8	42.7	41.2	42.3	41.3	40.5	37.2
Gavialis gangeticus	YPM R10514	India	31.0	31.0	30.2	29.3	28.3	27.3	27.1	27.6	30.3	31.0	31.4	31.8	32.8	32.1	32.6	33.1	31.8	31.3	31.5	30.0	29.7	27.6
Tomistoma schlegelii	FMNH 206755		33.1	33.1	33.9	32.9	33.7	32.1	30.6	32.3	35.0	35.8	37.7	37.8	37.9	38.7	39.7	41.2	41.6	41.5	41.7	40.3	40.0	36.1
Tomistoma schlegelii	UF 107493		38.0	37.5	37.8	36.9	36.4	35.0	36.2	36.1	34.0	39.4	36.2	36.7	36.9	38.4	38.1	40.1	41.0	40.0	40.1	38.9	39.8	37.3
Tomistoma schlegelii	USNM 52972	Indonesia, Borneo, Samarinda	35.6	36.0	35.4	34.8	34.4	34.2	32.2	33.4	33.6	33.0	32.4	32.9	34.3	35.0	35.4	37.3	36.7	37.0	37.3	37.1	37.1	32.5
Tomistoma schlegelii	UF 54210		27.1	26.9	27.1	27.4	24.9	25.2	25.5	26.2	27.6	28.4	29.2	27.9	28.2	28.7	29.3	29.1	31.1	30.2	29.1	28.3	27.2	25.6

Table S2. Measurements of centrum height (CH) in mm. Red color indicates estimated value.

Taxon	Specimen #	Locality	C3	C4	C5	C6	C7	C8	C9	D1	D2	D3	D4	D5	D6	D7	D8	D9	D10	D11	D12	D13	D14	D15
Alligator mississippiensis	AMNH 31563		27.5	27.2	26.8	27.2	28.2	28.6	28.7	28.3	29.6	31.7	31.3	31.0	32.7	32.0	32.4	29.6	30.6	29.3	29.6	29.7	28.9	29.2
Alligator mississippiensis	AMNH 43315	USA, Florida	23.8	23.4	23.0	23.9	24.3	24.6	25.0	24.3	25.9	27.3	25.7	26.1	25.9	26.1	26.2	25.3	25.3	25.0	24.9	24.6	23.8	24.0
Alligator mississippiensis	AMNH R43316		14.1	16.0	16.7	17.3	17.6	17.5	19.2	18.5	19.9	20.8	19.8	19.6	20.1	20.3	19.9	19.5	19.5	19.6	19.5	19.3	19.1	19.2
Alligator mississippiensis	YPM R10503	USA, Georgia, Chatham County	20.4	21.4	22.6	22.7	23.8	23.1	23.2	23.5	23.8	25.5	24.7	24.7	24.5	24.6	24.0	24.0	23.3	22.7	22.8	22.5	22.2	21.6
Alligator mississippiensis	YPM R17123	USA, Louisiana, Cameron Parish	12.2	11.9	12.6	12.1	12.6	12.7	12.5	12.3	12.9	13.7	14.0	13.2	13.8	14.0	13.7	13.6	13.5	13.8	13.4	13.5	13.0	12.8
Alligator sinensis	BMNH 1954.1.7.30		17.9	18.4	18.8	19.1	19.5	18.6	19.2	20.0	20.7	22.3	23.8	21.9	23.1	22.0	21.7	22.4	22.1	21.5	21.8	21.2	20.9	20.5
Caiman crocodilus	USNM 102874	Panama, Madden Lake	8.6	9.0	9.4	9.0	9.7	9.7	9.4	9.5	9.0	9.3	8.9	8.6	8.8	8.9	9.0	9.0	8.8	8.8	8.5	8.3	8.3	8.3
Caiman crocodilus	USNM 313860	Panama, Bocas del Toro	10.2	10.2	10.6	12.2	11.8	11.7	11.5	12.4	11.5	12.2	13.9	11.2	11.1	10.9	10.9	11.0	11.1	11.1	11.3	10.9	11.0	11.3
Caiman yacare	AMNH 97300	Bolivia, Beni	16.8	18.1	19.1	19.0	19.3	19.1	19.9	19.7	19.8	21.3	22.4	21.0	21.1	21.4	20.8	20.9	19.7	20.0	19.4	19.0	18.4	18.3
Caiman yacare	UF 121268	Paraguay, Pres. Hayes Dept.	20.0	18.2	19.3	20.0	20.1	21.2	22.4	23.5	23.6	24.4	24.7	23.8	23.5	23.0	24.5	23.3	23.3	22.9	22.5	21.8	21.1	20.1
Caiman yacare	UF 120653	Paraguay, Alto Paraguay	16.2	16.7	17.6	17.2	16.9	17.9	18.0	18.8	18.5	18.4	18.0	17.1	17.9	18.2	18.8	17.8	17.1	17.0	17.6	17.6	16.9	16.6
Melanosuchus niger	FMNH 218507	Ecuador, Napo Province	13.7	13.9	13.6	14.3	15.2	15.8	15.3	14.3	14.4	15.6	14.8	14.4	14.9	14.9	14.5	14.7	14.7	14.5	14.1	14.3	13.9	12.9
Melanosuchus niger	USNM 257786	Peru, Madre De Dios, Manu National Park	14.6	15.2	15.8	15.9	16.5	17.0	16.7	16.3	16.4	17.2	17.3	16.3	17.7	17.1	17.2	17.2	16.8	16.1	16.5	16.0	16.2	15.1
Paleosuchus palpebrosus	AMNH 78976	Colombia, Amazonas, Cano Negro	8.2	9.1	9.5	9.5	9.7	9.5	9.6	9.4	9.5	10.5	10.8	10.3	9.1	8.9	8.7	8.5	8.3	8.2	8.3	8.3	8.1	8.3
Crocodylus acutus	AMNH 7168		21.2	22.5	23.7	25.7	25.3	25.0	24.4	24.2	25.1	25.3	24.4	24.4	25.7	25.6	25.8	25.5	24.2	24.0	24.0	24.2	23.7	23.2
Crocodylus acutus	USNM 247943	Panama, Barro Colorado Island, Barbour Point	23.9	25.4	26.6	27.8	27.8	28.3	27.6	27.5	28.9	29.7	30.7	30.3	31.7	31.3	30.5	29.7	29.3	28.2	27.5	26.6	25.7	25.5
Crocodylus johnsoni	NTM JA076		12.0	12.0	13.2	14.0	13.8	14.2	14.0	13.8	13.9	13.9	14.4	13.6	13.7	13.9	13.6	13.4	13.0	13.0	12.6	12.2	11.8	11.6
Crocodylus johnsoni	NTM R25705		18.6	19.1	20.2	21.2	21.2	21.0	21.1	20.7	21.5	20.9	21.9	19.9	20.6	20.2	20.1	19.4	18.8	18.3	18.0	17.8	17.6	17.2
Crocodylus johnsoni	QM J58446	Australia, Queensland: Cooper Creek, ~6 km south of Windorah	14.5	15.8	17.1	17.4	18.0	17.8	18.4	18.2	18.2	18.3	18.9	18.3	18.4	18.4	18.0	17.5	17.1	16.9	16.7	16.2	16.0	15.8
Crocodylus johnsoni	QM J60590	Australia, Queensland: Amber Station, pool 1	10.6	11.6	11.9	12.7	12.6	12.5	12.1	12.1	12.5	12.6	12.2	11.5	12.2	12.0	12.3	12.2	11.7	11.2	11.5	11.5	11.5	11.1
Crocodylus palustris	FMNH 51691	India (captive)	18.0	18.3	19.5	19.8	19.2	18.5	18.7	18.8	19.7	20.7	20.4	20.6	20.7	20.2	20.7	19.7	18.9	18.8	18.3	18.2	17.6	17.9
Crocodylus porosus	FMNH 22026	India	32.4	34.5	36.7	36.7	37.2	36.3	35.6	36.1	36.4	38.2	39.0	38.9	39.2	38.6	37.6	37.2	36.7	35.1	35.4	33.9	34.5	36.1
Crocodylus porosus	USNM 61206	Indonesia, Celebes	30.4	31.1	32.7	33.7	33.6	33.2	33.6	32.7	34.5	36.0	36.6	34.9	35.3	35.3	34.7	34.9	34.6	33.8	33.8	33.1	32.7	31.4
Crocodylus rhombifer	AMNH 57773	Cuba	15.2	17.7	19.4	19.9	19.7	19.1	18.6	18.3	18.7	19.6	18.7	18.3	19.1	18.9	18.7	18.4	17.8	18.2	18.0	17.9	17.3	16.9
Crocodylus rhombifer	AMNH 77595		14.8	15.7	15.7	16.8	15.6	14.6	13.9	13.3	14.0	13.9	14.0	14.1	13.7	14.2	13.8	13.7	13.9	13.9	13.8	14.0	14.0	14.0
Osteolaemus tetraspis	AMNH 69057		11.6	11.7	13.0	13.2	13.6	13.2	13.0	13.0	13.4	13.2	13.4	12.8	12.2	12.1	12.3	12.2	12.2	12.1	12.0	11.8	11.7	11.7
Osteolaemus tetraspis	UF 33749?		11.2	11.1	11.7	12.1	12.3	12.1	12.0	12.3	12.6	12.8	12.9	12.4	12.1	11.9	11.6	11.3	11.2	11.3	11.3	11.3	10.9	11.0
Gavialis gangeticus	UF 70592		9.0	9.5	10.0	10.4	11.0	10.9	10.5	10.5	10.5	10.7	10.7	10.1	9.9	9.9	10.1	9.9	10.0	9.8	10.7	10.4	10.2	10.3
Gavialis gangeticus	USNM 576261		24.6	26.4	28.2	27.6	28.6	29.2	30.0	29.5	29.3	30.9	31.7	29.8	30.0	30.4	31.0	30.3	29.5	29.0	28.6	28.7	27.9	26.6
Gavialis gangeticus	YPM R10514	India	20.1	20.1	20.8	21.5	23.0	23.1	22.7	23.8	23.6	23.7	23.8	25.0	25.0	25.7	25.4	24.8	24.2	23.2	22.4	22.0	21.4	21.4
Tomistoma schlegelii	FMNH 206755		22.6	23.9	25.4	26.7	28.4	28.2	27.8	27.1	28.0	28.1	29.6	27.5	27.8	27.5	26.3	25.8	26.6	26.1	25.4	25.5	24.8	24.8
Tomistoma schlegelii	UF 107493		28.2	29.3	29.7	31.3	31.3	32.1	32.5	31.3	31.8	35.8	33.0	33.6	34.8	34.7	34.7	35.5	35.4	34.3	34.4	33.3	33.3	31.9
Tomistoma schlegelii	USNM 52972	Indonesia, Borneo, Samarinda	26.2	27.7	28.8	29.2	29.3	29.5	31.2	30.2	30.7	31.4	33.7	30.9	31.2	32.1	31.9	31.7	31.0	29.8	29.7	28.9	28.5	27.8
Tomistoma schlegelii	UF 54210		19.1	20.9	20.3	21.7	22.2	21.9	21.5	20.5	21.2	21.6	22.2	20.9	21.0	20.7	20.8	20.5	20.2	20.4	20.5	20.3	20.0	20.4

Table S3. Measurements of centrum width (CW) in mm. Red color indicates estimated value.

Taxon	Specimen #	Locality	C3	C4	C5	C6	C7	C8	C9	D1	D2	D3	D4	D5	D6	D7	D8	D9	D10	D11	D12	D13	D14	D15
Alligator mississippiensis	AMNH 31563		32.7	31.1	32.5	34.0	36.2	34.5	37.4	35.0	38.5	35.3	35.4	36.3	36.5	35.6	36.5	37.5	36.7	38.0	38.5	36.8	37.4	39.3
Alligator mississippiensis	AMNH 43315	USA, Florida	26.2	27.0	27.0	28.6	31.7	31.1	32.1	33.0	35.0	30.6	30.6	30.3	30.8	28.6	30.1	29.8	29.5	30.7	30.6	31.1	32.8	31.9
Alligator mississippiensis	AMNH R43316		17.9	18.7	19.4	21.0	21.9	22.5	24.0	24.3	26.6	22.5	21.9	21.9	21.7	21.3	21.7	22.3	22.8	23.2	23.5	23.8	25.2	25.8
Alligator mississippiensis	YPM R10503	USA, Georgia, Chatham County	21.4	22.6	23.9	26.0	27.7	27.0	27.5	29.2	30.9	24.5	24.3	25.2	26.1	25.8	25.9	26.6	27.2	26.7	26.7	27.7	28.4	28.1
Alligator mississippiensis	YPM R17123	USA, Louisiana, Cameron Parish	11.8	12.9	13.5	14.6	15.7	16.1	17.8	17.8	17.4	15.2	14.2	14.0	13.8	13.7	14.2	13.8	14.5	14.4	14.2	14.5	15.1	16.6
Alligator sinensis	BMNH 1954.1.7.30		18.7	19.5	20.1	21.6	23.0	23.9	25.1	25.7	26.2	25.1	24.0	24.8	23.4	25.0	25.2	24.8	25.9	25.8	26.1	26.9	26.4	27.8
Caiman crocodilus	USNM 102874	Panama, Madden Lake	9.3	9.7	9.8	10.4	11.0	12.3	12.6	12.8	11.6	10.8	10.8	11.1	11.2	11.3	11.2	11.4	11.9	11.8	11.8	12.4	12.6	12.6
Caiman crocodilus	USNM 313860	Panama, Bocas del Toro	11.1	11.4	11.8	12.2	12.9	13.2	14.2	15.0	15.1	13.3	13.7	13.7	14.3	13.8	14.3	13.9	13.9	14.3	14.4	14.4	14.2	15.2
Caiman yacare	AMNH 97300	Bolivia, Beni	17.4	18.0	19.1	19.5	21.3	22.0	22.0	24.2	23.5	23.8	24.0	24.3	24.4	24.0	23.7	22.8	22.8	23.2	23.2	22.4	23.2	25.9
Caiman yacare	UF 121268	Paraguay, Pres. Hayes Dept.	21.0	19.9	21.0	21.9	23.2	24.8	24.3	25.5	26.9	25.1	25.4	26.1	26.7	26.0	26.1	26.2	26.1	28.1	28.3	28.0	28.3	29.1
Caiman yacare	UF 120653	Paraguay, Alto Paraguay	16.3	16.4	17.0	17.4	18.4	19.6	19.7	19.9	22.5	21.3	21.2	21.6	21.3	21.4	21.0	21.3	22.2	22.4	22.6	22.6	22.0	23.1
Melanosuchus niger	FMNH 218507	Ecuador, Napo Province	15.4	14.9	15.7	16.1	18.1	18.9	20.0	20.2	19.6	17.8	17.6	17.3	16.9	16.8	17.2	17.4	17.1	17.7	18.2	18.7	18.7	19.4
Melanosuchus niger	USNM 257786	Peru, Madre De Dios, Manu National Park	17.3	17.3	18.3	19.2	19.0	20.3	21.6	22.1	21.9	18.4	19.1	18.4	18.1	17.8	17.9	18.3	18.7	19.1	20.1	21.0	20.2	21.4
Paleosuchus palpebrosus	FMNH 42703	Colombia, Villavicencio	8.5	7.9	8.0	8.3	8.6	9.2	9.3	9.7	9.7	9.2	8.8	8.8	8.7	9.1	9.3	9.3	9.4	9.3	9.5	9.6	9.8	9.7
Paleosuchus palpebrosus	AMNH 78976	Colombia, Amazonas, Cano Negro	9.9	9.7	10.1	10.1	10.7	11.7	12.3	12.8	12.9	11.1	10.3	10.5	11.0	11.4	11.5	11.5	12.0	12.1	12.1	12.2	12.6	12.3
Crocodylus acutus	AMNH 7168		23.4	26.9	27.8	28.6	29.1	29.5	30.0	28.3	29.9	30.7	29.8	27.9	28.7	28.9	28.5	28.6	28.9	28.6	28.5	28.5	28.6	30.2
Crocodylus acutus	USNM 247943	Panama, Barro Colorado Island, Barbour Point	27.0	29.3	32.2	35.1	36.7	38.3	38.5	37.3	37.0	32.0	30.8	30.7	30.3	30.7	31.3	31.4	31.9	33.0	33.3	32.7	32.6	32.7
Crocodylus johnsoni	NTM JA076		13.7	14.7	15.1	15.3	15.8	16.0	16.5	17.9	17.9	15.9	14.9	13.9	14.3	14.2	14.3	14.6	14.5	14.5	14.7	14.9	15.1	15.6
Crocodylus johnsoni	NTM R25705		20.2	21.8	22.6	24.0	25.5	26.0	27.2	29.0	28.5	25.9	23.4	22.4	22.4	22.6	22.7	22.6	22.8	22.8	23.0	22.6	23.9	25.2
Crocodylus johnsoni	QM J58446	Australia, Queensland: Cooper Creek, ~6 km south of Windorah	16.8	18.4	19.2	20.2	21.0	22.4	23.1	22.4	21.0	20.6	19.9	18.7	19.4	19.4	19.0	19.0	19.7	20.3	20.4	20.4	20.9	21.6
Crocodylus johnsoni	QM J60590	Australia, Queensland: Amber Station, pool 1	11.9	12.4	13.1	13.5	14.6	15.3	16.8	16.8	16.0	14.4	14.3	13.8	13.4	13.5	13.5	13.5	13.9	14.2	14.1	13.8	14.1	14.4
Crocodylus palustris	FMNH 51691	India (captive)	19.2	20.1	20.6	21.2	23.8	24.5	25.4	25.0	26.6	27.1	25.9	25.6	25.6	24.8	24.7	25.0	25.4	24.4	24.5	23.8	23.9	25.4
Crocodylus porosus	FMNH 22026	India	34.4	36.6	38.2	41.1	44.5	49.7	49.1	46.6	45.0	39.9	39.1	40.1	41.5	41.9	41.5	40.9	40.5	42.6	42.2	43.0	42.8	45.9
Crocodylus porosus	USNM 61206	Indonesia, Celebes	29.9	31.4	34.6	36.0	38.1	40.6	40.8	39.6	39.7	35.1	34.9	35.0	35.5	35.1	35.2	35.6	35.9	37.9	37.3	37.3	38.1	39.3
Crocodylus rhombifer	AMNH 57773	Cuba	17.4	19.8	21.3	22.0	23.7	24.3	24.0	23.2	23.5	23.0	22.4	21.3	21.2	20.7	20.8	21.3	21.4	21.0	20.8	21.3	22.2	23.6
Crocodylus rhombifer	AMNH 77595		15.9	17.1	18.0	20.7	21.4	22.4	20.3	22.4	22.2	21.8	20.1	20.3	20.0	19.6	19.3	19.9	19.9	20.4	19.6	20.8	21.4	22.7
Crocodylus rhombifer	FMNH 34677	Cuba	15.0	17.1	17.3	18.7	20.2	22.5	21.4	22.1	22.0	18.9	18.8	18.7	17.4	18.4	18.6	18.4	16.7	17.1	17.6	17.5	18.8	18.3
Osteolaemus tetraspis	AMNH 69057		12.5	12.7	13.2	13.4	14.5	15.7	15.6	16.3	16.1	15.1	14.6	14.8	14.7	14.9	14.6	14.8	15.2	15.6	15.1	14.8	15.0	15.0
Osteolaemus tetraspis	UF 33749?		12.5	12.5	12.8	14.1	14.6	15.0	15.7	15.3	14.9	14.9	14.3	14.4	14.3	14.7	14.9	15.0	15.1	14.4	14.6	14.4	15.0	15.0
Gavialis gangeticus	FMNH 82681		10.6	11.2	11.9	12.2	13.2	14.8	14.9	15.0	16.2	14.5	14.6	13.5	13.1	12.5	11.5	11.7	11.8	12.1	12.7	13.4	14.0	14.9
Gavialis gangeticus	FMNH 98864		10.4	11.1	11.3	11.5	12.1	12.8	13.7	14.4	15.0	13.9	13.8	13.2	13.6	13.2	13.6	13.2	13.2	13.7	13.7	14.0	14.1	14.2
Gavialis gangeticus	UF 70592		10.2	10.4	10.9	11.2	11.7	12.4	12.4	12.4	12.0	12.5	12.0	11.0	11.3	11.0	11.0	10.8	11.0	11.5	11.9	12.2	12.9	13.1
Gavialis gangeticus	USNM 576261		26.2	26.8	30.1	28.4	31.6	31.7	32.1	32.3	35.6	34.0	31.4	31.4	32.3	32.4	33.1	32.4	33.0	32.1	32.7	33.7	35.0	36.3
Gavialis gangeticus	YPM R10514	India	21.2	21.2	21.1	22.0	23.6	25.6	27.6	27.0	29.2	30.8	29.0	25.6	24.7	24.8	24.8	26.2	26.3	26.2	26.7	27.3	27.8	28.2
Tomistoma schlegelii	FMNH 206755		26.5	27.3	28.3	29.6	31.4	31.0	31.6	32.7	34.0	33.0	31.9	30.7	31.0	29.9	29.6	29.2	29.0	29.4	29.4	29.9	31.0	32.1
Tomistoma schlegelii	UF 107493		30.0	31.2	32.4	33.2	35.5	38.1	38.6	38.3	41.5	36.1	33.9	34.4	35.9	34.8	36.5	35.4	36.3	36.5	36.3	36.6	37.8	36.8
Tomistoma schlegelii	USNM 52972	Indonesia, Borneo, Samarinda	28.0	29.2	29.9	31.3	32.6	33.4	35.8	36.5	38.2	32.9	31.2	31.5	31.1	30.4	31.3	32.6	32.5	34.5	34.8	36.6	36.9	37.2
Tomistoma schlegelii	UF 54210		21.0	22.6	24.8	25.3	25.6	25.4	25.1	25.0	27.0	25.6	24.6	24.0	23.9	23.8	23.7	23.7	24.4	24.7	25.1	25.2	25.0	25.3

Table S4. Measurements of neural spine height (NSH) in mm. Red color indicates estimated value.

Taxon	Specimen #	Locality	C3	C4	C5	C6	C7	C8	C9	D1	D2	D3	D4	D5	D6	D7	D8	D9	D10	D11	D12	D13	D14	D15
Alligator mississippiensis	AMNH 31563		52.0	59.1	63.9	67.8	72.4	78.7	81.9	80.7	77.5	69.7	66.1	63.0	61.8	60.7	59.5	59.4	59.1	58.4	59.5	59.7	60.7	62.3
Alligator mississippiensis	AMNH 43315	USA, Florida	49.9	54.6	59.6	61.3	67.2	72.9	78.6	77.8	74.3	69.3	59.9	62.3	58.1	57.7	55.4	54.9	53.1	57.1	54.9	57.9	60.6	61.9
Alligator mississippiensis	AMNH R43316		36.5	41.1	42.9	43.8	47.8	52.4	56.8	58.2	54.3	53.3	50.3	48.0	47.1	45.0	45.3	44.4	43.1	45.4	45.0	45.5	46.8	49.1
Alligator mississippiensis	YPM R10503	USA, Georgia, Chatham County	47.0	50.9	50.2	52.7	55.1	62.1	65.3	61.5	57.8	54.1	52.3	50.6	48.1	47.6	46.9	47.1	46.4	46.5	46.2	46.5	49.5	49.9
Alligator mississippiensis	YPM R17123	USA, Louisiana, Cameron Parish	25.5	27.2	28.7	30.0	29.7	30.7	32.6	34.1	33.2	33.0	32.2	31.5	31.1	31.1	30.6	29.9	29.4	29.4	29.7	31.1	31.2	31.4
Alligator sinensis	BMNH 1954.1.7.30		39.3	43.7	46.7	48.2	50.0	52.5	54.1	57.3	52.4	52.4	51.0	48.4	50.9	48.8	48.8	47.1	47.9	46.6	46.8	48.3	47.9	47.0
Caiman crocodilus	USNM 102874	Panama, Madden Lake	18.9	20.5	21.7	22.0	23.6	25.6	27.4	25.8	24.1	23.0	22.2	22.1	21.4	21.4	20.5	20.2	21.1	19.8	20.6	21.1	22.0	22.0
Caiman yacare	AMNH 97300	Bolivia, Beni	44.2	48.4	52.8	52.2	53.9	62.1	65.1	44.8	54.1	49.1	46.7	45.1	43.4	42.6	42.1	40.8	41.1	42.0	43.4	44.3	44.8	46.8
Caiman yacare	UF 121268	Paraguay, Pres. Hayes Dept.	43.1	49.7	53.9	55.7	59.2	64.7	67.9	61.8	57.5	56.0	54.5	52.9	51.7	51.1	51.1	49.6	50.3	51.2	50.5	53.0	53.4	55.5
Caiman yacare	UF 120653	Paraguay, Alto Paraguay	33.4	37.9	38.3	42.3	43.7	48.7	50.6	47.4	45.2	43.6	42.8	41.0	39.6	38.6	39.0	40.0	40.1	41.0	39.7	41.8	40.7	44.2
Melanosuchus niger	FMNH 218507	Ecuador, Napo Province	29.6	29.6	31.8	32.2	34.7	39.8	41.1	37.6	36.3	35.9	35.8	34.7	34.8	35.7	35.5	34.5	34.1	32.9	33.0	33.5	33.0	33.4
Melanosuchus niger	USNM 257786	Peru, Madre De Dios, Manu National Park	30.1	33.1	34.5	36.1	39.8	43.0	44.9	42.4	40.8	39.8	39.4	39.4	39.3	39.1	38.5	38.6	38.5	37.2	37.6	37.2	38.1	38.9
Paleosuchus palpebrosus	FMNH 42703	Colombia, Villavicencio	13.6	15.1	16.8	16.5	17.5	19.9	21.2	17.5	17.5	15.9	14.7	15.5	14.6	14.7	15.3	14.9	15.0	14.9	15.7	15.6	15.9	16.8
Paleosuchus palpebrosus	AMNH 78976	Colombia, Amazonas, Cano Negro	17.6	18.5	20.3	22.2	23.9	26.7	28.3	27.0	24.7	22.9	21.9	21.7	21.1	20.6	20.2	20.0	19.8	19.9	19.5	20.4	20.9	20.7
Crocodylus acutus	AMNH 7168		46.7	51.9	51.8	55.2	58.9	59.6	65.2	66.1	61.8	59.0	55.8	53.1	51.2	49.4	49.3	48.4	48.7	49.7	49.7	50.0	51.1	51.2
Crocodylus acutus	USNM 247943	Panama, Barro Colorado Island, Barbour Point	51.4	54.5	58.2	63.0	64.1	65.9	74.2	69.1	66.2	64.2	62.9	60.1	58.4	57.4	56.9	56.1	55.8	54.5	54.7	55.7	56.3	55.9
Crocodylus johnsoni	NTM JA076		24.1	27.3	29.5	29.6	30.5	31.0	31.9	32.2	31.5	30.0	28.7	27.8	27.0	25.5	25.0	24.9	24.6	24.9	24.3	24.8	25.6	25.3
Crocodylus johnsoni	NTM R25705		43.3	47.4	47.8	49.5	50.3	51.6	53.8	55.2	52.5	49.7	46.7	43.9	41.9	41.2	40.5	40.4	39.1	40.5	41.5	40.8	42.8	42.5
Crocodylus johnsoni	QM J58446	Australia, Queensland: Cooper Creek, ~6 km south of Windorah	33.4	36.8	39.4	39.9	41.2	41.5	40.7	44.3	41.6	39.2	37.7	35.9	34.5	33.5	32.7	31.7	31.0	30.4	31.1	32.6	32.8	33.2
Crocodylus johnsoni	QM J60590	Australia, Queensland: Amber Station, pool 1	22.5	25.1	26.0	27.3	28.3	27.9	28.4	29.1	28.4	27.2	25.5	25.1	23.1	23.9	23.5	23.0	23.1	23.0	23.6	24.3	24.2	25.6
Crocodylus palustris	FMNH 51691	India (captive)	39.0	39.8	44.9	45.8	47.3	51.7	56.7	57.5	53.6	51.4	48.4	46.3	44.8	43.5	43.4	42.3	43.6	44.2	43.4	45.2	43.0	43.5
Crocodylus porosus	FMNH 22026	India	61.3	68.8	76.7	77.9	81.1	80.6	83.6	85.3	87.4	83.6	81.0	76.3	74.2	72.5	71.4	71.5	69.5	72.1	71.7	73.5	74.8	73.6
Crocodylus porosus	USNM 61206	Indonesia, Celebes	55.9	63.9	68.6	73.2	74.8	74.7	77.6	80.7	76.7	75.5	73.5	71.4	70.3	70.1	68.4	69.3	67.8	67.3	67.3	67.0	65.5	67.2
Crocodylus rhombifer	AMNH 57773	Cuba	37.7	42.7	45.3	45.7	46.4	46.8	46.2	47.8	45.0	42.3	40.9	39.6	38.2	37.7	37.2	37.5	38.4	39.1	39.3	38.1	37.3	35.1
Crocodylus rhombifer	AMNH 77595		34.0	35.6	37.4	39.8	41.9	42.2	42.5	42.0	41.5	39.7	36.7	37.4	36.1	35.3	34.9	35.6	36.9	38.3	37.3	38.8	36.8	36.0
Osteolaemus tetraspis	AMNH 69057		25.5	28.6	29.9	32.4	36.2	37.8	39.8	36.2	33.5	30.9	28.6	27.4	25.5	24.5	23.7	23.4	23.4	23.7	24.8	25.0	25.3	25.3
Osteolaemus tetraspis	UF 33749?		25.3	25.6	28.4	31.5	34.7	35.4	36.8	33.2	29.5	27.5	26.0	24.5	23.4	22.7	22.4	22.8	23.0	22.3	23.0	22.8	24.3	21.8
Gavialis gangeticus	UF 70592		14.6	17.1	16.2	17.1	18.1	19.5	21.4	22.4	23.3	22.8	22.3	22.2	21.3	20.9	21.2	20.4	20.5	20.4	20.6	21.5	21.2	20.9
Gavialis gangeticus	USNM 576261		49.3	55.8	59.5	57.8	62.5	63.6	69.0	73.2	72.0	72.5	70.2	68.8	66.6	65.3	63.2	63.3	61.7	60.0	61.3	61.3	61.3	61.3
Gavialis gangeticus	YPM R10514	India	37.9	37.9	38.4	40.6	42.0	41.8	45.3	48.7	50.4	51.8	51.1	49.8	48.3	46.9	45.5	44.9	44.8	44.2	43.4	45.8	45.6	47.1
Tomistoma schlegelii	FMNH 206755		37.2	53.8	58.1	64.0	68.9	69.7	76.2	79.0	75.7	74.4	70.5	69.3	66.1	65.2	65.2	62.5	62.6	62.5	62.9	64.3	66.2	63.5
Tomistoma schlegelii	UF 107493		41.3	55.7	67.7	76.4	81.1	84.8	85.4	84.8	81.2	79.1	79.4	76.2	74.1	72.9	75.9	72.5	73.4	74.2	74.1	73.7	70.5	70.5
Tomistoma schlegelii	USNM 52972	Indonesia, Borneo, Samarinda	47.2	53.1	58.8	64.5	66.7	72.0	73.9	73.9	69.9	66.0	64.1	61.4	60.9	58.6	57.0	56.2	55.7	54.2	54.4	54.8	56.4	56.0
Tomistoma schlegelii	UF 54210		38.2	43.1	41.7	50.1	55.8	58.6	61.3	59.9	58.3	57.5	55.3	55.0	45.4	52.6	50.7	50.6	50.0	50.2	49.9	50.2	51.5	52.7

Table S5. Measurements of interzygapophyseal length (IZL) in mm. Red color indicates estimated value.

Taxon	Specimen #	Locality	C3	C4	C5	C6	C7	C8	C9	D1	D2	D3	D4	D5	D6	D7	D8	D9	D10	D11	D12	D13	D14	D15
Alligator mississippiensis	AMNH 31563		47.3	43.8	45.6	45.9	42.0	39.6	42.6	47.2	54.2	58.8	58.0	58.6	59.3	56.2	58.0	59.6	60.0	60.8	61.0	63.2	62.2	34.4
Alligator mississippiensis	AMNH 43315	USA, Florida	39.8	37.8	36.0	34.7	33.1	33.6	33.6	43.2	49.3	50.8	50.4	51.1	52.2	53.0	53.1	52.8	51.9	51.9	55.0	56.2	58.0	29.5
Alligator mississippiensis	AMNH R43316		32.1	31.2	32.6	29.0	26.5	26.3	25.9	32.4	37.3	40.3	40.6	40.1	39.4	41.8	42.2	40.6	43.4	40.4	42.0	43.2	42.5	25.1
Alligator mississippiensis	YPM R10503	USA, Georgia, Chatham County	38.4	36.1	36.6	36.3	34.0	31.8	34.9	39.4	43.4	44.2	43.9	43.9	43.4	44.8	45.7	45.2	45.8	45.6	47.1	46.6	47.2	29.5
Alligator mississippiensis	YPM R17123	USA, Louisiana, Cameron Parish	20.6	22.0	21.5	20.6	20.2	18.7	19.9	21.4	25.6	26.9	27.0	26.7	26.7	26.8	26.2	25.6	27.9	26.8	27.7	28.0	27.5	18.8
Alligator sinensis	BMNH 1954.1.7.30		33.3	34.0	35.1	31.5	30.0	30.5	30.7	37.3	41.9	39.6	42.6	42.9	43.3	42.7	42.1	43.1	42.0	42.3	43.0	42.6	44.0	27.4
Caiman crocodilus	USNM 102874	Panama, Madden Lake	18.5	18.9	17.4	16.7	16.3	17.2	18.3	19.6	21.5	20.7	20.8	21.1	21.1	21.4	22.3	21.8	21.0	22.0	21.7	21.5	20.7	13.9
Caiman crocodilus	USNM 313860	Panama, Bocas del Toro	23.5	22.6	21.5	21.2	20.7	19.6	21.1	23.0	24.4	26.3	26.9	26.4	25.7	26.7	26.0	25.8	26.5	25.5	26.6	26.6	26.3	15.3
Caiman yacare	AMNH 97300	Bolivia, Beni	41.8	38.8	37.6	35.6	33.7	35.2	36.6	40.6	44.2	44.2	42.6	42.9	42.1	42.0	43.1	43.1	42.2	42.0	41.2	42.2	42.6	23.3
Caiman yacare	UF 121268	Paraguay, Pres. Hayes Dept.	43.6	41.7	37.3	39.0	38.9	37.3	40.1	47.1	47.1	47.4	45.1	44.9	46.1	44.1	46.1	44.5	44.4	45.3	45.2	47.3	46.1	28.5
Caiman yacare	UF 120653	Paraguay, Alto Paraguay	32.8	31.2	29.7	30.7	29.3	30.2	30.6	33.0	36.8	36.7	37.2	36.5	36.7	36.7	36.9	36.6	36.9	38.4	38.0	36.6	38.2	23.5
Melanosuchus niger	FMNH 218507	Ecuador, Napo Province	27.6	27.0	25.3	24.4	24.1	23.6	23.6	25.9	28.3	28.9	28.3	28.8	28.4	29.0	29.4	29.2	29.2	29.0	28.9	28.3	27.6	18.1
Melanosuchus niger	USNM 257786	Peru, Madre De Dios, Manu National Park	29.6	29.5	28.0	26.9	27.6	26.0	26.7	29.4	32.2	33.2	31.9	32.6	32.5	32.5	31.8	32.5	32.7	32.1	34.2	33.1	33.9	22.0
Paleosuchus palpebrosus	FMNH 42703	Colombia, Villavicencio	15.3	14.8	13.9	13.9	13.5	12.9	13.3	14.2	15.4	15.1	15.4	15.4	15.8	15.5	16.0	15.9	15.5	16.2	16.2	15.5	15.1	10.8
Paleosuchus palpebrosus	AMNH 78976	Colombia, Amazonas, Cano Negro	19.1	18.4	17.1	16.9	16.7	16.7	16.6	17.4	18.3	18.7	19.2	19.6	19.8	20.4	19.9	20.2	20.5	20.2	20.3	21.4	20.2	12.9
Crocodylus acutus	AMNH 7168		41.8	40.7	40.5	38.8	39.1	36.5	42.7	46.0	49.9	47.4	46.6	48.0	47.7	46.2	46.8	46.8	47.5	48.4	49.0	49.1	45.9	30.1
Crocodylus acutus	USNM 247943	Panama, Barro Colorado Island, Barbour Point	49.0	49.2	49.5	50.5	52.5	50.0	54.3	56.5	59.3	61.8	59.3	59.4	57.8	56.5	57.9	57.4	59.1	60.0	57.9	60.4	56.9	38.4
Crocodylus johnsoni	NTM JA076		25.2	24.8	23.3	23.3	23.0	22.0	24.0	23.2	25.7	26.4	25.4	25.1	24.5	24.6	25.2	25.4	25.6	25.7	26.1	27.1	27.9	18.9
Crocodylus johnsoni	NTM R25705		42.5	41.0	38.1	36.0	35.7	34.9	35.4	39.4	43.2	43.2	41.9	42.0	40.6	40.2	40.8	38.2	41.8	41.6	41.7	41.3	42.3	26.1
Crocodylus johnsoni	QM J58446	Australia, Queensland: Cooper Creek, ~6 km south of Windorah	30.1	29.4	28.5	27.5	26.3	26.9	27.6	30.7	31.6	33.5	30.6	30.2	30.7	30.0	31.6	31.2	32.4	31.0	32.5	34.2	34.0	23.2
Crocodylus johnsoni	QM J60590	Australia, Queensland: Amber Station, pool 1	24.6	22.4	21.1	20.5	19.6	19.3	20.5	22.3	23.6	23.1	22.7	21.8	22.6	22.7	22.9	22.4	23.8	23.2	24.9	25.5	25.7	18.0
Crocodylus palustris	FMNH 51691	India (captive)	34.0	31.1	31.6	30.9	30.1	29.4	31.5	33.4	38.1	38.9	39.8	37.6	38.9	38.2	39.5	39.3	39.9	38.4	40.1	40.0	37.3	23.4
Crocodylus porosus	FMNH 22026	India	53.3	52.8	50.0	51.9	51.9	48.4	53.8	58.6	63.8	64.7	66.3	67.8	66.5	66.7	65.8	65.9	66.6	66.9	66.6	68.6	72.8	37.2
Crocodylus porosus	USNM 61206	Indonesia, Celebes	51.8	47.8	47.1	46.3	47.7	47.0	48.9	53.4	57.2	58.7	61.8	59.6	57.7	58.2	60.7	61.3	62.6	64.4	64.6	63.6	62.0	37.6
Crocodylus rhombifer	AMNH 57773	Cuba	35.4	31.8	33.2	33.9	31.7	31.9	33.9	34.2	36.8	36.9	36.6	37.1	37.5	36.9	37.1	37.2	39.6	39.7	40.5	40.4	40.9	23.3
Crocodylus rhombifer	AMNH 77595		29.0	28.7	27.3	27.5	27.9	26.6	27.4	29.5	30.4	30.1	33.2	29.4	29.3	29.4	31.1	31.9	32.3	32.1	33.1	34.4	32.8	20.0
Crocodylus rhombifer	FMNH 34677	Cuba	27.0	25.9	26.5	26.3	25.6	26.7	28.1	27.4	29.9	31.3	31.6	32.7	31.3	32.3	32.6	33.2	29.4	31.7	32.7	32.3	32.6	20.8
Osteolaemus tetraspis	AMNH 69057		21.4	20.7	19.9	18.9	17.9	18.1	19.5	22.0	23.2	23.9	23.4	25.1	24.5	25.3	25.0	24.6	25.5	26.0	26.2	26.4	25.8	17.0
Osteolaemus tetraspis	UF 33749?		20.6	19.3	19.7	18.6	19.7	18.2	19.1	21.2	23.2	23.1	24.6	25.1	23.2	23.6	23.8	24.0	23.8	24.0	24.3	24.8	24.3	13.8
Gavialis gangeticus	AMNH 88316		31.1	30.3	31.4	30.8	31.4	31.9	32.2	33.7	33.8	34.3	34.7	35.5	35.7	37.0	36.2	36.8	37.1	37.1	36.1	36.8	34.5	16.8
Gavialis gangeticus	FMNH 82681		19.7	20.5	20.0	20.1	19.9	20.2	20.8	21.2	21.3	23.1	23.1	24.1	23.7	23.8	24.0	24.6	24.4	24.7	24.6	24.4	23.0	23.8
Gavialis gangeticus	FMNH 98864		20.1	19.4	20.7	20.1	21.0	21.5	20.6	20.4	21.5	21.8	21.1	21.7	22.1	21.8	22.1	22.6	22.3	23.4	22.8	23.7	22.8	16.4
Gavialis gangeticus	UF 70592		17.7	18.5	18.4	18.8	18.6	18.4	18.2	18.6	19.8	20.4	20.2	20.7	19.7	21.5	20.5	21.8	22.0	22.0	22.1	23.1	22.0	16.0
Gavialis gangeticus	USNM 576261		48.5	49.9	50.2	49.6	50.7	49.5	49.7	54.6	56.0	54.3	54.3	56.2	58.6	56.2	58.9	58.1	62.3	57.9	58.7	58.8	59.5	14.7
Gavialis gangeticus	YPM R10514	India	35.6	36.6	37.8	37.6	36.9	37.4	37.8	38.1	41.6	43.3	42.9	43.3	41.5	42.5	42.5	43.0	41.6	42.1	42.2	41.7	40.8	37.2
Tomistoma schlegelii	FMNH 206755		44.9	46.9	44.8	45.7	44.0	43.5	45.6	45.6	47.3	49.1	52.5	47.6	49.1	49.3	50.4	51.1	53.4	55.5	54.5	53.4	52.7	27.6
Tomistoma schlegelii	UF 107493		54.3	48.9	46.8	48.5	48.1	48.5	50.6	50.6	50.0	51.6	52.2	52.3	54.3	56.1	53.0	52.1	51.0	53.5	52.1	57.1	56.6	36.1
Tomistoma schlegelii	USNM 52972	Indonesia, Borneo, Samarinda	47.1	46.2	44.5	44.3	43.6	45.9	47.9	46.2	46.1	47.2	48.1	47.6	47.7	48.2	47.5	49.3	49.1	49.4	49.7	51.7	47.6	37.3
Tomistoma schlegelii	UF 54210		35.4	34.8	33.2	33.0	33.2	34.1	35.7	36.9	37.4	37.8	38.9	38.2	38.9	38.9	39.9	38.7	39.9	40.9	40.8	42.1	39.8	32.5

Table S6. Measurements of prezygapophyseal width (PZW) in mm. Red color indicates estimated value.

Taxon	Specimen #	Locality	C3	C4	C5	C6	C7	C8	C9	D1	D2	D3	D4	D5	D6	D7	D8	D9	D10	D11	D12	D13	D14	D15
Alligator mississippiensis	AMNH 31563		28.0	30.8	38.3	43.7	45.2	48.3	54.6	50.8	52.1	57.6	60.4	61.0	63.8	60.4	59.8	64.1	67.4	66.8	72.6	63.8	65.5	67.1
Alligator mississippiensis	AMNH 43315	USA, Florida	28.6	32.6	36.7	39.0	41.9	44.8	46.0	51.4	51.9	57.1	54.8	58.1	59.3	60.9	62.5	61.4	60.3	63.3	67.1	66.9	71.6	67.2
Alligator mississippiensis	AMNH R43316		18.0	22.1	25.5	28.6	31.5	34.1	34.2	34.2	35.6	38.4	40.0	41.1	40.6	43.1	44.9	45.3	46.4	48.6	48.5	49.1	50.1	47.5
Alligator mississippiensis	YPM R10503	USA, Georgia, Chatham County	22.3	24.2	27.5	33.0	34.9	37.2	39.1	40.0	43.1	48.4	48.2	51.0	51.2	51.9	54.1	53.4	53.4	52.9	52.5	52.9	54.4	54.2
Alligator mississippiensis	YPM R17123	USA, Louisiana, Cameron Parish	14.6	16.4	19.1	20.6	21.3	23.1	25.1	24.9	25.0	25.8	26.2	26.2	26.5	25.6	26.0	26.5	27.4	27.2	27.3	28.0	27.3	28.2
Alligator sinensis	BMNH 1954.1.7.30		22.1	26.2	32.5	32.1	37.0	38.1	39.4	39.3	39.2	35.7	44.4	41.3	43.7	41.9	40.5	41.8	42.9	43.6	44.3	45.3	44.4	46.6
Caiman crocodilus	USNM 102874	Panama, Madden Lake	10.8	13.0	14.7	15.4	16.2	16.8	16.3	16.8	18.4	18.9	20.6	20.9	21.2	21.4	20.5	20.6	21.2	20.9	21.3	21.7	21.3	22.3
Caiman crocodilus	USNM 313860	Panama, Bocas del Toro	12.4	14.7	18.4	19.2	20.7	20.1	19.7	19.2	20.8	20.5	21.8	23.1	23.6	25.4	24.2	25.8	26.1	26.1	26.6	26.8	25.4	26.2
Caiman yacare	AMNH 97300	Bolivia, Beni	25.8	27.7	34.2	34.9	34.4	37.1	36.6	37.6	39.5	42.1	45.3	47.3	45.3	47.2	48.4	50.7	48.0	47.7	46.8	46.9	45.8	42.2
Caiman yacare	UF 121268	Paraguay, Pres. Hayes Dept.	22.9	26.9	33.0	31.7	38.5	41.0	40.9	40.6	43.2	44.3	44.7	47.8	50.1	50.1	51.2	50.6	51.6	52.7	51.4	53.1	50.1	49.1
Caiman yacare	UF 120653	Paraguay, Alto Paraguay	20.2	23.6	27.0	27.2	29.6	32.1	31.5	32.0	32.9	35.0	36.8	35.1	36.7	37.1	37.3	39.4	39.3	39.6	39.6	39.8	40.6	38.4
Melanosuchus niger	FMNH 218507	Ecuador, Napo Province	17.4	20.5	22.2	23.9	24.1	24.6	24.6	25.4	24.8	24.7	24.6	26.7	26.3	25.7	26.3	26.5	26.3	26.4	25.8	25.5	27.1	26.7
Melanosuchus niger	USNM 257786	Peru, Madre De Dios, Manu National Park	17.0	20.8	25.9	27.2	26.5	28.0	28.4	27.2	27.8	27.0	28.7	29.9	29.8	30.1	29.2	29.0	29.7	27.9	30.0	30.9	30.3	31.1
Paleosuchus palpebrosus	AMNH 78976	Colombia, Amazonas, Cano Negro	10.9	13.1	14.7	16.1	17.2	18.0	17.1	15.5	16.3	16.8	18.5	20.0	20.8	22.2	22.6	22.0	22.0	21.7	20.7	21.2	20.6	20.0
Crocodylus acutus	AMNH 7168		22.4	23.7	27.2	30.1	35.2	41.0	44.0	45.5	48.9	46.5	48.0	47.5	48.2	47.6	52.6	55.7	54.0	53.8	52.1	50.6	50.4	50.3
Crocodylus acutus	USNM 247943	Panama, Barro Colorado Island, Barbour Point	27.7	32.2	38.7	40.7	45.3	48.5	48.9	51.8	55.4	56.2	57.6	59.4	60.2	61.4	60.3	59.2	59.7	60.6	59.1	61.0	66.9	64.7
Crocodylus johnsoni	NTM JA076		14.1	14.9	17.6	19.8	22.2	23.1	23.7	21.5	27.0	27.1	28.6	27.9	28.3	28.0	27.1	27.2	26.9	30.0	26.3	26.8	28.6	27.7
Crocodylus johnsoni	NTM R25705		21.0	25.1	28.4	32.5	35.1	35.8	37.3	36.7	40.4	40.2	41.7	41.4	41.9	40.6	41.6	43.3	43.0	43.1	43.7	44.9	43.4	43.1
Crocodylus johnsoni	QM J58446	Australia, Queensland: Cooper Creek, ~6 km south of Windorah	18.0	19.0	21.7	23.2	25.4	28.6	30.1	28.2	27.4	30.2	31.4	31.1	32.5	31.0	30.8	30.9	30.9	31.8	31.1	31.3	33.5	33.1
Crocodylus johnsoni	QM J60590	Australia, Queensland: Amber Station, pool 1	11.4	13.0	14.9	15.7	18.6	20.6	21.6	21.4	22.9	24.1	24.2	24.7	24.1	25.0	24.0	24.3	24.4	23.8	24.1	24.6	25.0	25.4
Crocodylus palustris	FMNH 51691	India (captive)	19.2	24.1	26.3	28.1	31.7	30.9	30.0	28.3	32.8	38.1	40.2	40.9	42.3	42.4	43.9	44.2	47.5	44.7	48.9	48.8	47.2	43.9
Crocodylus porosus	FMNH 22026	India	34.2	40.9	44.2	54.6	55.2	56.3	60.4	58.6	58.5	57.8	59.2	64.6	65.8	65.4	66.5	66.6	65.9	65.6	65.9	67.9	75.8	63.5
Crocodylus porosus	USNM 61206	Indonesia, Celebes	23.3	28.6	34.6	42.5	46.3	48.0	49.4	48.5	49.3	50.6	52.4	50.5	52.9	51.1	49.0	48.7	51.3	49.9	50.5	53.0	53.9	50.5
Crocodylus rhombifer	AMNH 57773	Cuba	18.3	21.6	24.6	26.1	29.4	31.6	33.9	33.5	37.6	39.7	41.6	42.6	44.1	44.5	45.2	43.8	44.5	44.1	43.1	43.9	43.5	42.9
Crocodylus rhombifer	AMNH 77595		16.4	20.2	23.5	25.0	26.3	27.4	26.9	27.3	30.4	32.0	36.9	34.6	34.5	35.4	35.3	37.1	37.6	38.7	37.2	39.5	38.6	35.2
Osteolaemus tetraspis	AMNH 69057		12.6	13.8	17.5	19.3	22.1	22.6	23.5	22.2	23.0	24.4	24.1	25.6	26.6	27.5	28.1	27.6	27.7	27.4	28.2	28.4	27.7	27.7
Osteolaemus tetraspis	UF 33749?		11.4	14.9	16.9	18.1	19.8	20.7	21.2	21.2	21.3	21.9	24.1	25.6	27.3	26.4	27.2	27.7	27.0	27.4	27.3	27.3	27.6	27.6
Gavialis gangeticus	AMNH 88316		18.8	17.3	20.3	20.0	19.3	20.1	20.6	19.4	20.0	17.3	16.8	16.2	16.5	17.5	17.8	17.0	15.5	16.1	16.7	19.6	17.5	15.8
Gavialis gangeticus	UF 70592		10.3	10.6	11.9	12.6	12.6	13.4	13.7	13.5	14.0	14.6	13.6	14.9	14.9	14.3	14.9	15.1	14.7	14.6	14.5	14.3	14.3	14.7
Gavialis gangeticus	USNM 576261		34.6	34.9	40.8	39.7	41.9	44.2	42.5	39.9	37.8	39.3	40.5	38.2	36.9	36.7	36.1	37.2	39.7	36.4	38.1	36.3	37.4	41.4
Gavialis gangeticus	YPM R10514	India	21.4	21.0	23.7	22.9	27.1	27.4	27.1	29.6	33.1	26.1	27.9	26.3	23.8	23.6	23.8	22.1	20.6	22.1	22.0	22.5	23.2	24.3
Tomistoma schlegelii	FMNH 206755		22.8	30.9	33.2	37.5	39.3	40.7	41.8	42.6	44.6	44.6	47.3	46.7	49.1	47.0	44.6	46.5	46.4	44.4	46.6	43.8	51.2	53.9
Tomistoma schlegelii	UF 107493		28.3	35.4	39.3	42.9	45.0	48.0	48.7	48.7	51.0	56.7	60.0	57.5	59.0	56.1	54.6	52.6	54.3	54.0	55.4	52.9	53.4	53.6
Tomistoma schlegelii	USNM 52972	Indonesia, Borneo, Samarinda	21.8	26.4	28.9	31.2	33.3	35.6	38.0	41.3	43.1	46.3	47.6	49.6	52.4	51.3	50.5	49.3	47.7	48.9	47.8	51.2	47.6	52.0
Tomistoma schlegelii	UF 54210		19.8	24.7	27.0	31.4	30.7	31.9	30.8	31.8	33.4	35.0	36.4	36.4	37.0	36.4	36.3	34.2	35.0	35.6	36.8	36.3	37.5	39.1

Table S7. Measurements of transverse process width (TPW) in mm. Red color indicates estimated value.

Taxon	Specimen #	Locality	C3	C4	C5	C6	C7	C8	C9	D1	D2	D3	D4	D5	D6	D7	D8	D9	D10	D11	D12	D13	D14	D15
Alligator mississippiensis	AMNH 31563		42.9	48.9	50.3	52.1	63.1	70.4	83.9	92.5	109.6	137.8	148.2	153.0	160.6	163.8	165.9	161.4	164.6	152.9	142.1	138.0	127.2	110.5
Alligator mississippiensis	AMNH 43315	USA, Florida	36.9	39.4	41.0	45.0	57.0	64.3	77.7	87.8	106.9	134.8	147.8	153.1	156.9	153.7	150.6	150.1	149.7	138.8	133.5	133.4	121.7	99.0
Alligator mississippiensis	AMNH R43316		27.6	30.1	29.7	33.5	41.4	48.1	58.6	64.9	77.8	96.6	103.8	106.8	111.1	112.3	114.5	111.9	110.2	102.2	99.7	92.3	81.7	69.6
Alligator mississippiensis	YPM R10503	USA, Georgia, Chatham County	33.1	37.5	38.2	42.3	47.8	54.2	65.9	77.4	97.9	117.9	127.5	131.2	135.8	138.8	138.7	134.5	130.2	117.2	110.3	105.3	95.9	78.1
Alligator mississippiensis	YPM R17123	USA, Louisiana, Cameron Parish	19.7	20.6	21.8	23.9	27.2	31.1	37.6	44.0	53.9	63.2	67.4	70.2	72.0	73.2	74.8	74.2	69.3	64.9	60.8	59.0	54.5	46.0
Alligator sinensis	BMNH 1954.1.7.30		29.8	33.1	35.2	39.2	44.6	52.7	60.1	69.5	88.5	106.7	117.8	122.8	121.1	122.2	123.8	123.8	119.0	108.0	103.1	98.2	89.7	75.5
Caiman crocodilus	USNM 102874	Panama, Madden Lake	17.6	17.2	18.5	20.3	22.2	26.3	31.6	38.2	48.8	55.2	59.1	60.3	60.3	59.2	58.6	58.1	53.8	53.5	51.8	50.5	44.4	44.4
Caiman crocodilus	USNM 313860	Panama, Bocas del Toro	20.8	22.1	23.1	25.0	28.3	31.2	35.5	43.1	50.4	63.1	70.7	74.6	76.3	74.6	71.2	70.6	70.3	67.3	67.0	65.5	61.7	53.2
Caiman yacare	AMNH 97300	Bolivia, Beni	35.9	37.3	36.1	39.8	43.8	52.4	64.8	83.6	104.8	125.5	133.8	140.2	143.2	144.0	143.0	138.7	135.0	126.8	120.0	118.3	115.5	99.2
Caiman yacare	UF 121268	Paraguay, Pres. Hayes Dept.	34.0	36.0	40.0	40.7	49.3	56.9	66.6	84.3	103.6	123.9	128.0	138.9	142.2	140.0	142.0	139.8	134.2	125.3	114.7	117.5	106.9	98.6
Caiman yacare	UF 120653	Paraguay, Alto Paraguay	28.2	29.4	30.9	31.6	38.0	48.2	55.1	66.2	80.8	95.2	104.3	106.1	107.8	107.3	104.4	107.1	102.1	93.7	96.0	92.9	93.2	80.2
Melanosuchus niger	FMNH 218507	Ecuador, Napo Province	22.7	22.1	23.9	26.8	29.1	36.6	43.4	52.0	59.3	76.6	80.7	87.5	90.8	89.5	90.8	91.6	87.0	80.2	73.4	69.7	69.1	61.6
Melanosuchus niger	USNM 257786	Peru, Madre De Dios, Manu National Park	26.2	25.9	26.7	29.0	31.3	39.1	48.9	59.8	71.5	88.4	96.2	99.5	101.6	102.0	101.8	101.8	95.8	89.2	83.2	75.2	77.7	72.2
Paleosuchus palpebrosus	AMNH 78976	Colombia, Amazonas, Cano Negro	17.4	17.3	18.5	19.9	22.2	27.2	31.0	36.8	44.6	52.7	60.5	64.3	65.8	65.8	65.5	64.8	60.9	56.2	53.7	50.8	48.7	42.2
Crocodylus acutus	AMNH 7168		41.9	55.8	57.8	50.5	53.7	60.0	79.8	90.7	97.2	114.8	129.1	135.7	136.3	139.4	141.1	143.9	134.0	132.6	124.6	121.4	110.4	94.5
Crocodylus acutus	USNM 247943	Panama, Barro Colorado Island, Barbour Point	45.8	50.4	52.3	58.1	63.1	71.0	86.5	95.5	102.8	124.2	135.3	142.7	147.5	151.4	151.2	153.6	156.6	153.1	146.8	141.6	140.8	141.0
Crocodylus johnsoni	NTM JA076		23.5	24.1	25.6	27.6	29.4	32.6	37.6	43.0	50.0	59.9	67.0	69.9	71.9	74.5	75.0	76.7	75.3	72.6	69.4	67.7	64.9	60.9
Crocodylus johnsoni	NTM R25705		36.0	35.3	36.6	38.8	42.4	51.8	61.4	71.2	81.5	97.2	106.0	109.6	113.8	116.6	119.0	119.3	114.8	104.8	102.8	100.4	93.0	90.1
Crocodylus johnsoni	QM J58446	Australia, Queensland: Cooper Creek, ~6 km south of Windorah	26.7	27.9	29.4	31.0	36.1	41.3	47.4	56.0	62.5	75.2	83.5	87.8	89.4	91.2	92.4	94.4	92.2	86.9	81.3	77.4	75.2	70.0
Crocodylus johnsoni	QM J60590	Australia, Queensland: Amber Station, pool 1	19.9	20.0	21.2	22.3	25.3	29.3	34.5	40.3	46.0	55.3	63.7	66.1	71.2	69.2	70.3	71.9	69.5	66.6	59.8	58.5	56.6	53.7
Crocodylus palustris	FMNH 51691	India (captive)	36.2	36.6	36.6	38.5	44.6	53.0	61.2	62.5	69.9	87.6	96.8	100.3	110.8	108.4	116.6	113.9	111.8	109.5	108.3	94.8	82.0	81.0
Crocodylus porosus	FMNH 22026	India	56.8	55.3	53.6	62.4	72.8	83.1	98.5	97.0	115.1	136.3	150.5	166.3	178.9	181.5	186.1	185.2	181.7	166.8	170.5	162.7	166.0	127.6
Crocodylus porosus	USNM 61206	Indonesia, Celebes	46.7	49.8	51.8	55.1	61.4	77.4	92.2	102.5	109.4	126.9	141.2	150.2	158.3	165.4	166.5	168.2	167.1	163.8	154.8	143.8	141.9	122.3
Crocodylus rhombifer	AMNH 57773	Cuba	28.8	30.8	31.8	35.5	43.6	52.5	63.0	68.9	75.5	86.5	93.5	98.6	102.9	103.6	104.1	103.5	105.1	94.4	91.2	87.6	84.6	68.9
Crocodylus rhombifer	AMNH 77595		25.9	27.5	29.3	32.3	37.6	42.9	52.2	56.3	58.9	68.8	73.8	75.5	79.0	83.3	85.2	88.3	88.4	85.2	81.5	73.7	65.9	59.0
Osteolaemus tetraspis	AMNH 69057		20.7	20.6	21.4	23.7	27.8	32.7	39.8	43.6	44.4	50.4	55.7	60.1	63.2	65.0	65.0	59.6	56.6	55.6	54.9	54.0	49.7	49.7
Osteolaemus tetraspis	YPM R16944	Cameroon	17.5	17.4	17.7	19.3	21.5	25.6	30.1	34.1	36.0	40.1	44.4	46.7	48.2	49.9	50.0	46.5	44.0	42.1	41.0	39.9	38.4	35.4
Osteolaemus tetraspis	UF 33749?		19.1	20.6	22.3	24.8	28.9	32.3	39.3	42.8	46.3	52.0	55.6	61.0	59.0	60.9	61.4	58.4	53.4	51.5	50.2	48.7	45.4	39.6
Gavialis gangeticus	UF 70592		16.6	15.8	14.9	16.9	18.1	23.4	26.7	28.4	32.9	43.0	52.4	58.5	59.4	65.7	62.2	64.2	67.0	62.5	55.4	50.8	51.0	47.6
Gavialis gangeticus	USNM 576261		50.6	48.9	51.8	49.6	56.9	71.8	82.3	93.2	111.4	140.4	166.2	180.6	188.4	197.1	201.7	202.7	200.1	189.7	172.4	162.7	155.1	149.8
Gavialis gangeticus	YPM R10514	India	33.1	31.6	32.1	34.4	37.8	50.7	58.0	60.3	66.6	79.6	96.0	115.5	132.1	137.8	139.0	141.8	142.2	134.8	125.2	114.4	111.5	111.5
Tomistoma schlegelii	FMNH 206755		46.9	47.7	49.5	54.3	61.4	72.2	84.1	94.9	108.3	124.1	145.1	167.3	176.7	180.7	183.6	185.5	187.3	185.3	164.0	142.6	146.6	138.5
Tomistoma schlegelii	UF 107493		46.4	46.8	51.6	57.5	63.3	80.4	90.0	101.7	114.8	134.9	156.5	165.9	171.6	176.0	177.8	175.6	186.0	159.1	173.7	149.1	140.1	123.5
Tomistoma schlegelii	USNM 52972	Indonesia, Borneo, Samarinda	40.6	41.0	41.2	46.3	55.2	62.3	72.0	85.3	101.0	118.5	143.4	162.6	168.6	172.5	172.9	176.5	176.7	166.9	147.6	147.0	141.8	130.4
Tomistoma schlegelii	UF 54210		34.8	35.5	39.7	41.3	43.2	49.9	56.5	63.6	72.0	82.8	101.7	114.0	119.4	122.4	124.4	127.7	127.6	124.7	111.1	109.8	108.2	95.9

Supplement to chapter IV

Geological background of *Toyotamaphimeia enshuensis*

The initial discovery of *Toyotamaphimeia enshuensis* dates back to late 1960s at a now-closed limestone quarry in Yage, Inasa-cho, Hamamatsu City, Shizuoka, Japan (Nakajima, 1983; Nojima, 2002). Owing to laborious collection work by Shizuoka University, Yokohama National University, Hamamatsu Kita High School, and many independent researchers, more than a thousand crocodylian fragments of had been collected over the following decade (Nakajima, 1983). The cave-hosted Yage Formation, which is equivalent to the Miyakoda Formation (Shikama & Shimaoka, 1955), can be subdivided into two parts: the lower part characterized by clay to middle-coarse grained sandstone intercalating a tephra bed, and the upper part characterized by yellowish brown clay containing subangular gravels (Tomida, 1978; Nojima, 2002; Nojima *et al.*, 2014). All crocodylian materials were recovered from the F3 bed is in the lower Yage Formation, which is composed of grayish white clay (Tomida, 1978; Nojima, 2002), and the overlaying tephra bed is correlated to the marine isotope stage 11-8.2 in the Middle Pleistocene (Nojima *et al.*, 2014). The lower Yage Formation yielded freshwater fishes (*Cyprinus carpio*, *Carrasius* sp., *Distoechodon* sp., and *Parasilurus* sp.), a turtle (*Ocadia sinensis*), and an otter (*Lutra* sp.) (Uyeno, 1965; Tomida, 1978; Nojima, 2002; Nojima *et al.*, 2007), other than a crocodylian (*T. enshuensis*). From F2 bed, which is approximately 1 m above the F3 bed, six diatom species (*Rhopalodea gibba*, *Coscinodiscus radiatus*, *Coscinodiscus lacustris*, *Melosira sulcata*, and *Hyalodiscus stelliger*) were reported (Nojima *et al.*, 2007). The upper Yage Formation has produced a number of terrestrial mammals (Cercopithecidae, Soricidae, Talpidae, Rhinolophidae, Cricetidae, Muridae, Leporidae, Canidae, Ursidae, Mustelidae, Felidae, Equidae, Cervidae, Suidae, Elephontidae, and Rhinocerotidae), birds (Galliformes, Passeriformes, and Accipitriformes), reptiles (Emydidae, Colubridae), frogs (Bufonidae and Hylidae), and a fish (Cyprinoidea) (Takai *et al.*, 1958; Tomida, 1978; Nojima, 2002; Handa, 2015). The paleoclimate during the deposition of the lower Yage Formation was considered as warm-temperate, based on the plant assemblage from the Washizu Mud Formation, which can be correlated to the lower Yage Formation (Nojima *et al.*, 2014).

Taxonomic remarks of *Toyotamaphimeia enshuensis*

Toyotamaphimeia enshuensis was preliminary examined by Nojima et al. (2007), and the new name *Yagesius yagesius* was proposed based on the comparison of skull table and teeth with an extant Malayan gharial and *Toyotamaphimeia* specimens from Osaka (Nojima *et al.*, 2007). However, the holotype they fixed was for “crocodylian fossils from Yage,” instead for the new name, and they did not explicitly state that the genus and species name was intentionally new, which violates ICZN Article 16 (ICZN, 1999). Moreover, the suggested holotype is neither labeled nor the institution of its deposition was given, contrary to the

recommendation in ICZN Article 72 (ICZN, 1999). Therefore, *Yagesius yagesius* is regarded as an invalid name.

Supplementary description

Skull

The partial rostrum (premaxillae, maxillae, nasals), near complete preorbital elements (lacrimals, prefrontals), complete skull table (frontals, parietals, postorbitals, squamosals), partial infratemporal and suspensorium elements (jugals, quadratojugals, quadrates), partial occipital elements (supraoccipitals and exoccipitals) are preserved (Fig. 1A, B).

The right premaxilla (Fig. 1A) is missing the dorsal posterior process and the floor of the narial canal medial to the alveoli. Its external surface is ornamented by shallow pits. The posterolateral border of the external narial opening is gently concave, and there is a small midline process projecting into the opening. Ventrally, third and fourth premaxillary alveoli are preserved, and both are similar in size.

Partial anterior to mid maxillae and the more complete right posterior maxilla are preserved (Fig. 1). The external surface of right posterior maxilla is sculptured by numerous longitudinal grooves. Medially, butt-joint suture for the nasal is straight and the suture for lacrimal is damaged. The palatal side of this portion (Supp. Fig. 1G, H) has six alveoli, and the occlusal pits are placed in line with the alveoli, contrasting to the overbite occlusal pattern of the posterior maxillary and dentary dentition in *Toyotamaphimeia machikanensis* (Aoki, 1983; Kobayashi *et al.*, 2006). The maxillary foramen for palatine ramus of cranial nerve V is relatively large, but smaller than the adjacent alveoli. The position of the foramen suggests that the alveoli in this fragment are from 8th to 13th tooth positions.

Nasals (Fig. 1) are missing the anterior extension and the posterior suture for the prefrontals and frontal. Both sides of nasals are parallel, while slightly widens posteriorly medial to lacrimals.

Lacrimals and prefrontals (Fig. 1) are nearly complete. The composite reconstruction shows that the lacrimal extends far anteriorly than the prefrontal, and the lacrimal is wider than the prefrontal. Both elements together form the anterior orbital rim, and the suture between them terminates near the anterior extremity of orbit. The external surface of both is ornamented by small pits, yet the anterior part of lacrimal is relatively smooth.

The frontal (Fig. 1) has anterior process separating the prefrontals and contacts with nasals, and the anterior extension of the process is shorter than prefrontals. The frontal-nasal contact (Supp. Fig. 1E, F) has a complex zig-zag sutural pattern, similar to *Penghusuchus pani* (Shan *et al.*, 2009). The interorbital space is near flat, and the upturn of the orbital rim is minimal. The width of the interorbital space is roughly twice wider than the interfenestral space. The external surface is heavily ornamented with circular to transversely wide pits.

The skull table (Supp. Fig. 1A, B) broadens posteriorly, and the anterolateral edge is rounded. The shape of supratemporal fenestra is sub-circular to anteroposteriorly long oval, and the shape varies both bilaterally and among specimens: the fenestra in HH709 (Supp. Fig. 1A, B) is sub-circular, whereas the one in HH712 is longer anteroposteriorly than wide. The fenestra is pointed lateral to the parietal-postorbital suture within the fenestra. The lateral and posterior bars of supratemporal fenestra are equally thick (Supp. Fig. 1A, B), unlike of derived gavialines and *T. machikanensis*, in which the posterior bar is extremely narrow.

The sutural contact of the parietal and frontal (Supp. Fig. 1A, B) is wavy, while largely concave anteriorly. The parietal-frontal contact is excluded from the supratemporal fenestrae. The medial rims of supratemporal fenestrae are upturned, and there is no apparent medial ridge between the fenestrae. The deep pits on the external surface have variously shaped, and those at the interfenestral space are larger than others.

The squamosal (Supp. Fig. 1A, B) forms the posterolateral part of skull table, and sculptured by pits with various shape and size. The squamosal-parietal suture is nearly straight and intersects with the middle part of the supratemporal fenestrae. Dorsally, the squamosal-postorbital suture is oriented anterolaterally, and it turns anteroventrally on the lateral side. On the lateral surface of the skull table, the shallow squamosal groove flares anteriorly. The squamosal borders the posterodorsal rim of the external otic aperture, which is bowed posteriorly.

The postorbital (Supp. Fig. 1A, B) forms the rounded anterolateral corner of the skull table, and the anterolateral rim of the supratemporal fenestra is straight. Its descending process, the dorsal half of the postorbital bar, is laterally compressed and missing the ventral extension.

The supraoccipital (Supp. Fig. 1A-D) is transversally wide triangular shape in occipital view. The lateral posterior tuberosities are not such prominent that they are barely visible posterior to the skull table in dorsal view. Between the tuberosities, there is a y-shaped median tubercle, and dorsolateral to the tuberosity, large crest-shaped posttemporal fenestrae open. Dorsally, the supraoccipital largely exposes on the posterior skull table at the level slightly lower than other skull table elements.

The exoccipitals are fragmentary and not informative.

The left jugal (Supp. Fig. 1I-K) is missing the anterior part and the ascending process of the postorbital. Its external surface is flat without a longitudinal ridge, and densely sculptured except for the portion near the jugal-quadratojugal suture. Medial surface of this element, anterior to the base of postorbital bar bears two large medial jugal foramina, of which the anterior one is larger. Ventrally near the jugal-ectopterygoid suture, a shallow concavity is present (Supp. Fig. 1K), which is much less prominent than that in *T. machikanensis*. It is uncertain whether the jugal or quadratojugal forms the posterior angle of the infratemporal fenestra because the jugal-quadratojugal suture intersection with the infratemporal fenestra is broken on both dorsal and ventral surfaces.

The left quadratojugal (Supp. Fig. 1I-K) is missing the narrow ascending process that would form the posterodorsal rim of the infratemporal fenestra. Immediately medial to the posterolateral angle of the fenestra, a small protrusion probably represents the base of the spina quadratojugalis. The jugal-quadratojugal suture ends well anterior to the quadrate condyles.

Both quadrates are largely damaged, while the preserved quadrate condyles indicate that the medial and lateral hemicondyles would be similar in depth.

Mandible

Although fragmentary, large portion of the mandible except for the coronoid is preserved (Fig. 1B).

Anterior dentary alveoli are widely spaced (Supp. Fig. 2G), and the dentary is laterally expanded at the second alveolus. All the alveoli are sub-circular in shape, and the first dentary alveolus projects anterodorsally. The right posterior dentary (Supp. Fig. 2H) preserves the widely and evenly spaced seven alveoli, contrasting to the more densely placed posterior mandibular alveoli in *T. machikanensis*. The shape of alveoli is sub-circular in anterior ones and more laterally compressed oval in posterior ones. The occlusal pits are placed in line with the alveoli. The posterior portion of the right dentary (Supp. Fig. 2A, B) is missing the dorsal and ventral process that would border the anterodorsal and anteroventral rim of the external mandibular fenestra. There are two shallow grooves extends horizontally, from the anterior end of the external mandibular fenestra, and from the anterior end of the surangular anterior processes.

The left splenial (Supp. Fig. 2E, F) is missing the anterior part of symphysis. The preserved portion shows that the symphysis extends the length of at least three adjacent alveoli, but the shape of the symphysis is uncertain. The right splenial exhibits the small foramen intermandibularis oralis near the caudal end of the symphysis, as in *G. gangeticus* and *T. machikanensis*.

The surangular (Supp. Fig. 2A-D) sends anterior processes posterior to the mandibular tooth row, of which the dorsal process extends further anteriorly. The dorsal surface of this element above the external mandibular fenestra is flattened, and lateral to the glenoid, there is a shallow depression. The surangular-angular sutural intersection with the external mandibular fenestra is not preserved. Posteriorly, the surangular laterally laps the glenoid, but its posterior extension is broken. Medially, the lingual foramen for the articular artery and alveolar nerve perforates surangular.

The right angular (Supp. Fig. 2A-D) sends the thin process anteriorly in the floor of the mandible, which is pinched off between the dentary and splenial anterior to the surangular's anterior processes. Posterior to the glenoid, the lateral surface is smoothed for the insertion of *M. pterygoideus ventralis* (Holliday & Witmer, 2007), and extends to near the caudal tip of

the retroarticular process. Medially, surangular-angular suture downturns ventrally and end near the tip of the articular descending process. The medial ascending lamina that would border the posterodorsal rim of the foramen intermandibularis caudalis is broken.

The descending process of the articular contacts with surangular by simple linear suture, and there is no prominent sulcus between them. The glenoid (Supp. Fig. 2C, D) is divided into two sulci, and the articular-surangular suture within the glenoid is linear. The retroarticular process is slender, which is roughly three times longer than the glenoid in dorsal view. The articular foramen aëreum is not observed because of the preservation condition.

Dentition

All teeth were isolatedly collected (Supp. Fig. 2J-O). Many of those teeth have roots, suggesting that they were shed after death. Tooth crowns are roughly divided into two morphotypes: strongly recurved slender conical crowns and short labiolingually compressed crowns with blunt apex. The first type is probably of premaxillary, anterior maxillary and anterior dentary teeth, and the second type is of posterior maxillary and dentary teeth, suggested by the observation of *T. schlegelii* (e.g., ZSM 200.1907; ZSM 210.1907). All crowns have mesial and distal carinae, and the crown surfaces are ornamented by numerous apico-basal striations.

Axial skeleton

The axial skeleton of *T. enshuensis* includes cervical, dorsal, sacral, and caudal vertebrae, cervical, dorsal, and sacral ribs, and chevrons. All the presacral centra except for the atlas and axis are procoelous.

The proatlas (Supp. Fig. 3A-C) is missing both posterolateral processes. Its anterior border is straight, and it widens posteriorly. The dorsal medial ridge is modestly developed, and the ventral tubercles are short and less than half the length of dorsal median ridge.

The left neural arch of atlas (Supp. Fig. 3D, E) has the anteromedially and the posteroventrally facing large facets for the articulation with the occipital condyle and the odontoid process of axis, respectively. Laterally, a tuberosity is present at the neck of the neural arch as in the *T. machikanensis*. The thin plate-like expansion medial to pre- and post-zygapophyses is broken.

The right atlanal rib (Supp. Fig. 3F, G) is missing the posterior half. It is convex laterally and concave medially, and on the lateral surface, a faint ridge extends posterodorsally. The articular surface is angled with respect to the dorsal and ventral rims of this element. The thin medial lamina ventral to the articular surface is not developed.

The axial centrum (Supp. Fig. 3H-J) is missing the odontoid process. Laterally, a ridge extends anteroventrally from the posterior part of the centrum, and leads to bifurcated

hypapophyses as in gavialines, which is placed in the anteroventral surface of the centrum. The forked hypapophysis is divided by the ventral medial keel.

The third or fourth cervical centrum (Supp. Fig. 3K-M) has large oval-shaped parapophysis lateroventrally near the concave intervertebral joint surface of the centrum. Ventrally, medial to the parapophyses, forked hypapophysis is present, which converges anteriorly with the ventral medial keel, as in the *T. machikanensis*. The keel is broadened and rugose anterior to the convex intervertebral joint surface of the centrum.

The posterior cervical vertebrae (8th and 9th: Supp. Fig. 4A, B and 4C, D) have long and horizontal diapophyses (transverse processes), with the tips of the processes rounded. The parapophyses are small and rounded, and placed in the ventral half of the centra. The pre- and post- zygapophyses are oval in shape and their axes are oriented anterolaterally and posterolaterally.

The third dorsal vertebra (Supp. Fig. 4E, F) has a modest hypapophysis that is placed anteriorly. The cross section of the transverse process is thin and anteroposteriorly long. The both prezygapophyses are closely spaced and circular in shape.

The first and second sacral vertebrae (Supp. Fig. 4G, H and 4I, J) are missing the neural spine. The first sacral centrum has anteriorly concave and posteriorly platy intervertebral joints. The fused ribs are triangular in cross section, and expanded distally. The second sacral centrum has platy anterior but convex posterior intervertebral joint surfaces unlike in typical crocodylians. The right rib is expanded distally, and the cross section is tear drop shape.

Pectoral girdle and forelimb

Pectoral girdle elements (scapulae, coracoids, and interclavicles), hemeri, ulnae and radii, radialia, some metacarpals and phalanges are preserved.

The scapula (Supp. Fig. 5A) is constricted at the neck, and the scapular blade is flared to the distal end. The anterior edge of the blade is concave, and the posterior edge is broken. The deltoid crest is thick and robust as in *Alligator*, *P. pani*, and *T. machikanensis*. The scapulocoracoid facet is tear drop shaped and tapers anteriorly.

The coracoid (Supp. Fig. 5B) is slender than scapula in lateral view. It is constricted ventral to the glenoid and the blade is flared distally. The anterior margin of the blade is concave, and the posterior margin is nearly straight. The large coracoid foramen is placed immediately ventral to the scapulocoracoid facet.

The interclavicle (Supp. Fig. 5C, D) is straight along the length, while some individuals have slight dorsoventral curvature in lateral view. It is narrow anteriorly, and widens posteriorly. The anterior end is flattened, yet the rest of the element is triangular in section due to the ventral ridge, which is more prominent in the posterior part. The dorsal surface is near flat in the anterior part, and concave in the posterior part.

The humerus (Supp. Fig. 5E, F) is bowed medially in posterior and anterior views. The humeral head is not prominent and is smoothly connected with the anterior and posterior tuberosities. The deltopectoral crest is weakly developed and its tip is blunted. The proximal edge of the crest is broadly concave. Dorsal to the deltopectoral crest, the humeral shaft surface is elevated and rugose, representing the insertion of *M. teres major* and *M. dorsalis scapulae*.

The ulnar shaft (Supp. Fig. 5G-I) is anteroposteriorly compressed, and widened towards the proximal end. The mediolateral width of the proximal end is more than twice wider than the mid part of the shaft. The proximal end is triangular in shape, and there is a large concavity in the anterior half of the proximal end, lateral to the olecranon process. The olecranon process is rounded.

The radial shaft (Supp. Fig. 5J-L) is anteroposteriorly wider than mediolaterally. Its proximal end is quadrangular and the surface is concave to fit the distal condyle of humerus. The anterior surface of the shaft, immediately distal to the proximal end, is elevated and rugose for the insertion of *M. humeroradialis*. The distal articular surface is tear drop shape.

The radiale (Supp. Fig. 5M-O) is hourglass shape in dorsal view, with the widened proximal and distal ends and the constricted mid part. On the dorsal surface, a sharp ridge is developed, and medial to this ridge, the dorsal surface is concave. The proximal end is crescent-shaped, and articular surface is extended on the lateral edge for receiving ulna. The distal end is pentagonal in outline.

Pelvic girdle and hind limb

Pelvic girdle elements (ilia, pubes, and ischia), femora, tibiae, fibulae, astragali, calcanei, some metatarsals and phalanges are preserved.

The dorsal margin of the iliac blade is broadly convex (Supp. Fig. 6A, B), and there is a prominent anterior process as in gavialines, *P. pani* and *T. machikanensis*. The blade is narrow posteriorly beyond the acetabulum, and the ventral edge is straight. The supuraacetabular crest is only faintly developed from the anterior end of the blade to the middle of the acetabulum.

The pubis (Supp. Fig. 6C) is triangular in outline in lateral view. Its proximal end is expanded and oval in shape, of which the lateral margin is more rounded than the medial one. It is cylindrical in section immediately distal to the proximal end, and flattened and flared more distally. The distal part is thicker anteriorly than posteriorly.

None of the preserved ischium (Supp. Fig. 6D) has complete proximal and distal ends. On the lateral shaft, a ridge extends from the proximal part to the posteroventral margin of this element.

The femoral shaft (Supp. Fig. 6E, F) is sigmoid, and the long axis of the femoral head is directed anteromedially with respect to the distal condyles. The fourth trochanter is placed

posteromedial surface of the proximal shaft, and distal to it, an oval depression represents the insertion of *M. adductor femoris*. Of the two distal condyles, lateral one is larger and extends more distally than the medial one.

Two of the preserved tibiae (Supp. Fig. 6G, H) are fractured in the mid shaft and the callus is formed, indicating that animals had survived the injuries for some time. The shaft is sub-circular in section in the proximal part, and mediolaterally thins towards the distal end. The proximal end is triangular in shape, and a shallow groove extends from the central to the posterior part, separating the lateral and medial condyles. The distal end is crescent shaped and divided into the anterior and posterior condyles by a shallow groove.

The fibula (Supp. Fig. 6I, J) is mediolaterally flat in the proximal part, and becomes more cylindrical distally. The anterolateral surface of the proximal shaft is rugose for the insertion of *M. iliofibularis*.

The astragalus (Supp. Fig. 6K-M) has flat articular facets for tibia and fibula in the proximal end. There are two shallow depressions on the anterior surface as in the *T. machikanensis*, and there is a single depression immediately posterodistal to the articular facet for tibia on the posterior surface.

The calcaneum (Supp. Fig. 6N, O) has a wheel shaped condyle, of which the more rounded dorsal facet articulates with fibula, and the flat ventral facet articulates with distal tarsal IV. Medial to the condyle, there is a socket joint for astragalus. The calcaneum tuber (posterodorsal process) is circular in shape, and the middle part of dorsal edge is grooved.

Among metatarsals I-III (Supp. Fig. 6P-R), metatarsal I is the thickest, and the metatarsal II is slightly thicker than the metatarsal III. The proximal end of the metatarsal I is oval in shape, and that of the metatarsal II and III are more dorsoventrally compressed, and are imbricated while articulated. In metatarsal I-III, the dorsolateral surface of the shaft near the proximal end is elevated and rugose.

Osteoderms

The flat, rectangular and mediolaterally wide osteoderms are of medial dorsal or pelvic osteoderms, usually with serrate joints on both sides (Supp. Fig. 7). Those osteoderms are densely sculptured without keel on the dorsal surface, and the anterior part is smoothed as overlapping facet. Similarly wide, flat without keel, but asymmetric osteoderms are probably from second medial row of dorsal or pelvic osteoderms. More rounded small ones are of probably lateral dorsal, caudal, or ventral osteoderms. Some of those small ones are with modest keels on the dorsal surface. The internal surface of all osteoderms is smooth, and very few numbers of small nutrient foramina open.

Character comparison

Toyotamaphimeia enshuensis shares unique axial characters with *Penghusuchus pani* from the Miocene of Taiwan and *T. machikanensis* from the Pleistocene of Japan: widely forked axial and third cervical hypapophysis, which is not known in other crocodylians to our knowledge. The bifurcated hypapophysis converges anteriorly and becomes a prominent boss in the third cervical in *P. pani* (Shan *et al.*, 2009), whereas this part is relatively smooth in *T. enshuensis* and *T. machikanensis* (Kobayashi *et al.*, 2006). The keel-like hypapophyses of posterior cervical vertebrae are rounded and do not extend beyond the anterior edge of centra in *T. enshuensis* and *T. machikanensis* (Kobayashi *et al.*, 2006), yet it project beyond the anterior edge of seventh through ninth cervical centra in *P. pani* (Shan *et al.*, 2009).

The sutural pattern of the antorbital part of skull in *T. enshuensis* is similar to *T. machikanensis*, but differs from *P. pani*. In both *T. enshuensis* and *T. machikanensis*, lacrimal extends far anteriorly to prefrontal, but in *P. pani*, both elements extend to nearly the same level (Kobayashi *et al.*, 2006; Shan *et al.*, 2009). The most bizarre feature uniting *Toyotamaphimeia* and *Penghusuchus*: seventh maxillary alveolus largest within the "first wave," cannot be observed in *T. enshuensis*.

T. enshuensis is relatively smaller in size compared to *P. pani* and *T. machikanensis*. Well preserved humeri of *T. enshuensis* [K10 (209 mm); T195 (212 mm); T196 (213 mm)] are shorter than that of *P. pani* (254.1 mm) and *T. machikanensis* (403 mm: Kobayashi et al., 2006). However, smaller size of *T. enshuensis* probably reflects their early growth stages: neurocentral suture of nearly all vertebrae in *T. enshuensis* is unfused, contrary to the completely closed suture of all vertebrae in *T. machikanensis* (Kobayashi *et al.*, 2006).

Nojima et al. (2007) argued that *T. enshuensis* differs from *T. machikanensis* in the following skull measurement ratios: 1) skull table length and width; 2) supratemporal fenestra and skull table areas; 3) supratemporal fenestra length and width; 4) supratemporal fenestra length and skull table width; 5) radius of curvature of the medial orbital rim and skull table width, and the slenderness and curvature of tooth crown.

However, use of the skull table measurements in *T. machikanensis* (MOUF 00001) is dismissed because of the reconstruction error: the region between the possible frontal-parietal suture and the interfenestral bar is filled with plaster in *T. machikanensis*. A direct observation of the specimen showed that the medial edge of the supratemporal fenestra is unnaturally angled at the plaster-interfenestral bar boundary, suggesting that the supratemporal fenestra, as well as the entire skull table shape was originally much anteroposteriorly shorter. Moreover, size-dependent change in the skull table and supratemporal fenestra shape should be taken into account. In the modern longirostrine crocodylians (*Gavialis gangeticus* and *Tomistoma schlegelii*), length-width ratio of the skull table changes significantly through growth, with wider skull table is attained in larger sized individuals. The supratemporal fenestra is narrow slit in small individuals, with the long-axis oriented anterolaterally (Iordansky, 1973; Dodson, 1975), while its long-axis orientation is altered to anteromedial

through growth, due to the internally-overhanged and straightened lateral edge of supratemporal fenestra, which gives more angular impression of the supratemporal fenestra.

Nonetheless, *T. enshuensis* (Supp. Fig. 1) is largely differs from *T. machikanensis* in the thickness of the lateral and posterior bars of supratemporal fenestra. Both bars are notably thicker and robust in *T. enshuensis* than *T. machikanensis*, and the latter is similar to *G. gangeticus* in having "thin crest" like posterior bar of supratemporal fenestra (Jouve et al., 2015; char. 179). In *G. gangeticus*, this feature is manifest in very large individuals, whereas smaller individuals that are comparable in size with *T. enshuensis* (HH709) have quite narrow posterior bar of supratemporal fenestra. The extremely narrow skull table behind supratemporal fenestra is characteristic to derived gavialines and *Dollosuchoides densmorei* from the Middle Eocene of Belgium (Brochu, 2007).

The use of tooth aspect ratio and curvature for the lower taxonomic level identification in crocodylians should be avoided because extant crocodylians, including *T. schlegelii*, are known to grow more robust teeth with growth. In addition, all the teeth measured by Nojima et al. (2007) are found isolatedly and thus their precise tooth positions are not clear.

The occlusal pattern of maxillary and dentary teeth of *P. pani*, *T. enshuensis* and *T. machikanensis* are quite contrasting: interfingering pattern in *P. pani* and *T. enshuensis*; overbite pattern in *T. machikanensis* (Aoki, 1983; Kobayashi *et al.*, 2006). Close examination of *T. machikanensis* revealed that the overbite pattern is limited to posterior maxillary and dentary dentition that gradually shift to interfingering pattern anteriorly. Meanwhile, observation of its extant relative, Malayan gharials (*Tomistoma schlegelii*) indicate that overbite occlusal pattern in posterior dentition is characteristic in large individuals with the skull length over 80 cm (e.g., BMNH 94.2.21.1; ZSM 370.1907). Given the young Malayan gharials clearly exhibit interfingering pattern, this is interpreted as size-dependent character change, perhaps caused by the packed posterior dentition in large individuals. It might also be true that the shift in the occlusal patterns over size is globally present in crocodylians: thus caution should be taken when scoring the occlusal patterns in very large individuals, considering the importance of this character in crocodylian phylogenetics.

The large excavation on the ventral jugal at the base of postorbital bar is present in *Toyotamaphimeia machikanensis*, which is absent in *T. enshuensis*, and is damaged in *P. pani*. The ventral jugal depression with bottom perforation, although not as prominent as in *T. machikanensis*, is often present in the extant crocodylian *Mecistops cataphractus* (e.g., IRSNB 17962; SMF 43977) and *Crocodylus intermedius* (e.g., FMNH 75660; SMF 55155). In those species, perforations at the bottom of the large depression leads to large internal room at the base of postorbital bar, and this room is interconnected with medial jugal foramen and dorsal jugal foramen. Compared with these extant crocodylians, *T. machikanensis* has considerably deep ventral jugal excavation. *T. enshuensis* has a shallow depression on the

ventral jugal as is generally in crocodylians, which is even shallower than that of *M. cataphractus* and *C. intermedius*.

The convex posterior articular facet of second sacral centrum in *T. enshuensis* is unique and not known in other members of Crocodylia, while diagnostic to the stem crocodylian *Isisfordia duncani* (Salisbury *et al.*, 2006). However, it could potentially be an abnormality because some captive individuals of extant crocodylians show platy to slightly concave anterior surface of first caudal centrum, and accordingly, caudal surface of second sacral centrum is platy [e.g., *A. mississippiensis* (AMNH 31563; AMNH 43315); *C. yacare* (AMNH 97300); *C. palustris* (FMNH 51691)].

Methods of postcranial metric comparison

We used the limb and vertebral metrics that show large disparity among recent forms to obtain systematic and functional inferences in the postcrania of East Asian "tomistomines," specifically a near completely preserved skeleton of *T. machikanensis*. Ulna length / humerus length ratio was acquired from 64 individuals of 17 modern crocodylian species (7 alligatorids; 8 crocodylids; 1 tomistomine; 1 gavialine) and the holotype of *T. machikanensis* (MOUF 00001). Forelimb propodial, epipodial and metapodal elements (humerus, ulna and radius, and metacarpals) are known to scale differently through growth in *A. mississippiensis* (Dodson, 1975; Livingston *et al.*, 2009), and thus similar forelimb scaling is expected in other crocodylian species. Therefore, we corrected the allometric scaling effect among the forelimb elements by using the equation $M_{adj} = M(L_s / L_o)^b$, where M_{adj} is the normalized length measurement, M is the original length measurement, L_o is geometric mean (GM) of humerus length (HL), ulna length (UL), and metacarpal III length (MCL) for each individual. L_s is the average L_o for all individuals, and b is the regression slope of $\log_{10}M$ on $\log_{10}L_o$ using all specimens (Elliott, Haskard, & Koslow, 1995; Pierce, Clack, & Hutchinson, 2011). GM of all forelimb elements are calculated as: $GM = (HL \times UL \times MCL)^{1/3}$. The normalized measurements are used to calculate the allometry-corrected UL / HL: UL_c / HL_c.

Zygapophyseal length (ZL) / pre-zygapophyseal width (PZW) ratio of posterior dorsal vertebrae (D6-D15) was calculated in 28 individuals of 14 modern crocodylian species (6 alligatorids; 6 crocodylids; 1 tomistomine; 1 gavialine) and the holotype of *T. machikanensis* (MOUF 00001), and the ratios were averaged for each individual. The average ZL / PZW of posterior dorsal vertebrae is functionally related with mediolateral intervertebral stiffness, and long relative ZL indicates increased intervertebral flexibility. Other potential morpho-functional metrics (e.g., dimension of centrum, zygapophyseal angle, neural spine height, and transverse process width) were not used in this study because of the small inter-specific and inter-group variation, but detailed species comparison of the comprehensive vertebral shape dataset is currently underway by the first author.

Difference in the mean of each metrics (UL_c / HL_c, ZL / PZW) among four groups of modern crocodylian (Alligatoridae, Crocodylidae, Tomistominae, Gavialinae) were examined using Tukey-Kramer test, although Tomistominae and Gavialinae include only one species each. Followingly, linear discriminant analysis was conducted using the four taxonomic groups as categories and each metric as a covariate, to predict the group belonging of *T. machikanensis*. All measurements were acquired by Tresna point digital caliper (Series SC02, ID 111-203, resolution = 0.01 mm), and statistical analyses were performed using JMP Pro 12.0.1 (SAS Institute Inc.).

Results of postcranial metric comparison

Tukey-Kramer test revealed that *Gavialis gangeticus* has significantly different UL_c / HL_c from alligatorid and crocodylid species. Near, but not significant difference between *G. gangeticus* and *Tomistoma schlegelii* is most likely due to small sample size ($n = 3$ for *G. gangeticus*, and $n = 2$ for *T. schlegelii*). For ZL / PZW, *G. gangeticus* is significantly different from all other groups. Linear discriminant analysis produced significant functions for UL_c / HL_c (Wilk's lambda = 0.483, F = 21.37, $p < 0.001$), and for ZL / PZW (Wilk's lambda = 0.171, F = 38.69, $p < 0.001$). Although 46.9 % and 53.6 % of the specimens are misclassified with each function, all *G. gangeticus* are correctly classified, and none of other species are misclassified as *G. gangeticus*. With each function, *T. machikanensis* is assigned to *G. gangeticus* category, with posterior probability of 0.952 and 0.923 respectively.

Characters and character states modified and newly added in the phylogenetic analysis

The morphological characters used in the phylogenetic analysis are based on Jouve et al. (2015), which is in large part derived from Brochu (1997a,b, 1999), with additional information (Benton & Clark, 1988; Norell & Clark, 1990; Buscalioni & Sanz, 1990; Clark, 1994; Brochu, 1997a, 2004a,b, 2006, 2010, 2011; Ortega *et al.*, 2000; Buscalioni *et al.*, 2001, 2011; Wu, Russell, & Brinkman, 2001; Hua & Jouve, 2004; Jouve, 2004; Salisbury *et al.*, 2006; Ősi, Clark, & Weishampel, 2007; Delfino *et al.*, 2008; Jouve *et al.*, 2008; Pol, Turner, & Norell, 2009; Shan *et al.*, 2009; Brochu & Storrs, 2012; Brochu *et al.*, 2012). The following are the character and character states modified and newly added in the current analysis.

19. Axial hypapophysis without (0) or with (1) deep fork (character states were switched from Jouve et al. 2015).

22. Scapular blade greatly flares dorsally, and fan shaped (0), minimally flares dorsally (1), or narrow and subparallel (2) [modified from Brochu 1999 (22), originally adapted from Benton and Clark 1988].

239. Axis odontoid process in anterior view: ventral portion (facets for axial rib parapophyses) narrower than the dorsal portion (facets for axial rib diapophyses) (0), or ventral and dorsal portions subequal in width (1). New.

240. Second sacral rib expands posteriorly to the level (0) or well beyond (1) the posterior end of centrum. New.

241. Metatarsal II longer (0) or shorter (1) than metatarsal III. New.

Morphological data matrix used in this study (66 taxa with 241 characters)

Bernissartia_fagesii ??11?1210?010????00??0?0?0000??00010101000?0?????0100??????110?0?00000100?2?000000101100302030 1?00?00110100100?000?000?0???0??????0??00??0100000010?00001???????00??000?0?0001000?0?0?0?00??0100001?0000000?0101000003?00?00000??01???00?1?00000?

Iharkutosuchus_makadii ??0???1???20??????110?1???210200?0?1000?3001120600?201?00?00?0?000000?00??0100???1000???1??0?0????00000100?1000????????0???00110000220001?01?1??0?0?1101014 1?0100010200210????0??01101000 1???10?1001????

Hylaeochampsa_vectiana ??1?????0200??1?0?000?01100600120???0?000100?0000?00??0101???0??000?1000000?0100?00?100?000??????????0?001??000?21?0?00??1??00001???0???0011?????0?210????????1101??0????10?1?0?0???

Allodaposuchus_precedens ??0?????120???1120000?0110?2?00??1?0??000100?00000?0???00011?000010?1?0010??110000001??0001???????0?0?000000??0?0?0?000?????010100?0??00000010?0110?????0??0000?0200????0?100?0???

Eothoracosaurus_mississippiensi ????????????????1????000??????00?00???0??40???0011?1??????0?0?0???2?1200?01021?00?1100050?1?03?00?00100000000000???01000?0?0?????1?00???111000100?1?00????????00??1001102?010110000??0100001 00?0230000?0021?0000?????00?0000002?2???00?11??0???

Eosuchus_lerichei ???0?1???????????1????????1???????0???????4????????11??????????0???201200?0?021?2?0110005011002?00?00?000?00000300?001000?0000????010?2?0?1110001 0??10113??????0?0?110100?0000010?100????0000101002300 0?0021200000?2?100?000010202???00?11000???

Eosuchus_minor ???1?1????0??????11??00?0?100??000000??0?0400000011110?0??00?2?00?02?1200?0102102001100050110 2?00000?00000000030???0100000000?0?1010020?0111000100?1?1?3???????000?10100?00000?0?100???1000010100230010 1?0?1?00000?2??00?00000??02???00?110?01??

Ocepesuchus_eoafricanus ??0?????1????0??????1???10?5??00??????00??0?????????????2???1?0???????????0???11??

00?????00?????????????1?0???0???0?0?1???????0001???????00???????0????????0?????00?
?0?????0?????0???
Thoracosaurus_macrorhynchus ??11?1?1??0??????11??????0??0????000???0??400??00?11?
??????0?100000201200?0102100101110050?1003??000011000000000000?1010?000000?0?
0?1000?0?111000100?10012???????000?1001100??00110100?10?000011100230000000213
00001??3?00?000001202???00?11000???
Thoracosaurus_neocesariensis ???1?1?1????0????11??????01?0???0000???0??40????01?11?
???????1?00?020120000102 1?0101100050?1003?000001100000000000?010?0000000000
0?000?0?111000100?1001????????000?100???0?000?1?10???1?000?1??00230000 1?0?1?00
001?23?00?0?000???2???00?110?01??
Aktiogavialis_portoricensis ??
????0???????0?1??????11???10????1??????2???120??0?????1?????0??00?????0001????????
?????????1??????????????0???????????10??????0011???????0??1?????0???1?????????????
?????????1???0???
Eogavialis_africanum ?????1??????0?????11?????????????0?????0?060??10?1111??????1?2
?000020020000102101101100050 1001002?020001200000000000000100000100?0?00100000
0101000100?101030??????000?100100000001012 01?110000111100230000110213000 01??
??00?000001202????0?110?0???
Argochampsa_krebsi ??11??????0??00???10?????0?????????0??????[46]????????11???????
???2????2?1200?000210110??10?5??1003?0??001100?00?000????01???00000???0?1010?1?
10100010???01?0???????0?0?1001200?000?0?111?10?011111000230000100213000 0??2??
0??0?0010002???00?110?0???
Piscogavialis_jugaliperforatus ??????????????????????????????????0?????6????0???11???
????0[12]?2????2?1200?000211210110005011?03?12?00?100?0000?00??001?00001000??00
1000???12100010??10103???????0?0?1001202111?2013?1?11?01?1111002300001002130 0
001??3?0??000000002???10?11000???
Ikanogavialis_gameroi ??????????????????????????????????????60???00??11??????0?2
?20?02?120????020?210??10?501?0?3?02?00?20???0?0?00???010?0?01???0??0??00???321
000100??01?3???????00????0?20?101020?3??????0?1111100230100100 21?00??1????0???0
000?202???10?110?0???
Siquisiquesuchus_venezuelensis ??????????????????1?????????????0?????????60?0??0??11
0?0???????2????2??2???0?021??1?1??0?50?1?0??02??01200??000?0?????10?0?0????0?????
00???321000100???1?????????00??1?0?20??1??20?3?????0000?111?02301?11?0?1?00?0??
???0????00????2????0?11??0???
Gryposuchus_colombianus ??1?0?????00?????1????000?????????????0?060000001111100
???00202000200200101021011010100501111 03?020001200000 00?0100001000001000000
1000???321000100?10103???????000?100?10[12]0100111311?1100111101002301011102 1
300001????00100000??021??10?110?0???

Gavialis_gangeticus
02110101100000000110000000100100000?0003000600000011110000100020000020020000
10210110111005011104002000120000000001000010000010000000100000031100010001010200000000000100120211102113111110011110010230101110213000010231001000001202000100110001000
Siwalik_Gavialis ????????????0??????????????????????????????60???0??????????????2?0000200200?01?2?0?101??00?01??04??20?012000?000?010????000001?000??01000???311????00?10102???????000?1001?021110?11311?11001111001023010111021300001????00?000001202???10?11000???
Borealosuchus_sternbergii ??0001?10?110000?11000000000100010000???000300?0001001??00?00200000001200001010000001001301101210?0000010000000000000?00011001000000101011?1?11100000001000102?????000?010011000?000010000011000100000000000000012000000????00?000001200???00?10000???
Borealosuchus_wilsoni ???????10???0????1???00000001???10000?20??10?0000?0010?0???011?000000120000102001001100301100200?00000100000?00?00000211??01????0??010011?1?111????0??1000????????000?0??01??0????0?10?????????10000020000?00?120?00?????0?0000012?????00?10??0???
Borealosuchus_formidabilis
00000101001100??01?000000000100010000?200030000?010010?00100120000000120020?0?020000001100301100200000010000000000000?021100?100000??010?1010111000000?10002???????000?0100110?000000100000110001010012000000011200000123000?00000120?????00?1000011?
Leidyosuchus_canadensis ????????????????1???????1?01???0111??110?300?011110??????????2?000000120000100000000100130210 11?000020010000001010000101010000?101?10?1?111000010?10001???????000?0?00110000000000?000100010010110000100102010000??3?00?0000112010??00?10010???
Diplocynodon_darwini
100000?000010100010 1?000?1141??00110112100101001111 01??000?1?2?00000112?0?01100000011013 1?1002?000002000000 00?101?000101?1000?0??12?10???111000010?10001???????000?011001?????0000000?0110??100001100000001 0?0?00012310 0?00001?20???00?100?0???
Caiman_crocodilus
10001100011001011101120111111000011112211122011111011010011102000110112101021111240000112121101000000211101000010101001010100000012211011021100001001021[12]01110110011011001000010000000001100010 0[01]002000[01]000102000001231000000000100000000100100 11
Alligator_mississippiensis
10001100010101001101111011111000011121311120100111111100001113000000112101 0

2101022000101212120000010021001000001011010101010000001221101101111000100100210110011001101100100000000000000011000100100010010001020100012310000000000100000000010010011

Brachychampsa_montana

10001??00111?10001?10?00011010000?10311110100?0111111???00?112?00?0011210102101013000001112120 1?000002000001000101000010101300000112110?1?111000110?10010???????000?01100100201?001000?011000110101110011001020100012?100?0000101010??00?10010???

Stangerochampsa_mccabei ??00?1?00?010????11??000?11010000101??110100?001??111?????12?011001121010210101000000121212 01?00?00200000?00101?0001?1?1300??????10???111000110?1?010???????000?011001002010001 00??011000110101110010001020000012?100?0000101010??00?10010???

Planocrania_hengdongensis ??0????01?11?????[12]?0???0?12?????010??0?0100030?1?01????002000?????01????????1????????10???0????11????00??0??????????00??0???00??????0010???11?00?1??02110000000 10?0000?????1??00001?1??????0?1???0???

Planocrania_datangensis ??11????????0?????12?????000?00?0?00?30?1?01?0??00210?????00??????0????1?00????0???0?????10001?0?????????????0???0?1?0????0100010???1??0??11002??0000000?0?00???????1??0?001???????00?12??0???

Boverisuchus_vorax ??000101??01???0?10??00000111??00010???100001?0??1?11????????2?00000?1200?0100002000100030010 01?000001100000000020?0000100?1000?1?102010???111001000?10001???????00?0?11001100010001 00?00110001000110?000000102000002?3?10?00001010????00?1?0?0???

Asiatosuchus_germanicus

001001?01100????1101?000?11?1???01?????1000???0001011???00??12?00000?1201?0100001000?10?10?10?1?000002000000011 30??000??0?100??1??01?10???0110000?0?10001?????????000?0110?10???10001?00?011???100?010000?0001020?000?2??00?0?001?10?????0?1?010???

Prodiplocynodon_langi ??0?????1200?0?001?10001?013?01?01?00??02000?0001130?00?01?01100001?1???10?10011000?00?10001???????0?0?011001?00???00100?00?1000100?0??000?00000201000????0??0000?12?0???00?12010???

Crocodylus_depressifrons ???000100???1????10??00001111??00110???11010??0001011?????112?00?000120100201102300100110 01?01?0020000?0011301?000010?1000?1?10?010?1?01100000001 00?2??????00???011001000000000000??01?000100?012000000010?0100?123101?00001110?????0?120?01??

Crocodylus_affinis
0000010001101100110100000111100001 10???1101000000101110000011200000001200?0
1011?2000100110010 01?0000020000000 1130?000000011000?1??01010???011000000?100
011??????010?011001000000001000001100010000120000000002000001231 01?00001?100
???00?12010???
Crocodylus_acer ??0???
?01200?0?02112000100110010 01?00?00?000?000103000000?01100011??01010?1?01100
0100?1000????????0?0?011001000 00?00100?00?100010000???000000?0200000????0??00
001??0????00?1?000???
Brachyuranochampsa_eversolei ??
??????2?0?????1200?0?021020001101100 1001??00002000?0?0?030??00?0?0?1?00?1?????
10???011000100?1000????????0?0?0110010?0?0?00100?00?100010010120000000020?00
0????0??00000?101???00?120?0???
Crocodylus_megarhinus ????????0????????1????????????????????101???000?011??????1
12?000000120002?02112?101?013001?01?010002100000 00?300000001011000?11?01010?
??011000000?1000????????010?011001?0????00100??01?000100?0??000?00000?0100????
?00?0000011?0???00?12010???
Harpacochampsa_camfieldensis ??
????????0????01?0?12?0211211???0?1?1???1?01???2?????????000?0??0?0?100?1????201?
???0010??0?0?0??00?2????????0?0??1?0?1?0?????0100?10?0000?00?0??000?00000?0?00????
?0??000??11????????1?0?0???
Kambara ????????????????1???????1?11??00110???110111?0001011??????112
?000000120112002112010100010110 01?0100121000000100000001011000111100020?010
101?011001010011?????010?000110011000000010??00110001000 0??000000010?00??????
?00?000001100????0?120?0???
Australosuchus_clarkae ?????1?0?????????1???????1??1???0?10???110111?000?011??????1
12?0000001????2002112210?00?1?11001?0?00021000?0000100?00101011000?11102010?
1?011000100010 0?11??????010????00100000001?00?0?????100?00200000010?0?0?????
?0??0000?1100???00?12??0???
Mecistops_cataphractus
100001000?001100?10100001112120001111131101110100101110010 0?020000000120011
002112010100110010020010002100100100300000101011000111101010111011000000110
002101010101010110011010000010000011000100001200000002120000112310000000111
0010000013010111
Crocodylus_porosus
111001101100100011010100011212000111123110111010010111001001120000000120011
002112010100110010010010002100100100300000001011000111101010111011001001110

00110101010101011001001000001000001100010000020000000002010011231000000001100101001012010111

Crocodylus_niloticus

10100100111010001101010011121200011112311011101001011100100112100000012001100211201010011001001001000210010010030000000101100011110101011101100000111000110101010101011001001000001000001100010000020000000002010011231000000001100101001012010111

Crocodylus_rhombifer

00100100111010001101010011111200011112311011101001011100100112000000012021100211201010011001001001001210010010030000000101100011110101011101100000111000110101010101011001000000000100?00110001000002000000010211000123100000000110000?0100012010111

Crocodylus_palaeindicus ????????????1????1??????????????1??????1011?0100??111?0??0112000000012001100211221010011 0?1001?0100021001?0100300?000010010001111010101110110000011?10001???????010?0?1001??0???001???00?1000100000?000?00000?0100????0??0000011?0???00?12?10???

Rimasuchus_lloydi ??1??????????????????0????0120?11002112010?00?1?011?1?0100021000?0000300??00?1011000?11101?10111011001000??10?1???????0?0??1?001?0????001????0??00?100?012000000010201000?????00?0000?11?0???00?12??0???

Voay_robustus ????????????1????10???????111??101?????1101110001101110 0??0112000000112021100211221010111001011?0100021001000103000000010?100011110101011101100100001100 1??????011101100100000000000000110001000012000000010211000?23100?0000001001??00?12010???

Osteolaemus_tetraspis ??1001100100100?1101010011111201011111111011100001011100100112000001120211002102010111110010101110002101000010300000011011000111101010111110010000110011010101011101100100000000000000011000100010200000001020000012310 0?000010100111001120100 11

Euthecodon_brumpti ????????????????????????????????????10???1?0411?000?021??????002110?02?1202110021110101101501?1003?01?00210010010030??00001011100?11101010???0110011000110 03???????011?0111111?0?0200000?00?0000111002300000000120000?????0??000001202???00?11010???

Euthecodon_arambourgi ??4????????????????????1?????1????1002112010?10?50?1?03?0?00021000?0000301??00?10?1100?1?101010111011001100??1003???????0???0?110?1??00?000?0??0?????101?023000000001?0000?????0??000001201???00?110?0???

Maroccosuchus_zennaroi ????????????????1????????????1???00110???1??30??00?1011??????112?00?0000201?000211221010001 0?1101?01?00210000100 13?0?0011?0?1000???001010

?1?01100010??10002??????0010?011?011?0000001000?01?000100001200?100202000??3?0??0?00011001??00?13010???
Kentisuchus_spenceri ??????????????????1?????????????????????????311?0?0???1??????1?2?0000??1200???021020?010001001101?0?000?100??100?30??0011???100011?????10???011000100?10002??????00?0?0?1001000100000100?001100010100??00?010020200?00??3?0??0000011?????00?13000???
Megadontosuchus_arduini ??????????????????1?????????????????1???????[35]???1?0??11?????0?2?00??0?0????0?021?20?0?10?1??1??1????00?1?????????????1????10???????1??0??20110001?????1?????????0???0?1?012???010?1????0?????1?1?0???0?0100?0?0???0?2??0?????00110?????0?1???0???
Dollosuchoides_densmorei
0010?1?00111?????1??????011????0010???????3???00?1111???????02?00??2?0200?0?021?20?1100010011102?11?00?000001?0?3???0011?0?1000???????10???011000100?100?2?????010?011001000000030??011000101001200001102020000012?100?00001?200???00?13001???
Thecachampsa_carolinensis ???001?01???1000?10??0?01??????00100???1?0531?00??011????002?00?02?0200?0?021?22?110001001?02?01?00?10010?00030??0010???10?????????0????11000100?100?3???????01??0110012?0?000??01?00?0000101001?0020?00013000011 2?100???0000200???00?1?1001??
Thecachampsa_antiqua
021001?000001000010??01011?11???01?0???1??531?????0111000????2000002?0200001021?22111000100?102?0100021000000030?000101?11000?1?001010???111000100?100031??????010?01?00120000000201?00?000010100120020100013000001????00?000000200???00?131001??
Penghusuchus_pani
00110?101100?0000111??10101011000000???0?040??00?1?1????00???2?00?02?0201????2??2??11??07?1?1????110021?000??0030??02100???????0?0??01011101100101?1010?????????00?001?0100000100?0??00110001??0010??20??0??300001123100??0001??11???0011010?11?
Yage_tomisotomine
0????1[01]1?1??1?00011??01?111111000000???100[345]00??0?1?11??????1?2?00?0??????????2??201[01]?00????1??[234]????00?10?0????0?????0??1??1?????????????????01??00???0????????????00???????0???0??02?????1????????????[12]????????0?????2?1?0????01?????????0?1???0???
Toyotamaphimeia_machikanensis
001101011111?1?0011??0101111110000000???000400?10?10?????00?102?00?02?020??0?021?2?1?1?007011?02?01?00210000000310??0?0???100??0?0??010???011000101?10103?

??????00??0?100100000?00300000110001110??0?00?00213000011231 00?0000?11?1???0
0?10?0011?
Tomistoma_cairense ??501?????01???????0?2?0
0002?0200?01?2??20?1100050?100?????00?100000?0?30?00010?011??0?1??01?10???011?
00?0???000?????????10???1??10??0100000??00110001??00??0000??0?131000?????????00
00??02???00?11?00???
Tomistoma_coppensi ??3??????1?11????????2?0
???2?12?????021?20101000 1??1[013]?2?0??0021?00???0?3???00???0?0??0???????10???01
100010???00?3???????0???011001000?0000000?00?10?010?001?0000?1121?0000????????
0000012 0?????0?11??0???
Paratomistoma_courti ??00?0?010????????0?2?
00?0??1???0?1?2??20?1?00????10?????000?10?0??????0?0?0?????0???10100?????1??11??
0?00??00??????????10?1?1????2??00???00????1?0001???0???0??1?????0????????0?????00?
?0?????0?????0???
Tomistoma_schlegelii
021001001100100011010000111111000110133110500010010110000000020000020120000
102102210110010111020110002100000010300000101011101111101010111011000100010
003101010101010110010000010000000011000111002000001112130000012310000000 02
1011100111010111
Tomistoma_lusitanica ??????????????????1??????????????????10???1??[35]?0?000101????????
?2?0000201200001021122?1110010?1002?0100021000000003000001010110 01?11101010
11?011000100?10003???????0?0?011001[12]??[01]00002?00001?00?10100[12]202?0?1121
310000????00?00000120????00?110?1???
Gavialosuchus_eggenburgensis ??????????????????1????????????????????????????????
????????0?????120??0?021?2??11?0020?1302???000?100??0?0?0???001????10?0???1????0
?0111100010???0??3???????0???0110011?000?00200??0??0001?100??02?0?1121?1000???
??0??00?001200???00?11??1???

Extant taxa used in the combined phylogenetic analysis

Nuclear and mitochondrial DNA sequences (7282 base pairs) of 9 individuals representing 9 extant species were selected from Oaks (2011), and used in the combined analysis. The following are the specimen ID numbers in Oaks (2011).

Alligator mississippiensis: LSUMZ_H 18733
Caiman crocodilus: LSUMZ_H 13962
Crocodylus porosus: LSUMZ_H 6758
Crocodylus niloticus: LSUMZ_H 21731
Crocodylus rhombifer: LSUMZ_H 21745
Mecistops cataphractus: LSUMZ_H 21718

Osteolaemus tetraspis: LSUMZ_H 6990
Tomistoma schlegelii: LSUMZ_H 21764
Gavialis gangeticus: LSUMZ_H 21748

Fig. S1. Skull of *Toyotamaphimeia enshuensis*. A, B, skull table (HH709) in dorsal view. C, D, skull (HH711) in occipital view. E, F, antorbital part of skull (HH710). G, H, right maxilla (HH586) in ventral view. I-K, left jugal-quadratojugal (HH753) in I, lateral, J, medial, K, ventral views. cn-V, maxillary foramen for palatine ramus of cranial nerve V; e, exoccipital; f, frontal; j, jugal; lpt, lateral posterior tuberosity; mjf, medial jugal foramina; p, parietal; pf, prefrontal; po, postorbital; qj, quadratojugal; soc, supraoccipital; sq, squamosal; stf, supratemporal fenestra. Scale bars are 2 cm.

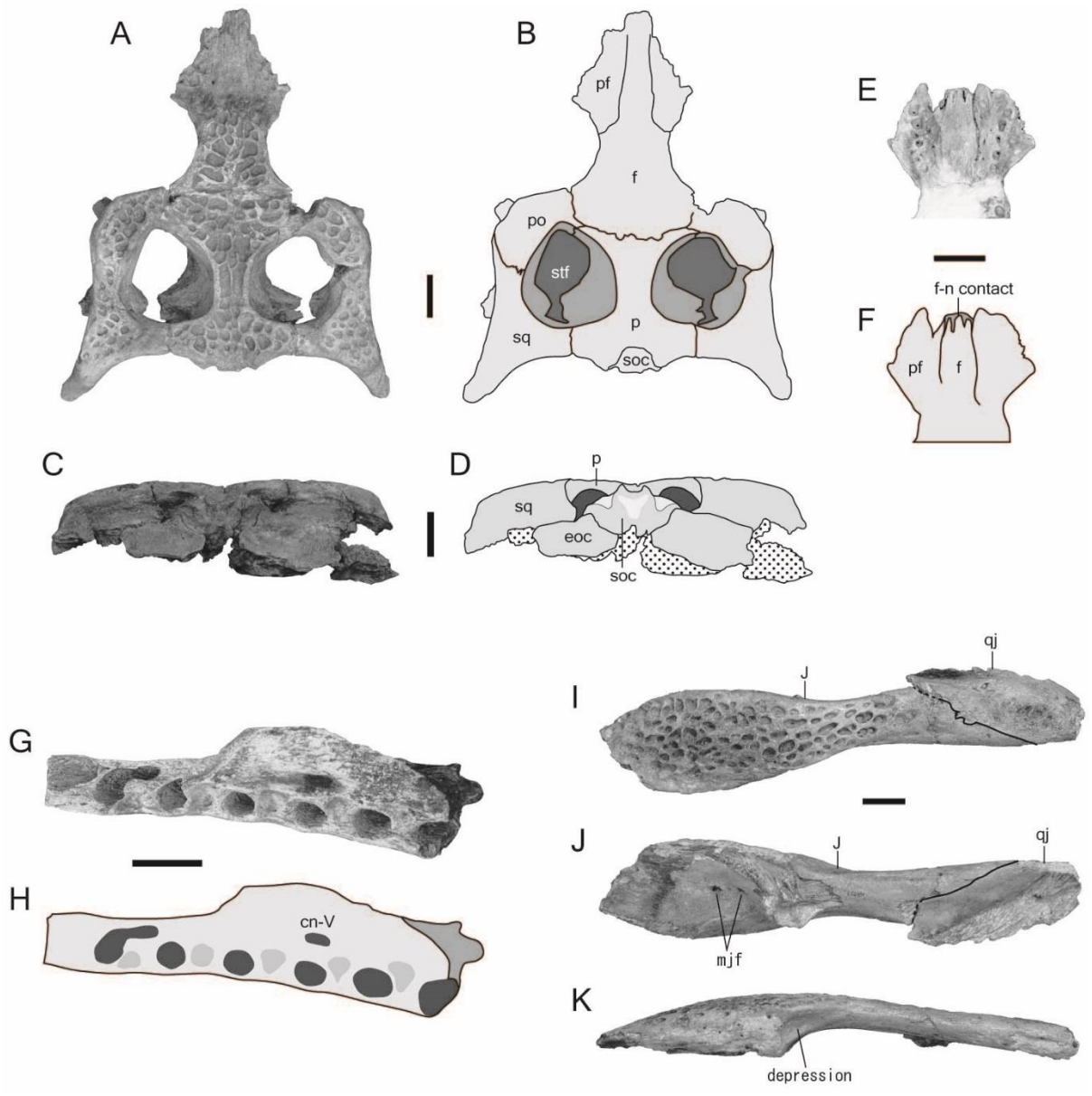


Fig. S2. Lower jaw and teeth of *Toyotamaphimeia enshuensis*. A, B, right posterior mandible (SU1) in A, B, lateral, C, D, dorsal views. E, F, left middle-posterior mandible (T225) in dorsal view. G, anterior dentary (HH589) in dorsal view. H, right posterior dentary (HH535) in dorsal view. I, right splenial (T134) in medial view. J-O, teeth (J, K: unnumbered; L, M; SU57; N, O; T108) in J, L, N, labial, and K, M, O, mesial or distal views. an, angular; art, articular; d, dentary; emf, external mandibular fenestra; fio, foramen intermandibularis oralis; sa, surangular; sp, splenial. Scale bars for A-I are 2 cm, and for J-O are 1 cm.

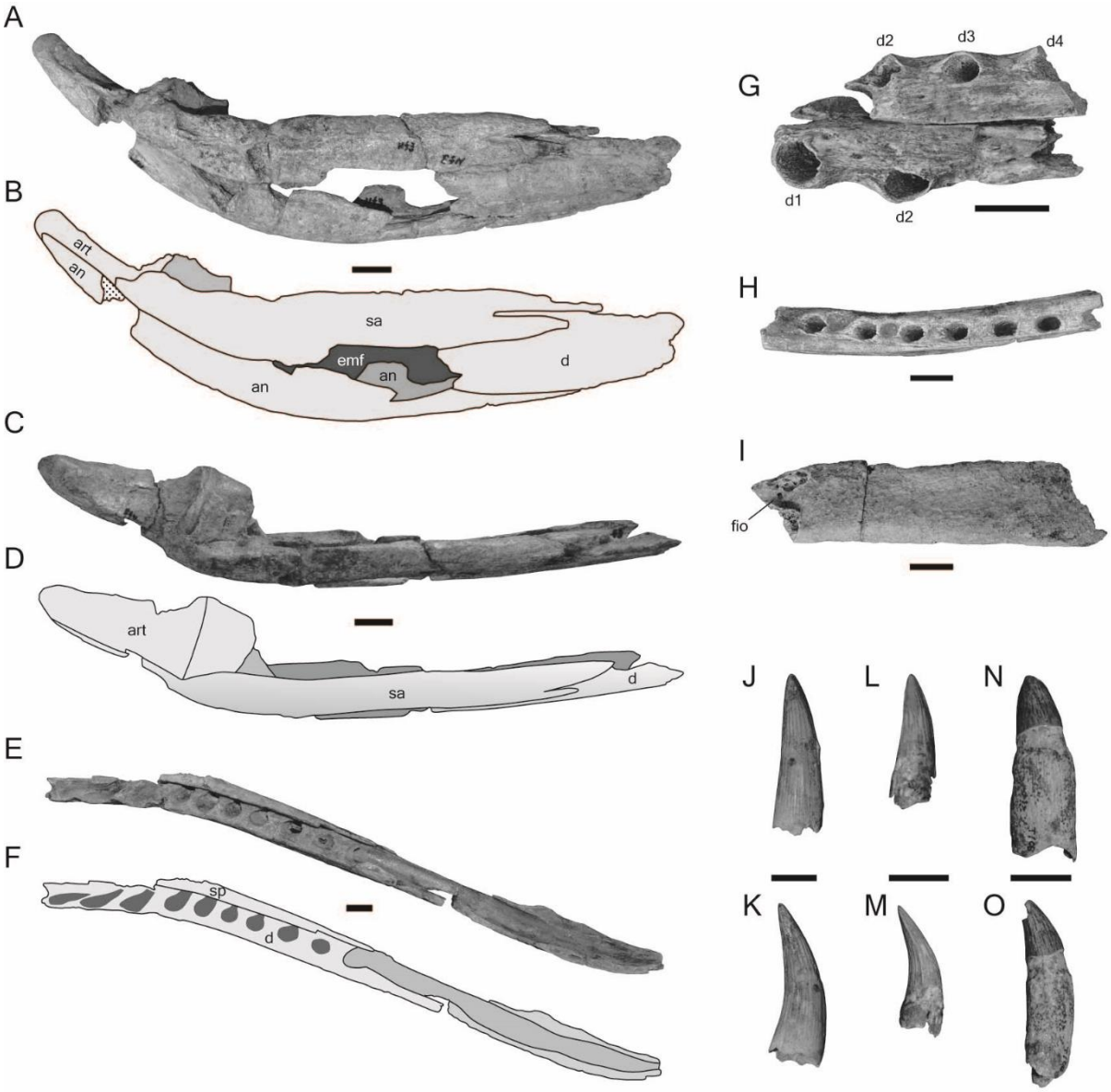


Fig. S3. Anterior cervical vertebrae and atlanal rib of *Toyotamaphimeia enshuensis*. A-C, proatlas (HAH137) in A, left lateral, B, dorsal, and C, ventral views. D, E, left neural arch of atlas (SU37) in D, lateral and E, anterior views. F, G, right atlanal rib (GMNH unnumbered) in F, lateral, and G, medial views. H-J, axial centrum (T114) in H, left lateral, and I, J, ventral views. K-M, fourth cervical centrum (HH376) in K, left lateral and L, M, ventral views. dmr, dorsal medial ridge; hp, hypapophysis; pp, parapophysis; vmk, ventral median keel; vtb, ventral tubercle. All scales are 2 cm.

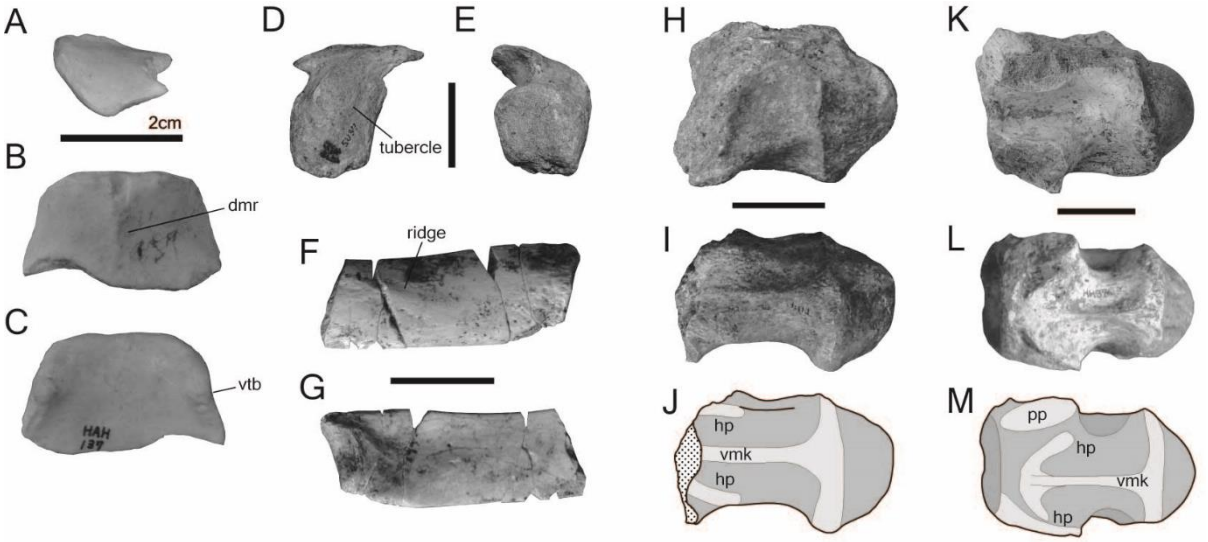


Fig. S4. Posterior cervical to caudal vertebrae of *Toyotamaphimeia enshuensis*. A, B, eighth cervical (K4) in A, dorsal and B, left lateral views. C, D, ninth cervical (K5) in C, dorsal and D, left lateral views. E, F, third dorsal (HH374) in E, dorsal and F, left lateral views. G, H, first sacral (HH414) in G, dorsal and H, left lateral view. I, J, second sacral (HH396) in I, dorsal and J, right lateral views. K, L, mid caudal (SU34) in K, dorsal and L, left lateral views. dp, diapophysis; hp, hypapophysis; pp, parapophysis. All scale bars are 2 cm.

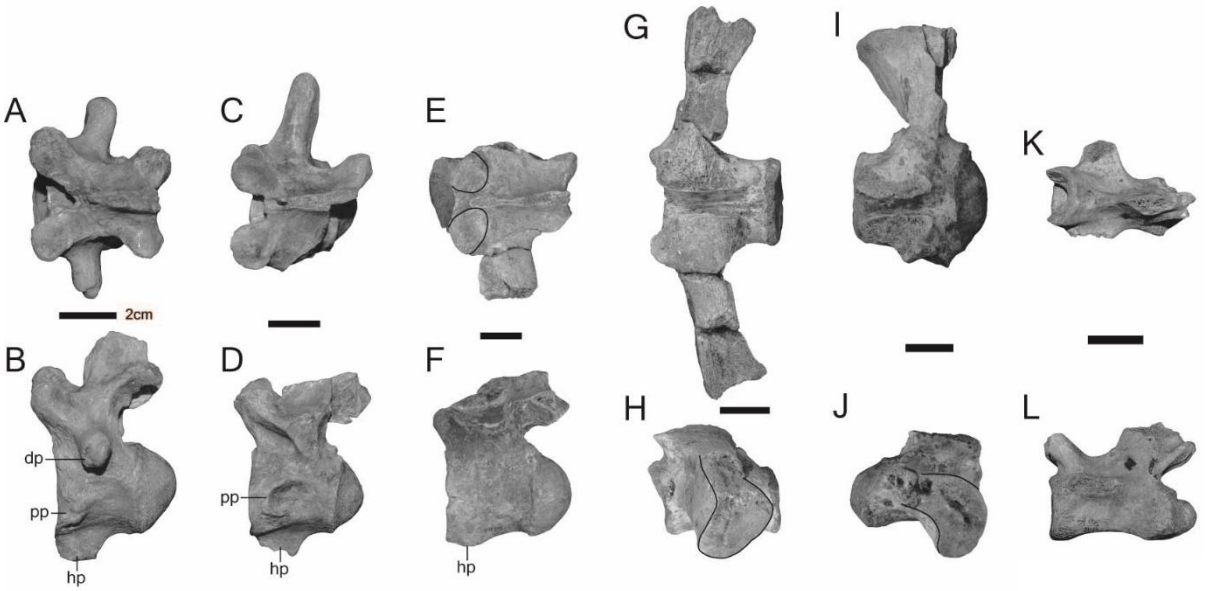


Fig. S5. Pectoral girdle and forelimb of *Toyotamaphimeia enshuensis*. A, right scapula (T203) in lateral view. B, left coracoid (HH715) in lateral view. C, D, interclavicle (HAH59) in C, left lateral, and D, ventral view. E, F, left humerus (K10) in E, lateral, and F, anterior. G-I, right ulna (HH13) in G, proximal, H, posterior, and I, lateral views. J-L, left radius (HH568-HH109) in J, proximal, K, posterior, and L, medial views. M-O, right radiale (HH782) in M, distal, N, dorsal, and O, proximal views. P, Q, right metacarpal I (T102) in P, dorsal, and Q, proximal views. cof, coracoid foramen; dc, deltoid crest; dpc, deltopectoral crest; op, olecranon process. All scale bars are 2 cm.

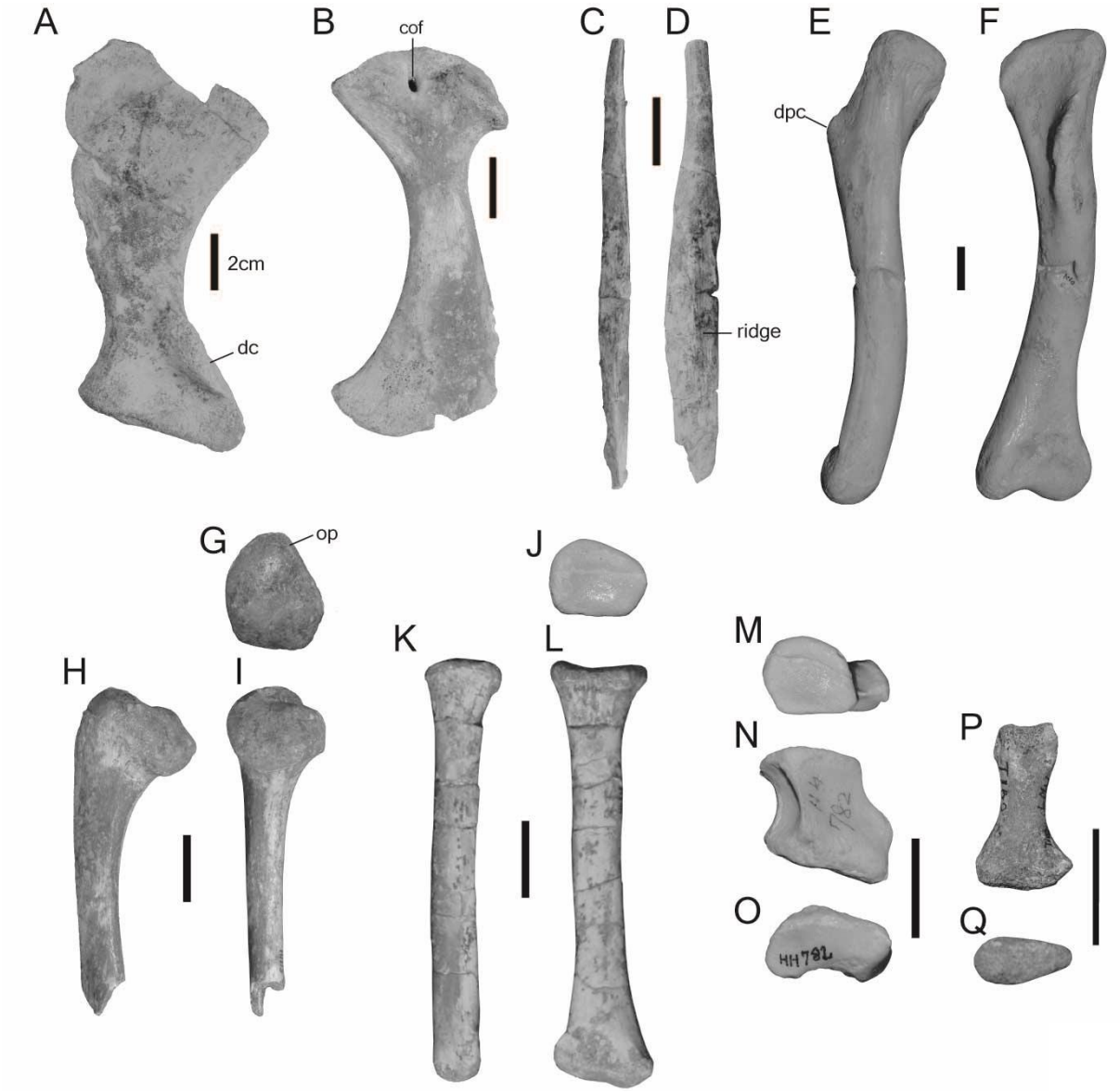


Fig. S6. Pelvic girdle and hind limb of *Toyotamaphimeia enshuensis*. A, B, right ilia (A: HH713; B: HH560) in lateral view. C, left pubis (HH475) in lateral view. D, left ischium (HH474) in lateral view. E, F, right femur (HH719) in E, lateral, and F, medial views. G, H, right tibia (HH1) in G, anterior, and H, lateral views. I, J, right fibula (T185) in I, lateral, and J, medial views. K-M, right astragalus (T36) in K, proximal, and L, posterior, and M, anterior views. N, O, right calcaneum (SU16) in N, proximal, and O, posterior views. P-R, right metatarsals [P: mt1 (HH582); Q: mt2 (HH580); R: mt3 (HH579)] in dorsal view. iac, iliac anterior process; 1, insertion of *M. adductor femoris*; 2, insertion of *M. iliofibularis*. All scale bars are 2 cm.

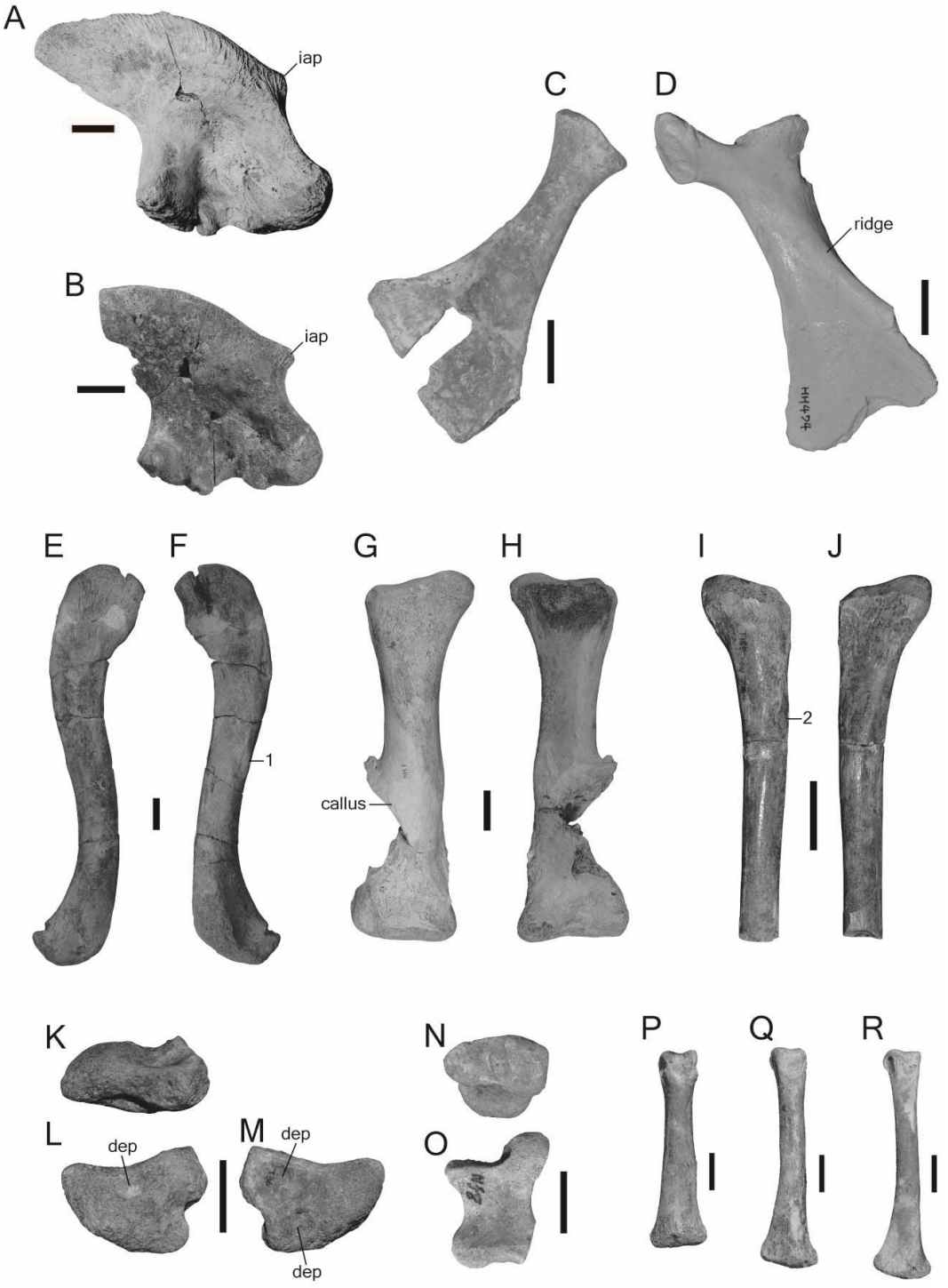


Fig. S7. Osteoderms of *Toyotamaphimeia enshuensis*. A, SH1; B, HH327; C, HH531; D, HH496; E, HH518; F, HH513; G, HH508; H, HH517; I, HH758; J, HH757, in external view. Scale bar is 2 cm.

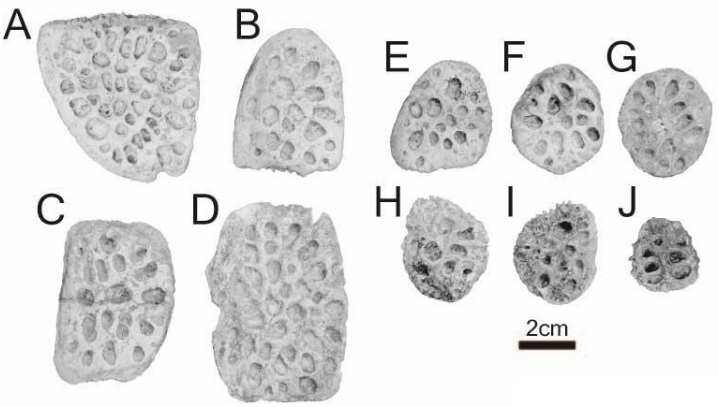


Fig. S8. A strict consensus tree obtained from the parsimony analysis of the morphology dataset without imposing topological constraint.

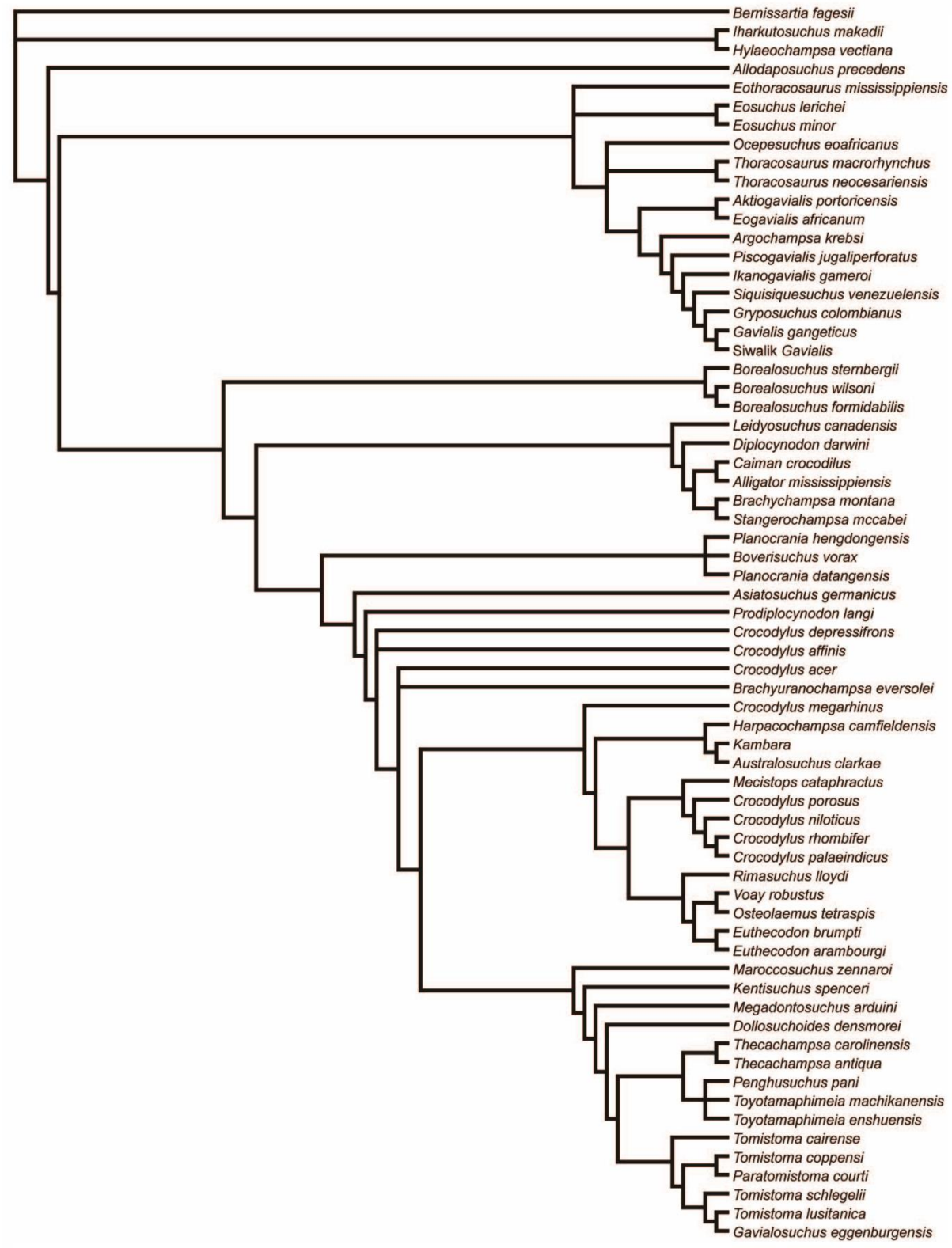


Fig. S9. A strict consensus tree obtained from the weighted parsimony analysis of the morphology dataset without imposing topological constraint. Potential rostrum shape correlates detected by the phylogenetic logistic regression were downweighted in this analysis.

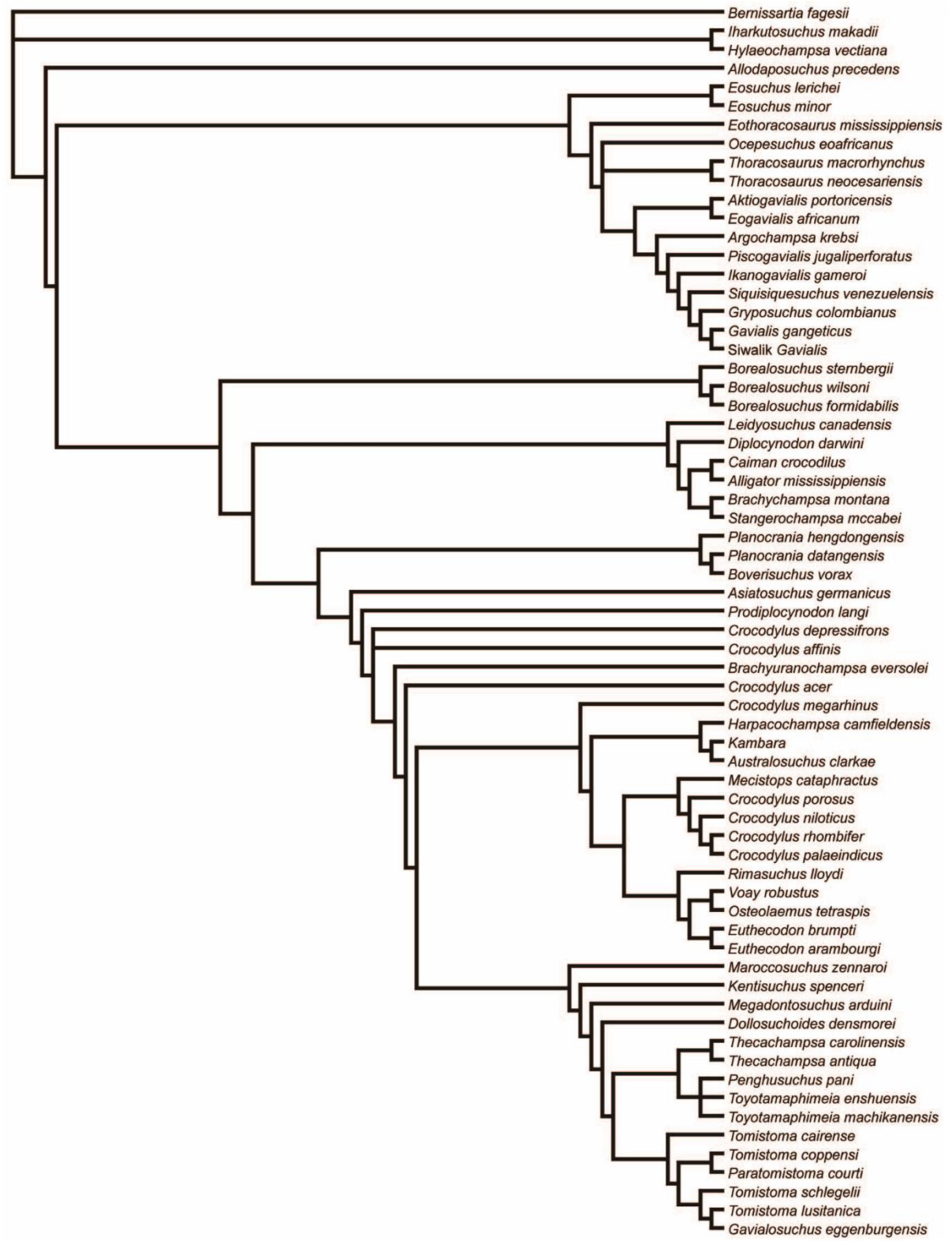


Fig. S10. A strict consensus tree obtained from the weighted parsimony analysis with the backbone constraint on modern taxa. Potential rostrum shape correlates detected by the phylogenetic logistic regression were downweighted in this analysis.

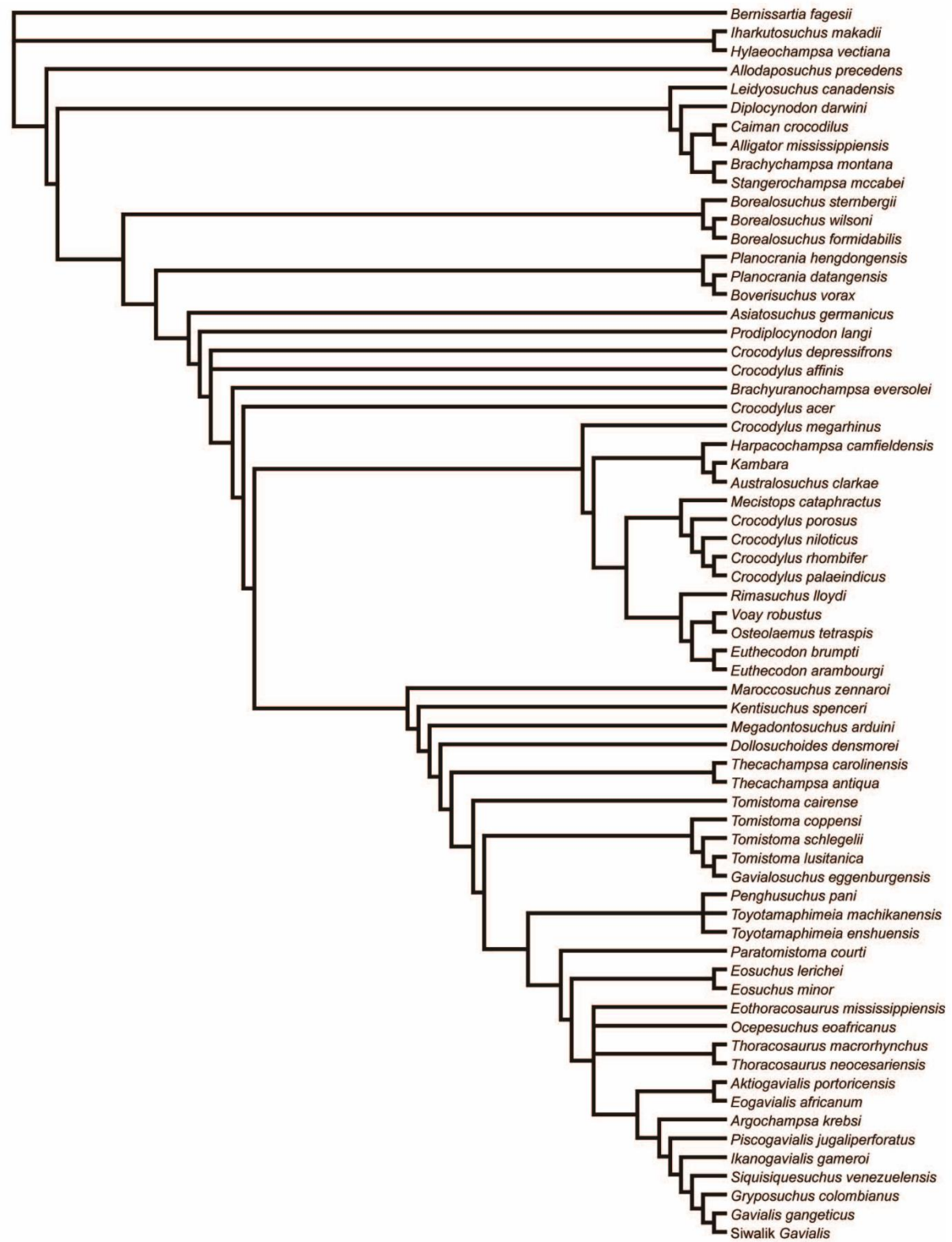
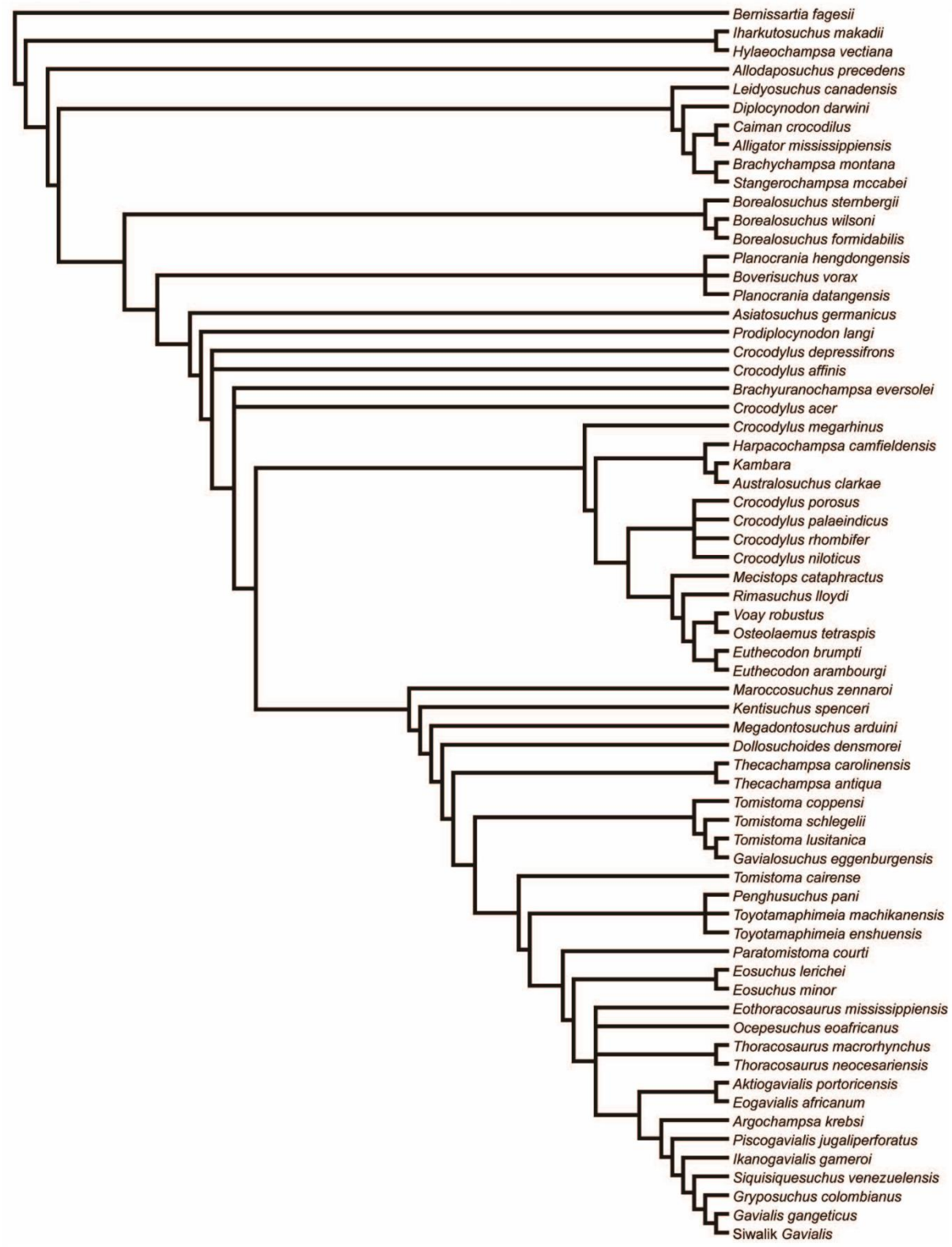


Fig. S11. A combined tree obtained from the parsimony analysis of morphology and molecular datasets.



Supplement to chapter V

Hyoid and postcranial description of the Kishiwada specimen (KSNHM-F7-6).

Hyoid

The anterior portion of the right ceratobranchial (Supp. Fig. 1A) is wide and parallel sided. On its convex lateral surface, a prominent ridge runs obliquely as in *Toyotamaphimeia machikanensis* (MOU F00001).

Postcrania

A cervical centrum is preserved (Supp. Fig. 1B and C). It is procoelous and shows the parapophyses that are positioned near the anterior end of the centrum. The ventral keel (hypapophysis) is prominent towards the anterior end. A right ninth cervical or an anterior dorsal rib (Supp. Fig. 1D) preserves a long capitulum. At the base of the capitulum, there is a small depression on the anterior surface, probably reflecting pathological condition. In the middle of the shaft, a low but long process projects anteriorly.

Several osteoderms are preserved (Supp. Fig. 1E–G), probably representing midline cervical, lateral dorsal, or lateral pelvic osteoderms. Those osteoderms are wider than long in general shape, with complex sutural facets on one side. The anterior edge is straight, but the posterior edge is convex in two of them (Supp. Fig. 1E and G). The anterior margin is smooth and thinning, representing an overlapping facet. There is no sagittal keel on the dorsal surface.

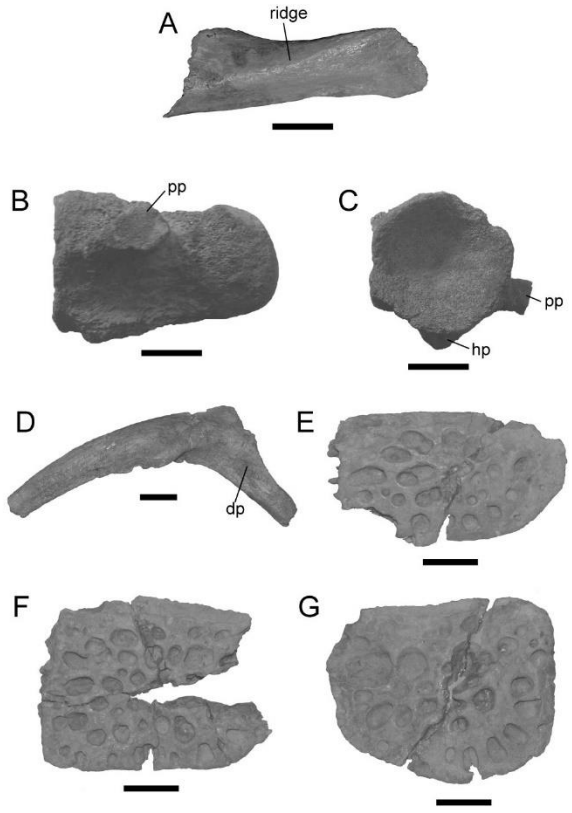


Fig. S1. KSNHM-F7-6 (Kishiwada specimen), A, right ceratobranchial in lateral view; B and C, cervical centrum in left lateral (B) and anterior (C) views; D, left ninth cervical or anterior dorsal rib in anterior view; E–G, osteoderms in dorsal view. dp, depression; hp, hypapophysis; pp, parapophysis. Scale bars are 2 cm.

The proximal shaft of the left pubis (Supp. Fig. 2C) is oval in section, and it is thinned distally. In the distal part, the shaft is thicker anteriorly. The left femur is relatively complete (Supp. Fig. 2A and B) and is 348 mm in length. The femoral head is twisted about 85 degrees relative to the distal condyles. Posterior surface distal to the head is rugose and grooved, representing the greater trochanter. Posteromedially on the mid shaft, an elevated and convex surface is the fourth trochanter. The distal condyles are incomplete and not informative.

The right humerus preserves most of the shaft and the distal end (Supp. Fig. 2D and E). Dorsally at the level of the deltopectoral crest, a large protuberance is present for the common insertion of *M. teres major* and *M. dorsalis scapulae*. The distal end is crushed and not informative.

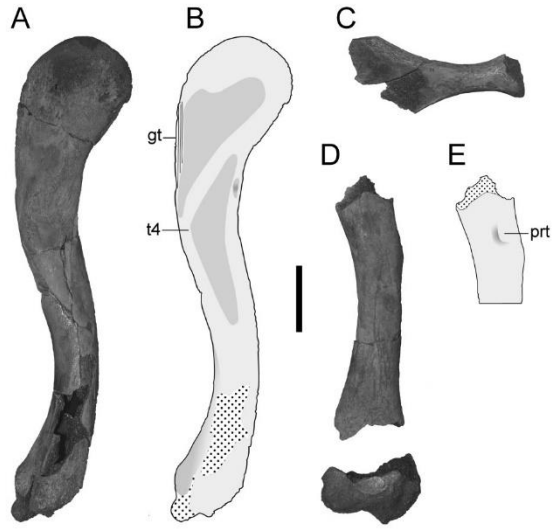


Fig. S2. KSNHM-F7-6 (Kishiwada specimen), A and B, left femur in medial view; C, left pubis in lateral view; D and E, right humerus in dorsal view. gt, greater trochanter; prt, protuberance; t4, fourth trochanter. Scale bar is 5 cm.

Character coding of *Penghusuchus pani* (NMNS-005645), *Toyotamaphimeia machikanensis* (MOU F00001), and the Kishiwada specimen (KSNHM-F7-6: *Toyotamaphimeia* cf. *machikanensis*) used in this study (238 Characters). Character description should be referred to Jouve et al. (2015).

Penghusuchus pani

00110?101100?0000111??1010101100000???0?040??00?1?1????00???2?00?02?0201????2??2??11??07?1?1????110021?000??0030??02100???????0?0??01011101?00101?1010?????????00?001?0100000100?0??00110001??0010??20??0??3000011231 00??0001??11???0011010?

Toyotamaphimeia machikanensis (MOU F00001)

00110101111?1?0011??0101111110000000???000400?10?10?????00?102?00?02?020??0?021?2?1?1?007011?02?01?00210000000031 0??0?0???100??0?0??010???0110001 01?10103???

????00??0?100100000?003000001100011100??0?00?002130000112310 0?0000?11?1???00?10?00

Kishiwada specimen (KSNHM-F7-6: *Toyotamaphimeia* cf. *machikanensis*)

??????????????????????????????1?????0???????400?10????????00?1?2?00????0????0?????2011?00????1???????0??10?0????0?????0?????1?????????01????01???0?0???????????????00?0????10???0??02????0????????????1?????????????????????????????????0?1???0

Table S1: Skull measurements in extant and fossil tomistomines for the comparison of rostral proportions (Fig. 7).

Taxon	Specimen #	Locality	Skull length (mm)	Skull width (mm)	Antorbital length (mm)	Width at anterior end of orbit (mm)	width at 5th maxillary alveolus (mm)	Rostral proportion (orbit)	Rostral proportion (M5 alveolus)
Tomistoma schlegelii	FMNH 11084	Sumatra, Upper Ogan River	135.3	42.5	98.3	21.1	9.0	0.215	0.092
Tomistoma schlegelii	ZSM 202/1907	Sumatra, Sultanat Deli, Batang K'wis	196.7	59.6	145.6	31.1	13.4	0.214	0.092
Tomistoma schlegelii	BMNH 1899.1.31.1	Borneo, Sadong River	344.6	117.2	256.7	53.7	23.5	0.209	0.092
Tomistoma schlegelii	SMF unknown	Sumatra	382.0	141.3	291.8	66.5	27.0	0.228	0.093
Tomistoma schlegelii	ZSM 232/1909	Sumatra, Sultanat Deli, Sungei Rampah	483.0	184.5	366.1	93.7	42.6	0.256	0.116
Tomistoma schlegelii	SMF 28135	Sumatra	499.0	209.9	379.3	103.2	48.7	0.272	0.128
Tomistoma schlegelii	USNM 52972	Borneo, Samarinda	510.0	220.1	399.0	102.9	48.6	0.258	0.122
Tomistoma schlegelii	ZSM 523/1909	Borneo, ohne Fundort	527.0	207.7	413.6	101.6	46.0	0.246	0.111
Tomistoma schlegelii	SMF 28134	Borneo	530.0	201.2	382.8	100.9	44.2	0.264	0.115
Tomistoma schlegelii	BMNH 48.10.31.19	Borneo	542.0	224.9	359.0	112.2	48.7	0.313	0.136
Tomistoma schlegelii	ZSM 200/1907	Central Borneo, Poetos Siban	557.0	232.4	423.6	110.9	46.6	0.262	0.110
Tomistoma schlegelii	ZSM 201/1907	Central Borneo, Sgei Mendalaim	562.0	228.8	435.0	119.0	49.9	0.274	0.115
Tomistoma schlegelii	BMNH 1860.11.6.8	Borneo	574.0	244.6	398.8	126.5	60.7	0.317	0.152
Tomistoma schlegelii	ZSM 203/1907	Central Borneo, Sgei Mendalaim	584.0	254.9	441.2	129.2	56.6	0.293	0.128
Tomistoma schlegelii	ZSM 385/1907	Central Borneo, Kapocasgebiet	590.0	240.1	444.8	119.1	52.6	0.268	0.118
Tomistoma schlegelii	ZSM 374/1907	Central Borneo, Kapocasgebiet	594.0	247.5	445.4	126.6	55.5	0.284	0.125
Tomistoma schlegelii	ZSM 371/1907	Central Borneo, Kapocasgebiet	602.0	237.3	463.6	120.3	50.2	0.259	0.108
Tomistoma schlegelii	USNM 211323	Indonesia, Kalimantan Sanggau, Kapuas River	665.0	289.4	469.8	143.2	69.2	0.305	0.147
Tomistoma schlegelii	ZSM 1/0	Borneo, ohne Fundort	674.0	311.4	501.8	165.0	79.0	0.329	0.157
Tomistoma schlegelii	ZSM 376/1907	Central Borneo, Kapocasgebiet	681.0	291.0	505.1	160.1	75.0	0.317	0.148
Tomistoma schlegelii	ZSM 252/1907	Central Borneo, Bika	686.0	323.0	516.4	175.2	89.4	0.339	0.173
Tomistoma schlegelii	ZSM 375/1907	Central Borneo, Kapocasgebiet	748.0	375.0	560.6	204.4	110.0	0.365	0.196
Tomistoma schlegelii	IRSNB 154C	Borneo	753.0	398.0	559.4	211.1	124.0	0.377	0.222
Tomistoma schlegelii	ZSM 372/1907	Central Borneo, Batang Leopar-Seen	767.0	367.0	540.9	205.8	113.7	0.380	0.210
Tomistoma schlegelii	USNM 211322	Borneo, Sarawak River	783.0	354.0	533.7	197.3	100.6	0.370	0.188
Tomistoma schlegelii	ZSM 370/1907	Central Borneo, Batang Leopar-Seen	812.0	392.0	584.4	233.3	132.9	0.399	0.227
Tomistoma schlegelii	BMNH 94.2.21.1	Borneo	839.0	409.0	608.8	250.0	142.6	0.411	0.234
Toyotamaphimeia machikanensis	MOU F00001	Toyonaka City, Osaka	1020.0	496.0	765.0	333.0	177.9	0.435	0.233
Kishiwada specimen (*Toyotamaphimeia* cf. *machikanensis*)	KSNHM-F7-6	Kishiwada City, Osaka		410.0		219.0			

Supplement to chapter VI

Table S1. Skull length and total length measuremens of *Alligator sinensis* acquired from literatures.

Skull length (mm)	Total length (mm)	Source
160	1230	Wermuth 1964
200	1550	Wermuth 1964
230	1750	Wermuth 1964
150	1250	Cong et al. 1998
154	1280	Cong et al. 1998
154	1300	Cong et al. 1998
166	1380	Cong et al. 1998

学 位 論 文 の 要 約

博士の専攻分野の名称　博士（理　学）　氏　名　　飯　島　正　也

学 位 論 文 題 名

Evolution of Ecology in Crocodylians: Morphometric and Phylogenetic Approach
（ワニ類の生態進化史の復元：形態計測・系統学的アプローチ）

ワニ類は白亜紀中ごろから陸棲・半水棲・水棲と複雑な適応進化をとげながら，水辺を支配してきた爬虫類の一グループである．ワニ類は，現生種の生態観察によって形態と生態を結びつけるエコモルフォロジー研究に最適であり，豊富な化石記録から数千万年スケールの進化史を追うことができる．一方でワニ類の系統分類は，分子・形態仮説が高次分類群レベルで対立しコンセンサスが得られていないため，その生物・進化学的理解を妨げていた．本研究では，１）食性・運動機能などのエコモルフォロジー研究，２）系統仮説の見なおしにより，ワニ類の生態進化史の復元を試みた．

ワニ類のエコモルフォロジー研究では，頭骨や体骨格から食性・運動機能と関連する部位を抽出し，化石種も含めてワニ類の生態の分化・進化パターンについて議論した．はじめに，食性に関連する頭部の形質を探索し，それらの形質の成長パターンを比較することにより，ワニ類（特にクロコダイル上科）の個体成長レベルの適応について議論した．食性に係る形質の中には，成長トレンドが全種共通である形質があり，ワニ類全体におけるサイズ依存の生力学的制約の存在を示唆した．一方で，一部の形質の成長パターンは種間で有意に異なり，これらは魚食化などの食性の特殊化と関連しているものと考えられる．

次に，運動機能に関連する四肢骨や脊椎の種間バリエーションやサイズと形態の関係を評価し，複数の機能システム（採餌，運動機能）の共進化を論じた．現生・化石ワニ類の前肢・後肢のプロポーションを比較すると，ワニ類の２大グループ（アリゲーター上科とクロコダイル上科）間に有意な差が見られた．アリゲーター上科はクロコダイル上科に対して比較的短い柱脚（上腕骨と大腿骨）をもち，２グループの運動能力の違いが示唆された．肢のプロポーションの分化，すなわち運動機能の分化は２グループが分岐して間もなく起こっていた．さらに，肢のプロポーションは頭骨の吻部形態と相関しており，運動・採餌機能の共進化が示された．脊椎形態とサイズの関係の観察からは，体サイズの増加に従って胴椎の椎体関節面が深く広く，また神経棘や横突起が長くなり，脊椎間の可動域が狭まることが分かった．これらのサイズ依存の形態変化は大型の個体が陸上での圧縮荷重や背腹方向の曲げモーメントに耐えうるための適応であり，ワニ類が個体の一生を通して陸上運動能力を保持していることを示す．脊椎形態の種間比較ではインドガビアルの特異性が明らかになった．インドガビアルでは頸椎・胴椎の分化が弱く，また頸椎の可動域が広くなっており，特異な採餌様式（水中での頭部の横運動）を反映しているものと思われる．頸椎の形態は吻部形態と相関しており，採餌能力を最適化するための，頭部と頸部の機能的統合であると考えられる．

ワニ類の系統関係の見なおしでは，系統問題解決の鍵となる日本のワニ化石の記載を行い，従来見過ごされがちであった体骨格形質の洗い出しを行った．日本のワニ化石を含む東アジアの中新世―更新世の“トミストマ類”は，ガビアル類に特有の先祖返り形質を多数有していた．新たなタクソン・形質データセットによる系統解析は依然として従来の形態系統仮説を支持したが，形態データを分子系統仮説にフィットさせた場合の樹長と数ステップしか変わらず，両者の有意差はなかった．新手法を用いて吻部との相関形質の重みを下げて解析した場合も，両者に有意差は顕れず，形態進化が分子仮説上で無理なく説明できることが初めて示された．分子仮説と整合性をもたせた樹上では，インドガビアルの系統で頭部や体骨格の形質が徐々に変化し，生態的に特殊化したことが分かった．